FINAL REPORT

Development of Parameters for the Collection and Analysis of LiDAR at Military Munitions Sites

ESTCP Project MM-0737

JANUARY 2010

Robert Selfridge
USACE

Environmental Security Technology Certification Program

Report Documentation Page

Form Approved
OMB No. 0704-0188

1. REPORT DATE **JAN 2010**	2. REPORT TYPE	3. DATES COVERED **00-00-2010 to 00-00-2010**

4. TITLE AND SUBTITLE **Development of Parameters for the Collection and Analysis of Lidar at Military Munitions Sites**	5a. CONTRACT NUMBER 5b. GRANT NUMBER 5c. PROGRAM ELEMENT NUMBER
6. AUTHOR(S)	5d. PROJECT NUMBER 5e. TASK NUMBER 5f. WORK UNIT NUMBER
7. PERFORMING ORGANIZATION NAME(S) AND ADDRESS(ES) **US Army Corps of Engineers,441 G Street NW,Washington,DC,20314-1000**	8. PERFORMING ORGANIZATION REPORT NUMBER
9. SPONSORING/MONITORING AGENCY NAME(S) AND ADDRESS(ES)	10. SPONSOR/MONITOR’S ACRONYM(S) 11. SPONSOR/MONITOR’S REPORT NUMBER(S)

12. DISTRIBUTION/AVAILABILITY STATEMENT
Approved for public release; distribution unlimited

13. SUPPLEMENTARY NOTES

14. ABSTRACT

15. SUBJECT TERMS

16. SECURITY CLASSIFICATION OF:			17. LIMITATION OF ABSTRACT	18. NUMBER OF PAGES	19a. NAME OF RESPONSIBLE PERSON
a. REPORT **unclassified**	b. ABSTRACT **unclassified**	c. THIS PAGE **unclassified**	**Same as Report (SAR)**	**378**	

Standard Form 298 (Rev. 8-98)
Prescribed by ANSI Std Z39-18

FIGURES

TABLES

APPENDICES

ACRONYMS

CADD	computer-aided drafting and design
CERCLA	Comprehensive Environmental Response, Compensation, and Liability Act
cm	centimeters
CSM	conceptual site model
DEM	digital elevation model
DoD	Department of Defense
DSM	digital surface model
DTM	digital terrain model
EMI	electromagnetic induction
ESTCP	Environmental Security Technology Certification Program
GIS	geographic information system
GPS	global positioning system
IMU	inertial measurement unit
INS	inertial navigation system
kHz	kilohertz
lidar	light detection and ranging
m	meters
MEC	munitions and explosives of concern
MRS	munitions response sites
OB/OD	open burn/open demolition
PDOP	position dilution of precision
pts/m^2	points per square meter
RAID	redundant array of independent disks
TIN	triangulated irregular network
UXO	unexploded ordnance
WAA	wide area assessment

ACKNOWLEDGMENTS

This project was made possible through funding provided by the Environmental Security Technology Certification Program. For their support and guidance to the US Army Corps of Engineers and URS on this project, we would like to express our sincere appreciation to:

- Dr. Jeffrey Marqusee, Director, Environmental Security Technology Certification Program and Strategic Environmental Research and Development Program
- Dr. Anne Andrews, Deputy Director, Environmental Security Technology Certification Program and Strategic Environmental Research and Development Program
- Dr. Herb Nelson, Munitions Management Program Manager, Environmental Security Technology Certification Program and Strategic Environmental Research and Development Program

We gratefully acknowledge the following for their technical review of drafts of the white papers and guidance document d included in the appendices:

- Terra Remote Sensing, Inc., especially Dave Neufeldt and Dave Mostyn
- Sky Research, especially Joy Rogalla and Tom Prescott
- Terrapoint, LLC, especially Kresimir Kusevic, Peggy Cobb, Claude Vickers, and DJ Lehto
- Karen Shuckman, URS and Instructor, Pennsylvania State University
- Bob Ryan, URS, formerly with Fugro EarthData

EXECUTIVE SUMMARY

The purpose of this project was to:

- Systematically investigate the effect of vegetation cover on the effectiveness of airborne lidar in munitions management
- Examine the effects of lidar point classification methods on lidar data density, along with implications for munitions sites
- Summarize the sources and magnitudes of lidar error, along with implications for munitions sites
- Evaluate the ability of current software packages to automatically identify ground features typical of munitions sites
- Summarize lessons learned from the Environmental Security Technology Certification Program (ESTCP) Wide Area Assessment (WAA) Pilot Program

This research project extends the earlier work with light detection and ranging (lidar) that was carried out by URS Corporation in Project 200534. Principal findings include the following:

Activity 1 – Systematically investigate vegetation effects

- Measures of vegetation height and density derived from lidar correlated reasonably well with standard measures for trees but not for grass.
- Vegetation caused a decrease in lidar density. At a series of vegetated test plots at the Former Camp Beale ESTCP demonstration site, up to 90% of laser pulses were determined to have returned from vegetation. Lidar data density was sufficient to model the ground surfaces under trees at this site, however the quality of the surface model was degraded under brush.
- Lowering the lidar data density at test plots affected feature detection. Lidar data at the higher densities tested (13.8 points per square meter [pts/m^2]) detected all of the features at the test plots, as verified by a field visit. Significant loss of feature detection began to appear between 6.9 pts/m^2 and 3.4 pts/m^2, with over two thirds of the features not visible at the lowest density level tested (0.8 pt/m^2).
- As lidar data density was lowered, ground feature detection rates declined, however, the effect varied: some features faded gradually as lidar density was lowered, while others did not disappear at all. There was some correlation between the rate of degradation and the size of the feature; that is, larger features tended to disappear more slowly. However, this correlation was not strong.
- The implications of the non-linear relationship between lidar data density and feature detection implies that there is no threshold lidar density at which no features will be detected. Rather, lower-density lidar will result in a lower degree of confidence.
- It appears that increasing lidar density will have a point of diminishing returns, after which additional lidar points will not reveal additional features.

- At 59 test plots, adding all of the lidar points within 40 cm of the vendor's ground surface revealed additional potential features at 36% (21) of the test plots. There was little to no negative impact to the quality of the ground surface model, even though this procedure added low vegetation and noise. This implies that modifying point classification methods to include more points in the ground surface model can potentially improve feature detection.
- Surface model cell size had a dramatic impact on detection of small features. At test plots where different cell sizes were tested, using smaller cell sizes both revealed additional small features and increased the clarity of the features shown. It appears to be appropriate to err on the side of smaller rather than larger grid cells.
- The positional accuracy of lidar points varies with many factors, with the largest instrument-based factors being flight height and distance from nadir of the laser signal. Lidar acquisitions at the ESTCP demonstration sites were conducted from 300 to 1,000 m, where instrument error is relatively low. Lidar collected at these sites met their contracted accuracy specifications, and subsequent acquisitions should successfully meet similar accuracy specifications. However, where accuracy is especially important, contract specifications may be adjusted to require the vendor to fly lower and/or use a narrower field of view.
- Positional error in lidar data will be higher on sites with steep terrain. Where appropriate, lidar accuracy can be assessed independently for major terrain types.
- Surveyed points used for calibration and quality control of lidar must be from a source of higher quality than the lidar data itself. Survey errors in control and calibration points can lead to incorrect assessment of data quality or errors in the entire lidar data set.
- Confidence levels for feature detection using lidar can be mapped. It is possible to map the number of ground returns per square meter, using either the vendor's classification or a re-classified data set. Site managers and regulators can use these maps to classify areas where insufficient lidar points reached the ground surface to characterize features of a given size.
- The results of this investigation point out the importance of receiving the entire lidar point data set for all lidar investigations. Because lidar data sets are very large, many vendors only deliver derived products such as ground surface models. By requiring delivery of the full data set, Government land managers can evaluate the approaches to point classification and to surface model creation used by the vendor, and make appropriate adjustments.
- There are advantages to conducting lidar data analysis, including creating surface models, in-house by Government end-users in-house, rather than having the vendor deliver them. Creating these products in-house can allow for experimentation with alternative methods. However, this requires that Government users have sufficient software tools and training to accomplish these tasks. Creating DEMs and DTMs in-house can be challenging, especially with high-density data sets where the number of points is very large. In such cases it may be appropriate for end-users to work with sample data sets to determine, in

consultation with vendors, the appropriate specifications for analysis products, and then request that the vendor create and deliver the final products.

Activity 2 – Evaluate current software packages

Current software products offer many useful tools for manipulating lidar data, but of those reviewed, only the HTFC software by Sandia National Laboratories was able to delineate craters from lidar-based surfaces. However, software for manipulating lidar is continuously being developed, and software vendors should be contacted periodically to review new developments. Government offices that use lidar data also should be contacted to determine which software products are currently in use and whether they are performing well.

Activity 3 – Summarize lessons learned from the ESTCP WAA Pilot Program

URS and USACE delivered a revised draft guidance document summarizing lessons learned to ESTCP and technical peer reviewers in July 2009. This document was revised based on ESTCP and peer review, and is submitted as Appendix D.

Cost Benefit Implications

Cost drivers for lidar and orthophoto acquisition are discussed in detail in the final reports for the ESTCP demonstration sites and for the Pilot Program as a whole. Additional conclusions from this investigation include:

- Cost for data acquisition at vegetated sites should not be significantly higher than for non-vegetated sites, except in exceptional circumstances. Lidar at vegetated sites should be collected at a higher density; however, with the introduction of higher-speed sensors (up to 250 kilohertz), appropriate data densities for vegetated sites will rarely require additional flight lines.
- The cost of orthophoto acquisition could be lower at vegetated sites, since at such sites orthophotos could be acquired with larger pixel sizes or omitted in favor of using pre-existing orthophotos.
- There should be little additional cost for changing data classification specifications to return more points to the ground surface model. At most, the vendor would charge for some initial tests of alternate processing methods, or for establishing an additional category for low lidar points. These additional costs should not be high.
- This project showed that feature detection rates did not go down substantially between the highest data density tested (13.8 pts/m^2) and half of that density (6.9pts/m^2). This suggests that it is unnecessary to collect extremely high lidar data densities. This may result in some cost savings.

1.0 INTRODUCTION

Earlier work supported by the Environmental Security Technology Certification Program (ESTCP) has shown that airborne light detection and ranging (lidar) can be a useful and cost-effective tool in the assessment and characterization of munitions response sites. The purpose of this research project is to:

- Systematically investigate the effect of vegetation cover on the effectiveness of airborne lidar in munitions management
- Examine the effects of lidar point classification methods on lidar data density, along with implications for munitions sites
- Summarize the sources and magnitudes of lidar error, along with implications for munitions sites
- Evaluate the ability of current software packages to automatically identify ground features typical of munitions sites
- Summarize lessons learned from the ESTCP Wide Area Assessment (WAA) Pilot Program

1.1 BACKGROUND

Many millions of acres of current and former Department of Defense (DoD) lands are potentially contaminated with military munitions or their components. On the majority of these sites, munitions are concentrated in specific ranges and training areas, while the remainder of the site is ordnance-free. Locating the site of contamination can be difficult, in part because historical records are often incomplete or inaccurate. The cost of traditional surveys using magnetometry and electromagnetic induction (EMI) can be very high, and this has driven the search for innovative methods to reduce costs.

This research project is an outgrowth of the WAA approach to site characterization and the ESTCP WAA Pilot Program. WAA is a procedure used to gather *"a preponderance of evidence that improves the understanding of the site and builds confidence in the conclusions. A suite of commercially available technologies provides data to:*

- *Identify areas of concentrated munitions use*
- *Collect information that will support decisions on areas with no indication of munitions presence*
- *Collect data to support planning, prioritization and contracting when a site ultimately must be cleaned up"* (Nelson et al. 2008)

Previous work by ESTCP demonstrated that lidar could be an effective addition to this combination, helping to detect and delineate munitions response sites (MRS), correcting the initial conceptual site model (CSM), and providing data in support of subsequent investigation. Results from lidar and orthophotos provided cross-validation of magnetometry and EMI data,

leading to higher confidence levels, and the combination of technologies employed in the pilot program was found to be cost-effective (Nelson et al. 2008).

The current demonstration extends ESTCP's earlier work with lidar that was carried out by URS Corporation in Project 200534.

1.2 OBJECTIVES OF THE DEMONSTRATION

This demonstration is an extension of the WAA Pilot Program, investigating and providing additional guidance to Government land managers on the appropriate use of lidar and orthophotography at munitions sites.

Activity 1: Systematically investigate vegetation effects on airborne lidar in munitions management

The objectives for this activity were to:

a. Examine the performance of lidar and orthophotography for detection of MRS and munitions and explosives of concern (MEC)-related features under a range of described vegetation conditions

b. Investigate the relationship between vegetation density and lidar point density, and its relationship to object detection

c. Provide guidance to Government land managers on the effects of vegetation conditions on the size, shape, and location of features that can be detected with lidar and orthophotography

d. Investigate the impact of lidar point classification methods on ground surface models and feature detection and determine whether changes to point classification methods would result in increased detection capability (this objective was added following the In-Progress Review meeting of February 2008)

e. Summarize the types and magnitudes of lidar error and their implications for the use of lidar at military munitions sites (this objective was added following the In-Progress Review meeting of October 2008)

Activity 2: Evaluate current software packages for their ability to automatically identify ground features typical of munitions sites

The objective for this activity was to:

a. Evaluate the ability of commercial, off-the-shelf software to identify MEC-related ground features from lidar data sets typical of munitions sites. Analyze features including craters at a variety of sizes from 2–5 meters (m) in diameter, along with bombing targets and other objects constructed from berms.

Activity 3: Summarize lessons learned from the ESTCP WAA Pilot Program

The objectives for this activity were to:

a. Accurately summarize the lessons learned during previous lidar and orthophotography testing at the ESTCP WAA demonstration sites, as well as the results of Activities 1 and 2, in a single guidance document

b. Provide peer review of the draft guidance document

c. Contribute useable and meaningful guidance to Government land managers considering the acquisition and use of lidar and orthophotography data in munitions management

1.3 REGULATORY DRIVERS

MEC remediation is generally conducted under the authority of the Comprehensive Environmental Response, Compensation, and Liability Act (CERCLA). With many millions of acres of land potentially contaminated, estimates of the cost of elimination of environmental liability under this statute at known and former DoD sites range as high as several hundred billion dollars. These potentially high costs have led to interest in developing innovative investigative or screening methods such as WAA, in order to reduce the costs of associated remediation activities.

2.0 TECHNOLOGY

This section provides an overview of lidar and orthophotography technology.

2.1 TECHNOLOGY DESCRIPTION

Lidar technology uses an airborne laser and sensor to map ground and non-ground surfaces. The laser and sensor are mounted in a helicopter or small aircraft, and Global Positioning System (GPS) and inertial measurement unit (IMU) equipment is used to locate the sensor in the air. The time of return of the laser signal allows for the accurate calculation of its point of reflection from the ground, buildings, or vegetation (Figure 1). Each laser return is classified as returning from the ground surface, vegetation, structures, or other objects.

Figure 1: Lidar System Operations

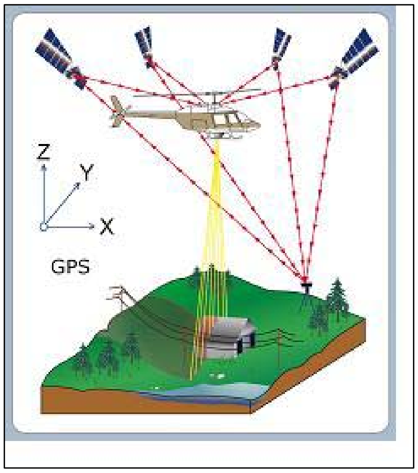

Lidar points have a vertical positional accuracy of approximately 15 centimeters (cm) on soft ground surfaces and a horizontal accuracy of approximately 60 cm, both compared to surveyed control points. Actual point-to-point variation is typically less than 15 cm. Accuracy is greater on relatively flatter and harder surfaces.

Once elevation data are collected in the form of lidar points, surface models are created and analyzed, and maps and analysis products are created. The surface modeling process can be conducted using standard Geographic Information System (GIS) software and methods, and much of the process can be automated.

Lidar has been become a standard tool for many applications that require detailed ground surface models. Its popularity is due to its ability to provide more accurate topographic data than other sources, at a reasonable cost compared to alternatives such as ground survey or photogrammetry.

An orthophotograph is a digital aerial photograph that has been geometrically corrected for topographic relief, lens distortion, and camera tilt. Individual digital images are assembled into a single mosaic, which is then corrected using sophisticated mathematical methods to permit the accurate spatial location of each photo pixel. This process, called orthorectification, allows the images to be used in a GIS or computer-aided drafting and design (CADD) system with other spatial data, such as contour lines or survey data (Nelson et al. 2008). While orthophotos are adjusted so that the pixels are spatially accurate, this only encompasses pixels representing the ground surface. Pixels representing the tops of buildings or tall trees can be slightly displaced (Appendix B).

Digital orthophotography has been available commercially since the early 1980s, with steady improvement in the resolution (i.e., pixel size) and precision (i.e., pixel placement) of the images as the technology of digital cameras, GPS, and IMU systems has advanced. Digital cameras have largely replaced film cameras in the productions of orthophotos (Dold 2008).

Airborne digital cameras have been integrated with lidar sensors successfully and, because the two sensors use the same GPS and Inertial Navigation System (INS), the two data sets can be integrated very accurately. Vendors generally guarantee a horizontal accuracy of three pixel widths compared to ground control for orthophotography, and spatial integration of orthophotos and lidar within two pixel widths.

Final orthophoto pixel size depends on the flight altitude and the camera specifications. For munitions sites, orthophoto pixel size is typically from 0.3 m (about 1 foot) down to 0.1 m (about 4 inches) (Nelson et al. 2008). Pixel sizes smaller than this generally are impractical because of the low flight elevations and slow flight speeds required to collect properly overlapping images, and the large numbers of images that would need to be combined into the image mosaic. Many areas also have existing orthophotography available, with pixels in the 0.5–1.0 m size range.[1]

A more complete description of lidar and orthophotography technology, including a discussion of system components, multi-return capabilities, and other characteristics, is provided in the ESTCP White Papers Errors in Lidar Data: Implications for Investigation of Military Munitions Sites (Appendix B) and Effects of Lidar Point Classification Methods on Surface Model Creation and Feature Identification (Appendix C).

2.2 TECHNOLOGY DEVELOPMENT

Between 2005 and 2007, ESTCP conducted a pilot program to test the effectiveness of a multi-technology approach to unexploded ordnance (UXO)/MEC WAA.

The first phase of the ESTCP program was carried out at seven sites. The first four were desert sites where the technologies were expected to perform well. The last three were sites with more challenging conditions and were chosen to test the limits of the various technologies chosen. The WAA Pilot Program examined the use of lidar, orthophotography, helicopter magnetometry, towed-array magnetometry, synthetic aperture radar, hyperspectral sensing, and statistically-based transect design.

At the five sites where lidar and orthophotos were tested, the results were positive. Lidar and orthophotos were used to locate berms, bombing targets, and individual craters, even where these features were highly eroded and could not be detected by ground-based field crews. The location of these features was used to correct the initial CSM, to refine the boundaries of MRS, and to support and help direct the use of subsequent technologies that directly detect ordnance. Example results are shown in Figure 2.

[1] States, cities and counties acquire orthophotos for a variety of purposes, not generally including detection of smaller objects. Consequently, these entities generally do not incur the considerably larger costs of higher-resolution orthophotos. These coarser images can nevertheless be useful on munitions sites with tree cover, where individual features are not visible and the primary use of the images will be overall mission planning.

Figure 2: ESTCP Demonstration Sites, Example Munitions-Related Features

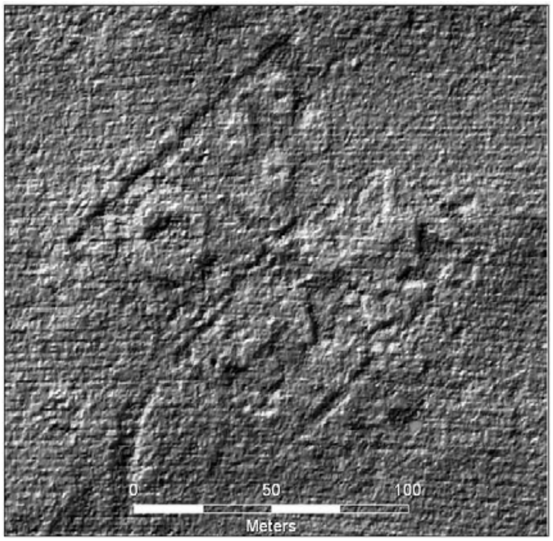

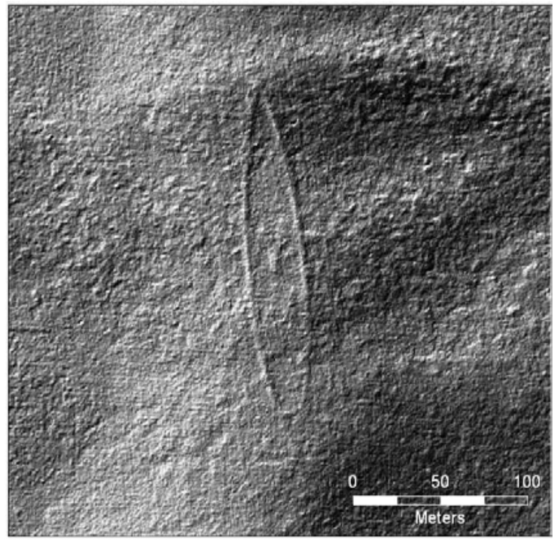

Kirtland Air Force Base Precision Bombing Range demonstration site. Bombing targets from the 1940s are visible in lidar-derived surface models. These targets are highly eroded and cannot be seen from the ground or in aerial photos.

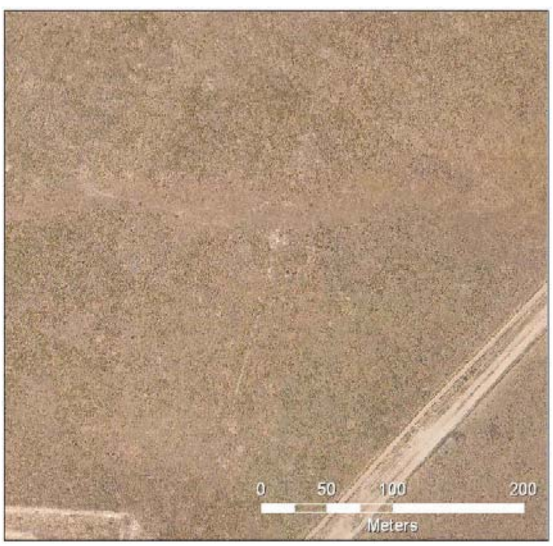

Kirtland demonstration site. Bombing target cross-hairs visible in 10-cm pixel orthophoto.

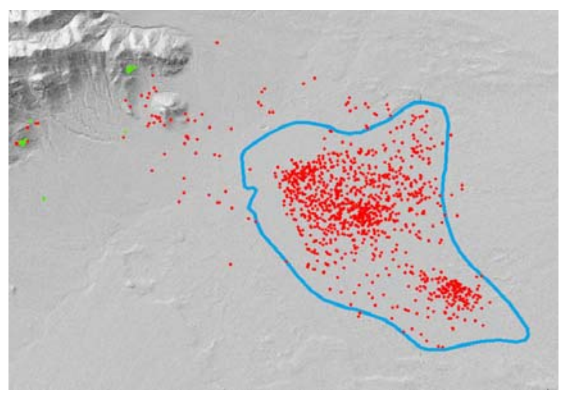

Victorville Demolition Bombing Range demonstration site. Potential crater locations outside of the original target area boundary.

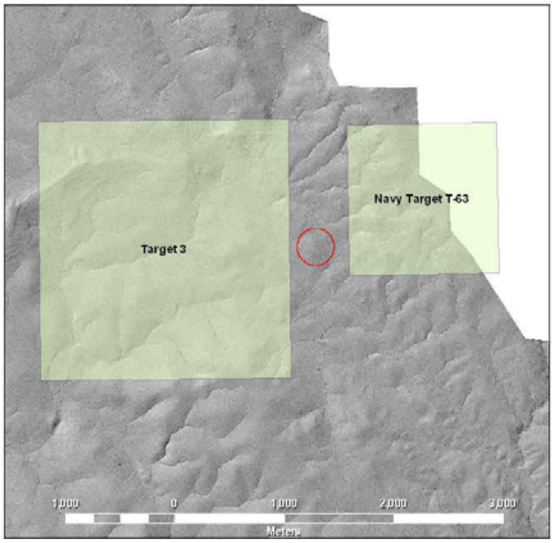

Former Camp Beale demonstration site, bombing target (red circle) located outside of mapped target locations based on historical records.

Pueblo Precision Bombing Range demonstration site, crater density map used to refine original MRS boundary. Source: ESTCP and Sky Research.

2.3 ADVANTAGES AND LIMITATIONS OF THE TECHNOLOGY

Lidar and orthophotography have the advantages and limitations discussed in Sections 2.3.1 and 2.3.2 compared to the current approach to creating CSMs through reviewing historic documents, ground-based geophysical surveys, and statistical modeling. These advantages and limitations were reported in URS's final reports for the ESTCP demonstration sites it examined (URS 2007 and 2008a) and for the overall program (Nelson et al. 2008), and are consistent with the findings of this demonstration.

2.3.1 Advantages of the Technology

Using lidar and orthophotos offers several advantages compared to the traditional approaches to site investigation:

- ***Rate of coverage.*** In an operational setting, data collection rates of 5,000 acres per day or higher can be expected for lidar and orthophotos. This compares favorably to typical collection rates of around 500 acres per day for helicopter-based magnetometry, 5 to 20 acres per day for towed-array magnetometry, and 1 to 5 acres per day for man-portable magnetometry.
- ***Enhanced planning and risk assessment.*** Because they can cover entire sites relatively quickly and at lower cost, these technologies can be used to locate and prioritize the use of more costly low-altitude or ground-based technologies.

- ***Ability to delineate MRS and MEC-related features.*** Lidar and orthophotography can, under some circumstances, successfully reveal MRS and MEC-related surface features even many years after their last use.
- ***Cross-validation.*** Lidar and orthophotos can cross-validate the results of other technologies, leading to enhanced confidence in results.
- ***Other benefits.*** Both technologies provide highly detailed topographic data that can be integrated into a facility's CADD or GIS system and used in subsequent phases of site investigation, site remediation, and range management.

2.3.2 Limitations of the Technology

The primary limitation of lidar and orthophotography is that neither technology can directly detect ordnance or MEC components, such as ferrous scrap. Consequently, lidar and orthophotos are not substitutes for technologies that directly detect ordnance, such as magnetometry or EMI. Rather, lidar and orthophotos are used to give a rapid assessment of potential areas of ordnance use, based on ground features such as target objects, crater fields, open burn/open demolition (OB/OD) areas, berms, or roads. Areas appearing to be free of evidence of munitions use in lidar and orthophotos still need to be surveyed with magnetometry or EMI; however, the initial level of effort with these technologies could potentially be reduced, and then adjusted depending on the initial results.

Lidar and orthophotos are best used as the first step in site investigation to quickly identify areas of potential contamination and other areas of interest and to help direct the application of subsequent technologies. Lidar and orthophotos will be less useful on sites that already have been well characterized using other methods, or on small sites that can be surveyed quickly using ground crews.

An additional limitation of orthophotos is their limited usefulness at highly vegetated sites. At such sites, orthophotos show only the tops of the vegetation, and will have limited usefulness. Lidar will provide useable surface models through many vegetation conditions, and will show severe degradation only where the vegetation is particularly dense. However, vegetation will lower the density of lidar returns from the ground surface and will thus lower confidence levels for detecting features under vegetation.

3.0 PERFORMANCE OBJECTIVES

URS's ESTCP Draft Demonstration Plan (URS 2008b) establishes performance objectives for the current demonstration. Table 1 lists these objectives plus additions related to white papers requested by ESTCP following the February and October 2008 In-Progress Review meetings.

Table 1: Performance Objectives

Performance Objective	Metric	Action to Achieve Metric	Sampling Frequency or Timing	Desired Result
Activity 1: Systematically Investigate Vegetation Effects – Field Data Collection				
Delineate vegetation classes using photos and lidar data	All major vegetation classes identified	Delineate from orthophotos followed by QA/QC review by qualified staff	Once at start of project	100% identification of all major vegetation classes
Calculate lidar ground and vegetation point percentages	Percentages accurately calculated on a per square meter basis using a 3 m cell size to show variation across the study area	Use of standard GIS calculation methods followed by QA/QC review	Once at start of project	100% of study area characterized
Calculate lidar data density variability	Density of ground lidar points and all lidar points accurately calculated on a per-meter basis to show variation across the study area	Use of standard GIS calculation methods followed by QA/QC review	Once at start of project	100% of study area characterized
Select representative field plots	Representative study areas selected	Select at least 50 plot locations, with plots distributed in all vegetation classes	Once at start of project	Plots placed in all vegetation classes
Collect field vegetation density data	Collect accurate data on vegetation conditions at each plot	Use standard forestry methods to determine vegetation density	Once	All field data collected to follow SOP
Collect field ground feature data	Collect accurate data on ground features at each plot	Incorporate field procedures into SOP, followed by QA/QC review	Once	All field data to follow SOP
Activity 1: Systematically Investigate Vegetation Effects – Data Analysis				
Step 1: Classify Vegetation				
Lidar ground point density vs. field vegetation density	Difference between vegetation density as measured by lidar and field methods	Standard GIS analysis methods, followed by QA/QC review	Once	Correlation should be highest in plots with a single, simple vegetation class such as grass or trees

Performance Objective	Metric	Action to Achieve Metric	Sampling Frequency or Timing	Desired Result
Lidar vegetation heights vs. field vegetation heights	Difference between vegetation heights as measured by lidar and field methods	Comparison of lidar and field data	Once – these may vary seasonally (for grasses) depending on the timing of the lidar survey and site visit)	Correlation should be within 5 feet for isolated trees
Step 2: Identify Ground Features				
Field ID of features vs. ID of features from lidar	Percentage detection and false alarm rate for features detected using lidar vs. field observation	Visual observation of lidar data followed by comparison of results of lidar and field observations	Once	Correlation should be 100% for features over 1 m in size in plots with no covering vegetation
Effects of lidar point density on feature detection	Number of features visible at successively lower point densities	Artificially lower point density through a series of levels, create surface models and examine the detection of features visible at the highest density	Once	Determine the lidar data density where detection falls off substantially
Step 3: Produce White Paper on Lidar Point Classification Methods				
Determine the percentage of lidar points misclassified as non-ground returns	Percentages of points classified as ground or non-ground in selected vegetation-free locations	Analyze in GIS to determine percentage values at selected test areas	Once	Determine magnitude of misclassification problem
Determine the source of misclassification of lidar points as non-ground returns	Clear understanding of the source of misclassification	Converse with vendors' data classification staff and examine software manuals for classification software	Once	Clear understanding of the source of misclassification
Examine the potential benefit of reclassification of lidar points	Approximate number and size of features visible after reclassification	Create new surface models using reclassified points and examine to determine whether additional features are visible	Once	Estimate of the potential benefit of point reclassification
White paper technical accuracy	White paper is technically accurate	Peer review by specialists from industry and universities	Once	Document will be technically accurate
White paper readability	Document is well written and understandable by non-specialists	Technical editing and QA/QC review	Once	Document will be understandable

Performance Objective	Metric	Action to Achieve Metric	Sampling Frequency or Timing	Desired Result
Step 4: Produce White Paper on Lidar Error				
White paper technical accuracy	White paper is technically accurate	Peer review by specialists from industry and universities	Once	Document will be technically accurate
White paper readability	White paper is well written and understandable by non-specialists	Technical editing and QA/QC review	Once	Document will be understandable
Activity 2: Evaluate Current Software Packages				
Prepare appropriate lidar data sets for subsequent testing	Accurate ID of ground features for testing	Visual inspection followed by QA/QC review	Once at start of project	100% confidence in test features to be given to vendors
ID of features using automated methods	Percent detection and false alarm rate of automated methods vs. visual inspection results	Compare results of visual inspection and automated methods	Once from each vendor	Percent detection will be highest for isolated, well-defined features. False alarm rate will be lowest for relatively flat, smooth ground surfaces.
Activity 3: Summarize Lessons Learned from the ESTCP WAA Pilot Program				
Usability	Guidance document applicable to the requirements of present and anticipated munitions management programs	Peer review by DoD program and policy staff	Once	Document will be useable
Technical accuracy	Guidance document is technically accurate	Peer review by specialists from industry and universities	Once	Document will be technically accurate
Readability	Guidance document is well written and understandable by non-specialists	Technical editing and QA/QC review	Once	Document will be understandable

DoD – Department of Defense
GIS – Geographic Information Systems
ID – identification
m – meter
QA/QC – quality assurance/quality control
SOP – standard operating procedure

4.0 SITE DESCRIPTION

No new sites were developed for this demonstration. Instead, lidar data from four ESTCP demonstration sites where lidar was collected previously were re-examined. These demonstration sites are described in the Final Report for the WAA Demonstration Project (Nelson et al. 2008). A summary of site characteristics is provided in Table 2.

Table 2: ESTCP Demonstration Sites

Name	Pueblo PBR	Kirtland AFB PBR	Victorville DBR "Y" and PBR 15	Former Camp Beale
Location	Pueblo, CO	Albuquerque, NM	Victorville, CA	Marysville, CA
Size (acres)	6,710	5,000	5,640	87,672
Date of acquisition	August 20–23, 2004	August 9–11, 2005	January 24–25, 2006 February 3–4, 2006	July 22–26, 2006
Lidar vendor	Sky Research	Terra Remote Sensing	Terra Remote Sensing	Terra Remote Sensing
Lidar data sets (#)	1	4	2	2
Overall lidar data density (pts/m^2)	5.16[a]	900 m North Block: 1.4 900 m South Block: 1.6 450 m north block: 5.2 450 m south block: 4.1 300 m east-west north block: 5.2 300 m north-south north block: 6.5 300 m flight 1 south block: 5.9 300 m flight 2 south block: 6.1	450 m flight: 4.8 300 m flight: 6.4	450 m flight: 13.8 300 m flight: 13.7
Orthophoto pixel size (cm)	18	12 / 20	10	10
Reference	Sky Research 2008	URS 2007	URS 2007	URS 2008a

a. Sky Research reported density as average point separation rather than average points per square meter. The reported point spacing of 0.44 m was converted to average points per square meter using the formula $D = 1/(s_a)^2$ where D is the density in points per square meter and s_a is the average separation in meters.
AFB – Air Force Base
DBR – demolition bombing range
PBR – precision bombing range
pts/m^2 – points per square meter

4.1 SITE SELECTION

4.1.1 Activity 1: Systematically Investigate Vegetation Effects

For Activity 1, URS used lidar and orthophotography data from a study area within the Former Camp Beale demonstration site in the Activity 1 analysis. This data set was chosen based on the following criteria:

- The study area contains several vegetation types, but vegetation is not too complex for an initial study of this type.
- The study area is located on public land within the Spenceville Wildlife Refuge. Because the site is public property with a single manager, site access was easier than with the multiple private property owners in the remainder of the Former Camp Beale site.
- The lidar data for the study area is very dense, and provides a useful "best case" test data set.
- Approximately 50 features of interest within the study area had been visited by field crews already. Data for these features included GPS location and a site photo.
- Because the study area is managed as a wildlife refuge, there had been no vegetation clearing since the lidar data was collected. Given the dry and undisturbed nature of the study area, vegetation conditions were likely to be relatively unchanged between lidar data collection in June 2006 and the field visit in September 2007.

The white paper on point classification (Appendix C) was based primarily on data from the Former Camp Beale demonstration site, along with discussion with vendors. However, its conclusions were verified by examining lidar data from the other ESTCP demonstration sites where lidar was collected, in addition to lidar data from two non-ESTCP sites.

The white paper on lidar error was based primarily on published literature and interviews, and did not involve site selection.

4.1.2 Activity 2: Evaluate Current Software Packages

Data from portions of the Kirtland and Victorville demonstration sites were used for the software test. The Victorville data set was chosen based on the following criteria:

- The craters at this target are large (up to 8 m in diameter), deep (up to 1 m) and are generally well defined in the lidar data. In addition to overlapping craters in patterns typical of crater fields, the data set contains many isolated, non-overlapping craters. These large, isolated craters provided a good "best case" data set for an initial software test.
- Because the craters are large and well defined, a comparison data set against which to judge the software results can be created with a high degree of confidence using visual inspection of the lidar and orthophotos.

The Kirtland data set included Target NDIA and Targets N2 and N3. This data was chosen based on the following criteria:

- Target NDIA is a high explosive bombing target containing a large number of small (2–3 m diameter), shallow (10–20 cm) craters. Because these craters are shallow and eroded, they are more difficult to distinguish from the normal variation in the ground surface. This data constitutes an appropriate complement to the simpler data from the Victorville site.
- Targets N2 and N3 contain large targets constructed from berms: a bull’s-eye target at N2, and a bull’s-eye target and a ship target at N3. These features can be seen clearly during visual inspection of the lidar data, but are highly eroded, often no more than 20 cm in height, and are not visible from the ground.

4.1.3 Activity 3: Summarize Lessons Learned from the ESTCP WAA Pilot Program

The deliverable for Activity 3 (Appendix D) summarizes lessons learned at the applicable ESTCP demonstration sites.

4.2 SITE HISTORY

The history and characteristics of each of the test sites, including munitions contamination, are described in the final report for the ESTCP WAA Pilot Project (Nelson et al. 2008). Site history is not available for the non-ESTCP sites that were examined in the white paper on point classification (Appendix C).

4.3 SITE GEOLOGY

Not applicable.

5.0 TEST DESIGN

5.1 CONCEPTUAL EXPERIMENTAL DESIGN

The demonstration was executed following the steps shown in Figure 3.

Figure 3: Conceptual Experimental Design Process

Item	Date of Completion
Initial planning meetings	6/15/2007
Demonstration plan, initial	7/1/2007
Field data collection	9/20/2007
Analysis of vegetation effects	2/1/2008
ESTCP Symposium	12/6/2007
Demonstration plan, revised	2/1/2008
Feature extraction software, downselect	2/15/2008
IPR	2/28/2008
Demonstration plan, revised 2	4/1/2008
White paper on point classification, draft	9/3/2008
Guidance document preliminary draft	10/3/2008
Interim Progress Report	11/1/2008
IPR	10/7/2008
ESTCP Symposium	12/4/2008
White paper in point classification, final	2/1/2009
White paper on lidar error, draft	5/1/2009
Feature extraction software, vendor contact and responses	5/1/2009
IPR	5/5/2009
Guidance document revised draft	7/13/2009
Final Report	1/31/2010

5.1.1 Activity 1: Systematically Investigate Vegetation Effects

Activity 1 was designed to establish performance criteria for lidar on vegetated sites using existing data. Activity 1 consisted of four steps.

Step 1: Classify vegetation. This part of the analysis compared the density and height of vegetation using lidar data to density and height measured in the field using standard forestry techniques. The field crew measured vegetation density using a spherical densitometer, tree height using a hand-held clinometer, and grass height using a tape measure (see Section 6.1.1). The field crew examined each plot to determine whether there were ground features visible that were not found in the lidar data, or features in the lidar data that were not found in the field.

Step 2: Identify ground features. This part of the analysis examined the effects of lowering the lidar data density on detection of ground features. The lidar data was decimated (artificially thinned) to simulate lower data collection densities, and the effects of this decimation on feature

detection were examined. URS created surface models at selected plots using the full lidar data sets and four decimated data sets, using the orthophoto data for the site as a cross-validation method where possible. URS then examined the surface models visually to determine whether the ground features at each test plot was visible at each decimation level.

Step 3: Produce White Paper on Lidar Point Classification Methods. At the In-Progress Review meeting in February, 2008, preliminary results were presented showing that in some cases, a significant number of lidar points on paved surfaces had been classified as non-ground returns. This result had the potential to lower the resolution of ground surface models. ESTCP requested a technical white paper examining lidar point classification methods, determining whether this phenomenon was unique to a single data set or vendor, and examining potential changes to classification methods. The white paper was based on re-examining data from all of the ESTCP demonstration sites and two non-ESTCP sites. In addition, URS conducted discussions with the two lidar vendors who provided data for the ESTCP demonstrations, Terra Remote Sensing and Sky Research, regarding point classification methods and potential alternative approaches. Technical peer review was provided by Terra Remote Sensing, Sky Research, and additional vender (Terrapoint, LLC), and URS internal experts. This white paper is included as Appendix C.

Step 4: Produce White Paper on Lidar Error. Following the October 2008 In-Progress Review meeting, ESTCP requested an additional technical white paper summarizing the sources and magnitudes of lidar error and their implications for the use of lidar at military munitions sites. This technical paper was based on existing literature; no original investigation was conducted. The white paper includes consideration of both lidar points and digital surface models. Technical peer review was provided by Terra Remote Sensing, Sky Research, and additional vender (Terrapoint, LLC), and URS internal experts. This white paper is included as Appendix B.

5.1.2 Activity 2: Evaluate Current Software Packages

Step 1: Evaluate existing commercial off-the-shelf feature extraction software packages. URS examined approximately 850 software products that advertised some ability to manipulate three-dimensional spatial data.[2] Criteria for further selection included:

- Will the software load and manipulate lidar point formats easily?
- Will the software handle large lidar data sets? What are the file size limits?
- What kind of processing speeds will the software achieve for creating surface models?
- Will the software output results be compatible with common GIS and CADD software?

[2] The source of the original list of software products was compiled by the US Army Topographic Engineering Center, which compiled "a summary of 3D terrain visualization software that may be relevant to LiDAR/ASLM users." Originally available at: http://www.tec.army.mil/TD/tvd/survey/index.html.

Based on this survey, URS selected 17 software packages for further evaluation. The manufacturers of the selected software packages were contacted and invited to participate in a test using a sample lidar data set containing data from both the Kirtland and Victorville demonstration sites. Software vendors were invited to report the number and type of features extracted, and to describe their capabilities, particularly for automated extraction.

Step 2: Testing software packages. Manufacturers of software packages that successfully identified features during Step 1 were to be invited to participate in a test using a larger and more complex lidar data set. Based on the results of Step 1, URS and the US Army Corps of Engineers recommended that this step not be undertaken (see Section 6.2).

5.1.3 Activity 3: Summarize Lessons Learned from the ESTCP WAA Pilot Program

In October 2008, URS submitted a preliminary draft guidance document to ESTCP summarizing the lessons learned through the WAA Pilot Program related to lidar and orthophotos, as well as the preliminary results from the first two activities of this demonstration. In July 2009, URS submitted a revised draft of the guidance document to ESTCP and technical peer reviewers. The final version appears as Appendix D.

5.2 SITE PREPARATION

Not applicable.

5.3 SYSTEM SPECIFICATION

Lidar system components are described in the white paper on lidar error (Appendix B).

5.4 CALIBRATION ACTIVITIES

Calibration activities are described in the final reports for the ESTCP demonstration sites (URS 2007 and 2008a) and the ESTCP Pilot Project Wide Area Assessment for Munitions Response final report (Nelson et al. 2008).

5.5 DATA COLLECTION

Lidar data collection is described in the final reports for each of the demonstration sites (URS 2007 and 2008a). Terra Remote Sensing collected lidar data at the Former Camp Beale demonstration site between September 10 and 13, 2007.

For field studies, URS selected 51 test plots in the Spenceville Wildlife Refuge in the southeast portion of the Former Camp Beale demonstration site. This area was selected because it contained a full variety of vegetation coverage ranging from bare ground with no grass or tree coverage to areas with field grass to areas with near-complete tree canopy closure. The Spenceville Wildlife Refuge is also public land, and site access was more easily obtained than for the remainder of the demonstration site. The test plots were circular and 15 meters in diameter.

The site visit team consisted of a staff member from the US Forest Service with background in evaluating percentage of crown cover using standard forestry techniques, a field technician to record the plot centers using resource-grade GPS and take site photos, and a UXO safety officer.

At each location, the site team recorded the date and time of the visit; percentages of brush, grass and tree cover; terrain slope; average height in inches of any grass or brush present; and took notes regarding features observed on the ground. The site team also took digital photos at each site facing north, south, east, and west. During a later site visit in April 2009, the team measured tree heights, which were not measured during the first site visit.

5.6 VALIDATION

The final reports for each of the demonstration sites (URS 2007 and 2008a) and the ESTCP Pilot Project Wide Area Assessment for Munitions Response final report (Nelson et. al. 2008) describe validation activities for the lidar data.

6.0 DATA ANALYSIS RESULTS

6.1 ACTIVITY 1: SYSTEMATICALLY INVESTIGATE VEGETATION EFFECTS

6.1.1 Step 1: Classify Vegetation

Vegetation Density

This activity compared vegetation density measured using standard field methods to that measured using the lidar data. The objective was to understand whether vegetation density as measured by lidar would correlate with vegetation density as measured using standard forestry instruments and methods. URS took field measurements at 50 circular 15-m diameter test plots using a spherical densitometer, an instrument that uses a curved mirror divided into a grid. The technician viewed the sky overhead in the mirror and counted the number of grid cells obscured by vegetation. The result is given as a percentage of crown closure; that is, the percentage of sky obscured by foliage. The spherical densitometer was chosen as a standard, low-cost forestry instrument most likely to be available to site managers.

For lidar, the vegetation density, or percentage of crown closure, was derived through a two-step process. First, lidar points representing the crown were classified by identifying and reclassifying all points within 0.4 m of the modeled ground surface. The remaining points represented returns from higher vegetation, and it appeared from visual inspection that the vast majority of these points were from the crown. Figure 4 shows an example of the lidar points at one of the test plots.

Next, the percentage of crown points was calculated based on a grid of 3-m cells. This cell size was selected as best matching the field conditions. When tested, smaller cells yielded too many cells with very low values due to gaps in the foliage, while larger cells were too large to show any variation at all. For each cell, the number of crown and non-crown points was counted, and percentages computed. Figure 5 shows an example of a vegetation density map for one of the test plots.

Finally, for each plot, an average vegetation density was derived, based on the percentage of crown points for the cells in the plot. These values were compared to the crown closure values measured in the field. Results are shown in Figure 6.

Figure 6 shows that correlation between lidar and field methods was reasonably good at lower data densities but that as vegetation density increased, lidar recorded lower vegetation densities than field measures. This result may be because of the difference in the visual perception of crown closure and the ability of lidar to penetrate small openings in the vegetation. This finding is consistent with the common observation that lidar will penetrate what at first appears to be very dense vegetation. In fact, such vegetation usually contains numerous small gaps where laser signals can penetrate to the ground.

Figure 4: Example Lidar Point Cloud

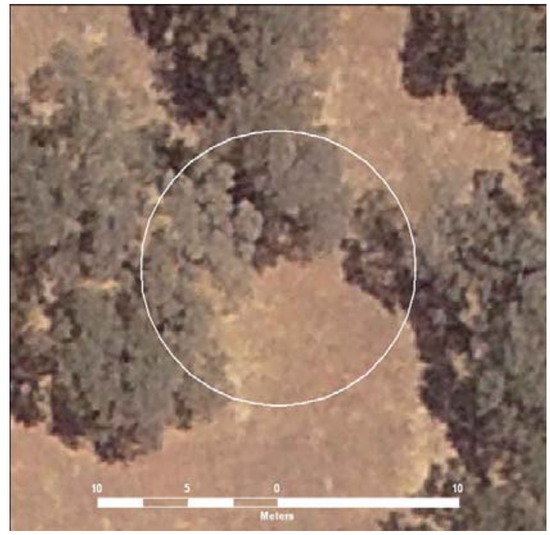

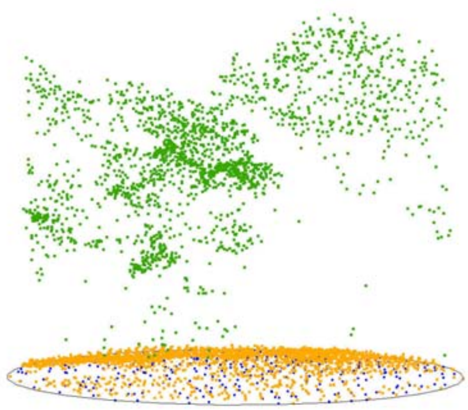

In the image to the left, the lidar points are color coded as:

Blue: vendor-classified ground points

Orange: points within 0.4 m of the vendor's ground surface

Green: remaining points assumed to be higher vegetation

Figure 5: Example Vegetation Density Map

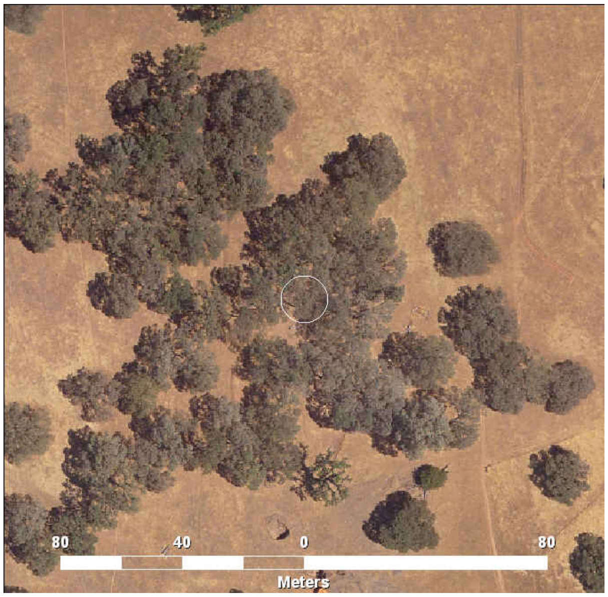

Test plot, orthophoto.

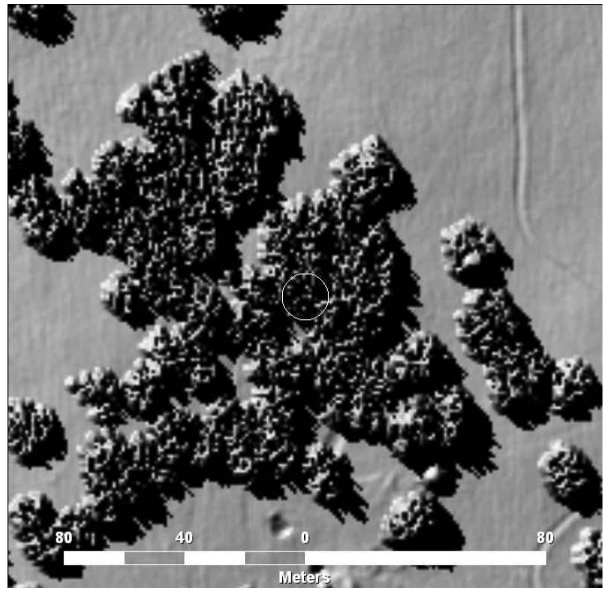

Test plot, DTM based on all lidar points.

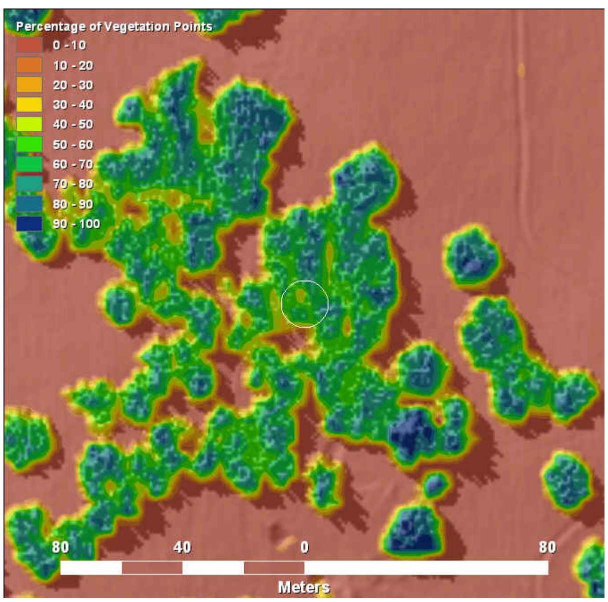

Test plot, vegetation density map (left), based on the percentage of laser returns from vegetation.

Figure 6: Vegetation Density, Lidar vs. Field Methods

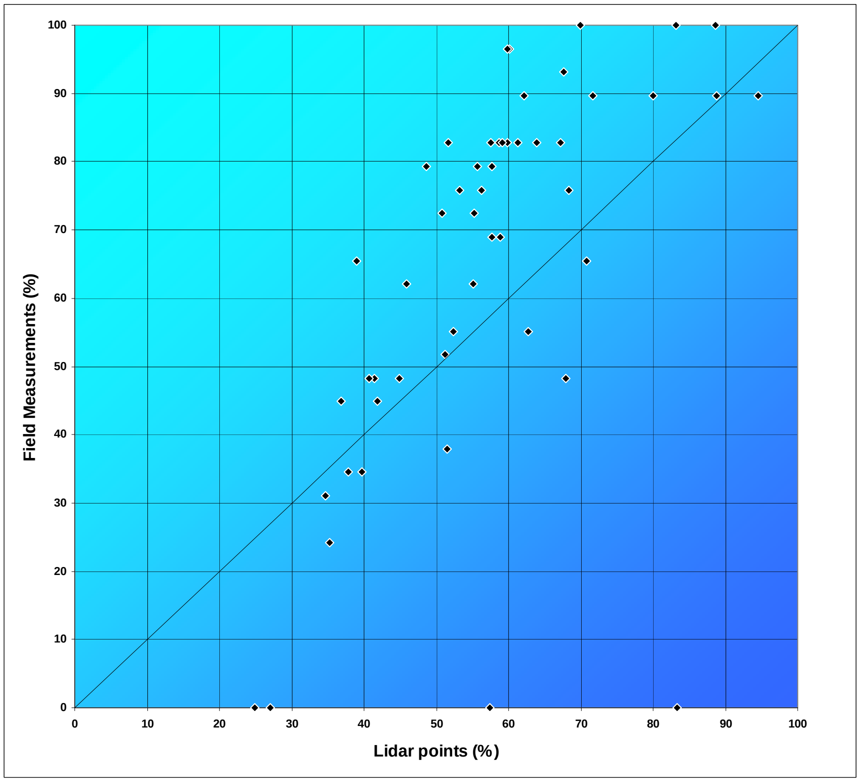

Tree Heights

During this part of the study, URS compared tree heights based on field measurements to those based on lidar, in order to confirm that site managers could use lidar to obtain relatively accurate tree height measurements. URS performed field measurement at the 50 test plots using a common trigonometric method used by foresters (Figure 7). Angles to the top of the tree and base of the tree were measured using a clinometer, a device that measures the angle above or below horizontal from a measured distance away. The combination of the angle and the distance from the tree yields the height of the tree through simple trigonometry. Distances were measured using a tape measure.[3]

[3] More accurate methods for measuring tree heights are available; for example, using laser range finders. However, the objective of this study was to mimic low-cost tools and methods most likely to be available to site managers. A positive result with these methods would eliminate the need for more costly, if more accurate, methods.

Figure 7: Trigonometric Estimation of Tree Heights

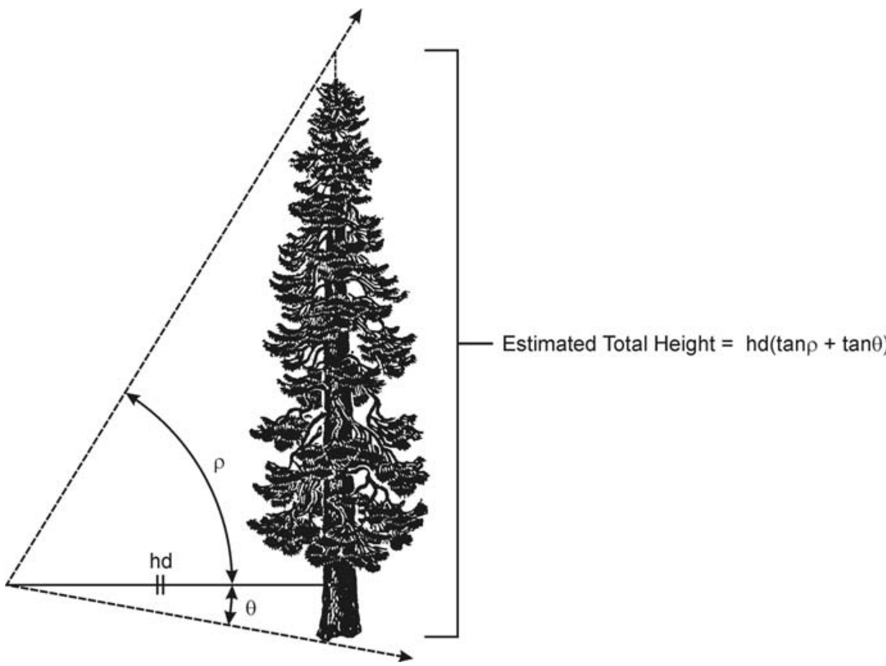

Field heights were compared to two different lidar height measurements. For the first, URS created a digital surface model (DSM) based on all lidar points, using a 1 m cell size. Cell values were interpolated from the heights of the lidar points above the ground surface (not their absolute elevations), and the cell with the highest value in the plot was taken to represent the tree height. For the second measurement, the lidar point with the highest height above the ground surface in the plot was taken as the tree height.

Figure 8 shows that the DSM provided a very poor correlation with field heights, but using the highest lidar point method showed good correlation. This result is consistent with numerous studies, which have shown that lidar can provide accurate measurements of individual tree heights in both deciduous and coniferous forests (Andersen et al. 2006, Lim et al. 2001).

Grass Heights

During this part of the study, URS compared the height of the tall grass under the trees based on field measurements to those based on lidar. Field teams used a tape measure to determine the average grass height in the field. Lidar heights were estimated using the lidar points less than 0.4 m from the modeled ground surface. Inspecting the point clouds showed that these low points are likely to include the vast majority of the returns from the grass area, and that lidar points above this height are most likely to be from tree trunks or branches (Figure 9).

Grass heights were estimated by using the highest “low vegetation” values in the plot. Figure 10 shows that lidar consistently and substantially under-measured the height of the grass compared to field measurement. It is possible that the relatively diffuse grass on the Former Camp Beale site did not have sufficient mass to cause a laser reflection until closer to the ground.

Figure 8: Tree Heights, Lidar vs. Field Methods

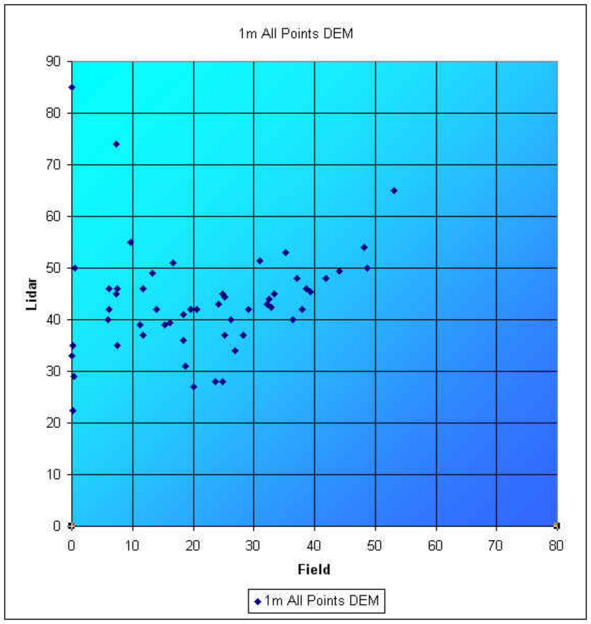

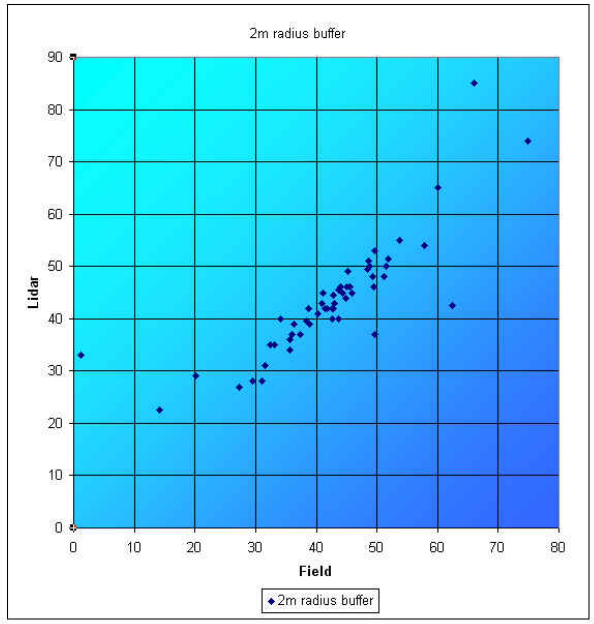

Tree heights, lidar compared to field methods. Left: results from lidar surface model method, right: results from highest lidar point method.

Figure 9: Example Grass Conditions and Lidar Point Cloud

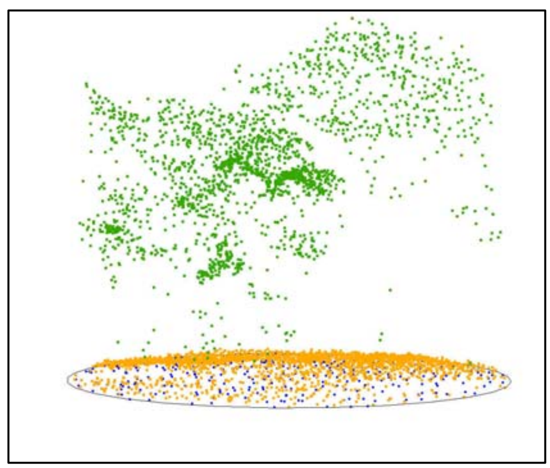

Example test plot, orthophoto and lidar point cloud.

Figure 10: Grass Heights, Lidar vs. Field Methods

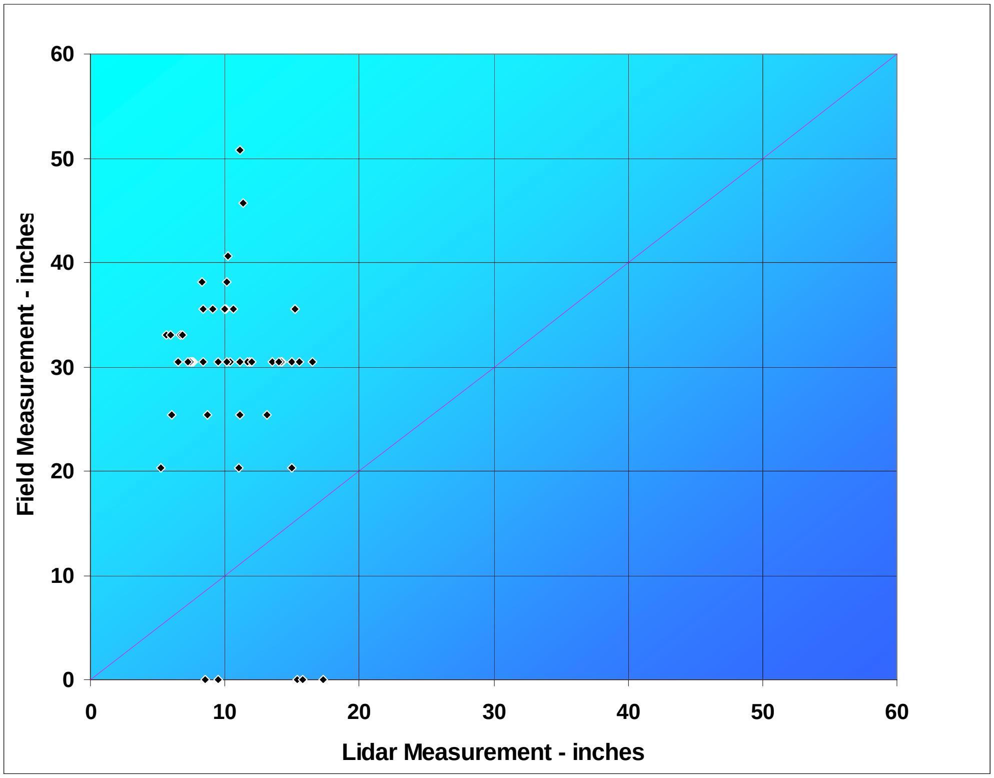

Only a few published studies were found on using lidar to measure low vegetation heights. Ritchie (1996) reported good agreement between lidar measurement and field measurement for desert scrub. However, the quoted studies were broad-level hydrologic studies and may not be comparable to the Former Camp Beale site. Genc et al. (2004) reported good agreement between lidar and field measurement of wetland vegetation in Florida, including low vegetation. However, the vegetation in question was not identified by species and did not appear to include grass.

6.1.2 Step 2: Identify Ground Features

Data Collection

During this part of the study, URS re-examined the Former Camp Beale data and examined the relationship between vegetation density and the size of features detected. Work at the Former Camp Beale site, as well as experience in the lidar industry generally, has shown that lidar can reveal features under tree cover. At the Former Camp Beale site, a variety of ground features were detected under trees, with the smallest features visible about 1 m in diameter. Figure 11 shows some representative features.

Figure 11: Example Feature Detection under Trees

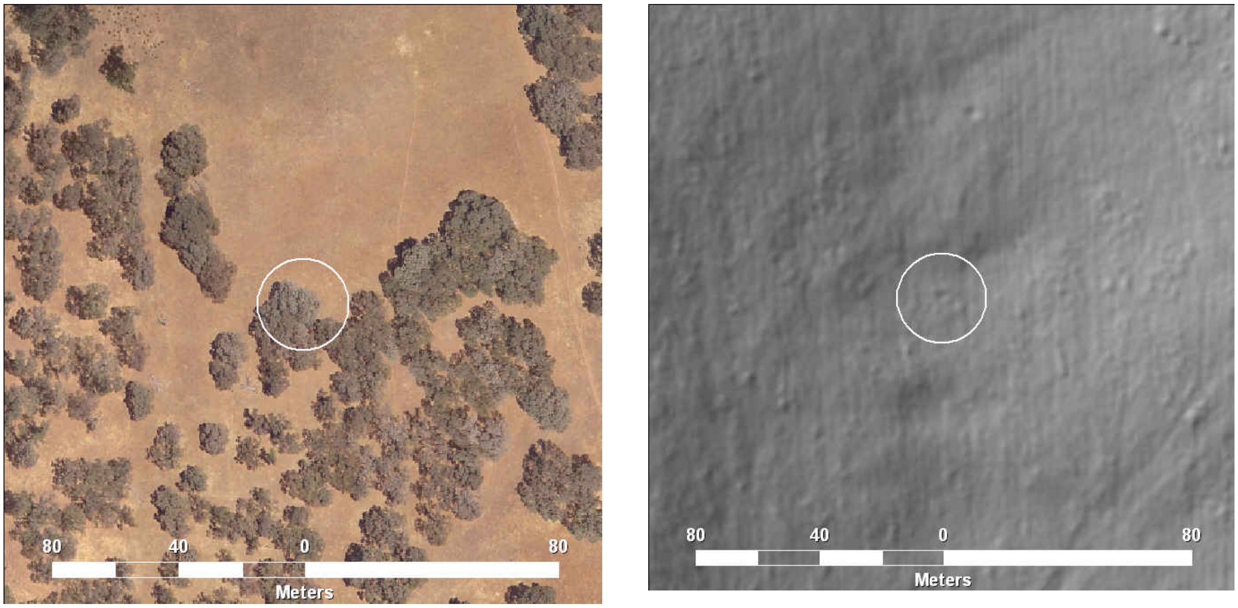

1.5 m feature, orthophoto and lidar surface model

3.3 m feature, orthophoto and lidar surface model

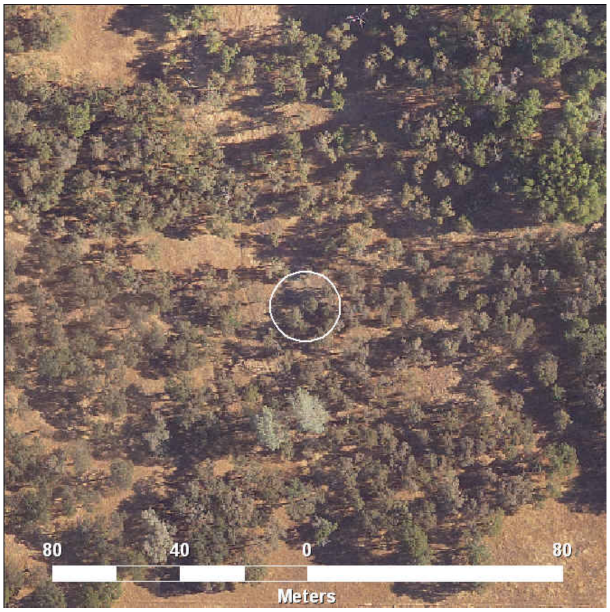

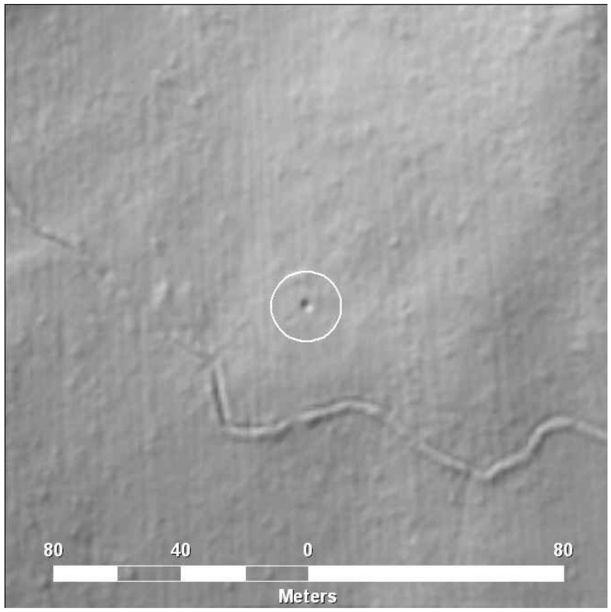

3.9 m feature, orthophoto and lidar surface model

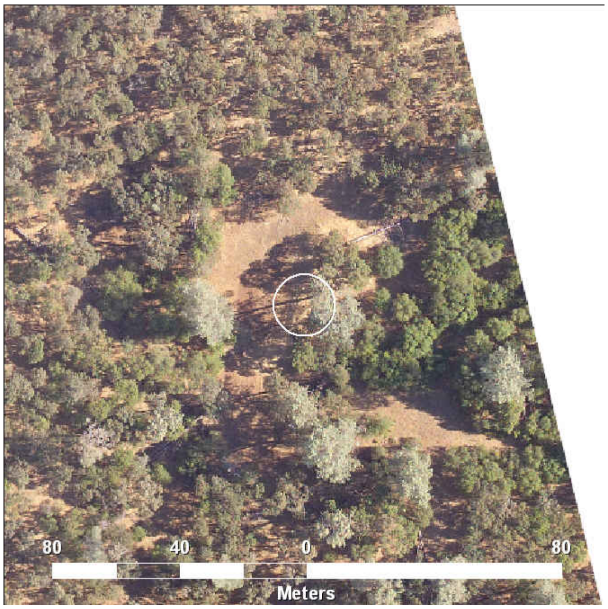

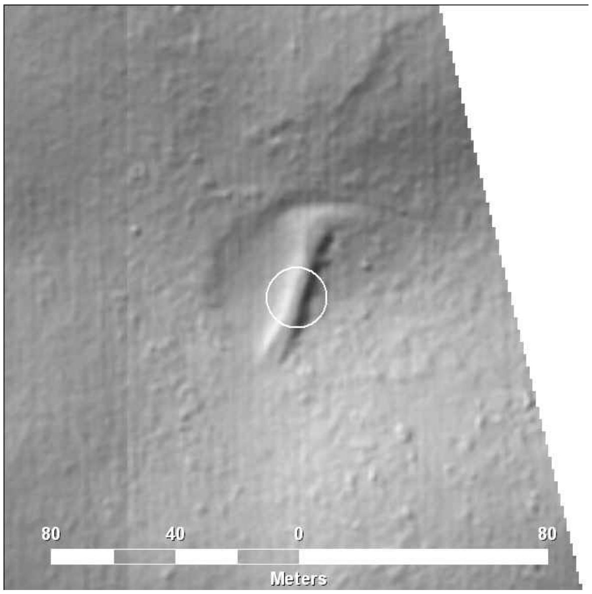

8.0 m (in width) feature, orthophoto and lidar surface model

During the field visit, the team visited 59 test plots, and took digital photos of 52 features in vegetation conditions ranging from completely open to the most dense tree cover on the site. Seven test plots had no visible features. No additional features were discovered that were not visible in the lidar data, indicating that lidar at the full data density had detected all of the ground features in the plots that could be seen by observers on the ground.

Effects of Lowering Point Density on Feature Detection

During this part of the study, URS examined the effect of lowering the lidar point density on feature detection. The objective was to determine a lidar point density below which ground features would cease to be visible. Fifty-two features were examined using successively lower lidar point density. The density of the original lidar data set was artificially lowered (decimated), using an algorithm that attributed every point so that datasets could be extracted by selecting every second, fourth eighth and sixteenth point. Using these classifications, lidar datasets were created with 1/2, 1/4, 1/8, and 1/16 of the original data density. Choosing points in this way mimicked the action of a slower mirror speed and pulse rate. New ground surface models were created using each of the four new datasets.[4]

Once the points were classified by decimation level, URS created new surface models and evaluated the visibility of the features in each. Three levels of visibility were used: clearly visible (green), barely visible (yellow), and not visible (red). These categories reflect the somewhat subjective nature of the determination. Table 3 shows a sample of the output of this exercise, and the results for all 52 test plots are included in Appendix E.

Table 3: Sample Analysis Output

		Density Level				
Feature size (m)	**Plot #**	**1 (13.8 pts/m^2)**	**2 (6.9 pts/m^2)**	**3 (3.4 pts/m^2)**	**4 (1.7 pts/m^2)**	**5 (0.8 pts/m^2)**
1.9	2					
2.6	13					
2.7	14					

m – meter
pts/m^2 – points per square meter

As expected, feature detection decreased with decreasing lidar point density. However, this decrease was uneven and varied considerably from one feature to the next. At one extreme, the visibility of some features declined evenly with decrease in data density (Figures 12 and 13). At the other extreme, some features barely degraded at all as density was lowered (Figures 14 and 16), even though the surrounding surface degraded significantly. This result is logical since even very low-density lidar data will still reveal features if the lidar points happen to fall in and near the feature. Images of each plot showing the orthophoto and the five surface models are included in Appendix F, Feature Detection and Point Decimation - Surface Model Results.

---

[4] For this demonstration, the original classifications as ground or non-ground returns from the full data set were retained.

Figure 12: Features Showing Steady Degradation, Example 1

Test plots, orthophotos

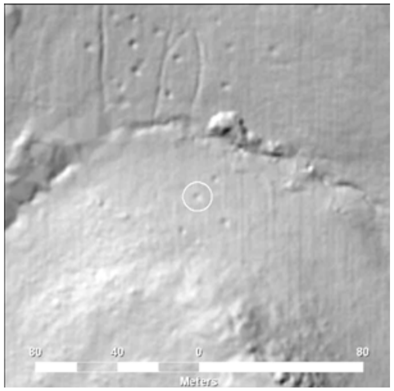

Level 1, original data. Average lidar data density: 13.8 pts/m^2

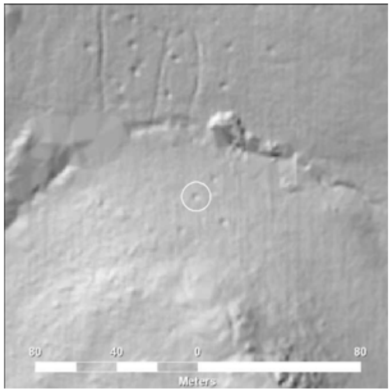

Level 2, average lidar data density: 6.9 pts/m^2

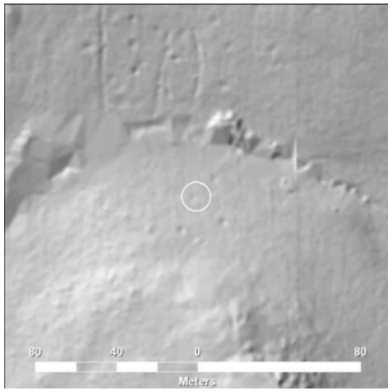

Level 3, average lidar data density: 3.4 pts/m^2

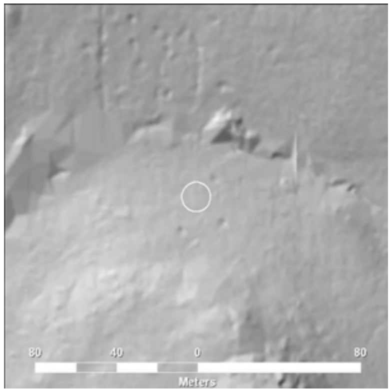

Level 4, average lidar data density: 1.7 pts/m^2

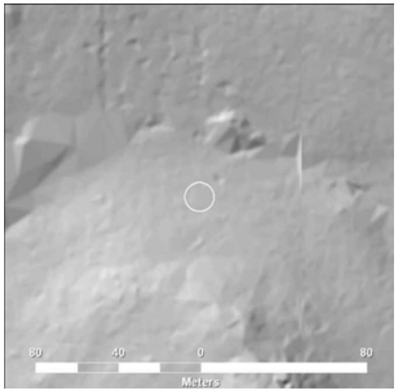

Level 5, average lidar data density: 0.8 pts/m^2

Figure 13: Features Showing Steady Degradation, Example 2

Test plots, orthophotos

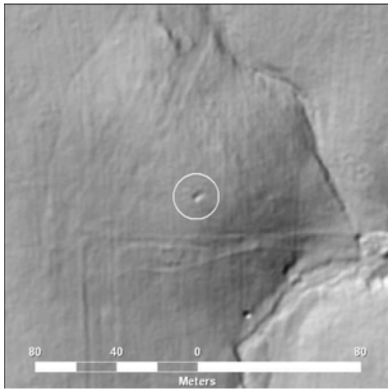

Level 1, original data. Average lidar data density: 13.8 pts/m^2

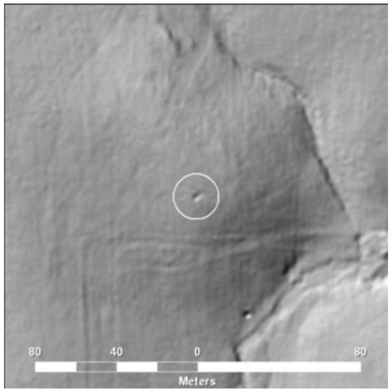

Level 2, average lidar data density: 6.9 pts/m^2

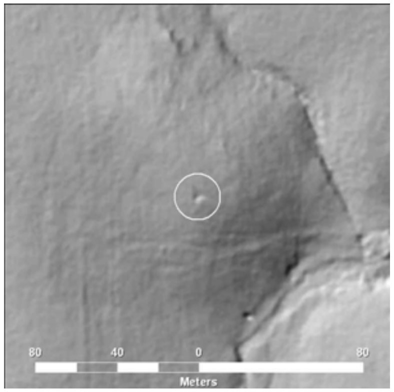

Level 3, average lidar data density: 3.4 pts/m^2

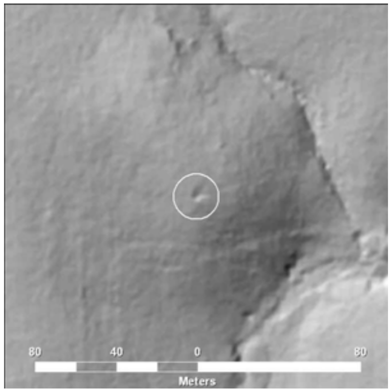

Level 4, average lidar data density: 1.7 pts/m^2

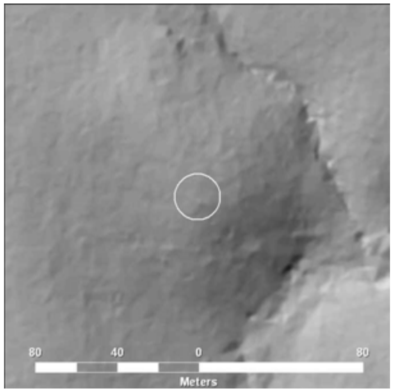

Level 5, average lidar data density: 0.8 pts/m^2

Figure 14: Features Showing Little or No Degradation, Example 1

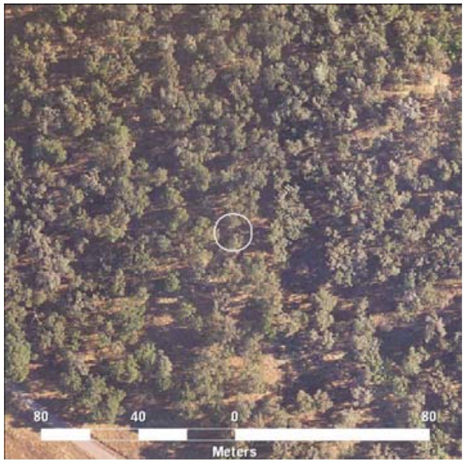

Test plots, orthophotos

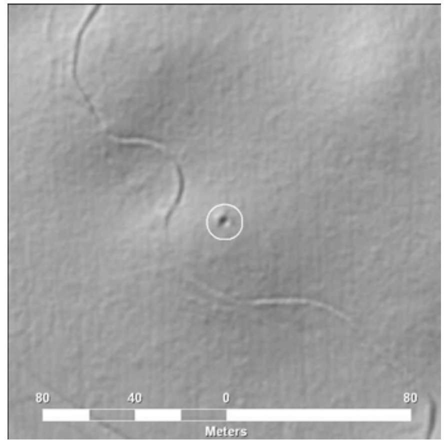

Level 1, original data. Average lidar data density: 13.8 pts/m^2

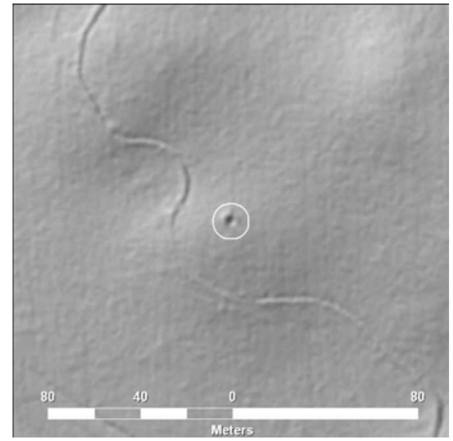

Level 2, average lidar data density: 6.9 pts/m^2

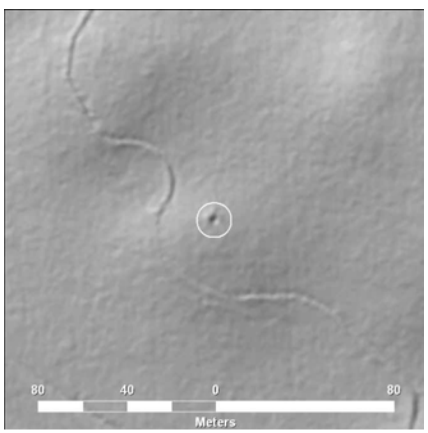

Level 3, average lidar data density: 3.4 pts/m^2

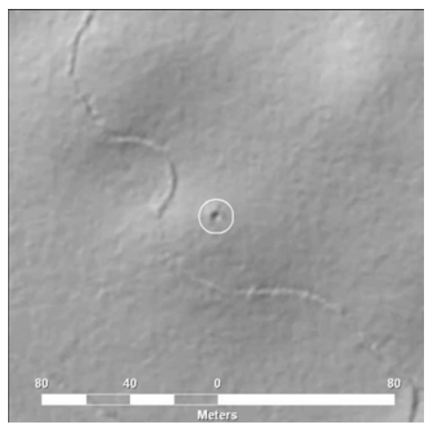

Level 4, average lidar data density: 1.7 pts/m^2

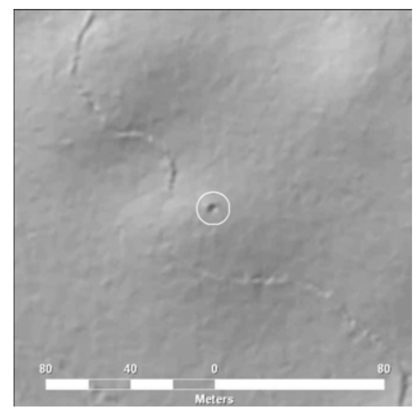

Level 5, average lidar data density: 0.8 pts/m^2

Figure 15: Features Showing Little or No Degradation, Example 2

Test plots, orthophotos

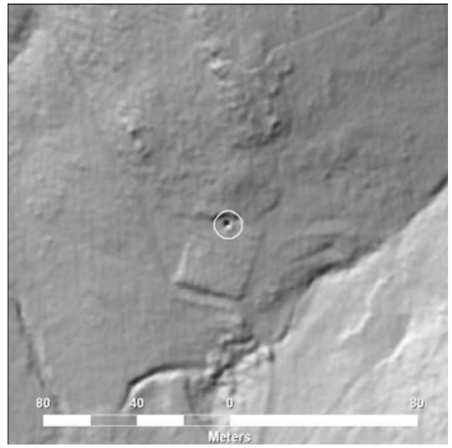

Level 1, original data. Average lidar data density: 13.8 pts/m^2

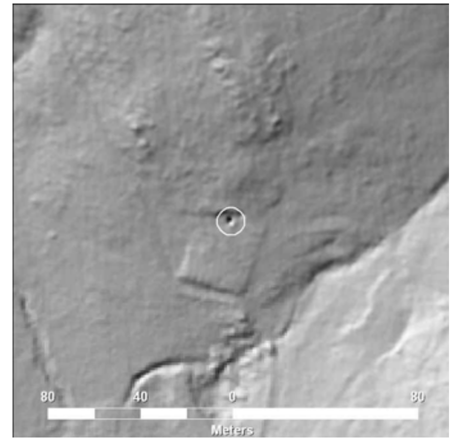

Level 2, average lidar data density: 6.9 pts/m^2

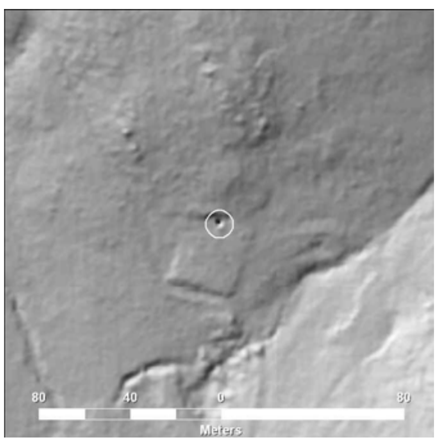

Level 3, average lidar data density: 3.4 pts/m^2

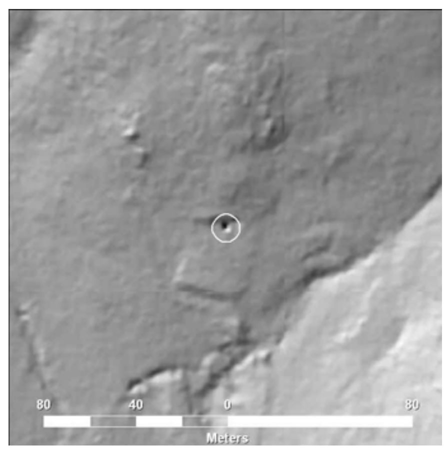

Level 4, average lidar data density: 1.7 pts/m^2

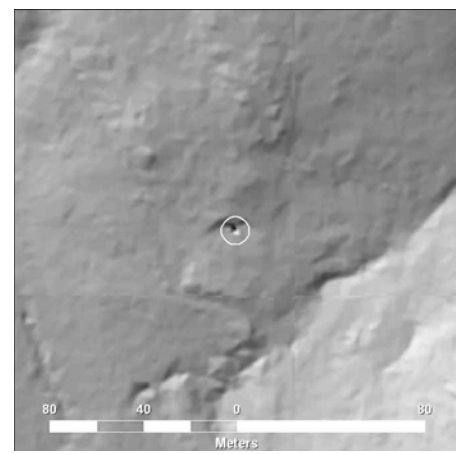

Level 5, average lidar data density: 0.8 pts/m^2

Figure 16 summarizes the results for the 52 features examined. Significant loss of feature detection begins to appear between level 2 (6.9 points per square meter [pts/m^2]) and level 3 (3.4 pts/m^2), with over two-thirds of the features not visible by level 5 (0.8 pts/m^2). There was some correlation between the rate of degradation and the size of the feature; that is, larger features tended to disappear more slowly. However, this correlation was not uniform.

Figure 16: Data Density and Feature Detection Summary

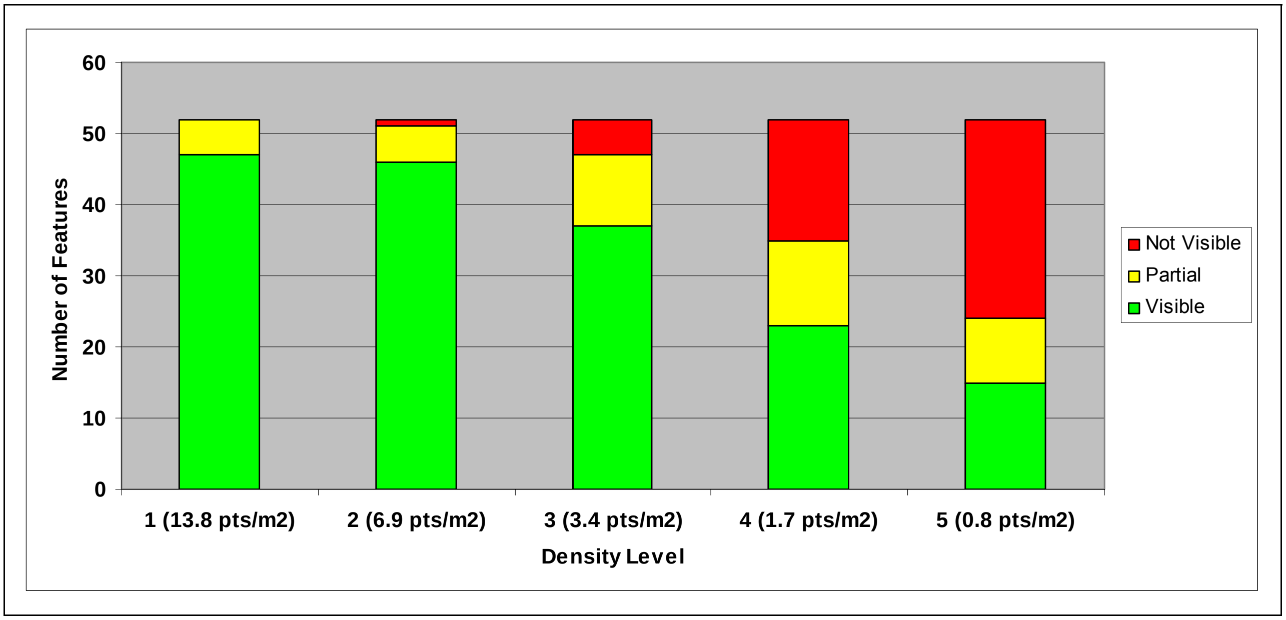

6.1.3 Step 3: Produce White Paper on Lidar Point Classification Methods

The final version of this white paper appears as Appendix C. Principal findings are summarized here.

In all lidar investigations, an important task is to distinguish laser signals that return from the ground from those that return from vegetation, buildings, or other objects. This task is carried out through the use of automated algorithms followed by inspection and editing by skilled operators.

This problem is most difficult in the case of lidar points close to the ground surface. Identifying returns from trees is relatively straightforward, but low brush and grass are more difficult, and results depend more on operator experience and judgment. For the lowest elevation lidar points, it can become very difficult to distinguish laser returns from an uneven ground surface or from low brush or grass. The problem of point classification on uneven ground surfaces has been observed for many years, as illustrated in Figure 17. Frequently, laser returns are classified as non-ground when orthophotos and other evidence indicate that they are most likely ground returns from uneven surfaces. In some cases, points will be classified as non-ground even when they are returned from relatively flat, un-vegetated surfaces. At the ESTCP demonstration sites, the phenomenon of laser returns incorrectly classified as non-ground points appeared, for

instance, in the incidence of points classified as non-ground that were returned from road surfaces (Figure 18).

Figure 17: Lidar Point Classification on Forest Roads

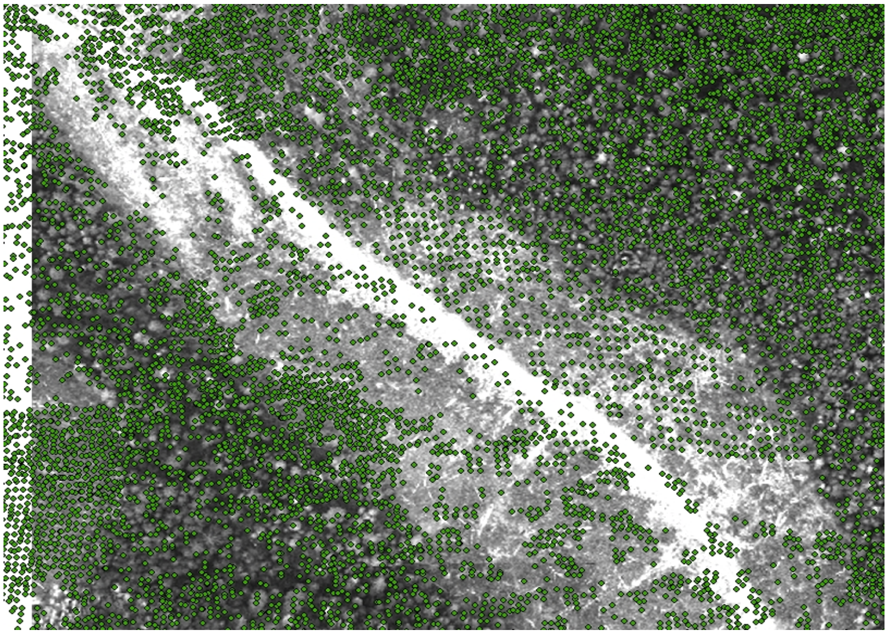

Lidar data collected in 2001 in a forest and timber harvest area in southeast Alaska. Green points, classified as non-ground returns, can be seen on the surface of the forest road where the photo shows no vegetation. It is difficult to determine whether these "non-ground" returns are artifacts of the classification process or result from the uneven surface of the dirt road.

Figure 18: Lidar Classification Results on Paved Road Surfaces

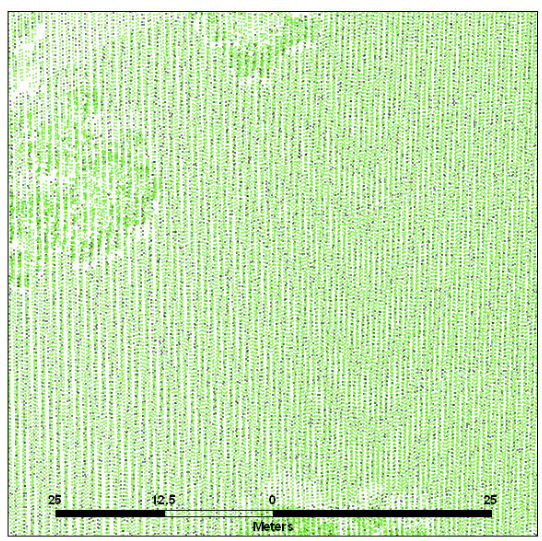

Orthophoto and classified lidar points for area portion of the Former Camp Beale demonstration site. At right, the vendor's

ground points are black, and the vendor's non-ground points are green. The road, which should not have any non-ground returns, shows many points classified as non-ground.

In response to this observation, ESTCP requested production of a white paper (Appendix C) describing the point classification process, with the goal of understanding whether this phenomenon was peculiar to the one data set examined or to the work of a single vendor, or was common to lidar data processing generally.

URS found that the phenomenon of over-classifying non-ground points was common to all of the ESTCP lidar data sets and both of the vendors used, and to the two non-ESTCP lidar data sets collected by other vendors. The percentage of non-ground classifications on road surfaces varied widely, ranging from 12% to over 95%. The percentage of lidar points misclassified as non-ground was higher in flight line overlap areas and other areas where the local density of lidar points was higher. As the overall density of lidar points increased, the rate of misclassification also increased. This higher rate of misclassification eliminated some of the advantage of collecting lidar at a higher density, since it was specifically the higher-density areas where misclassification was most common.

Misclassification of ground points was found to result from the interaction of standard software settings with the vertical error present in the lidar data. Classification methods rely in part on the angles between adjacent lidar points, with higher angles being used as an indicator of a non-ground reflection. In areas of high point density the lidar points are closer together, and even small height differences between points can be sufficient to cause the higher point to be classified as non-ground. Where lidar points are particularly close together, even height differences well within the 15-cm vertical accuracy specification can exceed the classification parameters (Figure 19).

Figure 19: Example Iteration Angles

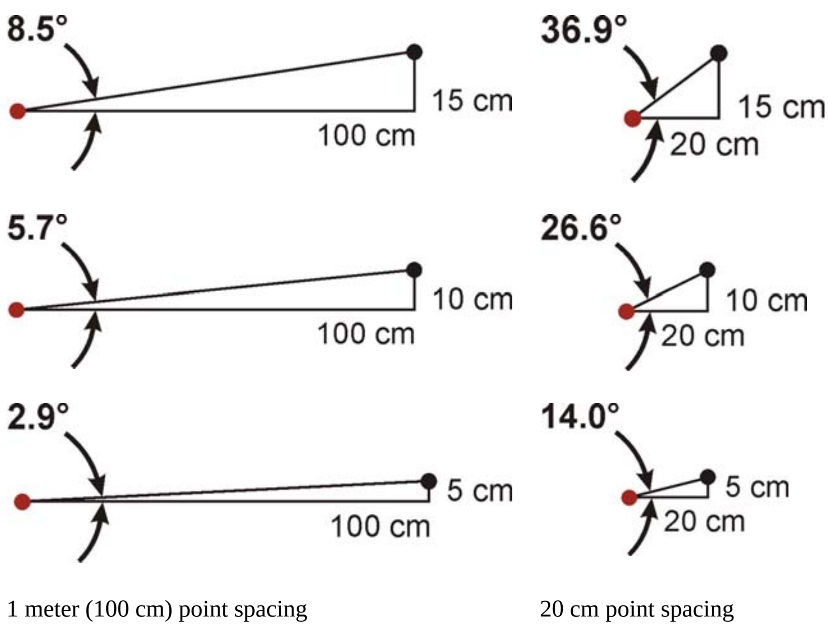

This phenomenon is described in greater detail in Appendix C.

The over-classification of non-ground returns does not, in itself, address the issue of the source of the vertical offsets which with the classification software is interacting. One vendor contacted pointed out that misclassification would be a predictable effect of errors in GPS or flight line-to-flight line data calibration, either of which would result in larger than necessary vertical discrepancies between points. This vendor noted that if the flight lines are vertically offset (due to calibration or GPS errors), then points associated with the higher flight line would be predictably classified as non-ground. This effect would be present even if the classification routine were well constructed. Reducing the misclassification effect should therefore include checks for successful calibration and GPS quality. (Sky Research, 2009). Other vendors concurred.

However, better calibration will not eliminate the residual inherent error between individual lidar points or lines of lidar points, which may lead to some misclassification depending on the parameters set up in the classification routine and the distance between the laser returns. Consequently, careful examination of point classification methods will remain desirable whenever lidar is used to detect and discriminate small ground features.

Adjusting the point classification parameters is easily accomplished by all vendors, and classification can be adjusted based on the needs of each particular lidar acquisition. Alternatively, the vendor can use their standard procedures, but also establish an additional classification for low lidar points. These points can be added to the ground surface model at a later date in order to increase the resolution of the surface model. A similar reclassification can be accomplished after the fact using standard GIS methods.

URS tested the effects of re-classifying all lidar points within 40 cm of the modeled ground surface at 59 test plots at the Former Camp Beale demonstration site. Adding the re-classified points back into the ground surface model increased the clarity of the ground features, and allowed the detection of additional small features at 36% (21) of 59 test plots (Figures 20 and 21).

Figure 20: Sample Point Reclassification Results

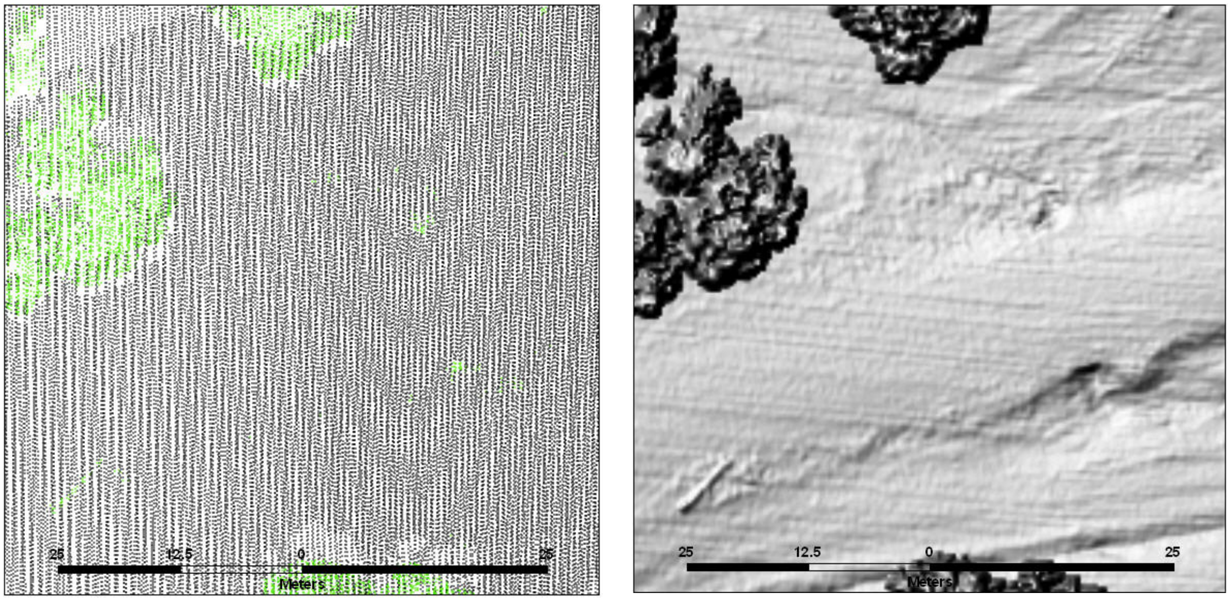

Initial point classification test area, points re-classified. Non-ground points within 0.4 m of the modeled ground surface were added to the ground classification. The remaining non-ground points appear to be reflections from trees and other objects on the ground. The image to the right is the digital surface model using the full lidar data set.

Adding all of the low points into the surface model, as was done for this test, also will add small surface features such as fallen tree trunks on the ground surface, which are not truly ground features. This was clearly evident at the Former Camp Beale demonstration site, especially when smaller grid cells were used (Figure 22). This method also will also add instrument noise, in the form of surface roughness resulting from vertical error in the lidar points that would be removed by standard approaches. However, noise did not noticeably change the appearance of the surface models at the test plots.

The objective of UXO/MEC surveys is to detect objects such as small craters. The major finding of the white paper was that re-classifying the lidar points had potential to increase the resolution of the ground surface model and the detection of small ground features. These results underscore the importance of adjusting the classification methods used for each site, experimenting with re-classification after the lidar data is delivered, and discussing point classification methods with the vendor in order to maximize the possibility of detection.

Figure 21: Surface Models Using Reclassified Points

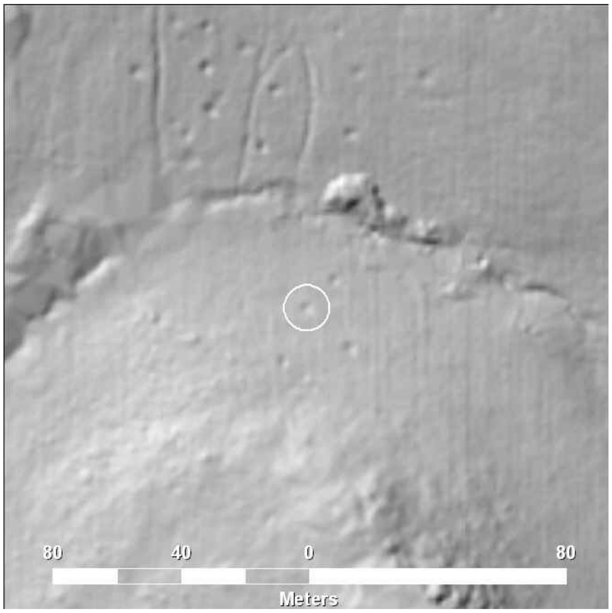

Plot 1: Vendor-classified points, 1 m grid size.

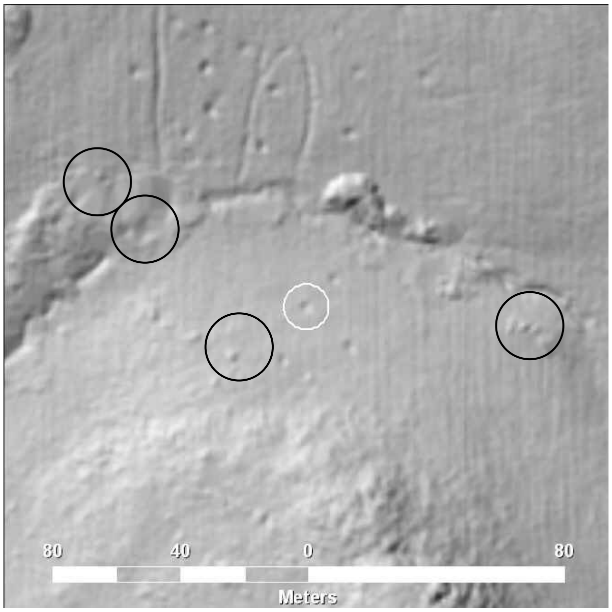

Plot 1: Re-classified points, 1 m grid size. Additional small objects are visible.

Figure 22: Tree Trunks on the Ground Surface

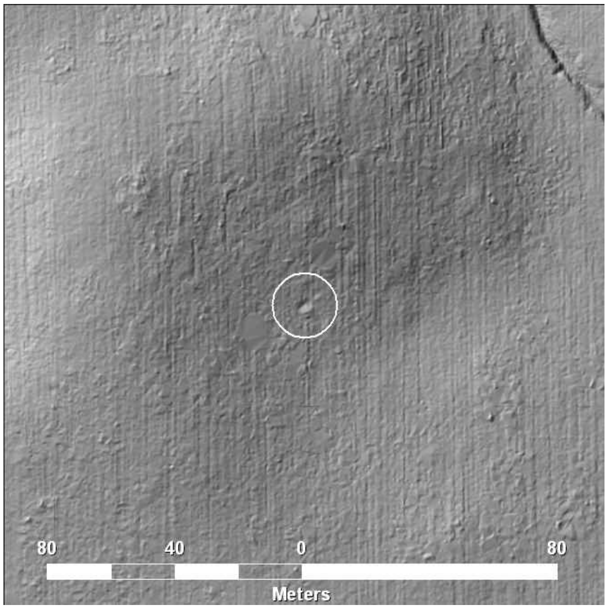

Plot 3: Vendor-classified points, 0.3m grid size. Tree trunks are faintly visible.

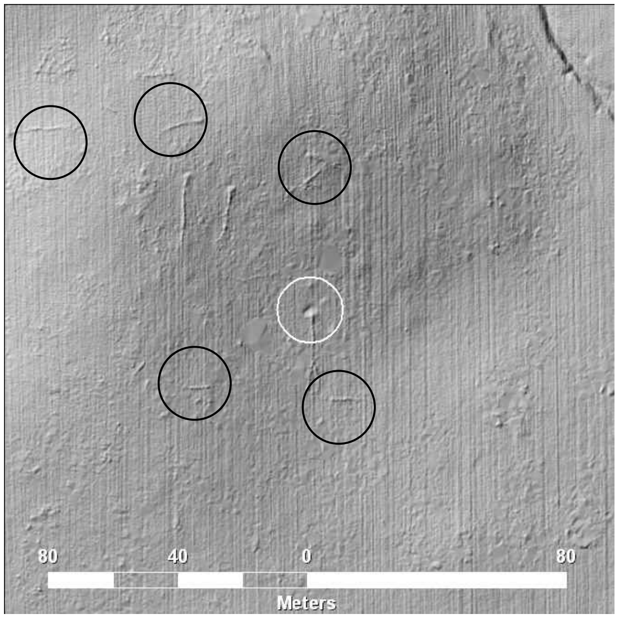

Plot 3: Reclassified points, 0.3m grid size. Many more tree trunks are visible, and all are more clearly defined.

6.1.4 Step 4: Produce White Paper on Lidar Error

The final version of this white paper appears as Appendix B. Principal findings are summarized here.

Error in Lidar Points

The positional error of lidar points is divided into horizontal (x, y) and vertical (z) error, and is typically expressed as the difference between lidar values and surveyed points established in the study area. A typical vertical accuracy specification is 5–10 cm for hard surfaces and open regular terrain; 15 cm for soft or vegetated surfaces and flat to rolling terrain; and from 30–50 cm on more extreme terrain (Ambercore 2008). Horizontal accuracy is typically 50–75 cm in all but extremely steep terrain.

Positional error in lidar points results primarily from a combination of equipment error and error resulting from site conditions. For equipment error, manufacturers and vendors typically report the positional error of lidar points for the entire lidar system, rather than for individual system components. When the system is calibrated and functioning correctly, equipment error varies with two main factors: the height of the sensor above the ground and the angle of the laser signal off directly vertical (nadir). A typical lidar system error curve is shown in Figure 23 for the Leica ALS60, a lidar system in common use. Figure 23 shows that horizontal (x,y) error is larger than vertical error, and increases more sharply than vertical error (z) with increasing height. Most lidar surveys at munitions sites are flown near at or below 1,000 m, where equipment error is relatively low.

Figure 23: Leica ALS60 Horizontal and Vertical Error Curve

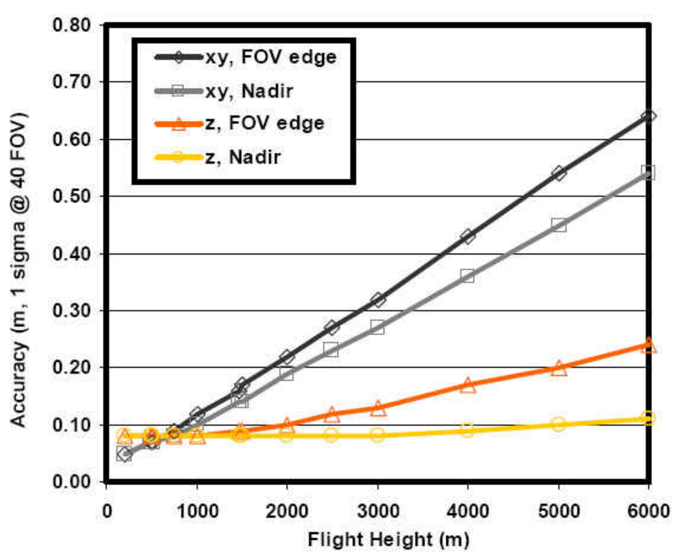

Source: see Appendix B.

A wide variety of site conditions can contribute to positional error in lidar data. Some conditions impact the entire data set, either by affecting the equipment directly or interfering with the GPS signal. Others, such as terrain roughness, may impact data from only part of the surveyed area. Site conditions that contribute the largest error to lidar positions include:

Slope. Lidar collected on steep terrain will be less accurate than that on flat terrain (Figure 24).

Figure 24: Effects of Slope on Lidar Point Error

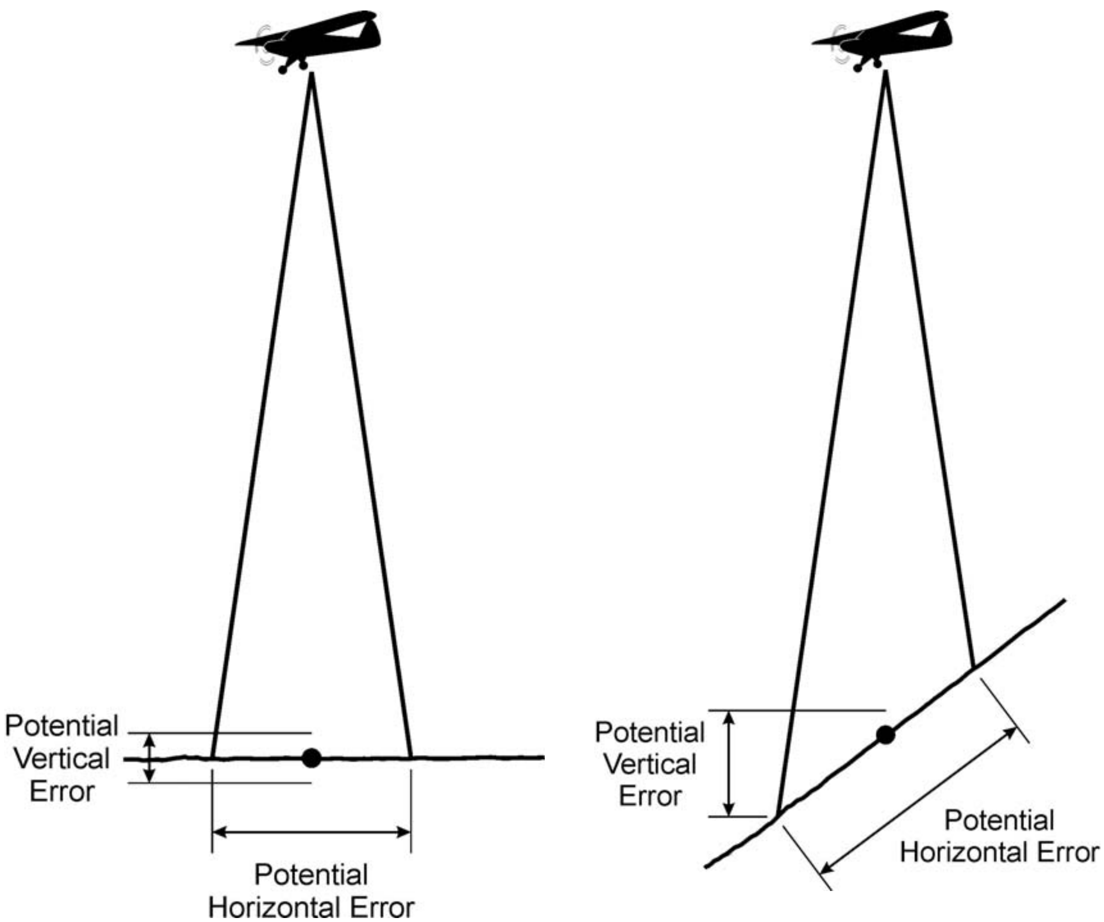

Slope compounds both horizontal and vertical error of lidar points.

This error arises in two ways:

- The lidar pulse spreads as the beam travels. The degree of beam divergence is affected by the characteristics of the laser combined with the flight height, with typical beam footprints between 10 and 100 cm in diameter.[5] Beam divergence creates an area of

[5] Formula for beam divergence is roughly: spot diameter at nadir = elevation (meters)*beam divergence (radians) (Baltsavias 1999). System manufactures report beam divergence factors from 0.22 to 1.0 mrad (Key 2009). Laser footprints would therefore range from 22 to 100 cm at 1,000 m flight elevations.

uncertainty as to the exact point where enough energy is reflected to trigger a return. On flat surfaces, this uncertainty may affect the horizontal location of the return, but will not affect the elevation value. On sloping surfaces, the area of the pulse footprint will be larger, and also will include a vertical error range.

- The horizontal error of the lidar location will be larger on sloped ground, and this horizontal error will magnify the vertical error compared to flat ground.

Ground surface. Some vendors guarantee higher accuracy on hard surfaces than on soft ground surfaces based on the fact that soft surfaces are often less clearly definable. Plowed fields or grassy areas, for instance, can have furrows or vegetation that would create error up to 10–20 cm (Terra Remote Sensing 2009).

Similarly, occasionally highly reflective surfaces will appear to be slightly raised in comparison to non-reflective surfaces, such as white painted centerlines on asphalt roadways. In such cases, it is likely that more reflective surfaces return sufficient energy to trigger a response more quickly than less reflective surfaces.

Vegetated conditions. Under vegetated conditions, it is common for the majority of laser signals to reflect from the vegetation rather than the ground surface. The lower density of lidar points under vegetation can lead to apparently lower accuracies of the individual lidar points. This is not because the accuracy of the individual lidar points is lower. Rather, the lower density of ground returns in vegetated areas means that survey points in such conditions will be compared to a coarser surface model.

Electromagnetic interference. Certain types of electromagnetic signals can affect lidar data collection, usually by interfering with the GPS signal. This can include:

- The on-board radio system
- High-intensity radar in the immediate area
- Geomagnetic activity, usually as a result of solar flares and other solar activity

Surface Model Creation and Display Methods

In practice, much of lidar data analysis is performed using surface models derived from the lidar points. The typical final products of lidar are digital models of the ground surface, both of the bare ground and the ground with vegetation and buildings included. Typical model types are digital elevation models (DEMs), DSMs, and digital terrain models (DTMs).

A DEM, as defined by the US Geological Survey, is a digital file consisting of terrain elevations for ground positions at regularly-spaced horizontal intervals that portrays the ground surface free of vegetation or human-created structures.[6] DEMs may be created using data from many sources in addition to lidar, including topographic maps, ground survey, photogrammetry, or synthetic aperture radar. In the context of lidar, the DEM is the product through which the irregularly-

---

[6] See: http://rockyweb.cr.usgs.gov/elevation/dpi_dem.html

spaced lidar points that the vendor classifies as returning from the ground surface are converted to a regularly-spaced grid of elevation values. This digital model can then be used in standard GIS or other software to produce hillshaded surfaces, contour lines, or other digital products.

Regularly spaced elevation files of this type also may be created using all returns, including those from buildings, trees and other features. The US Geological Survey refers to these as DSMs. The term DTM is used as a synonym for both DEM and DSM. In the lidar context, the term DTM is most frequently used to refer to the all-points surface model. Appendix B uses the term DSM for the all-points surface model including both ground and non-ground returns.

Factors Affecting Surface Models. The accuracy and usefulness of a surface model will depend on the accuracy of the lidar data from which it is created, and will be subject to the types of error that affect lidar points. However, the methods used to create the the model can impact both its accuracy and usefulness, with the factors examined including the point classification methods, interpolation method, choice of cell size and the methods for displaying hillshades.

Point classification methods. The point classification approach used by the lidar vendor should have no effect on the accuracy or precision of the individual lidar points, since classification takes place after the data is calibrated. However, methods that are biased toward creating clean, smooth ground surfaces can result in a lower data density of ground points, and this can result in lower accuracy compared to surveyed control.

Interpolation method. The technical problem in creating surface models from lidar points is to assign an elevation value to each regular grid cell from the semi-random distribution of lidar points. Various interpolation methods exist, and the method should be adapted to the specifics of each site. Limited testing of different interpolation methods for the ESTCP data showed only small differences. Further discussion of interpolation methods is found in Appendix C and in High Density Lidar and Orthophotography in UXO Wide Area Assessment (URS 2007), especially Appendix D of that document, GIS-Based Methods for Creating Ground Surface Models from Lidar Points.

Cell size. Choice of cell size can affect the detection of small surface features dramatically (Figure 25), with smaller cell sizes performing better.

Figure 25: Effects of Digital Surface Model Cell Size on Feature Detection

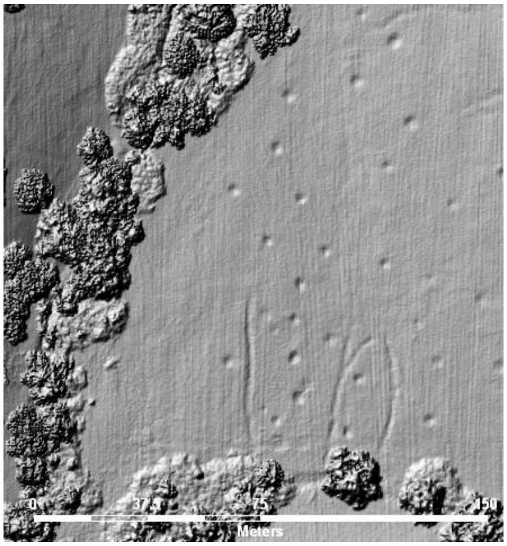

Former Camp Beale ESTCP demonstration site. Hillshade and DEM based on 0.3 m cells. Craters are approximately 3 m in diameter.

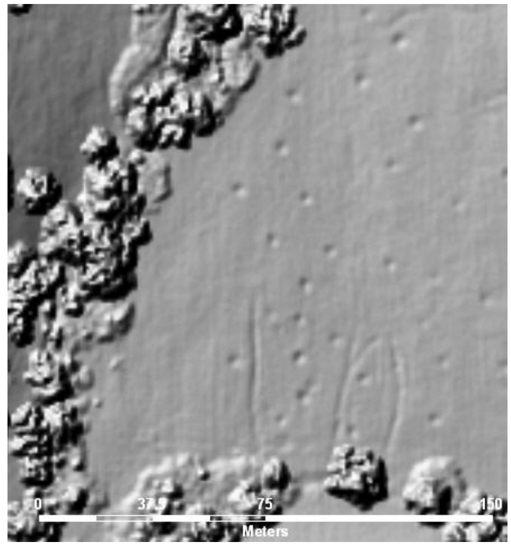

Hillshade and DEM based on 1.0 m cells

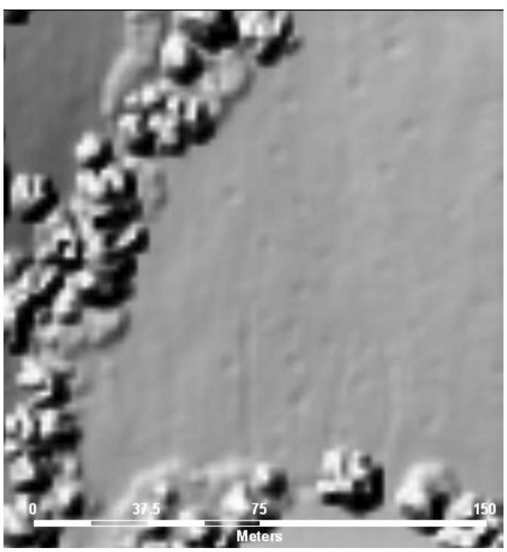

Hillshade and DEM based on 2.0 m cells

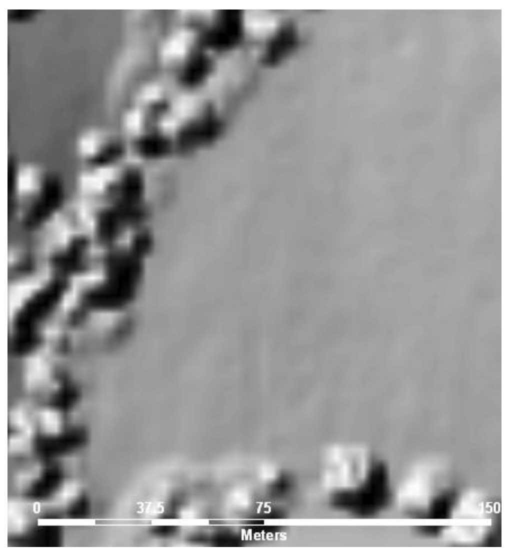

Hillshade and DEM based on 3.0 m cells

In discussing cell size, Smith et al. (2004) state that there has been little research into the effect of changing grid cell size other that that by Behan (2000), who found that the most accurate surfaces were created using grids that had a similar spacing to the original points. This conclusion makes sense intuitively since this procedure would result in a grid where each cell had, on average, at least one measured elevation. Discussion with vendors suggests that use of cells smaller than the average point spacing does not sacrifice accuracy (Kusevic 2009).

Using this logic, a ground surface model based on a lidar data set with approximately two ground points per meter (the average density of ground points classified by the vendor for the Former Camp Beale site) should contain approximately two cells per square meter, or be approximately 0.7 m on a side. The grid cells produced by URS for the Kirtland, Victorville, and Former Camp Beale sites were 1 m, and those produced by Sky Research for the Pueblo site were 0.5 m.

Adding more reclassified points to the ground surface model at three test plots at the Former Camp Beale site roughly doubled the number of ground points to approximately four ground points per square meter (Table 4). This opens the possibility of reducing the size of the grid cells. At this density, cell size equivalent to ground point spacing would be 0.5 m.

Table 4: Data Densities, Reclassified Points

Plot	1	2	3
Plot reference #	3977	4004	4088
Total lidar points	3,761,158	3,632,790	3,832,829
Vendor ground points	456,659	455,130	470,594
Reclassified ground points	975,812	898,548	1,034,459
All points density (pts/m^2)	15.04	14.53	15.33
Vendor ground points density (pts/m^2)	1.83	1.82	1.88
Reclassified ground points density (pts/m^2)	3.90	3.59	4.14

As a test, new surface models were created for these three plots using 0.3 m cells. These smaller cell sizes were intended as a preliminary test, and were probably somewhat smaller than justified by the densities of the reclassified points (Figure 26).

In each of these cases, the use of smaller grid cells revealed additional features, and showed the existing features with greater clarity. This result amplifies the potential benefit of reclassification. An examination of surface model cell size should be included in the analysis methods considered for each site.

Figure 26: Effects of Changing Grid Cell Size

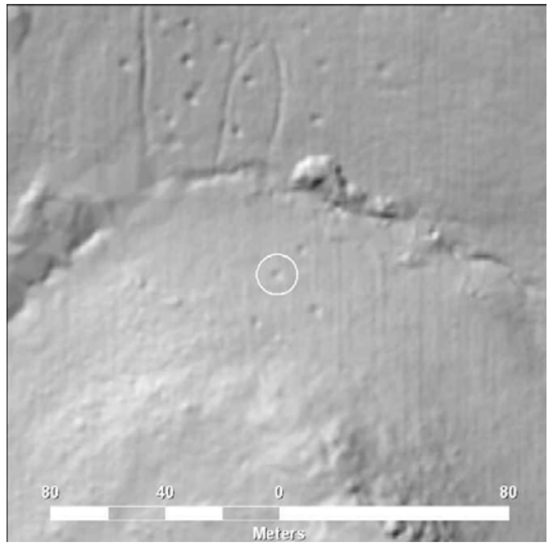

Test plot 1, orthophoto and original ground surface model, 1 m cells

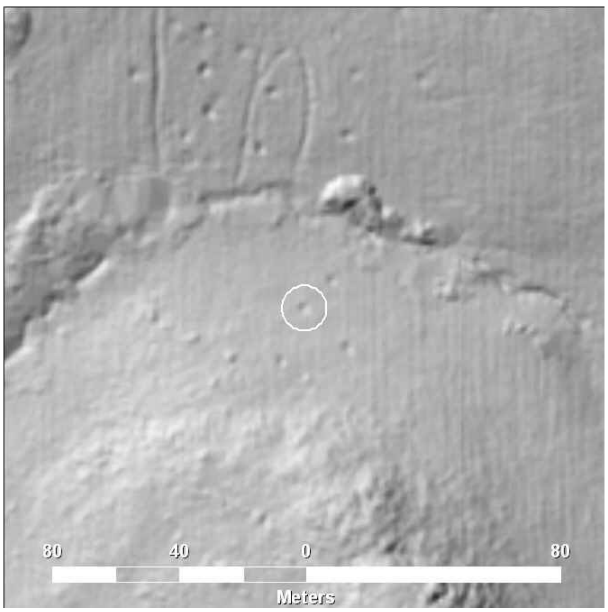

Reclassified 1 m cells

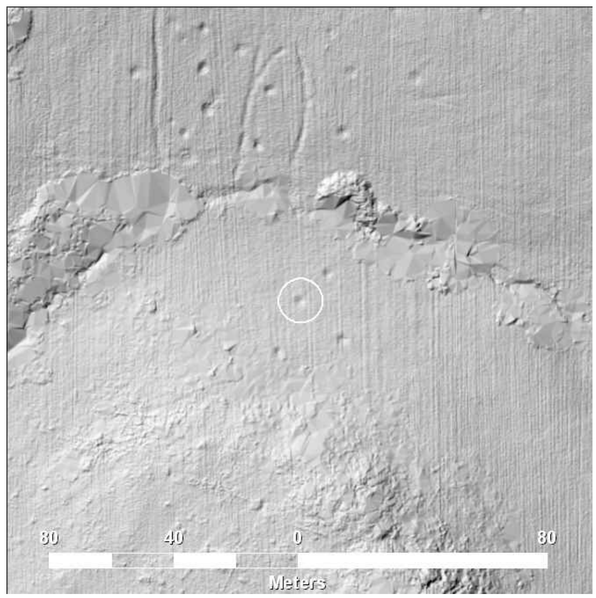

Reclassified 0.3 m cells

The smaller grid cell size shows better definition of small features and some possible additional features in the center right along the stream course.

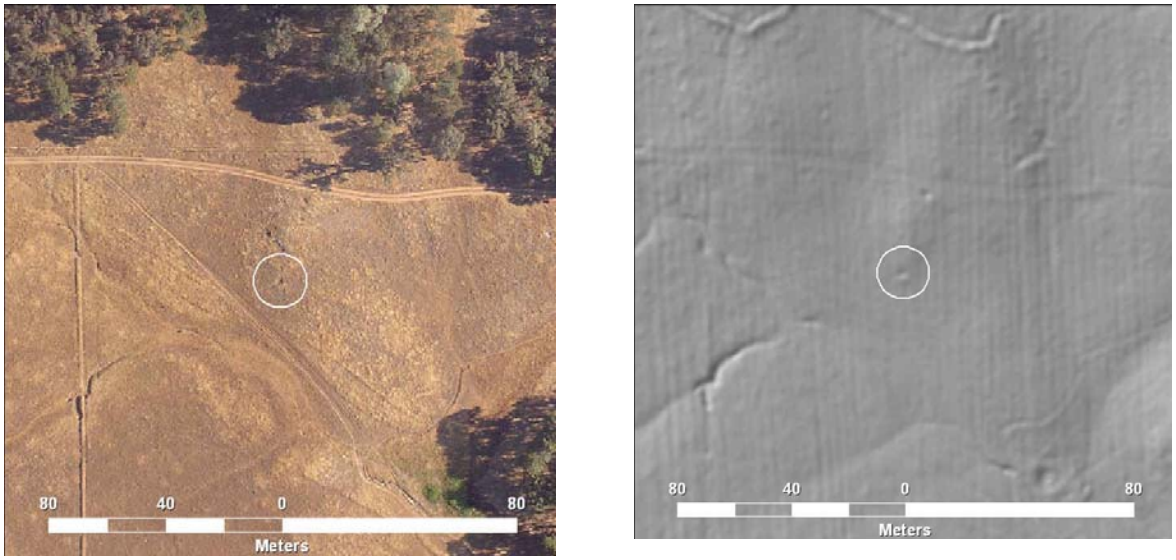

Test plot 2, orthophoto and original ground surface model, 1 m cells

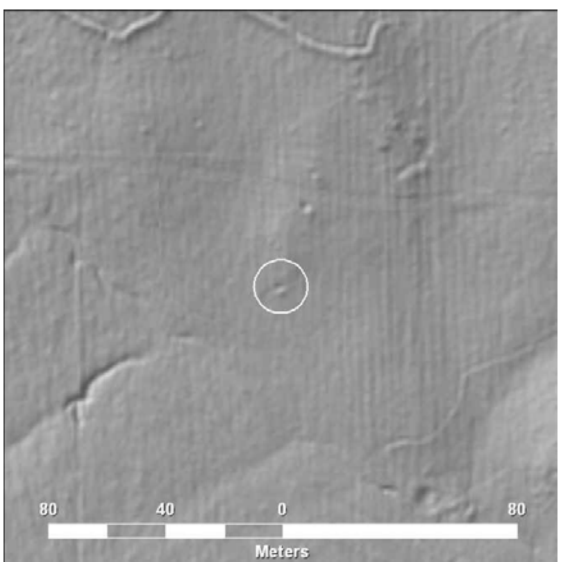

Reclassified 1 m cells

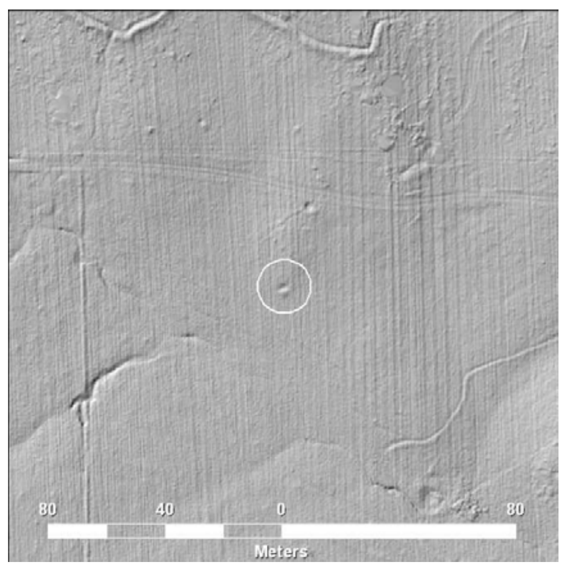

Reclassified 0.3 m cells

The smaller grid cell size shows some additional features in the upper left and shows the existing features with additional clarity.

Surface model display methods. DEMs and DTMs are usually displayed as hillshade images to enhance the visualization of surface features (Figure 27). ArcGIS, the most commonly used GIS software, contains dozens of settings that can affect the usefulness of these images, as do other software products that can produce hillshades. Different hillshade settings may be appropriate in some circumstances, and users need to work with analysts both to fully understand the goals of the survey and to experiment with appropriate settings.

Figure 27: Hillshade Display Method Examples

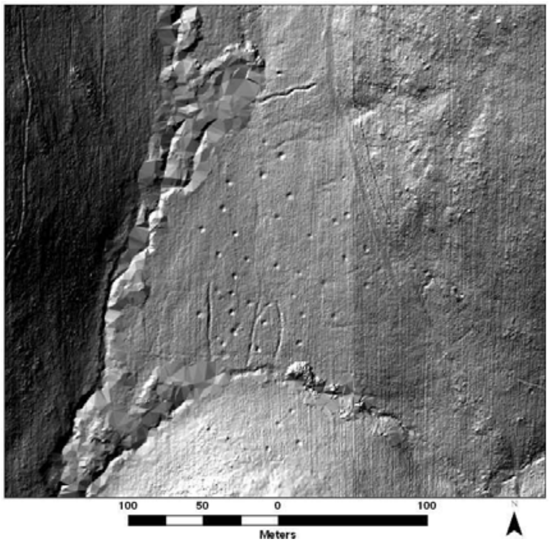

Former Camp Beale ESTCP demonstration site, hillshade image, ArcGIS default settings. The default settings are too dark in some areas to reveal the ground surface.

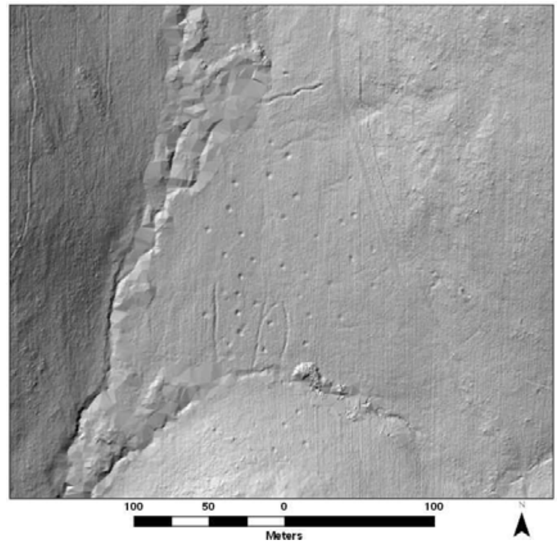

Hillshade image, alternate settings showing less dark grey area but also less contrast on the craters.

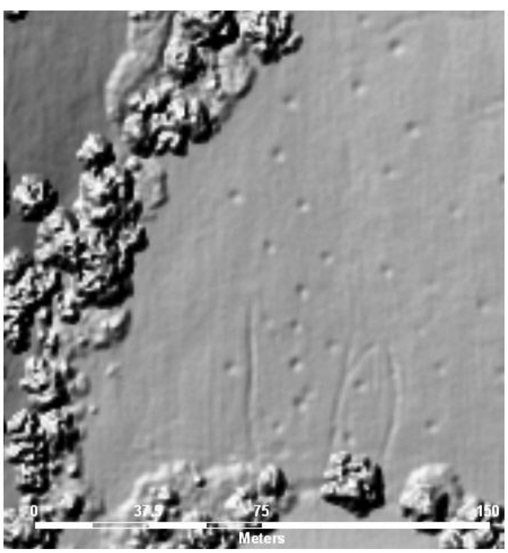

Hillshade image, "neutral" hillshade settings.

Hillshade image, contrast boosted, highlighting craters.

Implications for Munitions Sites

- The charts presented above show that the accuracy of lidar points varies primarily with flight height and distance from nadir. Lidar acquisitions at the ESTCP demonstration sites were conducted from 300 to 1,000 m, where instrument error is relatively low. Lidar collected at these sites met their contracted accuracy specifications, and subsequent

acquisitions in this range of flight height should successfully meet similar accuracy specifications. However, where accuracy is especially important, contract specifications may be adjusted to require the vendor to fly lower and/or use a narrower field of view.

- Positional error in lidar data will be higher on sites with steep terrain. Where appropriate, lidar accuracy can be assessed independently for major terrain types.
- Surveyed points used for calibration and quality control of lidar must be from a source of higher quality than the lidar data itself. Survey errors in control and calibration points can lead to incorrect assessment of data quality or errors in the entire lidar data set.
- Feature detection can be i by creating surface models using the smallest cell size justified by the density of lidar returns. Users should experiment with display methods.

6.1.5 Estimating Confidence Levels for Feature Detection Under Vegetation

Regardless of the overall point density achieved, lidar point density will always vary somewhat with terrain and will be lower under vegetation. These variation in lidar density will affect the confidence levels for detecting ground features over different parts of the site. One approach to determining confidence levels for feature detection is to map the density of lidar ground returns (Figure 28). Areas with no returns would be designated as areas where lidar would not detect ground features, with confidence levels increasing with the number of returns.

Figure 28: Preliminary Confidence Levels for Ground Features

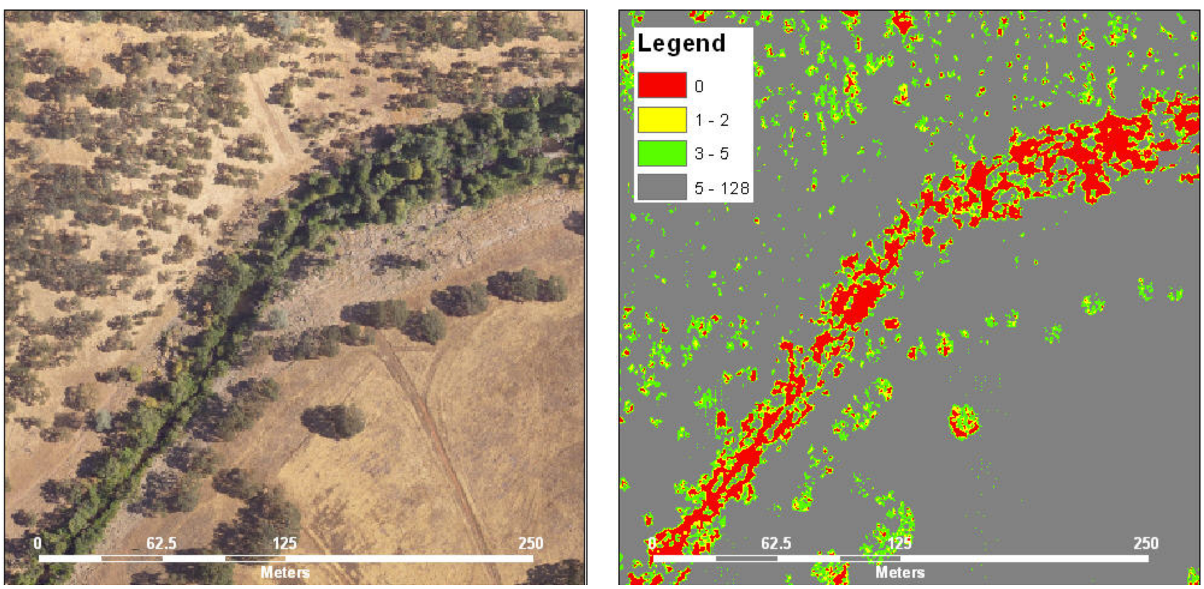

Former Camp Beale ESTCP demonstration site, point density map based on reclassified ground points. The legend shows ground points per square meter.

6.2 ACTIVITY 2: EVALUATE CURRENT SOFTWARE PACKAGES

URS examined a list of computer programs that manipulate three-dimensional data. Using the criteria listed in Section 5.1.2, seventeen software programs were selected for further evaluation (Table 5).

Software vendors were contacted and asked to participate. Of these, only four provided analysis results. URS reviewed the analysis results and discussed the findings with the vendor staff. In addition to these software packages, URS reviewed several free software products for viewing lidar points, and experimented with a tentative approach to crater detection developed by URS. These software packages were:

- LP 360 (and other free lidar viewers)
- Lidar analyst
- TLiD
- QT Modeler
- HTFC

Table 5: Software Packages Selected for Further Investigation

Software Name	Vendor
AcuScene	AcuSoft
Amber iQ	AmberCore Software
CARTERRA Analyst	Space Imaging
Creator Pro	MultiGen-Paradigm
GeoACE	US Army Corps of Engineers
Geospatial Analyst Suite	Visual Learning Systems
HTFC	Sandia National Labs
Lidar Analyst	Visual Learning Systems
LidarEngine	PCI Geomatics
Lidar Works	Technology Service Corporation
LIDAR XLR8R	Airborne 1
PolyWorks	InnovMetric
QT Modeler	Applied Imagery
Stratos98	RockWare
TerraScan	Terrasolid Oy
TLiD	Tiltan Systems Engineering
WinATLAS	KLT Associates

These software products all offer interesting capabilities for viewing and analyzing lidar data, and could be useful to Government staff using lidar (Figure 29). The free lidar viewers, although offering more limited functionality, also are appropriate tools for any regular user of lidar data.

However, with the exception of the Sandia National Laboratory HTFC software, none provided significant potential for automated detection of munitions-related features such as craters or bombing targets, nor did they provide scripting languages for the development of such capabilities by users.

The Sandia HTFC application was funded by ESTCP specifically for researching automated detection of munitions-related features from lidar data (Figure 30). Sandia investigated several algorithms for crater detection, embedding these in a user interface constructed in Visual Basic. Preliminary results were promising, as detailed in Sandia's report to ESTCP (Roberts and McKenna 2006).

At the May 2009 In-Progress Review meeting, URS and the US Army Corps of Engineers recommended that no further software testing be undertaken, and that any additional efforts be directed to further development of the Sandia HTFC application. This recommendation was based primarily on the fact that none of the commercially-available software applications reviewed can detect craters or other munitions features, and none offered scripting support that might allow such capability to be developed by users. Secondly, the HTFC application shows promise and could be developed reasonably rapidly should ESTCP wish to do so. If desired, the URS elevation difference approach could be tested by Sandia for possible inclusion in their application.

Figure 29: Software for Manipulating Lidar Data

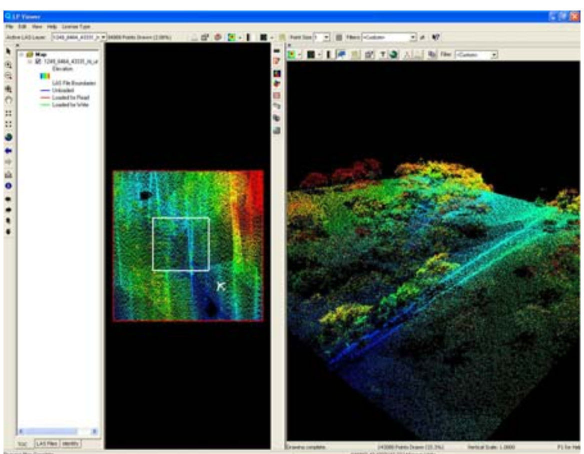

LP 360. Several free lidar viewers are available. None extract ground features but all display point clouds in ways that GIS products do not. The illustration above is from LP 360, an ArcGIS plug-in that works directly with the common .las file format and converts ascii format to .las.

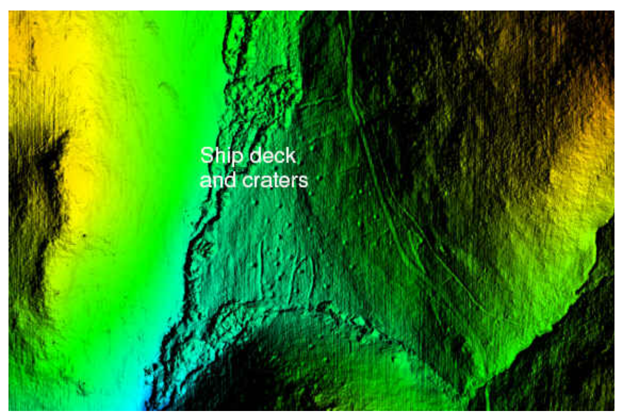

TLiD. TLiD provides a robust set of analysis tools for both surfaces and point clouds. The software is an ArcGIS plug-in, works directly with .las-format files, and identifies and extracts trees and buildings. It does not extract munitions features without additional programming, and no scripting capability is available.

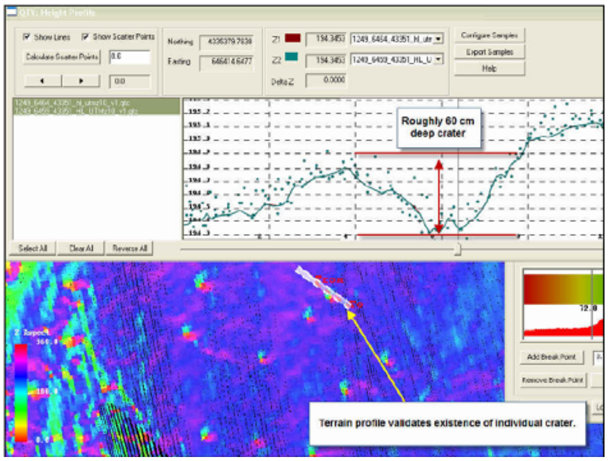

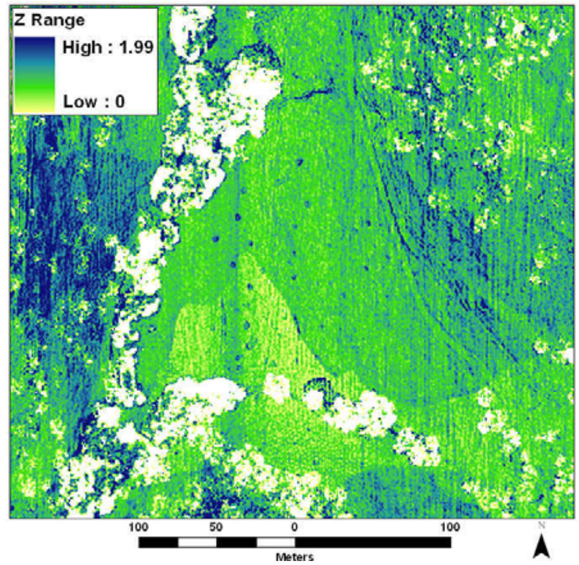

QT Modeler. QT Modeler provides a robust set of analysis tools for both surfaces and point clouds. The software is an ArcGIS plug-in and works directly with .las-format files. It does not extract munitions features without additional programming, and no scripting capability is available.

URS ΔZ Approach. URS tested a crater identification approach based on detecting local variations in ground surface elevation. The approach showed some promise in relatively flat terrain.

Figure 30: Sandia National Laboratories HTFC

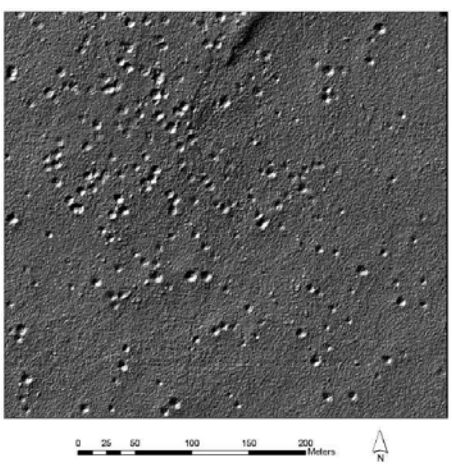

Figure 1. Shaded relief image of PA1 LIDAR data sample.

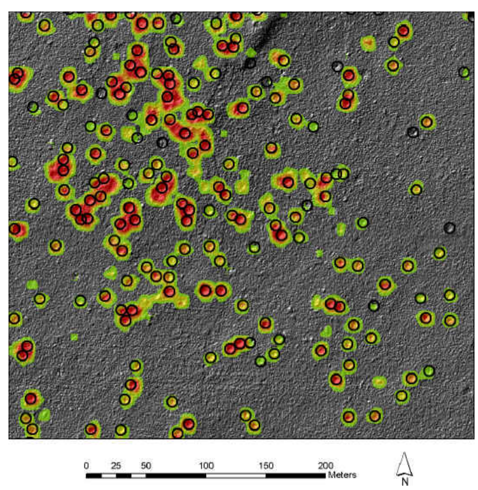

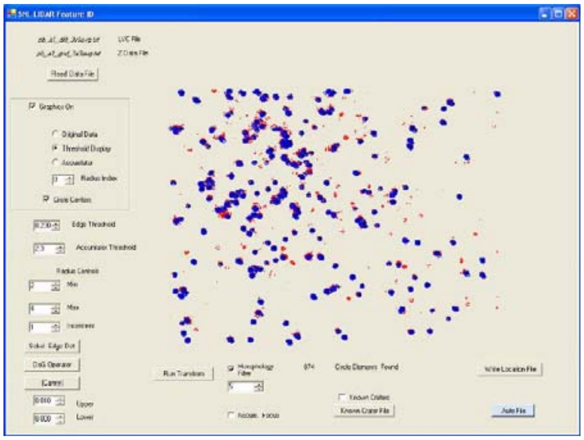

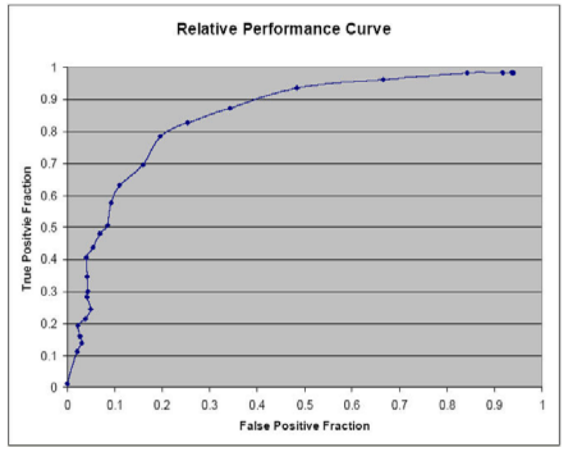

HTFC. Examples including test data, results of manual vs. automated output, and a portion of the user interface.

6.3 ACTIVITY 3: SUMMARIZE LESSONS LEARNED FROM THE ESTCP WAA PILOT PROGRAM

Appendix D contains the final guidance document presented to ESTCP in January, 2010.

7.0 PERFORMANCE ASSESSMENT

The performance objectives for this project were originally established in the Demonstration Plan (URS 2008b). Performance objectives were revised following the In-Progress Review meetings of February and October 2008, to reflect the addition of ESTCP's requests for the two white papers (Appendices B and C).

Actual performance compared to the performance objectives is summarized in Table 6. In summary, all of the performance objectives were accomplished except in the following two cases:

- Vegetation size classes were not mapped, since at the Former Camp Beale site, size classes had no clear boundaries and could not be mapped in a meaningful manner
- Correlation for grass heights between lidar and field measures could not be established

In addition, URS and USACE recommended that Activity 2, the software evaluation, be ended after the first round of evaluation.

This section details the principal findings of this demonstration.

Activity 1 – Systematically investigate vegetation effects

Lidar can perform well at vegetated sites, though vegetation will cause some decrease of lidar density and thus lower confidence in feature detection.

Lidar measures of vegetation height and density correlate reasonably well with standard measures.

Lowering the lidar data density affected the feature detection under vegetation. Significant loss of feature detection began to appear 6.9 pts/m^2 and 3.4 pts/m^2, with over two-thirds of the features not visible at the lowest density level tested (0.8 pts/m^2).

At lower densities, object detection rates were lower, but the effect is not completely predictable: some features faded gradually as lidar density lowered, while others did not disappear at all. These non-linear relationships are to be expected since any density of lidar points will show the features that happen to receive the laser reflections. There was some correlation between the rate of degradation and the size of the feature; that is, larger features tended to disappear more slowly. However, this correlation was not strong. Lidar data at the higher densities detected all of the features at the test plots, as verified by the field visit.

The implications of these non-linear relationships between lidar data density and feature detection include:

- There is no lidar density at which no features will be detected. Rather, lower-density lidar will result in a lower degree of confidence.
- Lidar density will have a point of diminishing returns, after which additional lidar points will not reveal additional features.

Table 6: Performance Objectives: Desired and Actual Results

Performance Objective	Metric	Action to Achieve Metric	Sampling Frequency or Timing	Desired Result	Actual Results
Activity 1: Systematically Investigate Vegetation Effects – Field Data Collection					
Delineate vegetation classes using photos and lidar data	All major vegetation size classes identified	Delineation from orthophotos followed by QA/QC review by qualified staff	Once at start of project	100% identification of all major vegetation classes	Partially accomplished. Vegetation heights were calculated for the study area. Vegetation size classes had no clear boundaries and could not be delineated meaningfully.
Calculate lidar ground and vegetation point percentages	Percentages accurately calculated on a per square meter basis using a 3 m cell size to show variation across the study area	Use of standard GIS calculation methods followed by QA/QC review	Once at start of project	100% of study area characterized	Accomplished. Percent of ground and vegetation returns was calculated based on vendor classification and revised classification.
Calculate lidar data density variability	Density of ground lidar points and all lidar points accurately calculated on a per-meter basis to show variation across the study area	Use of standard GIS calculation methods followed by QA/QC review	Once at start of project	100% of study area characterized	Accomplished. Densities for ground points and all points were calculated on a per-meter basis.
Select representative field plots	Representative study areas selected	Select at least 50 plot locations, with plots distributed in all vegetation classes	Once at start of project	Plots placed in all vegetation classes	Accomplished
Collect field vegetation density data	Collect accurate data on vegetation conditions at each plot	Standard forestry methods for stand exams for deteriorating vegetation density incorporated into SOP, followed by QA/QC review	Once	All field data collected to follow SOP	Accomplished

Performance Objective	Metric	Action to Achieve Metric	Sampling Frequency or Timing	Desired Result	Actual Results
Collect field ground feature data	Collect accurate data on ground features at each plot	Incorporate field procedures into SOP, followed by QA/QC review	Once	All field data to follow SOP	Accomplished
Activity 1: Systematically Investigate Vegetation Effects – Data Analysis					
Step 1: Classify Vegetation					
Lidar ground point density vs. field vegetation density	Difference between vegetation (crown) density as measured by lidar and field methods	Standard GIS analysis methods, followed by QA/QC review	Once	Correlation should be highest in plots with a single, simple vegetation class	Accomplished
Lidar vegetation heights vs. field vegetation heights	Difference between vegetation heights as measured by lidar and field methods	Comparison of lidar and field data	Once	Correlation should be within 5 feet for isolated trees	Partially accomplished. Correlation for tree heights was within desired results except for occasional outliers. Correlation for grass height was poor.
Step 2: Identify Ground Features					
Field ID of features vs. ID of features from lidar	Percentage detection and false alarm rate for features detected using lidar vs. field observation	Visual observation of lidar data followed by comparison of results of lidar and field observations	Once	Correlation should be 100% for features over 1 m in size in plots with no covering vegetation	Accomplished
Effects of lidar point density on feature detection	Number of features visible at successively lower point densities	Artificially lower point density through a series of levels, create surface models and examine the detection of features visible at the highest density	Once	Determine the lidar data density where detection falls off substantially	Accomplished

Performance Objective	Metric	Action to Achieve Metric	Sampling Frequency or Timing	Desired Result	Actual Results
Step 3: Produce White Paper on Lidar Point Classification Methods					
Determine the percentage of lidar points misclassified as non-ground returns	Percentages of points classified as ground or non-ground vs. actual point count in selected vegetation-free locations.	Analysis in GIS to determine percentage values at selected test areas to tally actual point classification distribution	Once	Understanding of the effects of classification methods on percentages of points classified as non-ground on vegetation-free surfaces	Accomplished
Determine the source of misclassification of lidar points as non-ground returns	Clear understanding of the source of misclassification.	Conversations with data classification staff and examination of software manuals for classification software	Once	Clear understanding of the source of misclassification	Accomplished
Examine the potential benefit of reclassification of lidar points to feature detection	Approximate number and size of features visible after reclassification	Create new surface models using reclassified points and examine	Once	Estimate of the potential benefit of point reclassification	Accomplished
White paper technical accuracy	Point classification white paper accurate	Peer review by specialists from industry and universities	Once	Document will be technically accurate	Accomplished. Document was subject to technical peer review by vendors familiar with classification methods and software.
White paper readability	Point classification white is well written and understandable by non-specialists	Technical editing and QA/QC review	Once	Document will be understandable	Accomplished
Step 4: Produce White Paper on Lidar Error					
White paper technical accuracy	White paper on lidar error is technically accurate	Peer review by specialists from industry and universities	Once	Document will be technically accurate	Accomplished

Performance Objective	Metric	Action to Achieve Metric	Sampling Frequency or Timing	Desired Result	Actual Results
White paper readability	White paper on lidar error is well written and understandable by non-specialists	Technical editing and QA/QC review	Once	Document will be understandable	Accomplished
Activity 2: Evaluate Current Software Packages					
Prepare appropriate lidar data sets for subsequent testing	Accurate ID of ground features for testing	Visual inspection followed by QA/QC review	Once at start of project	100% confidence in test features to be given to vendors	Accomplished.
ID of features using automated methods	Percent detection and false alarm rate of automated methods vs. visual inspection results	Compare results of visual inspection and automated methods	Once from each vendor	Percent detection will be highest for isolated, well-defined features. False alarm rate will be lowest for relatively flat, smooth ground surfaces.	Partially accomplished. Only one software product reviewed (Sandia National Labs HTFC) was able to automate feature detection. As this was an ESTCP-funded product, percent detection and false alarm rate were documented already. Based on these initial results, URS and USACE recommended that Activity 2 not proceed to further testing, and that ESTCP work directly with Sandia on further development.
Activity 3: Summarize Lessons Learned from the ESTCP WAA Pilot Program					
Usability	Guidance document applicable to the requirements of present and anticipated munitions management programs	Peer review by DoD program and policy staff	Once	Document will be useable	Pending

Performance Objective	Metric	Action to Achieve Metric	Sampling Frequency or Timing	Desired Result	Actual Results
Technical accuracy	Guidance document is technically accurate	Peer review by specialists from industry and universities	Once	Document will be technically accurate	Accomplished
Readability	Guidance document is well written and understandable by non-specialists	Technical editing and QA/QC review	Once	Document will be understandable	Accomplished

DoD – Department of Defense
GIS – Geographic Information Systems
ID – identification
m – meter
QA/QC – quality assurance/quality control
SOP – standard operating procedure
USACE – US Army Corps of Engineers

The performance of lidar can be improved compared to standard classification and display methods. Once a sufficiently dense lidar data set has been acquired, performance can be improved using the following approaches:

- Point classification methods can be adjusted to add more points into the ground surface model. The elevation cut-off for adding additional points probably should be established based on individual site conditions, but findings suggest that this method can increase the resolution of the ground surface model and justify the use of smaller grid cells, both of which have the potential to reveal additional ground features if present.
- Surface models can be created using the smallest grid cell size justifiable given the point density.

In practice, surface model development may be more conveniently accomplished in-house by Government end-users, rather than having the vendor deliver them. This is because in-house development can allow for experimentation with alternative methods. However, this requires that Government users have sufficient software tools and training to accomplish these tasks. Creating DEMs and DTMs in-house can be challenging, especially with high-density data sets where the number of points is very large. In such cases it may be appropriate to work with sample data sets to determine, in consultation with vendors, the appropriate specifications for these products, and then request that the vendor create and deliver the final products.

For lidar points, controlling error is primarily a function of standard quality control methods, and the accuracy of the lidar points is best assured by establishing and adhering to appropriate contract specifications during data acquisition. Specifications for lidar accuracy can be independently verified by end users.

Confidence levels for feature detection can be mapped. As shown in Figure 28, it is possible to map the number of ground returns per square meter, using either the vendor's classification or a re-classified data set. Site managers and regulators can use these maps to classify areas where insufficient lidar points reached the ground surface to characterize features of a given size.

Lidar vendors should always be asked to deliver the full lidar point set. Because lidar data sets are very large, many vendors only deliver derived products such as ground surface models (DEMs) and all-points models (DTMs). The results of this investigation underscore the importance of receiving the entire lidar point data set for all lidar investigations. Using this data, Government land managers can evaluate the approaches to point classification and to surface model creation used by the vendor, and make appropriate adjustments.

Activity 2 – Evaluate current software packages

Current software products offer many useful tools for manipulating lidar data, but of those reviewed, only the HTFC application by Sandia National Laboratories was able to detect craters. Users of lidar at munitions sites could consider funding the completion and distribution of the HTFC application.

Lidar software is being improved continuously. Vendors should be contacted periodically to review new developments. Government offices that use lidar data also should be contacted to determine which software products are currently in use and whether they are performing well.

Activity 3 – Summarize lessons learned from the ESTCP WAA Pilot Program

A revised draft guidance document (Appendix D) was delivered to ESTCP and technical peer reviewers in July 2009. The final version incorporating peer review is submitted with this report.

8.0 COST ASSESSMENT

8.1 COST MODEL

Cost models for lidar and orthophotos are presented in the final reports for the ESTCP demonstration sites (URS 2007 and 2008a) and for the ESTCP WAA Pilot Program (Nelson et al. 2008). The results of this demonstration led to small changes in the cost models, as described in Section 8.2.

8.2 COST DRIVERS

Cost drivers for lidar and orthophoto acquisition are discussed in detail in the final reports for the ESTCP demonstration sites and for the Pilot Program as a whole. Additional conclusions from this investigation include the following:

- Cost for data acquisition at vegetated sites should not be significantly higher than for non-vegetated sites, except in very exceptional circumstances. Lidar at vegetated sites should be collected at a higher density; however, with the introduction of higher-speed sensors (up to 250 kHz pulse repetition rate), appropriate data densities for vegetated sites will rarely require additional flight lines. Costs for processing the additional lidar data at vegetated sites may be somewhat higher based on the need for editing of the classification results by skilled operators.
- At vegetated sites, the cost of orthophoto acquisition could be lower since orthophotos could be acquired with larger pixel sizes or omitted in favor of using pre-existing orthophotos.
- There should be little additional cost for changing data classification specifications to return more points to the ground surface model. At most, the vendor would charge for some initial tests of alternate processing methods, or for establishing an additional category for low lidar points. These additional costs should not be high.
- This project showed that feature detection rates did not decline substantially between the highest data density tested (13.8 pts/m^2) and half of that density (6.9pts/m^2). This suggests that it is unnecessary to collect extremely high lidar data densities. This may result in some cost savings.

8.3 COST BENEFIT

The final reports for the individual ESTCP demonstration sites (URS 2007 and 2008a) and for the ESTCP WAA Pilot Program (Nelson et al. 2008) showed that lidar was a cost-effective addition to the range of WAA technologies. As summarized in Section 7, the current demonstration examined several potential ways to increase the effectiveness of lidar data. While most of these would not change the overall cost of using these technologies, each would increase the benefit to cost ratio.

9.0 IMPLEMENTATION ISSUES

As an airborne technology, implementation of lidar does not present significant regulatory challenges. Lidar and orthophotography rely on commercial off-the-shelf equipment, and there is a network of qualified vendors. There are few issues with equipment availability or skilled operators. Procurement issues discussed in this demonstration include establishing appropriate contract specifications, especially those related to point density specifications and point classification methods.

10.0 REFERENCES

Ambercore. 2008. White Paper on LiDAR Mapping. Terrapoint Division Offices. Available at: http://www.ambercore.com/files/TerrapointWhitePaper.pdf.

Andersen, Hans-Erik, Stephen E. Reutebuch, and Robert J. McGaughey. 2006. A rigorous assessment of tree height measurements obtained using airborne lidar and conventional field methods. *Canadian Journal of Remote Sensing* 32 (5): 355-366.

Baltsavias, E.P. 1999. Airborne laser scanning: basic relations and formulas. *ISPRS Journal of Photogrammetry & Remote Sensing* 54: 199–214.

Behan, A. 2000. On the Matching Accuracy of Rasterised Scanning Laser Altimeter Data. *International Archives of Photogrammetry and Remote Sensing* 33. Amsterdam.

Dold, Juergen. 2008. Technology is changing at blinding speed. *GIS Development, the Global Geospatial Magazine*. September. Available at: http://www.gisdevelopment.net/magazine/global/2008/september/42.htm.

Genc, L, B. Dewitt, S. Smith. 2004. Determination of Wetland Vegetation Height with Lidar. *Turkish Journal of Agriculture and Forestry* 28: 63-71.

Key, Hank. 2009. Airborne Lidar Sensors. Professional Surveyor Magazine, May. Available at: https://www.profsurv.com/assets/magazines/articles/70254/AirborneLidarSensors.pdf.

Jarvis, Beau. Terrapoint, LLC. Email with Dale Bennett, URS. August 19, 2009.

Lim, K., P. Treitz, A. Groot, B. St-Onge. 2001. Estimation of individual tree heights using LiDAR remote sensing. *Proceedings of the 23rd Canadian Symposium on Remote Sensing*. Sainte-Foy Quebec. pp 251-258.

Nelson, H., K. Kaye, and A. Andrews. 2008. ESTCP Pilot Project Wide Area Assessment for Munitions Response. Final Report. Environmental Security Technology Certification Program. July.

Ritchie, J.C. 1996. Remote sensing applications to hydrology: airborne laser altimeters. *Hydrological Sciences Journal* 41: 625-636.

Roberts, B.L. and S.A. McKenna. 2006. Identification of Munitions Range Related Features in Topographic LIDAR Data. ESTCP Project # 200325. Sandia National Laboratories. December.

Sky Research, Rogalla, Joy. Project Manager, Telephone conversation with Dale Bennett, URS. August 2008.

Sky Research. 2008. Demonstration of LiDAR and Orthophotography for Wide Area Assessment at Pueblo Precision Bombing Range #2, Colorado. Final Report. January.

Smith, S.L, D.A. Holland, and P.A. Longley. 2004. The Importance of Understanding Error in LiDAR Digital Elevation Models. *International Archives of the Photogrammetry, Remote Sensing and Spatial Information Sciences* 35: 996-1001.

Terrapoint, LLC. 2009. Letter re: Review of URS draft white paper on lidar error. July 6.

Terra Remote Sensing, Inc. 2009. Review of URS draft white paper on lidar error. June 23.

URS. 2007. High Density Lidar and Orthophotography in UXO Wide Area Assessment. August.

——. 2008a. Final Report Addendum for Former Camp Beale Demonstration Site. January.

——. 2008b. ESTCP Draft Demonstration Plan. Revision 0. Project Number 07 E-MM2-012/ MM-0737. Development of Parameters for the Collection and Analysis of LiDAR at Military Munitions Sites. January.

11.0 GLOSSARY

accuracy: The closeness of an estimated value to a standard or accepted value of a particular quantity.

anomaly: A geophysical signal from a detected subsurface object above geological background.

artifacts: In lidar, detectable surface remnants of buildings, trees, towers, telephone poles or other elevated features in a bare-earth elevation model. Also, detectable artificial anomalies that are introduced to a surface model via system-specific collections or processing techniques.

bathymetry: The measurement and study of water depths.

calibration: The process of identifying and correcting for systematic errors in hardware, software, or procedures.

conceptual site model (CSM): A description of site conditions that coveys what is known or suspected about the sources, releases and release mechanisms, contaminant fate and transport, exposure pathways, potential receptors, and risks.

contours: Lines of equal elevation on a surface. An imaginary line on the ground, all points of which are at the same elevation above or below a specified reference surface.

decimate: In the context of lidar, artificially lowering the density of the lidar data points in a manner that simulates the action of a slower lidar data sensor.

digital elevation model (DEM): A generic term for digital topographic and/or bathymetric data in all its various forms, but most often bare earth elevations at regularly spaced intervals in x and y directions. Regularly spaced elevation data are easily and efficiently processed in a variety of computer uses.

digital terrain model (DTM): Similar to DEMs, but they may incorporate the elevation of significant topographic features on the land and mass points and break lines that are irregularly spaced to better characterize the true shape of the bare earth terrain.

digital surface model (DSM): Similar to DEMs or DTMs, except they may depict the elevations of the top surfaces of buildings, trees, towers, and other features elevated above the bare earth.

electromagnetic induction (EMI): The physical process by which a secondary electromagnetic field is induced in an object by a primary electromagnetic field source.

Geographic Information System (GIS): A system of spatially referenced information, including computer programs that store, manipulate, analyze, and display spatial data.

Global Positioning System (GPS): Technology that computes the three-dimensional position of an object in space, for example the lidar sensor, using signals from at least four orbiting navigation satellites.

hillshade: A function used to create an illuminated representation of a surface, using a hypothetical light source, to enhance visualization effects.

horizontal accuracy: The positional accuracy of a dataset with respect to a horizontal datum.

Inertial Measurement Unit (IMU): Technology that uses gyroscopes and accelerometers to compute the roll, pitch, and heading of a moving object, for example a lidar sensor.

Inertial Navigation System (INS): A navigation aid that uses a computer and motion sensors (the IMU) to continuously calculate via dead reckoning the position, orientation, and velocity of a moving object without the need for external references.

light detection and ranging (lidar): An instrument system that measures distance to a reflecting object by emitting timed pulses of laser light and measuring the time between emission and reception of reflected pulses. The measured time interval is converted to distance.

magnetometry: The technique of measuring and mapping patterns of the earth's magnetic field as modified by geology or ferrous objects.

mrad: mRad is short for milliradians, a measure of the angle at which the laser beam expands with distance from its origin. A divergance of 1 mRad would be roughly equal to the beam expanding 1mm for every 1 meter it travels.

munitions and explosives of concern (MEC): Specific categories of military munitions that may pose unique explosives safety risk: unexploded ordnance, discarded military munitions, or munitions constituents such as TNT or RDX present in high enough concentrations to pose an explosive hazard.

nanometer: A unit of length equal to one billionth of a meter.

ordnance: Weapons of all kinds.

orthophotograph: A digital aerial photograph that has been geometrically corrected for topographic relief, lens distortion, and camera tilt.

orthorectification: The process by which the geometric distortions of an image are modeled and accounted for.

positional accuracy: The accuracy of the position of features, including horizontal and/or vertical positions.

redundant array of independent disks" (RAID) device: A device containing multiple hard drives, allowing computer users to achieve higher levels of storage reliability from low-cost and less reliable PC-class disk-drive components, through the technique of arranging the devices into redundant arrays.

root mean square error (RMSE): An accuracy assessment for measured data (e.g., lidar) calculated by taking the square root of the average of the set of squared differences between dataset values (i.e., lidar derived elevations versus field surveyed elevations).

triangulated irregular network (TIN): A set of adjacent, non-overlapping triangles computed from irregularly spaced points with x/y coordinates and z-values.

unexploded ordnance: Military munitions that have been primed, fused, armed, or otherwise prepared for action and that have been fired, dropped, launched, or placed in a manner constituting a hazard to operations, installations, or personnel; which remain unexploded.

vegetation removal: In lidar, the correction of reflective surface elevations so as to depict the elevation of the bare earth terrain beneath the vegetation.

vertical accuracy: The measure of the positional accuracy of a dataset with respect to a specified vertical datum.

wide area assessment: Rapid assessment of large tracts of potentially contaminated land to identify those areas with concentrated military munitions that require detailed characterization.

APPENDIX A
POINTS OF CONTACT

List all the important points of contact (POC) involved in the demonstration, such as co-investigators, sponsors, industry partners, and regulators. The list should include the following information: (1) full name; (2) complete mailing and/or FedEx addresses (if different); (3) telephone number, fax number, and e-mail address; and (4) the role of the individual in the project.

Use the tabular format below:

Name	**Organization**	**Phone Fax E-mail**	**Role in Project**
Bob Selfridge	ED-CS-D PO Box 1600 Huntsville, AL 35807-4301	256-895-1887	Co-Principal Investigator
Dale Bennett	URS Corporation 1501 4th Ave Suite 1400 Seattle WA 98101-1616	206-438-2026	Co-Principal Investigator
James Stewart	URS Corporation 1501 4th Ave Suite 1400 Seattle WA 98101-1616	206-438-2323	Lead Analyst

APPENDIX B
ESTCP WHITE PAPER: ERRORS IN LIDAR DATA: IMPLICATIONS FOR INVESTIGATION OF MILITARY MUNITIONS SITES

ESTCP White Paper

Errors in Lidar Data: Implications for Investigation of Military Munitions Sites

Project Number 07 E-MM2-012/MM-0737

Final

January 2010

Table of Contents

Figures

Acronyms

ASPRS	American Society of Photogrammetry and Remote Sensing
cm	centimeters
dB-Hz	decibel(hertz), band width relative to 1 Hz
DEM	digital elevation model
DoD	Department of Defense
DSM	digital surface model
DTM	digital terrain model
EMI	electromagnetic induction
ESTCP	Environmental Security Technology Certification Program
FEMA	Federal Emergency Management Agency
GIS	geographic information system
GNSS	Global Navigation Satellite System
GPS	global positioning system
Hz	hertz
IMU	inertial measurement unit
INS	inertial navigation system
km	kilometers
lidar	light detection and ranging
m	meters
MEC	munitions and explosives of concern
MRS	munitions response site
NMAS	National Map Accuracy Standard
NSSDA	National Standard for Spatial Data Accuracy
PDOP	position dilution of precision
ppm	parts per million
RMSE	root-mean-square error
TIN	triangulated irregular network
USGS	US Geological Survey
UXO	unexploded ordnance
WAA	wide area assessment

Acknowledgements

This project was made possible through funding provided by the Environmental Security Technology Certification Program. For their support and guidance to the US Army Corps of Engineers and URS on this project, we would like to express our sincere appreciation to:

Dr. Jeffrey Marqusee, Director, Environmental Security Technology Certification Program and Strategic Environmental Research and Development Program

Dr. Anne Andrews, Deputy Director, Environmental Security Technology Certification Program and Strategic Environmental Research and Development Program

Dr. Herb Nelson, Munitions Management Program Manager, Environmental Security Technology Certification Program and Strategic Environmental Research and Development Program

We gratefully acknowledge the following for their technical review of this paper:

- Terra Remote Sensing, Inc., especially Dave Neufeldt and Dave Mostyn
- Sky Research, especially Joy Rogalla and Tom Prescott
- Terrapoint, LLC, especially Kresimir Kusevic, Peggy Cobb, Claude Vickers, and DJ Lehto
- Karen Shuckman, URS and Instructor, Pennsylvania State University
- Bob Ryan, URS, formerly with Fugro EarthData

1 Introduction and Objectives

1.1 Introduction – Lidar in Wide Area Assessment

Many millions of acres of Department of Defense (DoD) lands are potentially contaminated with military munitions or their components. On the majority of these sites, munitions are concentrated in specific ranges and training areas. Locating the site of contamination can be difficult, in part because historical records are often incomplete or inaccurate.

Between 2005 and 2007, the Environmental Security Technology Certification Program (ESTCP) conducted a pilot program to test the effectiveness of a multi-technology approach to unexploded ordnance/munitions and explosives of concern (UXO/MEC) wide area assessment (WAA). The program included the use of light detection and ranging (lidar), orthophotography, helicopter magnetometry, towed-array magnetometry, and statistically-based transect design. The first phase of this program was carried out at three desert sites containing little or no vegetation and few non-military land uses: the Pueblo Precision Bombing Range site near Pueblo, Colorado; Kirtland Air Force Base Precision Bombing Range site near Albuquerque, New Mexico; and Victorville Demolition Bombing Range near Victorville, California. Subsequently, a second phase of the pilot program was added, including two new sites: the Former Camp Beale site near Marysville, California, and the Toussaint River site near Lake Erie. The Former Camp Beale site has more varied vegetation cover and land use types; the Toussaint River site is a shallow-water site and only a limited amount of land-based lidar was acquired.

At the three desert sites and the Former Camp Beale site, lidar was successfully used to identify munitions response sites, including bombing targets, berms, and firing points that were not detected using other technologies. At all four sites, lidar was used to detect small ground features such as potential craters. In many cases both the targets and the small ground features were highly eroded and not visible to ground crews.

At all four sites, the lidar investigation was able to supplement or correct the initial conceptual site model based on historical records review. This was accomplished through the discovery of preciously unknown targets, the correction of incorrect locations of known targets, and the definition of boundaries for known targets. Lidar also provided useful input to subsequent phases of site investigation, including information on slope and vegetation cover.

1.2 Problem Statement and Objectives

Error in the collection, processing, and interpretation of lidar data can lead to less accurate site characterization, with potential for “missed” ground features, difficulty in integrating lidar with other spatial data, and incorrect assessment of confidence levels in the data. An understanding of error in lidar data can contribute to appropriate expectations for the technology, and to the development of appropriate contract specifications.

Understanding lidar error is especially important since error in lidar data arises from different factors than error in magnetometry or electromagnetic induction (EMI), the most

common technologies used in geophysical investigations of munitions sites. Magnetometry and EMI are used to directly detect and map magnetic anomalies that may result from MEC, and each anomaly is reported and located individually. Error is understood as the discrepancy between the reported location of the magnetic anomaly and the true location of the object.

Lidar, by contrast, uses large arrays of laser reflections to model surfaces. The location of surface features (potential craters, for instance) is then inferred from characteristics of the entire surface. The accuracy of the location of features in the modeled surface rests on the accuracy and precision of the individual lidar points, but is influenced by other factors such as the density of the laser returns, the characteristics of the terrain, and the methods used to create the surface model. These factors can interact in complex ways.

This white paper presents a description of sources and magnitudes of error in lidar data, and the potential implications of such error for the use of lidar at military munitions sites. The objective of the paper is not to present the full range of scientific research on lidar error. Rather, it is intended as a guide for Government land managers who may acquire lidar. It identifies major sources of error, describes their implications for the use of lidar at munitions sites, and presents approaches for minimizing their impact.

The paper discusses:

- Factors affecting the accuracy and precision of the lidar points
- Error in GPS
- Factors affecting the accuracy of digital surface models
- Published map accuracy standards in common use

Quantitative measures of error are available primarily in the context of instrument error and terrain error. Factors affecting the digital surface models are important but more difficult to quantify.

This paper is based on published research and equipment specifications, along with interviews with lidar vendors and software providers. Examples are taken from lidar collected at ESTCP demonstration sites and other lidar data in the public domain. No original research was conducted for this paper

2 Accuracy and Precision of Lidar Points

Error in the use of lidar derives initially from the accuracy and precision of the individual lidar points.

2.1 Lidar Accuracy Specifications

Lidar vendors guarantee the accuracy of lidar points as a part of their contract documents, and vendors quote very similar guarantees across the industry. A typical accuracy specification quoted is 15 cm vertical and 50–100 cm horizontal.[1] Some vendors provide a more detailed specification such as the following:[2]. (All values are at 95% (two sigma or two standard deviations))

- Vertical: 15 centimeters (cm) hard surfaces and open regular terrain, 25 cm soft/vegetated surfaces, flat to rolling terrain, 30–50 cm soft/vegetated surfaces, hilly terrain
- Horizontal: 50–75 cm in all but extremely hilly terrain (depends on flying height and beam divergence

Lidar vendors guarantee the *accuracy* of the lidar data, that is, its correspondence to surveyed control. Accuracy, in contrast to precision, is the closeness of an estimated value to a standard or accepted correct value[3]. The accuracy value refers the size of the differences between the estimated and the standard value. In the context of lidar, the guaranteed accuracy refers to the correspondence of surveyed control points to either the individual lidar points closest to the surveyed point, or to the elevation of the lidar-derived surface model at that point.

2.2 Expressing Lidar Point Accuracy: Root Mean Square Error

Lidar vendors typically express their stated accuracies as root mean square error (RMSE) values. In calculating RMSE, the difference between data set coordinate values and the coordinate values from an independent source of higher accuracy for identical points are each squared and then averaged over the sample, after which the square root of the average is taken. Since the errors are squared before they are averaged, RMSE gives a relatively high weight to large errors compared to, for instance, an accuracy measure such as the mean absolute error, which gives the same weight to all values. This means that RMSE is most useful when large errors are particularly undesirable.

One weakness of RMSE is that, as a single number, it does not capture the spatial variability of lidar point error. As will be discussed in this paper, lidar error can vary with terrain and vegetation, and RMSE alone will not capture this variation. Useful supplements to the use of RMSE would include maps of principal terrain and vegetation types. Additionally, RMSE values are indications of the differences between the lidar

---

[1] See: http://www.airborne1.com/technology/LiDARAccuracy.pdf.
[2] Terrapoint, LLC, see: http://www.ambercore.com/files/TerrapointWhitePaper.pdf.
[3] The discussion in this section is adapted from Chapter 3 of *Digital Elevation Model Technologies and Applications: the DEM Users Manual* (Maune 2001).

points and survey control, and do not in themselves account for potential errors in the survey control points themselves.

RMSE values are generally quoted at the 68% (one sigma or one standard deviation) or 95% (two sigma or two standard deviations) level. This is because the error of some lidar points will always fall outside of the stated accuracy range.

When calculating the point accuracy, it is a common practice to eliminate from statistics all the points whose differences exceed a three sigma value. These points are considered outliers and are mostly present because the target points in the control and the lidar were wrongly associated. Such outliers are usually scarce, and the presence of a significant number of outliers may point to the existence of some systemic source of error in the data.

Formulas for computing horizontal and vertical RMSE are given in Attachment A.

2.3 Assessing the Accuracy of Lidar Points in the Field

Horizontal and vertical accuracy of lidar points are assessed differently. In measuring vertical accuracy, lidar vendors commonly survey a variety of locations in the study area, and compare these surveyed elevations to lidar elevations at the same points. Surveyed points are commonly established using static survey methods[4]. Some vendors will supplement static survey points with large numbers of additional points collected using kinematic Global Positioning System (GPS) survey methods, collected by driving along roads in the project area. Other vendors use small unmanned rover vehicles to collect large numbers of static points.

Surveyed points provide survey-grade data points of a higher accuracy than the lidar data to assess the accuracy of the lidar points. Vendors may perform vertical adjustments of the entire lidar data set to achieve a best possible fit to the control points[5], in which case the residual differences after this adjustment provide the quantitative estimate of the vertical error of the lidar data.

Methods and instrumentation chosen to collect the control points will directly influence the computed accuracy of lidar points. Since the accuracy of various methods, such as total station, static, and kinematic GPS, can vary from sub-centimeter to a decimeter level it is clear that different methods and adjustments will produce control points of different accuracy, directly influencing the accuracy estimation of the lidar points. Primary control points should have an accuracy at least one order of magnitude greater than the lidar points, and all control points should be reported with their method of collection and associated error.

---

[4] Vendors generally assume that these surveyed points are error-free, which in reality is not true. While more accurate than the lidar points, surveyed points are collected using techniques and instruments that are themselves subject to error, for instance total station, static and kinematic GPS have accuracies which vary from sub-centimeter to tens of centimeter. In practice, the estimated accuracy of the surveyed points should be reported along with the points themselves, and considered in evaluating the accuracy of the lidar points. (Personal communication, Terrapoint with Dale Bennett, June 2009).

[5] At least one vendor state that without such adjustment, vertical errors of the lidar data would routinely exceed the manufacturers reported maximum vertical error of 15 cm (Sky Research, 2009).

To evaluate horizontal accuracy, vendors compare the location of the lidar returns for objects in the study area whose real-world horizontal locations can be surveyed. These may include target objects placed with the surveyed points as in Figure 1, or larger objects. For example, lidar elevation values can be used to model the corners of buildings and other structures, or lidar intensity values can be used to model the edges of pavement (Figure 2). These lidar-based locations can then be compared to surveyed locations for the same objects.

Figure 1: Surveyed Control Points Used to Assess Vertical Error

Typical surveyed points used to evaluate vertical and horizontal accuracy.

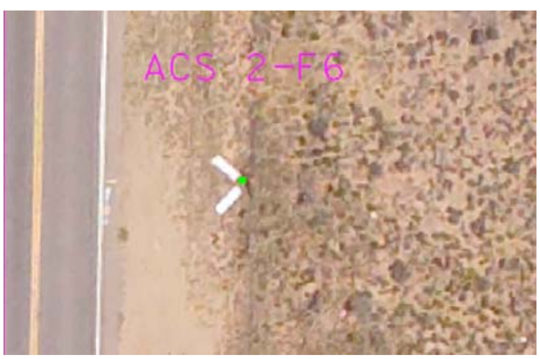

Survey target, with the-derived point added (green).

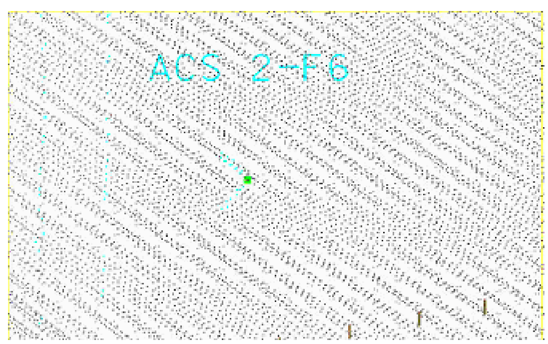

Lidar points classified by intensity. Blue points are reflections from the target legs. Green point is the derived intersection of the two panels, which is compared to the surveyed location.

Figure 2: Calibration Objects, Building Edges and Pavement Edges Used to Asses Horizontal Error

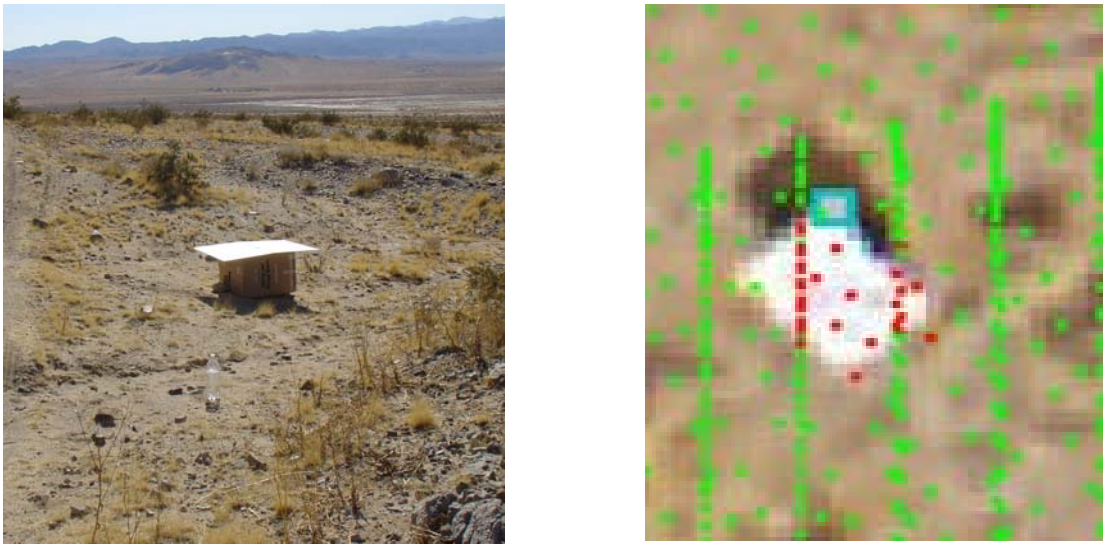

Lidar points reflecting on and around a pre-placed rectangular control surface. Lidar points are color-coded to show reflections from the ground surface (green) and those at or above the known height of the flat panel (red).

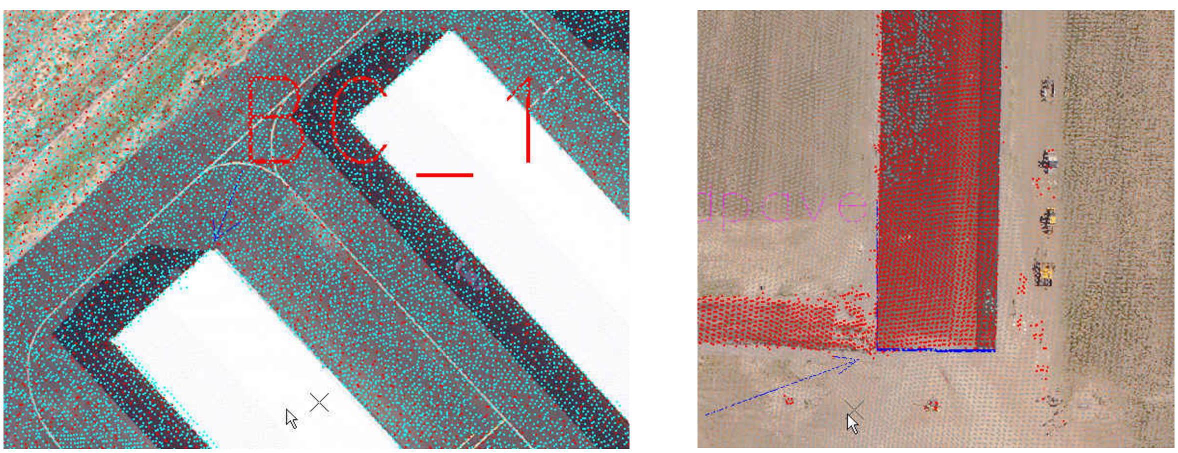

Lidar elevation values are used to model the edge of the building. The modeled location is compared to the surveyed location – not to the location in the orthophoto since this may be subject to different sources of error.

Lidar intensity values are used to model the edges of pavement (as in the runway above). Locations of pavement edges or corners are compared surveyed locations.

Horizontal and vertical accuracy are reported by vendors using standard quality control reports. Table 1 shows an example lidar vertical error report from a vendor, displaying

lidar-to-control-point vertical error for eight control points[6]. It shows an error of just over 10 cm or 0.104 meter (m) at the 95% confidence level.

Table 1: Example Lidar Vertical Error Report

Statistics					
Target	**Easting**	**Northing**	**Survey Elevation**	**Lidar Elevation**	**Difference**
TAR1	543461.243	3805793.824	827.486	827.440	-0.046
TAR2	542947.381	3807961.251	837.761	837.740	-0.021
TAR3	543747.347	3809712.492	833.970	833.930	-0.040
TAR4	545277.331	3809859.694	797.753	797.710	-0.043
TAR5	546671.936	3810138.520	846.280	846.230	-0.050
TAR6	547168.309	3808650.964	864.049	864.000	-0.049
TAR7	545682.049	3807795.187	784.720	784.650	-0.070
TAR8	546462.139	3805793.466	806.263	806.180	-0.083

Summary	
Average difference	-0.050[a]
Minimum difference	-0.083
Maximum difference	-0.021
RMSE of the elevation	+/- 0.053
2d RMSE of the elevation (95%)	+/- 0.104
Std-Dev. of the elevation	+/- 0.019

Source: Terra Remote Sensing (2007)

Surveyed and lidar elevations in this chart are reported in meters above the "height above the geoid", an elevation that roughly coincides with mean sea level. See Maune (2001) for additional discussion of elevation values in GPS and lidar.

a. This value points to a residual of some systemic error in the data. Once the systemic error is removed from the data, the RMSE and the standard deviation will converge.

2.4 Lidar Point Precision

Often confused with accuracy, precision is a measure of the tendency of a set of values to cluster about a number determined by the set. The usual measure of precision is the standard deviation or the standard error. Precision is distinguished from accuracy in that accuracy is a measure of the proximity of the "true" value usually as established by an independent means of at least an order of magnitude higher in accuracy. (This is the basis of using static survey techniques to establish control points for lidar.) Therefore, in order to be highly precise, a data set needs only to conform to itself, while to be accurate the data set must conform to an independently derived standard (Maune 2001).

If lidar precision were perfect, there would be no elevation differences, for instance, between lidar returns on a uniformly flat surface. In practice, precision is never completely perfect, and precision errors appear as the "corduroy" striping observable on

[6] Especially when large numbers of control points are collected, occasional control points will have large differences from the lidar data. It is common practice to eliminate such data from statistics as outliers, as long as such outliers are scarce. The presence of significant numbers of outliers points to the existence of some systemic source of error which should be investigated. (Personal communication, Terrapoint with Dale Bennett, June 2009).

flat, smooth ground surfaces, or the “lumpiness” observable on paved parking areas or roads (Figure 3).

Figure 3: Lidar Precision Error

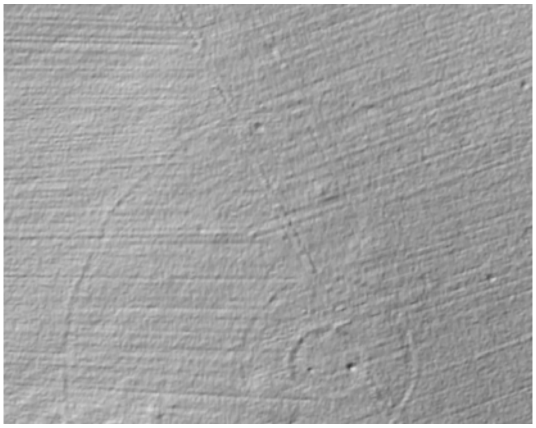

Surface model derived from lidar. “Corduroy” effect on relatively smooth, flat ground surface at Former Camp Beale ESTCP demonstration site.

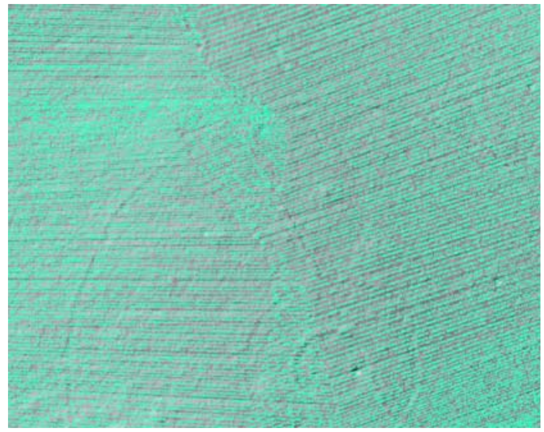

Same surface model as at left with superimposed lidar points, showing that the “corduroy” lines are congruent with the lines of lidar points.

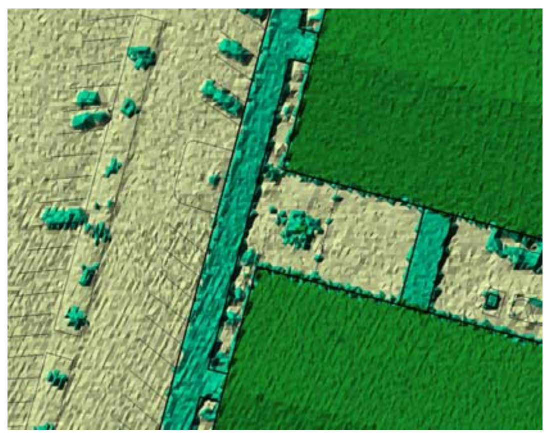

Orthophoto and lidar surface, municipal airport, Washington State. The lidar surface shows more “texture” than the flat surfaces of the parking lot and building roofs.

Small precision errors (under around 5 cm), arise from small errors in the sensor system and represent the inherent limits of the technology. Larger precision errors, including corduroy striping, also may be caused by other factors, including calibration errors, oversampling the data, moderate to severe turbulence, asymmetrical spot spacing, excessive noise in the sensor apparatus, and GPS error. According to some vendors, the most common cause of larger precision errors such as corduroy striping is calibration error. Calibration errors are caused by a systematic “drift” in the IMU (roll, pitch, crab), which remains fairly uniform over the course of a day. Calibration errors are corrected for in post-processing. Calibration must be performed after each collection and is the primary method for increasing precision of lidar data. The process works by assessing the precision, or the internal agreements among successive passes, over a series of

properly aligned symmetrical targets and then developing a set of coefficients to correct for the consistent offset observed in the data. Assuming high quality GPS data, when calibration is performed properly, the range in elevation values over (for example) a perfectly flat surface will be the same for one flight line as it is for multiple passes over the same target. If this internal agreement is not consistent then a calibration error should be suspected. Because calibration must be performed on each data set and because the effects of a poor calibration are always substantial, it must be assumed that calibration is among the top contributors to poor precision and therefore the cause of the corduroy striping[7].

Assessing the precision of lidar points. Lidar system manufacturers generally report overall accuracies for the system as a whole. No results have been located for precision measurements alone, such as bench tests of ranging error under fully controlled conditions, and in practice isolating the contribution of all of the factors contributing to precision error would be difficult to achieve. However, precision of lidar under field conditions can be roughly assessed by examining the elevation values of adjacent lidar points or rows of points on reasonably flat surfaces such as parking lots, roads, or building roofs.

URS conducted an evaluation using a set of 12 lines of lidar points at the Former Camp Beale ESTCP demonstration site (Figure 4). The site chosen was a road surface, appearing from the orthophoto to be in good condition, and located parallel to the flight lines and thus perpendicular to the lines of laser returns. The assumption of this small test is that by using a small lidar data set with points located close together on a reasonably flat surface; the influence of terrain changes along the road would be minimized, resulting in a rough snapshot of precision[8].

The distance between the vertical lines of points in Figure 4 was from 5–19 cm, with the total distance along the road of approximately 3 m. Mirror speed during data acquisition was 30 hertz (Hz), so the 12 lines of lidar points in the test set were collected in approximately 0.4 seconds, and were thus based on either one or two GPS readings.

---

[7] Sky Research, 2009.
[8] The test could be improved by choosing a more truly flat surface at an area with vertical scan angles, which were not controlled in this data.

Figure 4: Precision in Adjacent Lidar Points

Lidar points on road surface, Former Camp Beale ESTCP demonstration site.

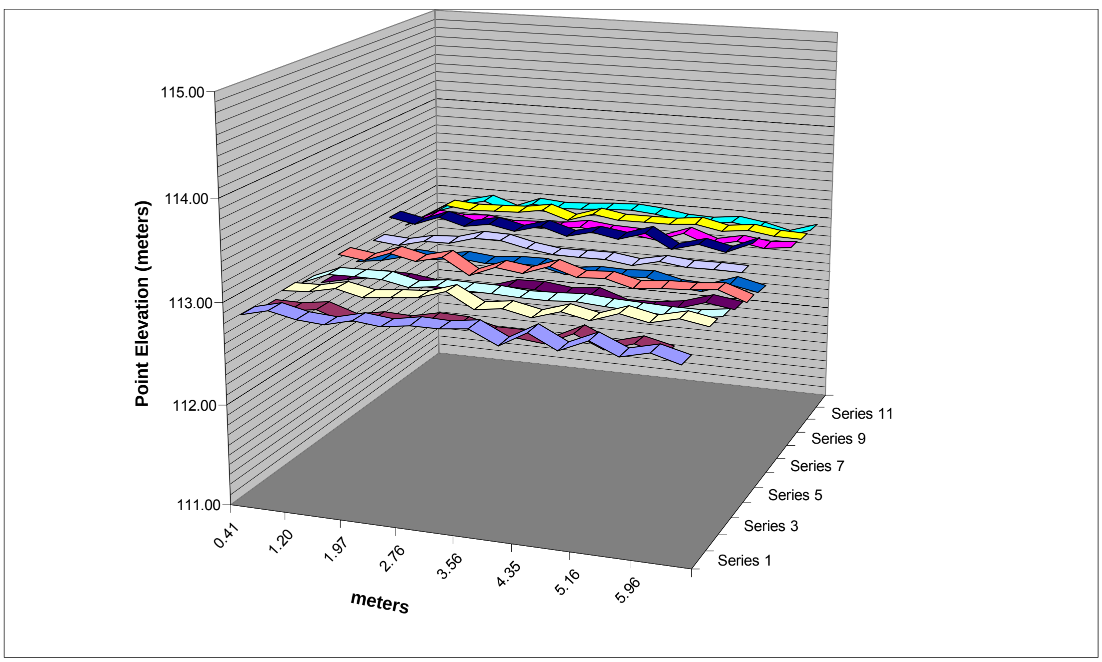

Elevation differences along and between adjacent lidar points.

The test showed the following results:

- Average point-to-point difference along the lines of points of 5.1 cm (minimum 0, maximum 16 cm)
- Average point-to-point difference between the lines of points of 7.4 cm, (minimum 0, maximum 21 cm), measured as the elevation difference between the lidar point and the nearest lidar point on the adjacent line

Some of this discrepancy between lidar point elevations is likely due to unevenness of the road surface itself; however, this test appears to indicate the approximate level of point-to-point error. These results are consistent with informal examination of “corduroy” striping in flat desert surfaces of the ESTCP demonstration sites, where lines of lidar points causing the “corduroy stripes” appear to have an elevation difference of approximately 5–8 cm.

2.5 Sources of Lidar Point Error

Several factors influence the accuracy and precision of individual lidar points. In most cases, the magnitude of each error source is not well documented, since vendors and manufacturers generally report error values for the system as a whole.

2.5.1 Instrument Error

Broadly, instrument error refers to the difference between the value given by an instrument and the “actual” values, based on the accuracy and precision of the measuring instrument. In the context of lidar, instrument error consists of deviations from positional values, generally as determined by GPS-based survey methods, contributed by each physical component of the system. Instrument error can impact both accuracy and precision.

System components. In order to establish the location of the lidar points, the lidar sensor system must establish the location of the sensor in space and the distance and angle from the sensor to the point of reflection of the laser pulse.

The position of the aircraft is determined using the GPS and Inertial Navigation System (INS). The GPS samples the aircraft location based on the position of at least four orbiting navigation satellites, at rates between one and ten times per second. Vendors report that error in the location of the aircraft is primarily GPS error, with the most serious source of GPS error being the momentary loss of sufficient satellite data to establish locations accurately.

The INS calculates the position of the aircraft between GPS locations. The primary input to the INS is from the Inertial Measurement Unit (IMU).). The IMU works by detecting the changes to rates of acceleration, along with rotational attributes such as pitch, roll, and yaw. The IMU generally contains three accelerometers and three gyroscopes, each placed in orthogonal positions so that data is collected in all three planes. Current IMUs record these changes at 200 hertz (Hz) (200 samples per second). The IMU adds a small error component in each plane. This error results from the accumulation of small errors as positions are continually re-calculated. These small errors accumulate until the aircraft’s position is updated from the GPS.

The laser system consists of a laser, a receiver, and a mirror that directs each pulse towards the ground surface. Lidar systems typically use lasers with wavelengths of 1,000 to 1,500 nanometers. The mirror system may be rotating or oscillating depending on the manufacturer. The receiver is a passive device that is tuned to the frequency of the laser, which records a signal when the amplitude of light in that frequency exceeds a threshold value. The sensor also records the energy level of the return, which is referred to as its intensity value. The threshold energy value that will trigger a return may or may not be adjustable, depending on the manufacturer.

The receiver can record multiple returns from each laser pulse. In vegetated conditions, part of the laser return may be reflected from branches and other sub-canopy features, leaving the remainder of the signal to be reflected from the ground surface. The limitation of the multi-return capability is that there must be sufficient time between returns for the sensor to reset. This time is generally between 3 and 20 nanoseconds and depending on the sensor used, a distance of between 0.5 and 3 m[9]. Thus, multiple returns cannot be recorded in low vegetation.

The final components of the sensor system are the power source, the hardware- and software-based control system, and the data storage equipment (consisting of multiple high-speed hard drives).

The lidar system has some parameters that can be varied, all within the equipment specifications of each manufacturer. These include power level, laser pulse rate, mirror speed, and scan angle or field of view. Vendors report that the primary parameters that are varied are pulse rate and scan angle.

A relatively recent development in lidar technology is the analog or “full wave form” laser receiver, available from several manufacturers. In contrast to the approach described above, the analog receiver records a continuous level of energy values once the amplitude passes the threshold value. The shape of this energy return curve can be analyzed and multiple return values derived in a more interactive manner. Analog receivers create much larger data sets than traditional sensors, and more advanced software is needed to process the output. Analog sensors are typically used for analyzing vegetation rather than modeling the ground surface, and appear to offer little advantage at most munitions sites. Since analog receivers are not commonly used at sites similar to military munitions sites, this paper does not describe them in further detail. However, error in these systems appears to derive from similar sources and to have similar magnitudes as the systems described here.

Overall instrument package error. Manufacturers and vendors typically report error for the entire system, expressed as the difference between the positions of individual lidar points compared to surveyed positions. Reported error for two example systems is presented below. Both systems are in common use in the industry and represent typical error values. This section assumes that the instruments are calibrated and used appropriately and are functioning correctly.

- ***Optech Canada ALTM 3100EA.*** Optech is one of the largest builders of lidar systems at the time of this report. The Optech product reviewed is a complete instrument package. Its published accuracy specifications assume a 50° field of

[9] Terra Remote Sensing personal communication, 2009

view in standard atmospheric conditions. Operational altitudes are between 80 to 3,500 m above ground level. Although not shown in Figure 5, vertical accuracy are stated to be between 5 and 20 cm.

Horizontal accuracy varies with altitude; the formula for horizontal error is: 1/5,500 x altitude (m above ground level). Both horizontal and vertical error is given at one standard deviation. Horizontal accuracy values vary from under 10 cm to over 60 cm depending on flight height, as illustrated in Figure 5.

Figure 5: Optech ALTM 3100EA Horizontal Error Curve

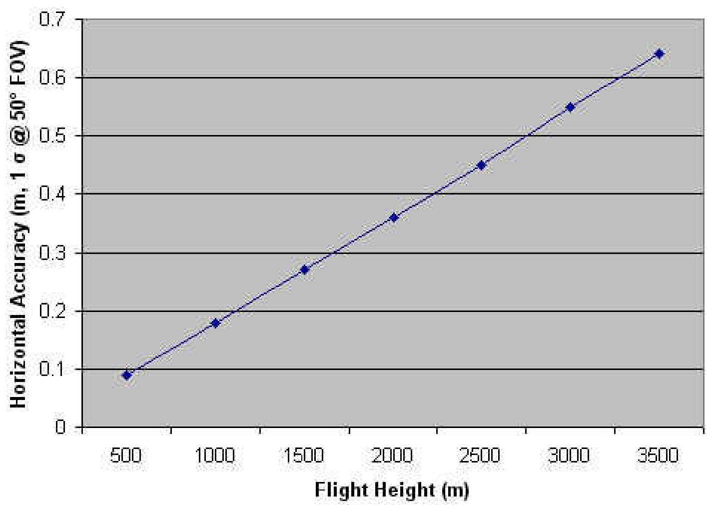

- ***Leica Geosystems ALS60 Airborne Laser Scanner.*** Leica is another major builder of lidar systems and the Leica ALS60 is also a complete instrument package. Leica published the accuracy specifications shown in Figure 6; their estimates are based on a 40-degree field of view and a nominal 5 cm GPS error.

Figure 6: Leica ALS60 Horizontal and Vertical Error Curve

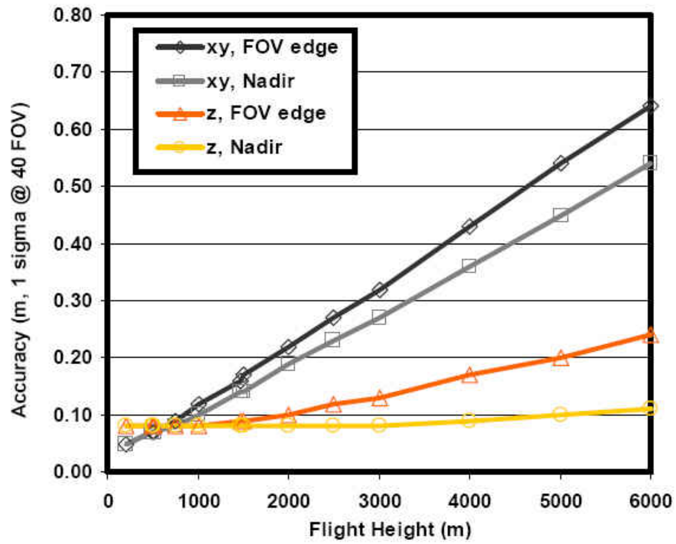

The Leica chart is more complete that the Optech chart, and shows that both horizontal and vertical error increase not only with flight height, but with distance from nadir. The chart shows that vertical (z) error ranges from under 10 cm to over 20 cm depending on flight height and distance from nadir, and that horizontal (x,y) error ranges from around 5 cm to over 60 cm, again depending on flight height and distance off nadir.

The Leica chart shown above is not in accord with the observation by Hodgson and Bresnahan (2004), which states that *"horizontal error is often reported to be approximately 1/1,000th of the flying height AGL [above ground level] on most systems."* Rather, the Leica chart shows horizontal error at 1,000 m AGL of approximately 1/10,000th of the flight height.

These error relationships are assumed to be roughly similar for all lidar systems, based on the similarity in the technology used and the relative consistency in the accuracies guaranteed by vendors in their contract documents. .Within the overall instrument error charts presented above are a variety of subcategories of error caused by individual system components. Manufacturers typically do not specify the error contribution of each component (Glennie 2007), however, types of error are further described in Habib and Van Rems (2009).

Site Conditions. Error from site conditions refers to the impact of local site conditions on the accuracy and precision of the lidar points, and thus on all of the resulting products. A wide variety of local conditions can create error in lidar data. Some conditions impact the entire data set, either by affecting the equipment directly or interfering with the GPS signal. Others, such as terrain roughness, may impact only part of the survey area. Site conditions that can contribute to lidar error include:

Slope. Lidar collected on steep terrain will be less accurate than that on flat terrain (Figure 7).

Figure 7: Effects of Slope on Lidar Point Error

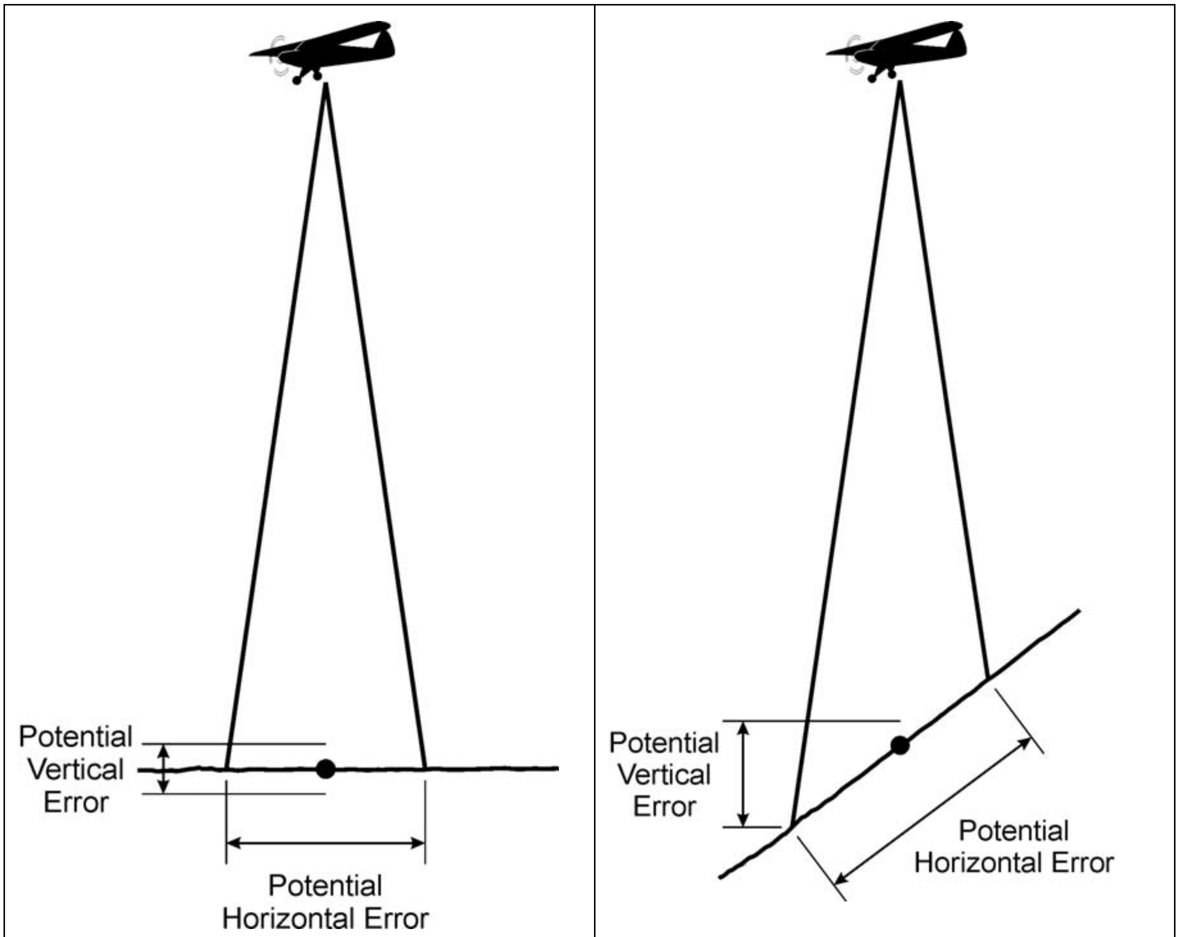

Slope compounds both horizontal and vertical error of lidar points.

This error arises in two ways:

- The lidar pulse spreads as the beam travels. The degree of beam divergence is affected by the characteristics of the laser combined with the flight height, with typical beam footprints between 10 and 100 cm in diameter[10].

  Beam divergence creates an area of uncertainty as to the exact point where enough energy is reflected to trigger a return. On flat surfaces this uncertainty may affect the horizontal location of the return, but will not affect the elevation

---

[10] Formula for beam divergence is roughly: spot diameter at nadir = elevation (meters)*beam divergence (radians) (Baltsavias 1999). System manufactures report beam divergence factors from 0.22 to 1.0 mrad (Key 2009). Laser footprints would therefore range from 22 to 100 cm at 1,000 m flight elevations.

value. On sloping surfaces, the area of the pulse footprint will be larger, and will also include a vertical error range.

- The horizontal error of the lidar location, caused by both beam divergence and the error inherent in the GPS, IMU and other components, will be larger on sloped ground. Further, on sloped ground the horizontal error will magnify the vertical error versus flat ground. The maximum amount of elevation error introduced is a function of surface slope, with:

  Elevation Error = tan α x Horizontal Displacement

Studies have shown that slope errors in lidar horizontal and vertical locations increased consistently with increasing slope (Hodgson et al 2005, Bowen and Waltermire 2002, Maling 1989).

Interaction of slope and scan angle. At the edges of the scan, the laser signal will approach the ground at an angle. This can either multiply or cancel the effect of the ground slope. Some experimentation has been done with estimating the combined impact of terrain, incidence angle and beam width (Schaer, et.al. 2007).

Ground surface. Some vendors guarantee higher accuracy on hard surfaces than on soft ground surfaces; this is based on the fact that soft surfaces are often less clearly-definable. Plowed fields or grassy areas, for instance, would have furrows or vegetation that would create error up to 10 – 20 cm (Terrapoint, 2009).

Similarly, it is occasionally observed that highly reflective surfaces will appear to be slightly raised in comparison to non-reflective surfaces, such as white painted centerlines on asphalt roadways. It is possible that more reflective surfaces are returning sufficient energy to trigger a response more quickly than less reflective surfaces.

Vegetation conditions. Under vegetated conditions, it is common for the majority of laser signals to reflect from the vegetation rather than the ground surface (Figure 8), the lower density of lidar points under vegetation will lead to lower confidence levels for the accuracy of the lidar points, since the elevation of the laser reflection will be compared to a more coarse surface model.

Electromagnetic interference. Rarely, certain types of electromagnetic signals can affect lidar data collection. This can include the on-board radio system, which can interfere with GPS antenna performance, and external sources. External interference was noted at the Former Camp Beale ESTCP demonstration site. Beale Air Force Base, which is adjacent to the demonstration site, is the site of one of three installations that are part of the Phased Array Warning System (PAWS), a radar system designed to detect and track sea-launched ballistic missiles. The high-intensity radar signals from this installation disrupted the GPS time signal used by the lidar system, initially rendering the data unusable. The effect was noted within several kilometers of the radar station and at altitudes up to approximately 500 m. The problem was noted during the daily quality assurance/quality control checks on the first day of data collection. A sample of the data was sent to the vendor's office, and a solution was developed to re-insert the correct GPS times. Interestingly, lidar was subsequently collected at Beale Air Force Base without problems, since lidar data collection took place at a higher altitude outside of the influence of the radar system.

Figure 8: Percentages of Laser Points Reflecting from Vegetation

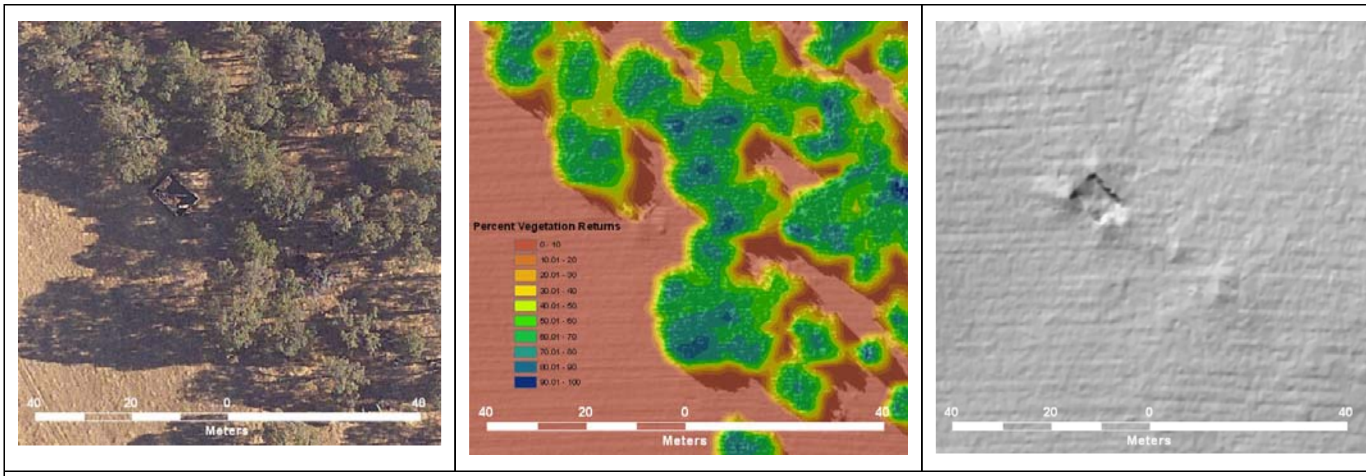

Percentage of lidar points reflected from vegetation, darker green and blue areas have higher percentages of vegetation returns. Although ground detail is visible under the tree cover, the lower number of ground returns will result in lower confidence in these areas.

Weather and temperature. Weather and temperature conditions can affect the ability to collect lidar data, but should not affect the accuracy or precision of the lidar data itself.

2.5.2 Operator Error

Potential areas where actions of the operator can impact lidar products are potentially numerous and can include the following (Sky Research, 2009):

- Improper planning that can cause an asymmetric distribution of points on the ground
- Failure to inform the pilots when they are offline, which can result in holes in the data
- Collection during periods of elevated position dilution of precision (PDOP) that exceed contract specifications, which may result in noisy or inferior GPS data
- Exceeding roll restrictions that can manifest in a poor position and orientation solution

There are many sources for operator error, including inexperience or improper training, momentary lack of judgment, inattentiveness, or distraction. Operator error also may result from incomplete information, as when the operator does not fully understand the purpose of the lidar survey. Operator error is difficult, if not impossible to quantify.

The standard approach to eliminating operator error is through the application of training programs to reduce error and quality control programs to detect and correct errors. Most vendors have well developed training and quality assurance programs, and the impact of serious operator error is generally small. This is particularly true in regard to all processes that impact the positional accuracy of the lidar data, where operator error may cause the vendor to fail to meet contract specifications.

2.6 Implications for Munitions Investigations

Instrument Error. The charts presented above show that the accuracy of lidar points varies primarily with flight height and distance from nadir. Lidar acquisitions at the ESTCP demonstration sites were conducted from 300 to 1,000 m, where instrument error is relatively low. Lidar collected at these sites met their contracted accuracy specifications.

At the ESTCP demonstration sites, features with elevation differences less than 10 cm were successfully detected, including bombing targets and potential craters (URS 2007). These features were detected despite the fact that the vertical accuracy specification was 15 cm. This is most likely due to the fact that vertical precision error is generally lower than accuracy error.

Subsequent acquisitions in this range of flight height should successfully meet similar accuracy specifications. However, where accuracy is especially important, contract specifications may be adjusted to require the vendor to fly lower and/or use a narrower field of view.

Site Conditions. Slope is the site factor with the most direct impact on the accuracy of the individual lidar points, and this impact can be relatively severe. The effects of slope and other site conditions such as vegetation cover are generally documented by placing additional calibration points in all major terrain types. Data calibration would still be performed using the most accurate points, i.e. those on flat, un-vegetated surfaces, with remaining points used for quality control and accuracy evaluation.

Operator Error. Most operator error can be controlled through applying accuracy specifications to the lidar data. Serious operator error will result in data that fails to meet specifications, and which will therefore not be accepted. However, an important supplement to contract specifications is to be sure that data collection and processing staff (not just contracting staff or management) fully understand the goals of the survey and the objects to be detected, so that collection and processing methods can be appropriately adjusted.

3 GPS Error

GPS error is a component of the overall lidar system error discussed above. Error in GPS is discussed separately for two reasons. First, vendors report that GPS error is the largest source of error in the day-to-day use of lidar technology. Second, GPS error affects not only the positional accuracy of the lidar points, but the accuracy of field data, including both calibration points and the reported locations of features in the field.

3.1 Theory of Operation

The United States GPS system is based on a network of 32 satellites operated by DoD; the system has been operational since 1978. The satellites are stationed in six orbital rings, with approximately circular, non-geostationary orbits with radii of 26,560 kilometers and orbital periods of approximately 11.9 hours. A complementary system is the Russian GLOASS system, which was planned for 24 satellites.[11] Similar systems are planned by China (Wikipedia 2009a) and the European Union (Wikipedia 2009b). Some GPS receivers are configured to receive signals from both satellite groups, and accuracy of such dual systems is reported to be higher (Clarkin 2007)[12].

Each GPS satellite sends out two carrier waves, and each also transmits a unique "Coarse Acquisition, pseudo-random noise" code, which is stored in the library of GPS receivers and which modulates the first carrier wave.

A GPS receiver must lock onto and track at least four satellites in order to determine a position on the earth. A minimum of three receivers are needed to determine the x, y and z coordinates (more are desirable) and a fourth is required to solve for clock error between the atomic clocks aboard the satellites and the less accurate clocks built into the receivers.

"Differential correction" is a method of reducing systematic positional error by applying corrections from outside sources. The most common form of differential correction is achieved through the use of a stationary GPS base station at a surveyed location. The base station monitors its location based on the satellites visible at each interval, and then calculates the difference between this measured location and its surveyed location. These differences are then applied to field locations recorded by the receiver. When this differential correction is done in real time it is referred to as real time kinematic differential correction, and when the differences are applied following data collection it is referred to as post-processed differential correction. Accuracies quoted here assume the use of differential correction except for recreation grade receivers.

3.2 GPS Error Sources

Potential sources of GPS error have been summarized in several sources. The following discussion is taken from Clarkin (2007). System specifications provided by

[11] As of February 2009, the system was reported to have 20 satellites, of which 19 were operational and one was undergoing maintenance (Wikipedia 2009c).
12 A description of the GLONASS system (provided by a receiver manufacturer) can be found at: http://www.novatel.com/Documents/Papers/GLONASSOverview.pdf

manufacturers include combined error from all of these sources, and little quantitative data was located regarding the relative contribution of each of these sources separately. Factors contributing to GPS error include:

- ***Ionospheric delay.*** The ionosphere is a portion of the atmosphere that ranges from 50–1000 kilometers (km) and contains gases that are ionized by solar radiation. The production of electrons from these gasses, measured as total electron content, cause delays in the propagation of satellite signals causing errors on the order of 10–20 m (Grewal et al. 2001). Although dual-frequency users can easily resolve this problem, ionospheric models still need to be developed for single-frequency users (Le and Tiberius 2006). Dual-frequency receivers nearly eliminate ionospheric effects by comparing the propagation of the signal at two frequencies (Leick 2003). Because the delay induced by the ionosphere is known to be inversely proportional to the square of frequency, ionospheric range error can be estimated accurately by comparing the times of arrival of the L1 and L2 signals (Grewal et al. 2001).
- ***Tropospheric delay.*** The troposphere is the lower part of the earth's atmosphere and also can delay the propagation of Global Navigation Satellite System (GNSS) signals, due to dry gasses and water vapor refracting the signals. The error is far less than that of ionospheric delay (1–3 m) and generally can be eliminated by differential correction and modeling (Grewal et al. 2001).
- ***Multipathing.*** Multipathing refers to the reflection of satellite signals off of objects or surfaces, producing signals of multiple ranges arriving at a GNSS receiver. Reception of satellite signals from multiple pathways, in addition to direct reception paths, can cause large coarse acquisition code ranging errors of up to approximately 10 m and degrade the ambiguity resolution process required in carrier-phase ranging (Grewal et al. 2001). Since multipathing effects are specific to receiver location, these errors cannot be reduced by differential correction. Piedallu and Gegout (2005) found that errors caused by multi-path signals due to signal reflections off trees were much greater than the errors that differential corrections could reduce. They contended that in forest environments, the multipath of the signal caused by the tree stand is the main error source.
- ***Elevation angle.*** Elevation angle is the angle between a satellite signal and the horizon. It is well known that the signal received at a low elevation angle will be more affected by multipath, ionosphere, and troposphere errors and receiving antenna gain patterns (Parkinson and Spilker 1996, Le and Tiberius 2006). The effect of low elevation angle can be even more severe when collecting GNSS information in heavily forested environments. For environmental field studies, it is a rule of thumb that satellites lower than 10–15 degrees above the horizon should not be used for positioning because of atmospheric refraction (Johnson and Barton 2004). Most receivers have an elevation mask setting that can be used to specify the lowest elevation angle that will be accepted.
- ***Satellite constellation and position dilution of precision.*** Position dilution of precision (PDOP) is a quality measure of satellite geometry. When the satellites contributing to a GNSS position are spread out, they provide a low PDOP value and a strong geometry for a better solution. When satellites are close together,

they provide high PDOP values and weaker solutions. Both theory and research have shown that accuracy decreases as PDOP increases (Karsky et al. 2001), so filtering out occupations with high PDOP values can be very important when taking GNSS positions. This is especially important in obstructed environments. Piedallu and Gegout found that in closed environments (coppice and high forest) the positioning errors increase linearly or according to an exponential model with the PDOP (Piedallu and Gegout 2005). Most receivers have a PDOP mask setting that can be used to specify the highest PDOP that will be accepted.

- ***Signal-to-noise ratio.*** Signal-to-noise ratio is the ratio of satellite signal strength to the strength of the surrounding noise measured in band width relative to 1 Hz (dB-Hz). The canopy has been shown to have a substantial effect on total signal loss and the reduction of signal-to-noise ratio (Karsky et al. 2001). Rodriguez-Perez et al. (2006) also found that positional accuracy was affected by stand density because of the lowering of signal-to-noise ratio and signal interception caused by the electromagnetic waves penetrating the stem and canopies. However, other research has found that a vegetation canopy may produce complete attenuation to little or no apparent effect on the signal pathway (Gerlach and Jasumback 1989). Furthermore, GNSS signals become unusable when the ratio falls below approximately 25 dB-Hz (Grewal et al. 2001). Most receivers have a signal-to-noise ratio mask setting that can be used to specify the highest PDOP that will be accepted.
- ***Geomagnetic activity.*** Geomagnetic activity refers to natural variation in the earth's magnetic field, usually as a result of solar flares and other solar activity. During periods of high geomagnetic activity the GPS phase can be affected to the point where the receiver cannot perform phase measurements with enough precision for centimeter level accuracy. It is good practice to check government web sites for geomagnetic activities prior to data collection[13].
- ***Occupation length and logging rate.*** Occupation length refers to the amount of time spent recording data at a GNSS point (and consequently the number of observations that will be averaged to determine the final position. Occupation lengths in GNSS research range from 1 minute up to 24 hours (Sawaguchi et al. 2003). Logging rate, which is the frequency of GNSS positions recorded, is closely associated with occupation length. For instance, Piedallu and Gegout 2005) found that positioning errors decrease linearly with the logarithm of the number of points taken into account when carrying out the measurement. Sawaguchi et al. (2003) found that over 1,000 logged positions/sample numbers (~17 minutes) were needed to achieve a precision to within 1 m. Comparatively, Naesset (2001) found in one study that the accuracy of GNSS point positions did not seem to improve beyond 15 minutes of observation. The National Geodetic Survey also states that experiments show that multipathing can take 10 minutes or more to average out in recording an observation. However, Hasegawa and Yoshimura (2003) found that the probability of resolving ambiguities in carrier-phase solutions significantly improved up to an observation period of 30 minutes or slightly more.

[13] See, for instance, the NOAA Space Weather Prediction Center at http://www.swpc.noaa.gov/forecast.html.

GPS field practices are designed to minimize these error sources.

3.3 Receiver Categories

There are three broad categories of GPS receivers on the market. The first is recreation or consumer grade, available from manufacturers such as Magellan and Garmin. These receivers generally cost under $1,000 and use the coarse-acquisition code to obtain rough positions. Positional accuracies are quoted as 3–5 m in open areas[14]. Manufacturers do not quote accuracies for obstructed areas such as under vegetation canopy for any type of GPS receiver (Clarkin 2007); however, Wing and Eklund (2007) found these recreation-grade receivers to be capable of accuracies within 10 m under closed canopies and 7 m under young forest in western Oregon.

The second grade of receiver is generally referred to as resource or mapping grade receiver; examples include the Trimble Pathfinder ProXTR or ProXH. These receivers generally cost under $5,000 and usually receive single-frequency carrier wave signals in addition to the coarse-acquisition code. Accuracy in the open is quoted as sub-meter down to around 30 cm[15]. Researchers have found single-frequency receivers to achieve error between 0.2 and 6 m under vegetation, depending on conditions (Clarkin 2007).

The third grade of receiver is referred to as survey grade; these receivers cost $20,000 or more and receive both carrier wave frequencies, achieving sub-centimeter accuracy in open conditions. Hasegawa and Yoshimura (2003) found that survey grade receivers achieve accuracies of 0.02–0.4 m under dense canopy. Naesset (2001) found a survey-grade dual frequency receiver had mean positional accuracies of 0.08–1.35 m under dense canopy.

3.4 Implications for Munitions Investigations

Implications of GPS error for munitions investigations fall into three categories: implications for lidar points, for calibration and quality control, and for field investigations.

3.4.1 Implications for Lidar Points

The published accuracy specifications for lidar systems include assumptions regarding the contribution of GPS error. (Some are explicitly stated, such as the 5 cm quoted for the Optech system in Section 2.5.1). As long as GPS error does not exceed assumed values quoted by vendors, the resulting lidar data should be within contracted accuracy specifications. Monitoring positional accuracy levels should be part of the vendor's daily quality assurance/quality control procedures.

3.4.2 Implications for Calibration and Quality Control

---

[14] For example, see http://www.magellangps.com/products/product.asp?segID=425&prodID=1916 for the Magellan Triton 2000 series, a high-end hand-held model.

[15] For example, see http://www.trimble.com/pathfinderproxt.shtml or http://store.elecdata.com/trimble/pathfinder_proxh_receiver.aspx. For example, the Trimble R8 GNSS, a commonly-used GPS system in both static GPS and real time kinematic surveying, has published accuracy specifications of ±5 mm +0.5 ppm horizontally and ±5 mm +1 ppm vertically for static GPS applications, and ±1 cm +1 ppm horizontally and ±2 cm +1 ppm vertically for real time kinematic applications. See Trimble R8 GNSS System Datasheet, http://trl.trimble.com/docushare/dsweb/Get/Document-140079/022543-079H_TrimbleR8GNSS_DS_0309_LR.pdf.

Surveyed points used for calibration and quality control must be from a source of higher quality than the lidar data itself. Errors in the calibration points can lead to incorrect assessment of data quality or errors in the entire lidar data set. Standard practice in establishing calibration points includes:

- Using survey-grade GPS operated by qualified staff
- Choosing flat sites to minimize the effects of slope between surrounding control point and nearest lidar points
- Choosing open sky sites, which are essential to GPS quality
- Choosing calibration points in all major terrain types
- Reporting estimated error of all calibration and control points

The only one of these that is not standard practice is the placement of calibration points in all major terrain types, where in practice the number of calibration points established will vary with the type of survey. Since the accuracy of lidar points can be affected by terrain (see Section 2.5), investigations at munitions sites should specify that calibration points will be established in each major terrain type.

<u>Implications for field investigations</u>. Munitions-related features such as potential craters are generally at least 2 m in diameter. In most field work, resource-grade GPS, with its sub-meter accuracy, should be able to locate these features with sufficient accuracy to compare the with lidar data, as long as open-sky conditions are present.

At vegetated sites, however, the locations of features collected by field crews must be treated with more caution, since GPS accuracy can be degraded under vegetation. As shown in Figure 9, resource-grade GPS can sometimes suffer significant inaccuracies at vegetated sites.

Figure 9: Potential Error in Resource-Grade GPS in Vegetated Conditions

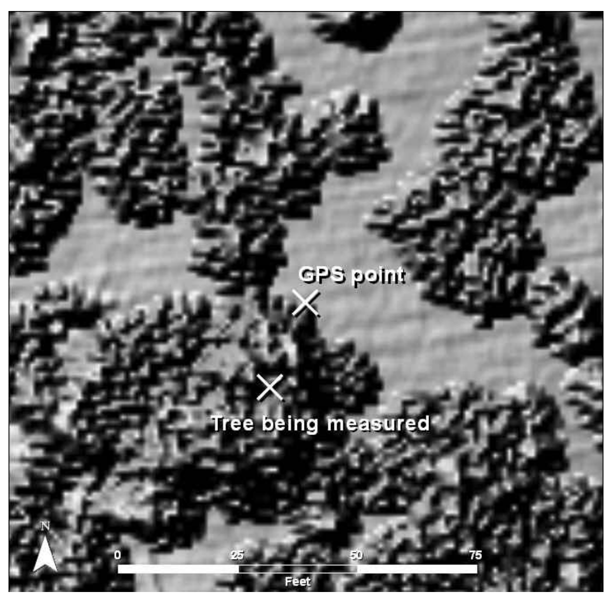

GPS point acquired for tree height investigation, Former Camp Beale ESTCP demonstration site, orthophoto left and

lidar digital surface model right. The GPS point is approximately 6 m from the highest lidar point in the tree being measured. GPS locations were acquired using resource-grade GPS. While most GPS points acquired at this site were more accurate than the point shown, several of the 51 points acquired showed errors of this magnitude.

For field investigations in vegetated conditions, other methods, beyond the scope of this paper, may need to be used.

4 Digital Elevation Models and Digital Surface Models

In practice, much of the analysis of lidar data is performed using surface models derived from the lidar points. Error in the use of lidar data should therefore include a discussion of potential error arising from the creation of surface models. This type of error may be quantified by comparing the elevation of the model to the elevation of the lidar points used to generate the model.

4.1 Using Lidar Points to Create Digital Surface Models

The typical final products of lidar are digital models of the ground surface, both of the bare ground and the ground with vegetation and buildings included. Typical model types are digital elevation models (DEMs), digital surface models (DSMs) and digital terrain models (DTMs).

A DEM, as defined by the US Geological Survey (USGS), is a digital file consisting of terrain elevations for ground positions at regularly spaced horizontal intervals that portrays the ground surface free of vegetation or human-created structures[16]. DEMs may be created using data from many sources in addition to lidar including topographic maps, ground survey, photogrammetry, or synthetic aperture radar. In the context of lidar, the DEM is the product through which the semi-random mass lidar points that the vendor classifies as returning from the ground surface are converted to a regularly-spaced grid of elevation values. This digital model can then be used in standard Geographic Information System (GIS) or other software to produce hillshaded surfaces, contour lines, or other digital products.

Regularly spaced elevation files of this type also may be created using all returns, including those from the tops of buildings, trees and other features. The USGS refers to these as DSMs. The term DTM is used as a synonym for both DEM and DSM. In the lidar context, the term DTM is most frequently used to refer to the all-points surface model. This paper uses the term DSM for the all-points surface model created using both ground and non-ground returns.

Figure 10 shows an example of the lidar point cloud, DSM and DEM for an example site.

4.2 Error Sources in Digital Models

Error in the DEM can be defined as the discrepancy between the elevation values of the DEM cells compared to surveyed values at the same locations. Error in the elevation values of the DEM cells also affects the horizontal error of features in the ground surface model, since it is the elevation differences between adjacent DEM cells that create edges that allow the user to infer the location of features.

[16] See: http://rockyweb.cr.usgs.gov/elevation/dpi_dem.html

Figure 10: Digital Surface Models and Digital Elevation Models

	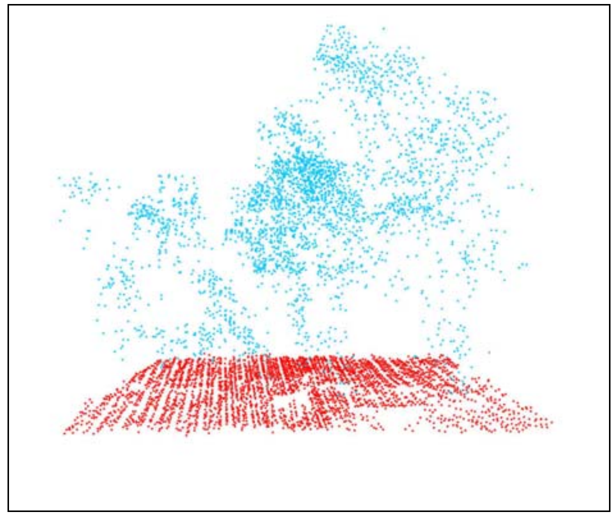
Aerial orthophoto, Former Camp Beale ESTCP demonstration site.	Laser reflections, classified as ground (red) and non-ground (blue). Modified vendor classification.
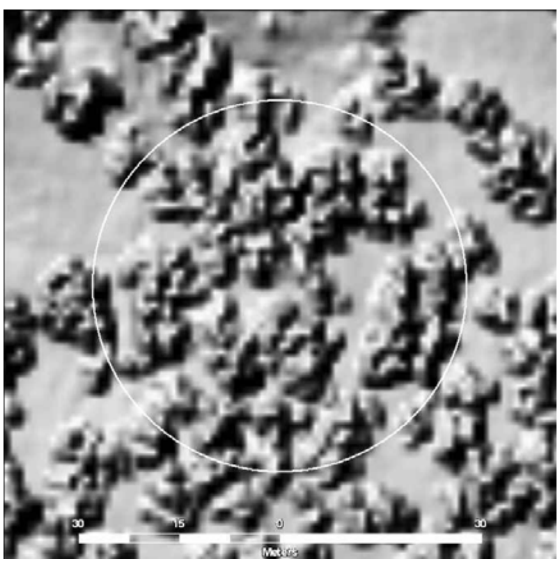	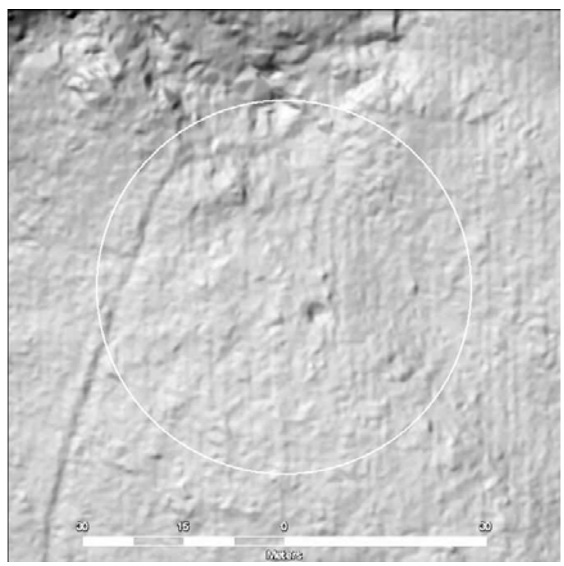
Digital surface model using all laser reflections.	Digital elevation model using ground reflections only.

Ultimately, the accuracy of the DEM consists of its accurate depiction of the true ground surface. Accuracy of a DEM will depend on the accuracy of the lidar data from which it is created, and will be subject to the types of error that affect lidar points. However, additional error can be introduced to DEMs through the methods used to create the DEM itself, including:

- The choice of the points classified as ground or non-ground returns

- The choice of interpolation method from the lidar points to the DEM cell elevations
- The choice of cell size

Each combination of these choices may be more accurate in a particular application.

4.2.1 Point Classification Methods

The point classification approach used by the lidar vendor should have no impact on the accuracy or precision of the lidar points, since classification takes place after the data is calibrated. However, methods that are biased towards creating clean, smooth ground surfaces can result in a lower data density of ground points, and this may result in fewer detections of small ground features.

Earlier work under this contract demonstrated that point classification methods in common use can over-classify lidar returns as non-ground (USACE and URS 2009). This phenomenon is a result of classification routines that interact with small elevation differences between nearby lidar points. The phenomenon is most common in areas of especially dense lidar data. Including more points in the ground surface model allowed detection of additional small surface features compared to the vendor's original ground surface model.

Interviews indicated that vendors are capable of modifying point classification methods increase the number of points classified as ground, and to adapt data collection and calibration methods to minimize elevation differences between points. Therefore, in the context of lidar surveys of military munitions sites, the most critical method for minimizing error resulting from point classification methods is to assure that vendors have a clear understanding of the goals of the lidar survey, how these differ from the use of lidar for other applications, and how methods will be adapted.

4.2.2 Digital Surface Model Interpolation Method

In a DSM, each cell of a regularly-spaced grid is assigned an elevation value. This elevation value is interpolated from the semi-random lidar points in and near the grid cell. There are two general approaches to this process. The first approach is to interpolate the surface model directly from the lidar points; the second is to create a Triangulated Irregular Network (TIN) using every individual lidar point, and to then interpolate the surface model from the TIN.

Interpolation is performed using one of a variety of mathematical approaches. Interpolation methods are classified as:

- Deterministic methods such as inverse distance weighting, which assume that each input point has a local influence that diminishes with distance
- Spline-based methods that fit a minimum-curvature surface through the sample points
- Geostatistical methods such as kriging that take into account both the distance and the statistical relationship among the sample points

Surveys of DEM interpolation methods have concluded that none of the interpolation methods is universally superior for all kinds of data sources, terrain patterns or

purposes. Inverse distance weighting is generally thought to be suitable for lidar data, since it works well for dense and evenly-distributed points (Liu 2008).

Little investigation has been done on the effects of different interpolation methods at munitions sites or for detection of small surface features. Earlier work by URS examined DEM creation methods using the data from the Kirtland Air Force Base Precision Bombing Range ESTCP demonstration site (URS 2007). The points in the area surrounding 1.5 and 1.0 m diameter test craters were extracted and used to create a series of surfaces using four methods. Deterministic, inverse distance weighted interpretation from the TIN showed the calibration craters somewhat more clearly than surfaces directly interpolated using other methods; however, the differences between the methods were not large, especially given the small size of the craters examined.

4.2.3 Cell Size

Choice of cell size can affect the detection of small surface features dramatically (Figure 11).

Figure 11: Effects of Digital Surface Model Cell Size on Feature Detection

<table>
<tr>
<td>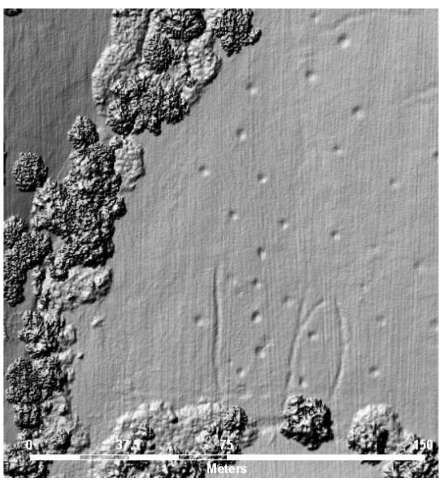
</td>
<td>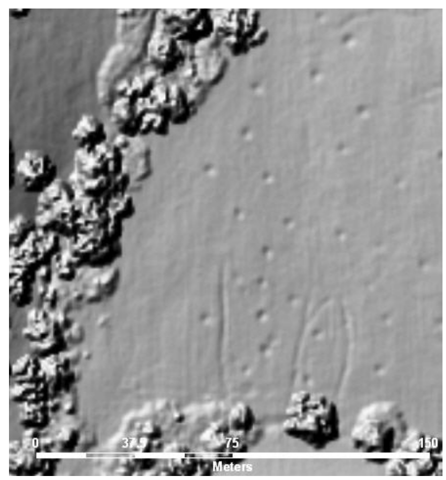
</td>
</tr>
<tr>
<td>Hillshade and DEM based on 0.3 m cells. Craters are approximately 3 m in diameter. Former Camp Beale ESTCP demonstration site.</td>
<td>Hillshade and DEM based on 1.0 m cells</td>
</tr>
</table>

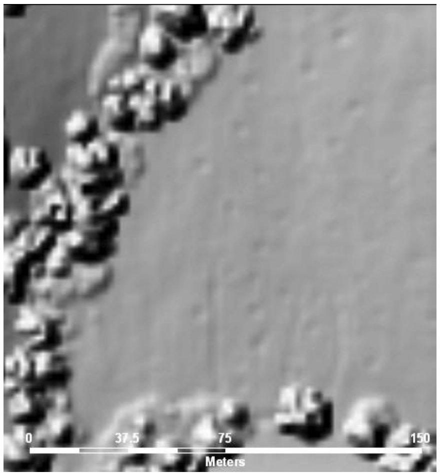	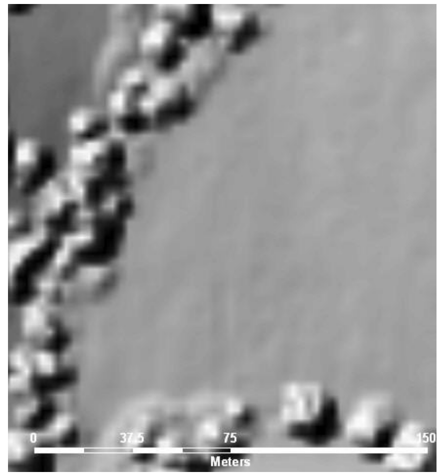
Hillshade and DEM based on 2.0 m cells	Hillshade and DEM based on 3.0 m cells

In Figure 11, images created with smaller cell sizes showed the potential craters with the best resolution. Visibility of these features decreased with increasing cell size, and at a cell size of 2 meters the features were essentially undetectable.

It is not always appropriate to use the smallest possible cell size. State-wide or region-wide lidar data sets typically have point density of 1–2 pts/m^2 and DEM cell sizes of 1-2 m[17]. The low data density and coarse surface representation of these surveys obscure much fine ground surface detail and would not be appropriate for munitions sites. Nevertheless, the resulting data is completely acceptable for its intended purpose of mapping surficial geology or large-scale stormwater runoff or flooding patterns. In fact, in modeling surface water runoff, a highly detailed ground surface model often will result in incorrect flow patterns when used in standard models, and the surface must be artificially smoothed or modeled with a larger cell size (Zandbergen 2006)

However, in investigations of munitions sites, the goal of the survey is to detect small surface features. In this application, surface models should be created using the smallest cell size that can be justified by the density of the lidar data. Vendors contacted uniformly recommended that cell size be kept as small as justified by average point spacing.

4.2.4 Display Methods

DEMs and DTMs are usually displayed as hillshaded images to enhance the visualization of surface features (Figure 12). ArcGIS, the most commonly used GIS software, contains dozens of settings that can affect the usefulness of these images. Different hillshade settings may be appropriate in some circumstances, and users need to work with analysts both to fully understand the goals of the survey and to experiment with appropriate settings.

---

[17] For example, see the metadata for the Puget Sound Lidar Coalition at http://pugetsoundlidar.ess.washington.edu/lidardata/metadata.html, or for the Pennsylvania PAMAP program at http://www.pamap.info/faq/lidar.htm#FAQ0110.

4.2.5 Topographic Break Lines

One important characteristic of lidar is that this technology does not record topographic break lines (Figure 13). This means that the apparent edges of features cannot always be regarded with great confidence. The absence of break lines can have serious impacts on the creation of contour lines (especially along shorelines or edges of roads) and on the operation of hydraulic models. In applications where break lines are important, these can be acquired through ground survey or other appropriate methods and added as inputs to the creation of the DEM.

Figure 12: Hillshade Display Method Examples

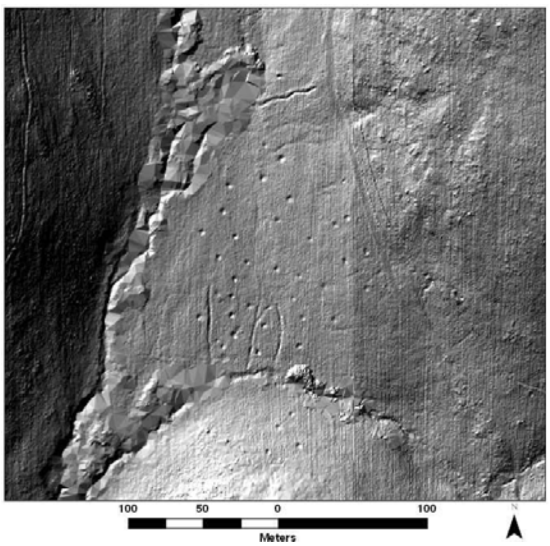	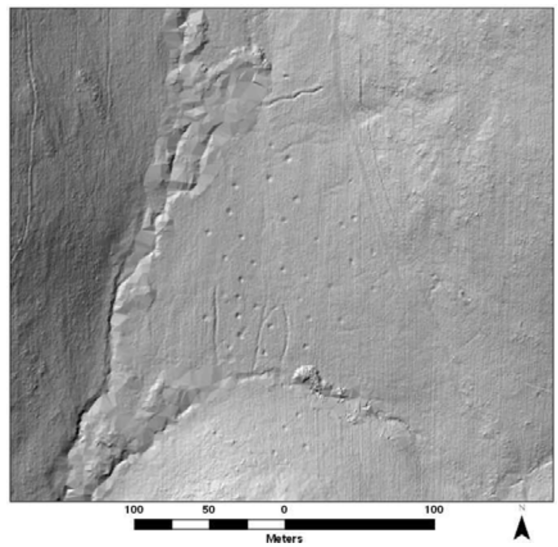
Hilshade image, ArcGIS default settings, former Camp Beale ESTCP demonstration site. The default settings are too dark in some areas to reveal the ground surface.	Hillshade image, alternate settings showing less dark grey area but also less contrast on the craters

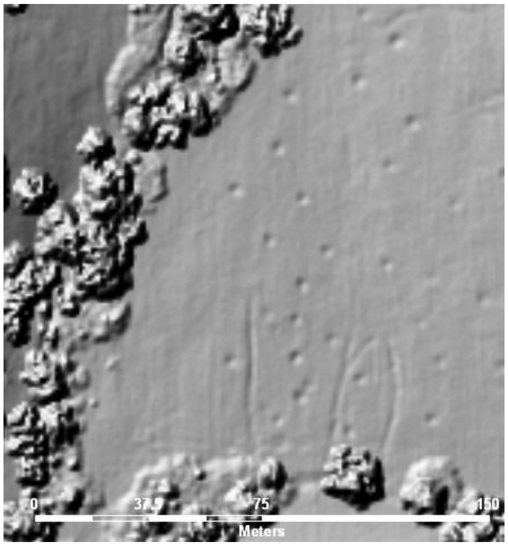	
Hillshade image, "neutral" hillshade settings	Hillshade image, contrast boosted, highlighting craters

Figure 13: Absence of Topographic Break Lines in Lidar-Derived DEMs

	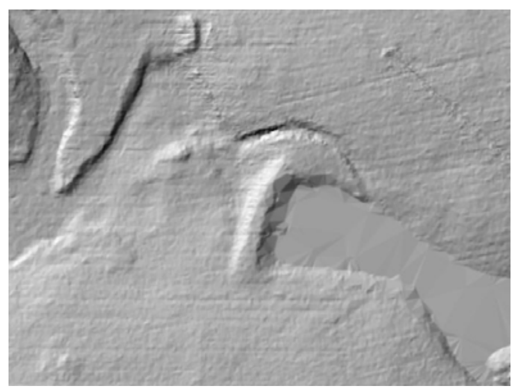
The small dam is visible under the trees in the lidar surface model. However, the edges of the dam cannot be precisely determined from the lidar data alone since there is no guarantee that laser signals will fall exactly at the edges. Former Camp Beale ESTCP demonstration site.	

4.3 Lidar-Derived Contour Lines

Contour lines also are a typical product of lidar data, and contour line creation introduces additional technical choices, along with further idealization of the original data. Users are often surprised that lidar-based contours can look highly irregular and jagged, rather than the smooth contours that are usually found on topographic maps. This effect is a result of the detailed lidar ground surface being interpreted through computer methods rather than a human operator (Figure 14).

Smooth contour lines can be created from lidar data using a variety of methods; however, these should be approached with some caution and adjusted to the particular

project needs. Caution is required because computer-based methods for creating smooth contour lines may remove small ground features that may be important.

4.4 Implications for Munitions Sites

Creation and display of DEMs and DSMs for military munitions sites should be adapted to the detection of small ground features, a use of lidar that is different from many other applications of the technology. Site managers should be prepared to experiment with appropriate methods; however, general approaches should include:

- Point classification methods should be discussed with the vendor's processing staff and adapted to maximize the number of points included in the ground surface model
- Some experimentation should be conducted to determine the most appropriate methods for interpolating cell elevation values
- DEM and DSM cell sizes should be kept as small as justifiable by the density of the data collected
- DEM and DSM display methods should be adjusted for maximum clarity

Lidar data is available for many parts of the country; however, the existing lidar sets are often not appropriate for munitions investigations. This is because the available DEMs are created with cells that are too large to detect small surface features, and because the underlying lidar data is generally not sufficiently dense to justify a smaller cell size.

Figure 14: Contour Lines from Lidar Surface Models

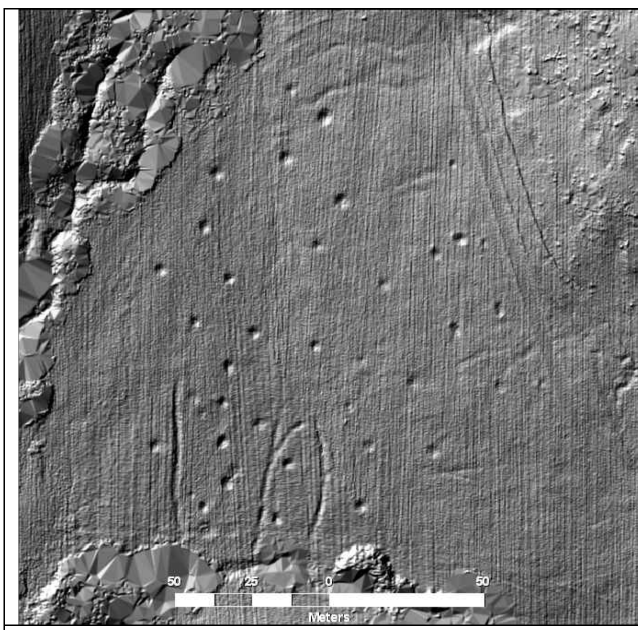

DSM, Former Camp Beale ESTCP demonstration site.

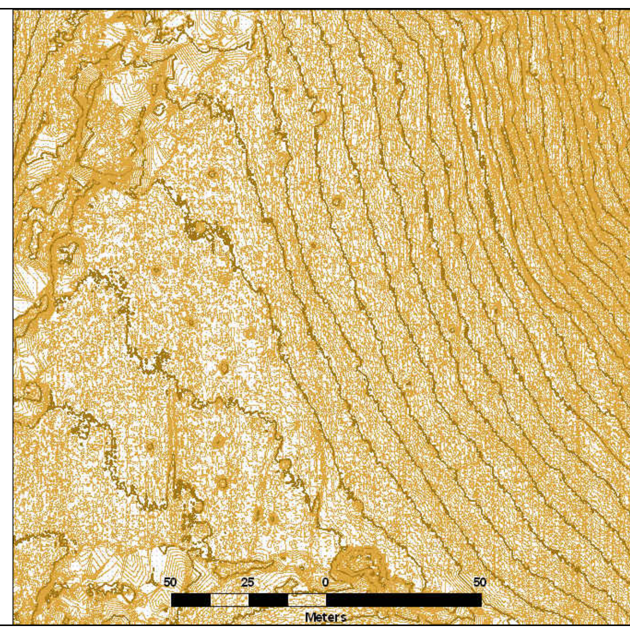

1 m (black) and 10 cm (brown) contour lines created from original DEM with 0.3 m cell size. Contour lines show craters but are very jagged.

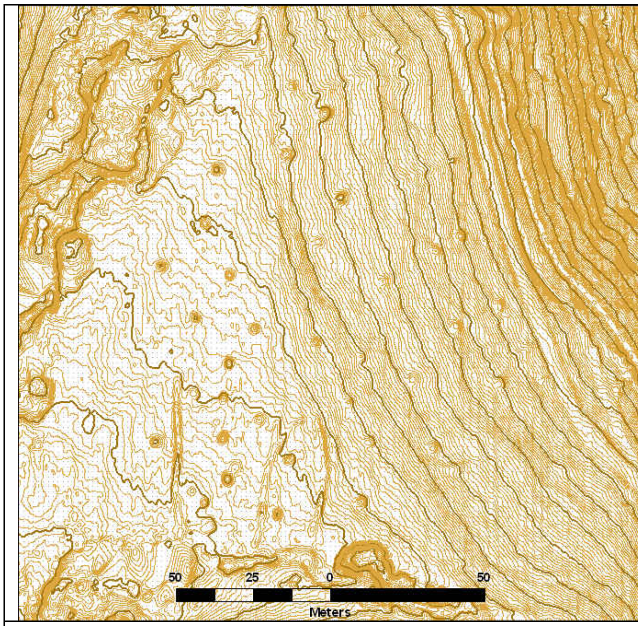	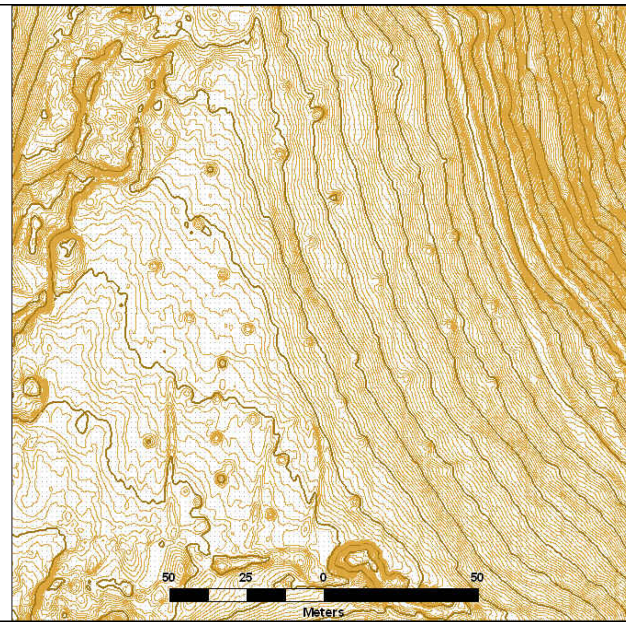
1 m (black) and 10 cm (brown) contour lines created from DEM after application of ArcGIS “filter” command (3 passes). Contour lines are somewhat smoothed.	1 m (black) and 10 cm (brown) contour lines created from DEM after application of ArcGIS “filter” command (5 passes). Contour lines are more smoothed.

5 Published Map Accuracy Standards

Published accuracy standards are commonly applied to products derived from lidar, including DEMs and contour lines. These accuracy standards derive historically from map accuracy standards for photogrammetry. In photogrammetric mapping, such as for the production of topographic maps, the vertical accuracy of the printed contour lines is largely a function of the flying height of the aircraft and the characteristics of the mapping camera used. Early map accuracy standards, therefore, consisted of required flight altitudes and camera specifications to create contour lines of a desired interval. A standard reference describes this, for example, as: *"if a client needed 2' contours, a typical flying height for acquisitions of aerial photography is 4,000 feet above mean terrain when using a mapping camera with a 6" focal length: if a client needed 5-foot contours, a typical flying height is 10,000 feet,"* (Maune 2001, p 63).

Non-photogrammetric methods, such as sonar, lidar, or synthetic aperture radar, are less dependent on flight altitude to determine the accuracy of the data. Map accuracy standards have begun to evolve in response to the emergence of these technologies, and this evolution is still underway. Users of lidar may encounter any of the standards described in this section.

5.1 National Map Accuracy Standard

The oldest map accuracy standard still in common use, the National Map Accuracy Standard (NMAS) was published in 1947 by the US Bureau of the Budget[18]. The NMAS defined horizontal and vertical accuracies for contour maps with a published scale and contour interval. Vertical accuracy is generally defined such that *"not more than 10 percent of the elevations tested shall be in error more than one-half the contour interval."* However, apparent vertical accuracy may be decreased based on permissible horizontal error for a map of that scale.

Lidar vendors are often required to meet NMAS accuracy standards, especially where contour lines are one of the requested deliverables. However, it is important to note that the NMAS predated the development of DEMs, and it does not contain a mechanism for evaluating the accuracy of either lidar points or DEMs. At least one standard reference recommends that NMAS not be used for evaluating and reporting the vertical accuracy of DEMs (Maune 2001).

5.2 American Society of Photogrammetry and Remote Sensing Standard

In 1990, the American Society of Photogrammetry and Remote Sensing (ASPRS) published the ASPRS Interim Accuracy Standards for Large Scale Maps (ASPRS 1989), with the expectation that these standards would form the basis for revision of the NMAS. The ASPRS Standard postdates the introduction of DEMs but still applies to graphic contour maps with a published scale and contour interval. Like the NMAS, vertical accuracy may be adjusted based on horizontal accuracy.

[18] See: http://egsc.usgs.gov/isb/pubs/factsheets/fs17199.html.

Unlike the NMAS, the ASPRS Standard defines horizontal and vertical accuracy in terms of RMSE from checked points, using check surveys of a higher accuracy. As with the NMAS, the ASPRS Standard is most appropriately applied to contour maps, and standard sources recommend that it not be used for evaluating and reporting the accuracy of DEMs (Maune 2001).

5.3 National Standard for Spatial Data Accuracy

In 1998, the Federal Geographic Data Committee endorsed and published a set of standards that included the National Standard for Spatial Data Accuracy (NSSDA). The NSSDA was developed to evaluate and report the accuracy of digital geospatial data, including DEMs (Maune 2001). For both horizontal and vertical accuracy, the NSSDA establishes accuracy as the area of uncertainty within which the true value falls 95% of the time. (The area of uncertainty is circular for horizontal uncertainty and linear for vertical uncertainty [FGDC 1998]). The NSSDA postdates the development of DEMs and can replace the NMAS for digital geospatial data including DEMs.

Unlike the MNAS and ASPRS Standard, accuracy is computed in terms of ground distances as opposed to map distances. Reported accuracy values reflect all uncertainties, including those introduced by geodetic control coordinates, compilation, and final computation. Apparent vertical errors in DEMs are not offset by permissible horizontal errors.

However, the NSSDA does not define threshold accuracy values, stating that *"Agencies are encouraged to establish thresholds for their product specifications and application and for contracting purposes."* This lack of threshold accuracy values may account for the persistence of the use of NMAS and ASPRS Standard, which do contain threshold values for acceptable accuracy.

5.4 Federal Emergency Management Agency

Lidar users may encounter the accuracy standard established by the Federal Emergency Management Agency (FEMA 2003). The FEMA standard is a variation of the NSSDA with an agency-specified accuracy threshold, and with an emphasis on contour lines for flood plain mapping. The FEMA standard calls for DEMs with a minimum 5-m post spacing, and a vertical RMSE of 15 cm, evaluated separately for all (normally 3–5) land cover types representative of the floodplain being mapped.

5.5 Lidar Contour Lines and Map Accuracy Standards

The creation of contour lines from lidar data introduces important issues regarding the relationship of lidar accuracy and density to the contour interval chosen and the certification of contour line elevations. As a general rule, smaller contour line intervals require lidar data that is denser and more accurate.

One standard source for guidance on accuracy standards for contour lines and other elevation data is the ASPRS guidelines (ASPRS 2004).[19] In terms of setting accuracy

---

[19] Online at:
http://www.asprs.org/society/committees/lidar/Downloads/Vertical_Accuracy_Reporting_for_Lidar_Data.pdf.

standards for contour lines, ASPRS points out that contour lines are produced through a series of technical steps, each of which has the potential to introduce error. Consequently, contour line accuracy should be specified for the contours themselves, and not be confused with accuracy of the lidar points. The guidelines conclude that *"Specifying accuracy of the final product(s) requires the data producer to ensure that error is kept within necessary limits during all production steps."*

Table 2 shows the ASPRS-recommended general correspondence between contour line interval and data accuracy.

Table 2: Recommended Correspondence Between Contour Line Interval and Data Accuracy

NMAS Equivalent Contour Interval (feet)	NSSDA $RMSE_{(z)}$ (cm)	NSSDA $Accuracy_{(z)}$ (cm)	Reference Data Accuracy Required for "Tested to Meet" (feet)
0.5	0.15 ft or 4.60 cm	0.30 ft or 9.10 cm	0.10
1	0.30 ft or 9.25 cm	0.60 ft or 18.2 cm	0.20
2	0.61 ft or 18.5 cm	1.19 ft or 36.3 cm	0.40
4	1.22 ft or 37.0 cm	2.38 ft or 72.6 cm	0.79
5	1.52 ft or 46.3 cm	2.98 ft or 90.8 cm	0.99
10	3.04 ft or 92.7 cm	5.96 ft or 181.6 cm	1.98

ASPRS recommends that in contracting for lidar data production, the required vertical accuracy should be specified in terms of $Accuracy_{(z)}$ in the third column of the table. That is, production of 1-foot contour lines would require a vertical accuracy of 0.60 foot or 18.2 cm.[20] Most well-controlled lidar data sets should at least meet this standard.

However, it is important to note that vertical error is not evenly distributed within the lidar data set. As described in Section 2.5, vertical error will be lower in flat, open areas and higher in rugged terrain or areas of greater vegetation cover. Consequently, in applications where contour line accuracy is critical, it may be appropriate to require reporting of lidar accuracies separately for different ground cover categories. This would require placement of appropriate survey controls in each ground cover type.

Vendors contacted generally reported procedures that agreed with the ASPRS standards. Vendors reported that they occasionally received requests for 1-foot contour lines. To comply with such requests required, they felt, a point density of at least 2 to 3 points per square meter with 5 to 6 points being better, and with control points distributed through all ground cover types. They further reported that they would not create 1-foot contour lines for steep or very uneven ground surfaces, where horizontal error in the lidar data would result in unacceptable vertical error.

Creation of 1-foot or smaller contour lines is possible with some lidar data sets, but presents special problems and ground survey may be more appropriate. Users of lidar data occasionally specify accuracy sufficient to create 0.5 foot contour lines. At the time of this paper, only a few vendors would undertake work at this accuracy level, which is accomplished by flying at extremely low altitudes with very high point densities the most accurate equipment available.

---

[20] Vertical accuracy, in this case, would be determined using the formula $Accuracy_{(z)} = 1.9800*RMSE_{(z)}$, assuming normally distributed error. See ASPRS Guidelines, p. 3 (ASPRS 2004).

5.6 Implications for Munitions Sites

At military munitions sites, map accuracy standards could be used to assure the successful spatial integration of lidar data with other spatial data such as field surveys, magnetometry and EMI data. However, since earlier map accuracy standards were designed for production of contour lines on paper maps, it would be most appropriate to use a more modern standard such as the NSSDA, with the addition of a specific accuracy threshold such as that adopted by FEMA.

6 Summary and Implication for the Use of Lidar at Munitions Sites

6.1 Lidar in Wide Area Assessment

The ESTCP Wide Area Pilot Program demonstrated that lidar which met its stated accuracy specifications can make a cost-effective contribution to characterizing munitions sites. The use of lidar at the ESTCP demonstration sites provided corrections to the initial conceptual site model at each site investigated, including locations and revised boundaries for munitions response sites (MRSs). At the ESTCP demonstration sites, features with elevation differences under 10 cm were successfully detected, including bombing targets and potential craters. The ESTCP program managers used lidar data to plan the deployment of follow-on technologies, and integrated lidar data with spatial data from all of the other data sources.

6.2 Controlling Lidar Error

Lidar error is discussed in terms of the lidar points, associated use of GPS, and creation of digital models.

6.2.1 Lidar Points

It is important to remember that the objective of the lidar survey is not to detect individual munitions items, but rather to delineate MRSs and to focus the use of follow-on technologies such as magnetometry and EMI. Further, the features being identified, such as potential craters, are larger than individual ordnance items identified by magnetometry and EMI. Consequently, the level of positional error that can be tolerated in lidar points is potentially somewhat higher than those for individual ordnance items, and allows the use, for instance, of DEMs and DTMs with 0.3 – 1.0 m cell sizes. Based on the results at the ESTCP demonstration sites, it appears highly likely that the vendors' standard guaranteed accuracy levels are sufficient for lidar points.

Controlling error of the lidar points is primarily a function of the vendor's quality control methods. With few exceptions, accuracy of the lidar points is best assured by establishing and adhering to appropriate contract specifications as part of the contract for data acquisition. Specifications for horizontal and vertical accuracy, along with those for flightline to flightline integration, can be verified by the vendor as part of its standard quality assurance/quality control report, and can be independently verified by end users.

However, in applications where higher accuracy is required, Government end users may require lower flight elevations and a narrower field of view, at some increase in cost.

6.2.2 GPS

GPS error has implications for the accuracy of the lidar points themselves, and GPS is also used to establish calibration points and locations of features in the field.

Lidar points. As long as GPS error does not exceed assumed values quoted by vendors, the resulting lidar data should be within contracted accuracy specifications. Monitoring GPS quality and other factors affecting positional accuracy should be part of the vendor's daily quality assurance/quality control procedures.

Calibration and quality control. Standard practice in establishing calibration points includes:

- Using survey-grade GPS operated by qualified staff
- Choosing flat sites to minimize the effects of slope between surrounding control point and nearest lidar points
- Choosing open sky sites, which are essential to GPS quality
- Choosing calibration points in all major terrain types

Field investigations. In most field work, resource-grade GPS, with its sub-meter accuracy, should be able to locate munitions-related ground features with sufficient accuracy to compare with the lidar data, as long as open-sky conditions are present. At vegetated sites, resource-grade GPS may not provide positions of sufficient accuracy, and other methods may be necessary. .

6.2.3 Digital Models

In the creation of digital models, vendors and Government end users have several options to assure that DEMs and DTMs best serve the needs of the site investigations:

- Vendors should be required to meet tight calibration standards to minimize elevation differences that may result in over-classification of non-ground points. Optimum point classification methods for munitions sites have not yet been developed; however, the appropriate principle is to retain the largest number of points possible in the ground classification, even at the cost of including some additional surface noise.
- In creating DEMs and DTMs, vendors and Government end users should use the smallest cell size consistent with data density.
- Vendors and end users should consider experimenting with interpolation methods.

In practice, creating DEMs and DTMs is more conveniently accomplished by Government end-users in-house, rather than having the vendor deliver them, since creation in-house can allow for experimentation with alternative methods. However, this requires that Government end-users have sufficient software tools and training to accomplish these tasks. Creating DEMs and DTMs in-house can be challenging, especially with high-density data sets where the number of points is very large. In such cases it may be appropriate to work with sample data sets to determine, in consultation with vendors, the appropriate specifications for these products, and then request that the vendor create and deliver the final products.

7 References

American Society of Photogrammetry and Remote Sensing (ASPRS). 1989. ASPRS Interim Accuracy Standards for Large Scale Maps. July.

———. 2004. ASPRS Guidelines—Vertical Accuracy Reporting for Lidar Data. May 15.

Baltsavias, E.P. Airborne laser scanning: basic relations and formulas. *ISPRS Journal of photogrammetry and Remote Sensing* 54.

Bowen, H. and R.G. Waltermire. 2002. Evaluation of light detection and ranging (lidar) for measuring river corridor topography. *Journal of the American Water Resources Association* 38(1): 33-41.

Clarkin, Tobey. 2007. Modeling Global Navigation Satellite System Positional Error under Forest Canopy based on LIDAR-Derived Canopy Densities. Thesis submitted in partial fulfillment of the requirements for the degree of Master of Science. University of Washington.

Federal Emergency Management Agency (FEMA). 2003. Guidelines and Specifications for Flood Hazard Mapping Partners – Appendix A, Guidance for Aerial Mapping and Surveying.

Federal Geographic Data Committee (FGDC). 1998. Geospatial Positioning Accuracy Standards Part 3: National Standard for Spatial Data Accuracy. FGDC-STD-007.3-1998.

Gerlach, F.L. and A.E. Jasumback. 1989. Global Positioning System Canopy Effects Study. 8971 2234. Missoula, MT: US Department of Agriculture, Forest Service, Missoula Technology and Development Center.

Glennie, Craig. 2007. Rigorous 3D Error Analysis of Kinematic Scanning LIDAR Systems. *Journal of Applied Geodesy,* 1 (2007) 147-157.

Grewal, M.S., L.R. Weill, and A.P. Andrews. 2001. *Global Positioning Systems, Inertial Navigation, and Integration.* John Wiley & Sons, Inc. New York, NY.

Habib, Ayman and Jim Van Rems. 2008. Quality Assurance and Quality Control of LiDAR Systems and Derived Data. American Society of Photogrammetry and Remote Sensing (ASPRS) Lidar Committee, Draft Best Practice documents, April 29, 2008. Available at: http://www.asprs.org/society/committees/lidar/AKAM_LiDAR_Calibration.pdf. Accessed June, 2009.

Hasegawa, H. and T. Yoshimura. 2003. Application of dual-frequency GPS receivers for static surveying under tree canopies. *Journal of Forest Research* 8:103-110.

Hodgson Michael E., John Jensen, George Raber, Jason Tullis, Bruce A. Davis, Gary Thompson, and Karen Schuckman. 2005. An evaluation of lidar-derived elevation and terrain slope in leaf-off conditions. *Photogrammetric Engineering & Remote Sensing* 71(7):817-823.

Hodgson, M.E. and P. Bresnahan. 2004. Accuracy of airborne lidar derived elevation: empirical assessment and error budget. *Photogrammetric Engineering and Remote Sensing*, 70(3): 331-339.

Johnson, C.E. and C.C. Barton. 2004. Where in the world are my field plots? Using GPS effectively in environmental field studies. *Frontiers in Ecology and the Environment* 2(9): 475-482.

Karsky, D., K. Chamberlain, S. Mancebo, D. Patterson and T. Jasumback. 2001. Comparison of GPS Receivers Under a Forest Canopy After Selective Availability Has Been Turned Off. Missoula, MT, USDA Forest Service Technology & Development Program: 1-23.

Key, Hank. 2009. Airborne Lidar Sensors. Professional Surveyor Magazine. May. Accessed at: https://www.profsurv.com/assets/magazines/articles/70254/AirborneLidarSensors.pdf.

Le, A.Q. and C. Tiberius. 2006. Single-frequency precise point positioning with optimal filtering. *GPS Solutions.* D01 (10.1007): s10291-006-0033-9.

Leick, A. 2003. *GPS Satellite Surveying.* John Wiley and Sons, Inc. New York, NY.

Liu, Xiaoye. 2008. Airborne LiDAR for DEM generation: some critical issues. *Progress in Physical Geography* 32(1): 31-49.

Maling, D.H. 1989. *Measurements from Maps*, Pergamon Press, New York, N.Y. section 2.5

Maune, D.F., editor. 2001. *Digital elevation model technologies and applications: the DEM Users Manual.* The American Society for Photogrammetry and Remote Sensing (ASPRS), Bethesda.

Mostyn, David. Data Processing Manager, Terra Remote Sensing, Inc. Phone conversations with Dale Bennet, URS. 2008.

Naesset, E. 2001. Effects of Differential Single- and Dual-Frequency GPS and GLONASS Observations on Point Accuracy under Forest Canopies. *Photogrammetric Engineering & Remote Sensing* 67(9):1021-1026.

Parkinson, B. and J. Spilker. 1996. Global Positioning System: Theory and Applications, Vol. 1. Washington, AIAA.

Piedallu, C. and J.C. Gegout. 2005. Effects of Forest Environment and Survey Protocol on GPS Accuracy. *Photogrammetric Engineering & Remote Sensing* 71(9): 1071-1078.

Rodriguez-Perez, J.R., M.F. Alvarez, E. Sanz, and A. Gavela. 2006. Comparison of GPS Receiver Accuracy and Precision in Forest Environments. *Practical Recommendations Regarding Methods and Receiver Selection.* Shaping the Change, XXIII FIG Congress, Munich, Germany.

Sawaguchi, I., K. Nishida, M. Shishiuchi, and S. Tatsukawa. 2003. Positioning precision and sampling number of DGPS under forest canopies. *Journal of Forest Research* 8:133-137.

Schaer, Philipp, Jan Skaloud, S. Landtwing and Klaus Legat. Accuracy Estimation for Laser Point Cloud Including Scanning Geometry. Presented at: 5th International Symposiaum on Mobile Mapping Technology, Padova (Italy), May 29-31, 2007. Accessed at: infoscience.epfl.ch/record/116146/files/**schaer**_philipp.pdf. Accessed June 2009.

Sky Research, 2009. Review Comments, DRAFT Errors in LiDAR Data: Implications for Investigation of Military Munitions Sites. September 22.

Terrapoint, 2009. Review of DRAFT Errors in Lidar Data: Implications for Investigation of Military Munitions Sites. January 20 and June 23, 2009

Terra Remote Sensing, Inc. 2007. Lidar to Control Point Comparison Report for Kirtland AFB PBR ESTCP Demonstration Site. April 1.

Terra Remote Sensing, Inc. 2009. Review of DRAFT Errors in Lidar Data: Implications for Investigation of Military Munitions Sites. July 3.

URS. 2007. Final Report: High Density LiDAR and Orthophotography in UXO Wide Area Assessment (ESTCP #200534). August.

US Army Corps and Engineers and URS (USACE and URS). 2009. ESTCP White Paper: Effects of LiDAR Point Classification Methods on Surface Model Creation and Feature Identification. Project Number 07 E-MM2-012/ MM-0737. January.

Wikipedia. 2009a. Compass navigation system. Accessed at: http://en.wikipedia.org/wiki/COMPASS_navigation_system.

———. 2009b. Galileo (satellite navigation). Accessed at: http://en.wikipedia.org/wiki/Galileo_positioning_system.

———. 2009c. GLONASS. Accessed at: http://en.wikipedia.org/wiki/GLONASS.

Wing, M.G. and A. Eklund. 2007. Performance Comparison of a Low-Cost Mapping Grade Global Positioning Systems (GPS) Receiver and Consumer Grade GPS Receiver under Dense Forest Canopy. *Journal of Forestry* 105(1):9-14.

Zandbergen, Paul A. 2006. The effect of Cell Resolution on Depressions in Digital Elevation Models. *Applied GIS* 2(1):04.1–04.35.

Attachment A
Formulas for Calculating Horizontal and Vertical Root Mean Square Error

The following formulas are used to compute horizontal and vertical root mean square error (RMSE) and horizontal and vertical accuracy at the 95% confidence level. For example, these formulas are used in reporting accuracy based on the map accuracy standards such as the National Standard for Spatial Data Accuracy (NSSDA), discussed in Section 4.3.

Horizontal Root-Mean-Square Error and Accuracy

$RMSE_x = sqrt[\sum(x_{data\ I} - x_{check\ I})^2/n]$

$RMSE_y = sqrt[\sum(y_{data\ I} - y_{check\ I})^2/n]$

Where:

$X_{data\ I}$, $y_{data\ I}$ are the coordinates of the *Ith* check point in the dataset

$X_{check\ I}$, $y_{check\ I}$ are the x coordinates of the *Ith* check point in the independent source of higher accuracy

n is the number of check points tested

I is an integer ranging from 1 to n

Horizontal error at point I is defined as:

$Sqrt[(x_{data\ I} - x_{check\ I})^2 + (y_{data\ I} - Y_{check\ I})^2$

Horizontal RMSE ($RMSE_r$) is:

$RMSE_r = sqrt[\sum((x_{data\ I} - x_{check\ I})^2 + (y_{data\ I} - y_{check\ I})^2)/n]$

$= sqrt[RMSE_x^2 + RMSE_y^2]$

Computing accuracy according to the NSSDA when $RMSE_x = RMSE_y$

$RMSE_r = sqrt(2 * RMSE_x^2) = sqrt(2 * RMSE_y^2)$

$= 1.4142 * RMSE_x = 1.4142 * RMSE_y$

In the use of these formulas “It is assumed that systematic errors have been eliminated as best as possible. If error is normally distributed and independent in each the x- and y-component and error for the x-component is equal to and independent of error for the y-component, the factor 2.4477 is used to compute horizontal accuracy at the 95% confidence level” (Greenwalt and Schultz 1968). When these conditions apply, horizontal accuracy, $Accuracy_r$, may be computed by the formula:

$Accuracy_r = 2.4477 * RMSE_x = 2.4477 * RMSE_y = 2.4477 * RMSE_r/14142$

$Accuracy_r = 1.7308 * RMSE_r$

Vertical Root-Mean-Square Error and Accuracy

$RMSE_z = sqrt[\sum(z_{data\ I} - z_{check\ I})^2/n]$

Where:

$z_{data\ I}$, is the vertical coordinate of the Ith check point in the dataset

$z_{check\ I}$, is the vertical coordinates of the Ith check point in the independent source of higher accuracy

N is the number of points being checked

I is an integer ranging from 1 to n

As with horizontal accuracy, "It is assumed that systematic errors have been eliminated as best as possible. If vertical error is normally distributed, the factor 1.9600 is applied to compute linear error at the 95% confidence level" (Greenwalt and Schultz 1968). Therefore, vertical accuracy, $Accuracy_z$, reported according to the NSSDA shall be computed by the following formula:

$Accuracy_z = 1.9600 * RMSE_z$

Reference

Greenwalt, C.R. and M.E. Schultz. 1968. Principles and Error Theory and Cartographic Applications. *ACIC Technical Report* No. 96. St. Louis, Mo. Aeronautical Chart and Information Center, U.S. Air Force.

APPENDIX C
ESTCP WHITE PAPER: EFFECTS OF LIDAR POINT CLASSIFICATION METHODS ON SURFACE MODEL CREATION AND FEATURE IDENTIFICATION

ESTCP White Paper

Effects of Lidar Point Classification Methods on Surface Model Creation and Feature Identification

Project Number 07 E-MM2-012/MM-0737

Final

January 2010

Table of Contents

Figures

Tables

Acronyms

AFB	Air Force Base
CAD	computer-aided drafting
cm	centimeters
CSM	conceptual site model
DBT	Demolition Bombing Target
DEM	digital elevation model
DoD	Department of Defense
DTM	digital terrain model
ESTCP	Environmental Security Technology Certification Program
GPS	global positioning system
IMU	inertial measurement unit
INS	inertial navigation system
kHz	kilohertz
lidar	light detection and ranging
m	meters
MEC	munitions and explosives of concern
MRS	munitions response site
PBR	Precision Bombing Range
PDOP	position dilution of precision
pts/m^2	points per square meter
QC	quality control
TIN	triangulated irregular network
UXO	unexploded ordnance
WAA	wide area assessment

Acknowledgements

This project was made possible through funding provided by the Environmental Security Technology Certification Program. For their support and guidance to the US Army Corps of Engineers and URS on this project, we would like to express our sincere appreciation to:

- Dr. Jeffrey Marqusee, Director, Environmental Security Technology Certification Program and Strategic Environmental Research and Development Program
- Dr. Anne Andrews, Deputy Director, Environmental Security Technology Certification Program and Strategic Environmental Research and Development Program
- Dr. Herb Nelson, Munitions Management Program Manager, Environmental Security Technology Certification Program and Strategic Environmental Research and Development Program

We gratefully acknowledge the following for their technical review of this paper:

- Terra Remote Sensing, Inc., especially Dave Neufeldt and Dave Mostyn
- Sky Research, especially Joy Rogalla and Tom Prescott
- Terrapoint, LLC, especially Kresimir Kusevic, Peggy Cobb, Claude Vickers, and DJ Lehto
- Karen Shuckman, URS and Instructor, Pennsylvania State University
- Bob Ryan, URS, formerly with Fugro EarthData

1 Introduction and Summary of Key Findings

1.1 Introduction

Many millions of acres of Department of Defense (DoD) lands are potentially contaminated with military munitions or their components. On the majority of these sites, munitions are concentrated in specific ranges and training areas. Locating the site of contamination can be difficult, in part because historical records are often incomplete or inaccurate.

Between 2005 and 2007, the Environmental Security Technology Certification Program (ESTCP) conducted a pilot program to test the effectiveness of a multi-technology approach to unexploded ordnance/munitions and explosives of concern (UXO/MEC) wide area assessment (WAA). The program included the use of light detection and ranging (lidar), orthophotography, helicopter magnetometry, towed-array magnetometry, and statistically-based transect design, in a comprehensive, sequential approach. The first phase of this program was carried out at three desert sites containing little or no vegetation and few non-military land uses. Subsequently, a second phase of the pilot program was added, including two new sites: the Former Camp Beale site near Marysville, California, and the Toussaint River site near Lake Erie. The Former Camp Beale site has more varied vegetation cover and land use types; the Toussaint River site is a shallow-water site.

This white paper is a follow-up to the investigation of the ESTCP demonstration sites where lidar data was collected. At these sites, lidar met the objectives of the demonstration:

- Lidar was used to identify munitions response sites (MRS) such as bombing targets, berms, and firing points
- The results of the lidar investigation were used to supplement or correct the initial conceptual site model (CSM) based on historical records review
- Lidar data provided useful input to subsequent phases of site investigation, including information on slope and vegetation cover

Further examination of the lidar data for the ESTCP demonstration sites showed that there may be potential to improve the resolution of the lidar surface models by improving the way lidar returns are classified. An important part of the use of lidar is the classification of laser signals as returning from ground or non-ground surfaces. At all of the ESTCP sites where lidar was used, some of the lidar points classified as returning from non-ground surfaces appeared to be returns from ground. If classification could be modified to include more of these points in the ground surface model, the ground surface could be portrayed with higher resolution, and the ability to detect small features could be increased.

A preliminary draft of this paper presented the results of re-analysis of the lidar data for the Former Camp Beale demonstration site. Following review by ESTCP of the methodology used, data from six additional sites were analyzed, and results are presented in this draft.

1.2 Objectives

This white paper examines the methodologies in use for classification of laser returns, the possibility that some laser returns are being incorrectly classified as non-ground, and potential benefits of including more of the lidar points in the digital elevation model (DEM) representing

the ground surface. The findings and conclusions of this paper are intended to contribute to contract specifications and analysis methods that can be used by Government site managers who are planning to use lidar.

Key questions examined include:

- How do lidar vendors distinguish reflections from the ground or other objects such as vegetation?
- What point classification results were achieved at the ESTCP demonstration sites?
- Would different classification methods improve the resulting surface models and lidar feature detection?
- If so, how great is the difference and how much extra effort is required?

1.3 Summary of Key Findings

At the ESTCP demonstration sites, a significant number of laser returns from the ground surface appear to have been classified as non-ground. Visual examination showed that some returns from paved surfaces were classified as non-ground. Samples from a total of 11 data sets from the four sites where lidar was collected showed that from 15 to over 95 percent of the ground returns may have been classified as non-ground depending on the sample area examined.

The phenomenon of laser returns from the ground being classified as non-ground appears to result from the operation of the standard TerraSolid software used for point classification, especially as it interacts with small elevation differences between lidar points. The TerraSolid software uses a sophisticated set of automated algorithms for classifying laser returns. An initial surface model is first created using the lowest points in the data set, after which points are added iteratively if they meet pre-set parameters intended to prevent the addition of points that form “spikes” characteristic of vegetation or buildings. An important parameter in this process is the angle between each new point examined and the nearest already-included point.

Point classification results can be influenced by increasing either the spatial discrepancies between the lidar points, as when flight lines are not tightly calibrated, or by increasing the density of lidar returns. When the density of lidar returns increases, the laser returns are closer together and the angle formed by any new point will be larger, even when the new point is only slightly above the already-modeled surface. When laser returns are sufficiently close, this increase in angle can be large enough that very small elevation variations, within the noise level of the equipment, can cause points to be classified as non-ground.

In most lidar surveys, classifying numerous points as non-ground is acceptable and even desirable. This is because the resulting ground surface will be smoother and points will be misclassified only in areas where the overall density is higher than needed to generally characterize the ground surface. However, this method may not be appropriate where the objective of the survey is to detect small objects.

For the six sites and 11 lidar data sets examined, the percentage of laser returns classified by the vendor as non-ground was calculated for a series of test areas. Where possible, test areas were located on paved surfaces where all “non-ground” classifications could be assumed to be artifacts of the classification process. On sites with no paved surfaces, test areas were placed in areas of sparse and uniform vegetation.

At the four ESTCP sites (nine data sets), the percentage of laser returns classified as non-ground ranged from approximately 15 percent to over 95 percent. For all but one of the data sets, the rate at which points were classified as non-ground increased very closely with increasing overall density of lidar points, and visual inspection showed that points were classified as non-ground at much greater rates in areas of flight line overlap. Further, the operation of the classification software held the density of ground returns to a maximum of around 2.5 points per square meter (pts/m^2), regardless of the overall point density (which ranged as high as 41 pts/m^2).

At the two non-ESTCP sites (two data sets), the overall data density was lower than for the ESTCP sites (between 0.78 and 1.55 pts/m^2 compared to between 1.69 and 41.50 pts/m^2 for the test areas at the ESTCP sites). Both non-ESTCP test areas included paved roads, and examination of the data showed that the rate of classification as non-ground on road surfaces was much lower than for the ESTCP sites, between 3.34 and 15.36 percent. The lower rate of misclassification may be a result of the overall lower point density which resulted in greater distances between the laser returns. However, some laser returns from paved surfaces were still classified as non-ground, and the mechanism appeared to be the same as at the ESTCP sites.

Classification errors of this kind can be partially eliminated by lowering the degree of spatial displacement in the laser returns, both between one point and the next and between one flight line and the next. Vendors contacted commented that the primary emphasis in reducing the amount of spatial displacement should be to achieve the best possible calibration of the data set, especially from one flight line and the next. However, some degree of displacement is inevitable due to site conditions and instrument accuracy limitations, and local areas of high density can occur for other reasons than flight line overlap. Lidar surveys aimed at detecting small surface features should therefore also consider adjustments to the classification methods used.

The TerraSolid software includes numerous settings that can be varied at will to increase the number of points classified as ground. Modification of these settings should not result in increased time or effort. Potential modifications range from specific changes to individual classification parameters to bulk classification of all laser returns within a given distance of the original modeled surface as ground. Classification could be modified either to directly classify more points as ground returns or to establish a new classification for “low” lidar points in addition to the vendor’s original ground classification.

Notwithstanding the relative ease of changing the classification parameters, a change of classification is valuable only if it results in enhanced feature detection. A test reclassification was performed, using a series of 59 test areas at the Former Camp Beale site. New surface models were created using all laser returns within 0.4 meters (m) of the ground surface. This value was chosen as a means to include the maximum number of additional points for an initial determination of increased ability to reveal features, with the understanding that both low vegetation and noise also would be included. The test areas all included ground features visible in the initial surface model based on the vendor’s classifications, typically large depressions. All but three of these features were under partial or full tree cover.

The surface models from the vendor’s classification were compared to those using the reclassified points. At 21 of the test areas (36 percent), the new surface models showed additional potential features. These features were all small and poorly-defined, and most could not be conclusively identified. However, these additional potential features did indicate areas

for further investigation. The larger features in the surfaces created with the reclassified points also were somewhat better defined in the reclassified surfaces.

As a second test, the size of the grid cells in the surface models for nine test areas was changed from 1 m to 0.3 m (1 foot), using both the vendor's original classifications and the reclassified points. The smaller grid cells yielded a more sharply-defined ground surface. The reclassified surfaces showed additional small features in a manner similar but not identical to the 1 m cell sizes, with the smaller cell sizes showing more additional features.

As a third test, new surfaces were created using a different approach to surface model creation. At all of the ESTCP demonstration sites, surface models were created by first creating a Triangulated Irregular Network (TIN) using every laser return as the vertex of the triangles. Surface models were then created from the TINs. This method was chosen since it uses every available laser return to create the initial model from which the surfaces are derived. The alternative to this method is to use one of several methods to mathematically interpolate surfaces directly from the points. Interpolated surfaces were created for three test areas, using both 1 m and 0.3 m cell sizes. At two of the three test areas, the interpolated surfaces showed more features than the TIN-derived surfaces. The reason for this difference is not clear, and further investigation would be warranted.

Finally, the 1.5 m and 0.3 m test craters at the Former Camp Beale site were examined, using the models created from the vendor-classified points and the reclassified points. Since the test craters were located in an area with no tall vegetation, the reclassified points included all of the lidar points. The more dense data showed the test craters more clearly, and included additional noise. However, no new features were visible using the full data set, and in neither case were the smallest (0.30 m) test craters seen.

These findings lead to the following recommendations for subsequent use of lidar at munitions sites:

- Lidar remains a useful tool in WAA, and should be included where appropriate to the site.
- Vendors should be asked to describe potential point classification approaches prior to each survey, and should be requested to adjust classification parameters depending on the objectives of the survey.
- Vendors should be required to deliver the full lidar data set, including all points classified as non-ground returns, to the Government. If all points are delivered, Government land managers can evaluate the classification methods used and can experiment with other approaches to classification as warranted.
- Government land managers may consider requesting an additional classification from the vendor, including more potential ground returns. This would allow the vendor's initial classifications to be used for applications where achieving a smooth ground surface was more important (such as creating contour lines), while using the "enhanced" classifications for investigation of munitions-related features.

2 Overview of Lidar Data Processing Steps

This section outlines the components of the lidar data collection system and the steps through which the original sensor output is converted to lidar x, y, z locations. This information is not intended to be comprehensive, and is included as background to the discussion of point classification methods. This section is based on published research, user manuals for standard software packages, and interviews with vendors.

2.1 Collecting Lidar Data and Creating Lidar Points

2.1.1 Sensor Components

In order to establish the location from which the laser signal is reflected, the lidar system must answer two basic questions: 1) where is the aircraft located and 2) what is the distance and angle to the point of reflection of the laser pulse?

Locating the aircraft. The position of the aircraft is determined using the Global Positioning System (GPS) and Inertial Navigation System (INS).

- The GPS samples the aircraft location at regular intervals (one to ten times per second), based on received signals from a minimum of four orbiting navigation satellites. GPS position inaccuracies are due to errors in calculating the exact time, the ranges to the individual satellites and noise. The standard method to limit the effects of correlated errors (e.g., propagation delays that will be similar for reasonably close points) in the GPS signal is to establish an independent static GPS base station at a known location to provide error correction information. If sufficiently close, the reference station (static) will experience the same propagation and timing errors as the GPS on board the aircraft (kinematic). Because the reference is fixed and its location is known, correlated GPS errors can be isolated from the signal, a solution developed, and the solution applied to kinematic GPS data in post processing to help refine the position of the aircraft. (Sky Research 2009)
- The INS calculates the position of the aircraft between GPS locations. The primary input to the INS is from the Inertial Measurement Unit (IMU). The IMU works by detecting the changes to rates of acceleration, along with rotational attributes such as pitch, roll, and yaw. The IMU generally contains three accelerometers and three gyroscopes, each placed in orthogonal positions so that data is collected in all three planes. Current IMUs record these changes at 200 hertz (Hz) (200 samples per second). The IMU adds a small error component in each plane. This error results from the accumulation of small errors as positions are continually re-calculated. These small errors accumulate until the aircraft's position is updated from the GPS.

Locating the laser pulse. Lidar systems measure the time of return of a laser pulse. The laser system consists of a laser, a receiver, and a mirror that directs each pulse toward the ground surface. Lidar systems typically use lasers with wavelengths of 1,000 to 1,500 nanometers. Pulses are directed to the ground by a mirror system, which may be rotating or oscillating, depending on the manufacturer.

The receiver is a passive device that is tuned to the frequency of the laser, which records a signal when the amplitude of light in that frequency exceeds a threshold value. The sensor also records the energy level of the return, which is referred to as its intensity value. The threshold energy value that will trigger a return is typically set by the manufacturer and is not adjustable.

The sensor can record multiple returns from each laser pulse. In vegetated conditions, part of the laser return may be reflected from branches and other sub-canopy features, leaving the remainder of the signal to be reflected from the ground surface. The limitation of the multi-return capability is that there must be sufficient time between returns for the sensor to reset. This time is generally between three and 20 nanoseconds depending on the sensor used, a distance of between 0.5 m and 3 m. Thus, multiple returns cannot be recorded in low vegetation.

A relatively recent development in laser technology is the analog or “full wave form” laser receiver. In contrast to the approach described above, the analog receiver records a continuous level of energy values once the amplitude passes the threshold value. The shape of this energy return curve can be analyzed and multiple return values derived in a more interactive manner. Analog receivers create larger data sets than traditional sensors, and more advanced software is needed to process the output. Analog sensors are typically used for analysis of vegetation rather than modeling the ground surface and appear to offer little advantage at munitions sites.

The final components of the sensor system are the power source, the hardware- and software-based control system, and the data storage equipment (consisting of multiple high-speed hard drives).

2.1.2 System Settings

The lidar system has some parameters that can be varied, all within the equipment specifications of each manufacturer. These inSclude:

- ***Power level.*** The power of each laser pulse is adjustable up to the maximum power of the system.
- ***Pulse rate.*** The maximum pulse rate, or the number of laser signals per second, has increased steadily as the technology has evolved, from four to 10 kHz in the mid-1990s to as much as 250 kHz at the time of this report. Pulse rates are typically adjustable.
- ***Mirror speed.*** The oscillation or rotation speed of the mirror is adjustable independently of the laser pulse rate.
- ***Scan angle.*** The maximum scan angle of the mirror off nadir is adjustable. In combination with the aircraft altitude, the scan angle controls the width of the data collection swath.

Vendors report that the primary parameters that are varied are pulse rate and scan angle.

Flight altitude and air speed determine the average along-track point spacing, while scan and flight altitude determine the average across-track point spacing.

The relationship of laser pulse rate to system performance is not always straightforward. This is because the power system of the laser is finite, and as a result, as the pulse rate is increased, each individual laser pulse will necessarily have less power. It is possible to design a combination of flight altitude and pulse rate that will cause the return signal to be too weak to trigger the receiver and record a return. This limitation is especially notable in vegetated

conditions, where the success of the survey will depend on recording multiple returns. Multiple returns have less power since they reflect only part of the laser pulse. In practice, vendors will adjust power levels, pulse rates, and fight altitude to maximize the performance of the system. Numerous low-intensity returns or failing to get returns over less reflective surfaces such as blacktop during data collection may indicate that power should be increased, altitude lowered, or pulse rate reduced.

2.1.3 Sensor Output

The output of the sensor system is a series of data values recorded by the GPS, INS, mirror system, and receiver. These data values record the action of each of these components, each with a time record. The GPS and INS records allow the calculation of aircraft location, the mirror system records the angle of each laser pulse, and the receiver records the time and intensity of each return. Timestamps for each record allow the data to be assembled and the x, y, and z locations that become the lidar points created.

2.1.4 Calibration and Data Validation

Calibration. System calibration begins just prior to the data collection flights. Test flights are conducted over calibration features with known dimensions. Flights are conducted at several headings. On return to the office, the results of these test fights are used to establish correction values for pitch, roll, and yaw so that the features remain constant at all headings. In a well-calibrated data set, the average vertical offset between overlapping flight lines should be at or near the inherent noise level of the data, typically around 3-4 cm at one sigma (Sky Research, 2009).

Data validation. During the mission, a set of surveyed validation points is established on the ground within the data collection area. These points are used in post processing to vertically adjust the laser data to known ground heights. Establishing a higher number of control points will in most cases increase accuracy.

As one indicator of overall data quality, the variance of the laser data is calculated by comparing the height from a set of individual validation points with the height of the nearest laser return. In some cases, a high degree of variance may be an indicator of poor data processing. Terrain setting, quality of ground survey points, location of ground survey targets (flat ground vs. uneven ground), and density of the laser data points are all factors that may affect this value as well. It is therefore important that great care be taken when collecting data for validation points and that the location of these points be chosen carefully (Sky Research, 2009).

The number of surveyed points collected varies considerably between vendors and there appears to be no industry standard. Some vendors establish three to four static survey points; others supplement static points with vehicle-mounted GPS surveys on roads in the study area; others use remote-controlled rovers to establish up to many hundreds of static survey points.

On return to the office, the lidar data is compared to the surveyed points to validate the lidar data values by comparing the height of the surveyed points with the height of the nearest laser return. Sources of vertical error in the laser data include changes in atmospheric conditions, residual GPS errors, noise inherent to the apparatus, and calibration. The lidar data can be adjusted to achieve a “best fit” to the control points; some vendors commented that failure to do so may result in vertical accuracy errors of up to 0.5 meter (Sky Research, 2009).

A high degree of variance between lidar data and survey points may indicate poor data calibration. If calibration values are incorrectly established, the lidar values and the surveyed values will not match. If the lidar data is not consistent throughout the site, the pitch, roll, and yaw values would then be examined and recalculated, or other potential sources of error examined. However, terrain setting, quality of ground survey points, location of ground survey targets (flat ground vs. uneven ground), and density of the laser data points are all factors that may affect this value as well. It is therefore important that validation points be located carefully, preferably on smooth, flat areas where terrain variation will not affect the comparison between lidar elevations and validation point elevations.

2.1.5 Exporting the Lidar Values

Once the data are calibrated and validated, x, y, z values can be exported to various formats that can be read by GIS, computer-aided drafting (CAD), or geophysical programs. Export can take place before or after classification, and can include any of the data collected with the return, such as the GPS time, intensity, scan angle, and flight line number (if this is recorded).

2.2 Classifying the Lidar Points

2.2.1 The Problem: Distinguishing Ground Returns from Non-Ground Returns

In all lidar investigations, an important task is to distinguish laser pulses that return from the ground from those that return from vegetation, buildings, or other objects. This task is carried out through the use of automated algorithms followed by inspection and editing by skilled operators.

This problem is most difficult in the case of lidar points close to the ground surface. Identification of returns from trees is relatively straightforward, but low brush and grass are more difficult, and results depend more on operator experience and judgment. Orthophoto images provide an important cross-verification resource for the operator in these cases.

At the lower detection limit of the technology, it can become very difficult to distinguish laser returns from an uneven ground surface from those from low brush or grass. The problem of point classification on uneven ground surfaces has been observed for many years, as shown in Figure 1.

Figure 1: Lidar Point Classification on Forest Roads

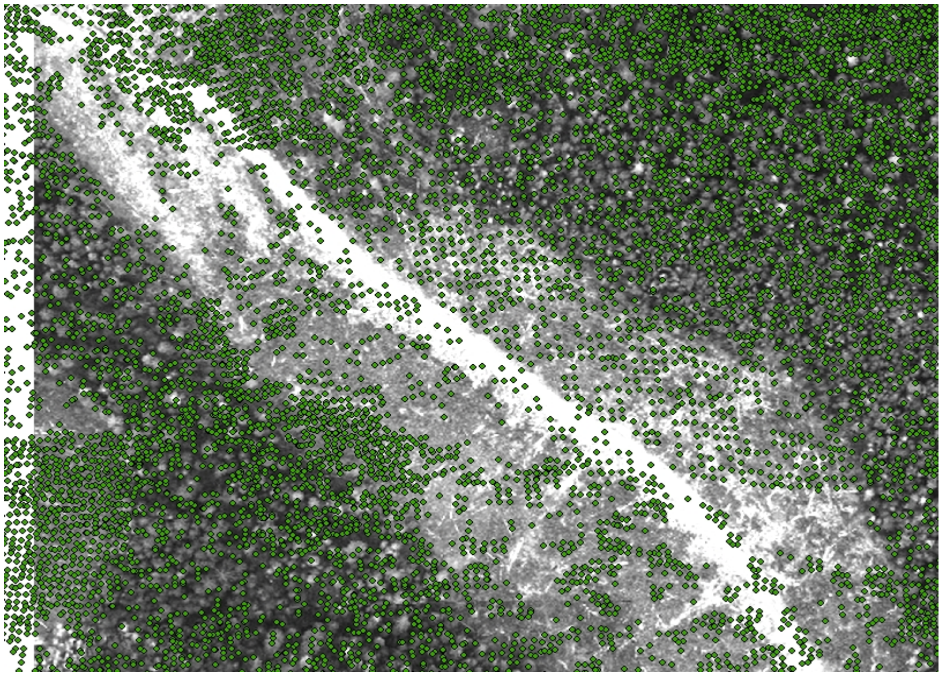

Lidar data collected in 2001 in a forest and timber harvest area in southeast Alaska. Green points, classified as non-ground returns, can be seen on the surface of the forest road where the photo shows no vegetation. It is difficult to determine whether these "non-ground" returns are artifacts of the classification process or result from the uneven surface of the dirt road.

2.2.2 Overview of Potential Classification Approaches

Prior to the early 2000s, vendors typically developed proprietary custom software for point classification, based on a variety of different approaches. These approaches varied in their success, and the development of faster laser sensors that produced higher data densities occasionally led to unexpected negative results, as shown in Figure 2.

Figure 2: Early Lidar Point Classification Errors, Alaska

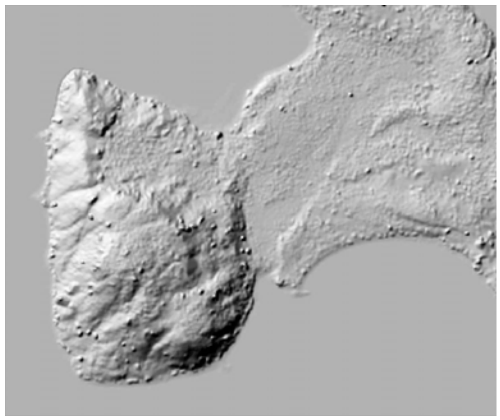

Lidar data collected in 2001 in a southeast Alaska forest. This was the first data collection flight by a new 20kHz sensor system, considered very high-speed at the time, which had replaced a 4kHz system. The DEM shows the output of the automated classification algorithm developed for the earlier, slower system. The DEM shows numerous “spikes” caused by reflections from trees not removed by the automated algorithm.

Because lidar vendors developed proprietary classification algorithms, there is little published literature available about the methods used. The small amount of published material outlines the following general approaches:

- ***Block-minimum algorithm.*** In theory, the ground returns should be the lowest points in a lidar data set. This observation suggests the use of a block-minimum function to separate ground from non-ground returns. The algorithm would establish a block size and separate the lowest points in that block as potential ground returns. The algorithm could be adjusted along various parameters such as block size and establishment of specified elevations above the initial surface within which points would be classified as ground returns. Implementation of block minimum functions have been described by Kilan et al. (1996), and Hansen and Vögtle (1999). Haugerud and Harding (2001) observed that proprietary algorithms then in use by some North American lidar vendors appeared to be block-minimum algorithms.
- ***Iterative Differential algorithm.*** Anderson, Reutebuch and McGaughey (Anderson, et.al. 2006) modified a method described by Kraus and Pfeifer (1998). This is an iterative method that begins by computing an initial surface model using the average elevation of all returns within a 1 m x 1 m grid cell. This initial surface model is computed using all returns from both vegetation and ground. For each iteration, difference values are computed as the difference between the return elevation and the modeled elevation at that point. Ground

returns are more likely to be below the modeled surface, and thus have negative differences. Vegetation returns are more likely to have small negative or positive differences. These residual values are used to compute weights for each return using a weight function. Cells with no ground returns are flagged as holes in the intermediate surface and filled through interpolation from surrounding cells. Each iteration results in a new intermediate surface model. The authors reported that five iterations were sufficient to remove vegetation while preserving laser returns that defined ground features, while additional iterations began to remove ground features. These authors performed an additional final step of adding all points within 15 centimeters (cm) of the intermediate surface to the values used to interpolate the final ground surface model. This method was also described by Kraus and Pfeifer (2001).

- ***No-multiple return algorithm.*** The absence of multiple returns suggests that the laser signal has reached the ground surface, at least locally. A potential approach would be to require that there be no multiple returns within a specified contiguous area. Haugerud and Harding (2001) tested an algorithm of this type and found that it rarely misidentified bare-earth reflections as tree canopy and did not falsely reject points within large bare-earth areas. However, this algorithm does not provide information about the ground surface beneath the tree canopy, since there will seldom be a large enough contiguous area with no multiple returns to give meaningful results.
- ***De-spike algorithm.*** A de-spike algorithm proceeds from the observation that a ground surface should be relatively smooth compared to non-ground objects such as trees or buildings. The algorithm searches for points that define local areas of strong ground curvature, and removes them iteratively until a smooth ground surface is left. Haugerud and Harding (2001) tested a de-spike algorithm using data from a large lidar survey in Washington state, and this algorithm was later adopted by the lidar vendor engaged in the survey. The de-spike algorithm was found to create surfaces that look realistic and to match reality where surveyed ground control existed. The algorithm retained a larger number of points than the block-minimum algorithms tested, and appeared to retain more points than commercial block-minimum algorithms. The algorithm removed small buildings and most bridges, but did not remove large, low buildings which created large flat surfaces. Haugerud and Harding reported several disadvantages of the de-spike algorithm, including long computation times[1], removal of some points at the intersection of surfaces such as the toe of highway cuts, and sensitivity to negative blunders in the lidar data.[2]

---

[1] Possibly due to its implementation in ArcGIS.

2 Haugerud and Harding observed (as have others) that many lidar surveys contain a few points that are dramatically lower than their surroundings and clearly not reflected from actual ground features. If these blunders are not removed, they appear in the surface model as conical pits in the ground surface. Positive blunders are also observed, possibly resulting from laser returns from birds or aerosols in the atmosphere. These appear as very tall “spikes” and would be removed by a de-spike algorithm.

2.2.3 Current Classification Methods and Software

Beginning in the early 2000s, most vendors began to use the same suite of software applications for processing lidar data, including point classification. This set of programs is produced by the Finnish company TerraSolid[3], and is implemented as an add-on to Bentley Microstation, a commonly-used CAD program. Some of the more important modules in the TerraSolid software suite include:

- ***TerraScan:*** Used to import the sensor output, create data points, and classify data points (Soininen 2005). The TerraScan Viewer is also available, with a more limited set of tools for viewing and modeling lidar points.
- ***TerraModeler:*** Used to validate laser points and create surface models that are used to create contours, elevation models, profiles and cross sections, volumes, etc.
- ***TerraMatch:*** Used to resolve survey parameters and correct for roll, pitch, heading, and elevation changes between flight lines.
- ***TerraSurvey:*** Used to import survey data, display profiles, and perform data quality control (QC) functions.
- ***TerraPhoto:*** Used to process and rectify digital images to create orthophotos, including using lidar data as part of the rectification process.

TerraScan, the module used for point classification, uses a sophisticated de-spike approach, with a variety of adjustable parameters. The initial classification takes place in two steps:

- ***Selecting low points.*** This step creates a temporary ground surface using the lowest points in the data set. Each point in the data set is examined, and its elevation is compared to all other points within a specified horizontal distance. The lowest point is classified as ground. The routine can also search for groups of low points rather than single points. This step includes routines to eliminate isolated negative or positive blunders[4].
- ***Adding points to the ground surface model.*** This step classifies ground returns by iteratively adding points to the initial temporary ground surface. The routine starts by using the low points selected in the first step to create a triangulated surface model, with the vertices of the triangles at the modeled ground surface. Because these are the lowest points in the data set, the remaining points are all higher than this initial ground surface. The model iteratively adds a new laser point to the triangulated model.

Four parameters influence the results of point classification:

- ***Maximum building size.*** This parameter sets the largest area in which the program will select an initial low point. If the setting is too small, low points will be established on large flat surfaces such as building roofs. If the setting is too

---

[3] See: http://www.terrasolid.fi/en/products

[4] At approximately the time TerraScan became the most popular lidar processing software, negative and positive blunders largely stopped appearing in the lidar data delivered from vendors.

large, natural features such as small hills, stream channels, or ditches will be missed.

- ***Iteration Angle.*** This parameter sets the maximum angle from the nearest point already in the ground surface model. A low value is more appropriate for flatter sites with gradually changing topography, while a higher maximum angle would be appropriate for steeper or more rugged terrain.
- ***Iteration distance***. This parameter sets the maximum value for the height of a potential point above the existing ground surface model. As with iteration angle, low values are more appropriate for flatter sites and higher values are more appropriate for steeper sites.
- ***Terrain angle***. Defines the "steepest allowed slope in ground terrain". The terrain angle is especially important in the "first-cut" or the first routine used to delineate the ground model, which all other ground classification routines will use as their reference. If this value is set too low, subsequent routines will stand little chance of correctly classifying ground in steep terrain. If set too high, vegetation may erroneously be classified as ground. The terrain angle should be selected to match the unique conditions present in each terrain model.

Final editing by the operator is used to correct for errors that remain following the automated process. The overall process is shown in Figure 3.

Figure 3: Lidar Point Classification Process

	Real-world ground, shrubs, trees, buildings and power lines.
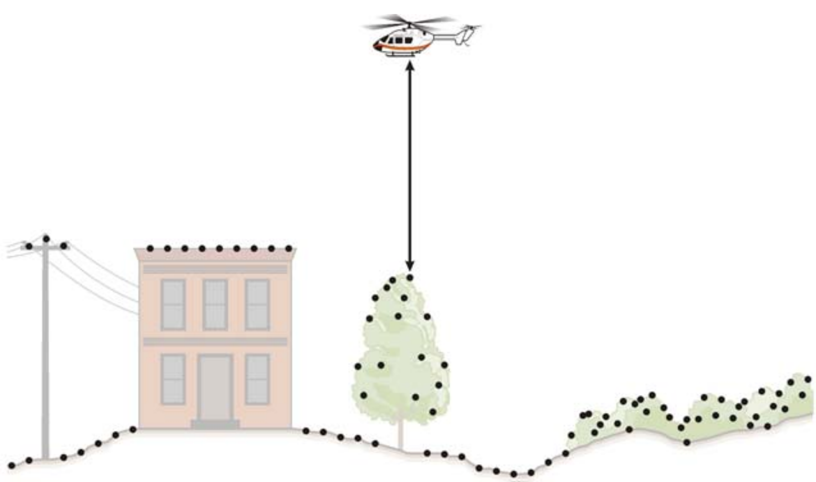	Laser reflections are returned from all of these surfaces. Use of the data requires classification as ground- or non-ground returns.

Figure 3: Lidar Point Classification Process (continued)

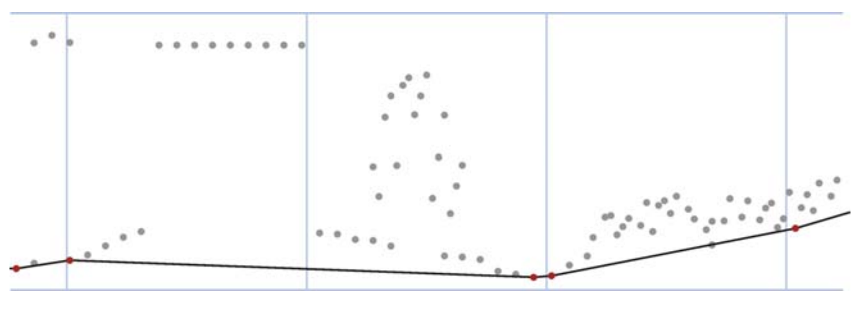	The first classification steps in TerraSolid are to: • Establish maximum building size (blue lines). • Identify initial low points (red points) for each area. • Using the initial low points, create the initial ground surface model.
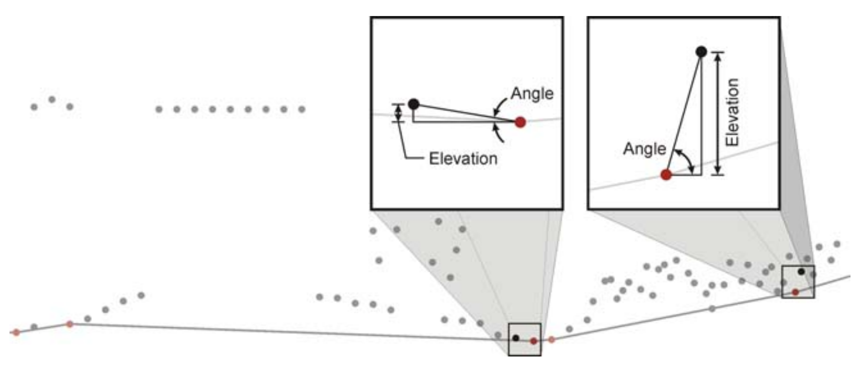	The next step is to evaluate each remaining point for addition. Evaluation is based on the elevation above the existing surface model and the angle with the closest already-accepted point. In this sketch, the point on the left would be classified as ground and the point on the right as non-ground.
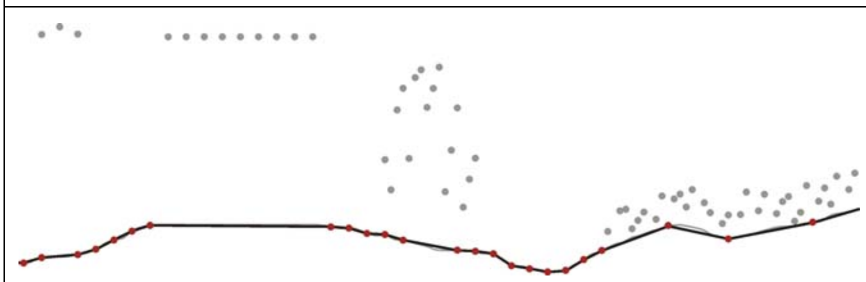	The final ground classifications are used to create the DEM representing the modeled ground surface. When done well, the modeled surface closely corresponds to the actual ground conditions.

TerraSolid's automated algorithms will classify points with varying degrees of success, depending on the fit between the parameter settings and the terrain type being surveyed. No one combination of parameter settings will be optimum for all sites or even all parts of the same site. Frequently, the operator will divide the site into a series of terrain types, each with somewhat different settings. The labor tradeoff between subsequent hand editing and establishing additional terrain types is a function of operator experience. As many clients prefer to see a "smooth" ground surface, most vendors by default tailor the parameter settings for each terrain type so that the resulting ground is a smooth as possible while still conforming to the project's accuracy and density specifications.

Several approaches would permit larger numbers of points to be classified as ground, including establishing different iteration elevations or angles. TerraSolid also will permit bulk classification of all points within a given elevation of the initial surface as ground, regardless of iteration angle. All of these approaches would result in a more detailed ground surface, although such approaches could also include additional roughness from system noise, variations in the ground surface, and low vegetation.

A classification scheme that resulted in more ground points could be produced either in place of or in addition to the vendor's initial classification approach. Establishing an additional classification cateogory ("near ground" in addition to "ground" "non-ground") would allow Government land managers to use the initial classifications in those applications where a smoother ground surface was desirable, such as for creating contour lines, while allowing for creation of more detailed surface models for studies of potential munitions-related features, where the addition of some additional surface roughness could be acceptable.

3 Point Classification Results at Six Sites

This section describes the results of lidar point classification at the four ESTCP sites where lidar data was collected, along with two non-ESTCP sites. Since more than one lidar flight was conducted at some ESTCP sites, a total of 11 lidar data sets were examined. The objectives of this section are to determine the percentage of lidar points that were classified as non-ground returns, and the processes that account for the classification results.

3.1 Results – Former Camp Beale Demonstration Site

The Former Camp Beale site is located near Marysville, California. Data was acquired as part of the ESTCP WAA Pilot Program in July 2006. Lidar was collected and processed by Terra Remote Sensing, Inc.

3.1.1 Lidar Point Patterns

Lidar is collected in a series of overlapping flight lines. The amount of flight line overlap is determined by project requirements and flight conditions. All of the three vendors contacted plan for a minimum overlap of 15 to 50 percent, but in practice, overlap may vary considerably during the survey based on flight conditions (Figure 4).

Figure 4: Flight Line Overlap

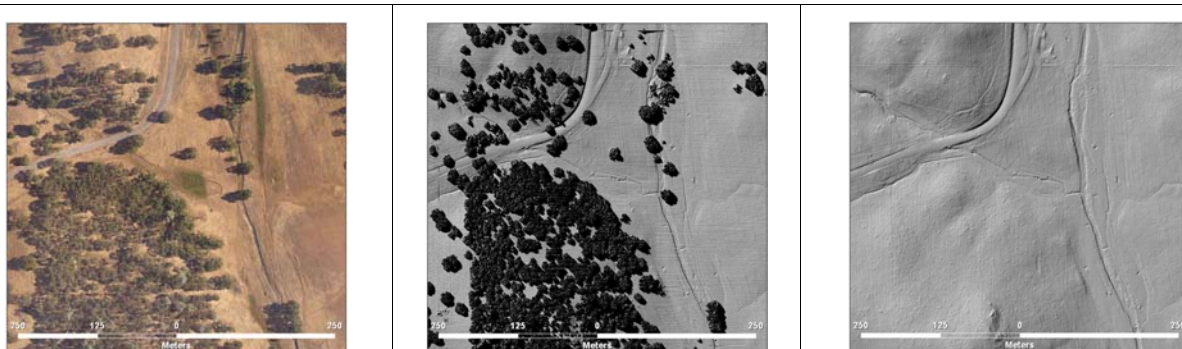

Example area. Images show orthophoto, digital terrain model (DTM) created from all lidar points, and DEM created from ground points only.

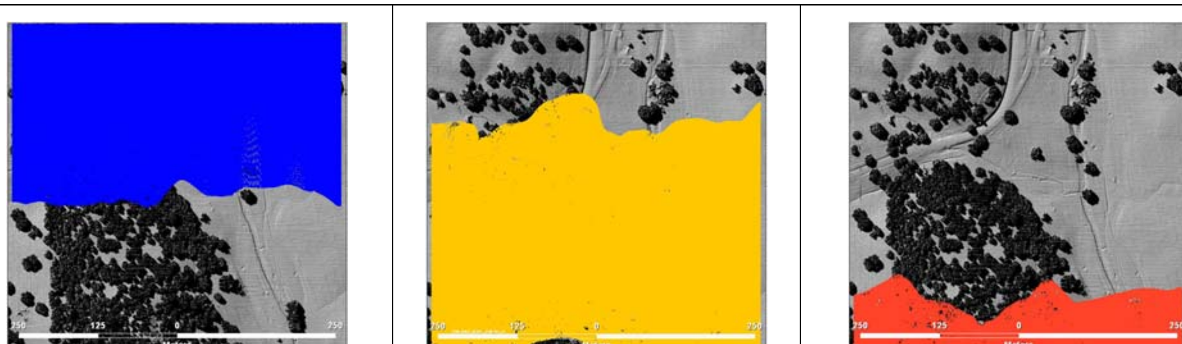

Lidar points from overlapping flight lines. The aircraft traveled east - west. The impact of wind conditions can be seen at the edges of the flight lines.

As the mirror sweeps back and forth, lidar points fall in roughly parallel lines, perpendicular to the direction of the flight line (Figure 5).

Figure 5: Lidar Point Patterns

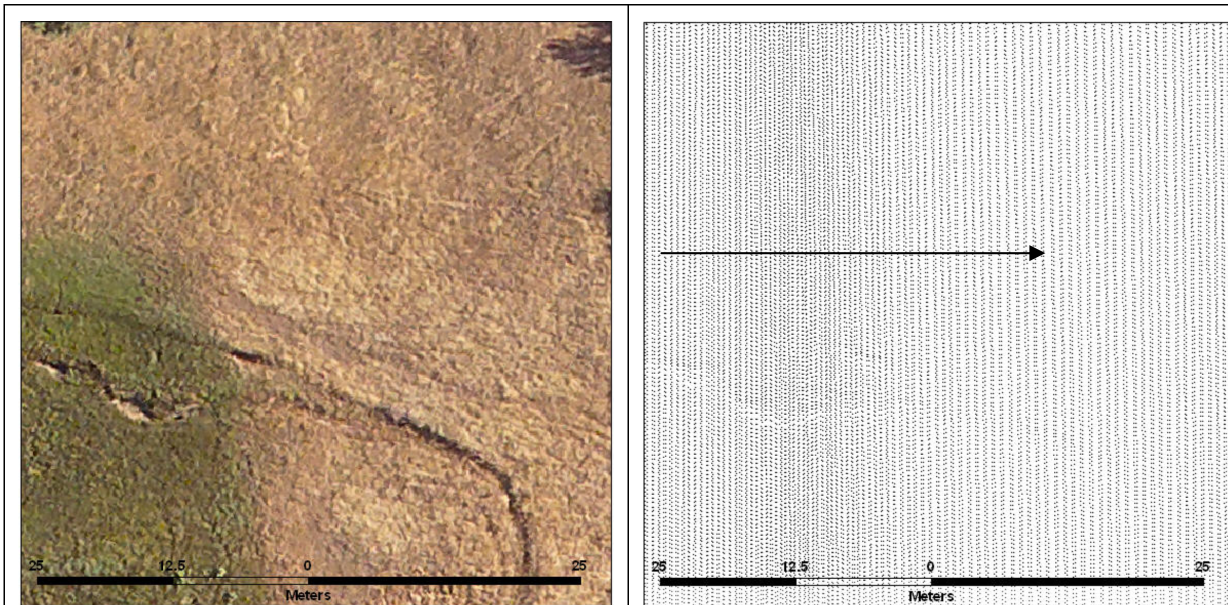

Test area showing lines of lidar points perpendicular to the direction of the flight line. The flight lines reach the ground in a long "z" pattern as the sensor sweeps back and forth and the aircraft moves forward; however, since the lines are long compared to the angle, they appear as roughly parallel.

Objects such as trees change the patterns of lidar points, and such objects can create small "shadowed" areas. These areas are caused by the angle of approach of the lidar points toward the ground surface. The effect is clearly seen in areas of flight line overlap where the "shadow" effect is different for each flight line (Figure 6). These shadowed areas can generally be eliminated through overlapping flight lines.

3.1.2 Lidar Data Density Variations

All lidar points. Lidar point density varies with flight line overlap and flight conditions (URS 2007a). For the Former Camp Beale site, point density variations were illustrated by creating density grids in which each 1 m cell was labeled with the number of lidar points in the cell. These grids clearly show the higher point density in areas of flight line overlap, and also show higher data density where the aircraft pitches into the wind. These appear as bands of higher density perpendicular to the flight line direction, often giving the appearance of "curtain folds" (Figure 7).

Figure 6: Effects of Vegetation on Lidar Point Patterns

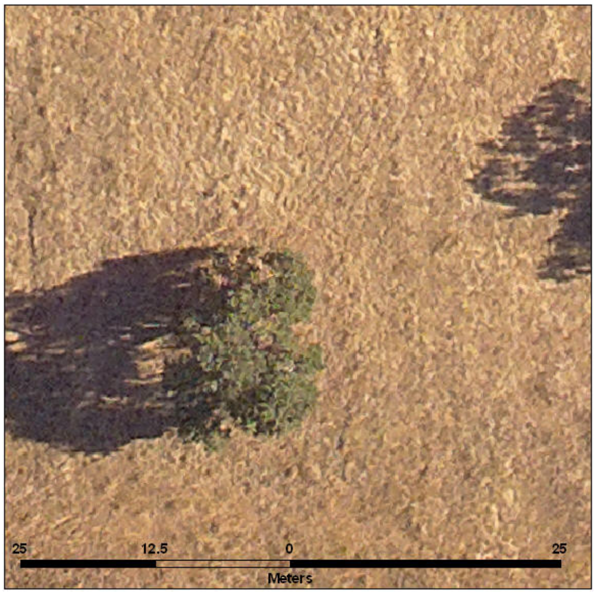

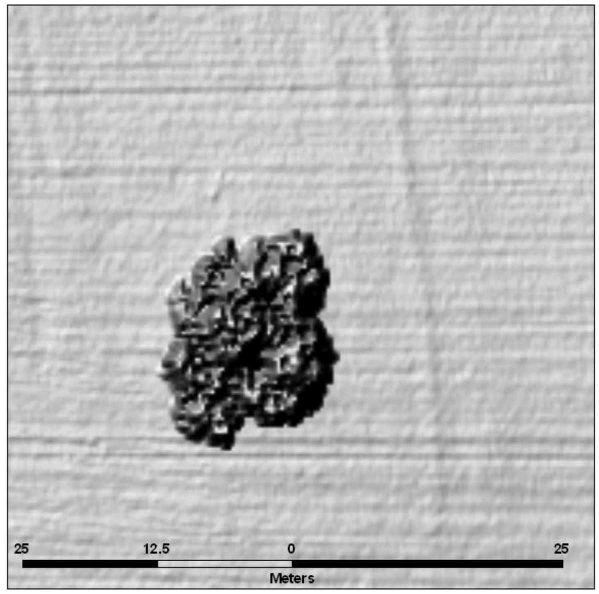

Effects of trees on lidar point patterns. Orthophoto and all-points DTM.

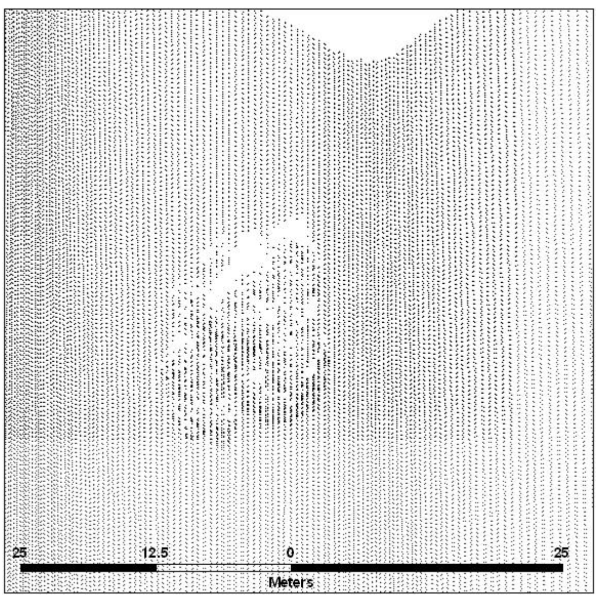

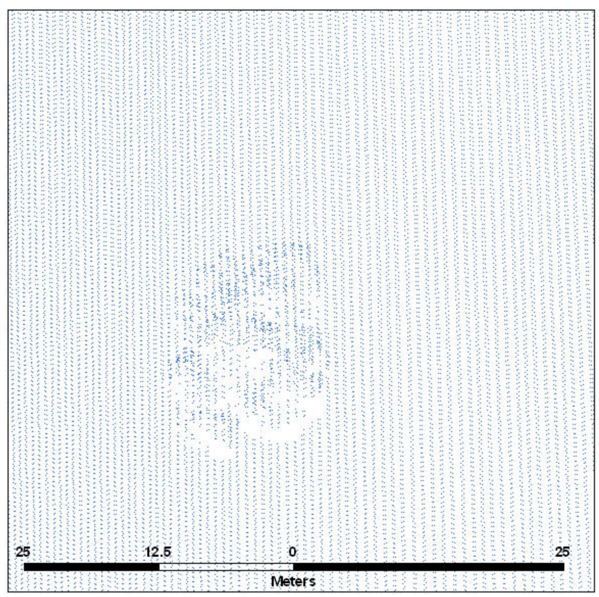

Changes in lidar point patterns, overlapping flight lines. The tree in the image on the left is near the north extent of the flight line, the same tree in the image to the right is near the center of the flight line. Small shadowed areas can be seen where no lidar points reach the ground, and these shadowed areas are different for each flight line..

Figure 7: Lidar Data Density Grids

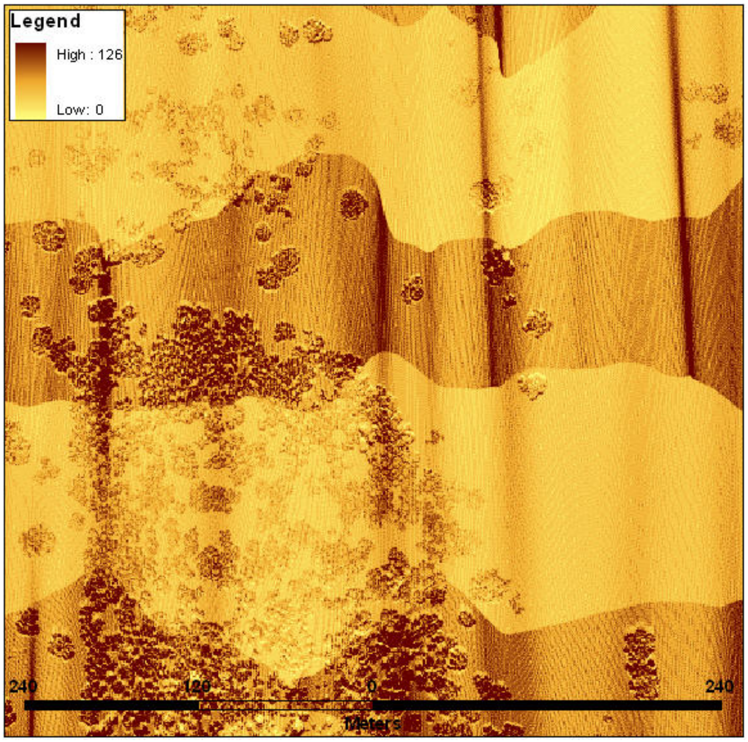

Data density grids, same data block as Figure 4.

Darker colors indicate higher data density. Areas of higher density correspond to areas of flight line overlap and also appear where the aircraft pitched and rolled, creating "curtain" effects.

The overall point density for the Former Camp Beale site was 13.8 pts/m^2.

Values for this block:

- Maximum:126 pts/m^2
- Minimum: 0 pts/m^2
- Mean:12.42 pts/m^2
- Standard deviation: 6.47 pts/m^2

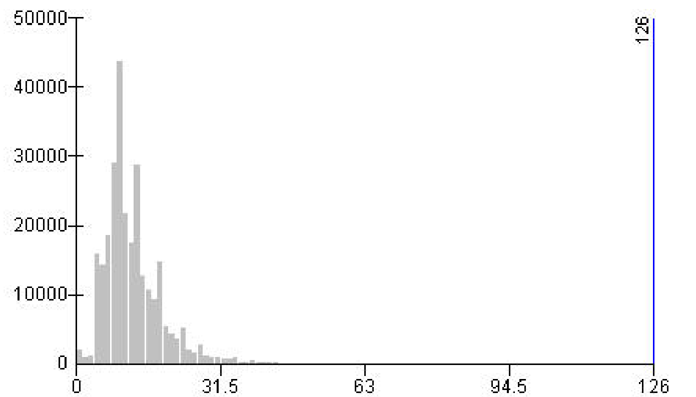

The histogram shows that while the maximum value is 126 pts/m^2, the highest values are outliers. The majority of the values are between 0 and 31 pts/m^2, with the most common values near the overall average density of 13.8 pts/m^2.

Point density variations are further illustrated in Figure 8.

Figure 8: Lidar Point Density Variation

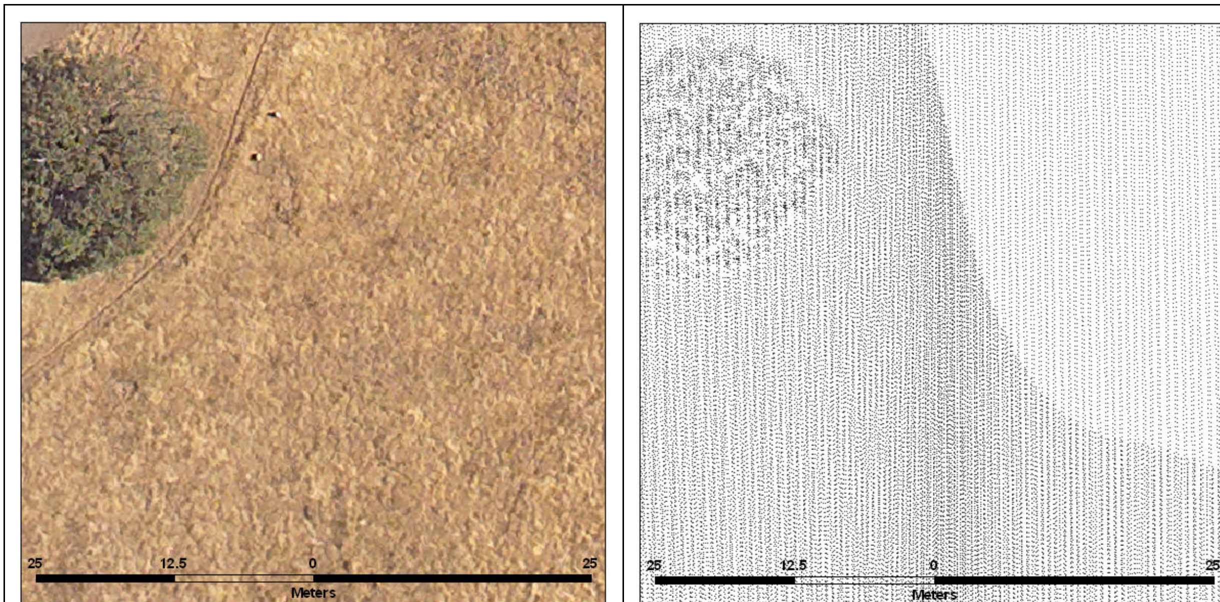

Point density test area, orthophoto and lidar points.

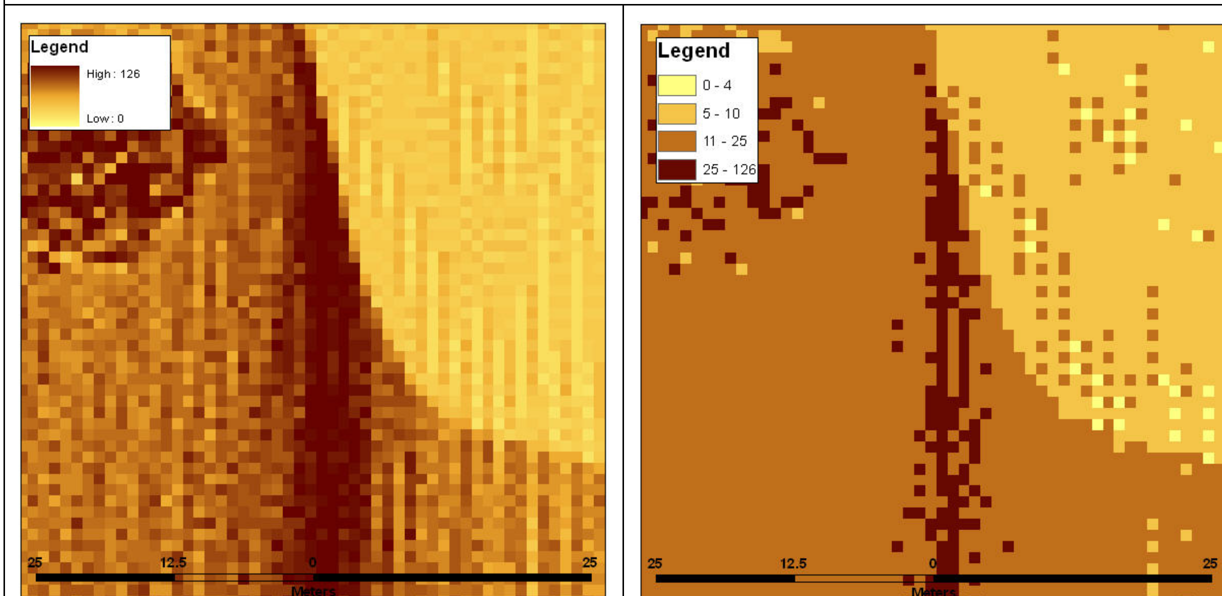

Point density images. The image on the left shows a color ramp between minimum and maximum values; the image on the right shows the same data classified in bands of: 0–4, 5–10, 11–25, and 26–126 pts/m^2. The image on the right shows that in the non-overlap area (upper right), most cells have between 5 and 10 pts/m^2, and in the flight line overlap area (lower left) most cells have between 11 and 25 pts/m^2. The area of aircraft pitch (the center "stripe") often has over 25 pts/m^2.

Ground returns. The density of ground returns can be mapped in a manner similar to the all-points maps shown. Figure 9 shows the same area as Figures 7 using only returns classified by the vendor as ground. In Figure 9, the contrast between all-points density and ground-points density is dramatic. The maximum point density was decreased from 126 total points to 8

ground pts/m^2. Areas of extremely high point density have been eliminated. The mean value for all points in the test block is 12.42 pts/m^2, which is roughly comparable to the value for the entire demonstration site of 13.8 pts/m^2. The overall density of ground points is much lower, at 1.78 pts/m^2. Variability is also lower for the ground points, as illustrated by the fact that the ground point density map is relatively uniformly colored while the all-points image highly variable.

Tthe density of the vendor-classified ground returns did not show higher density in areas of flight line overlap or aircraft pitch and roll. This lower variability of the ground points is initially puzzling since ground points should, intuitively, be more dense in areas of flight line overlap and should be higher in areas of aircraft pitch in the same way as overall point density.

.

Figure 9: Lidar Data Density – All Points and Ground Points

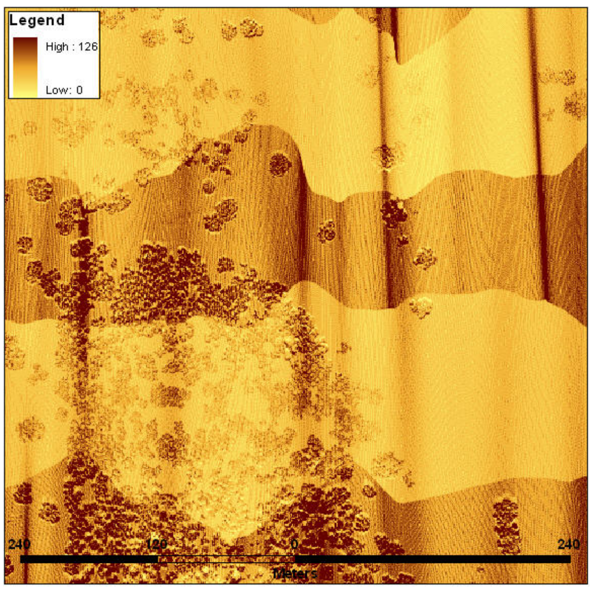	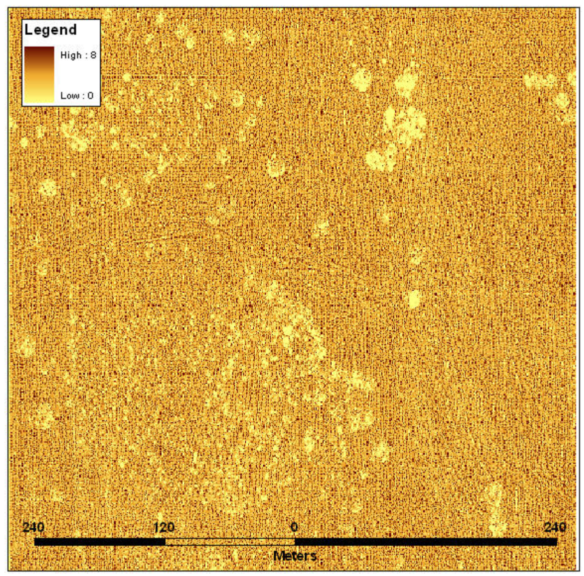
All points: Minimum: 0 pts/m^2 Maximum: 126 pts/m^2 Mean: 12.42 pts/m^2 Standard deviation: 6.47	Vendor-classified ground points only: Minimum: 0 pts/m^2 Maximum: 8 pts/m^2 Mean: 1.78 pts/m^2 Standard deviation: 1.07

Figure 9: Lidar Data Density – All Points and Ground Points (continued)

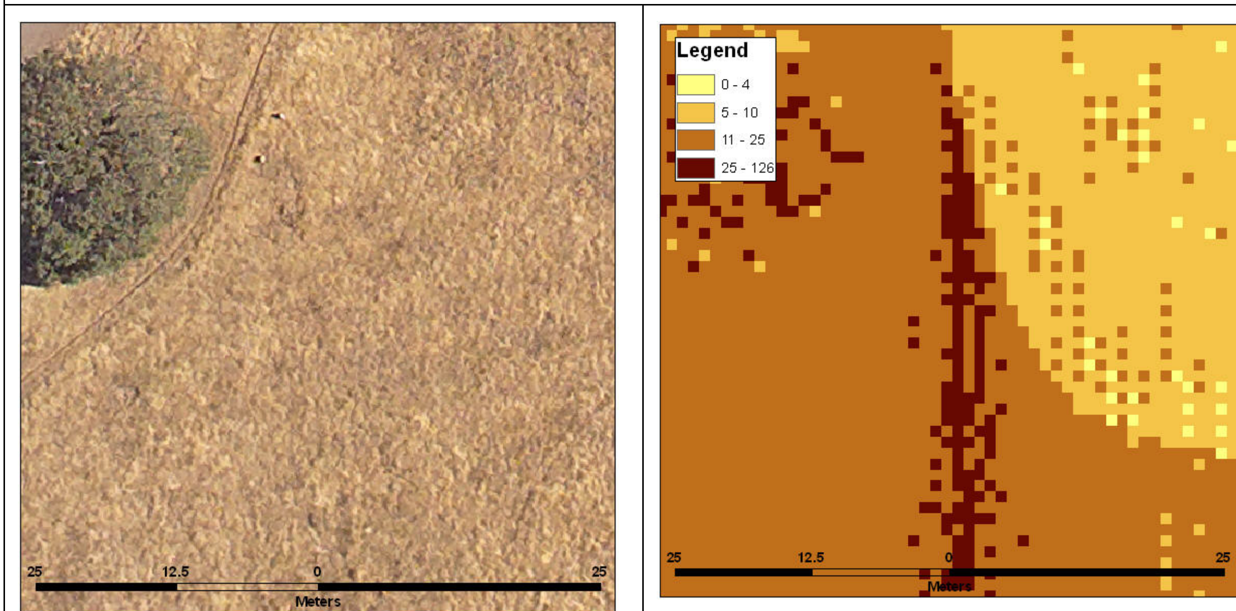

Point density test area, repeated from Figure 8. The image on the right shows density for the full lidar data set.

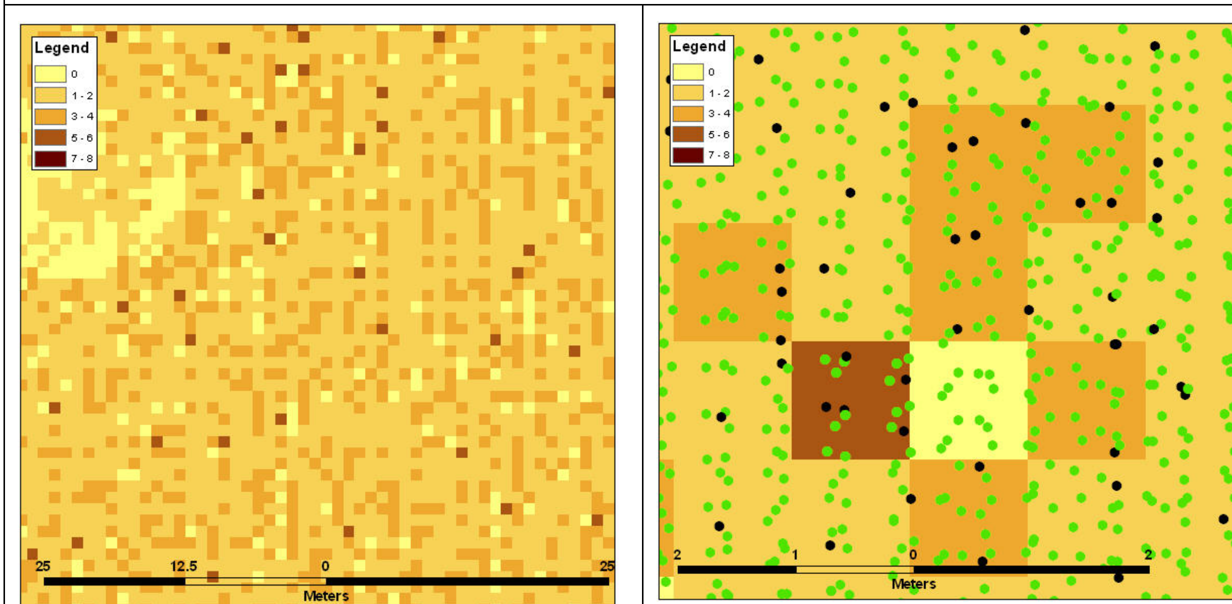

Density for the ground points only, same area. The image on the right shows the vendor's ground points (black) and non-ground points (green).

3.1.3 Point Classification

Initial observations. At the Former Camp Beale site, many lidar points appeared to have been classified as "non-ground" returns, even in areas where there is little or no apparent vegetation.

Figure 10 shows an area of paved road surface with the lidar points for the same area color coded by ground or non-ground returns.

Figure 10: Lidar Classification Results on Paved Road Surfaces

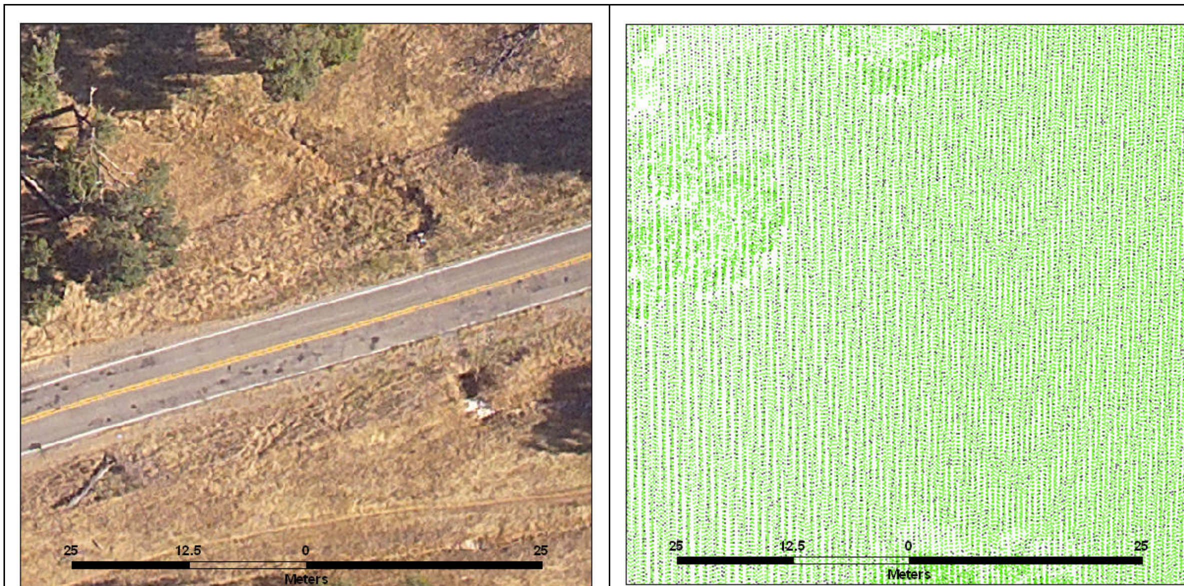

Orthophoto and classified lidar points for the initial point classification test area. In the image on the right, the vendor's ground points are black, and the vendor's non-ground points are green. The road, which should not have any non-ground returns, is not visible.

This image shows that the road—where there are no true "non-ground" returns—has many returns classified by the vendor as non-ground. Further, the classification for the paved surface appears to be similar to the sparsely-vegetated areas on either side of the road. In both areas, it appears that a large number of points classified as non-ground could have been classified as ground returns.

The points classified as non-ground are generally not used in the creation of lidar-based surface models. However, these points were not "lost", since the vendor provided the full lidar data set.

Test areas. In response to these initial findings, a series of 14 test areas was chosen, all on paved roads where site photos showed no overhanging vegetation. In these areas, all "non-ground" lidar returns were assumed to be artifacts of the classification process. For each site, the number of ground and non-ground returns was measured, and point density calculated for all points and "ground" points. Test areas were chosen in both areas of flight line overlap and non-overlap. The results are shown in Table 1.

Table 1: Former Camp Beale Test Area Results

Area ID	Area (m^2)	Number of Points			Percentage		Density (pts/m^2)	
		Total	Ground	Non-Ground	Ground	Non-Ground	All	Ground
1	516	1,399	715	684	51.1	48.9	2.71	1.39
2	398	1,276	606	670	47.5	52.5	3.21	1.52
3	2,200	7,815	3,494	4,321	44.7	55.3	3.55	1.59
4	492	1,913	704	1,209	36.8	63.2	3.89	1.43
5	871	6,614	1,887	4,727	28.5	71.5	7.59	2.17
6	524	4,966	916	4,050	18.4	81.6	9.48	1.75
7	763	7,732	1,453	6,279	18.8	81.2	10.13	1.90
8	784	8,098	1,358	6,740	16.8	83.2	10.33	1.73
9	2,477	29,463	4,908	24,555	16.7	83.3	11.89	1.98
10	1,450	20,440	2,729	17,711	13.4	86.6	14.10	1.88
11	662	9,902	1,333	8,569	13.5	86.5	14.96	2.01
12	539	9,340	2,256	7,084	24.2	75.8	17.33	4.19
13	2,118	40,297	4,046	36,251	10.0	90.0	19.03	1.91
14[a]	431	17,888	828	17,065	4.6	95.4	41.50	1.92

a. This test area included both fight line overlap and aircraft pitch, which resulted in a very high overall point density.

One result of this test was that the percentage of laser returns classified as non-ground increased closely with the increase in overall density. A single “background” rate of non-ground classification cannot be developed, since the rate of non-ground classification varies with overall point density.

A second result is that as the overall data density rose from 2.7 to 41.5 pts/m^2, ground point density rose much more modestly, from around 1.4 to around 2.2 pts/m^2 (with only one outlier).

3.1.4 Vertical Distribution of Non-Ground Points

Initial observations. Most of the points classified as “non-ground” appear to be close to the ground surface. As an initial test, lidar points for the same area were re-classified to include all of the points that are within 0.4 m of the ground surface in the “ground” classification. Figure 11 shows that this approach added almost all of the points to the ground surface except those reflecting from trees or higher ground features.

Figure 11: Initial Point Reclassification Test – Former Camp Beale

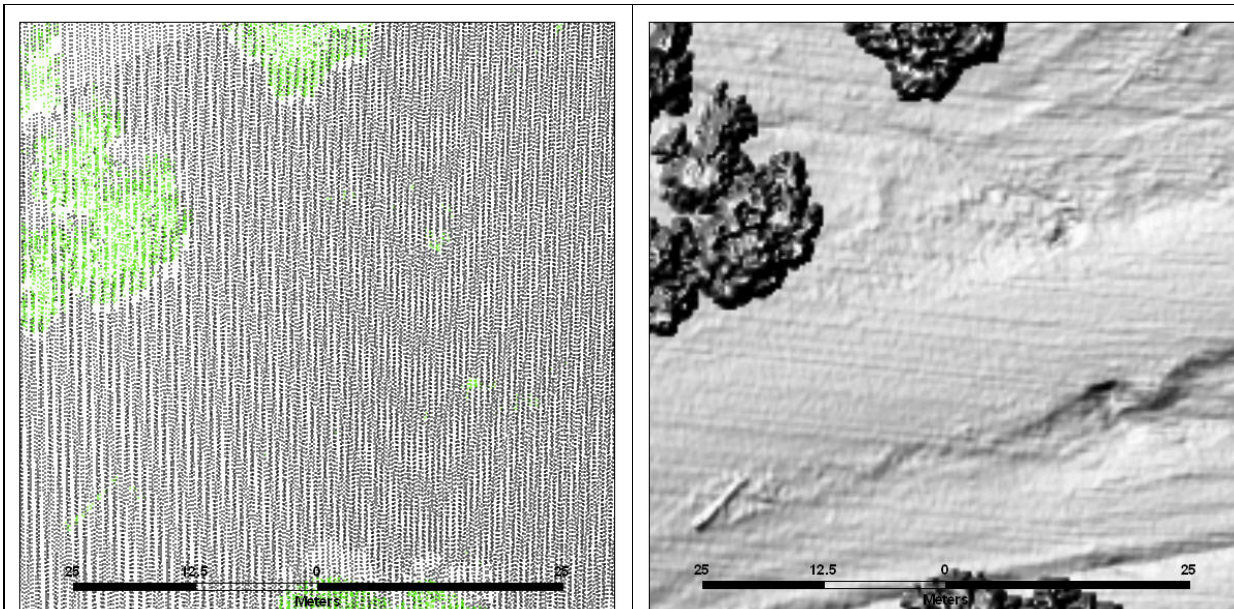

Initial point classification test area, points re-classified. “Non-ground” points within 0.4m of the modeled ground surface were added to the “ground” classification. The remaining “non-ground” points appear to be reflections from trees and other objects on the ground. The image to the right is the DTM using the full lidar data set.

Test areas. The vertical distribution of the “non-ground” returns was examined for six of the point density test areas. The areas examined were all paved surfaces with no apparent overhanging vegetation or unpaved road shoulder. Non-ground returns were measured for their distance above or below the surface model created from the points classified as ground returns. Four elevation classes were established: +/- 5 cm, between +/- 5 and 10 cm, between +/- 10 and 15 cm, and greater than 15 cm. For each of the test areas, the majority of the “non-ground” returns were within 10 cm of the modeled surface (Table 2). Only a small number (between 3.1 and 15.3 percent) were more than 15 cm from the modeled surface.

Table 2: Elevation Distribution for Non-Ground Points – Former Camp Beale

Test Area ID	Area (m^2)	Number of Points – Non-Ground	Elevation Class (%)			
			<= +/- 0.05 cm	> 0.05 and <= 0.10 cm	> 0.10 and <= 0.15 cm	> 0.15 cm
1	398	670	58.8	30.4	8.4	2.4
2	763	6,279	35.4	37.0	20.8	6.8
4	539	7,084	24.3	36.4	24.0	15.3
7	492	1,209	53.8	32.6	10.4	3.1
8	662	8,569	29.2	36.0	23.0	11.8
10	1,450	17,711	27.3	35.4	25.1	12.3

The elevation distribution of the non-ground returns is illustrated in Figure 12. The general elevation distribution of non-ground points appears to extend to the relatively un-vegetated area off the road surface.

Figure 12: Elevation Distribution for "Non-Ground" Points– Former Camp Beale

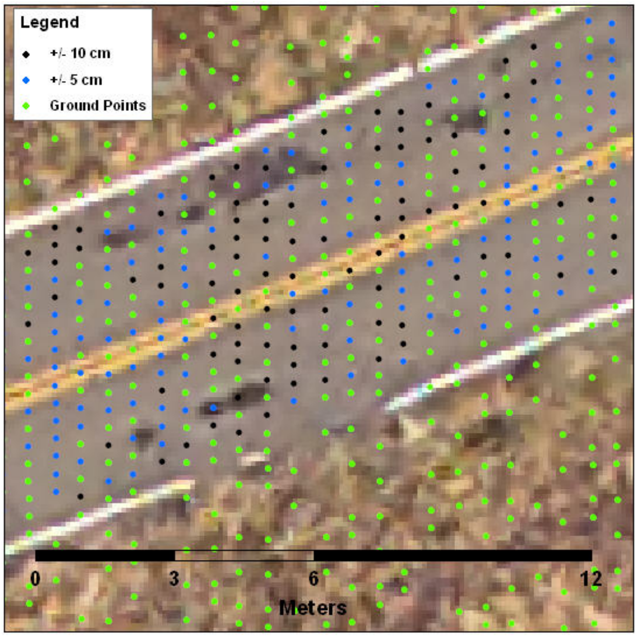

Vertical distribution of non-ground returns. There were no points further than 10 cm from the modeled ground surface in this area.

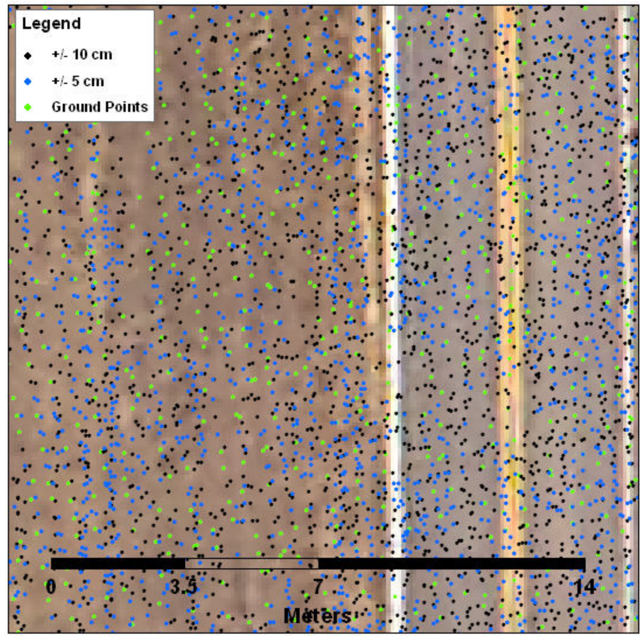

Vertical distribution of non-ground returns, on and off paved surface. There were no points further than 10 cm from the modeled ground surface in this area.

These results suggest that at least the majority of the points classified as non-ground could be added back to the ground surface model with little risk of including low vegetation or other "true" non-ground features.

3.2 Results at Additional Sites

Lidar data from six additional sites was examined to determine whether the same types of effects would be found. Sites included:

- ***Kirtland Air Force Base (AFB) Precision Bombing Range (PBR).*** Data collected by Terra Remote Sensing in August 2005. Four lidar data sets were collected.
- ***Victorville Demolition Bombing Target (DBT) "Y".*** Data collected by Terra Remote Sensing in January 2006. Two lidar data sets were collected.
- ***Pueblo PBR.*** Data collected by Sky Research in August 2004 (Phase I) and August 2005 (Phase II). One lidar data set was collected.
- ***Former Camp Beale Sky Research.*** In May 2006, Sky Research collected lidar data for Beale AFB. Data collection involved some overlap with the Former Camp Beale demonstration site. One lidar data set was collected.
- ***Puget Sound Lidar Coalition, Portland Area.*** Data collected by Terrapoint in 2004. One lidar data set was collected.
- ***Puget Sound Lidar Coalition, Snohomish County.*** Data collected by Terrapoint in 2003. One lidar data set was collected.

The two Puget Sound sites were collected at a lower data density, since their primary purpose was not to detect small surface features. They are included to represent the work of an additional lidar vendor and a lower point density. The sites selected are not intended to be a comprehensive survey of lidar data sets, but rather to be an overview to determine whether results appear similar to those at the ESTCP sites. Results are described in the sections below.

3.2.1 Kirtland Air Force Base Precision Bombing Range

Four lidar flights were conducted at this site, as part of an investigation of point density required to detect features.

Point density maps. Figure 13 shows point density for the full point data set and for ground points alone for one of the 300 m flights conducted at this site. Results for all four flights were similar and are discussed in Appendix C to the ESTCP Final Report for this demonstration site (URS 2007a).

Figure 13: Point Density Maps – Kirtland AFB PBR

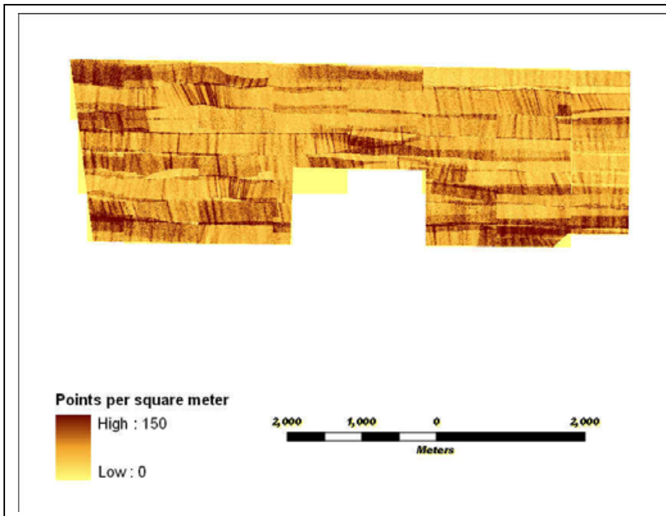

Density map, all points

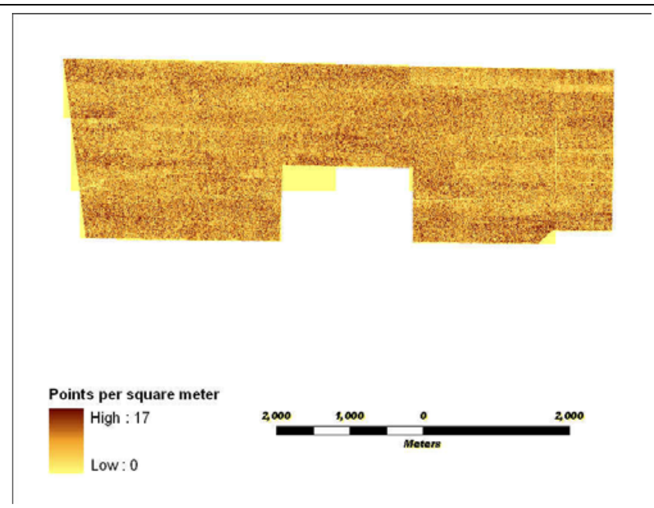

Density map, ground points only

Test areas. Tables 3 through 6 show the results for 10 test areas, each 50 m x 50 m. These areas were selected to represent both flightline overlap and non overlap areas for all four of the lidar flights conducted. The Kirtland site did not contain any paved roads, so it was not possible to select test areas where non-ground classification would be assured to be classification artifacts. However, vegetation conditions did not vary noticeably over the site, so in theory the percentage of vegetation returns should be consistent for all test areas and for all lidar flights.

Table 3: Kirtland AFB PBR Test Area Results
900 m Flight

Area ID	Area (m^2)	Number of Points			Percentage		Density (pts/m^2)	
		Total	Ground	Non-Ground	Ground	Non-Ground	All	Ground
1	2,500	4,222	2,970	1252	70.35	29.65	1.69	1.19
2	2,500	4,566	2,929	1637	64.15	35.85	1.83	1.17
3	2,500	4,831	2,923	1,908	60.51	39.49	1.93	1.17
4	2,500	4,839	3,313	1,526	68.46	31.54	1.94	1.33
5	2,500	4,886	3,355	1,531	68.67	31.33	1.95	1.34
6	2,500	4,921	3,389	1,532	68.87	31.13	1.97	1.36
7	2,500	6,190	3,577	2,613	57.79	42.21	2.48	1.43
8	2,500	6,392	3,901	2,491	61.03	38.97	2.56	1.56
9	2,500	6,473	3,902	2,571	60.28	39.72	2.59	1.56
10	2,500	6,658	3,086	3,572	46.35	53.65	2.66	1.23

Table 4: Kirtland AFB PBR Test Area Results
450 m Flight

Area ID	Area (m^2)	Number of Points			Percentage		Density(pts/m^2)	
		Total	Ground	Non-Ground	Ground	Non-Ground	All	Ground
1	2,500	7,430	4,342	3088	58.44	41.56	2.97	1.74
2	2,500	9,569	4,950	4619	51.73	48.27	3.83	1.98
3	2,500	10,367	4,977	5,390	48.01	51.99	4.15	1.99
4	2,500	12,261	5,392	6,869	43.98	56.02	4.90	2.16
5	2,500	19,513	5,827	13,686	29.86	70.14	7.81	2.33
6	2,500	21,690	6,451	15,239	29.74	70.26	8.68	2.58
7	2,500	22,371	5,573	16,798	24.91	75.09	8.95	2.23
8	2,500	25,342	6,351	18,991	25.06	74.94	10.14	2.54
9	2,500	27,438	6,154	21,284	22.43	77.57	10.98	2.46
10	2,500	34,190	6,461	27,729	18.90	81.10	13.68	2.58

Table 5: Kirtland AFB PBR Test Area Results
300 m Flight East-West Flight Lines

Area ID	Area (m^2)	Number of Points			Percentage		Density (pts/m^2)	
		Total	Ground	Non-Ground	Ground	Non-Ground	All	Ground
1	2,500	8,199	4,347	3852	53.02	46.98	3.28	1.74
2	2,500	10,410	4,521	5889	43.43	56.57	4.16	1.81
3	2,500	13,247	5,397	7,850	40.74	59.26	5.30	2.16
4	2,500	14,929	4,940	9,989	33.09	66.91	5.97	1.98
5	2,500	15,464	5,468	9,996	35.36	64.64	6.19	2.19
6	2,500	17,701	4,961	12,740	28.03	71.97	7.08	1.98
7	2,500	21,792	6,402	15,390	29.38	70.62	8.72	2.56
8	2,500	24,642	6,604	18,038	26.80	73.20	9.86	2.64
9	2,500	25,053	6,484	18,569	25.88	74.12	10.02	2.59
10	2,500	25,749	6,778	18,971	26.32	73.68	10.30	2.71

Table 6: Kirtland AFB PBR Test Area Results
300 m Flight North-South Flight Lines

Area ID	Area (m^2)	Number of Points			Percentage		Density (pts/m^2)	
		Total	Ground	Non-Ground	Ground	Non-Ground	All	Ground
1	2,500	8306	4,500	3806	54.18	45.82	3.32	1.80
2	2,500	9052	4,734	4318	52.30	47.70	3.62	1.89
3	2,500	9486	4,884	4,602	51.49	48.51	3.79	1.95
4	2,500	10479	5,004	5,475	47.75	52.25	4.19	2.00
5	2,500	11513	5,321	6,192	46.22	53.78	4.61	2.13
6	2,500	11680	5,407	6,273	46.29	53.71	4.67	2.16
7	2,500	13855	5,948	7,907	42.93	57.07	5.54	2.38
8	2,500	14954	6,553	8,401	43.82	56.18	5.98	2.62
9	2,500	16055	6,089	9,966	37.93	62.07	6.42	2.44
10	2,500	21650	6,403	15,247	29.58	70.42	8.66	2.56

Comparison with previous data sets. As with the Former Camp Beale data, the density map for the full data set clearly shows the effects of flight line overlap, and this effect is largely absent in the density map based on the vendor's ground points (Figure 13). Ground point density is much less variable than overall density (Tables 3 through 6). As overall point density went up, the percentage of non-ground classifications also went up. As at Former Camp Beale, the ground point density was generally no higher than 2.5 pts/m^2, even when overall density was as high as 13.68 pts/m^2.

3.2.2 Victorville Demolition Bombing Target "Y"

Two lidar flights were conducted at this site.

Point density maps. Figure 14 shows point density for the full point data set and for ground points alone, for one of the two lidar flights conducted at this site. Results for both flights are similar and are discussed in Appendix C to the ESTCP Final Report for this demonstration site (URS 2007a).

Figure 14: Point Density Maps – Victorville DBT "Y"

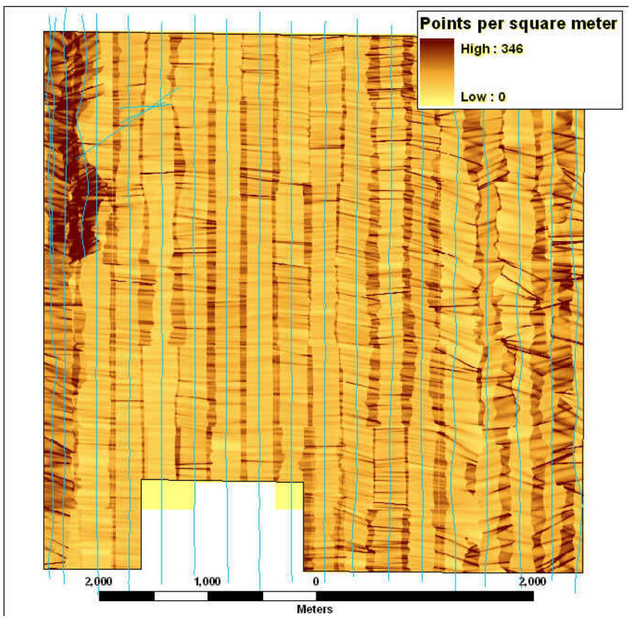

Density map, all points

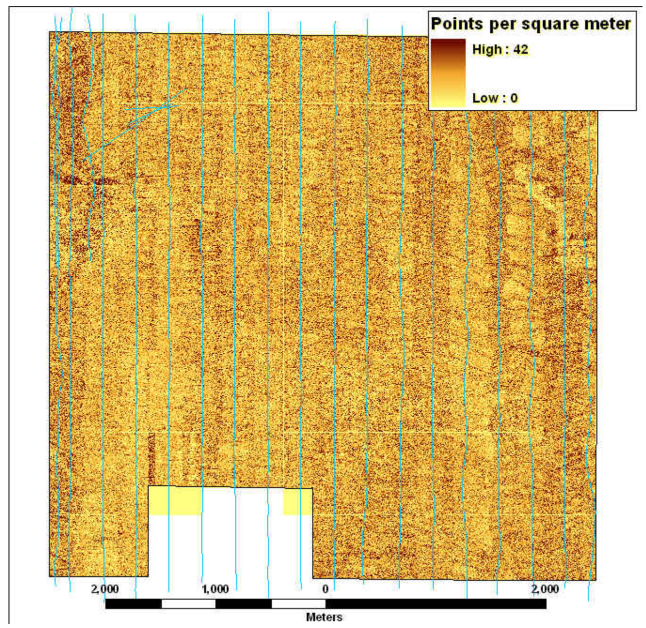

Density map, ground points only

Test areas. Tables 7 and 8 show the results for 10 test areas, each 25 m x 25 m. As with the Kirtland site, the Victorville site did not contain any paved roads, so test areas were chosen in open areas. However, the site does not contain tall vegetation, and vegetation conditions do not vary noticeably over the site, so in theory the percentage of vegetation returns should be consistent for all test areas, and for all lidar flights.

Table 7: Victorville DBT "Y" Test Area Results
300 m Flight

Area ID	Area (m^2)	Number of Points			Percentage		Density (pts/m^2)	
		Total	Ground	Non-Ground	Ground	Non-Ground	All	Ground
1	625	2,335	1,441	894	61.71	38.29	3.74	2.31
2	625	2,826	1,490	1,336	52.72	47.28	4.52	2.38
3	625	2,851	1,274	1,577	44.69	55.31	4.56	2.04
4	625	2,964	1,248	1,716	42.11	57.89	4.74	2.00
5	625	3,219	1,420	1,799	44.11	55.89	5.15	2.27
6	625	3,518	1,535	1,983	43.63	56.37	5.63	2.46
7	625	4,175	1,410	2,765	33.77	66.23	6.68	2.26
8	625	5,059	1,506	3,553	29.77	70.23	8.09	2.41
9	625	5,725	1,829	3,896	31.95	68.05	9.16	2.93

10	625	7,247	1,859	5,388	25.65	74.35	11.60	2.97

Table 8: Victorville DBT "Y" Test Area Results
450 m Flight

Area ID	Area (m^2)	Number of Points			Percentage		Density (pts/m^2)	
		Total	Ground	Non-Ground	Ground	Non-Ground	All	Ground
1	625	1,789	1,071	718	59.87	40.13	2.86	1.71
2	625	1,910	1,100	810	57.59	42.41	3.06	1.76
3	625	2,085	1,099	986	52.71	47.29	3.34	1.76
4	625	2,345	978	1,367	41.71	58.29	3.75	1.56
5	625	2,456	1,190	1,266	48.45	51.55	3.93	1.90
6	625	3,614	1,219	2,395	33.73	66.27	5.78	1.95
7	625	4,839	1,433	3,406	29.61	70.39	7.74	2.29
8	625	5,362	1,451	3,911	27.06	72.94	8.58	2.32
9	625	5,568	1,558	4,010	27.98	72.02	8.91	2.49
10	625	5,601	1,376	4,225	24.57	75.43	8.96	2.20

Comparison with previous data sets. As with the Former Camp Beale and Kirtland data, the density map for the full data set clearly shows the effects of flight line overlap and aircraft motion, which is largely absent in the density map based on the vendor's ground points. As with the other sites, the percentage of non-ground returns increased roughly with overall point density, and ground point density is no higher than 2.49 pts/m^2, even when overall density was as high as 8.96 pts/m^2.

3.2.3 Pueblo Precision Bombing Range

One lidar data set was acquired at the Pueblo site.

Point density maps. Figure 15 shows point density for the full point data set and for ground points alone.

Figure 15: Point Density Maps – Pueblo PBR

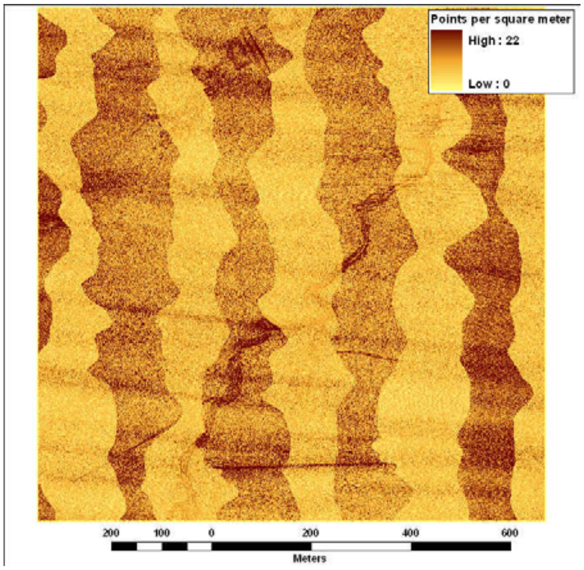

Density map, all points

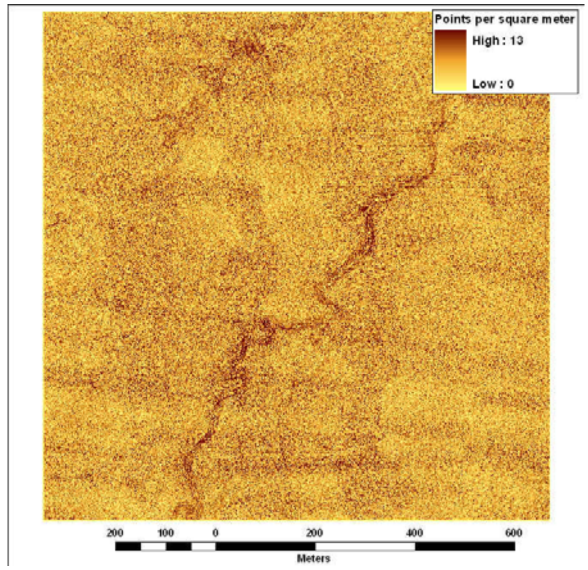

Density map, ground points only

Test areas. Table 9 shows the results for 15 test areas, each just over 50 x 50 m. Like the Kirtland and Victorville sites, the Pueblo site did not contain any paved roads, so it was not possible to select test areas where non-ground classification would be certain to be classification artifacts. However, the site does not contain high vegetation, and vegetation conditions do not vary noticeably over the site, so in theory the percentage of vegetation returns should be consistent for all test areas.

Table 9: Pueblo PBR Test Area Results

Area ID	Area (m^2)	Number of Points			Percentage		Density (pts/m^2)	
		Total	Ground	Non-Ground	Ground	Non-Ground	All	Ground
1	2,500	5,232	4,580	652	87.54	12.46	2.09	1.83
2	2,500	5,626	4,352	1,274	77.36	22.64	2.25	1.74
3	2,500	6,330	5,036	1,294	79.56	20.44	2.53	2.01
4	2,500	8,496	6,660	1,836	78.39	21.61	3.40	2.66
5	2,500	10,843	5,794	5,049	53.44	46.56	4.34	2.32
6	2,500	11,728	5,962	5,766	50.84	49.16	4.69	2.38
7	2,500	13,894	7,481	6,413	53.84	46.16	5.56	2.99
8	2,500	14,117	5,511	8,606	39.04	60.96	5.65	2.20
9	2,500	16,142	7,858	8,284	48.68	51.32	6.46	3.14
10	2,500	16,283	5,654	10,629	34.72	65.28	6.51	2.26

The effect of flight line overlap on point classification can be seen in Figure 16, which shows the surface model created from all lidar returns, and the same image with the individual lidar points coded black for ground returns and green for non-ground returns. This image shows an area of flight line overlap on the left side of the image. The overlap area shows a higher number of green (non-ground) returns.

Figure 16: Flight Line Overlap Area – Pueblo PBR

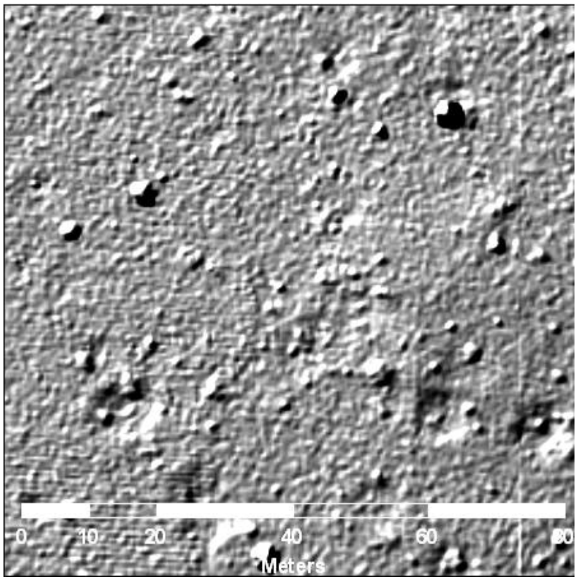	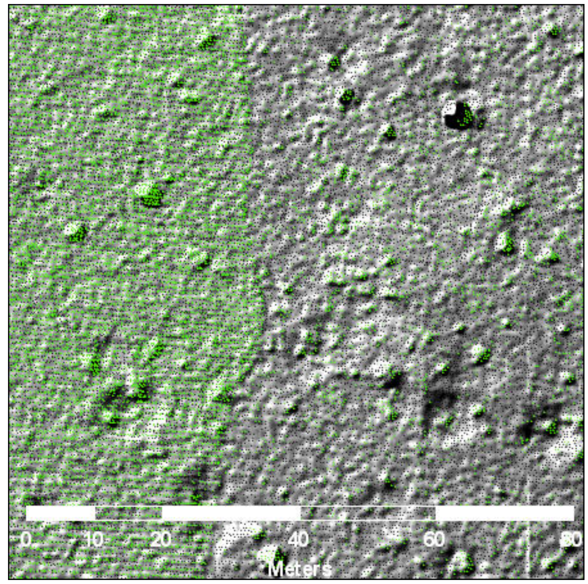
All points surface model	All points surface model with lidar points. Flight line overlap area to the left. Non-ground returns are green.

Comparison with previous data sets. As with the previous data sets examined, the density map for the full data set clearly shows the effects of flight line overlap, and this effect is largely absent in the density map based on the vendor's ground points. As with the other sites examined, the percentage of non-ground returns increased roughly with overall point density.

One difference from the three data sets collected by Terra Remote Sensing is that in the Pueblo data examined above, the maximum all-points density is lower: 22 pts/m^2 compared with 346 pts/m^2 in the Victorville data. This may be because the lidar data at Pueblo was collected using a fixed-wing aircraft, which was subject to less pitching due to wind than the helicopter used at the other sites, where areas of aircraft pitch appear to account for the very high data densities occasionally seen. (The lower rate of aircraft pitch can be seen in the all-points density map as an absence of "curtain fold" effects.)

3.2.4 Former Camp Beale/Sky Research

The ESTCP data for the Former Camp Beale site was collected by Terra Remote Sensing; however, Sky Research collected lidar data at Beale AFB, directly to the west. Sky Research's data extended a small distance onto the Former Camp Beale site, providing a complementary view of the same area. One lidar data set was collected.

Point density maps. Figure 17 shows point density for the full point data set and for ground points alone.

Figure 17: Point Density Maps – Former Camp Beale/Sky Research

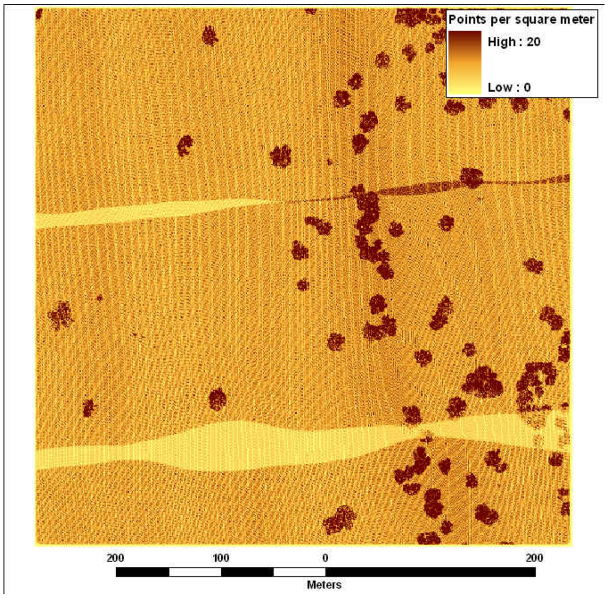	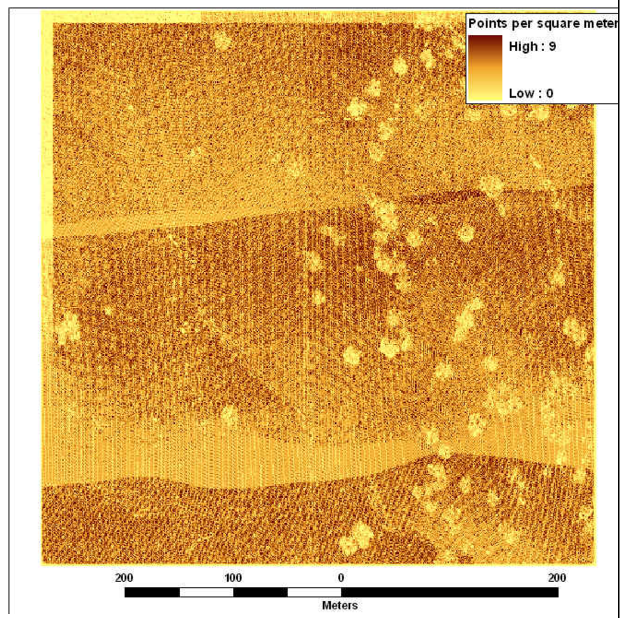
Point density map, all points	Point density map, ground points only.

Test areas. Table 10 shows the results for 10 test areas, each 50 m x 50 m. The test areas were placed to avoid tall vegetation.

Table 10: Former Camp Beale/Sky Research Test Area Results

Area ID	Area (m^2)	Number of Points			Percentage		Density (pts/m^2)	
		Total	Ground	Non-ground	Ground	Non-ground	All)	Ground
1	2,500	9976	8444	1532	84.64	15.36	3.99	3.38
2	2,500	10654	8316	2338	78.06	21.94	4.26	3.33
3	2,500	11435	9794	1641	85.65	14.35	4.57	3.92
4	2,500	11739	7121	4618	60.66	39.34	4.70	2.85
5	2,500	11755	9903	1852	84.25	15.75	4.70	3.96
6	2,500	11814	9329	2485	78.97	21.03	4.73	3.73
7	2,500	12011	9489	2522	79.00	21.00	4.80	3.80
8	2,500	12052	8507	3545	70.59	29.41	4.82	3.40
9	2,500	12140	9854	2286	81.17	18.83	4.86	3.94
10	2,500	16667	7793	8874	46.76	53.24	6.67	3.12

Figure 18: Lidar Points on Road Surface – Former Camp Beale/Sky Research

Orthophoto

Lidar points, ground (black) and non-ground (green), vendor classification

Comparison with previous data sets. In this data set, the overall data density map shows the effect of flight line overlap and aircraft motion. Unlike in the other data sets examined, these effects persist in the ground point density model. Based on conversations with Sky Research staff, this may be a result of more successful efforts to spatially integrate data from one flight line to the next, resulting in less spatial displacement (Sky Research 2009).

Table 10 shows that the effects observed at the other ESTCP sites are less evident. While the percentage of points classified as non-ground does increase with overall density, this effect is much less pronounced and there are many more outliers. The percentage of returns classified as non-ground does vary between approximately 15 and 53 percent in areas with relatively consistent vegetation conditions. Figure 18 shows some non-ground points on a paved surface, indicating that although the effect is less pronounced than at the other ESTCP sites, there are nevertheless some returns from the paved surface being classified as non-ground.

3.2.5 Puget Sound Lidar Coalition, Portland Area

Lidar data was collected for this area by TerraPoint in 2004. One lidar data set was collected.

Point density maps. Figure 19 shows point density for the full point data set and for ground points alone.

Figure 19: Point Density Maps – Puget Sound Lidar Coalition, Portland Area

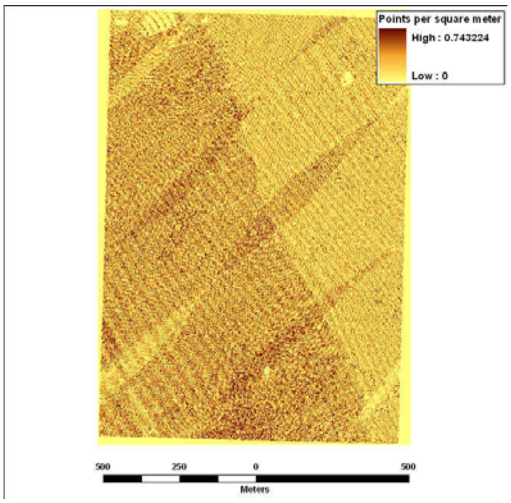

Point density map, using all points

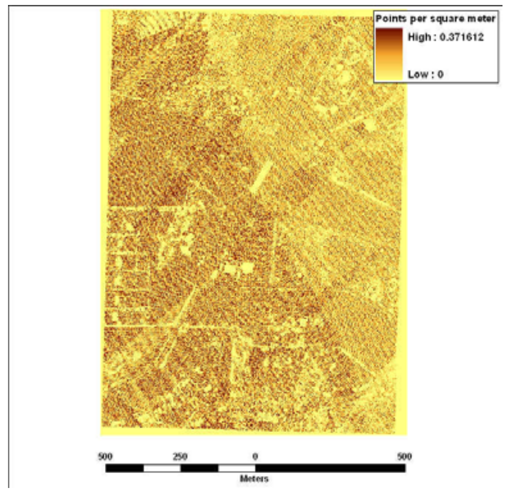

Point density map, ground points

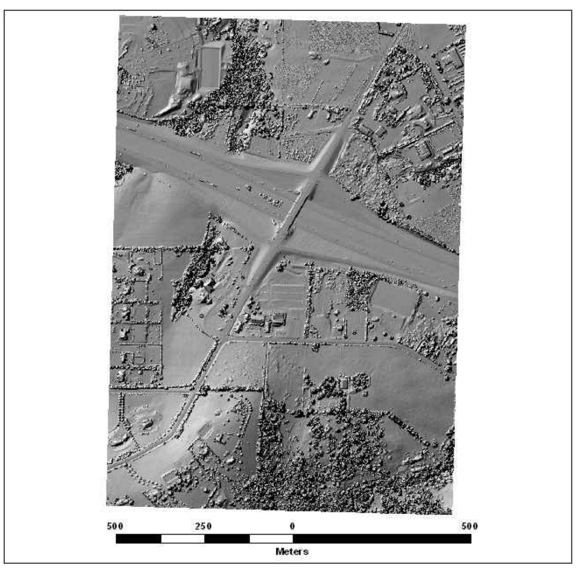

All-points surface model

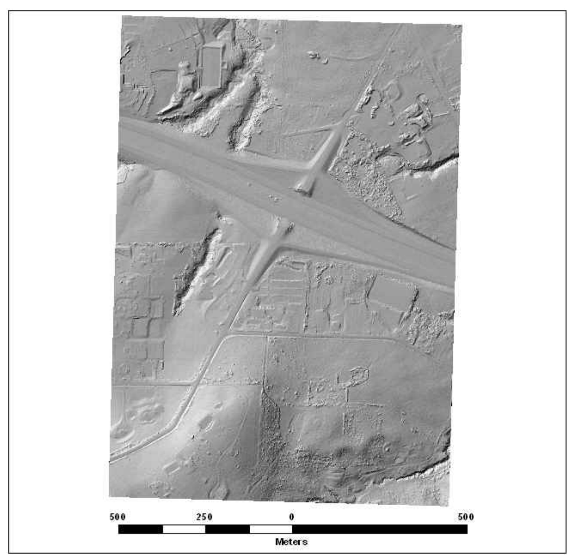

Ground points surface model

Test areas. Table 11 shows the results for 10 test areas, each just under 30 m x 30 m. The test areas were placed on roads where the full lidar data sets showed that no vehicles were present.

Table 11: Puget Sound Lidar Coalition, Portland Area Test Area Results

Area ID	Area (m^2)	Number of Points			Percentage		Density (pts/m^2)	
		Total	Ground	Non-Ground	Ground	Non-Ground	All	Ground
1	883	689	666	23	96.66	3.34	0.78	0.75
2	883	691	663	28	95.95	4.05	0.78	0.75
3	883	694	666	28	95.97	4.03	0.79	0.75
4	883	695	626	69	90.07	9.93	0.79	0.71
5	883	703	671	32	95.45	4.55	0.80	0.76
6	883	706	681	25	96.46	3.54	0.80	0.77
7	883	732	639	93	87.30	12.70	0.83	0.72
8	883	1,036	953	83	91.99	8.01	1.17	1.08
9	883	1,044	971	73	93.01	6.99	1.18	1.10
10	883	1,102	997	105	90.47	9.53	1.25	1.13

Comparison with previous data sets. As with the all of the data sets examined, the effects of flight line overlap are evident in the overall density maps. These effects are still somewhat evident in the density map for ground points, although results are somewhat complicated by the presence of trees and buildings in this complex suburban area.

The classification results are somewhat different from the ESTCP sites. First, a much smaller percentage of returns were classified as non-ground, and while this percentage does increase with overall point density, there are many more outliers. These results may be related to the lower overall point density of this data set, and the much smaller range of overall point density, from 0.78 to 1.25 pts/m^2. This area may also have had particularly good data calibration between flight lines.

3.2.6 Puget Sound Lidar Coalition, Snohomish County

Lidar data was collected for this area by TerraPoint in 2003. One data set was collected.

Point density maps. Figure 20 shows point density for the full point data set and for ground points alone.

Figure 20: Point Density Maps – Puget Sound Lidar Coalition, Snohomish County

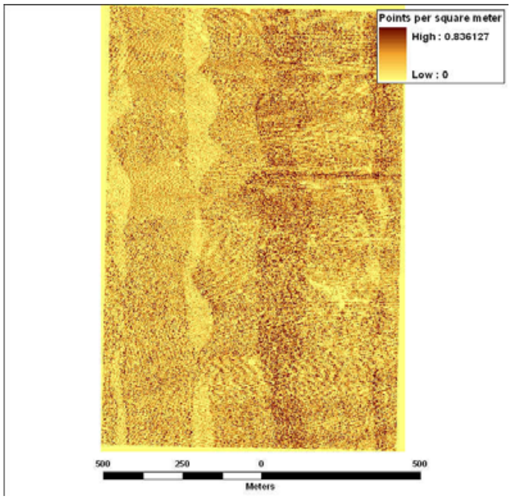	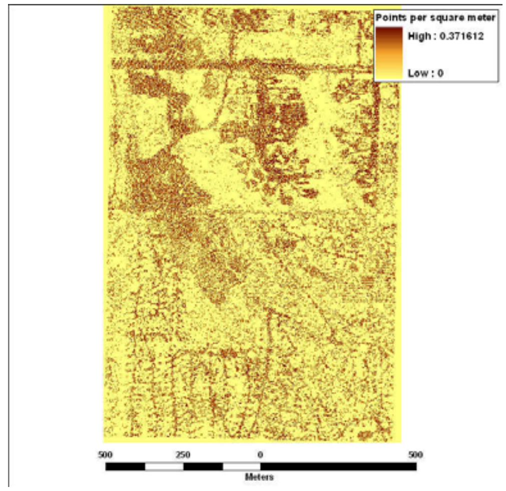
Point density map, all points	Point density map, ground points
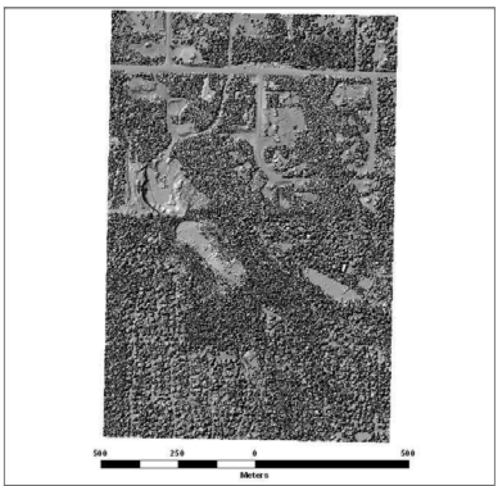	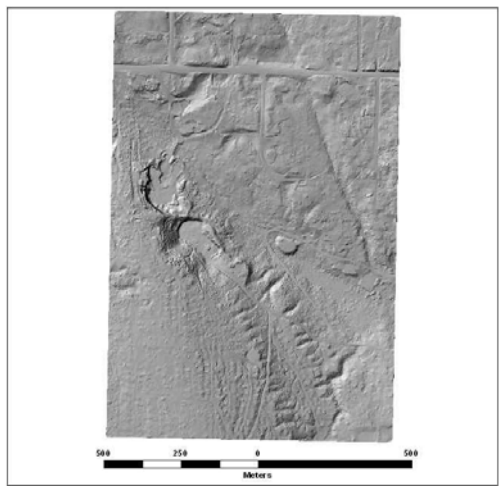
All points surface model	Ground points surface model

Test areas. Table 12 shows the results for 10 test areas, each just over 20 m x 20 m. The test areas were placed on roads where the full lidar data sets showed that no vehicles were present.

Table 12: Puget Sound Lidar Coalition, Snohomish County Test Area Results

Area ID	Area (m^2)	Number of Points			Percentage		Density (pts/m^2)	
		Total	Ground	Non-Ground	Ground	Non-Ground	All	Ground
1	402	338	300	38	88.76	11.24	0.84	0.75
2	402	385	225	160	58.44	41.56	0.96	0.56
3	402	404	355	49	87.87	12.13	1.01	0.88
4	402	421	323	98	76.72	23.28	1.05	0.80
5	402	489	341	148	69.73	30.27	1.22	0.85
6	402	490	315	175	64.29	35.71	1.22	0.78
7	402	511	357	154	69.86	30.14	1.27	0.89
8	402	564	377	187	66.84	33.16	1.40	0.94
9	402	605	420	185	69.42	30.58	1.51	1.05
10	402	623	391	232	62.76	37.24	1.55	0.97

**Figure 21: Lidar Points on Road Surface –
Puget Sound Lidar Coalition, Snohomish County**

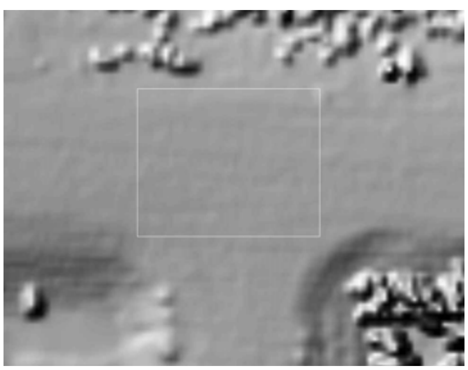

Surface model, all points

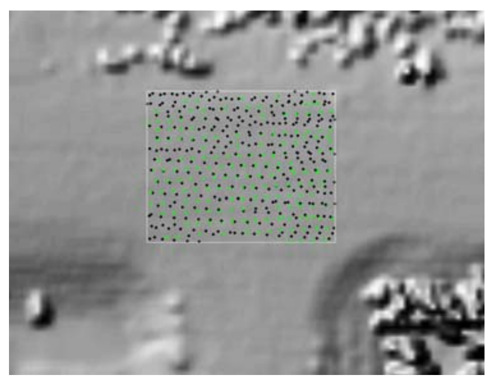

Lidar points on road surface, color-coded by ground (black) and non-ground (green)

Comparison with previous data sets. As with all of the lidar data sets examined, the full data sets shows the effects of flight line overlap. This effect is largely absent from the density map for ground points. This may be an effect of heavy vegetation and buildings in this complex suburban area. As with the Portland area data, the range of overall lidar density is lower than for the ESTCP sites, from 0.84 to 1.55 pts/m^2.

While the number of non-ground returns is lower than for the ESTCP sites, it remains a significant portion (often over 30 percent) of the overall lidar points, given that the test areas are on roads with no vegetation. However, the correlation between overall lidar density and the percentage of points classified as non-ground is less clear than for the ESTCP sites. At both this site and the Portland site, the weaker correlation may be the result of the lower overall density.

3.3 Analysis

Based on discussions with processing staff at the three vendors contacted, it appears that the large number of returns classified as non-ground in high density and flight line overlap areas is likely the result of the operation of TerraSolid's algorithms, interacting with small vertical errors between lidar points.

In part, this effect results from the fact that when point density is higher, the lines of laser points will be closer together, as shown in Figure 22.

Figure 22: Lidar Point Spacing Differences

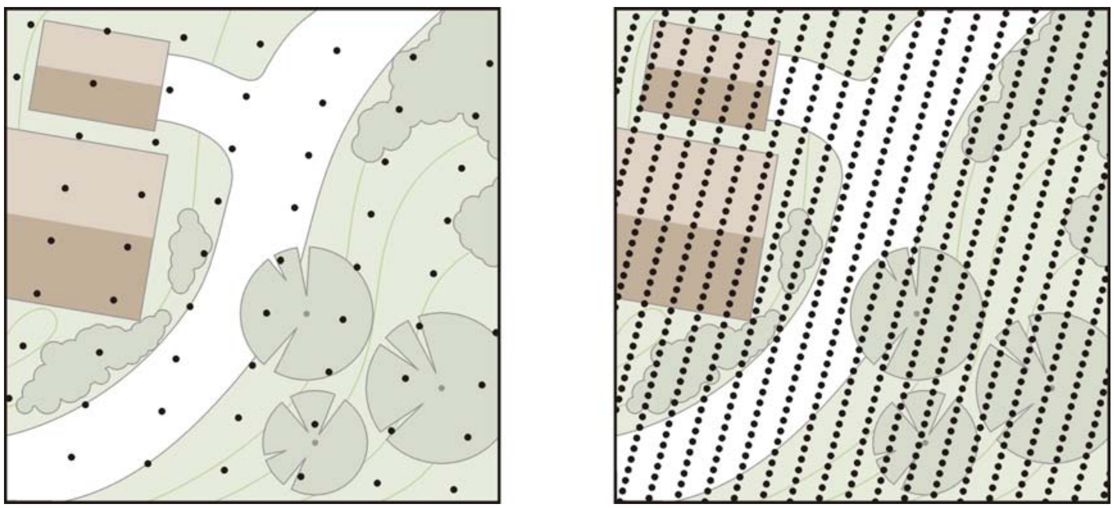

Lower-density lidar, average point spacing of 1m x 1.5m.	Higher density lidar, average point spacing of 0.2m x 0.4m.

When laser points are closer together, the angle formed by any new point with the existing model will be larger. When laser returns are sufficiently close, this increase in angle can be large enough so that very small elevation variations, within the noise level of the equipment, can cause points to be classified as non-ground.

Figure 23 shows the difference in iteration angle that results from decreasing the distance between the lines of points in this manner. Iteration angle was calculated for lines of laser points 100 cm apart vs. 20 cm apart, with elevations of 15, 10, and 5 cm above the initial surface. These elevations were chosen because the stated lidar vertical accuracy of lidar points is typically 15 cm, the typical flight line-to-flight line error is around 10 cm, and the elevation difference between sequential lines of lidar points is often around 5 cm.

All of the vendors contacted believe that this effect accounts for the large number of points classified as non-ground. This conclusion is consistent with the results described earlier, showing that as overall density increased, the classification algorithms classified an increasing percentage of points as non-ground. This also may account for the weaker effects seen in the Puget Sound Lidar Coalition data, which was acquired at lower overall densities.

Figure 23: Example Iteration Angles

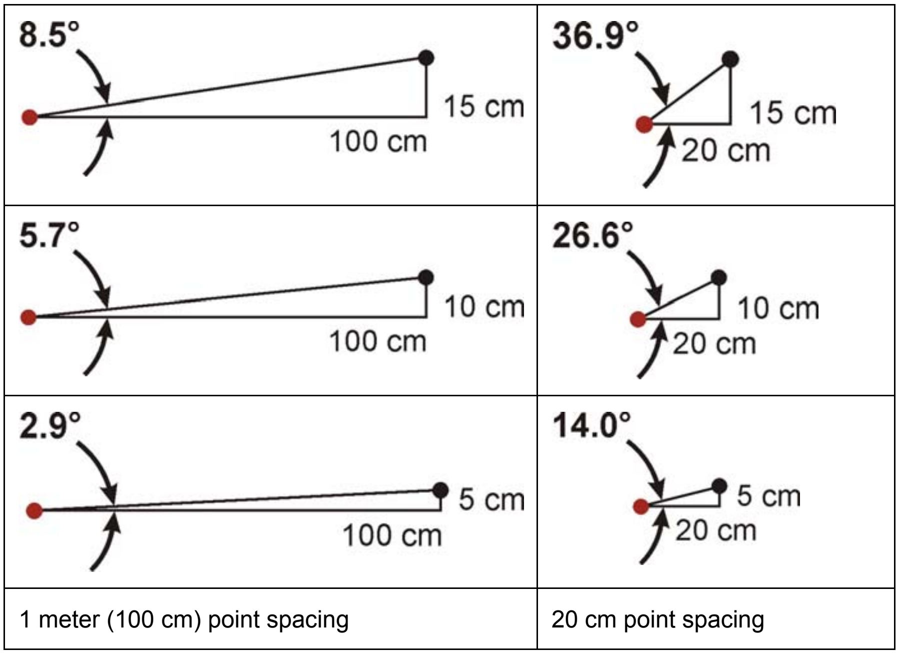

The over-classification of non-ground returns does not, in itself, address the issue of the source of the vertical offsets which with the classification software is interacting. One vendor contacted pointed out that misclassification would be a predictable effect of errors in GPS or flight line-to-flight line data calibration, either of which would result in larger than necessary vertical discrepancies between points. This vendor noted that if the flight lines are vertically offset (due to calibration or GPS errors), then points associated with the higher flight line would be predictably classified as non-ground. This effect would be present even if the classification routine were well constructed. (Sky Research, 2009)

Reducing the misclassification effect should therefore include checks for successful calibration and GPS quality. Striations or “corduroy” effects in the lidar surface models (as in Figure 24) may be another indicator of poor calibration, poor GPS data, or a noisy platform and should be cause for further checks.

However, better calibration will not eliminate the inherent error between individual lidar points or lines of lidar points, which may lead to some misclassification depending on the parameters set up in the classification routine and the distance between the laser returns. Consequently, careful examination of point classification methods will remain desirable whenever lidar is used to detect and discriminate small ground features.

4 Results of Increasing Ground Point Density on Feature Detection

This section examines the results of a preliminary reclassification of the lidar points to add more of the “non-ground” points back into the lidar surface model. The objective of this test was not to develop a recommended reclassification method. Rather, this test was intended to determine whether adding the maximum possible number of points back into the surface model would improve feature detection enough to warrant further investigation.

4.1 Potential Reclassification Methods

TerraScan allows two straightforward approaches to changing point classification. First, iteration distance could be increased and/or iteration angle could be lowered, and second, all points within a given distance of the initial surface could be classified as ground.

Either of these approaches would classify more points as ground returns, and could increase the resolution of the resulting surfaces. Both would add noise due to small measurement errors and low vegetation. Noise effects have been documented in earlier work, and have been seen in lidar models of smooth ground surfaces at the ESTCP WAA demonstration sites, as shown in Figure 24.

Figure 24: Noise Effects in Lidar Surface Models

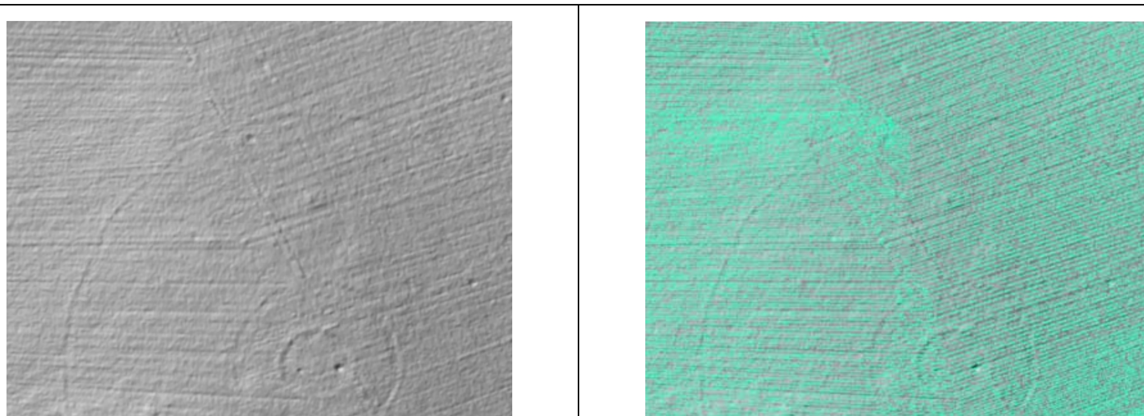

Former Camp Beale site. Surface noise appears as “corduroy” effect. Addition of the lidar points to the image (right) shows that the “corduroy” lines are associated with the small elevation differences (approximately 5 cm) between the lines of lidar points.

4.2 Reclassification Test

Methodology. For this initial test, 59 test areas were established where the original lidar surface models showed ground features such as individual potential craters. In all but three of these plots, the identified features were either completely or partially under tree cover. Features under tree cover were chosen since this is where reclassification would have the most utility. (Features in the open can always be examined using the full lidar data set.)

The lidar points at the Former Camp Beale site were reclassified such that all points within 40 cm of the ground surface using the vendor-classified points were reclassified as ground points. This distance was chosen based on specific conditions of this site to include as many points as

possible without adding higher vegetation. These operations were performed using ArcGIS, and mimic the similar process in TerraScan.

Lidar surface models were created using the reclassified points. The surface models using the reclassified points were compared to those made using the vendor's original classification. The aim of the examination was to determine 1) whether the existing features showed more clearly in the reclassified surface, and 2) whether additional features were visible.

Results. New surface models using the reclassified points showed the previously-identified features in somewhat greater detail, and revealed potential additional features at 21 of the 59 plots (36 percent). It should be emphasized that these potential features were all small, and none were shown with great clarity. Some may be debris lying on the ground. These additional features did, however, indicate areas where additional investigation would be warranted. A representative sample of the initial results is shown in Figure 25. The full data set, including orthophotos for each of the test areas, is shown in Appendix A.

Figure 25: Surface Models Using Reclassified Points – Initial Comparisons

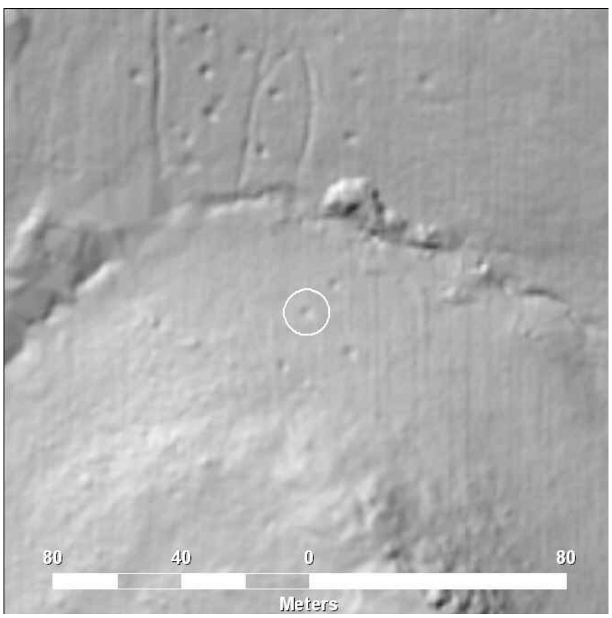	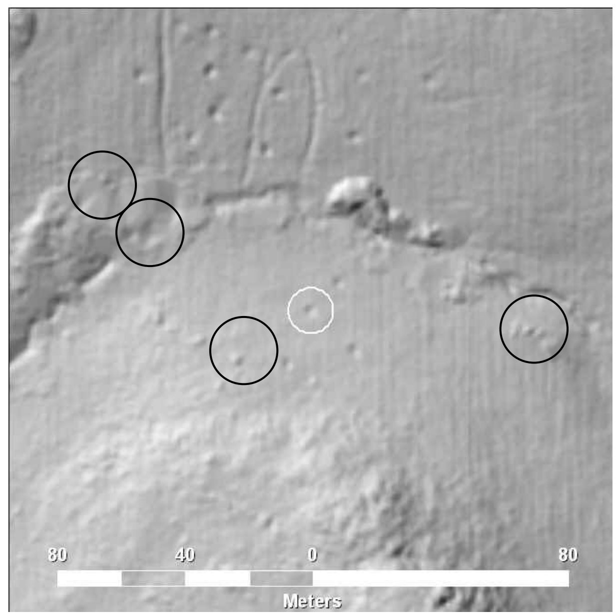
Plot 1: Vendor-classified points.	Plot 1: Re-classified points.

Figure 25: Surface Models Using Reclassified Points – Initial Comparisons (continued)

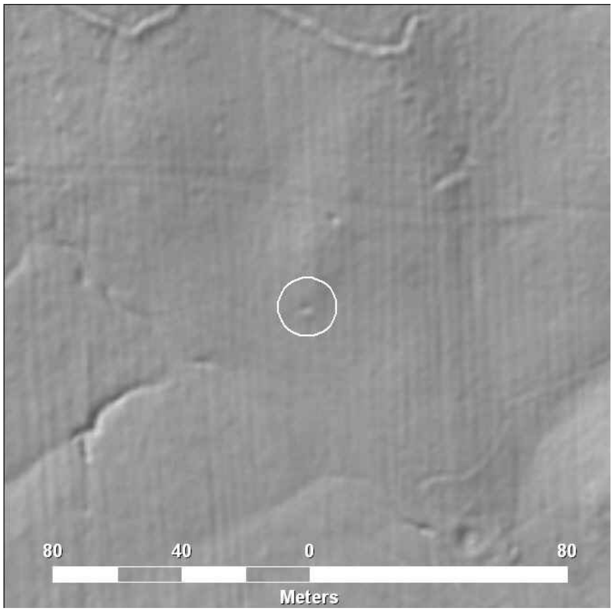

Plot 2: Vendor-classified points.

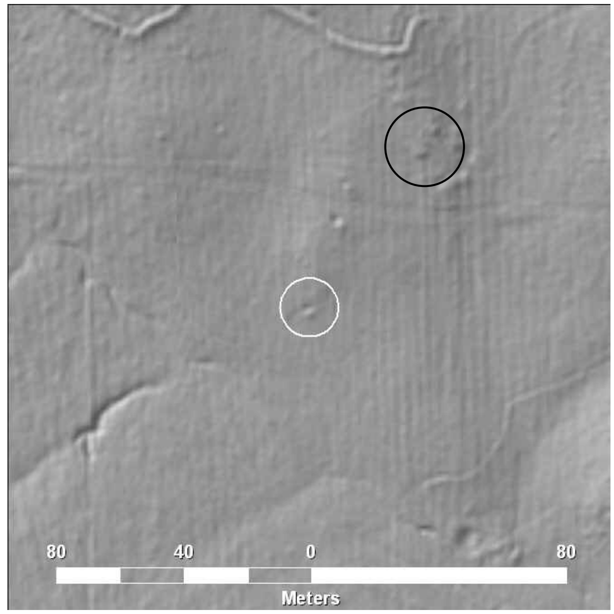

Plot 2: Re-classified points.

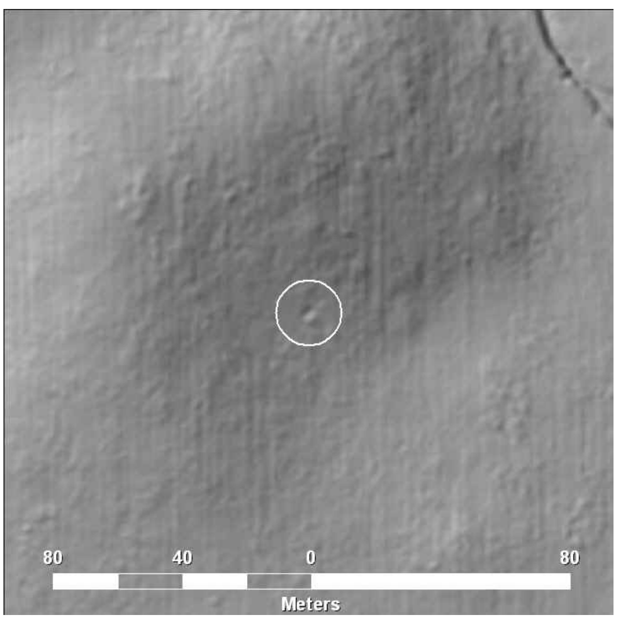

Plot 3: Vendor-classified points.

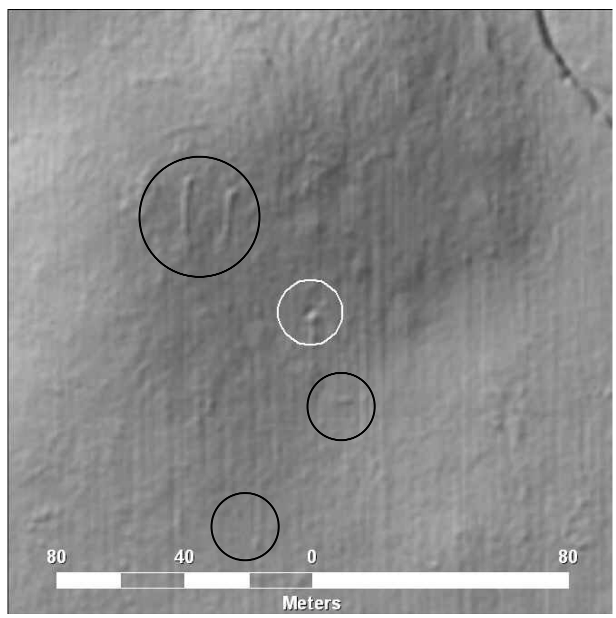

Plot 3: Re-classified points.

Figure 25: Surface Models Using Reclassified Points – Initial Comparisons (continued)

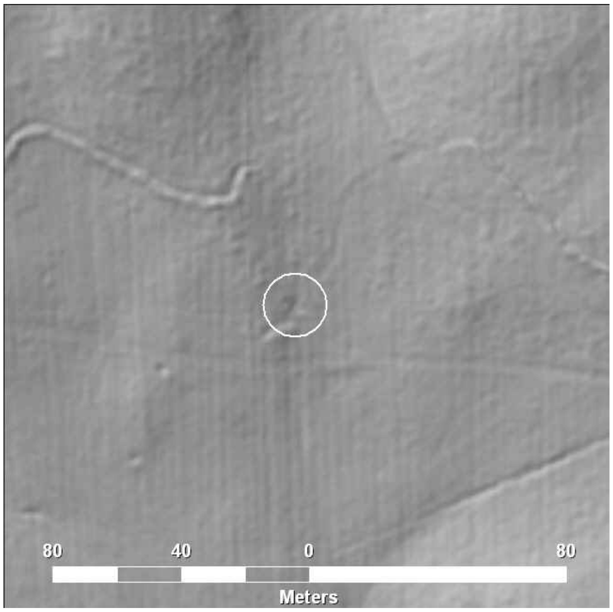

Plot 4: Vendor-classified points.

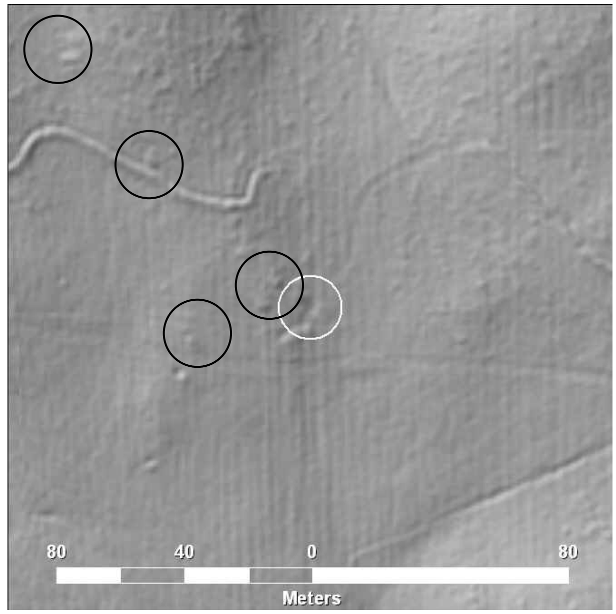

Plot 4: Re-classified points.

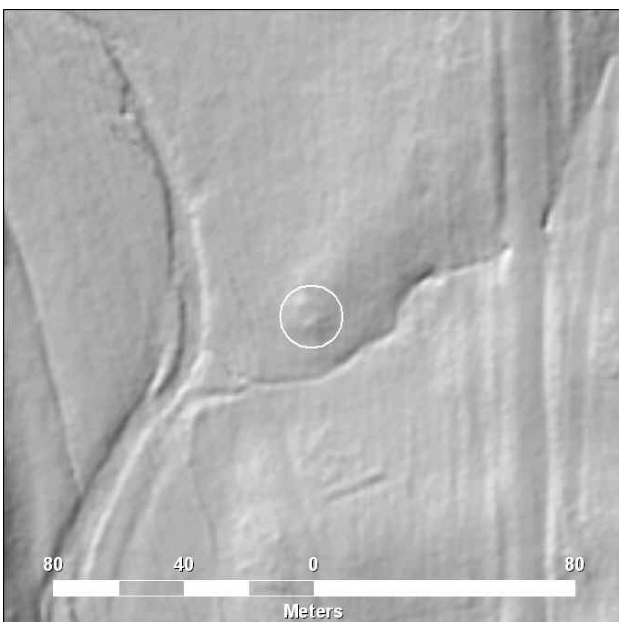

Plot 5: Vendor-classified points.

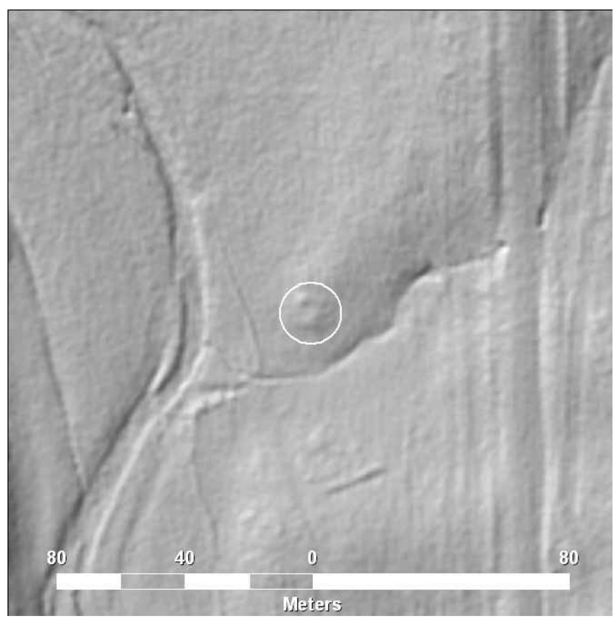

Plot 5: Re-classified points.

Figure 25: Surface Models Using Reclassified Points – Initial Comparisons (continued)

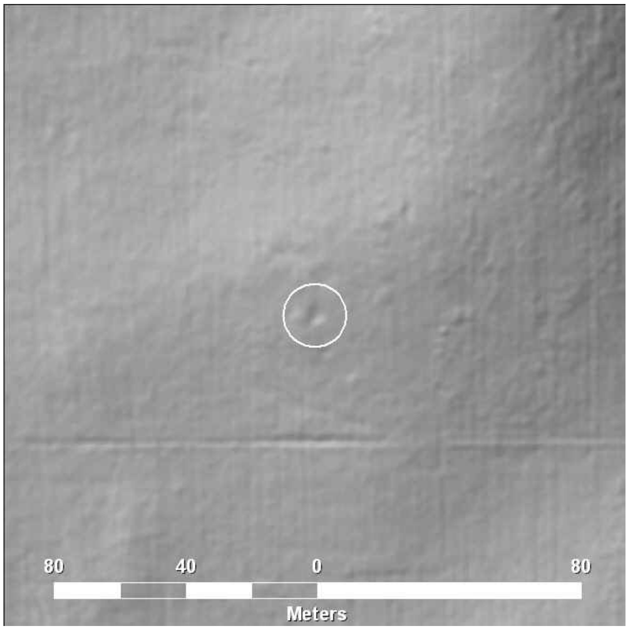

Plot 6: Vendor-classified points.

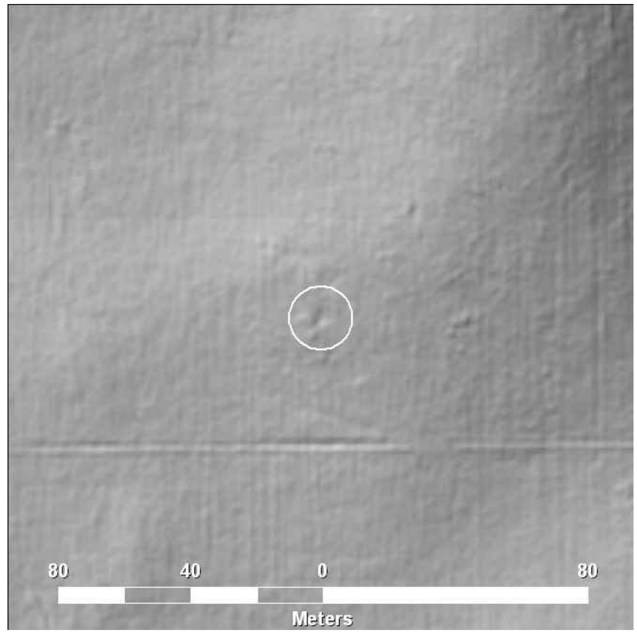

Plot 6: Re-classified points.

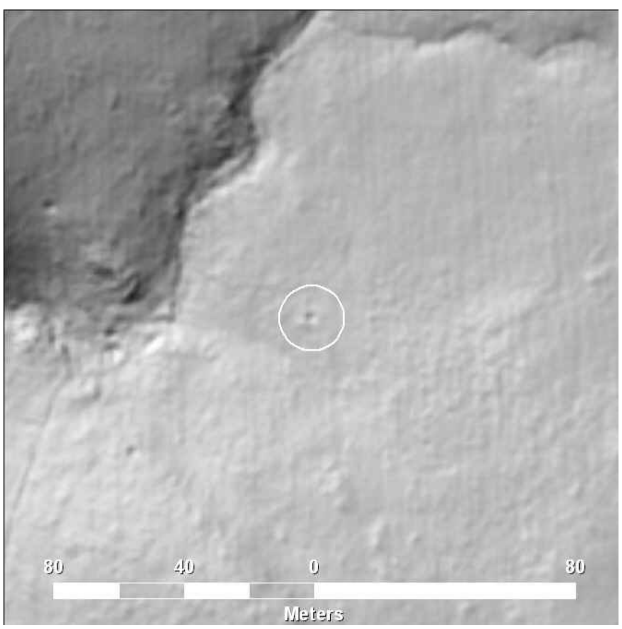

Plot 7: Vendor-classified points.

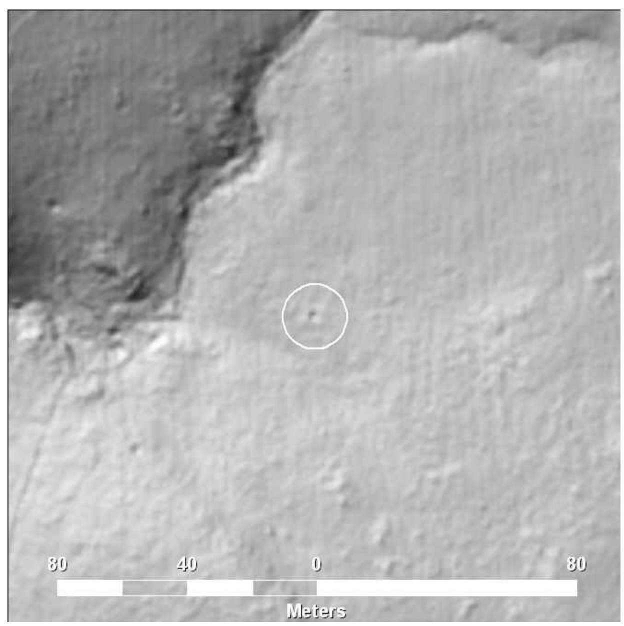

Plot 7: Re-classified points.

Figure 25: Surface Models Using Reclassified Points – Initial Comparisons (continued)

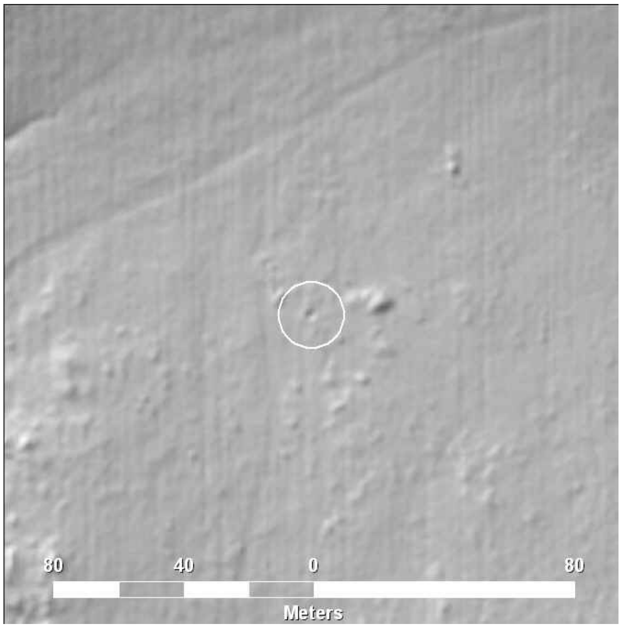

Plot 8: Vendor-classified points.

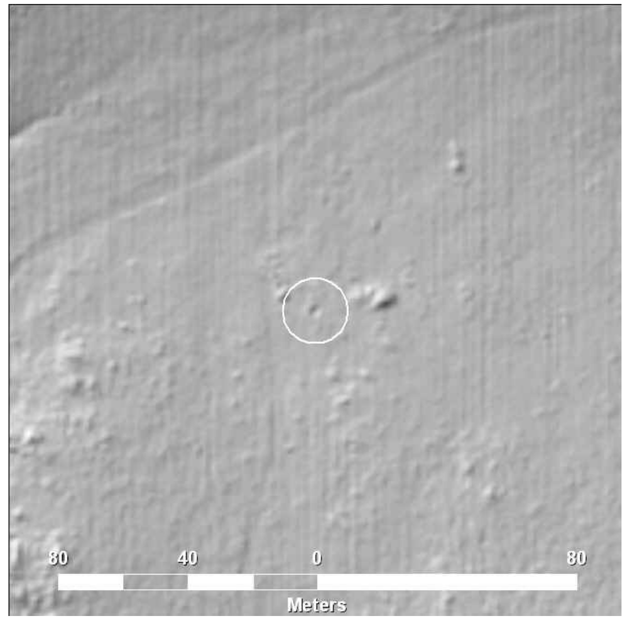

Plot 8: Re-classified points.

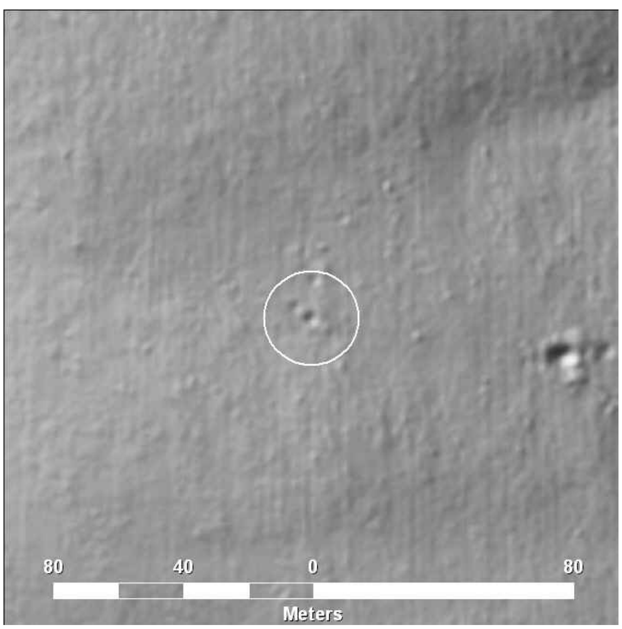

Plot 9: Vendor-classified points.

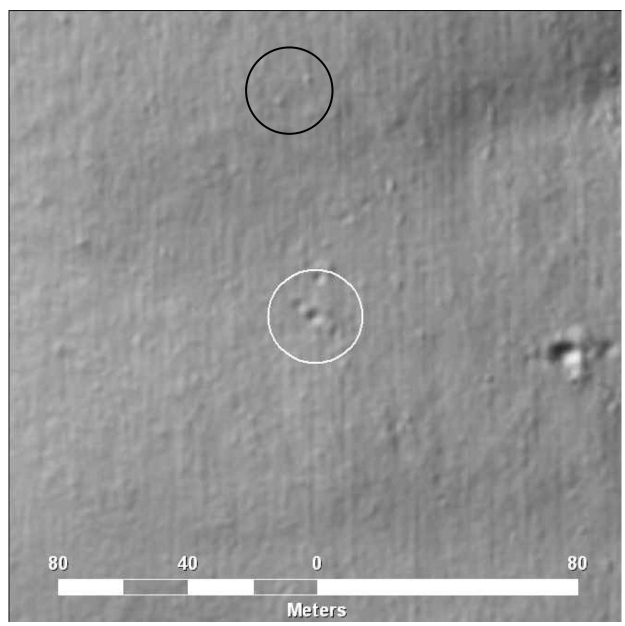

Plot 9: Re-classified points.

As a second test, the surface models for nine test areas were re-created using a 0.3 m (1-foot) cell size rather than the original 1.0 m cell size used for all of the ESTCP demonstration sites. Surface models can be created with cells of any size, and smaller cells will yield more sharply-

defined features. This ability is limited by the density of the underlying data, and in some cases the additional detail can be misleading.

New surface models were created using both the vendor's classification and the reclassified data. In this test, the 0.3 m cells showed the features with more clarity, as expected. The surfaces created with the reclassified points showed additional small features in the same manner as those at the 1.0 m cell size. The pattern of additional small features detected was somewhat different, with more features detected using the smaller cell size (Figure 26). Some of the additional features appeared to be downed tree trunks, although most could not be clearly identified.

Figure 26: Surface Models Using Reclassified Points – Comparisons Using Smaller Cell Sizes

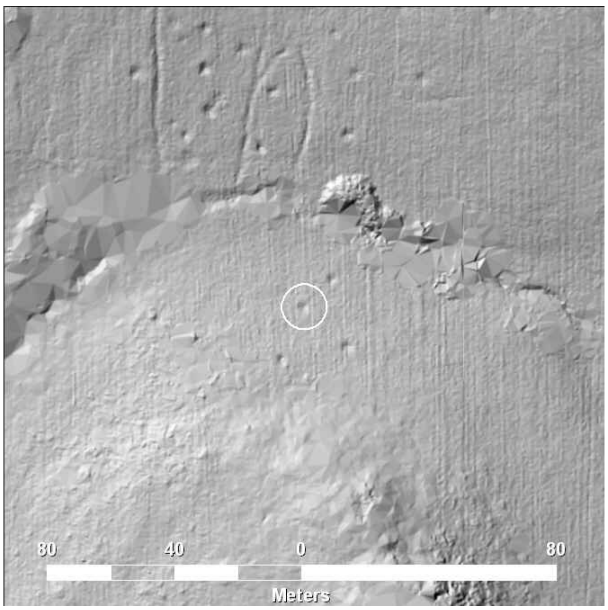	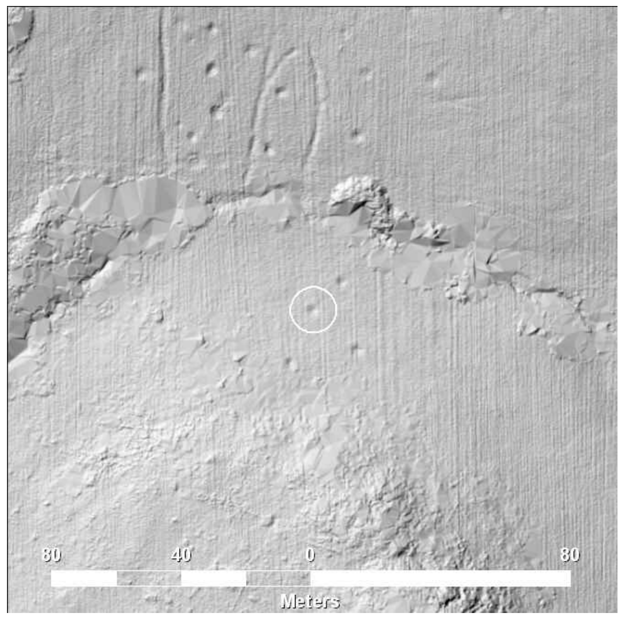
Plot 1: Vendor-classified points, 0.3m grid size.	Plot 1: Reclassified points, 0.3m grid size.

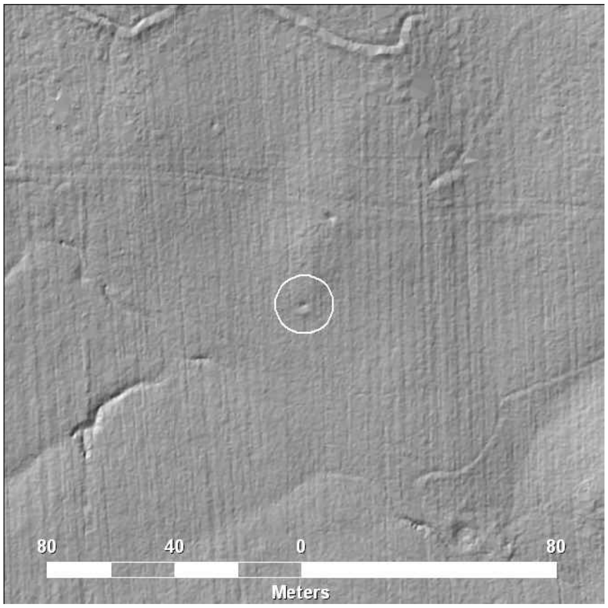	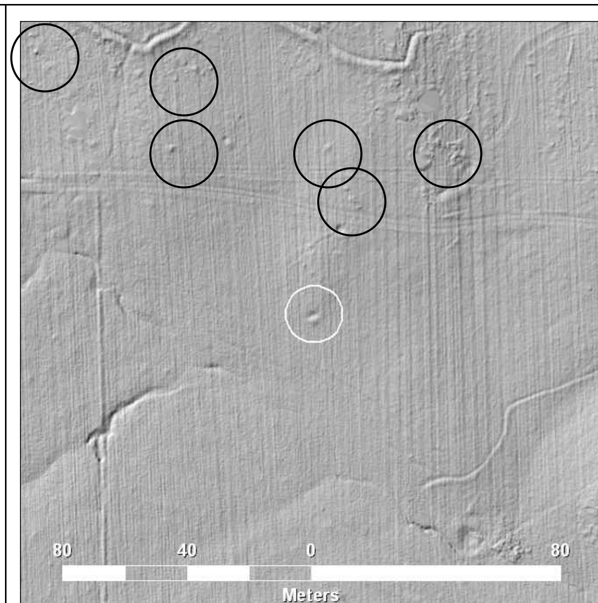
Plot 2: Vendor-classified points, 0.3m grid size.	Plot 2: Reclassified points, 0.3m grid size.

**Figure 26: Surface Models Using Reclassified Points –
Comparisons Using Smaller Cell Sizes (continued)**

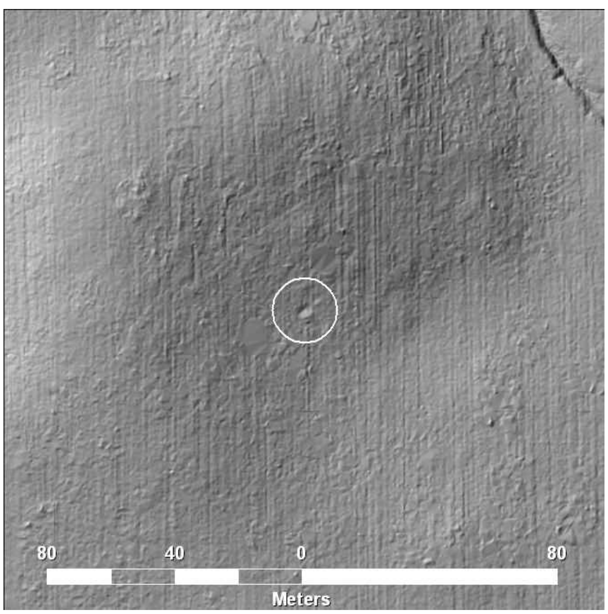	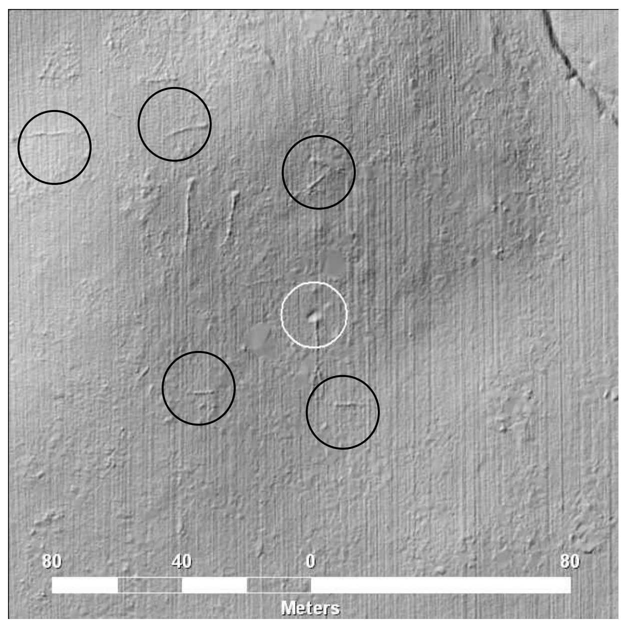
Plot 3: Vendor-classified points, 0.3m grid size.	Plot 3: Reclassified points, 0.3m grid size.

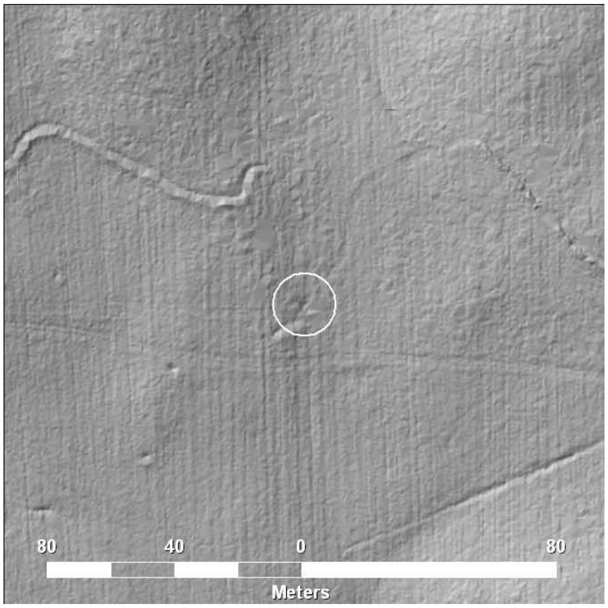

Plot 4: Vendor-classified points, 0.3m grid size.

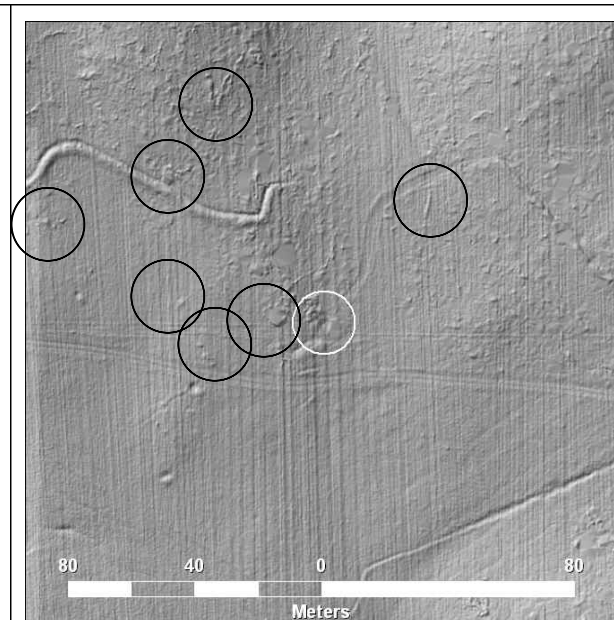

Plot 4: Reclassified points, 0.3m grid size.

Figure 26: Surface Models Using Reclassified Points – Comparisons Using Smaller Cell Sizes (continued)

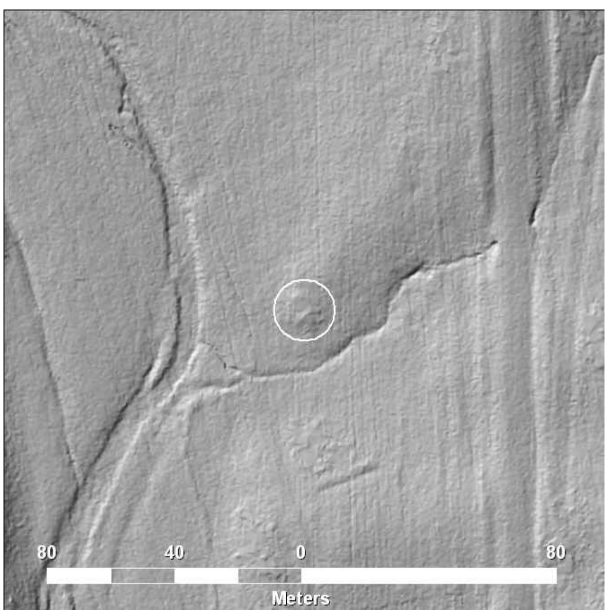

Plot 5: Vendor-classified points, 0.3m grid size.

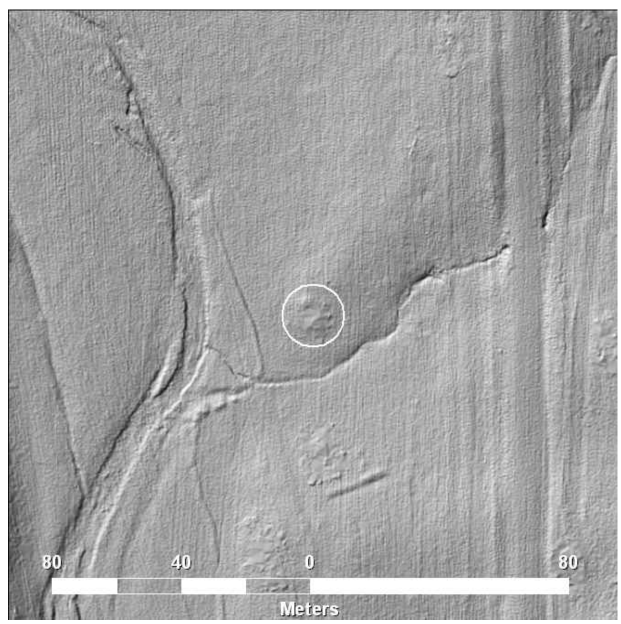

Plot 5: Reclassified points, 0.3m grid size.

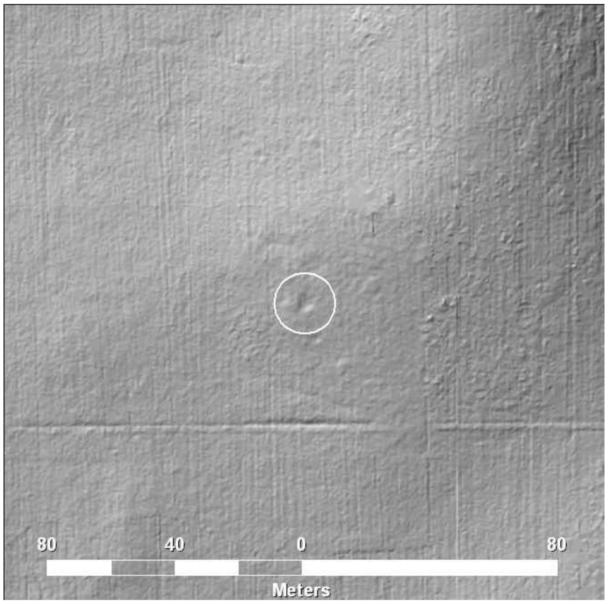

Plot 6: Vendor-classified points, 0.3m grid size.

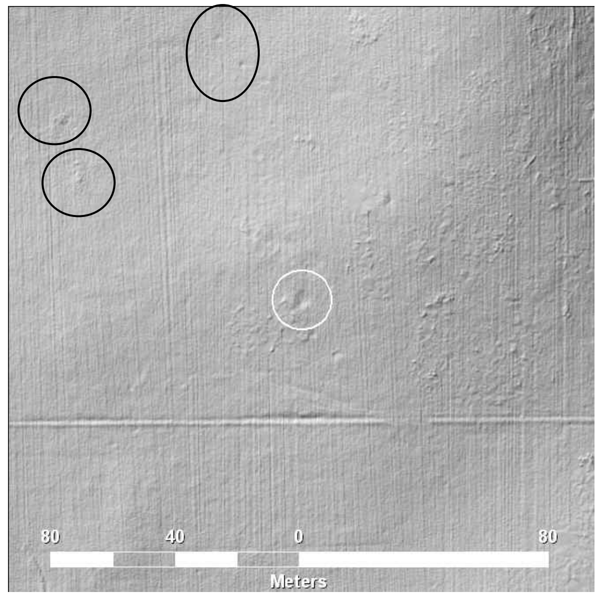

Plot 6: Reclassified points, 0.3m grid size.

Figure 26: Surface Models Using Reclassified Points – Comparisons Using Smaller Cell Sizes (continued)

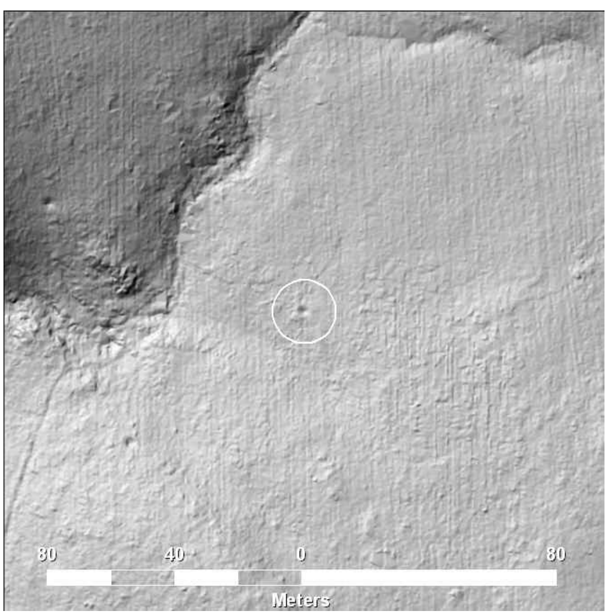

Plot 7: Vendor-classified points, 0.3m grid size.

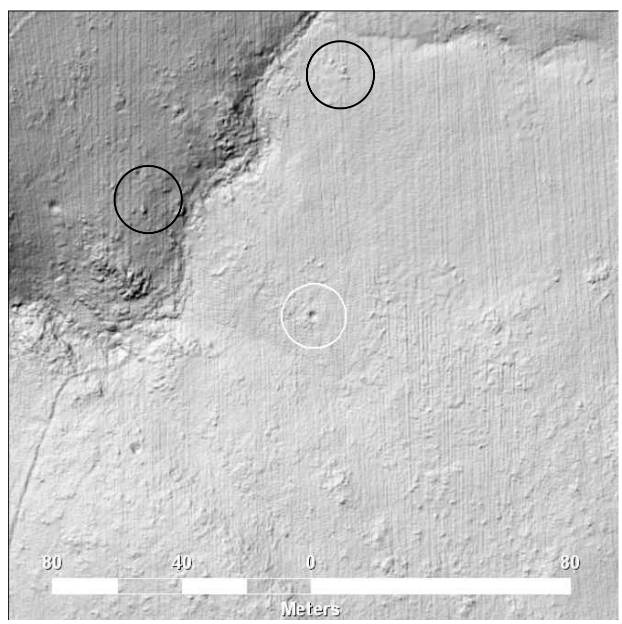

Plot 7: Reclassified points, 0.3m grid size.

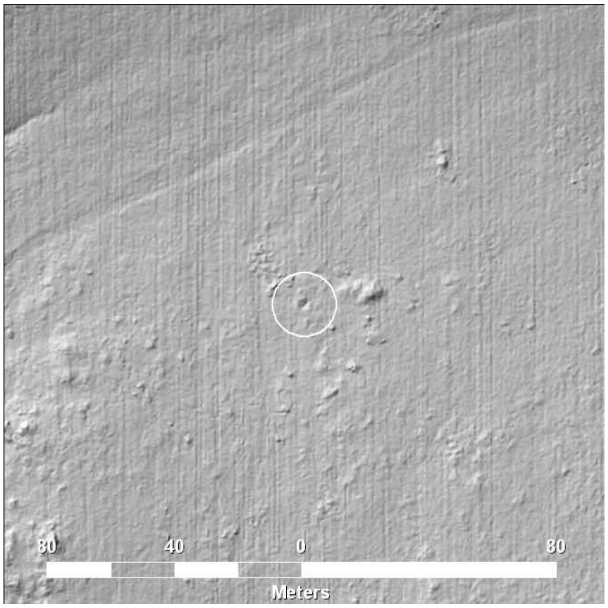

Plot 8: Vendor-classified points, 0.3m grid size.

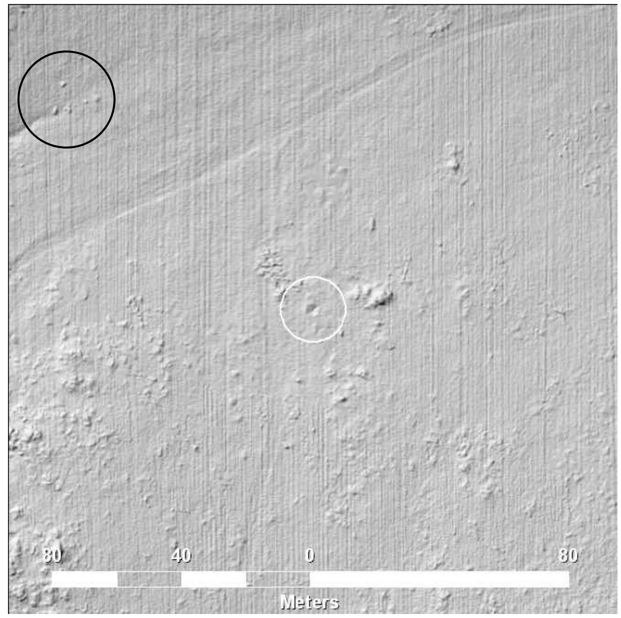

Plot 8: Reclassified points, 0.3m grid size.

Figure 26: Surface Models Using Reclassified Points – Comparisons Using Smaller Cell Sizes (continued)

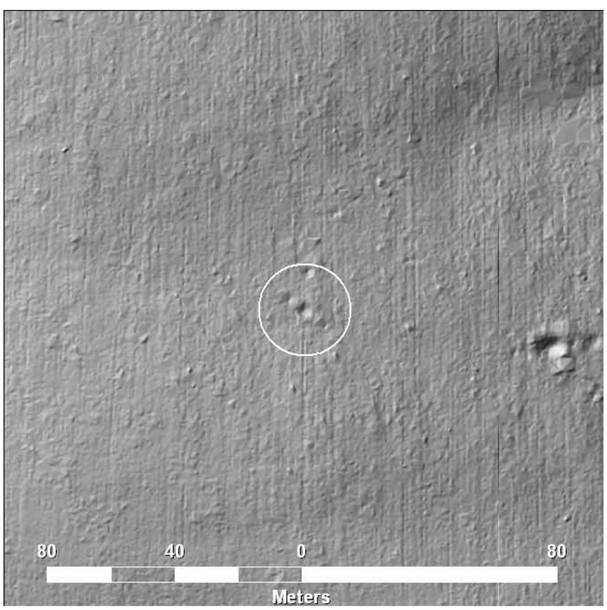

Plot 9: Vendor-classified points, 0.3m grid size.

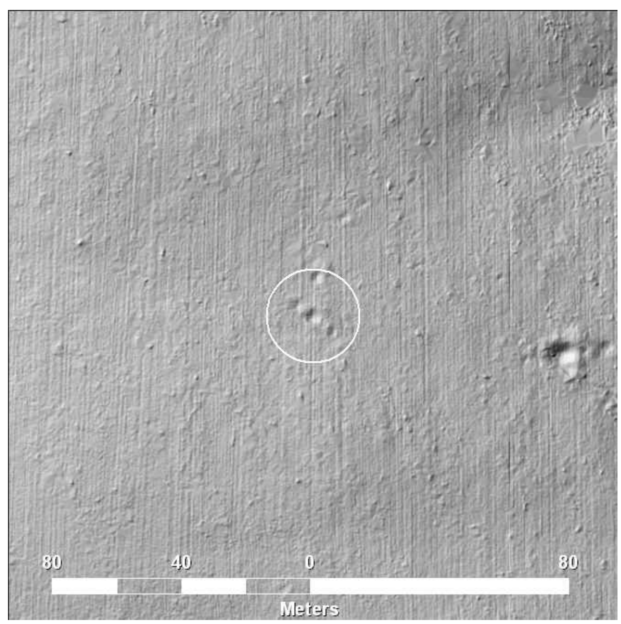

Plot 9: Reclassified points, 0.3m grid size.

A third comparison was made between the vendor-classified and reclassified data by changing the process for creating the ground surface models. At all of the ESTCP demonstration sites, surface models were created by first creating a TIN using every laser return as the vertex of the triangles. Surface models were then created from the TINs. This method was chosen since it

uses every available laser return to create the initial model from which the surfaces are derived. The alternative to this method is to use one of several methods to mathematically interpolate surfaces directly from the points.

Several interpolation approaches were compared to the TIN method during the Kirtland AFB PBR demonstration site investigation, and no significant difference was found (URS 2007b). For the Former Camp Beale data, surfaces were created for three test areas using ArcGIS Inverse Distance Weighted interpolation method, using the default settings. This comparison was repeated using a 1.0 m and a 0.3 m cell size.

Unlike the Kirtland data, the interpolated surfaces showed more features than the TIN-derived surfaces at two of the three test areas. The reason for this difference between the Former Camp Beale data and the Kirtland data is not clear, and further investigation would be warranted.

As with the TIN-derived surfaces, using the reclassified points showed the existing features more clearly, and showed additional small features (Figure 27). Changing the cell size to 0.3 m resulted in clearer definition of the features that were shown (Figure 28)

Figure 27: Surface Models Using Reclassified Points – Comparisons Using Interpolated Surfaces, 1.0 m cell size

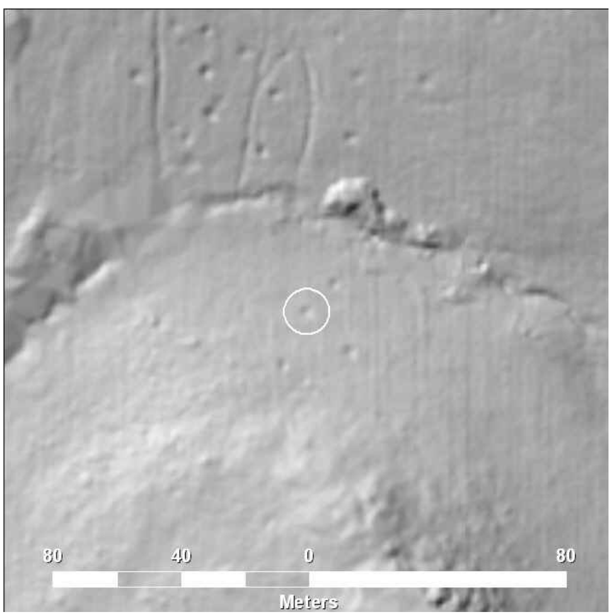	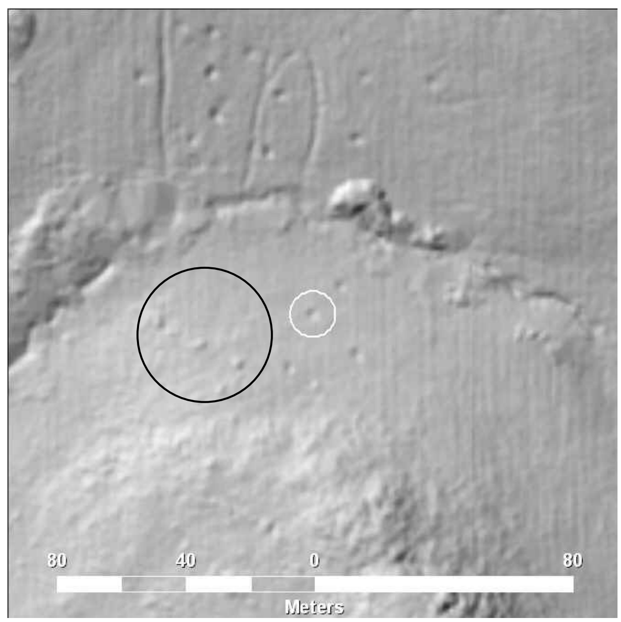
Plot 1: Vendor classified points, TIN-derived surface. Repeated from Figure 26.	Plot 1: Reclassified points, TIN-derived surface. Repeated from Figure 26.

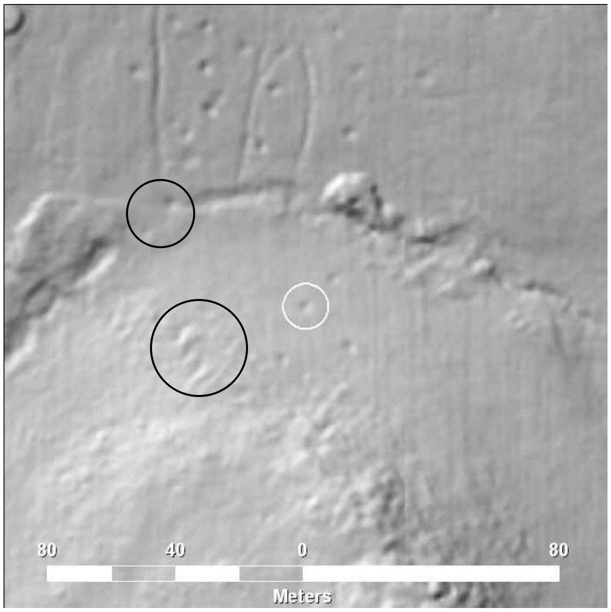

Plot 1: Vendor classified points, interpolated surface. The interpolated surface shows some features not visible in the TIN-derived surface above.

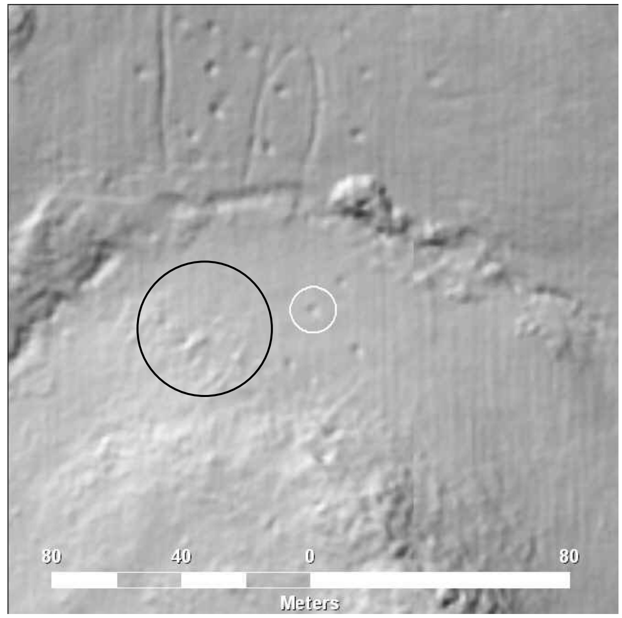

Plot 1: Reclassified points, interpolated surface. The interpolated surface gives a different interpretation of the three small features shown in the TIN-derived surface above.

Figure 27: Surface Models Using Reclassified Points – Comparisons Using Interpolated Surfaces, 1.0 m cell size (continued)

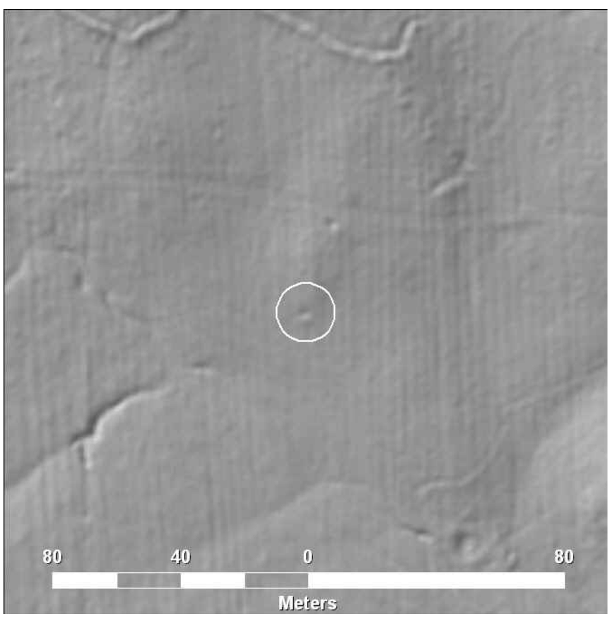

Plot 2: Vendor classified points, TIN-derived surface. Repeated from Figure 26.

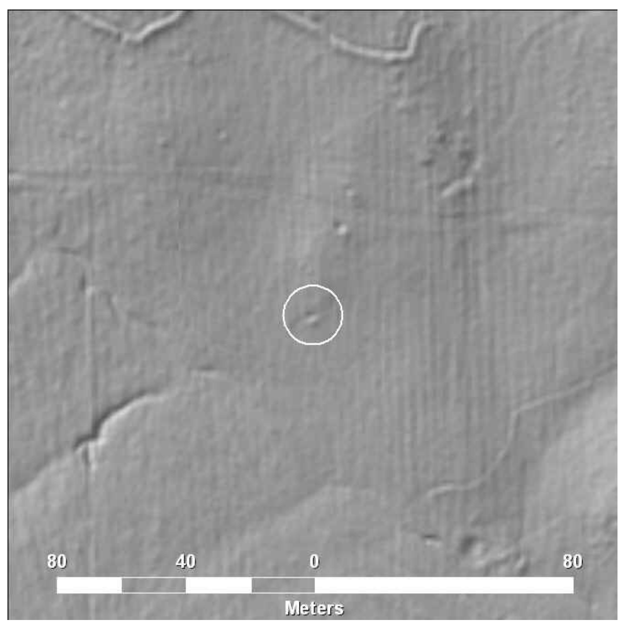

Plot 2: Reclassified points, TIN-derived surface. Repeated from Figure 26.

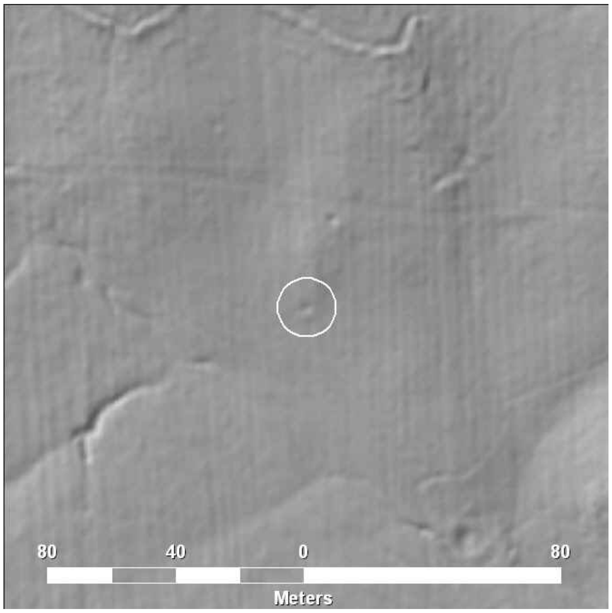

Plot 2: Vendor classified points, interpolated surface. The TIN and interpolated surfaces are similar.

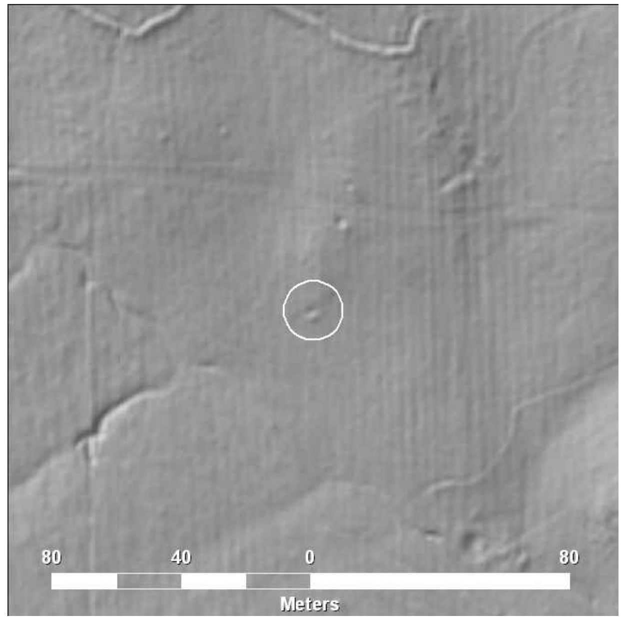

Plot 2: Reclassified points, interpolated surface.

Figure 27: Surface Models Using Reclassified Points – Comparisons Using Interpolated Surfaces, 1.0 m cell size (continued)

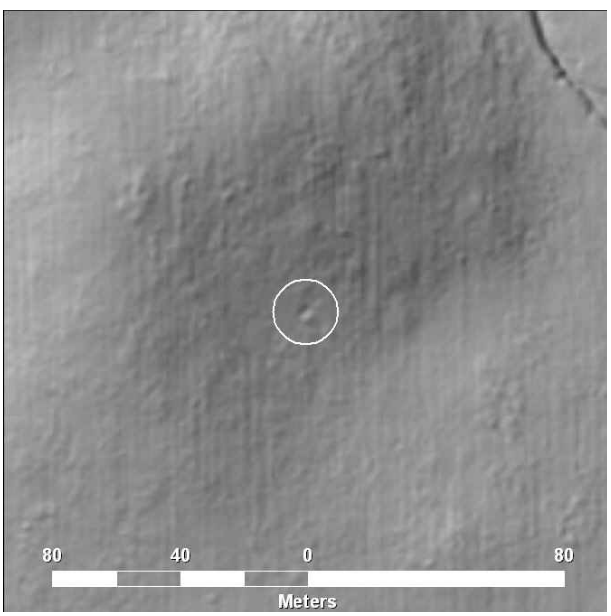

Plot 3: Vendor classified points, TIN-derived surface. Repeated from Figure 26.

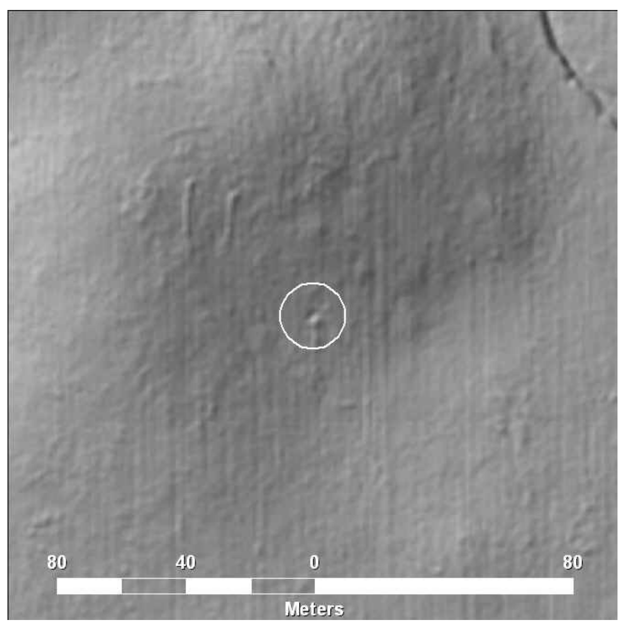

Plot 3: Reclassified points, TIN-derived surface. Repeated from Figure 26.

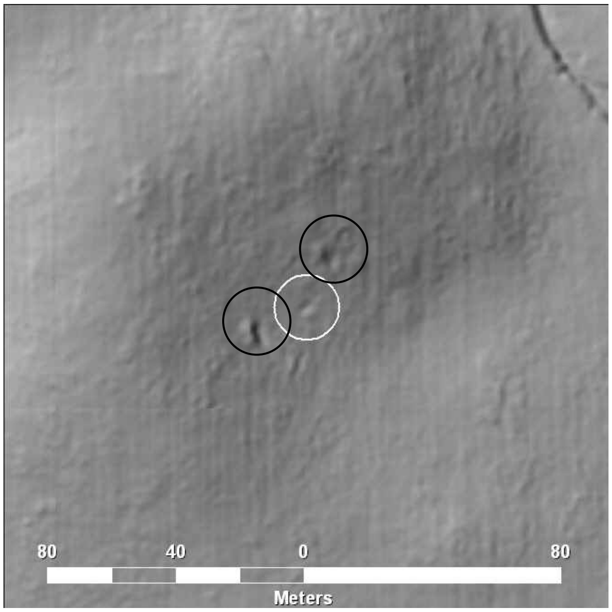	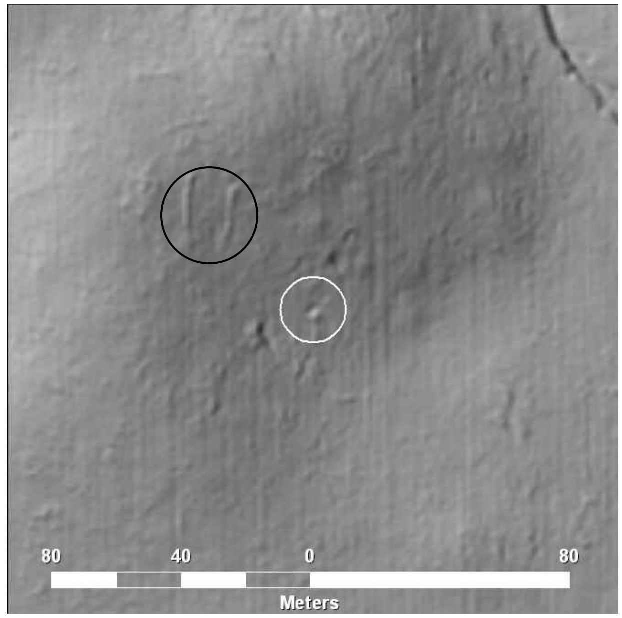
Plot 3: Vendor classified points, interpolated surface. The interpolated surface shows features not visible in the TIN-derived surface above.	Plot 3 – Reclassified points, interpolated surface. As with the TIN-derived surface above, the interpolated surface shows what appears to be down trees.

Figure 28: Surface Models Using Reclassified Points – Comparisons Using Interpolated Surfaces, 0.3 m cell size

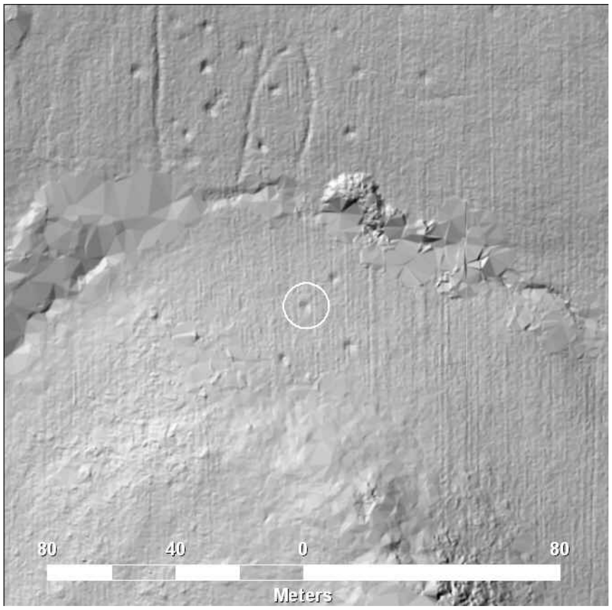	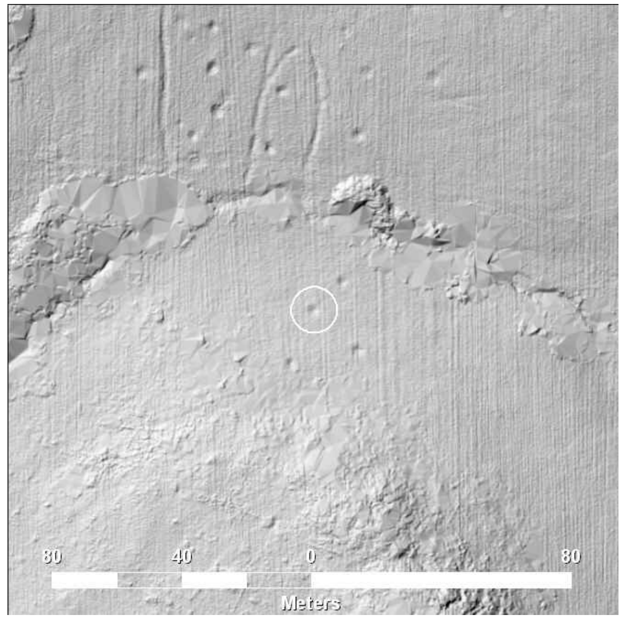
Plot 1: Vendor classified points, TIN-derived surface, 0.3m cell size. Repeated from Figure 27.	Plot 1: Reclassified points, TIN-derived surface, 0.3m cell size. Repeated from Figure 27.
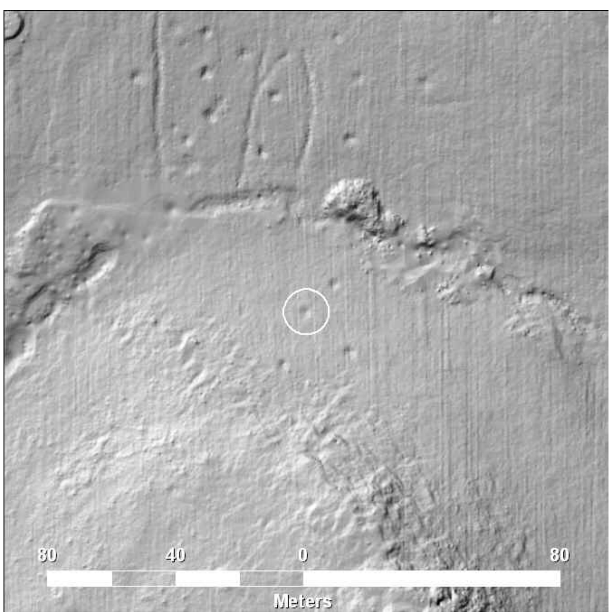	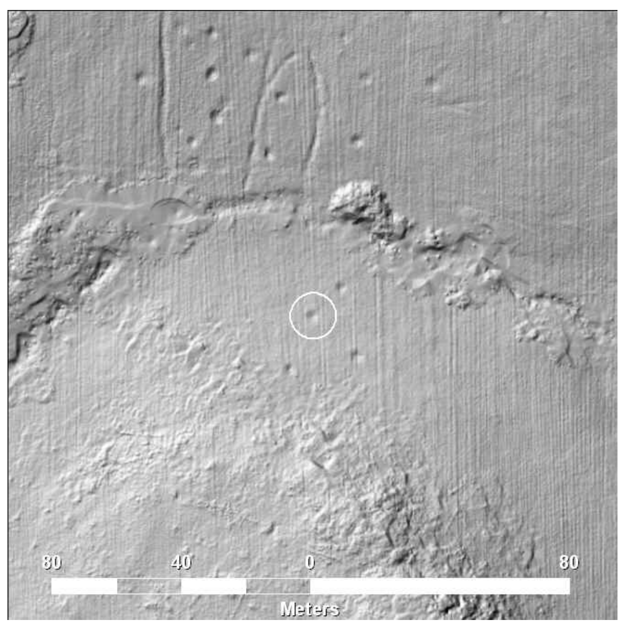
Plot 1: Vendor classified points, interpolated surface, 0.3m cell size.	Plot 1: Reclassified points, interpolated surface, 0.3m cell size.

**Figure 28: Surface Models Using Reclassified Points –
Comparisons Using Interpolated Surfaces, 0.3m cell size (continued)**

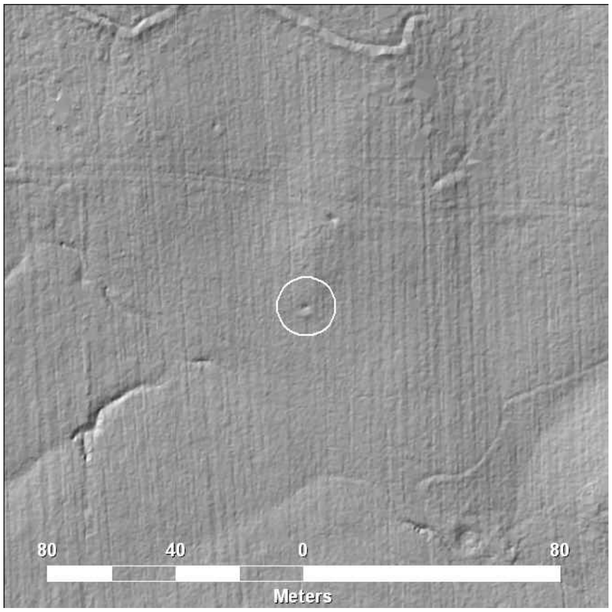

Plot 2: Vendor classified points, TIN-derived surface, 0.3m cell size. Repeated from Figure 27.

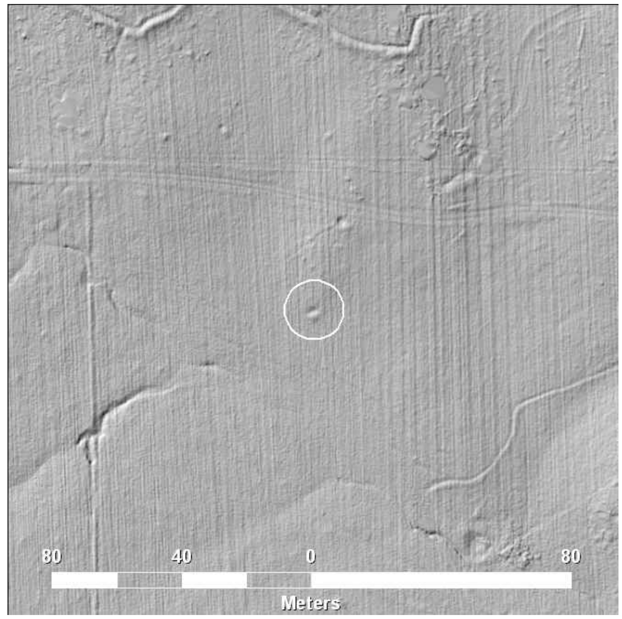

Plot 2: Reclassified points, TIN-derived surface, 0.3m cell size. Repeated from Figure 27.

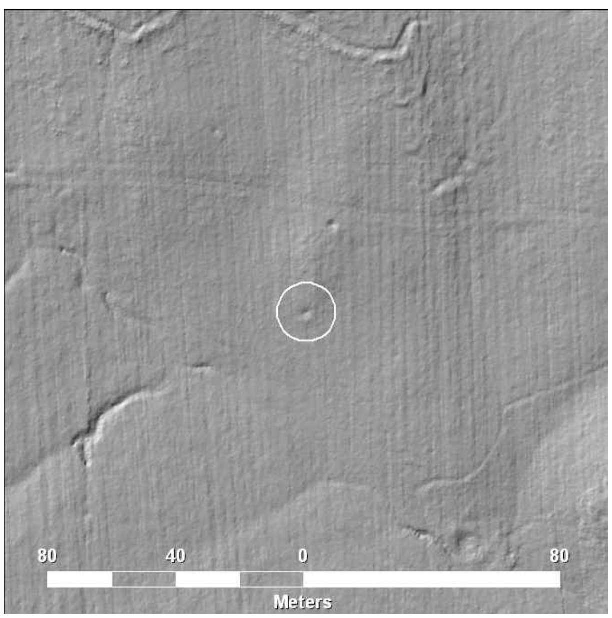

Plot 2: Vendor classified points, interpolated surface, 0.3m cell size. As with the 1.0m cells, the TIN and interpolated surfaces are similar.

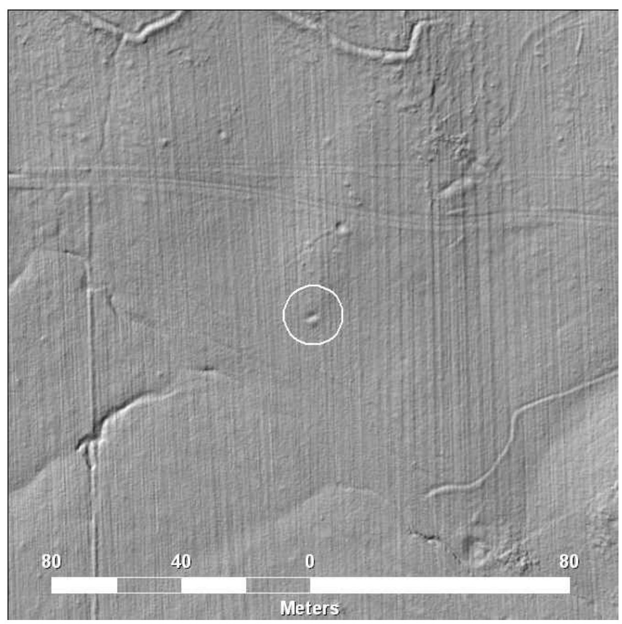

Plot 2: Reclassified points, interpolated surface, 0.3m cell size.

**Figure 28: Surface Models Using Reclassified Points –
Comparisons Using Interpolated Surfaces, 0.3m cell size (continued)**

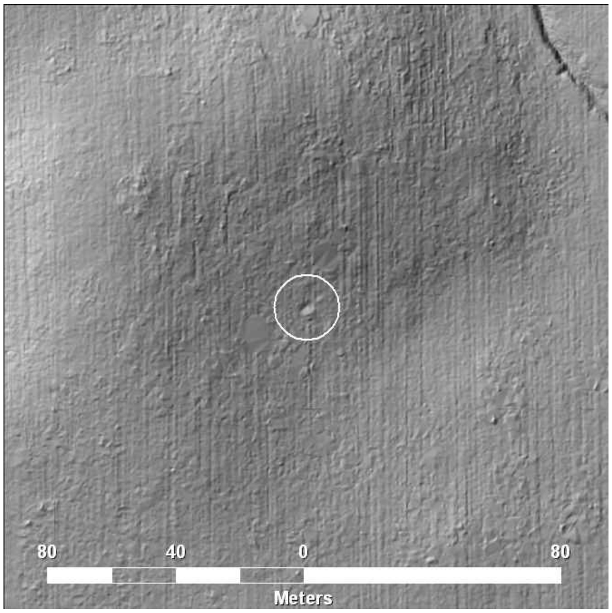

Plot 3: Vendor classified points, TIN-derived surface, 0.3m cell size. Repeated from Figure 27.

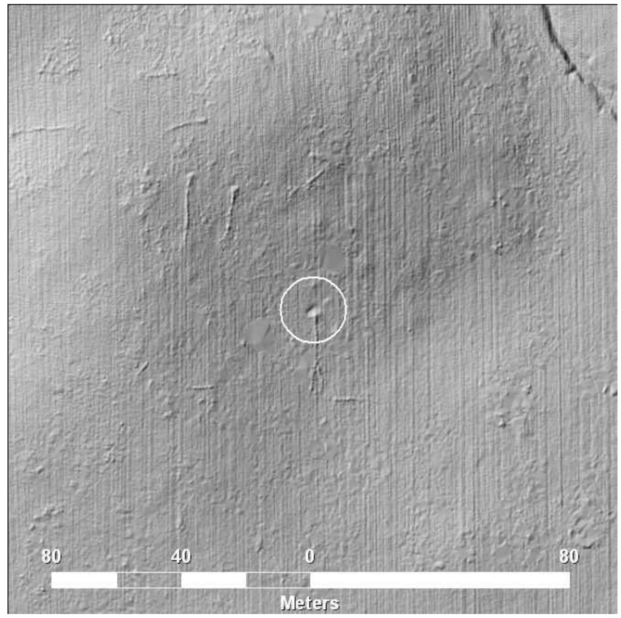

Plot 2: Reclassified points, TIN-derived surface, 0.3m cell size. Repeated from Figure 27.

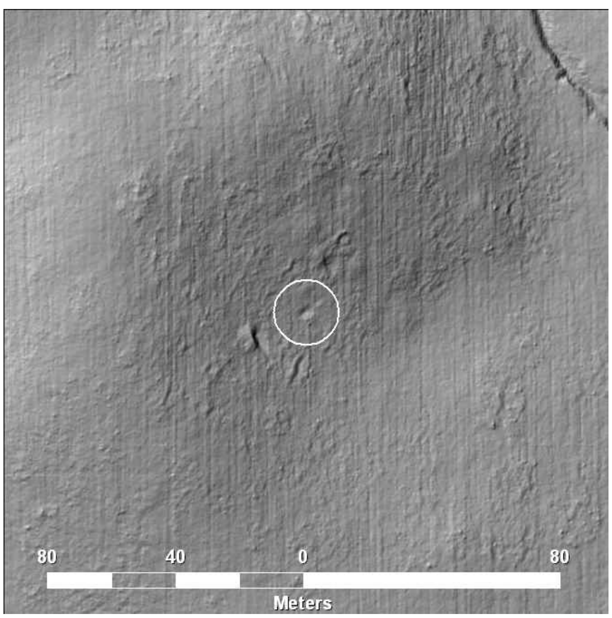

Plot 3: Vendor classified points, interpolated surface, 0.3m cell size. As with the 1.0m cells, the interpolated surface shows features not visible in the TIN-derived surface.

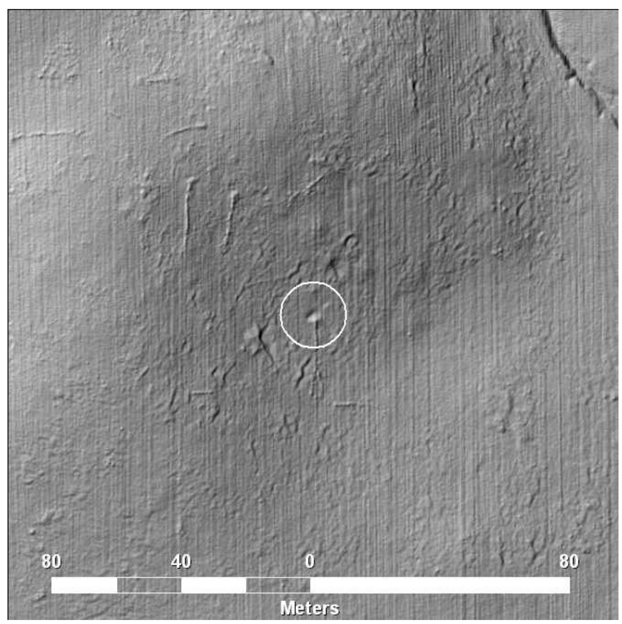

Plot 3: Reclassified points, interpolated surface, 0.3m cell size.

A final comparison was made between the all-points and ground-points surface models in the area of the 1.5 and 0.3 m test craters that were established as part of the lidar investigation at the Former Camp Beale site. The test craters were established in an area with little to no vegetation, so reclassification would be equivalent to using the full data set. As with the other comparisons, the features were somewhat more clearly defined using the reclassified points and the surface included more noise (the corduroy lines). However, no additional features were seen (Figure 29).

Figure 29: Surface Model Compound: Test Craters

Left: Former Camp Beale test craters, orthophoto.

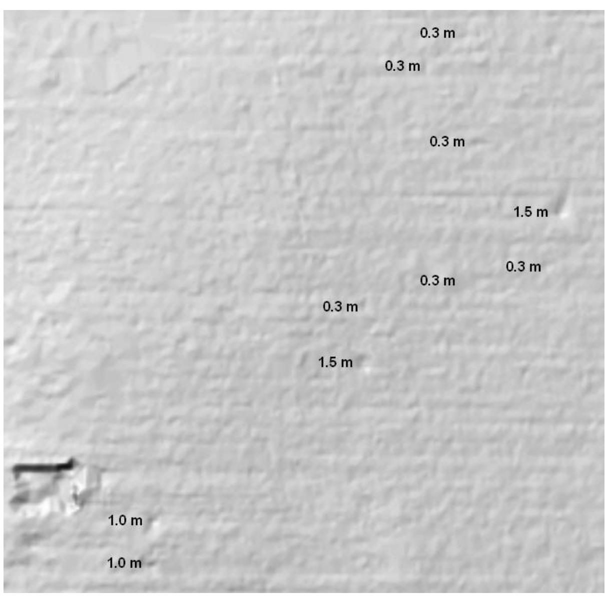

Former Camp Beale test craters, surface model based on vendor-classified ground points.

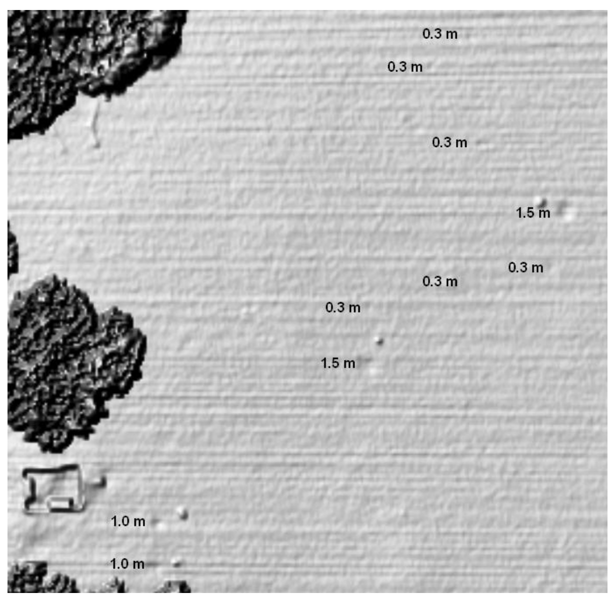

Former Camp Beale full lidar data set. Features are more clearly defined, but no additional features are seen. Noise effects are more visible.

5 Conclusions

Lidar has been shown to be an effective tool for UXO/MEC WAA. The focus of this investigation is to determine whether adjustments to the point classification can increase the detection capability and thereby increase the effectiveness of this technology. Preliminary results indicate that some increase in detection capability can be achieved.

At the Former Camp Beale demonstration site, large numbers of laser returns from the ground surface were classified by the vendor as non-ground. This effect correlated strongly with the density of the lidar points. In local areas of very high lidar point density, over 90 percent of the points were classified as non-ground, even on paved road surfaces. The effect appears to be the result of commonly-used point classification algorithms interacting with local areas of high lidar data density.

This interaction of the point classification methods with increased lidar point density has the effect of reducing the effectiveness of newer, faster sensors. Newer equipment produces a higher number of laser pulses per second, but at least on some sites, much of this additional data could be classified as non-ground.

The practical impact of this over-classification of non-ground points will depend on the site. At desert sites with little vegetation, the effect will be smaller since the ground surface can be modeled using the full lidar data set. At sites with more vegetation, the ground surface must be modeled using the ground returns in order to eliminate vegetation (or buildings), and the effect will be more pronounced.

The effect can be eliminated by changing the settings in the standard classification software. Doing so would add additional points to the ground surface model, along with additional noise. An additional approach, not tested in this paper, would be to reduce the vertical discrepancies in the lidar data closer to the inherent noise level. It is logical to suspect that tighter calibration, especially between flight lines, could reduce misclassification and result in a larger number of points classified as ground, even without changing the point classification routine.

A preliminary test of reclassifying the lowest points as ground returns showed that reclassification may reveal some additional features. These additional features are all small, since the vendor-classified ground points are sufficiently dense to reveal larger features. Most of these features could not be identified, and some appeared to be debris such as down tree trunks.

These results indicate that adjustment of the vendor’s classification methods to increase the density of the surface model would be worthwhile. This is especially the case since such adjustment would not increase processing time or cost. The reclassification test also showed that methods used to create the surface models may be more relevant to feature detection than shown in previous investigations.

Because lidar data sets are very large, many vendors only deliver derived products such as ground surface models (DEMs) and all-points models (DTMs). The results of this investigation suggest that the Government should receive the entire lidar point data set for all lidar investigations. Using this data, Government land managers can evaluate point density patterns, apparent calibration success and the approaches to point classification to surface model creation used by the vendor, and make appropriate adjustments. T

6 References

Anderson, Hans-Erik, Stephen E. Reutebuch, and Robert J. McGaughey. 2006. A Regorous Assessment of Tree Height Measurements Obtained Using Airborne LIDAR and Conventional Field Methods. *Canadian Journal of Remote Sensing* 32(5): 355-366.

Hansen, W. and T. Vögtle. 1999. Extraktion der Geländeoberfläche aus flugzeuggetragenen Laserscanner-Aufnahmen. *Photogrammetrie Fernerkkundung Geoinformation*: 229–236. Cited in Haugerud and Harding (2001).

Haugerud, R.A. and D.J. Harding. 2001. Some Algorithms for Virtual Deforestation (VDF) of LIDAR Topographic Survey Data. *International Archives of Photogrammetry and Remote Sensing* XXXIV, Part 3/W4, Commission III: 211–217.

Kilian, J., N. Haala, and M. Englich. 1996. Capture and evaluation of airborne laser scanner data. *International Archives of Photogrammetry and Remote Sensing* XXXI, pt. B3: 383–388. Vienna, Austria.

Kraus, K. and N. Pfeifer. 1998. Determination of terrain models in wooded areas with airborne laser scanner data. *ISPRS Journal of Photogrammetry and Remote Sensing* 53: 193–203.

———. 2001. Advanced DTM Generation from Lidar Data. *International Archives of Photogrammetry and Remote Sensing* 34: 23–30.

Sky Research. 2009. Comments on ESTCP White Paper: Effects of LiDAR Point Classification Methods on Surface Model Creation and Feature Identification. Rogalla, Joy and Tom Prescott,. January 5.

Soininen, Arttu. 2005. TerraScan User's Guide. March 10. Available at www.terrasolid.fi/en.

URS Corporation. 2007a. Final Report, High Density Lidar and Orthophotography in UXO Wide Area Assessment, Kirtland and Victorville Demonstration Sites. Appendix C: Variation in Lidar Data Density and Potential Effect on Feature Identification. April.

———. 2007b. Final Report, High Density Lidar and Orthophotography in UXO Wide Area Assessment, Kirtland and Victorville Demonstration Sites. Appendix D: GIS-Based Methods for Creating Ground Surface Models from Lidar Points. April.

APPENDIX D
DRAFT GUIDANCE DOCUMENT: USING LIDAR AND ORTHOPHOTOS IN UXO WIDE AREA ASSESSMENT

Draft Guidance Document

Using Lidar and Orthophotos in UXO Wide Area Assessment

Project Number 07E-MM2-012/MM-0737

Final

January 2010

Table of Contents

Figures

TABLES

APPENDICES

Acronyms

ASPRS	American Society for Photogrammetry and Remote Sensing
CADD	computer-aided design and drafting
CSM	conceptual site model
DEM	digital elevation model
DoD	Department of Defense
DSM	digital surface model
DTM	digital terrain model
EMI	electromagnetic induction
ESTCP	Environmental Security Technology Certification Program
FEMA	Federal Emergency Management Agency
GIS	geographic information system
GPS	global positioning system
Hz	hertz
IMU	inertial measurement unit
INS	inertial navigation system
kHz	kilohertz
lidar	light detection and ranging
MRS	munitions response sites
NMAS	National Map Accuracy Standards
OB/OD	open burning/open detonation
PDOP	position dilution of precision
QA/QC	quality assurance/quality control
RAID	redundant array of independent disks
RMSE	root mean square error
TIN	triangulated irregular network
USGS	US Geological Survey
UXO	unexploded ordnance
WAA	wide area assessment

Acknowledgements

This project was made possible through funding provided by the Environmental Security Technology Certification Program. For their support and guidance to the US Army Corps of Engineers and URS on this project, we would like to express our sincere appreciation to:

- Dr. Jeffrey Marqusee, Environmental Security Technology Certification Program and Strategic Environmental Research and Development Program Director
- Dr. Anne Andrews, Environmental Security Technology Certification Program and Strategic Environmental Research and Development Program Deputy Director
- Dr. Herb Nelson, Munitions Management Program Manager, Environmental Security Technology Certification Program and Strategic Environmental Research and Development Program

We gratefully acknowledge the following for their technical review of drafts of this document:

- Terra Remote Sensing, Inc., especially David Neufeldt and David Mostyn
- Sky Research, especially Thomas Prescott and Joy Rogalla
- Terrapoint, LLC, especially Kresimir Kusevic, Shiva Shenoy, Joe Sackett and Beau Jarvis
- Karen Shuckman, URS and Instructor, Pennsylvania State University
- Bob Ryan, URS, formerly with EarthData, (now Fugro EarthData, Inc.)

1 Introduction to Lidar and Orthophotography

1.1 Objectives

This guidance document is intended to assist Government site managers who are considering the use of light detection and ranging (lidar) and orthophotography at munitions sites. The document summarizes lessons learned and describes suggested contract specifications and analysis methods for these technologies.

Lidar and orthophotography are airborne technologies that can be used to give a rapid assessment of site conditions. In the context of munitions management, lidar and orthophotos have been used to locate surface features that may indicate historic munitions use including bombing targets, crater fields, open burning/open detonation (OB/OD) areas, and smaller individual items such as craters, bunkers, and firing points.

Lidar and orthophotos are most appropriately used at the beginning of the site assessment process. These technologies are capable of assessing large areas for which historical data may be incomplete, providing an additional layer of data that can corroborate or correct historical records. The data may be used to improve the accuracy of the conceptual site model (CSM) and to prioritize and focus the use of more expensive technologies that directly detect munitions components.

1.2 Overview of Lidar and Orthophoto Technologies

1.2.1 Lidar

Airborne lidar is a well-established technology for modeling ground surfaces. The technology was first developed in the late 1960s and early 1970s, and has been used for modeling ground surfaces since the mid 1980s. Lidar has been in wide commercial use since the early 1990s, and the accuracies and limitations of lidar for surface modeling are well documented.

Lidar is based on measuring the time of return for a laser pulse from the laser to the sensor. The lidar system is mounted in a helicopter or small aircraft, and Global Positioning System (GPS) and Inertial Measurement Unit (IMU) technology are used to locate the sensor in the air. Measuring the time of return allows for the accurate calculation of the point of reflection of the laser signal from the ground, buildings, or vegetation (Figure 1).

When the laser pulse approaches the ground it is wide enough that part of the pulse may reflect from an object, while the remainder of the pulse continues to the ground or another object. Sensors can detect these multiple reflections from a single laser pulse, which increases the probability of sampling the ground surface through gaps in vegetation. Automated algorithms followed by operator inspection are used to categorize each data point as returning from the ground surface, vegetation, structures or other objects.

Lidar points have a vertical positional accuracy of approximately 15 cm and a horizontal accuracy of approximately 60 cm, both compared to surveyed control points. Accuracy will be greater at lower altitudes and on relatively flatter and harder surfaces.

Figure 1: Lidar System Operations

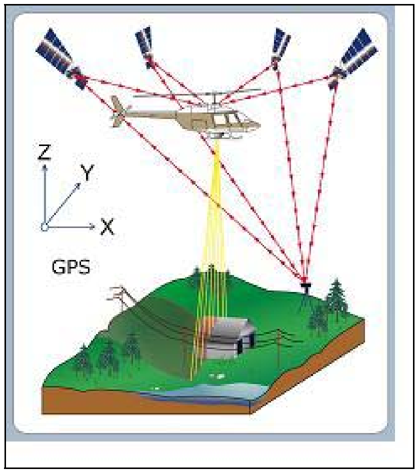

Once elevation data are collected in the form of lidar points, surface models are created and analyzed, and maps and analysis products generated. Although specialized software now exists, most analysis of lidar data can be conducted using standard Geographic Information Systems (GIS) software and methods, and some of the process can be automated.

Lidar has been become a standard tool for many applications that require detailed ground surface models, including seismic and geohazard studies; corridor and siting studies for pipelines, power lines, roads, and railroads; floodplain and other hydrology studies; and land management programs. The popularity of lidar is due to its ability to provide more accurate topographic data than other typically-available sources (such as the US Geological Survey [USGS] maps and digital data) at a reasonable cost compared to alternatives such as ground survey or photogrammetry.[1] Each application of lidar will have appropriate specifications for data collection, processing and analysis. Investigation of munitions sites using lidar and orthophotography will similarly call for appropriate specifications that may differ from other applications.

1.2.2 Orthophotography

An orthophotograph is a digital aerial photograph that has been geometrically corrected for topographic relief, lens distortion, and camera tilt. Individual digital images are first combined into a mosaic, and then the composite image is spatially corrected using sophisticated mathematical algorithms including the use of terrain data, such as data from lidar. This process, called orthorectification, allows for the accurate spatial location of each photo pixel, and this allows the images to be used in a GIS or computer-aided design and drafting (CADD) system with other spatial data such as contour lines, survey data, or the results of other investigations such as magnetometry. While orthophotos are adjusted so that the pixels are spatially accurate, this only refers to pixels representing the ground surface. Pixels representing the tops of buildings or tall trees can be slightly displaced.

[1] For instance, a recent paper examined USGS 10-m digital elevation data for the area near Seattle, Washington, and concluded that errors in the digital data would have a significant effect on standard equations for earthquake-triggered landslide assessment (Haneberg 2006).

Digital orthophotography has been commercially available since the early 1980s, with steady improvement in the resolution (i.e., pixel size) and precision (i.e., pixel placement) of the images as the technology of digital cameras, GPS, and IMU systems has advanced. Digital cameras have largely replaced film cameras in the production of orthophotos (Dold 2008).

Airborne digital cameras have been integrated with lidar sensors successfully, and because the cameras and lidar sensors use the same GPS and Inertial Navigation System (INS), the two data sets can be accurately integrated. Vendors generally guarantee a horizontal accuracy of three pixel widths compared to ground control for orthophotography, and spatial integration within two pixel widths for orthophotos and lidar.

Final orthophoto pixel size depends on flight altitude and camera specifications. For munitions sites, orthophoto pixel size is typically from 0.3 m (about 1 foot) down to 0.1 m (about 4 inches) (Nelson et al. 2008). Smaller pixel sizes than this are generally impractical due to the low flight elevations and slow flight speeds required to collect properly overlapping images, and the large numbers of images that would need to be combined into the mosaic. Many areas also have existing orthophotography available at lower resolution, with pixels in the 0.5 m – 1.0 m range.[2]

1.3 System Components

1.3.1 Lidar

Lidar systems are manufactured by several vendors worldwide, the largest of which are Optech, based in Canada, and Leica, based in Switzerland and the US. Other vendors include IGI Ltd. in Germany and Laseroptronix in Sweden. In addition, some lidar vendors assemble their own systems using standard components. Since the 1990s, lidar system development has primarily focused on increasing laser pulse rate, adding the ability to receive multiple returns from each laser pulse, and recording the intensity of each return. Each lidar system has slightly different performance specifications; however, both commercial off-the-shelf systems and vendor-built systems appear to function reliably and to meet their published specifications if used and functioning correctly. A typical lidar system is shown in Figure 2.

Lidar system components are designed to determine the position of the aircraft and the distance and angle to the point of reflection of the laser pulse. The position of the aircraft is determined using GPS and INS. GPS uses the position of at least four orbiting navigation satellites to sample the aircraft location. Measurements are taken between one and ten times per second, depending on the manufacturer and model in use (Terrapoint, 2009). Vendors report that error in the location of the aircraft is primarily GPS error, and that the most serious source of GPS error is momentary loss of satellite data sufficient to establish locations accurately (Terra Remote Sensing, 2008).

[2] States, cities and counties acquire orthophotos for a variety of purposes, not generally including detection of smaller objects. Consequently, these entities generally do not incur the considerably larger costs of higher-resolution orthophotos. These coarser images can nevertheless be useful on munitions sites with tree cover, where individual features are not visible and the primary use of the images will be overall mission planning.

Figure 2: Helicopter-Mounted Lidar and Orthophoto System

GPS antenna and lidar and orthophoto sensor pod.

Images courtesy of Terra Remote Sensing, Inc.

Operator control panel, system control and backup components.

The INS calculates the position and orientation of the aircraft between GPS locations. The primary input to the INS is from the IMU, which detects and records the rate of acceleration along with changes in rotational attributes such as pitch, roll, and yaw. The IMU generally contains three accelerometers and three gyroscopes, placed in orthogonal positions so that data is collected in all three planes. Current IMUs record these changes at 100 – 2,000 hertz (Hz) (samples per second). Small errors in the IMU positions accumulate due to IMU drift as positions are continually re-calculated until the aircraft's position is updated from the GPS.

The lidar sensor system consists of a laser, a receiver, and a mirror that directs each pulse toward the ground surface. Lidar systems typically use lasers with wavelengths of 1,000 to 1,500 nanometers. The mirror system may be rotating or oscillating, depending on the manufacturer.

The receiver is a passive device that is tuned to the frequency of the laser, which records a signal when the amplitude of light in that frequency exceeds a threshold value. The threshold value that will trigger a return is typically set by the manufacturer and is not adjustable. The position of the laser reflection is calculated using the time of return combined with the known angle of the pulse.

The sensor also records the energy level of the return, which is referred to as its intensity value. This value will be higher from more reflective surfaces. Intensity values can be used to create quick and spatially accurate black-and-white images of the surface (Figure 3), and can be used to detect some site conditions that are not based on elevation, such as the boundary between paved and unpaved surfaces.

Figure 3: Lidar Intensity Image

Lidar intensity image, with grey-scale values based on the energy of the lidar return. More reflective surfaces are lighter.

The sensor can record multiple returns from each laser pulse. In vegetated conditions, part of the laser return may be reflected from branches and other features, leaving the remainder of the signal to be reflected from the ground surface (Figure 4). The limitation of the multi-return capability is that there must be sufficient time between returns for the sensor to reset. This time is generally between three and 20 nanoseconds depending on the sensor used, a distance of between 0.5 m and 3 m. Thus, multiple returns cannot be recorded in low vegetation.

Figure 4: Lidar Multi-Return Capability

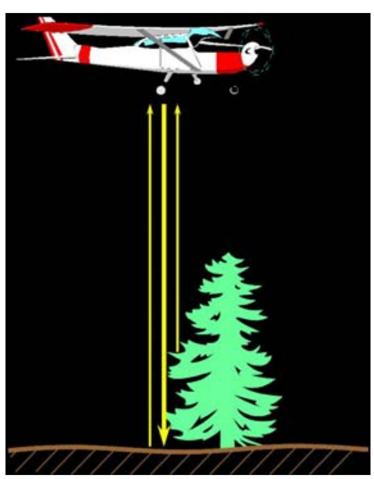

A relatively recent development in laser component technology is the analog or "full wave form" laser receiver. In contrast to the approach described above, the analog receiver records a continuous level of energy values once the amplitude passes the threshold value. The shape of this energy return curve can be analyzed and multiple return values derived in a more interactive manner. Analog receivers create larger data sets than traditional sensors, and more advanced software is needed to process the output. The number of vendors using analog receivers was small but increasing at the time of this report.

Lidar systems in current use also include bathymetric lidar systems that can map shallow underwater surfaces. Bathymetric lidar systems use a blue-green laser signal that will penetrate water, often in conjunction with a red wavelength laser that reflects from the water surface. The time difference between the two signals is used to determine water depth (Optech 2008). Bathymetric lidar systems are capable of measuring water depths to a maximum of approximately 50 m; however, success of the system is limited by many factors, including water turbidity and the reflectivity of the bottom surface. Bathymetric lidar systems are less commonly used than terrestrial systems and costs tend to be considerably higher. However, where applicable, bathymetric lidar can provide data on the nearshore environment where the water is too shallow to map using sonar or other on-water geophysical survey methods.

The final components of the sensor system are the power source, the hardware- and software-based control system, and the data storage equipment (consisting of multiple high-speed hard drives).

The lidar system has some parameters that can be varied within the equipment specifications of each manufacturer. These include:

- ***Power level.*** The power of each laser pulse is adjustable up to the maximum power of the system. Maximum power levels are set by the manufacturer to be safe for humans and wildlife.
- ***Pulse rate.*** The maximum pulse rate, or the number of laser signals per second, has increased steadily as the technology has evolved, from 4 to 10 kilohertz (kHz) in the mid-1990s to as much as 250 kHz at the time of this report. Pulse rates are typically adjustable.
- ***Mirror speed.*** The oscillation or rotation speed of the mirror can be controlled independently of the laser pulse rate.
- ***Scan angle.*** The maximum angle of the mirror off nadir is adjustable. In combination with the aircraft altitude, the scan angle controls the width of the data collection swath.

Vendors report that the primary parameters that are varied are pulse rate and scan angle.

In theory, higher pulse rate systems should provide more laser reflections and therefore more detailed surface models. However, the relationship of laser pulse rate to system performance is not always straightforward. This is because the power system of the laser is finite, and therefore, as the pulse rate is increased, each individual laser pulse will necessarily have less power. It is possible to design a combination of flight altitude and pulse rate that will cause the return signals to be too weak to trigger the receiver and record a return. This limitation is especially notable in vegetated conditions, where

the success of the survey will depend on recording multiple returns. Multiple returns have less power since they reflect only part of the laser pulse. In practice, vendors should monitor power levels, pulse rates, and flight altitude in order to maximize the performance of the system. During data collection, numerous low-intensity returns, or failing to get returns over less reflective surfaces such as blacktop, indicate that power should be increased, altitude lowered, or pulse rate reduced.

1.3.2 Orthophotography

The orthophoto system consists of a digital camera, with a clock timer to record the time of exposure. The time record allows of the location of the image center to be calculated using data from GPS and INS.

Since the mid-1990s, camera image size has advanced from 1,500 pixels across an image to approximately 4,500 pixels. This has allowed for increased flying heights and a reduced number of images for a given area, with consequent cost savings. Cameras with image sizes of 4,000 by 4,000 pixels or greater are often favored (at the time of this report), since the width of the digital image is similar to the typical width of the lidar swath.

2 LIDAR AND ORTHOPHOTOS IN MUNITIONS MANAGEMENT

Many millions of acres of Department of Defense (DoD) lands are potentially contaminated with military munitions or their components. On the majority of these sites, munitions are concentrated in specific ranges and training areas, while the remainder of the site is ordnance-free. Locating the site of contamination can be difficult, in part because historical records are often incomplete or inaccurate. The cost of traditional surveys using magnetometry and electromagnetic induction (EMI) can be very high, and this has driven the search for innovative methods to reduce costs.

2.1 The ESTCP Wide Area Assessment Pilot Project

Between 2005 and 2007, the Environmental Security Technology Certification Program (ESTCP) conducted a pilot program to test the effectiveness of a multi-technology approach to unexploded ordnance (UXO) WAA. The objective of WAA is to “quickly and cost effectively assess 100% of a potentially contaminated site. Beginning with historical records, a CSM is used to record the best understanding of the site. The WAA is a means to gather a preponderance of evidence that improves our understanding of the site and builds confidence in the conclusions. A suite of commercially available technologies provides data to:

- Identify areas of concentrated munitions use
- Collect information that will support decisions on areas with no indication of munitions presence
- Collect data to support planning, prioritization and contracting when a site must ultimately be cleaned up” (Nelson et. al. 2008)

The ESTCP program examined the use of lidar, orthophotography, helicopter magnetometry, towed-array magnetometry, synthetic aperture radar, hyperspectral sensing, and statistically-based transect design.

At the demonstration sites where lidar and orthophotos were tested, the results were positive. Lidar and orthophotos were used to locate berms, bombing targets, and individual craters, even where these features were highly eroded and could not be detected by ground-based field crews (Figure 5). The location of these features was used to correct the initial CSM, to refine the boundaries of munitions response sites (MRS) and to support and help direct the use of subsequent technologies that directly detect ordnance. Results from lidar and orthophotos provided cross-validation of magnetometry and EMI data, leading to higher confidence levels, and the combination of technologies employed in the pilot program was found to be cost-effective (Nelson et al. 2008).

Figure 5: ESTCP Demonstration Sites, Example Munitions-Related Features

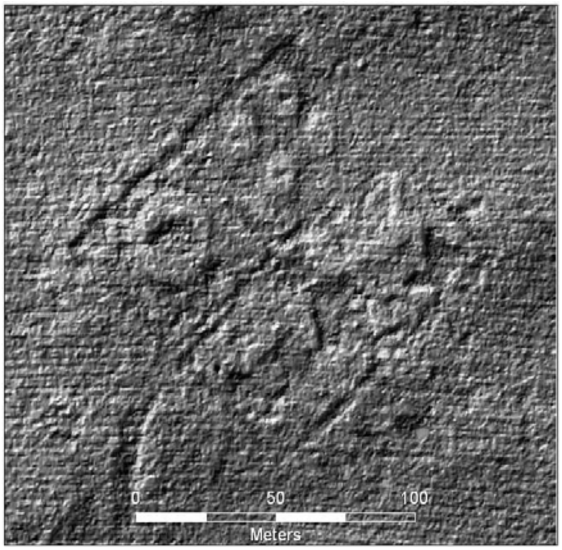

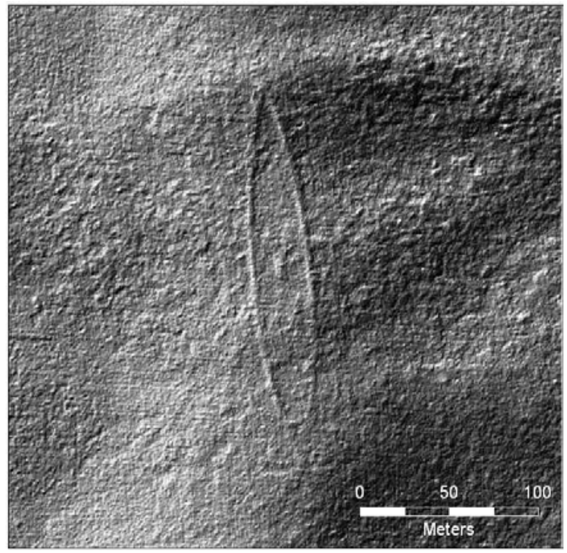

Kirtland Air Force Base Precision Bombing Range ESTCP demonstration site, bombing targets from the 1940s visible in lidar-derived surface models. These targets are highly eroded and cannot be seen from the ground or in aerial photos.

Kirtland site, bombing target cross-hairs visible in 10-cm pixel orthophoto.

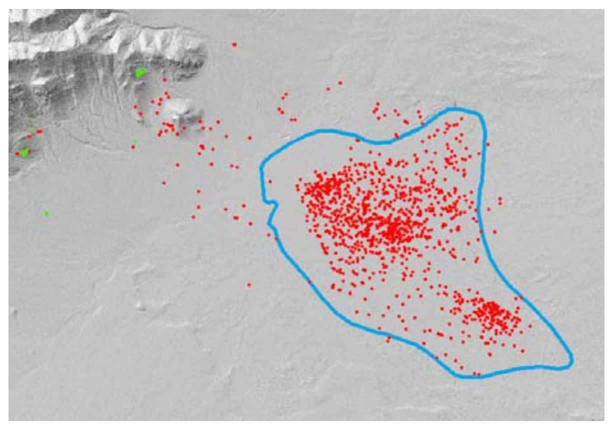

Victorville Demolition Bombing Range ESTCP demonstration site, crater locations outside of the original dry lake bed target area.

<table>
<tr><th colspan="2">Figure 5 continued</th></tr>
<tr><td>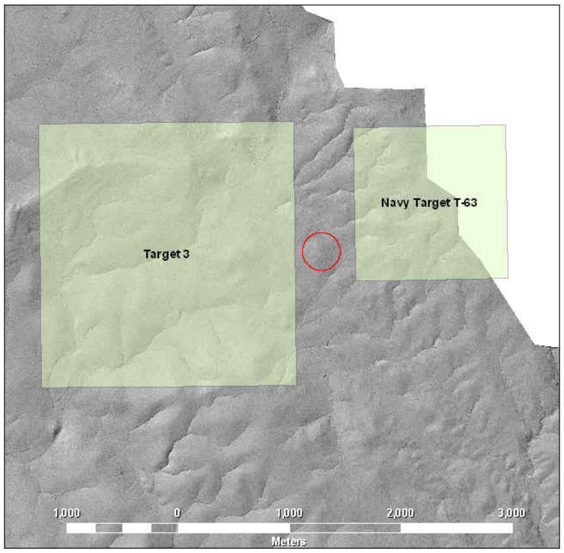
</td><td>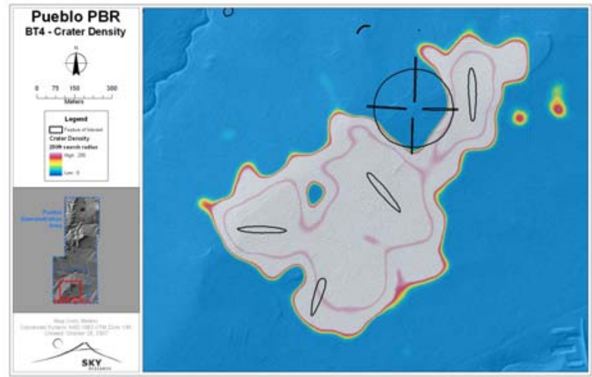
</td></tr>
<tr><td>Former Camp Beale ESTCP demonstration site, bombing target (red circle) located outside of mapped target locations based on historical records.</td><td>Pueblo Precision Bombing Range ESTCP demonstration site, crater density map used to refine original MRS boundary.</td></tr>
</table>

2.2 Advantages of Lidar and Orthophotos at Munitions Management Sites

Using lidar and orthophotos offers several advantages as a supplement to more traditional approaches to site investigation.

- ***Rate of coverage.*** In most operational settings, data collection rates of 5,000 acres per day or higher can be expected for lidar and orthophotos, and collection rates of up to 20,000 acres are possible. This compares favorably to typical collection rates of around 500 acres per day for helicopter-based magnetometry, 5 to 20 acres per day for towed-array magnetometry, and 1 to 5 acres per day for man-portable magnetometry.
- ***Enhanced planning and risk assessment.*** Because they can cover entire sites relatively quickly and at lower cost, these technologies can be used to locate and prioritize appropriate areas for use of more costly low-altitude and ground-based technologies.
- ***Ability to delineate MRS and UXO-related features.*** Lidar and orthophotography can, under some circumstances, successfully reveal MRS and UXO-related surface features even many years after their last use.
- ***Cross-validation.*** Lidar and orthophotos can cross-validate the results of other technologies, leading to enhanced confidence in results.
- ***Other benefits.*** Both technologies provide highly detailed topographic data that can be integrated into a facility's CADD or GIS system and used in subsequent phases of site investigation, site remediation, and range management.

2.3 Limitations of Lidar and Orthophotos at Munitions Management Sites

The primary limitation of lidar and orthophotos is that neither technology can directly detect ordnance or UXO components, such as ferrous scrap. Consequently, lidar and orthophotos are not substitutes for technologies (such as magnetometry or EMI) that directly detect ordnance. Rather, lidar and orthophotos are used to give a rapid assessment of potential areas of ordnance use, based on ground features such as target objects, crater fields, OB/OD areas, berms, or roads. Areas of suspected munitions use can then be prioritized for additional survey. However, areas appearing to be free of evidence of munitions use in lidar and orthophotos will still need to be surveyed with magnetometry or EMI at a level sufficient to demonstrate that they are actually ordnance-free.

Lidar and orthophotos are best used as the first step in site investigation to quickly identify areas of potential contamination and other areas of interest and to help direct the application of subsequent technologies. Lidar and orthophotos will be less useful on sites that have been fully characterized already using more traditional methods, or on small sites where the full site can be surveyed quickly using ground crews.

An additional limitation of both lidar and orthophotos is that both are affected by vegetation. At vegetated sites, orthophotos will show only the tops of the vegetation and thus are of limited utility in characterizing the ground surface. Lidar will provide useable surface models under many vegetation conditions, and will only show severe degradation where the vegetation is particularly dense. However, vegetation will lower the density of lidar returns from the ground surface and will thus lower confidence levels for detecting features under vegetation. Vegetation effects are discussed in more detail in Section 4.2.

3 ACQUIRING LIDAR AND ORTHOPHOTO DATA

3.1 Pre-Mission Planning

Pre-mission planning is an essential part of the successful use of lidar and orthophotos.

Establishing the study area boundary. The lidar vendor must be provided with an accurate study area boundary in order to plan flight lines and estimate costs. In addition to any paper maps sent, the study area should be delivered as an electronic file with spatial coordinates. ESRI[3] shape files or AutoCAD drawing files with spatial coordinates are the most common formats. Files provided for planning should be accompanied by documentation defining the sources of the information, and any specifications associated with the data so this information can be carried throughout the process.

Establishing survey control requirements. The project survey network is a series of points established with survey-grade GPS techniques, and referenced to local survey control. The number of control points to be established depends on the level of validation required, with the understanding that error may not be distributed equally throughout the site. At a minimum, validation points should be located in each major terrain type, and control points should be collected at an accuracy which is an order of magnitude higher than the lidar points. See further discussion of survey control in Section 3.2.

Clarifying projection and datum requirements. Lidar data will be integrated with other project spatial data, and therefore should be delivered in the projection and datum that is being used by other team members. On large projects, it is a reasonably common problem for different subcontractors to operate with data in different projections. This is especially problematic in the case of lidar because the data sets are very large, making re-projection time-consuming and difficult. It is more effective to give the vendor clear direction as to the projection and datum as part of the contract specifications.

Flight line planning. Flight lines are planned using custom software to achieve planned flight line overlap and lidar point densities. Flight line overlap is designed to allow the lidar signals at the extreme edge of the swath to be discarded. Such signals are less vertical and thus are more likely to be obstructed from reaching the ground surface by vegetation, and the points are somewhat more widely spaced and slightly less accurate. Flight line overlap also helps to prevent data gaps when the aircraft makes minor course deviations due to wind, a common occurrence especially with helicopters. Flight lines should be designed to produce a relatively symmetrical distribution of laser returns on the ground surface, which assists in the reliable detection of small objects.

Establishing data density requirements. Selecting appropriate lidar and orthophoto data densities is important since these have a strong impact on both cost and performance. Density specifications for both technologies should be adjusted to the specifics of each site. See the discussion of data density in Section 4.1.

Field logistics. During the planning phase, arrangements are made for aircraft, aircraft fuel, and a hanger in which to install the equipment. If the study area is sufficiently far from the nearest airport, it may be necessary to establish secondary landing areas, GPS

[3] ESRI is the producer of ArcGIS, the most commonly-used GIS program in the United States.

base stations, or fuel sources. Secondary landing areas may be appropriate for helicopter surveys. At active sites, pilot briefings may be required and will need to be scheduled. During the planning phase, arrangements also are made for housing and work space for the data collection crew. Site access problems are identified and resolved, including ground access to establish survey control points and permission to enter the air space over the site. Contingencies for weather. During the planning phase, site weather conditions are assessed and the mission plan adjusted to include an appropriate contingency for weather delays. Lidar and orthophotos cannot be collected in wind, rain or snow. Choosing the airframe. Lidar may be acquired either from helicopters or small fixed-wing aircraft. There is generally only a small difference between the two airframes in cost or performance and the choice can usually be left to the vendor. In practice, some performance factors include:

- Fixed-wing aircraft generally fly somewhat faster and at higher altitudes and therefore achieve somewhat higher data collection rates, along with somewhat larger orthophoto pixel sizes, generally 12 to 20 cm. If 10 cm pixel sizes are required, it may be necessary to use helicopters.
- Helicopters can sometimes fly under low cloud cover that may make fixed-wing acquisition difficult or impossible. In coastal areas with frequent cloud cover, using helicopters may be advantageous for this reason. Helicopters also may be advantageous for maintaining a fixed altitude in mountainous areas.
- Helicopters make turns more easily and can follow irregular project area boundaries with greater efficiency.
- Helicopters can fly lower and more slowly than fixed-wing aircraft, thus achieving higher point densities without flying multiple passes.

A second consideration in choosing an airframe is the use of local versus vendor-owned aircraft and pilots. Some vendors own and operate their own aircraft and provide their own pilots, others rent local aircraft. The choice can usually be left to the vendor.

- Local pilots will generally be more familiar with local weather conditions, airports, restricted air spaces, and flight operational controls. This can be an advantage in areas with unpredictable or difficult weather conditions, or where restricted air space requires advance permission and coordination.
- Vendor-provided pilots will generally have more experience at collection lidar and orthophoto data, which requires staying on line, at speed and at altitude in order to maintain data quality and safety.
- Aircraft owned by the lidar vendor must be mobilized to the project site, which can be time-consuming and lead to costly delays due to weather and border crossings. In contrast, use of a rented aircraft involves shipping only the sensor equipment. Local aircraft, however, can be difficult to rent during periods of strong local demand, and must be verified to meet the technical requirements of the lidar system, such as an adequate and reliable power system.

Project schedule. The data acquisition schedule is based on expected data collection rates, mobilization requirements, and quality control procedures. For most projects, a collection rate of 5,000 acres per day can be used for planning purposes; however,

collection rates up to 20,000 acres per day are achievable, particularly with fixed-wing aircraft. Individual sites should be evaluated for site-specific problems. These can include site boundaries that require short flight lines and multiple turns, or restricted air space where flights may be conducted only during specified hours. For all projects, an additional day should be planned at the end of the survey for re-acquiring any missed areas or areas where the data appear to be problematic.

Safety. Lidar and orthophoto data collection is generally governed by the same safety rules and considerations as any small aircraft mission. Local aircraft vendors or lidar vendors who operate their own aircraft should provide a standard safety plan as part of their qualifications. One safety problem that has been encountered occasionally is data collection that occurs near an existing airport, where planned flight lines may conflict with existing air traffic patterns. All flight lines should be reviewed carefully with local airport managers and other knowledgeable sources to avoid such hazards. For collection near existing airports, a Notice to Airmen may be issued to notify other pilots of the activity in the area.

Delivery products. During mission planning, the delivery products and data formats should be clearly specified and agreed upon. Vendors should be required to deliver the full lidar data set, in addition to any derived products such as contour lines or surface models. The choice of file format and maximum data file size should be determined by the software and hardware in use by the facility receiving the data.

Permitting and other access constraints. Lidar and orthophoto surveys generally do not present problems with permitting and site access, since the only ground access requirement is for establishing survey control. However, access to local air space at some active military bases can occasionally require extensive coordination and should be investigated well in advance. For international projects, the IMU is US military dual use technology, and international use requires a permit pursuant to the International Traffic in Arms Regulations, Code of Federal Regulations Sections 123.1 and 123.9(c). This regulation restricts use of lidar and orthophotos in some countries. In addition, foreign countries may have limitations on the use of these technologies in some sensitive areas (particularly border and military areas) and some require data processing be done in-country and limit outside access to data. For international projects, sufficient time must be allowed for permitting and shipping requirements,generally at least two weeks to ensure that the IMU will arrive at the destination.

3.2 Field Data Acquisition

Field communication. Communication with the vendor during data collection is critical to the success of the survey. During data collection, site conditions often force modification of mission plans, and decisions often must be made quickly. Vendors should be in daily contact with the Government project manager or other representative throughout the field effort, and all decisions should be reviewed by both the vendor and the Government before decisions are finalized. The Government representative must be available full-time during the field effort. Daily field reports are generally submitted to document the day's activities and note any problems encountered or resolved, site visitors, etc.

Mobilization. During mobilization, the lidar equipment is shipped to the site, installed on the aircraft to be used, and tested. Installation typically requires less than one day. The data collection crew also establishes a work area where data can be processed during

the daily quality assurance/quality control (QA/QC) review. Fuel is placed on site if needed.

Establish survey control points and other calibration items. Just prior to data collection, control points are established. Primary control points are established using static survey methods, additional surveyed points may be established using static and/or kinematic methods. Fiberglass targets can be placed with the control points for verification of horizontal positional accuracy and lidar-to-orthophoto alignment. Often, conditions in the field will require some deviation from planned control point locations. This is acceptable as long as an adequate network of control points is maintained.

It is often desirable to establish other calibration items in addition to control points. The most common are vertical control structures and simulated craters at a variety of sizes. Detection of these calibration objects can be used in a manner somewhat analogous to the use of geophysical prove-out areas in traditional geophysical munitions investigations. Current best practice is to take a digital photo of all static control points and other calibration objects, and to survey the location of all calibration items.

Sensor calibration. Before data acquisition begins, test flights are conducted over calibration features with known dimensions. Calibration flights are conducted at several headings. On return to the office, the results of these test fights are used to establish correction values for pitch, roll, and yaw so that the features remain constant at all headings. The results of sensor calibration flights should be recorded as part of the vendor's QA/QC report. Calibration results should be checked daily. Calibration coefficients change over time (on the scale of days) and their suitability should be assessed for each individual data set. Long deployments (several days to many weeks) may require multiple unique sets of calibration coefficients to account for small yet consistent drift of the IMU.

Data acquisition flights. The efficiency of the data acquisition process will depend primarily on the distance to the nearest fuel source and the percentage of the flight spent turning vs. acquiring data. Data acquisition also can be affected by air temperatures over 100^{o} F during the summer months, which can affect equipment performance and reduce the hours of operation. During flights, the operator should monitor the quality of the data being received and make any needed corrections to operating conditions to assure data quality.

In-field QA/QC review and re-flight. All vendors have software with which the field crew can examine the data, and daily review to assess data quality and identify any problems is a standard and essential part of field activities. Identifying missed areas or data quality problems allows for correction in the field prior to demobilization, usually by re-flying missed areas or areas of poor-quality data. Correcting problems of this kind while the crew is still in the field avoids the substantial costs and delays of re-mobilization and re-acquisition.

Documentation of the field activities is an important part of the QA/QC process. Documentation should include site photos, calibration records, flight logs showing time and date of each flight line, and the results of the daily QA/QC review.

3.3 Post-Mission Data Processing

Once the data arrives from the field, the vendor performs a series of steps to produce lidar points and orthophoto images that are ready for use in the GIS, CADD, or geophysical software environment.

3.3.1 Lidar

Calibration. On return to the office, the results of the calibration fights are used to establish calibration values for pitch, roll, and yaw so that the features remain constant at all headings. These correction values are applied either to the entire lidar data set, or if multiple calibration coefficients are developed, each will be applied to the appropriate portion of the lidar data.

Flight line integration. Data from different flight lines are adjusted to achieve the closest possible fit to each other and to the project control points. This calibration process is used to correct, to the extent possible, minor positional error from one flight line to the next, and to detect any major positional errors. This calibration is essential to assure that lidar points will be positionally accurate throughout the project area. Small discrepancies will always remain between the data from one flight line to the next; this is acceptable as long as the discrepancies fall within the contract specifications. Large discrepancies between flight lines that cannot be corrected may indicate serious equipment or data collection problems and may require re-acquisition.

QA/QC review. As part of the calibration procedure, the vendor should perform basic QA/QC review of the alignment of the lidar data to the control points. This review forms the basis for validating the location of the lidar data. If vertical control structures and simulated craters have been established, detecting these items should be part of this QA/QC review.

Lidar point classification. Once the lidar data are calibrated, the ground surface is derived from the entire lidar point data set, and remaining points are classified as vegetation, buildings, and other objects, depending on the needs of the project. Classification is done through automated algorithms followed by inspection and editing. Inspection and editing by qualified analysts is essential to creating a quality ground surface model.

Point classification methods can affect the density of ground points and thus the resolution of the ground surface model. Typical software settings tend to favor creation of smooth ground surface models, and can result in some ground points being misclassified as non-ground in order to keep the surface model smooth. Point classification methods can be adjusted to add more points to the ground surface model, and work at the ESTCP demonstration sites has shown that this may increase the resolution of the surface model and somewhat increase detection of small objects (URS 2009a). When the objective of the survey is to detect objects such as small craters, it is important to discuss point classification methods with the vendor in order to maximize the possibility of detection.

Data delivery. Once the lidar points have been created, they are delivered by the vendor, along with any additional products such as surface models. Data delivery requires several decisions:

- ***Format.*** Lidar points can be delivered in several different formats. The most common are ASCII text files and the LAS file format. LAS is a binary format that

was specifically designed for lidar data. LAS files are considerably smaller than equivalent ASCII files, and LAS files can be viewed directly in many software products without conversion. ArcGIS requires a third-party extension to directly view and process LAS files, or they can be converted to ESRI shapefiles using free tools that can be found on the internet. In the ArcGIS environment, LAS files also can be converted to a special ArcGIS feature class type called a multipoint feature class. The multipoint feature class, however, does not allow direct access to the file attributes, thus preventing any kind of analysis, manipulation, or reclassification based on attribute values of the lidar points. ASCII text files, usually in space, tab or comma-separated format have the advantage of being universally accepted. The files are much larger, although these files compress well into much smaller archive formats such as ZIP, RAR, LZH, GZ, etc.

- ***Delivery.*** Lidar data should be delivered using a DVD, flash drive, or portable hard drive, depending on the size of the data set. Ftp is a potential method of data transfer, but often leads to problems. Ftp transfer is generally very slow given the size of lidar files, and it is possible for data files to become corrupted during transfer.
- ***Data tiles.*** Lidar and orthophoto file sizes can be very large, and data is generally delivered in tiles. It is important that the lidar vendor deliver the data in tile sizes, and resulting data files, that can be managed efficiently. File sizes present a tradeoff: larger tiles result in larger data files, which are harder to open, examine, process, copy, or move, but large numbers of smaller files can be confusing and difficult to manage. File sizes should be determined by the software and hardware capabilities of the receiving installation.
- ***Overlapping vs. non-overlapping blocks.*** Lidar can be delivered in blocks with or without overlap. Non-overlapping blocks will generally result in data gaps between blocks if they are processed separately and recombined in the analysis stage (URS 2007). If processing in separate blocks is desired, all vendors can deliver overlapping blocks upon request, but this is not always the default so this requirement should be included in the contract specifications. As an alternative, it may be possible to avoid data gaps between blocks by using the ESRI multipoint feature class, or a software package other than ArcGIS, to load all of a project area's lidar data into a single file for creating surface models.
- ***Lidar point attributes.*** Lidar points should include several attributes in addition to the x, y, and z values. These include values for:
  - ***Class:*** The vendor's classification of the point as a ground or non-ground return.[4]
  - ***Intensity:*** The strength of the signal returned.
  - ***Flight line:*** The code for an individual flight line. It is useful to view data from individual flight lines, especially as a means to diagnose problems with the data.

---

[4] Vendors can use more complex classification schemes if desired, including classification as vegetation, buildings, or power lines.

- ***Collection date and time:*** These are values for GPS week and GPS time that are collected automatically as part of system operations.

The vendor should provide documentation of all attribute codes, such as the values to indicate ground and non-ground returns and the format used for the collection date or flight line number.

3.3.2 Orthophotos

Once the individual digital images are collected, vendors create orthophotos by building a mosaic of the individual images, transforming the consolidated image to the delivery datum and projection, orthorectification using the lidar data, color balancing, and trimming to the delivery tiles. While some of these processes can be automated, creating high quality orthophoto images requires a large amount of operator time, especially for creating the image mosaic. Consequently, orthophotos with smaller pixel size are more expensive and time consuming to create, since they involve manipulating larger numbers of smaller images.

Orthophotos should be delivered in tiles sized to keep the files at a useable size. This size limit should be determined based on the software in which the data will be used.

3.3.3 Post-Mission Quality Control Report

At the conclusion of data processing, the vendor performs a series of QC checks based on the contract specifications, and these are summarized in a QC report. This report is typically submitted with the data. The QC report should include, at a minimum:

- Accuracy of the control points
- Position dilution of precision during data collection
- Data collection specifications
- Root mean square values for orthophoto triangulation
- Locations of control points and GPS base stations
- Site photos of the data collection process and control points
- Equipment calibration results
- Achieved swath width
- Achieved swath overlap
- Achieved point density
- Achieved flight altitudes
- Achieved flight lines (as CADD or shape files)
- Lidar vertical positional accuracy compared to controls
- Lidar horizontal positional accuracy compared to controls
- Orthophoto horizontal positional accuracy compared to controls
- Orthophoto positional accuracy compared to lidar
- Results of lidar data integration between flight lines

3.4 Receiving and Working with Lidar and Orthophoto Data

3.4.1 Data Management

Lidar and orthophoto data sets can be very large, and managing these large data sets requires several important considerations.

File naming system. Vendors typically deliver lidar point data and orthophotos as a series of tiles or blocks sized to keep the file size manageable. A large site can require several hundred data blocks, and the difficulty of keeping these data sets organized for a large site should not be underestimated. Having a well-defined file naming system is essential. Consistent file naming also is required in the use of automated scripts for batch processing.

Data storage. The large data sets produced by lidar and orthophotos make backup and storage an ongoing problem for many users. These data sets can sometimes be too large to back up using an organization's existing tape backup system, and some form of independent backup and storage must be maintained. The optimal solution is generally a dedicated server with tape backup of adequate size. Where this is too expensive, an alternative is to use a small, portable "redundant array of independent disks" (RAID) device, which are available at relatively low cost. RAID devices are generally acceptable as storage; however, they sometimes present problems of data corruption if they are used for data processing. Processing should be performed on the local machine where possible and copied to the RAID device for storage.

Additional files. Because the data are delivered in blocks, the vendor must produce and deliver a block index file for each data set. Other required files include the surveyed locations of all control points and calibration structures, line files for all achieved flight lines, and the QA/QC report. The format of these ancillary files should be compatible with the software that will be used to view and analyze the data.

GIS products. Although the initial data sets are large, the final GIS products from lidar such as point files and digital elevation models (DEMs) are smaller, and are within the capability of normal GIS programs to process, analyze, and display. This may not be the case for CADD and geophysical programs, and exporting files from the GIS to these software environments requires additional planning and may require clipping the data to smaller tiles.

3.4.2 Creating GIS Products from Lidar Points

Lidar data arrives from the vendor as a table of values in one of several text file formats (Figure 6). These data must be converted to a useable format, generally in a GIS program, before they can be reviewed and analyzed. Products to be created include point files based on the individual lidar points, models of the ground surface (DEMs), and digital terrain models (DTMs) based on all lidar returns, along with hill shaded views created from both. The lidar vendor will provide these products along with the point data if requested; however, where the receiving facility has GIS capabilities these products may be produced in-house. Surface models, hillshades, and contour lines can be created and displayed in many different ways, each of which will affect the utility of the products. Commonly, several different approaches will be tested, and different products will be created for specific parts of the analysis. The advantage of creating these products in-house is that these choices can be made explicitly, and different approaches

can be tested more easily, assuming that the appropriate equipment and operators are available.

ESRI's ArcGIS software is the product that facilities most commonly use for creating and analyzing lidar data, and it will function adequately for most tasks. Basic GIS products are created using standard GIS data processing methods. In the ESRI GIS environment, these processes can be automated using scripts written in AML, Python, or Visual Basic. Once basic GIS products are created from the lidar data, products appropriate to other software packages, such as CADD or geophysical software, can be exported at will.

Other software tools are available for more specialized analysis tasks, and in some cases these may offer capabilities that ArcGIS does not provide.

Figure 6: Lidar System Output

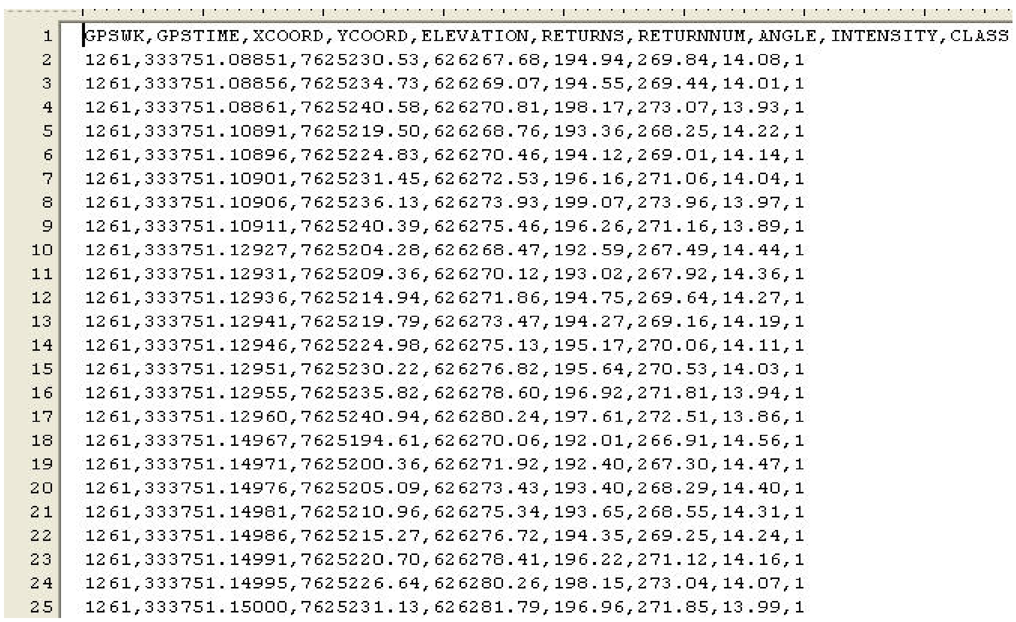

```
GPSWK,GPSTIME,XCOORD,YCOORD,ELEVATION,RETURNS,RETURNNUM,ANGLE,INTENSITY,CLASS
1261,333751.08851,7625230.53,626267.68,194.94,269.84,14.08,1
1261,333751.08856,7625234.73,626269.07,194.55,269.44,14.01,1
1261,333751.08861,7625240.58,626270.81,198.17,273.07,13.93,1
1261,333751.10891,7625219.50,626268.76,193.36,268.25,14.22,1
1261,333751.10896,7625224.83,626270.46,194.12,269.01,14.14,1
1261,333751.10901,7625231.45,626272.53,196.16,271.06,14.04,1
1261,333751.10906,7625236.13,626273.93,199.07,273.96,13.97,1
1261,333751.10911,7625240.39,626275.46,196.26,271.16,13.89,1
1261,333751.12927,7625204.28,626268.47,192.59,267.49,14.44,1
1261,333751.12931,7625209.36,626270.12,193.02,267.92,14.36,1
1261,333751.12936,7625214.94,626271.86,194.75,269.64,14.27,1
1261,333751.12941,7625219.79,626273.47,194.27,269.16,14.19,1
1261,333751.12946,7625224.98,626275.13,195.17,270.06,14.11,1
1261,333751.12951,7625230.22,626276.82,195.64,270.53,14.03,1
1261,333751.12955,7625235.82,626278.60,196.92,271.81,13.94,1
1261,333751.12960,7625240.94,626280.24,197.61,272.51,13.86,1
1261,333751.14967,7625194.61,626270.06,192.01,266.91,14.56,1
1261,333751.14971,7625200.36,626271.92,192.40,267.30,14.47,1
1261,333751.14976,7625205.09,626273.43,193.40,268.29,14.40,1
1261,333751.14981,7625210.96,626275.34,193.65,268.55,14.31,1
1261,333751.14986,7625215.27,626276.72,194.35,269.25,14.24,1
1261,333751.14991,7625220.70,626278.41,196.22,271.12,14.16,1
1261,333751.14995,7625226.64,626280.26,198.15,273.04,14.07,1
1261,333751.15000,7625231.13,626281.79,196.96,271.85,13.99,1
```

Sample lidar point locations in ASCII comma-delimited format. Data fields are included for GPS week, GPS time, x, y, and z coordinates, number of returns for this pulse, return number for this return, scan angle, intensity value, and classification code for ground vs. non-ground return.

Creating point files. Point files are the first product to be created from the lidar positional locations. All of the fields in the original text file can be used in subsequent analysis, and should be kept as attributes of the resulting points. For instance, retaining the flight line number as an attribute of the lidar points allows flight line overlap to be inspected (Figure 7). The lidar points also can be examined to show variations in data density, as discussed in Section 4.1.

Creating surface models. The most common products created from lidar data are surface models, either of the ground surface alone (DEMs) or of the ground surface plus vegetation, buildings and other features (DSMs). As discussed in Section 4.3.5, surface models can be created in a variety of ways and these methods should be adapted to the needs of each survey.

Creating contour lines. Contour lines also are a typical product of lidar data, and contour line creation introduces some important technical choices (Figure 8). Users are often surprised that lidar-based contours look highly irregular and jagged, rather than the smooth contours that are usually found on topographic maps. This effect is a result of the detailed ground surface being interpreted through computer methods rather than by human operators, as in photogrammetry. Smooth contours can be created from lidar data; however, these should be approached with some caution, and adjusted to the particular project needs. Caution is required because computer-based methods for creating smooth contour lines can sometimes remove small ground features (such as craters or fault scarps) that may be important for the project.

Figure 7: Lidar Flight Line Overlap

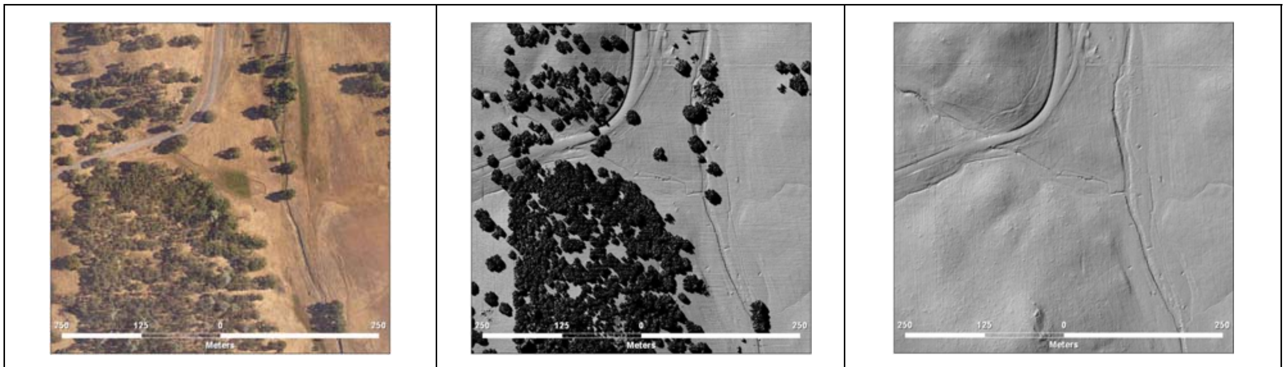

Example area for lidar flight line effects. Images show an orthophoto DTM created from all lidar points, and a DEM created from ground points only.

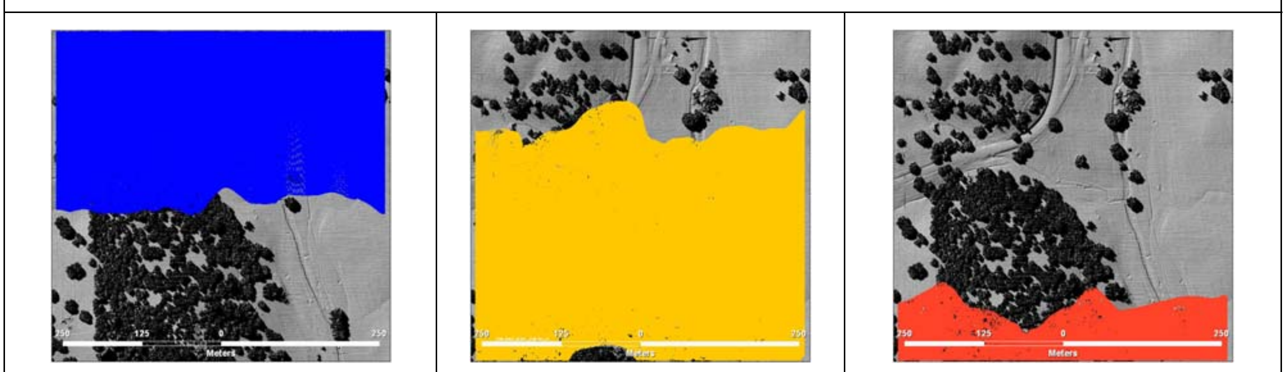

Lidar points from overlapping flight lines. The aircraft traveled east to west (right to left). The impact of wind conditions can be seen at the edges of the flight lines.

GIS or CADD programs can create contour lines at any interval. However, contour lines cannot be certified as accurate unless the underlying data meets specific requirements. As a general rule, creating smaller contour line intervals requires lidar data that are denser and more accurate.

One standard source for guidance on accuracy standards for contour lines and other elevation data is the American Society for Photogrammetry and Remote Sensing (ASPRS) publication *ASPRS Guidelines: Vertical Accuracy Reporting for Lidar Data* (ASPRS 2004). In terms of setting accuracy standards for contour lines, ASPRS points out that contour lines are produced through a series of technical steps, each of which has the potential to introduce error. Consequently, contour line accuracy should be

specified for the contours themselves, and should not be confused with accuracy of the lidar points. The guidelines conclude that “Specifying accuracy of the final product(s) requires the data producer to ensure that error is kept within necessary limits during all production steps.”

Figure 8: Lidar-Based Contour Lines

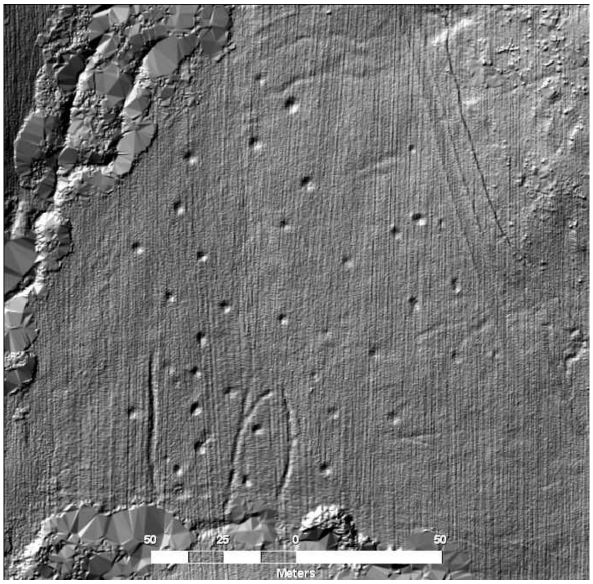

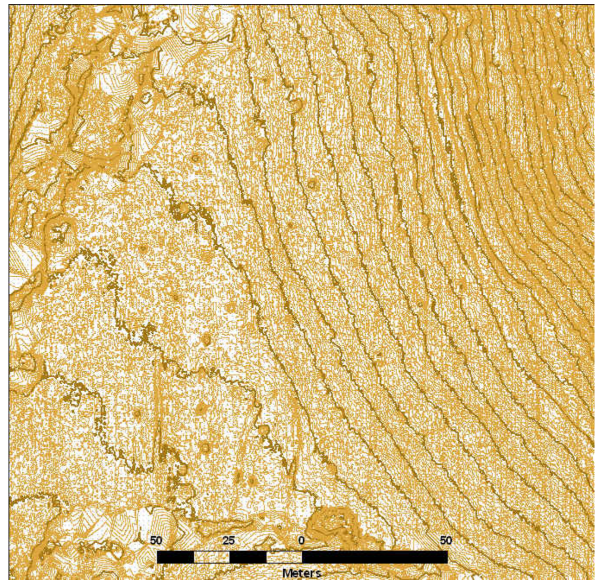

Former Camp Beale ESTCP demonstration site, ground surface model and original, contour lines without smoothing.

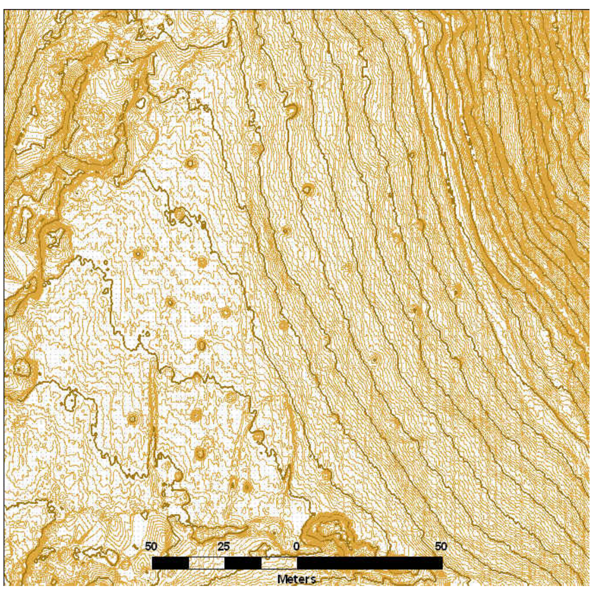

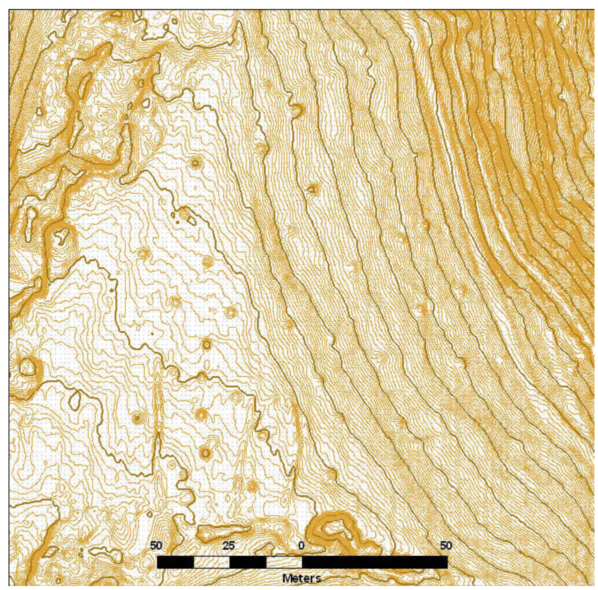

Former Camp Beale ESTCP demonstration site. Contour lines increasingly smoothed.

Contour line accuracy is sometimes certified in reference to the National Map Accuracy Standards (NMAS) or equivalent (NDEP 2004). Often, contour line accuracy is required

to be certified by licensed professionals such as surveyors or photogrammetrists. The NMAS, referring to vertical accuracy, states:

> *"Vertical accuracy, as applied to contour maps on all publication scales, shall be such that not more than 10 percent of the elevations tested shall be in error more than one-half the contour interval. In checking elevations taken from the map, the apparent vertical error may be decreased by assuming a horizontal displacement within the permissible horizontal error for a map of that scale."*

At least one standard reference notes that the NMAS was developed before the advent of DEMs, and recommends that DEMs generally should not be certified to NMAS standards (ASPRS 2001). This could apply to contour lines created from lidar data, since the contour lines would be created from the lidar-based DEM.

An important consideration in creating contour lines is that vertical error will be lower in flat, open areas and higher in rugged terrain or areas of greater vegetation cover. Consequently, in applications where contour line accuracy is critical, it may be appropriate to require separate reporting of lidar accuracies for different ground cover categories. This would require placement of appropriate survey controls in each ground cover type.

Vendors contacted reported that they regularly produced 2-foot contour lines that met ASPRS standards, and occasionally received requests for 1-foot contour lines. They felt that creation of 1-foot contour lines required a point density of at least two to three points per square meter, with five to six points being better, and with control points distributed through all ground cover types. Most vendors further reported that they would not create 1-foot contour lines for steep or very uneven ground surfaces, where horizontal error in the lidar data would result in unacceptable vertical error. At the time of this report, a small number of vendors would produce contour lines at 0.5-foot intervals; however, such surveys require extremely high-accuracy equipment, very low flight elevations, and very high point densities.

3.4.3 Independent Quality Control

Once basic GIS products have been created, the lidar data can be inspected for data quality problems. The lidar vendor's QC report should not substitute for this independent review of the quality of the lidar data. This section reviews steps in the inspection process.

Inspecting for artifacts. As surface models are created, they should be inspected for both small and large artifacts. "Small" artifacts are defined as those that are within the stated horizontal and vertical accuracy of the data. These are generally the result of precision error as described in Section 4.3.3. Small artifacts of this type cannot be eliminated entirely, and do not affect the level of analysis needed for most projects. Large artifacts are those that exceed the data accuracy specification, and these can indicate improper data calibration, editing, or processing. Errors of this type can require re-processing or even re-acquisition to correct.

Verifying point density. Point density is verified by calculating the total number of points collected per square meter for the project area as a whole. In practice, lidar density varies considerably with such factors as flight line overlap, as discussed in Section 4.1.3. Overall point density should therefore be understood as a measure of the

proper functioning of the equipment and compliance with general contract specifications. In some applications, it may be appropriate to specify minimum acceptable point densities for smaller areas of a specified size or for each major terrain type, as discussed in Section 4.7.

Verifying positional accuracy. Vertical and horizontal accuracy are verified separately. Vertical accuracy is verified by comparing the surveyed elevation of the control points to the elevation of the lidar data. Horizontal accuracy is verified by comparing the horizontal location of a surveyed object that can also be detected in the lidar data. Points used could include the survey targets, or surveyed points can be placed at the corners of buildings, paved surfaces, or other natural or cultural objects that will be clearly visible in the lidar elevation or intensity data. Lidar-to-orthophoto alignment is verified by comparing the surveyed control point locations to their locations in the orthophotos.

3.4.4 Identifying and Analyzing Ground Features

At munitions sites, most analysis is aimed at detecting and interpreting ground features, and is performed by examining surface models. In some cases, it may be useful to view the lidar points, in either two or three dimensions.

Identifying and evaluating ground features. Generally, personnel with experience in munitions sites identify ground features by visually inspecting the surface models and orthophotos. Some features are easily identified as munitions-related. These include bombing targets, crater fields, and OB/OD areas (Figure 9).

Figure 9 Unambiguous Munitions-Related Ground Features

Practice bombing target, Victorville, CA ESTCP demonstration site.

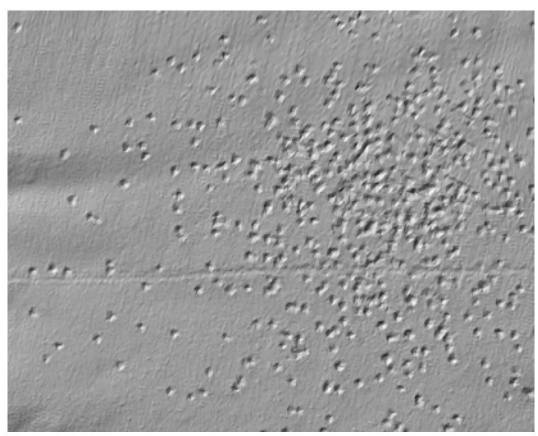

Crater field, Naval Bombing Range Boardman, OR.

Other ground features are ambiguous, and their presence is an indication that further investigation is required using technologies such as magnetometry or EMI. Ambiguous features include individual crater-shaped objects that may result from ordnance use, other human activities, or natural ground variations (Figure 10).

Figure 10: Ambiguous Ground Features

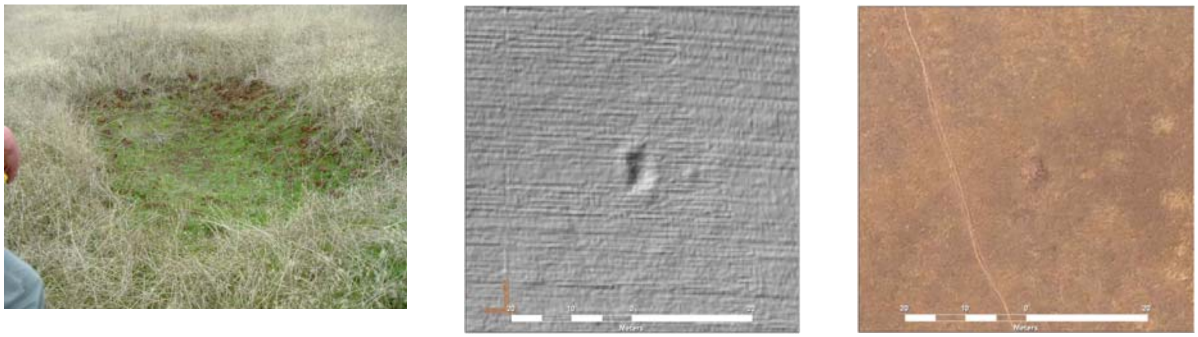

Former Camp Beale ESTCP demonstration site. Ground feature with negative magnetic response.

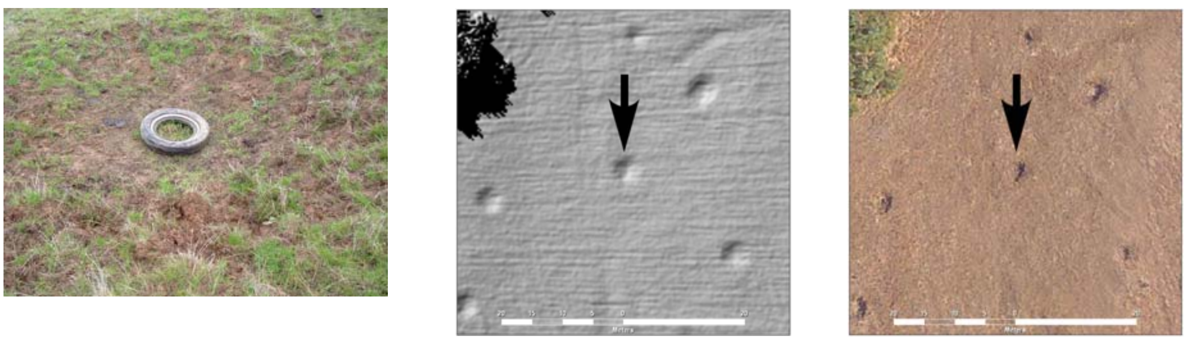

Former Camp Beale ESTCP demonstration site. Ground feature with positive magnetic response.

In-office evaluation of potential ground features is typically conducted in several steps. First, the entire set of potential munitions-related features is identified, either by GIS analysts or using automated feature extraction methods. The aim of this first step is to identify all potential man-made features, being as inclusive as possible.

Second, potential features are compared to the historic information in the CSM, Archive Search Report, or other available documents. Staff familiar with the type of ordnance used on the site should contribute to this comparison.

Finally, the individual features are examined by staff who are familiar with type or ordnance uses on the site and the size and shape of the expected features, using the orthophoto and lidar data. The aim is to identify those features that are most clearly related to ordnance use, those that are clearly not ordnance-related, and those that require further investigation.

The results of the in-office evaluation can be used to correct or confirm the historic data, to modify the boundaries of MRS, and to identify ambiguous features for further field verification. Once complete, the evaluation is used to focus and prioritize the following stages of the site investigation.

4 Factors Affecting Performance of Lidar and Orthophotos

The performance of lidar and orthophotos is affected by a variety of site conditions and processing choices. These will affect both the expectations for the technologies and the appropriate contract specifications for each site.

4.1 Data Density Effects

An important decision in acquiring lidar and orthophoto data is the density of the data to be collected. For both technologies, data density directly affects both the detection ability of the technology and the cost of collecting and processing the data. Orthophoto data density is expressed as the size of the orthophoto pixels. Lidar data density is expressed as either the average number of points per square meter or the average spacing between lidar points. Unlike orthophoto pixel size, lidar data density can vary considerably over the ground surface. In areas of lower lidar density, confidence in detection will be lower for small ground features.

4.1.1 Orthophoto Pixel Size

The size of the orthophoto pixels has a strong effect on feature detection capability. Figure 11 compares 10 cm and 20 cm pixel orthophotos showing simulated craters at the Kirtland Air Force Base ESTCP demonstration site. These small features are much more clearly visible in the 10-cm image. The 1.0 m simulated craters are visible in the 10-cm pixel image on the left. The 0.3-m craters are visible, but can only be distinguished from the surrounding vegetation due to the regularity of their pattern. Isolated ground features of this size would not be distinguishable.

Figure 11: Orthophotos with Simulated Craters – 10 cm and 20 cm pixels

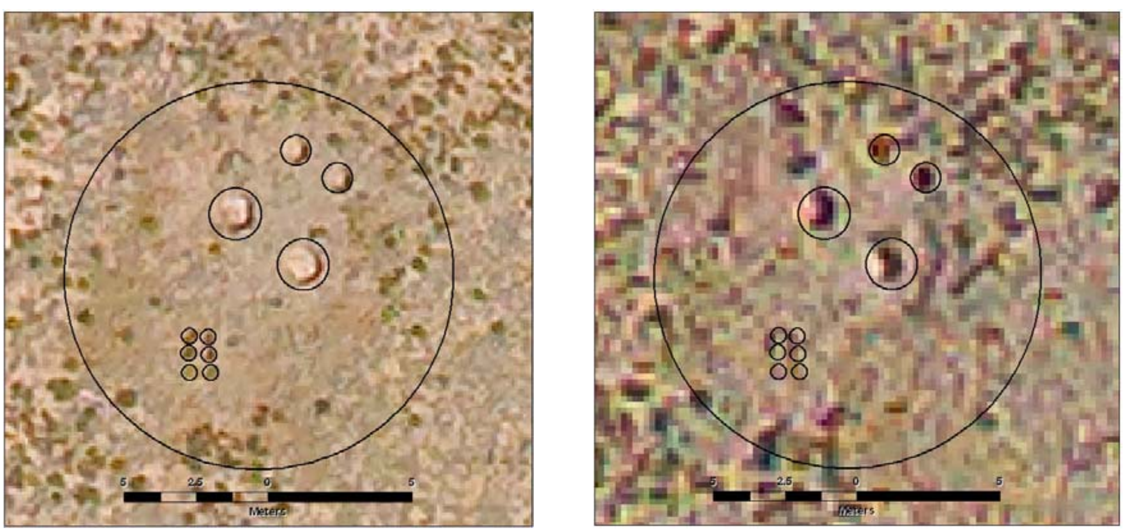

Kirtland Air Force Base ESTCP demonstration site, 10 cm (left) and 20 cm (right) pixel orthophoto with simulated craters at 0.3, 1.0, and 1.5 m diameters.

The advantage of smaller pixel sizes is not limited to small objects. At the Former Camp Beale ESTCP demonstration site, a 1,000-foot diameter bull's-eye target was visible in

the 10 cm orthophotos acquired for the project, but was not visible in a previously-available 30 cm pixel orthophoto (Figure 12).

Figure 12: Orthophotos with Bombing Target – 10 m and 30 cm pixels

Former Camp Beale ESTCP demonstration site, bull's-eye aiming target: 10 cm (left) and 30 cm (right) pixel orthophotos. The target is visible in the 10 cm pixel orthophoto but not in the 30 cm pixel version.

4.1.2 Lidar Data Density and Feature Detection Limits

Work at the ESTCP demonstration sites showed that densities of four points per square meter and higher were sufficient to characterize the simulated craters at the 1.0 m and 1.5 m sizes, at least in open areas. Higher point densities tested showed ground features with more clarity, but did not reveal more features (URS 2007 and 2008). For most munitions investigations, four to five points per square meter should be considered as a minimum recommended point density, with higher density desirable for more vegetated sites. However, simulated craters at 0.3-m (1-foot) diameter were not detected reliably at any of the lidar densities tested (Figure 13) (URS 2007 and 2008). Even at the highest data densities tested, the lines of lidar points could miss the 0.3-m diameter craters. At the few areas where the 0.3-m craters were detected, they were very hard to distinguish from the normal variations in the ground surface, and probably would not have been noted if their locations had not been surveyed previously.

4.1.3 Variations in Lidar Data Density

Lidar vendors report lidar data density as the average number of points per square meter, or the average spacing between points, based on the entire site. However, in practice, lidar point density varies considerably over the site, based on factors such as flight line overlap and wind conditions that cause the aircraft to pitch, roll, and yaw. Variation in overall lidar point density can be clearly seen using point density maps, where cells are color-coded by the number of lidar points per square meter (Figure 14).

Figure 13: Lidar Point Patterns and Detection of Small Features

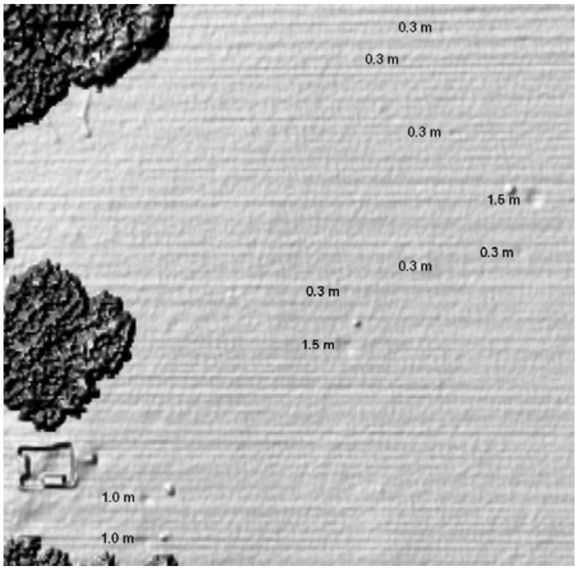

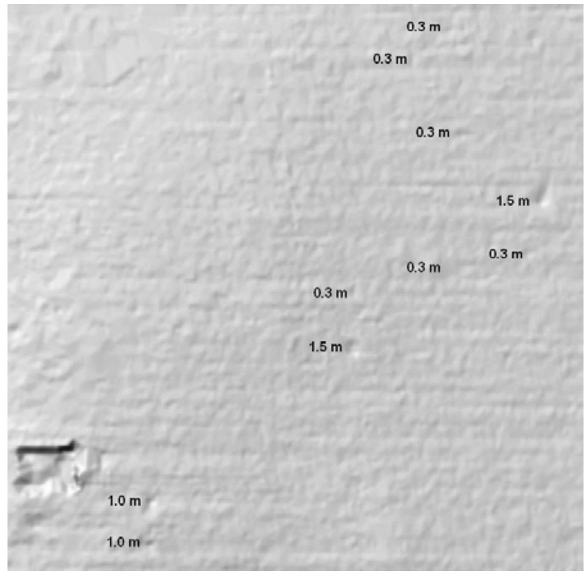

Simulated craters, Former Camp Beale ESTCP demonstration site. Overall lidar data density of 13.8 points per square meter. All points surface model (left) and ground point surface model (right).

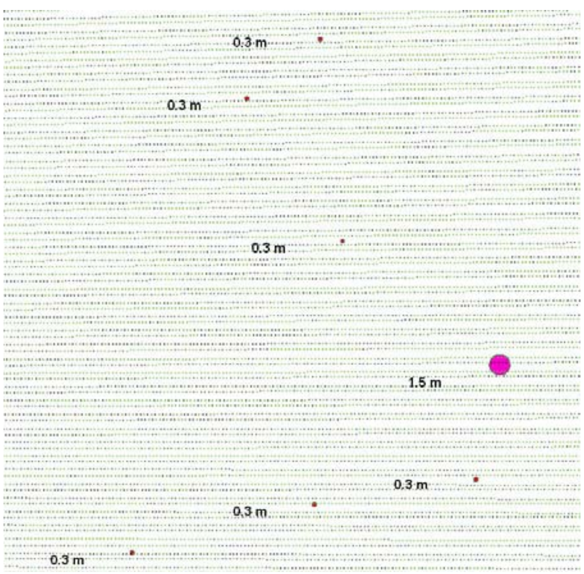

Lidar points for area shown above. The 1.5 m test crater is large enough to intersect several lines of lidar points. The 0.3 m test craters are small enough to fit between the lines of lidar points.

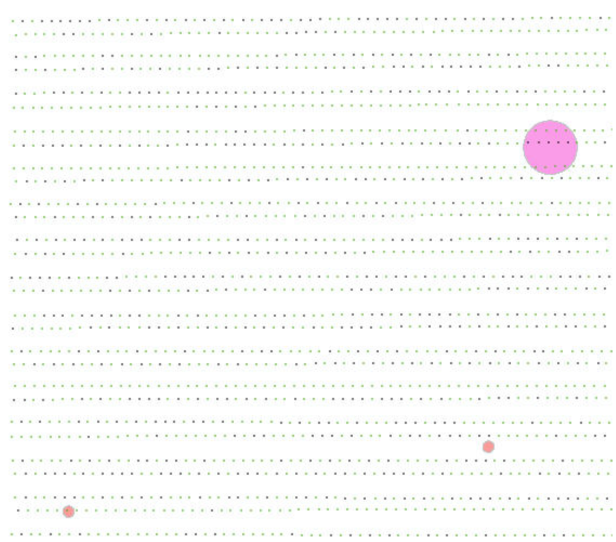

Closer view of image to left showing lidar points, 1.5 m and 0.3 m test craters.

Figure 14: Lidar Point Density Variation

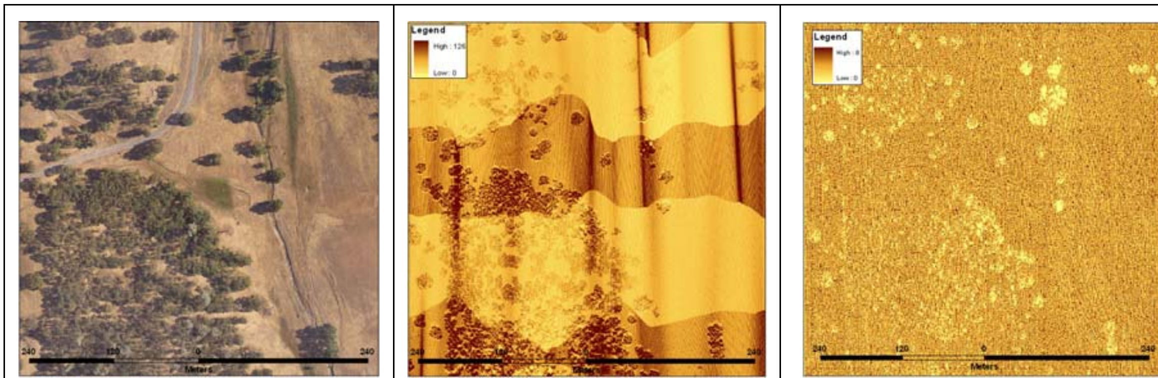

Former Camp Beale ESTCP demonstration site. Point density maps based on all lidar points (center) and ground points only (right). The all points image shows flight line overlap effects (dark horizontal bands) and aircraft pitch (narrow dark vertical bands). The ground points image shows the effects of point classification method (disappearance of flight line overlap and wind effects) and of vegetation (lower density under trees).

4.1.4 Estimating Confidence Levels for Feature Detection

Regardless of the overall point density achieved, lidar point density will always vary somewhat with terrain and will be lower under vegetation. This will affect the confidence levels for detection of ground features over different parts of the site. One approach to determining confidence levels for feature detection is to map the density of lidar ground returns (Figure 15). Areas with no returns would be designated as areas where lidar would not detect ground features, with confidence levels increasing with the number of returns.

Figure 15: Preliminary Confidence Levels for Ground Features

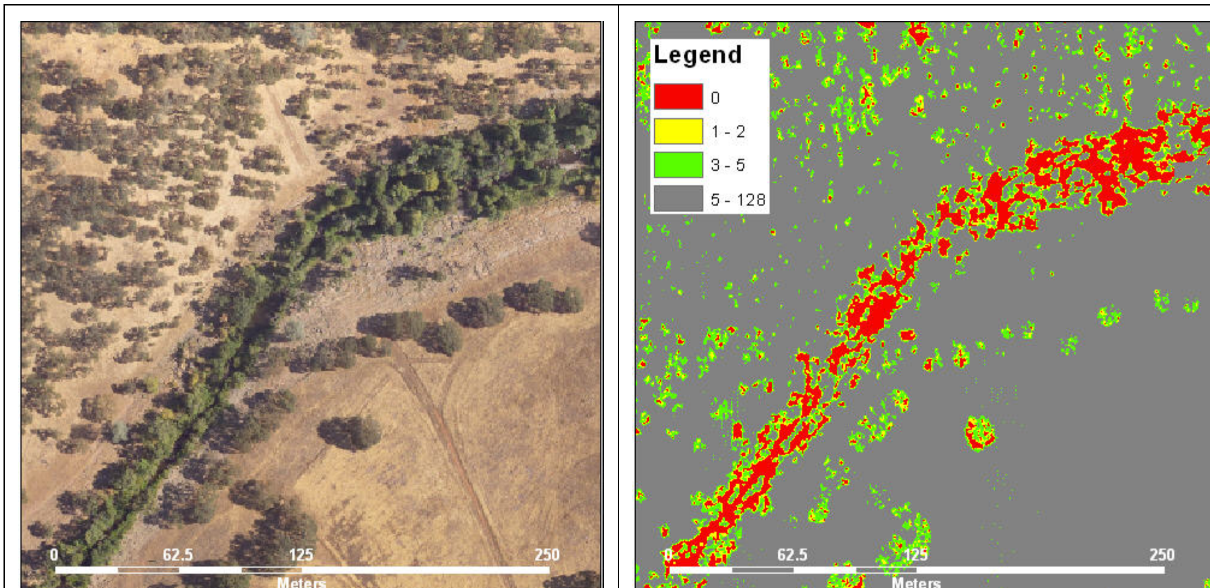

Former Camp Beale ESTCP demonstration site. Point density map based on reclassified ground points, (vendor's ground points plus "low" points within 40 cm of the original ground surface). Scale is in ground points/m^2.

4.2 Vegetation Effects

4.2.1 Lidar

Laser signals do not penetrate vegetation; however, lidar often can be used successfully in most vegetated conditions (Figure 16). This is because the laser will produce a sufficient number of signals to penetrate the many small gaps in the foliage. The ability of lidar to "look through" vegetation is enhanced by the fact that modern lidar sensors can receive multiple returns from the same laser pulse.

Figure 16: Lidar Surface Models under Trees

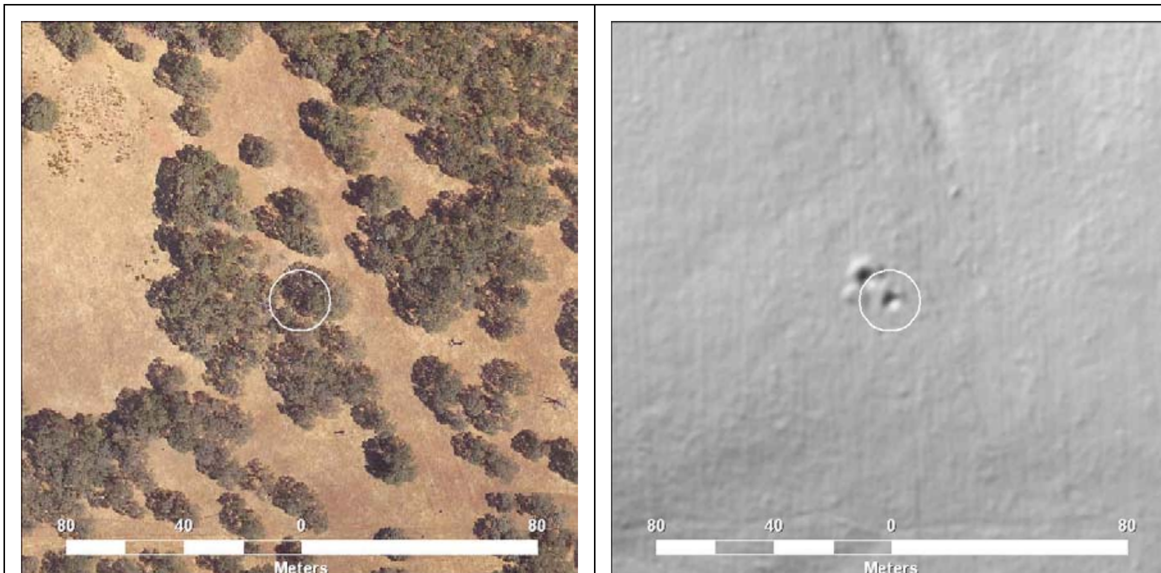

Former Camp Beale ESTCP demonstration site. Orthophoto and lidar-based surface model.

Nevertheless, higher-density vegetation will always result in fewer laser points reaching the ground surface, and thus in a less dense ground model. This is particularly true for low, dense brush (Figure 17 and 18).

4.2.2 Orthophotos

Orthophotos do not look through vegetation; consequently at highly vegetated sites orthophotos will not be useful for detecting ground features. At such sites, it may be appropriate to use pre-existing orthophotos, which are available from many sources. While pre-existing orthophotos often have larger pixels sizes than those collected specifically for munitions investigations, they are still appropriate for general site maps.

Figure 17: Lidar Surface Models in Brush

Former Camp Beale demonstration site, orthophoto and lidar in mixed vegetation. The lidar image is detailed under the tree cover to the left, but degraded in the thick brush to the lower right.

Figure 18: Percentages of Vegetation Returns

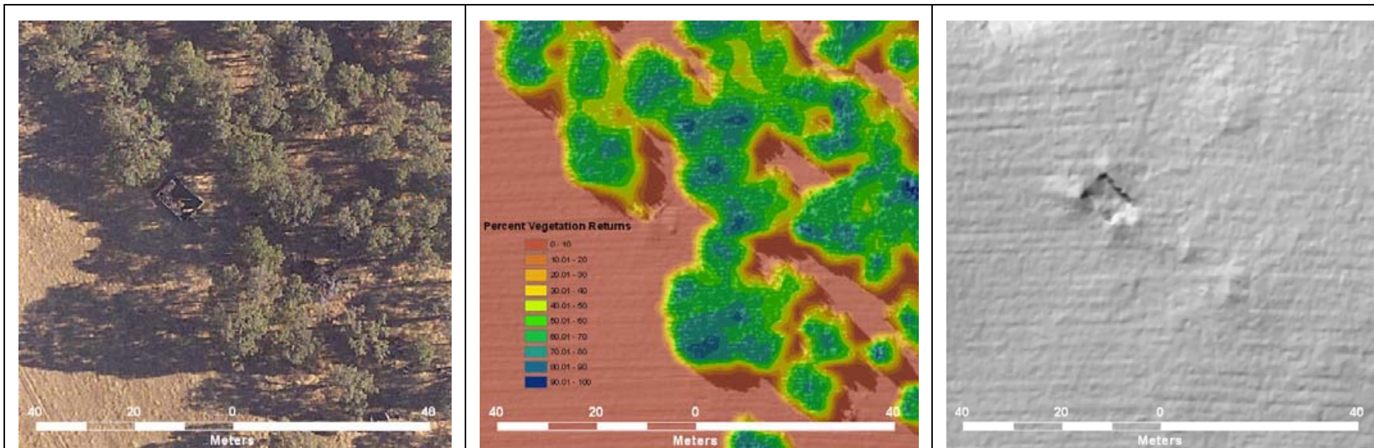

Percentage of lidar points reflected from vegetation – darker green and blue areas have higher percentages of vegetation returns. Although much ground detail is visible under the tree cover, the lower number of ground returns will result in lower confidence in these areas.

4.3 Accuracy and Error in Lidar Data

Error in the collection, processing, and interpretation of lidar data can lead to less accurate site characterization, with potential for both false negatives and false positives in the detection of ground features, difficulty in integrating lidar with other spatial data, and incorrect assessment of confidence levels in the data. An understanding of error in lidar data can contribute to appropriate expectations for the technology, and to the development of appropriate contract specifications.

Understanding lidar error is especially important since error in lidar data arises from different factors than error in magnetometry or EMI, the most common technologies used in geophysical investigations of munitions sites. Magnetometry and EMI directly detect and map magnetic anomalies that may result from UXO, and each anomaly is reported and located individually. Error is understood as the discrepancy between the reported location of the magnetic anomaly and the true location of the object.

Lidar, by contrast, uses large arrays of laser reflections to model surfaces. The location of surface features (potential craters, for instance) is then inferred from characteristics of the entire surface. The accuracy of the location of features in the modeled surface rests on the accuracy and precision of the individual lidar points, but is influenced by other factors such as the density of the laser returns, the characteristics of the terrain, and the methods used to create the surface model. These factors can interact in complex ways.

4.3.1 Lidar Point Accuracy

Lidar vendors guarantee the accuracy of lidar points as a part of their contract documents, and vendors quote very similar guarantees across the industry. A typical accuracy specification quoted is 15 cm vertical and 50–100 cm horizontal.[5] Some vendors provide a more detailed specification such as the following[6]. (The following values are at 95% [two sigma or two standard deviations]).

- ***Vertical:*** 15 cm hard surfaces and open regular terrain, 25 cm soft/vegetated surfaces, flat to rolling terrain, 30–50 cm soft/vegetated surfaces, hilly terrain
- ***Horizontal:*** 50–75 cm in all but extremely hilly terrain (depends on flying height and beam divergence

Lidar vendors guarantee the *accuracy* of the lidar data, that is, its correspondence to surveyed control.[7] Accuracy, in contrast to precision, is the closeness of an estimated value to a standard or accepted correct value.[8] The accuracy value refers the size of the differences between the estimated and the standard value. In the context of lidar, the guaranteed accuracy refers to the correspondence of surveyed control points to either the individual lidar points closest to the surveyed point, or to the elevation of the lidar-derived surface model at that point.

Lidar vendors typically express their stated accuracies as root mean square error (RMSE) values. In calculating RMSE, the difference between data set coordinate values and the coordinate values from an independent source of higher accuracy for identical points are each squared and then averaged over the sample, after which the square root of the average is taken. Since the errors are squared before they are averaged, RMSE gives a relatively high weight to large errors compared to, for instance, an accuracy

[5] See: http://www.airborne1.com/technology/LiDARAccuracy.pdf

[6] , Available from Terrapoint, LLC. See: http://www.ambercore.com/files/TerrapointWhitePaper.pdf

[7] Surveyed control points are often assumed to be free of error, which in really will not be true since control points are surveyed using techniques and instruments that are themselves subject to error. Control points, therefore, should be reported with an appropriate error measure, which can be considered in evaluating the accuracy of the lidar points.

[8] The discussion in this section is adapted from Chapter 3 of Digital Elevation Model Technologies and Applications: The DEM Users Manual (ASPRS 2001).

measure such as the mean absolute error, which gives the same weight to all values. This means that RMSE is most useful when large errors are particularly undesirable. The error of some lidar points will always fall outside of the stated accuracy range. Consequently, RMSE values are generally quoted at the 68% (one sigma or one standard deviation) or 95% (two sigma or two standard deviations) level.[9]

One weakness of RMSE is that, as a single number, it does not capture the spatial variability of lidar point error. As discussed in Section 4.3.4, lidar error can vary with terrain and other factors, and RMSE alone will not capture this variation. Useful supplements to RMSE would include maps of principal terrain and vegetation types, and calculation of error for each principal terrain type separately. This is the approach used by the Federal Emergency Management Agency (FEMA) in its accuracy specification for lidar collected in support of FEMA's flood mapping program (FEMA 2003).

4.3.2 Assessing the Lidar Point Accuracy

Horizontal and vertical accuracy of lidar points are assessed differently. To measure vertical accuracy, lidar vendors commonly survey a variety of locations in the study area, and compare these surveyed elevations to lidar elevations at the same points. Surveyed points are commonly established using static survey methods. Some vendors will supplement static surveyed points with large numbers of additional points collected using kinematic GPS survey methods, collected by driving along roads in the project area. Other vendors use small unmanned rover vehicles to collect large numbers of static points.

To evaluate horizontal accuracy, vendors compare the location of the lidar returns for objects in the study area with real-world horizontal locations that can be surveyed. These may include target objects placed with the surveyed points as in Figure 19, or larger objects. For example, lidar elevation values can be used to model the corners of buildings and other structures, or lidar intensity values can be used to model the edges of pavement (Figure 20). These lidar-based locations can then be compared to surveyed locations for the same objects. These same objects can be used to assess lidar to orthophoto alignment.

Figure 19: Surveyed Points Used to Assess Lidar Vertical Error

[9] Formulas for calculating RMSE can be found in ASPRS (2001).

Typical surveyed points used to evaluate vertical and horizontal accuracy.

Figure 20: Objects Used to Asses Lidar Horizontal Error

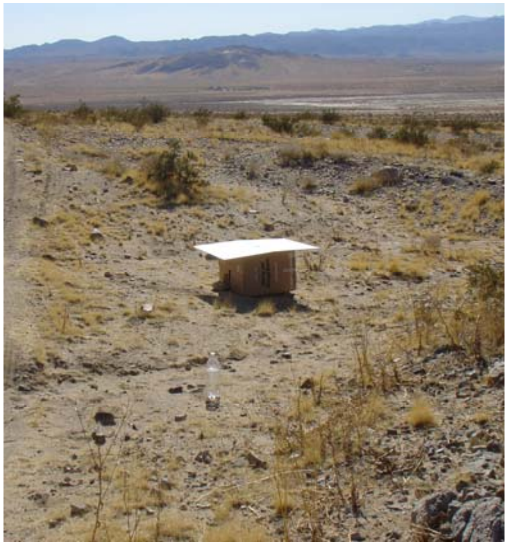

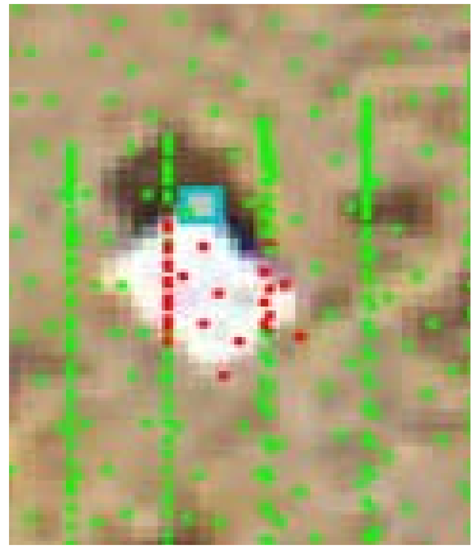

Lidar points reflecting on and around a pre-placed rectangular control surface. Lidar points are color-coded to show reflections from the ground surface (green) and those at or above the known height of the flat panel (red).

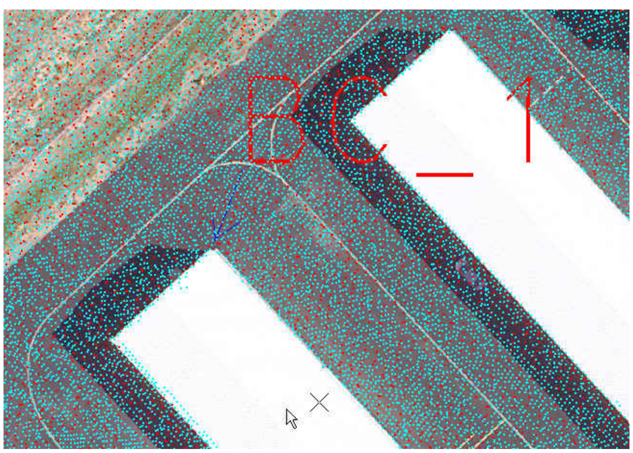

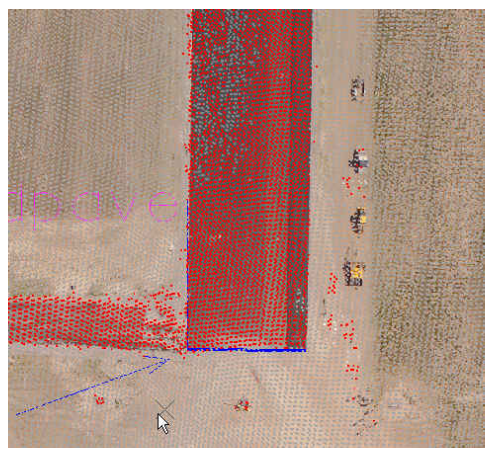

Lidar elevation values are used to model the edge of the building. The modeled location is compared to the surveyed location – not to the location in the orthophoto since this may be subject to different sources of error.

Lidar intensity values are used to model the edges of pavement (as in the runway above). Locations of pavement edges or corners are compared surveyed locations.

Surveyed control points provide survey-grade data points of a higher accuracy than the lidar data to assess the accuracy of the lidar points. Vendors may perform vertical adjustments of the entire lidar data set to achieve a best possible fit to the control points[10], in which case the residual differences after this adjustment provide the

[10] At least one vendor state that without such adjustment, vertical errors of the lidar data would routinely exceed the manufacturers reported maximum vertical error of 15 cm (Sky Research, 2009).

quantitative estimate of the vertical error of the lidar data. The surveyed points are also used to validate the accuracy of the lidar system and to validate the lidar calibration values.

Both surveyed control points and lidar point locations depend on GPS to determine locations. It is therefore important not to have too great a distance between the study area and the nearest GPS base station that will be used for post-processing. Generally, 50 kilometers is considered a reasonable limit, after which the accuracy of the lidar data begins to degrade. Most airports have GPS base stations; however, a closer base station should be established for sites located at a sufficient distance from the airport. In remote areas where established GPS base stations are scarce or non-existent, lidar acquisition may require support from helicopters to establish control points and additional base stations in or near the project area.

Horizontal and vertical accuracy are reported by vendors using standard quality control reports. Table 1 shows an example lidar vertical error report from a vendor, displaying lidar-to-control-point vertical error for eight control points. It shows an error of just over 10 cm or 0.104 meter (m) at the 95% confidence level.

Table 1: Example Lidar Vertical Error Report from a Vendor

Statistics					
Target	**Easting**	**Northing**	**Survey Elevation**	**Lidar Elevation**	**Difference**
TAR1	543461.243	3805793.824	827.486	827.440	-0.046
TAR2	542947.381	3807961.251	837.761	837.740	-0.021
TAR3	543747.347	3809712.492	833.970	833.930	-0.040
TAR4	545277.331	3809859.694	797.753	797.710	-0.043
TAR5	546671.936	3810138.520	846.280	846.230	-0.050
TAR6	547168.309	3808650.964	864.049	864.000	-0.049
TAR7	545682.049	3807795.187	784.720	784.650	-0.070
TAR8	546462.139	3805793.466	806.263	806.180	-0.083
Summary					
Average difference			-0.050		
Minimum difference			-0.083		
Maximum difference			-0.021		
RMSE of the elevation			+/- 0.053		
2d RMSE of the elevation (95%)			+/- 0.104		
Std-Dev. of the elevation			+/- 0.019		

Source: Terra Remote Sensing

Surveyed and lidar elevations in this chart are reported in meters above the "height above the geoid", an elevation that roughly coincides with mean sea level. See ASPRS (2001) for additional discussion of elevation values in GPS and lidar.

4.3.3 Lidar Point Precision

Often confused with accuracy, precision is a measure of the tendency of a set of values to cluster about a number determined by the set. The usual measure of precision is the

standard deviation or the standard error. Precision is distinguished from accuracy in that accuracy is a measure of the tendency to cluster about a value, such as a surveyed point, which is not determined by the data set but specified in some other manner (such as ground survey). Therefore, in order to be highly precise, a data set needs only to conform to itself, while to be accurate the data set must conform to an independently derived standard (ASPRS 2001).

If lidar precision were perfect, there would be no elevation differences, for instance, between lidar returns on a uniformly flat surface. In practice, precision is never completely perfect, and precision errors appear, for instance, as the "texture" observable on paved parking areas or roads (Figure 21). Precision error of this type may arise from small errors in the sensor system, and to this extent reflects the inherent limits of the technology at its current state of development, or precision errors may arise from insufficiently tight calibration, which can lead to higher than necessary vertical distances between lidar points.

Figure 21: Lidar Precision Error

Orthophoto and lidar surface, municipal airport, Washington State. The lidar surface shows more "texture" than the orthophoto on the flat surfaces of the parking lot and building roofs.

4.3.4 Sources of Lidar Point Error

Several factors influence the accuracy and precision of individual lidar points. In most cases, the magnitude of each error source is not well documented, since vendors and manufacturers generally report error values for the system as a whole.

Instrument error. Broadly, instrument error refers to the difference between the value given by an instrument and the "actual" values, based on the accuracy and precision of the measuring instrument. In the context of lidar, instrument error consists of deviations from positional values, generally as determined by GPS-based survey methods, contributed by each physical component of the system. Instrument error can impact both accuracy and precision.

Manufacturers and vendors typically report error for the entire system, expressed as the difference between the positions of individual lidar points compared to surveyed positions. Reported error for one commonly-used lidar system, the Leica Geosystems ALS60 Airborne Laser Scanner, is presented below. This system is comparable to

others in common use and represents typical error values. The error curves are based on a 40-degree field of view and a nominal 5 cm GPS error.

Figure 22 shows that vertical (z) error ranges from under 10 cm to over 20 cm depending on flight height and distance from nadir, and that horizontal (x,y) error ranges from around 5 cm to over 60 cm, again depending on flight height and distance off nadir. Most lidar collected at munitions sites has been collected at flight heights of 300–1,000 m, where both horizontal and vertical error is lower.

Figure 22: Leica ALS60 Horizontal and Vertical Error Curve

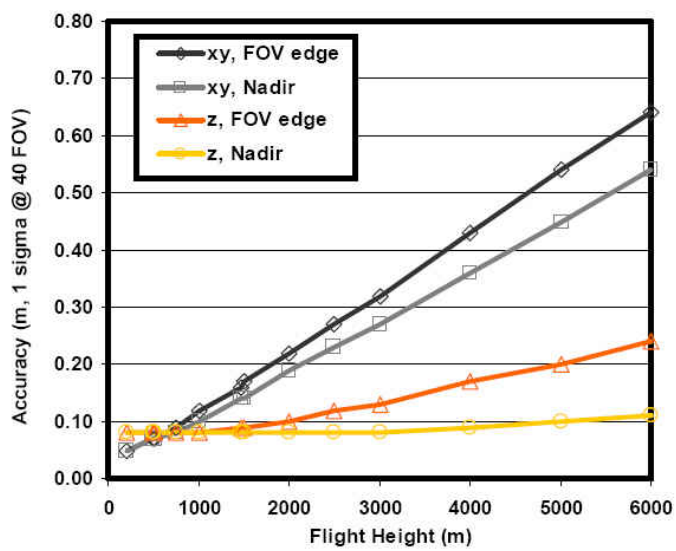

Site Conditions. A wide variety of local conditions can create error in lidar data. Some conditions affect the entire data set, either by affecting the equipment directly or interfering with the GPS signal. Others, such as slope, may affect only part of the survey area. Site conditions that can contribute to lidar error include:

- ***Slope.*** Lidar collected on steep terrain will be less accurate than that on flat terrain (Figure 23). This error arises in two ways:
  - The lidar pulse spreads as the beam travels. The degree of beam divergence is controlled by the characteristics of the laser combined with the flight height, with typical beam footprints between 10 and 100 cm in diameter.[11] Beam divergence creates an area of uncertainty as to the exact point where enough energy is reflected to trigger a return. On flat surfaces this uncertainty may affect the horizontal location of the return, but will not affect the elevation value. On sloping surfaces, the area of the pulse footprint will be larger, and will include a vertical error range.

[11] The formula for beam divergence is roughly: spot diameter at nadir = elevation (meters)*beam divergence (radians) (Baltsavias 1999). System manufactures report beam divergence factors from 0.22 to 1.0 mrad (Key 2009). Laser footprints would therefore range from 22 to 100 cm at 1,000 m flight elevations.

- The horizontal error of the lidar location, caused by both beam divergence and the error inherent in the GPS, IMU, and other components will be larger on sloped ground. Further, on sloped ground the horizontal error will magnify the vertical error versus flat ground. The maximum amount of elevation error introduced is a function of surface slope, with: Elevation Error = tan α x Horizontal Displacement.

Figure 23: Effects of Slope on Lidar Point Error

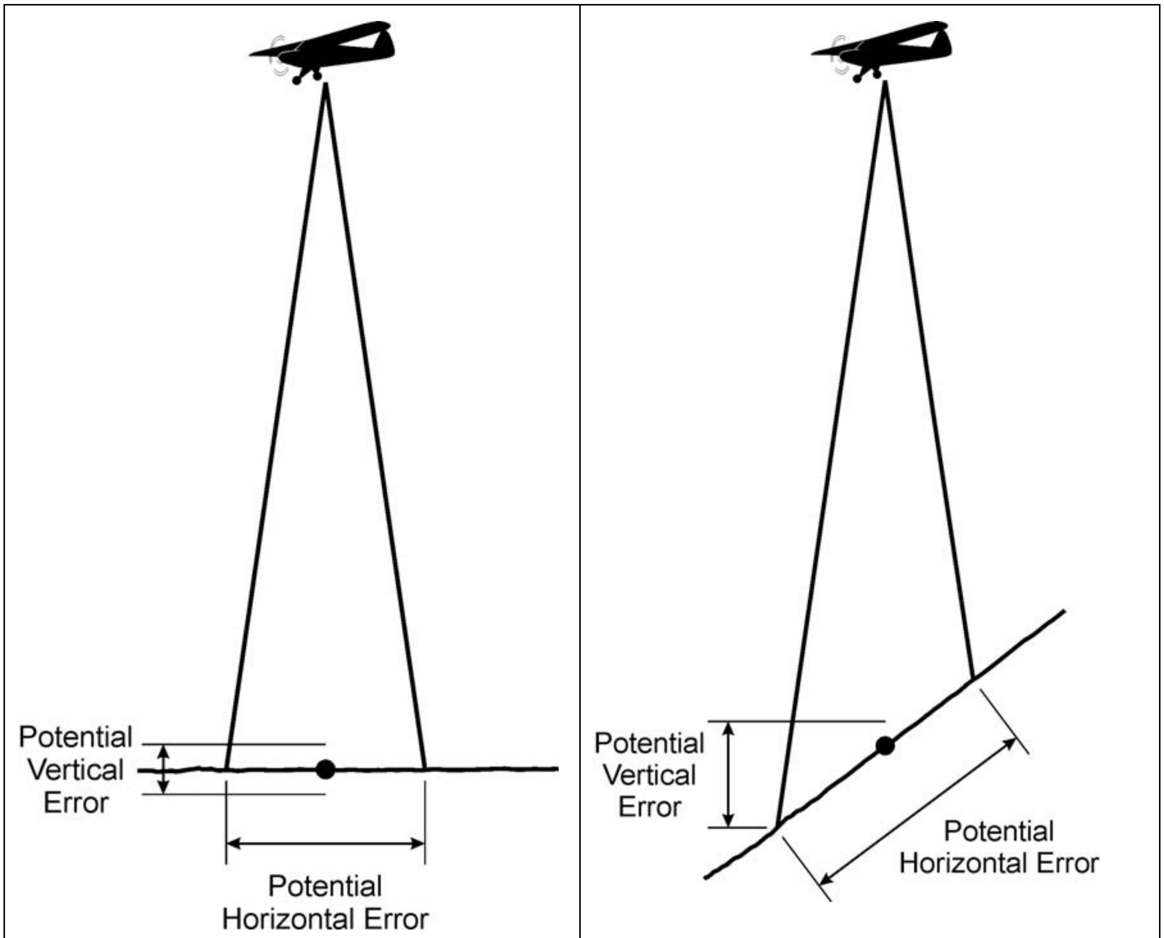

Slope compounds both horizontal and vertical error of lidar points.

- ***Type of ground surface.*** Some vendors guarantee higher accuracy on hard surfaces than on soft ground surfaces; this is based on the fact that soft surfaces are often less clearly-definable. Plowed fields or grassy areas, for instance, have furrows or vegetation that would create error up to 10–20 cm compared to use of a survey pole (Neufeldt 2009).

  Similarly, highly reflective surfaces occasionally appear to be slightly raised in comparison to non-reflective surfaces, such as white painted centerlines on asphalt roadways. It is possible that more reflective surfaces are returning sufficient energy to trigger a response more quickly than less reflective surfaces.

- ***Vegetation conditions.*** Under vegetated conditions, it is common for the majority of laser signals to reflect from the vegetation rather than the ground surface (Figure 18). The lower density of lidar points under vegetation will lead to lower confidence levels for detection of small features. The accuracy of the individual lidar points under vegetation should not be affected; however, the ground surface model will be coarser, which may lead to more discrepancy between the modeled surface and surveyed points at any particular location.
- ***Electromagnetic interference.*** Rarely, certain types of man-made electromagnetic signals can affect lidar data collection. Such interference was noted at the Former Camp Beale ESTCP demonstration site. Beale Air Force Base, which is adjacent to the demonstration site, is the site of one of three installations that are part of the Phased Array Warning System radar system, designed to detect and track sea-launched ballistic missiles. The high-intensity radar signals from this installation disrupted the GPS time signal used by the lidar and orthophoto sensors, initially rendering the data unusable. The effect was noted within several kilometers of the radar station and at altitudes up to approximately 500 m. The problem was noted during the daily QA/QC checks on the first day of data collection. A sample of the data was sent to the vendor's office, and a solution was developed to re-insert the correct GPS times. Interestingly, lidar was subsequently collected at Beale Air Force Base without problems, since lidar data collection took place at a higher altitude outside of the influence of the radar system.
- ***Geomagnetic activity.*** A different form of electromagnetic interference, geomagnetic activity refers to natural variation in the earth's magnetic field, usually as a result of solar flares and other solar activity. During periods of high geomagnetic activity the GPS phase can be affected to the point where the receiver cannot perform phase measurements with enough precision for centimeter level accuracy. It is good practice for vendors to check Government web sites for geomagnetic activities prior to data collection.
- ***Weather and temperature.*** Weather and temperature conditions can affect the ability to collect lidar data, but should not affect the accuracy or precision of the lidar data itself.

4.3.5 Creating Surface Models

In practice, much of the analysis of lidar data is performed using surface models derived from the lidar points. Several factors influence the usability of lidar-based surface models; some are due to error and others to technical choices that may be inappropriate to the site.

The typical final products of lidar are digital models of the ground surface, both of the bare ground and the ground with vegetation and buildings included. Typical model types are DEMs, digital surface models (DSMs), and DTMs.

A DEM, as defined by the USGS, is a digital file consisting of terrain elevations for ground positions at regularly-spaced horizontal intervals that portrays the ground surface free of vegetation or human-created structures.[12] DEMs may be created using data from

[12] See: http://rockyweb.cr.usgs.gov/elevation/dpi_dem.html

many sources in addition to lidar, including topographic maps, ground survey, photogrammetry, or synthetic aperture radar. In the context of lidar, the DEM is the product through which the semi-random mass lidar points that the vendor classifies as returning from the ground surface are converted to a regularly-spaced grid of elevation values. This digital model can then be used in standard GIS or other software to produce hillshaded surfaces, contour lines, or other digital products.

Regularly spaced elevation files of this type also may be created using all returns, including those from the tops of buildings, trees and other features. The USGS refers to these as DSMs. The term DTM is used as a synonym for both DEM and DSM. In the lidar context, the term DTM is most frequently used to refer to the all-points surface model. This paper uses the term DSM for the all-points surface model including both ground and non-ground returns.

Error in the DEM can be defined as the discrepancy between the elevation values of the DEM cells compared to surveyed values at the same locations. Error in the elevation values of the DEM cells also affects the horizontal error of features visible in the ground surface model, since it is the elevation differences between adjacent DEM cells that create edges that allow the user to infer the location of features.

Factors Affecting Surface Models. The accuracy and usefulness of a surface model will depend on the accuracy of the lidar data from which it is created, and will be subject to the types of error that affect lidar points. However, the usefulness of the model can be impacted by the methods used to create the model itself, including:

- The choice of the points classified as ground or non-ground returns
- The choice of interpolation method from the lidar points to the individual cell elevations
- The choice of cell size

Point classification methods. The point classification approach used by the lidar vendor should have no effect on the accuracy or precision of the lidar points, since classification takes place after the data is calibrated. However, methods that are biased towards creating clean, smooth ground surfaces can result in a lower data density of ground points, and this can result in fewer detections of small ground features.

Interpolation method. The technical problem in creating surface models from lidar points is to assign an accurate elevation value to each regular grid cell from the semi-random lidar points. There are two general approaches to assigning these values. The first approach is to interpolate the cell values directly from the lidar points. There are a variety of mathematical approaches to such interpolation available in GIS programs and other software.[13]

The second approach is to create a triangulated irregular network (TIN) using every individual lidar point. The TIN is then used to create the surface model, again using one of the interpolation methods described above. Either approach can be employed using the ground points only or both the ground and vegetation points.

[13] These methods are described in detail in references such as the ArcGIS help files.

Both of the above approaches produce useable surfaces, with each method having its own particular advantages and shortcomings. However, the TIN method appears to be the most common approach at the time of this document (Figure 24).

Cell size. Choice of cell size can affect the detection of small surface features dramatically (Figure 25), with smaller cell sizes performing better. Vendors and researchers suggest that cell size be no larger than the average ground point spacing, and that use of cells smaller than the average point spacing may not sacrifice accuracy.

Display methods. Surface models are usually displayed as hillshaded images to enhance the visualization of surface features (Figure 26). ArcGIS, the most commonly used GIS software, contains dozens of settings that can affect the usefulness of these images. Different settings may be appropriate in some circumstances, and users need to work with analysts both to fully understand the goals of the survey and to experiment with appropriate settings.

Figure 24: Process Steps for TIN-Based Lidar Surface Models

<table>
<tr><td>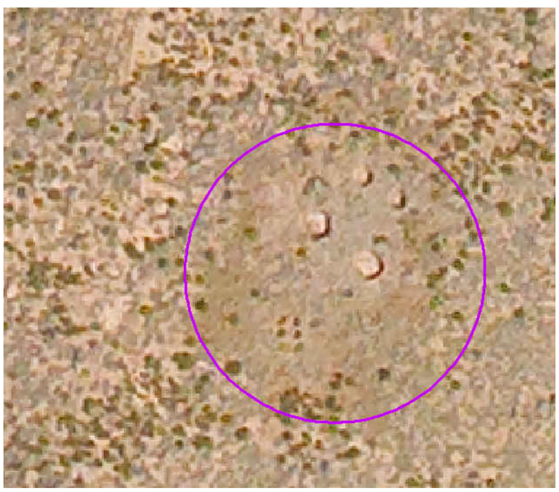</td><td>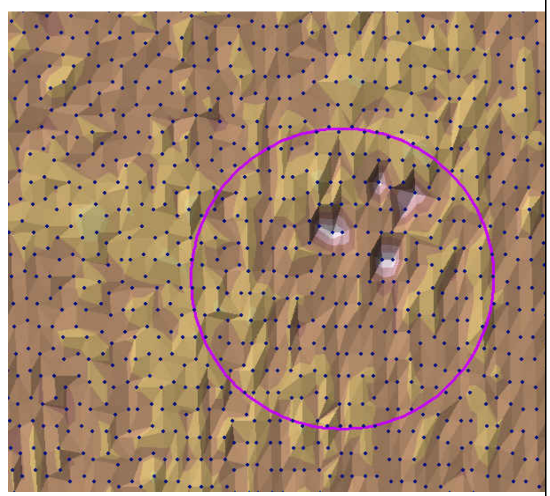</td></tr>
<tr><td>Kirtland AFB ESTCP demonstration site, orthophoto showing simulated craters.</td><td>TIN and lidar points. Each lidar point represents one vertex in the network of triangles.</td></tr>
</table>

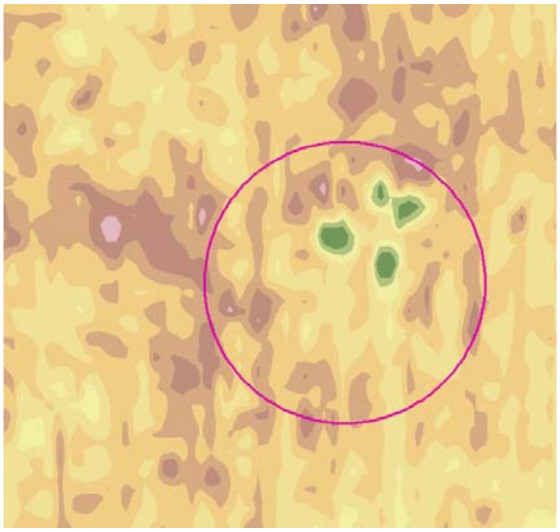	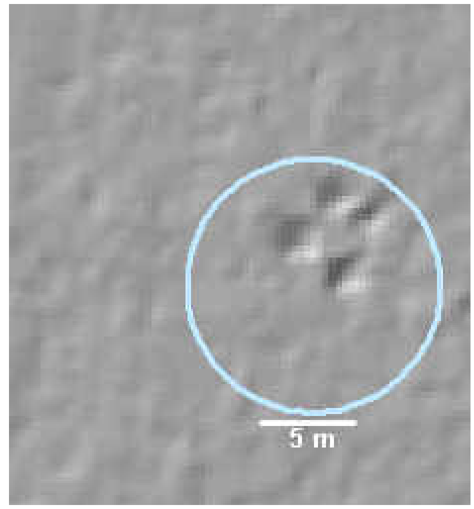
DEM created from the TIN, above right.	Hillshade created from the DEM, left.

Figure 25: Effects of Surface Model Cell Size on Feature Detection

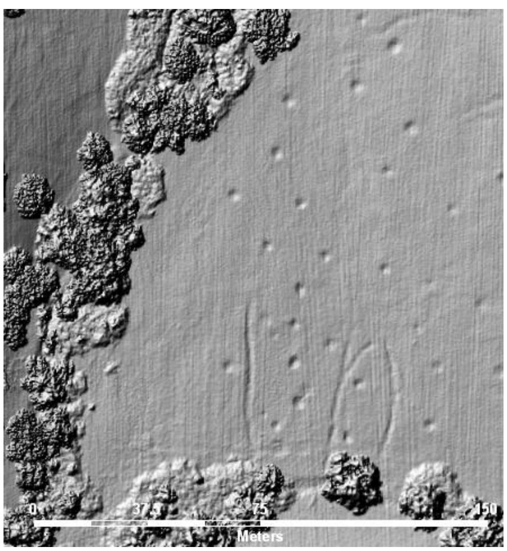	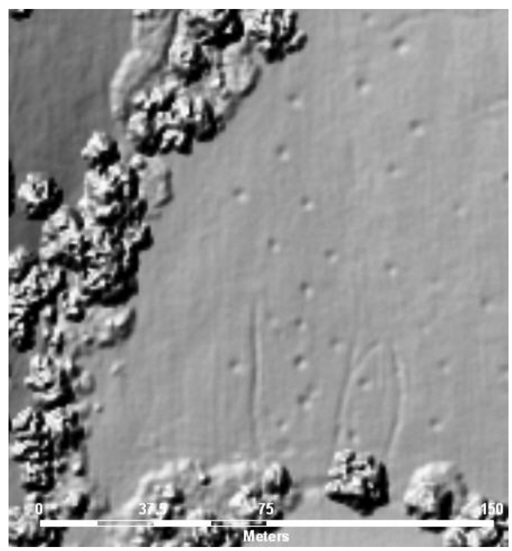
Former Camp Beale ESTCP demonstration site. Hillshade and DEM based on 0.3 m cells. Craters are approximately 3 m in diameter.	Hillshade and DEM based on 1.0 m cells

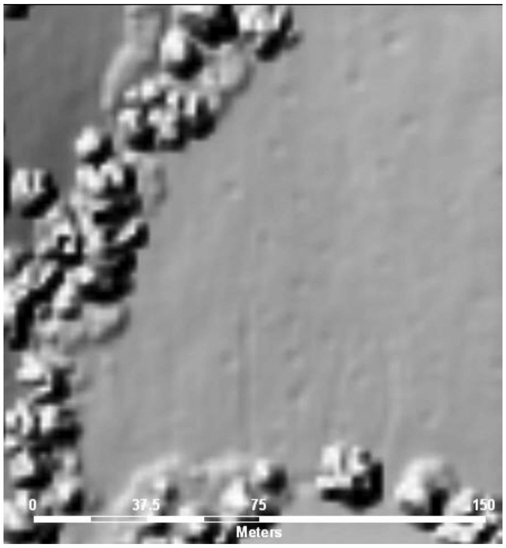	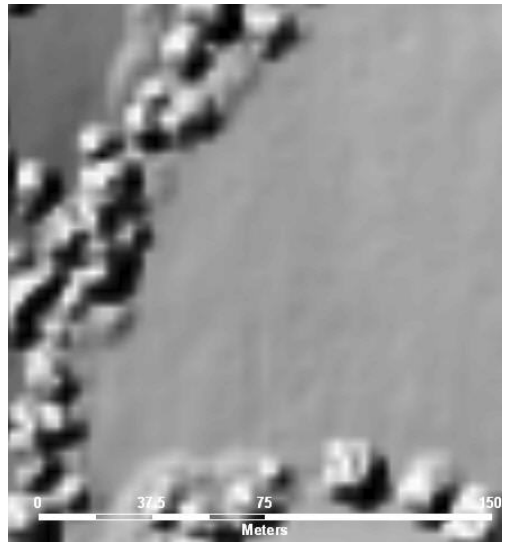
Hillshade and DEM based on 2.0 m cells	Hillshade and DEM based on 3.0 m cells

Figure 26: Hillshade Display Method Examples

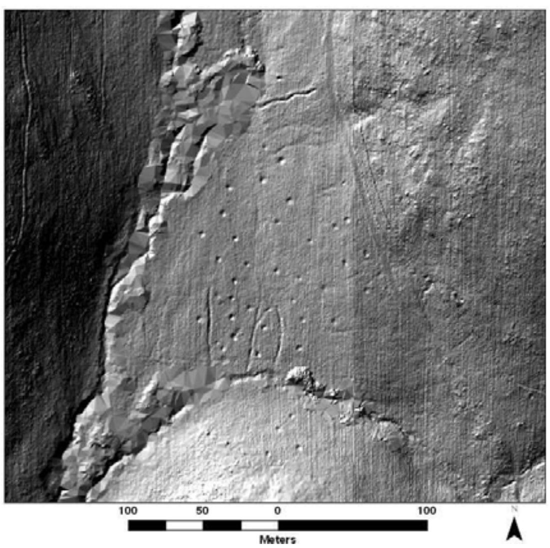	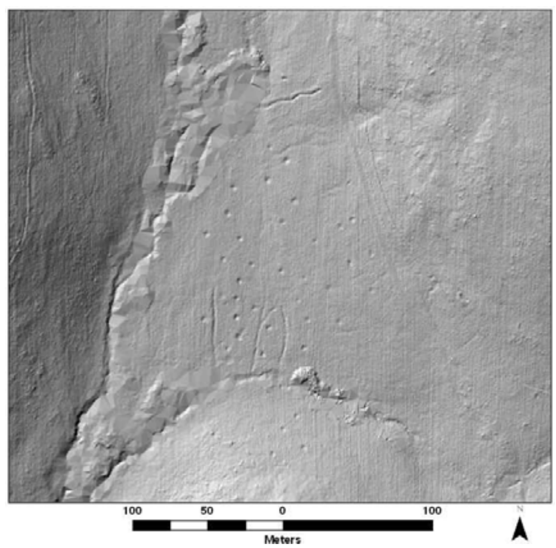
Former Camp Beale ESTCP demonstration site, hilshade image, ArcGIS default settings. The default settings are too dark in some areas to reveal the ground surface.	Hillshade image, alternate settings showing less dark grey area but also less contrast on the craters

<table>
<tr><td>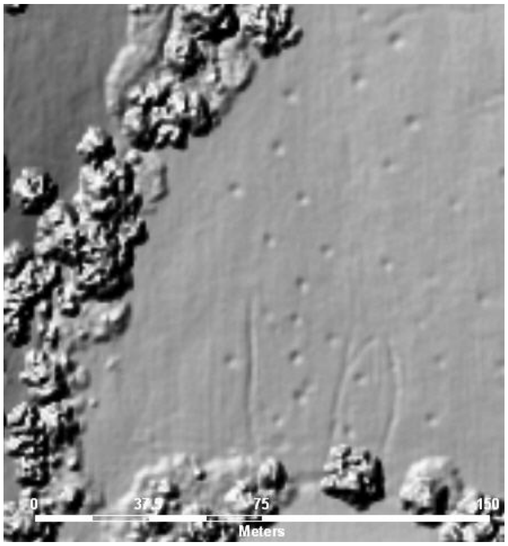
</td><td>
</td></tr>
<tr><td>Hillshade image, “neutral” hillshade settings</td><td>Hillshade image, contrast boosted, highlighting craters but obscuring other detail</td></tr>
</table>

4.4 Accuracy and Error in Orthophotos

Positional error in orthophotos can be expressed as the difference between the apparent location of the orthophoto pixel and its true ground location. Positional error is specified in contract documents and verified by comparing objects in the image to surveyed locations, as discussed in Section 4.3.2.

In addition to positional error, there are a number of other quality issues that can arise in the creation and use of orthophotos, including:

- ***Color balance.*** Vendors will sometimes have a difficult time achieving a good color balance among the numerous digital images in the mosaic. While it is difficult to establish a rigorous contract specification, color balance should be inspected on receipt of the orthophotos and any problems discussed.
- ***Position of base vs. top of objects.*** In parts of the image that are not directly under the aircraft, the image will include portions of the sides of tall objects such as trees and buildings. In such cases, the top of the image is not located directly over the base of the object, and while the base of the object will be correctly spatially located, the top will appear slightly offset (Figure 27). This is a limitation of the technology which should be understood by users.

Figure 27: Apparent Misalignment of Tops of Buildings in Orthophotos

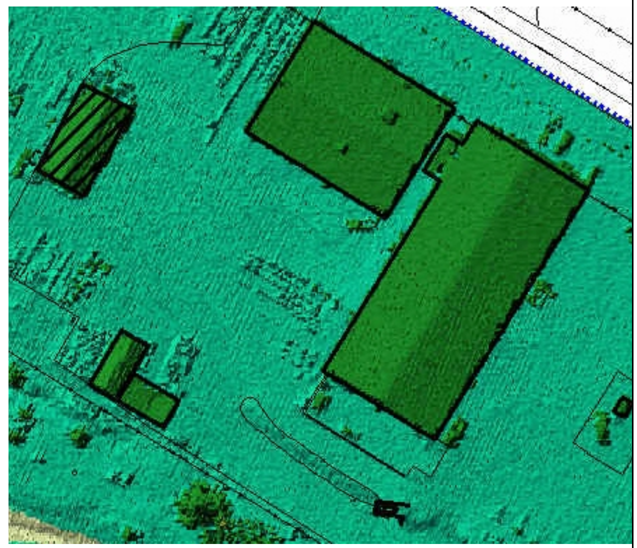

Airport site, Washington State. Orthophoto and lidar compared to surveyed building locations. The orthophoto on the left shows slight apparent misalignment of the top of the buildings compared to surveyed locations, while the lidar image on the right (color coded by elevation) shows better alignment.

- ***"Leaning" trees.*** Another implication of portions of the image being off-nadir is that groups of objects, most often trees, can appear to lean, sometimes in paradoxical ways. This problem is greater with larger image sizes, where the off-nadir angle will be greater, and also in steep terrain. The problem can be minimized by skillful assembly of the image mosaic, but cannot be eliminated entirely.
- ***Shadows.*** Shadows in orthophotos can sometimes be extreme and can obscure ground features. Shadows can be minimized by collecting imagery at times of day and times of the year when the sun is close to overhead, and vendors will normally plan data acquisition for such times when possible. For relatively flat munitions sites without tall vegetation, however, images collected at low sun angles can have some advantages since the resulting shadows will highlight small craters, dirt roads, and other faint objects (Figure 28).

Figure 28: Shadows in Orthophotos

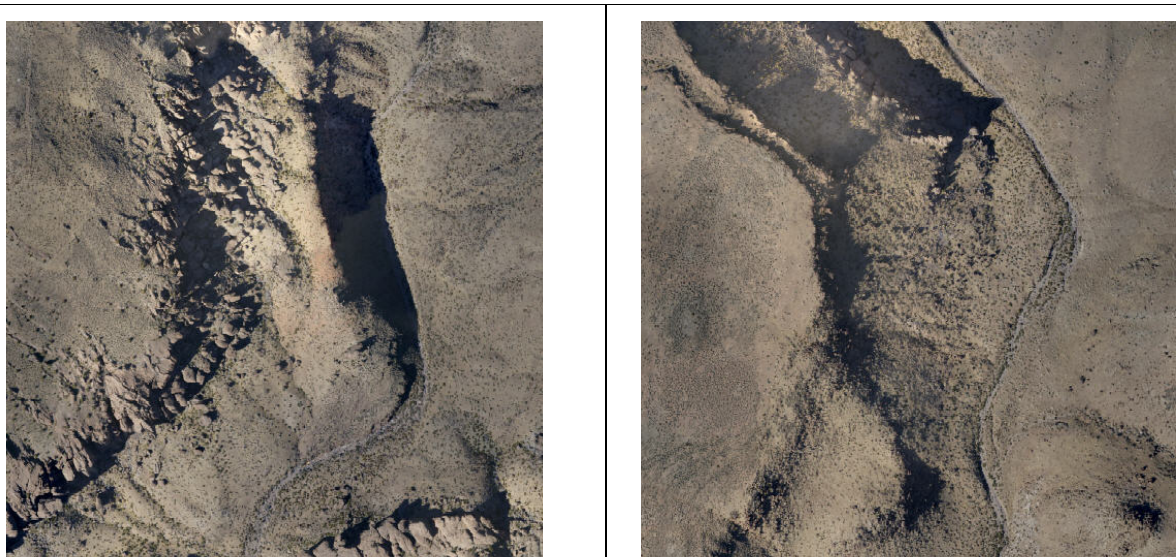

Nevada desert site: steep canyons create deep shadows in the orthophotos; these areas are largely unusable. Images could have been improved by flying during higher sun angle.

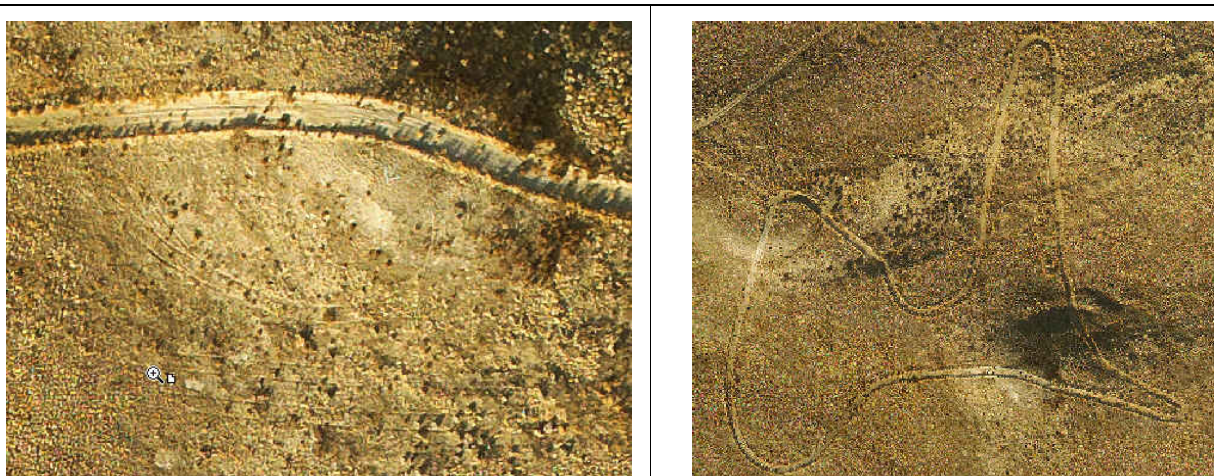

Navy Range Boardman, OR: orthophotos taken at low sun angle, shadows enhance the visibility of ground features. Left, vehicle tracks can be seen to the south of the dirt road. Right, the road is much more visible as a result of the shadowing at its edges, which would not have been present if the sun had been at or near nadir.

4.5 Operator Error

Potential areas where actions of the operator can affect lidar products include mission planning, field data collection practices, data calibration, and lidar point classification. There are many sources of operator error, including inexperience or improper training, momentary lack of judgment, inattentiveness, or distraction. Operator error also may result from incomplete information, as when the operator does not fully understand the purpose of the lidar survey. Operator error is difficult or impossible to quantify.

The standard approach to eliminating operator error is through the application of training programs to reduce error and quality control programs to detect and correct errors. Most vendors have well-developed training and QA programs, and the impact of serious operator error is generally small. This is particularly true in regard to all processes that impact the positional accuracy of the lidar, where operator error may cause the vendor to fail to meet contract specifications.

4.6 GPS Error

GPS error is a component of the overall lidar system error discussed above. Error in GPS is discussed separately first, since vendors report that GPS error is the largest source of error in the day-to-day use of lidar technology, and second, since GPS error affects not only the positional accuracy of the lidar points, but the accuracy of field data, including both calibration points and the reported locations of features in the field.

There are three broad categories of GPS receivers on the market. Each has a different level of positional accuracy, and this should be accounted for in reporting the positions established in the field. GPS accuracy is degraded under vegetation for all types of equipment. Receiver types include:

- Recreation or consumer-grade GPS, which have quoted positional accuracies of 3–5 m in open areas.[14] Manufacturers do not quote accuracies for obstructed areas such as under vegetation canopy for any type of GPS receiver (Clarkin 2007); however, Wing and Eklund (2007) found recreation-grade receivers to be capable of accuracies within 10 m under closed canopies and 7 m under young forest in western Oregon.
- Resource or mapping-grade receivers, which have a quoted accuracy in the open as sub-meter down to around 30 cm.[15] Researchers have found these single-frequency receivers to achieve error between 0.2 and 6 m under vegetation, depending on conditions (Clarkin 2007).
- Survey grade receivers, which achieve sub-centimeter accuracy in open conditions. Hasegawa and Yoshimura (2003) found that survey grade receivers achieve accuracies of 0.02–0.4 m under dense canopy. Naesset (2001) found a survey-grade dual frequency receiver had mean positional accuracies of 0.08–1.35 m under dense canopy.

4.7 Summary: Implications for Use of Lidar and Orthophotos

The preceding sections have several implications for the use of lidar and orthophotos at munitions sites.

---

[14] For example, see http://www.magellangps.com/products/product.asp?segID=425&prodID=1916 for the Magellan Triton 2000 series, a high-end hand-held model.

[15] See http://www.trimble.com/pathfinderproxt.shtml or http://store.elecdata.com/trimble/pathfinder_proxh_receiver.aspx. For example, the Trimble R8 GNSS, a commonly-used GPS system in both static GPS and real time kinematic surveying, has published accuracy specifications of ±5 mm +0.5 ppm horizontally and ±5 mm +1 ppm vertically for static GPS applications, and ±1 cm +1 ppm horizontally and ±2 cm +1 ppm vertically for real time kinematic applications. See Trimble R8 GNSS System Datasheet, http://trl.trimble.com/docushare/dsweb/Get/Document-140079/022543-079H_TrimbleR8GNSS_DS_0309_LR.pdf.

Implications for calibration and quality control. Errors in the surveyed calibration points can lead to incorrect assessment of data quality or errors in the entire lidar data set. Surveyed points used for calibration and quality control must be from a source of higher quality than the lidar data itself. Standard practice in establishing calibration points includes:

- Using survey-grade GPS operated by qualified staff.
- Choosing flat sites to minimize the effects of slope between surrounding control point and nearest lidar points.
- Choosing open-sky sites, which are essential to GPS quality.
- Choosing calibration points in all major terrain types. Actual data calibration will be performed using the highest quality surveyed points, which may exclude points in especially rugged or soft terrain. However, points in all terrain types will be used for quality control and accuracy evaluation.

GPS error in field surveys. In most field work, resource-grade GPS, with its sub-meter accuracy, should be able to locate munitions-related ground features with sufficient accuracy to compare the with lidar data, as long as open-sky conditions are present. At vegetated sites where GPS error can be larger, more complex methods to locate positions may be needed.

Surface models. In the creation of digital surface models, vendors and Government end users have several options to assure that surface models best serve the needs of the investigation:

- Vendors should be required to meet tight calibration standards to minimize elevation differences that may result in over-classification of non-ground points. Optimum point classification methods for munitions sites have not yet been developed; however, the appropriate principle is to retain the largest number of points possible in the ground classification, even at the cost of including some additional surface noise.
- In creating DEMs and DTMs, vendors and Government end users should use the smallest cell size consistent with data density.
- Vendors and end users should consider experimenting with interpolation methods.

In practice, creating DEMs and DTMs is more conveniently accomplished by Government end-users in-house, rather than having the vendor deliver them, since creation in-house can allow for experimentation with alternative methods. However, this requires that Government end-users have sufficient software tools and training to accomplish these tasks. Creating DEMs and DTMs in-house can be challenging, especially with high-density data sets where the number of points is very large. In such cases it may be appropriate to work with sample data sets to determine, in consultation with vendors, the appropriate specifications for these products, and then request that the vendor create and deliver the final products.

5 Costs and Contracting Considerations

5.1 Factors Affecting Cost

Costs for lidar and orthophoto surveys are variable and depend on site-specific factors. However, a planning-level cost of between $10 and $30 per acre is typical at the time of this report (URS 2009b). This cost includes acquiring lidar in the range of four to six points per square meter, orthophotos at a 10–20 cm pixel size, creating standard GIS products, and performing QA/QC review and initial analysis. Table 2 presents the principal factors affecting estimated cost, and whether these factors also affect performance.

Table 2: Factors Affecting Cost and Performance

Parameter	Value	Cost Impact	Performance impact
Data density	Orthophotos not collected	Cost approximately 25% lower than the range quoted	Project must rely on pre-existing orthophotos
	Orthophotos ~ 20 cm pixels or larger	Cost on the lower end of the range quoted	Orthophtos appropriate for overall site maps but limited usefulness for individual object detection
	Orthophotos ~10 cm pixels	Costs on the higher end of the range quoted	Orthophotos appropriate for both overall site maps and individual object detection
	Lidar ~ 4-6 pts/m^2	Costs on the lower end of the range quoted	Surface models appropriate for detection of target objects and larger individual objects
	Lidar ~ 8-10 pts/m^2	Costs on the higher end of the range quoted	Surface models appropriate for detection of target objects and larger numbers of individual objects
Weather	Clear	Cost not affected	Data quality not affected
	Wind, rain, or snow	Additional labor and per diem for each day that weather prevents data collection	Data cannot be collected in wind, rain, or snow
	Summer temperatures over 100° F	Cost of additional labor, per diem and aircraft rental due to shorter data collection flights	Data quality not affected, but data collection limited to early morning hours

Parameter	Value	Cost Impact	Performance impact
Vegetation	No vegetation or low grass	No impact	Lidar: no impact Orthophotos: no impact
	High grass and light brush	No impact	Lidar: no impact Orthophotos: no impact
	Medium brush and some trees	No impact	Lidar: some degradation in surface models in brush, no impact in light tree cover Orthophotos: will not show areas beneath trees or brush
	Medium to heavy trees	No impact	Lidar: surface models show some degradation in heavy trees Orthophotos: limited usefulness in areas of medium to heavy trees
	Full canopy	No impact	Lidar: surface models show severe degradation Orthophotos: limited usefulness
Terrain	Rugged (steep, rocky)	No impact	Lidar: positional accuracy will be somewhat lower in steep, rough terrain Orthophotos: very steep terrain can cause shadowing, plan data collection for hours when the sun is directly overhead
	Rolling (hills, ravines, ruts)		
	Level (wide, open, flat)		
Surface clutter	Uncluttered through heavily cluttered	No impact	No impact from surface clutter
Geology	Localized or regional ferrous rocks or soil	No impact	No impacts from ferrous rocks or soil
Survey site shape	Rectangular vs linear or irregular	Linear or irregular shapes may require additional flight lines	Lidar: no impact Orthophotos: no impact

5.2 Cost Strategies

There are several strategies for cost management in lidar and orthophoto surveys:

- Occasionally, projects may be scheduled to share mobilization costs between completely unrelated projects. It is worthwhile to stay in touch with vendors who may be working in the same area to see if projects can be combined.

- All needed areas should be acquired at once. Lidar and orthophotos are less expensive per unit area to acquire if collected in larger areas, where mobilization costs may be shared over more area and multiple mobilizations can be avoided.
- Lidar and orthophotos should be acquired together if both data sets will be needed. Acquiring data concurrently can achieve both cost savings and better data integration.
- Lidar and orthophotos may be used in both the site assessment and cleanup phases of site project, as well as in ongoing site management. As such, it may be possible to share the cost of the survey between different programs or funding sources.

There are some aspects of a project where it is not appropriate to economize:

- ***Data calibration, data inspection, and other data processing steps.*** Automated algorithms can perform most (but not all) data processing steps; however, review by experienced operators is essential to insure data quality. Vendors should be asked to describe their calibration, integration, point classification and orthophoto creation process in their proposals, and extremely low bids should be scrutinized with care to be sure that process steps by experienced operators are not being slighted.
- ***Adequate survey control.*** Establishing sufficient survey control is relatively inexpensive and provides the essential means of data adjustment and verification of data positional accuracy. Survey control should not be minimized except where field work poses a safety risk to the crew.
- ***QA/QC review in the field.*** Field QA/QC review is important to avoid the risk of having to re-mobilize and re-acquire data in the event that bad data is collected. This is true even if the cost of correcting poor quality data falls to the vendor, since re-acquisition after demobilization can causes significant delay. The schedule should always include time for in-field QA/QC review and re-acquisition of any missed or erroneous areas while the crew is still in the field.

5.3 Additional Contracting Considerations

The lidar/orthophoto industry is in some flux at the time of this report, with some firms consolidating and new firms emerging. The level of experience among vendors varies substantially, with some firms having more or less experience, or experience only in a particular market, such as flood plain mapping, the electric power industry, or other applications. Vendors with no experience with munitions sites should not necessarily be excluded from consideration, since most vendors use equipment that will perform well for a variety of projects. However, the wide variety of experience makes it important to work closely with all vendors to make sure that they understand the unique requirements of munitions investigations.

A discussion of vendor qualifications should include examples of the vendor's performance when data collection or processing did not go as planned. For instance, the vendor should, if possible, provide customer contacts as to its willingness to re-acquire or re-process areas of bad data in the event of equipment problems or failure to meet project specifications (Appendix A).

Lidar vendors are often booked far in advance, and may need several months of advance notice to plan a survey. Therefore the general rule is to contact vendors as early in the planning process as possible to reserve time. Occasionally, vendors will be able to accommodate projects on short notice if they have gaps in their schedules or if other projects are cancelled.

It is appropriate to present contract specifications to several vendors and request cost and technical proposals. Generally, vendors should be requested to describe their technical approach, and to invite the vendor to present alternative approaches that the vendor feels will meet the project needs better.

In addition to the example data specifications discussed in Appendix B, the following additional contract provisions should be considered:

- ***Contingencies for weather delays.*** In coastal areas especially, weather can cause severe delays. Vendors should be asked about their contingencies for bad weather, and whether there will be an extra charge for weather delays once mobilization has occurred.
- ***Replacement of poor quality data.*** Typically, lidar and orthophoto acquisition contracts specify that the vendor will replace out-of-specification data at the vendor's cost with data that meets the contract specifications. Major errors that cause the data not to meet the contract specifications can result in substantial re-processing or even re-acquisition. Minor errors include delivery of occasional corrupt data files or data blocks in an incorrect projection and datum.

  Given the amount of data involved in a large lidar and orthophoto survey, delivery of an occasional bad file is tolerable and probably inevitable. Errors of this type are acceptable as long as they are infrequent and data is promptly replaced. Nevertheless, it may be reasonable to stipulate that after delivery of an agreed-upon number of poor quality data files, the vendor will be penalized.

6 REFERENCES

American Society for Photogrammetry and Remote Sensing (ASPRS). 2001. Digital Elevation Model Technologies and Applications: The DEM Users Manual. D. Maune, ed.

———. 2004. ASPRS Guidelines: Vertical Accuracy Reporting for Lidar Data. May 24. Available at: http://www.asprs.org/society/committees/LiDAR/Downloads/Vertical_Accuracy_Reporting_for_LiDAR_Data.pdf.

Baltsavias, E.P. 1999. Airborne laser scanning: basic relations and formulas. *ISPRS Journal of Photogrammetry and Remote Sensing* 54(2-3): 199–214.

Clarkin, Tobey. 2007. Modeling Global Navigation Satellite System Positional Error under Forest Canopy based on LIDAR-Derived Canopy Densities. Thesis submitted in partial fulfillment of the requirements for the degree of Master of Science. University of Washington.

Dold, Juergen. 2008. Technology is changing at blinding speed. *GIS Development, the Global Geospatial Magazine*, September. Available at: http://www.gisdevelopment.net/magazine/global/2008/september/42.htm.

Federal Emergency Management Agency (FEMA). 2003. Guidelines and Specifications for Flood Hazard Mapping Partners – Appendix A, Guidance for Aerial Mapping and Surveying.

Haneberg, W. 2006. Effects of Digital Elevation Model Errors in Spatially Distributed Seismic Slope Stability Calculations: An Example from Seattle, Washington. *Environmental & Engineering Geoscience* Vol. XII: 247-260. August.

Hasegawa, H. and T. Yoshimura. 2003. Application of dual-frequency GPS receivers for static surveying under tree canopies. *Journal of Forest Research* 8:103-110.

Key, Hank. 2009. Airborne Lidar Sensors. *Professional Surveyor Magazine*, May. Available at: https://www.profsurv.com/assets/magazines/articles/70254/AirborneLidarSensors.pdf.

Naesset, E. 2001. Effects of Differential Single- and Dual-Frequency GPS and GLONASS Observations on Point Accuracy under Forest Canopies. *Photogrammetric Engineering & Remote Sensing* 67(9):1021-1026.

National Digital Elevation Program (NDEP). 2004. Guidelines for Digital Elevation Data, Version 1.0. Part 5, National Map Accuracy Standards. May 10. Available at: http://www.ndep.gov/NDEP_Elevation_Guidelines_Ver1_10May2004.pdf.

Nelson, H., K. Kaye, and A. Andrews. 2008. ESTCP Pilot Project Wide Are Assessment for Munitions Response. Final Report. Environmental Security Technology Certification Program. July.

Neufelt, David. 2009. Letter re: of URS draft white paper on lidar error. Terrapoint, LLC. July 6.

Optech Inc. 2008. Marine Survey. Accessed September 30. Available at: http://www.optech.ca/shoalsfeatbens.htm.

Sky Research. Telephone conversation with Dale Bennett, URS. August 2008.

Terrapoint LLC, 2009. Review of Draft URS white paper on lidar error. June 23.

Terra Remote Sensing, Inc. Terra Remote Sensing, Inc. Phone conversations with Dale Bennet, URS and review of draft white paper on lidar point classification. 2008.

URS. 2007. High Density Lidar and Orthophotography in UXO Wide Area Assessment. August.

———. 2008. Final Report Addendum for Former Camp Beale Demonstration Site. January.

———. 2009a. ESTCP White Paper: Effects of Lidar Point Classification Methods on Surface Model Creation and Feature Identification. Draft Final. January.

———. 2009b. Wide Area Assessment Cost-Benefit Analysis: Active Army Military Munitions Response Program. May.

Wing, M.G. and A. Eklund. 2007. Performance Comparison of a Low-Cost Mapping Grade Global Positioning Systems (GPS) Receiver and Consumer Grade GPS Receiver under Dense Forest Canopy. *Journal of Forestry* 105(1):9-14.

7 GLOSSARY

accuracy: The closeness of an estimated value to a standard or accepted value of a particular quantity.

anomaly: A geophysical signal above geological background from a detected subsurface object.

artifacts: In lidar, detectable surface remnants of buildings, trees, towers, telephone poles or other elevated features in a bare-earth elevation model. Also, detectable artificial anomalies that are introduced to a surface model via system-specific collections or processing techniques.

bathymetry: The measurement and study of water depths.

calibration: The process of identifying and correcting for systematic errors in hardware, software, or procedures.

conceptual site model (CSM): A description of site conditions that coveys what is known or suspected about the sources, releases and release mechanisms, contaminant fate and transport, exposure pathways, potential receptors, and risks.

contours: Lines of equal elevation on a surface. An imaginary line on the ground, all points of which are at the same elevation above or below a specified reference surface.

digital elevation model (DEM): A generic term for digital topographic and/or bathymetric data in all its various forms, but most often bare earth elevations at regularly spaced intervals in x and y directions. Regularly spaced elevation data are easily and efficiently processed in a variety of computer uses.

digital terrain model (DTM): Similar to DEMs, but they may incorporate the elevation of significant topographic features on the land and mass points and break lines that are irregularly spaced to better characterize the true shape of the bare earth terrain.

digital surface model (DSM): Similar to DEMs or DTMs, except they may depict the elevations of the top surfaces of buildings, trees, towers, and other features elevated above the bare earth.

electromagnetic induction (EMI): The physical process by which a secondary electromagnetic field is induced in an object by a primary electromagnetic field source.

Geographic Information System (GIS): A system of spatially referenced information, including computer programs that store, manipulate, analyze, and display spatial data.

Global Positioning System (GPS): Technology that computes the three-dimensional position of an object in space, for example the lidar sensor, using signals from at least four orbiting navigation satellites.

hillshade: A function used to create an illuminated representation of a surface, using a hypothetical light source, to enhance visualization effects.

horizontal accuracy: The positional accuracy of a dataset with respect to a horizontal datum.

Inertial Measurement Unit (IMU): Technology that uses gyroscopes and accelerometers to compute the roll, pitch, and heading of a moving object, for example a lidar sensor.

Inertial Navigation System (INS): A navigation aid that uses a computer and motion sensors (the IMU) continuously calculate via dead reckoning the position, orientation, and velocity of a moving object without the need for external references.

light detection and ranging (lidar): An instrument system that measures distance to a reflecting object by emitting timed pulses of laser light and measuring the time between emission and reception of reflected pulses. The measured time interval is converted to distance.

magnetometry: The technique of measuring and mapping patterns of the earth's magnetic field as modified by geology or ferrous objects.

nanometer: A unit of length equal to one billionth of a meter.

ordnance: Weapons of all kinds.

orthophotograph: A digital aerial photograph that has been geometrically corrected for topographic relief, lens distortion, and camera tilt.

orthorectification: The process by which the geometric distortions of an image are modeled and accounted for.

positional accuracy: The accuracy of the position of features, including horizontal and/or vertical positions.

redundant array of independent disks" (RAID) device: A device containing multiple hard drives, allowing computer users to achieve higher levels of storage reliability from low-cost and less reliable PC-class disk-drive components, via the technique of arranging the devices into arrays for redundancy.

root mean square error (RMSE): An accuracy assessment for measured data (e.g., lidar) calculated by taking the square root of the average of the set of squared differences between dataset values (i.e., lidar derived elevations versus field surveyed elevations).

triangulated irregular network (TIN): A set of adjacent, non-overlapping triangles computed from irregularly spaced points with x/y coordinates and z-values.

unexploded ordnance: Military munitions that have been primed, fused, armed, or otherwise prepared for action and that have been fired, dropped, launched, or placed in a manner constituting a hazard to operations, installations, or personnel; which remain unexploded.

vegetation removal: In lidar, the correction of reflective surface elevations so as to depict the elevation of the bare earth terrain beneath the vegetation.

vertical accuracy: The measure of the positional accuracy of a dataset with respect to a specified vertical datum.

wide area assessment: Rapid assessment of large tracts of potentially contaminated land to identify those areas with concentrated military munitions that require detailed characterization.

APPENDIX A

SAMPLE PROJECT SPECIFICATION CHECKLIST

Contract specifications should be reviewed to be sure that they address the following topics:

1. Proposal Due Date
2. General Project Description
3. Project Schedule Requirements
4. Project Specifications
   - Project size
   - Project area general location
   - Project area boundaries
   - Project area configuration: corridor versus area, general size, number and size of separate areas
   - Requirements related to on-site logistics, access and project coordination
5. Lidar Specifications
   - Lidar data density required (overall and within smaller areas as appropriate)
   - Horizontal and vertical accuracy
   - Lidar flight line integration specification
6. Field QA/QC Requirements
   - Field assessment of ground data density
   - Field assessment of data overlap and coverage
   - Criteria for scope modifications/additions
7. Orthophoto Specifications
   - Orthophotos required or not
   - Orthophoto pixel size
   - Orthophoto to lidar alignment specification
8. Survey Control Requirements
9. Data Delivery Projection and Datum
10. Deliverables
    - Data delivery format
    - Data delivery medium
    - Supporting files including block index, attribute description, mission and QA/QC report
11. Proposed Technical Approach:
    - Proposed flight platform (helicopter v fixed wing aircraft)
    - Sensor description
    - Laser pulse rate

- Planned flight altitude
- Proposed flight line overlap
- Proposed control point network
- Point classification methods
- Other relevant details

APPENDIX B

SAMPLE REQUEST FOR PROPOSALS

The following represents some sample language for a request for proposal for a lidar and orthophoto survey. This language is intended as a starting point, and should be adapted to fit the needs of each particular project.

Request for Proposals, Lidar and Orthophoto Survey in Support of UXO Wide Area Assessment at [SITE NAME]

Proposal due date: close of business [DATE].

AGENCY (Government) is soliciting proposals for acquisition of lidar and orthophoto data for a project near [GENERAL LOCATION]. The objective of the lidar/orthophoto survey is to support site assessment and cleanup activities related to the historic use of the site as a military bombing range [OR OTHER AS APPROPRIATE]. A further objective is to support ongoing site management. Project award will be made based on technical qualifications, cost, and ability to meet the attached delivery schedule.

1. Project Specifications

1.1. Project site size: approximately [XX] acres, approximately [XX] acres, approximately [XX] by [YY] kilometers.

1.2. Project area location and project boundaries: Project areas are shown in attached ESRI shape files.

1.3. Lidar data density. Lidar point density specifications are designed to detect craters and other objects of approximately 1 meter in diameter. Vendor will acquire lidar data at a minimum of 5 points/m^2. Lidar point density will be calculated based on total points versus total area for each separate area; however lidar data density shall not fall below 3 points/m^2 for any 500 x 500 m area.

1.4. Lidar data specifications:

- Lidar data will have a vertical accuracy of +/- 15 cm and a horizontal accuracy of +/- 60 cm root mean squared error, compared to the established survey control points.
- Flight line to flight line calibration error for lidar points will not exceed 12 cm root mean squared error.
- Lidar will be acquired for 100% of the site.
- Lidar point classification will be sufficient to create surface models free of trees and large vegetation, and all small vegetation which can be distinguished from natural ground features.

1.5. Orthophoto data: Digital photography will be acquired for this project concurrently with lidar.

- Orthophotos will be acquired at 10 cm pixel size [OR OTHER SIZE DEPENDING ON THE SITE].
- Orthophotos will be spatially accurate to within 3 pixel widths compared to surveyed control points.

1.6. Control and calibration structures. Vendor will independently occupy a survey control point at the airport used for flight operations. Stationary or kinematic survey control points shall be established throughout the

project area sufficient to demonstrate the required vertical and horizontal accuracy for each major terrain type on the site. The vendor shall provide a plan for survey control acquisition for approval prior to mobilization.

1.7. Delivery projection and datum. Vendor will deliver lidar in [SPECIFY], the same projection and datum as the attached shape files showing project area boundaries.

1.8. On-site coordination. Vendor will be responsible for all on-site logistics. No flight access constraints are known for the site [OR SPECIFY KNOWN SITE CONSTRAINTS].

1.9. Project coordination. Vendor will coordinate with the Government throughout the project. Deviations from agreed specifications will only be undertaken after prior consultation with the Government, which will be confirmed in writing or via email. The Government will supply an on-call point of contact for consultation during field acquisition to preclude delays in the acquisition program.

1.10. Field QA/QC Specifications. Vendor will perform QA/QC checks for complete coverage, data density and estimated spatial accuracy prior to demobilization, and will re-acquire all areas that are missed or where data appears not to meet the specifications stated in this Scope of Work.

1.11. Intellectual property. The Government shall have unrestricted rights to all delivered reports and data. The Government will place reports and lidar data in the public domain. This specification shall not restrict the ability of the Vendor to resell data or derivative products.

2. Project Schedule

Data collection shall begin no later than [DATE], and data delivery to the Government shall be complete no later than ten weeks following the end of data collection. [DELIVERY DATE WILL BE ADJUSTED FOR SITE SIZE] However, earlier data collection and delivery is desirable, and vendor selection will depend in part on proposed schedule for mobilization, data collection, and data delivery.

3. Deliverables

3.1. Lidar data format: All lidar data points will be delivered as ASCII comma-delimited files with a .csv extension, with values for northing, easting, elevation, intensity, flight line, gps date and time, and classification as ground or non-ground return. Lidar point data will be delivered in blocks representing 1 square kilometer, or other tiling system as mutually agreed. Lidar data may be delivered in phases as mutually agreed. Data blocks will overlap by a minimum of 10 meters.

3.2. Orthophoto data. Orthophotos will be delivered in .geotiff format, in blocks no larger than 1GB in size, or other tiling arrangements as mutually agreed.

3.3. Block index. A lidar and orthophoto block index will be provided in ESRI shape file or other agreed-upon format.

3.4. Delivery medium: lidar point data will be delivered via external hard drive.

3.5. Acquisition and QA/QC report. Vendor will deliver data acquisition and QA/QC reports sufficient to demonstrate compliance with all

specifications in this Scope of Work. The QA/QC report shall be delivered concurrently with the last shipment of lidar and orthophoto data.

4. Proposed Costs and Schedule

Cost Items: (Costs in US Dollars)

Item	Amount ($)
Mobilization/Demobilization	
Data Acquisition	
Data Processing	
Data Analysis	
Total	

Proposed mobilization date:

Proposed delivery date(s) for lidar data:

5. Technical Approach

Please briefly describe your technical approach including:

- proposed flight platform (helicopter v fixed wing aircraft) and reason for selection
- make and type of sensor
- planned laser pulse rate
- planned flight altitude
- flight line overlap
- conceptual control point network
- proposed point classification methods and how these will be optimized to the goals of the survey
- suggested technical modifications to better meet the goals of the survey

APPENDIX E
FEATURE DETECTION AND POINT DECIMATION – ANALYSIS RESULTS

Appendix E
Feature Detection and Point Decimation – Analysis Results

In this table the plots are ordered by feature size.

Feature Size (m)	Plot #	Lidar ref #	Decimination Level 1	2	3	4	5	Veg %	Notes	Lowest level visible
			Average Point Density (pts/m^2)							
			13.8	6.9	3.4	1.7	0.8		**Average pt density**	
1.9	2	4004						0	The feature is very faint throughout and gone by 4.	3
2.6	13	3978						0	The feature is largely gone by 3, but because it is surrounded by a cleaner set of features, it could probably still be identified. The feature is completely gone in 4 and 5.	3
2.7	14	3991						11.4	The feature is clear throughout	5
2.9	16	3953						55.7	The feature in 1 through 3 is difficult to distinguish from background noise. At 4 and 5, the feature is completely gone.	3
2.9	4	4007						34.2	The feature is discernable in 1 and 2, and gone by 3.	2
2.9	15	5351						34.1	The feature remains distinguishable as such until it disappears completely in 5.	4
3.1	19	5461						35	The feature is relatively clear through 3 and could possibly be picked out in 4, but has degraded enough in 5 to make it invisible.	4
3.1	18	5718						33.7	The feature is fairly clear through 3 but disappears in 4 and 5	3
3.2	1	3977						0	The feature is largely gone by 3, but because it is surrounded by a cleaner set of features, it could probably still be identified. The feature is completely gone in 4 and 5.	3
3.3	21	4089						42.1	The feature is clear through 3, but disppears completely in 4.	3

3.3	20	5924						28.7	The feature is clear throughout	5
3.5	22	5738						57.7	The feature is fairly clear through 4 but is gone in 5	4
3.7	23	5512						45.4	The feature looks reasonably clear in 1 and 2 but has degraded enough in 3 to look more like surface texture. It is gone from 4 and 5.	2
3.8	24	5463						48.3	The feature is very clear through 4 but disappears completely in 5.	4
3.8	7	5466						36.3	The feature seems reasonably clear in 1 and 2 but looks like surface texture in 3 and has completely disappeared in 4.	3
3.8	8	5580						43.8	The feature is clear through 4 but has essentially disappeared in 5.	5
3.8	25	5719						61.5	The feature is clear in 1 and 2, fairly clear in 3 and 4, but badly degraded in 5	4
3.9	26	5465						38.6	The feature looks relatively clear through 3 but has degraded enough in 4 to possibly be mistake for background noise. It has completely disappeared in 5.	4
4.0	27	5740						39	The feature is clear through 3 but fades somewhat into the surface texture in 4 and 5.	5
4.2	3	4088						46.3	The feature looks like something in 1 and 2. By 3, feature looks like background noise, and is gone completely from 4 and 5.	3
4.3	29	5615						52.9	The feature is reasonably clear throughout	5
4.3	30	4077						73.8	The feature continues to be visible until it disappears completely in 5.	4
4.3	44	5350						67	Even though the feature changes shape considerably by 5, it still looks like something worth investigating.	5

4.5	31	4001						38.5	The feature is clear throughout	5
4.5	32	5468						63.4	The feature is clear throughout	5
4.6	6	4086						47.8	The feature is more visible on the ortho that it does in any of the surface models. It might be noticeable through 3, but not in 4 or 5.	3
4.7	33	4014						47.7	The feature changes shape entirely in 3, but still might be considered to be something. It has degraded further in 4 and gone in 5.	4
4.8	34	5521						50.2	The feature is reasonably clear in 1 and 2 but has essentially disappeared in 3, 4, and 5.	2
4.8	9	5743						42.7	The feature is clear through 3 but is pretty much gone in 4 and 5.	3
5.1	35	5569						53.5	The feature is clear through 3 but is beginning to look like normal surface texture in 4 and 5.	5
5.2	37	3965						43.2	The feature survives the decimination process but changes shape considerably. The feature is slightly visible in the ortho, but probably only because there is a white circle around. It.	5
5.2	36	5736						38.9	The feature is fairly clear through 3 but has degraded in surface texture by 4 and 5	4
5.3	38	5644						53	Even though the feature fades somewhat, it is still discernable through level 4.	4
5.3	39	5675						51.7	The feature is relatively clear through 3, but fades into the surface texture in 4 and 5.	3
5.6	40	5715						54.9	The feature is clear through 3, fairly clear in 4, but badly degraded in 5.	5
5.8	41	4033						37.4	The feature is clear throughout.	5

5.8	42	5717						47	The feature is clear throughout	5
6.2	43	5613						51.1	The feature is clear through 4, but disappears in 5.	4
6.5	45	5678						47.5	The feature remains clear throughout though it changes shape considerably by 5.	5
7.1	46	3975						44.6	The feature has changed shaped considerably in 3, but still appears to be a hole in the ground. Not visible in 4 or 5.	3
8.0	47	5609						62.8	The feature is large enough to reamin clear throughout	5
8.2	49	4029						51.2	The feature doesn't entirely disappear but by 3 it has started looking like a natural surface feature.	5
8.2	48	5921						47	The feature remains clear through 3, but has degraded badly in 4 and 5.	5
8.6	50	5735						51.5	The feature is clear throughout	5
8.7	51	5679						55.5	The surface feature, such as it is, remains discernable through 3 and somewhat so in 4, but all but disappears by 5.	4
8.8	52	4030						41	The feature contiunes to be something worth noting until 5 where it is no longer visible.	4
10.3	53	5739						46.9	Feature is clear throughout.	5
10.4	54	5913						60.2	The feature looks like it may be something noteworthy in 1 and 2, is less noticable in 3 and 4, and has disappeared in 5.	2
11.3	55	5923						36.5	The feature is clear throughout	5

12.2	56	5583						43.2	The feature is reasonably clear throughout	5
14.3	57	4035						46	The feature is visible throughout though quality decreases.	5
	59	4068						63.3	The faint dimple of a feature disappears completely in 2 and is never seen again	1

Plot # 1

Feature size: 3.2 m
Vegetation Density: 0 %

Lidar block reference number: 3977

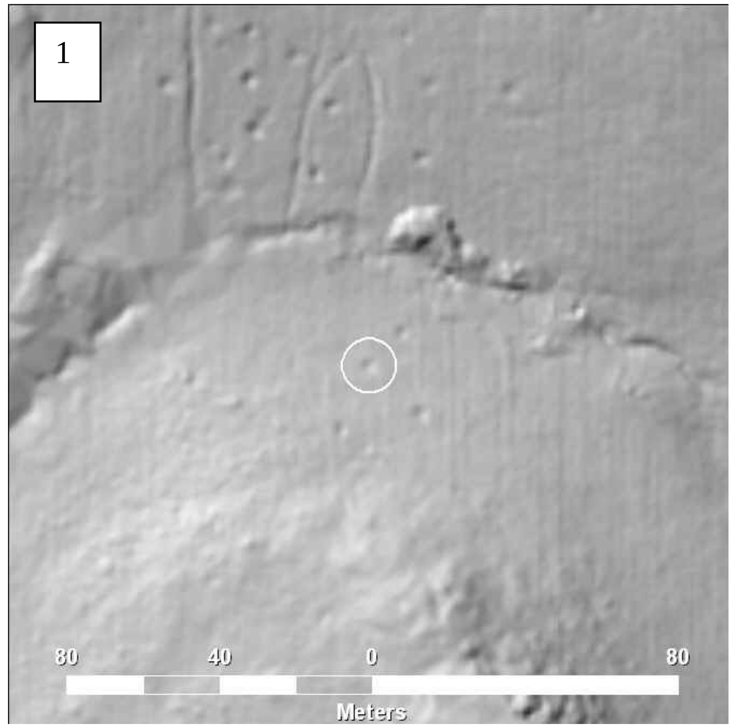

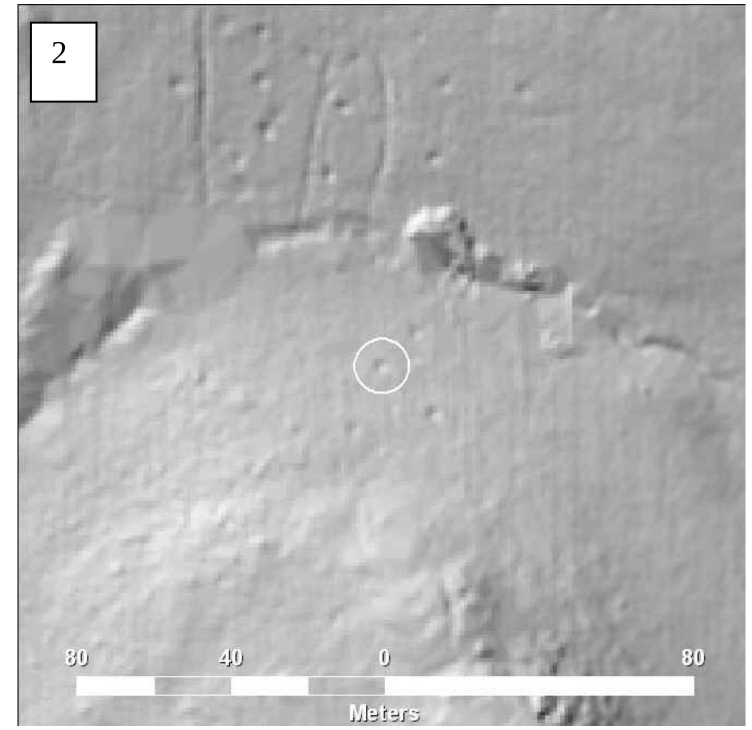

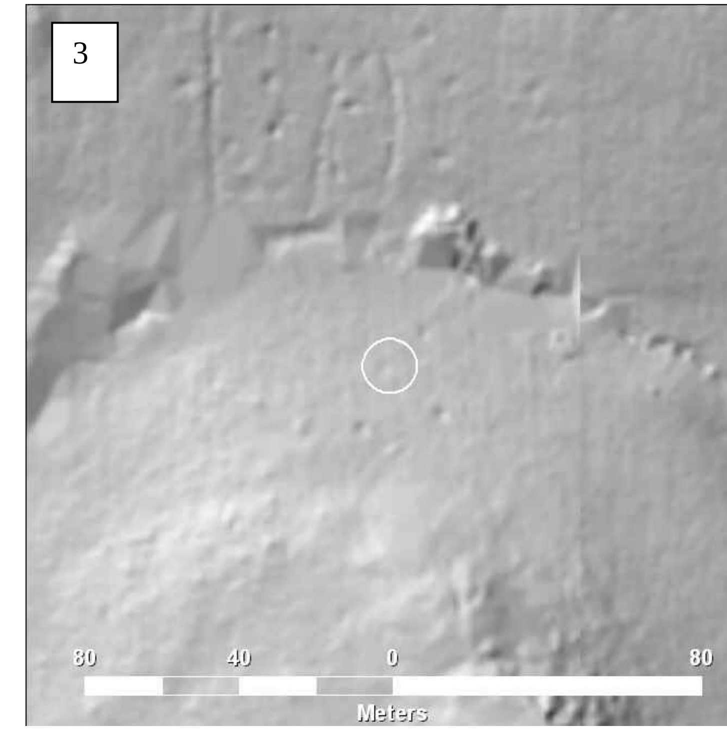

Decimation Levels:
1: 13.8 pts/m^2 (original)
2: 6.9 pts/m^2
3: 3.4 pts/m^2
4: 1.7 pts/m^2
5: 0.8 pts/m^2

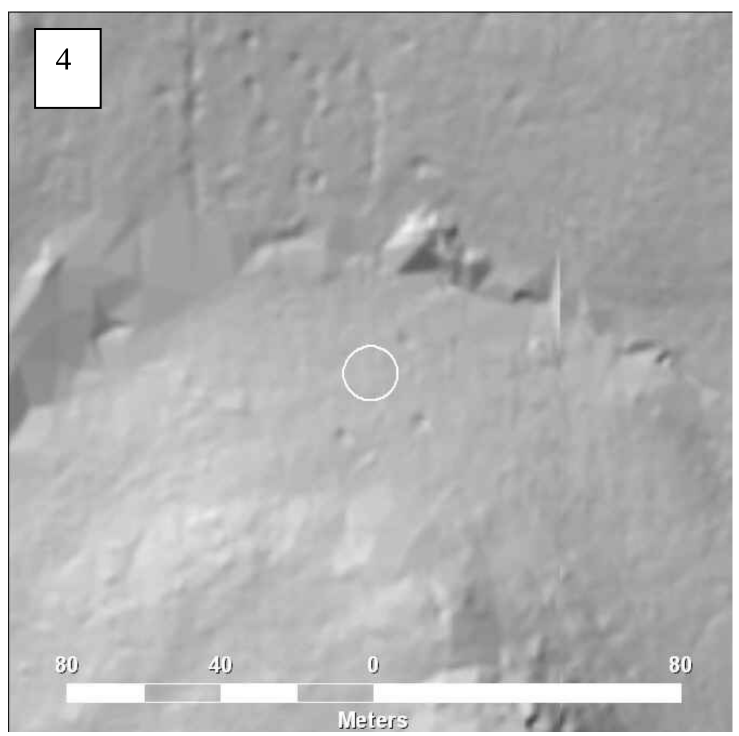

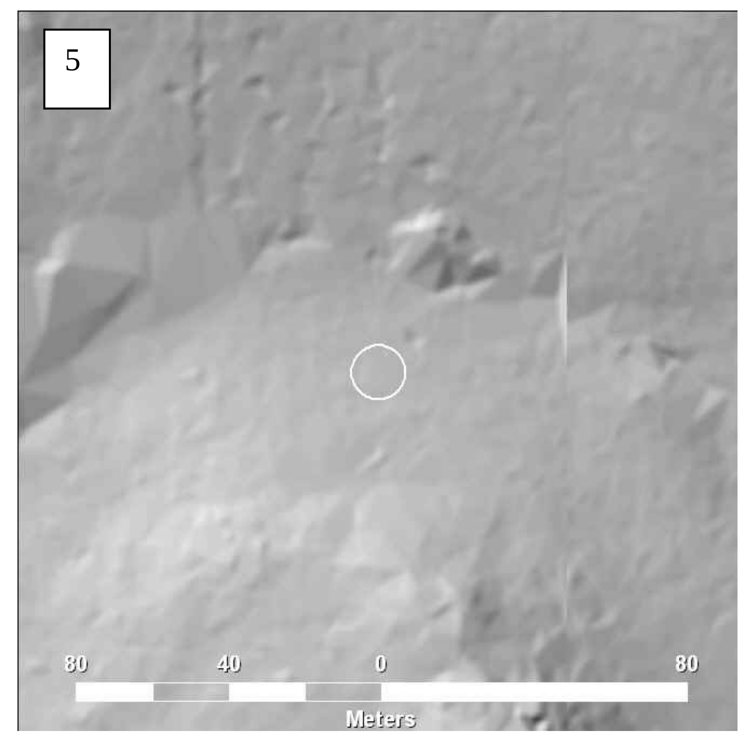

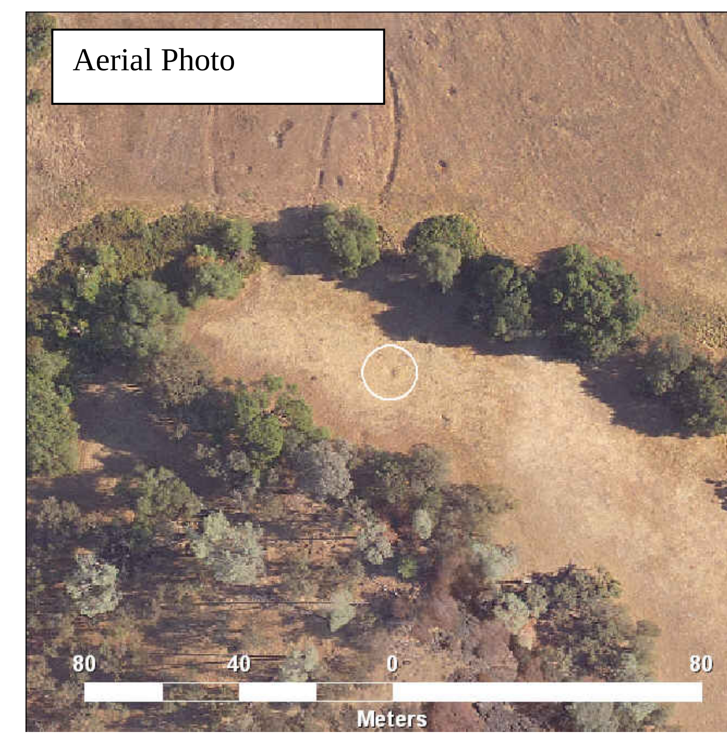

Plot # 2

Feature size: 1.9 m
Vegetation Density: 0 %
Lidar block reference number: 4004

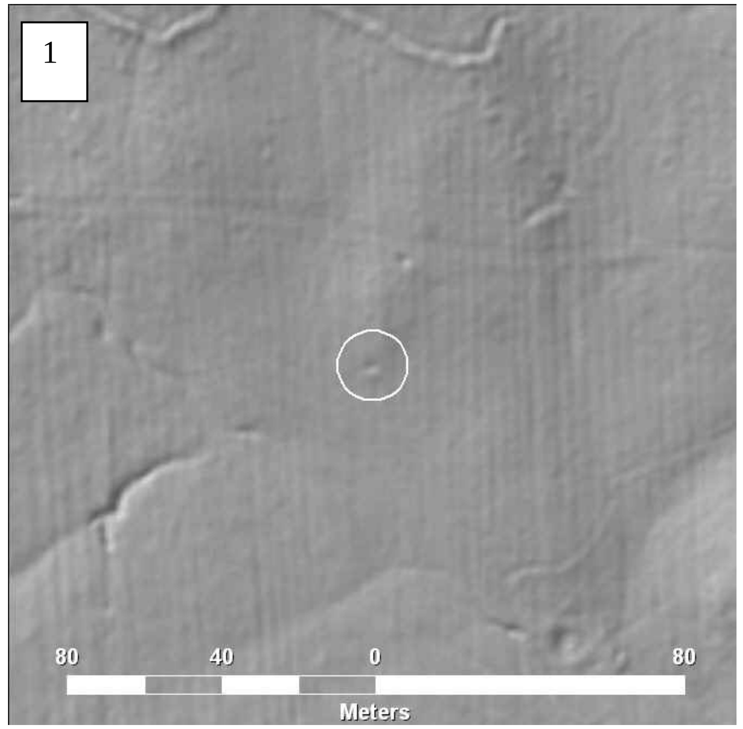

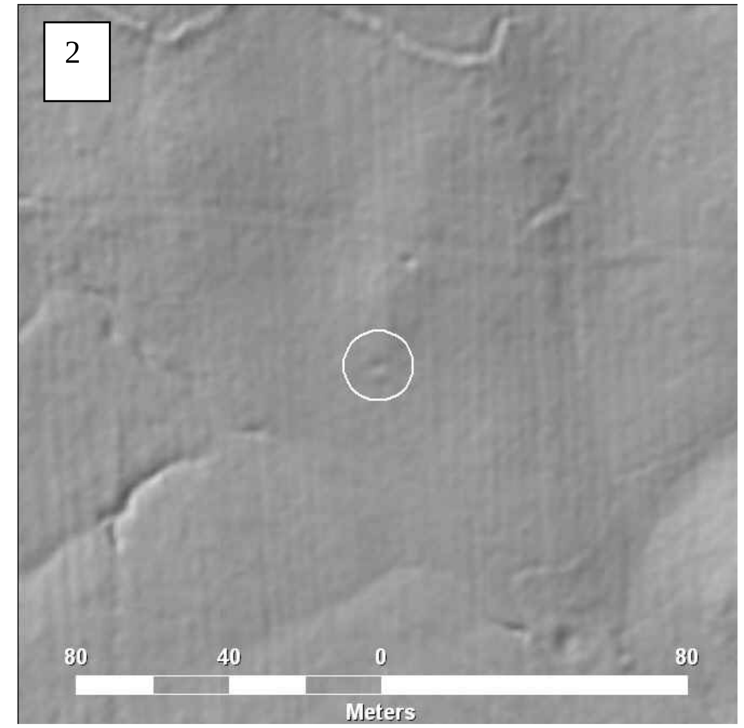

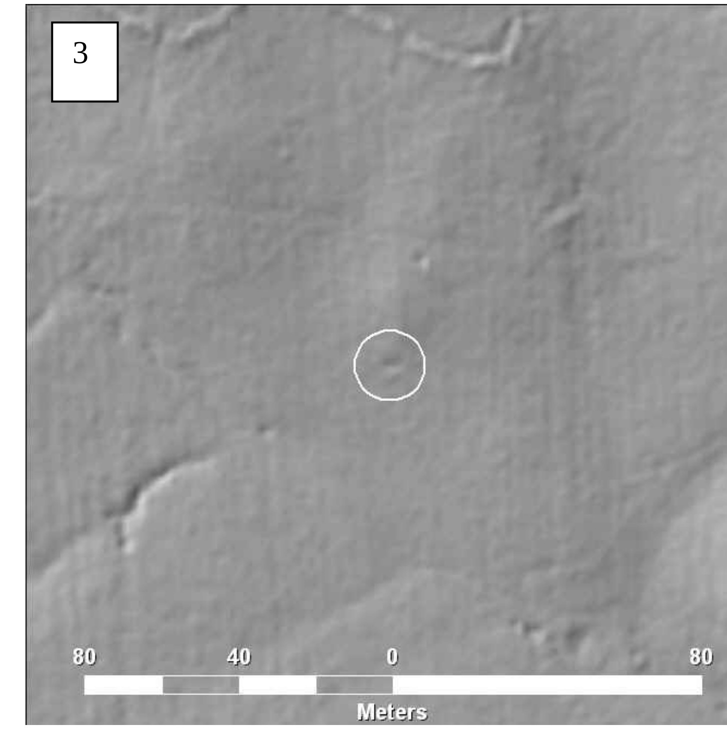

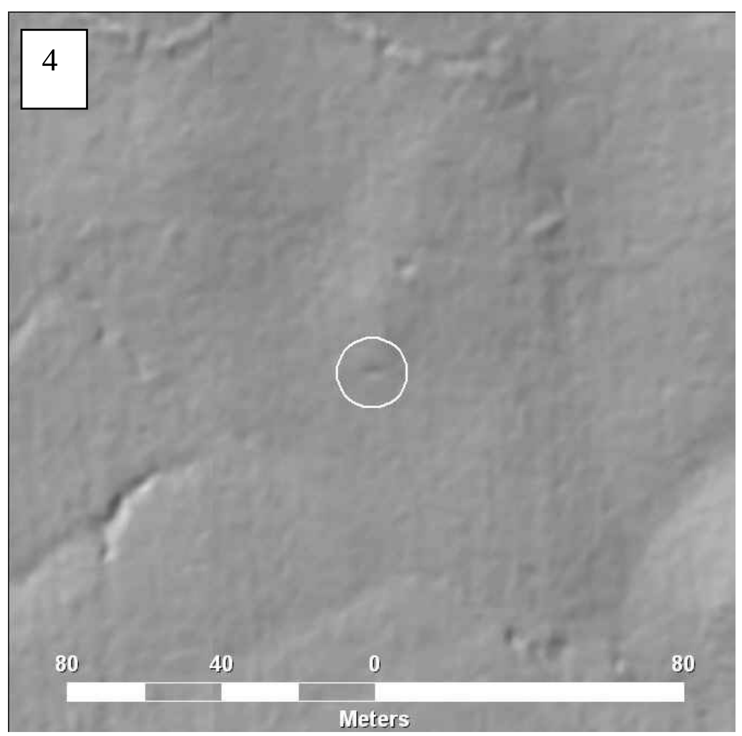

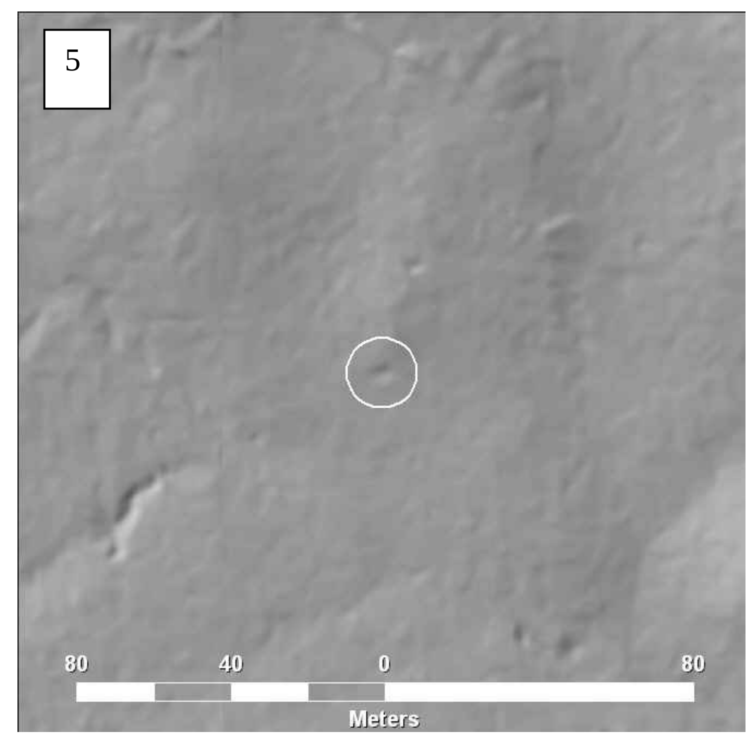

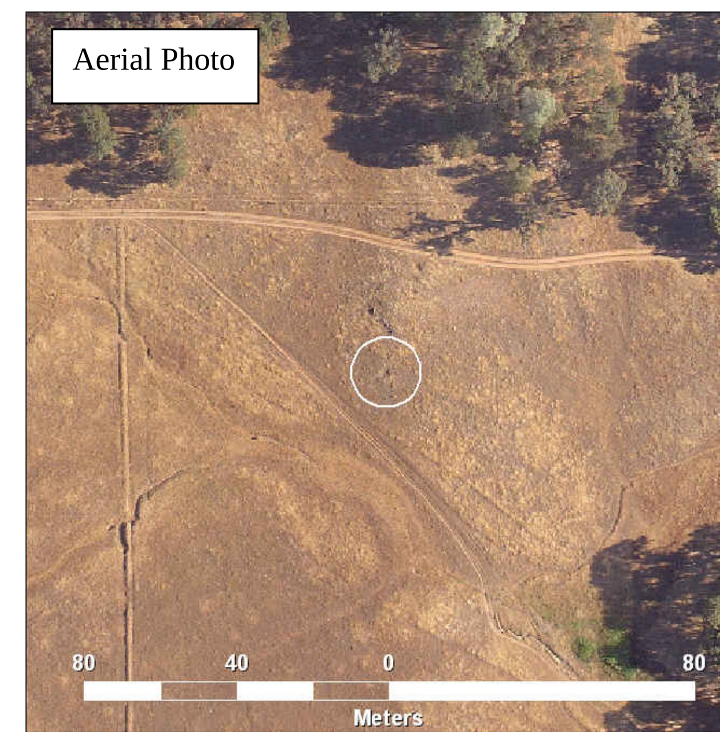

Plot # 3

Feature size: 4.2 m
Vegetation Density: 46.4 %
Lidar block reference number: 4088

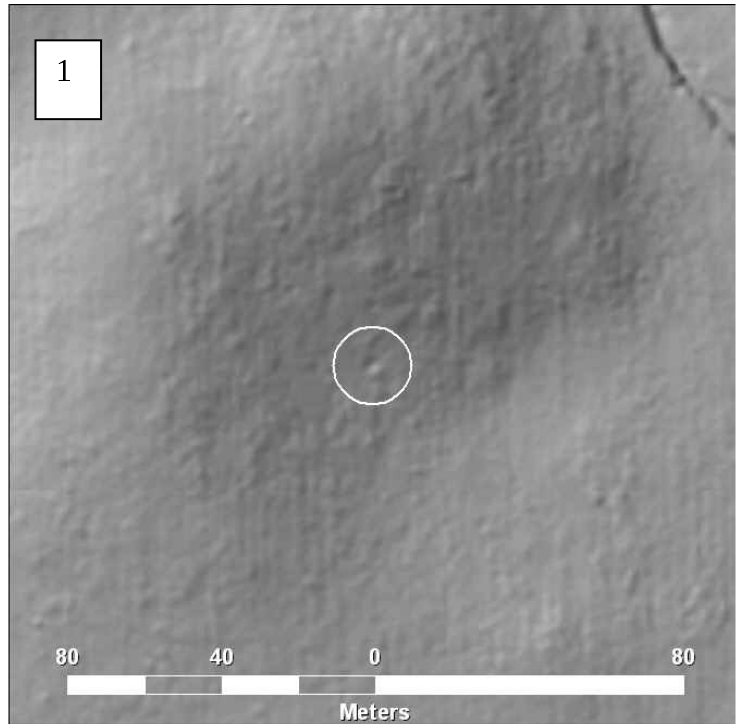

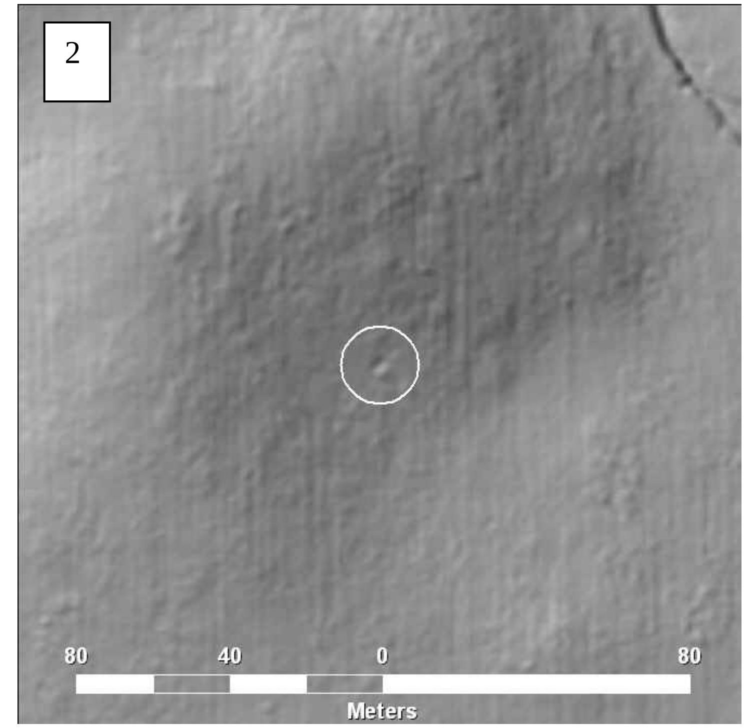

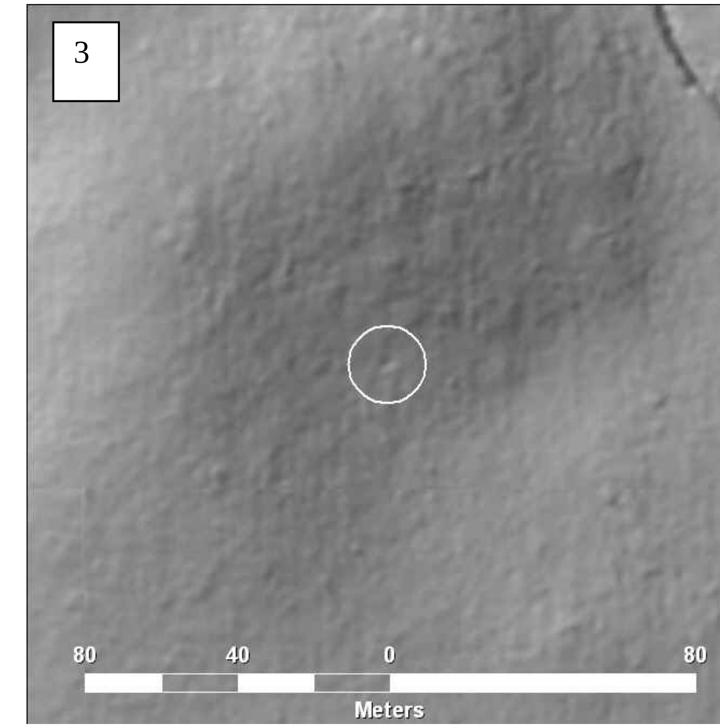

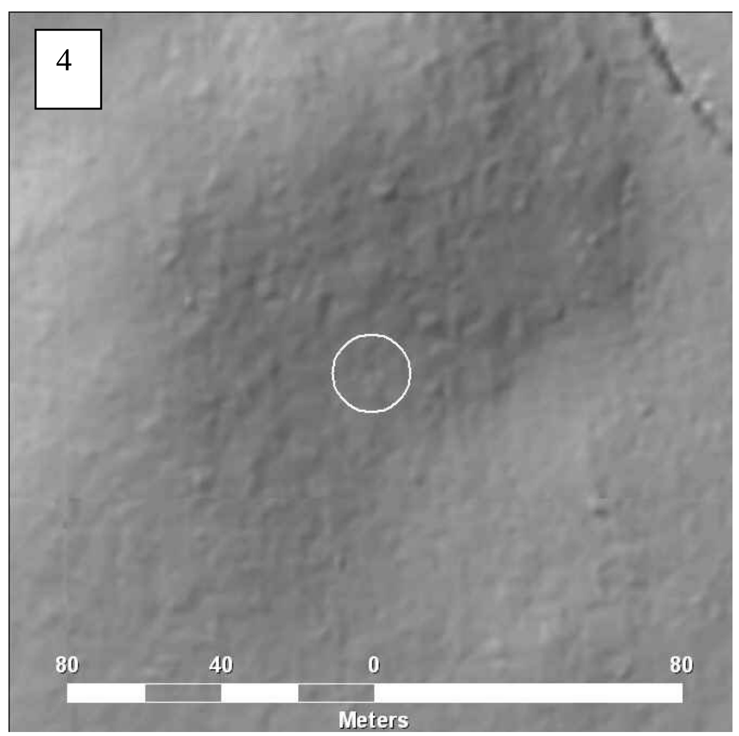

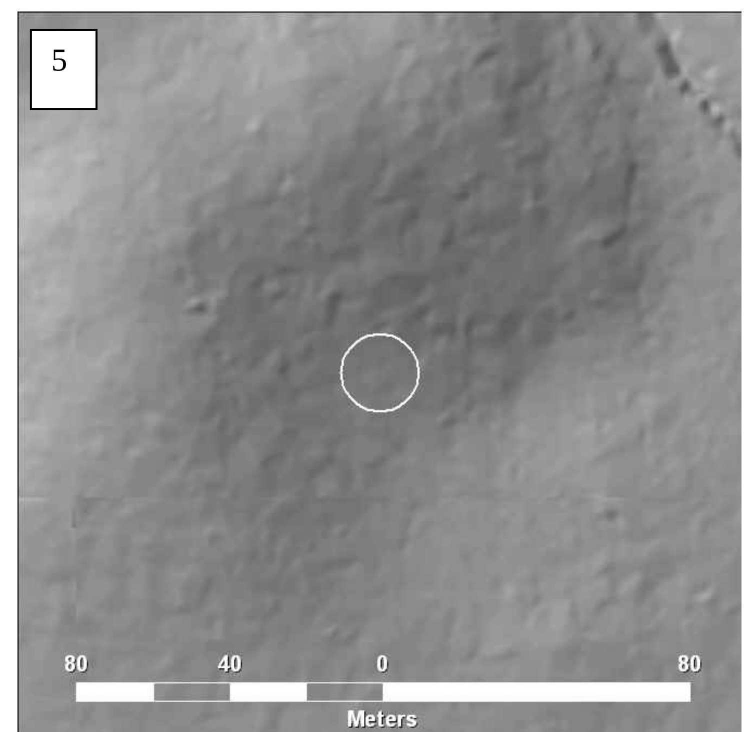

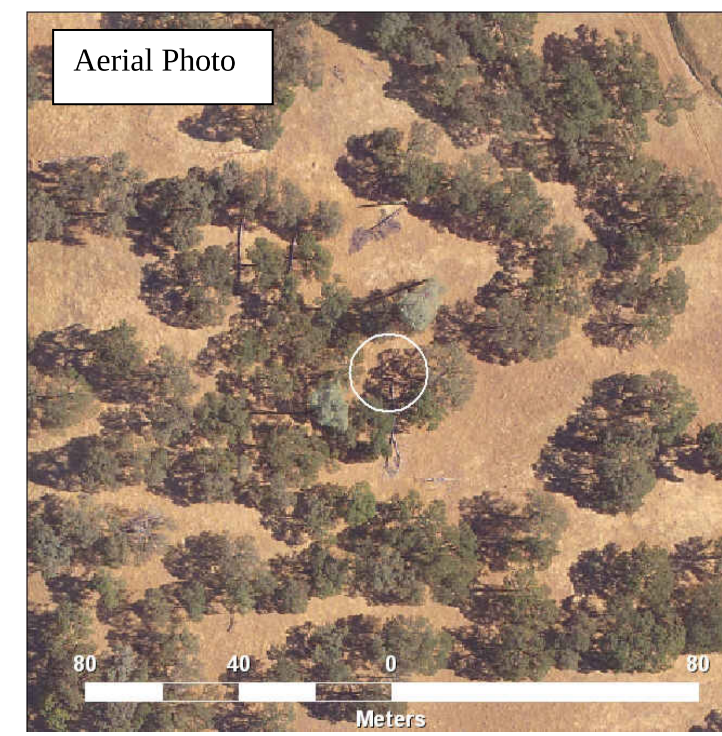

Plot # 4

Feature size: 2.9 m
Vegetation Density: 34.16 %
Lidar block reference number: 4007

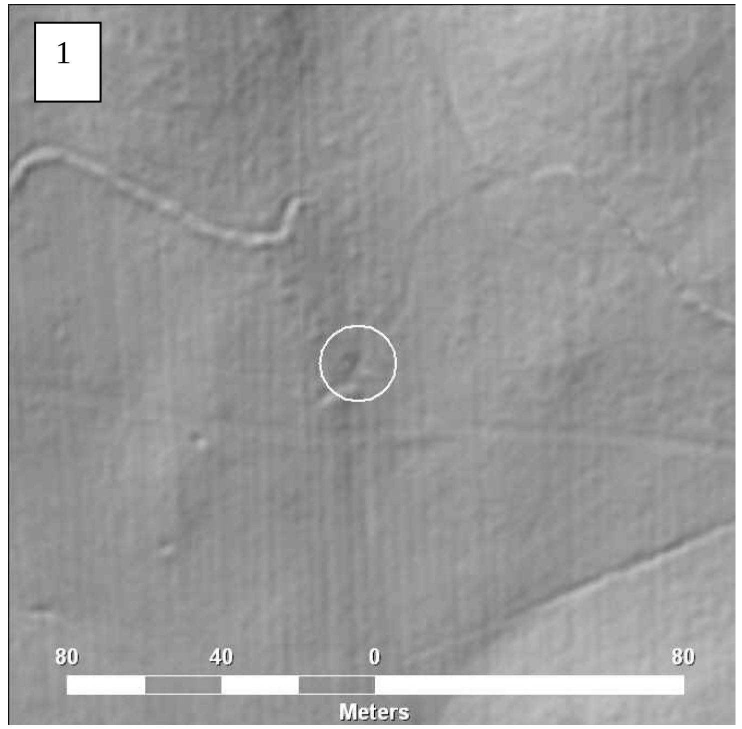

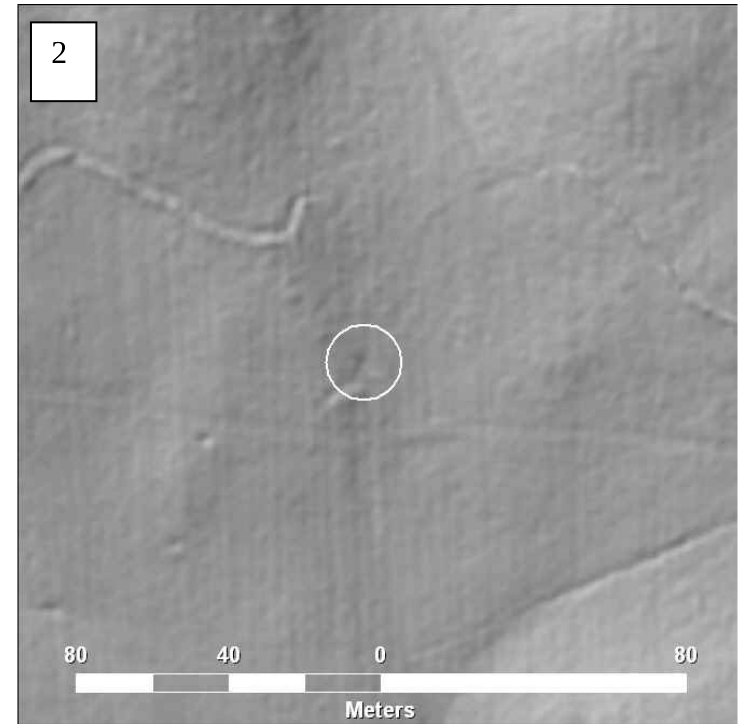

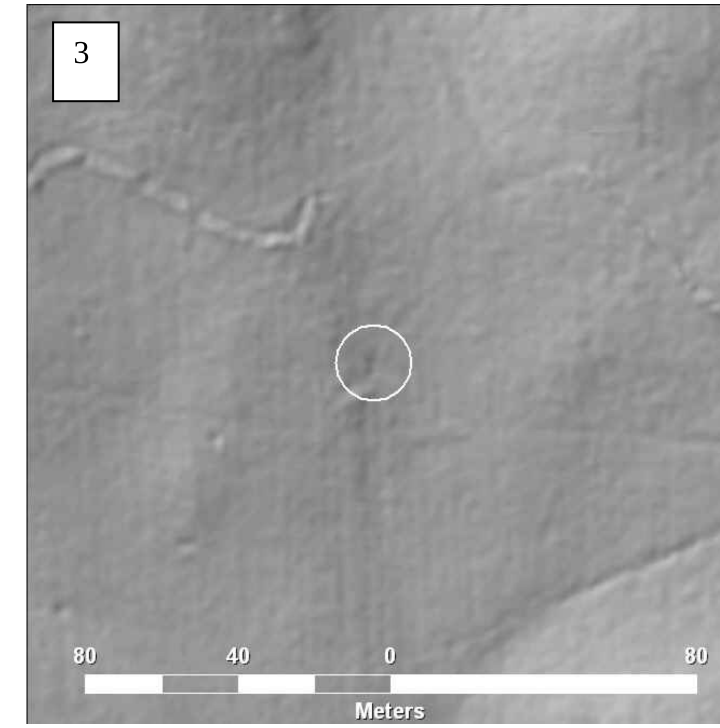

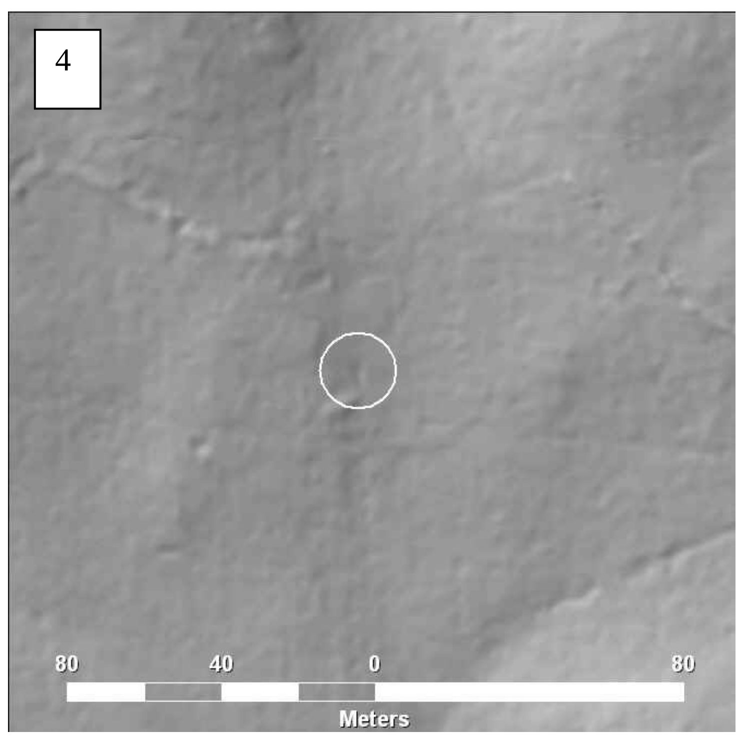

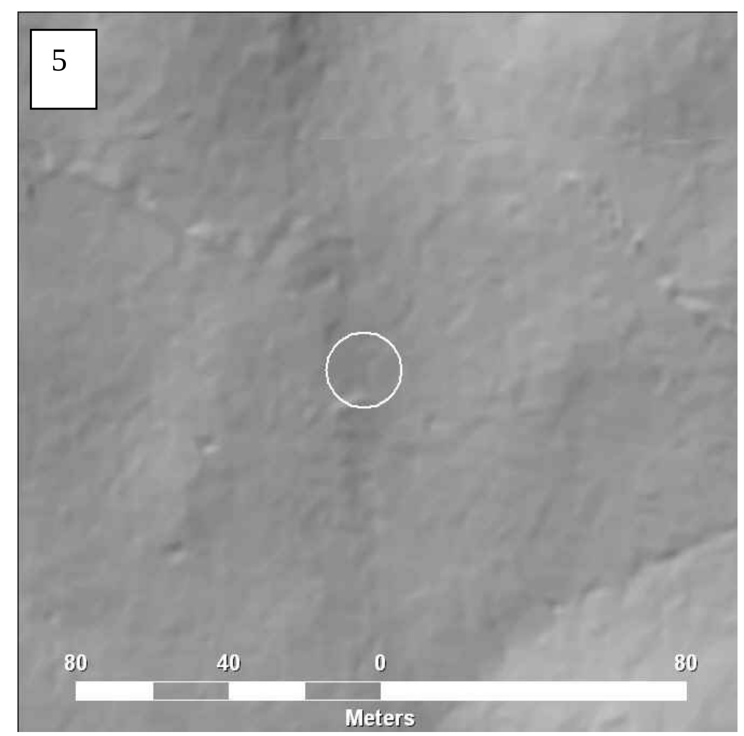

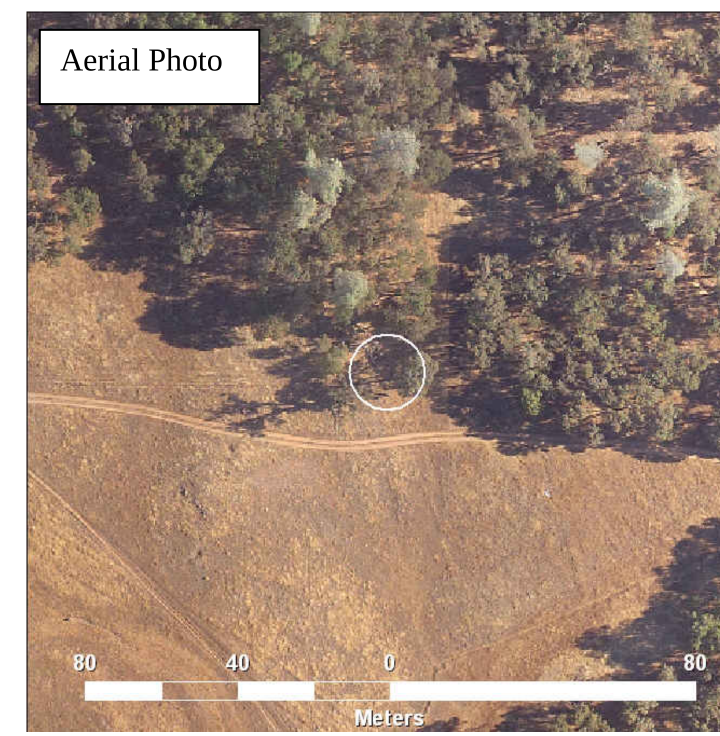

Plot # 5

Feature size: 4 m
Vegetation Density: 47.44 %
Lidar block reference number: 4065

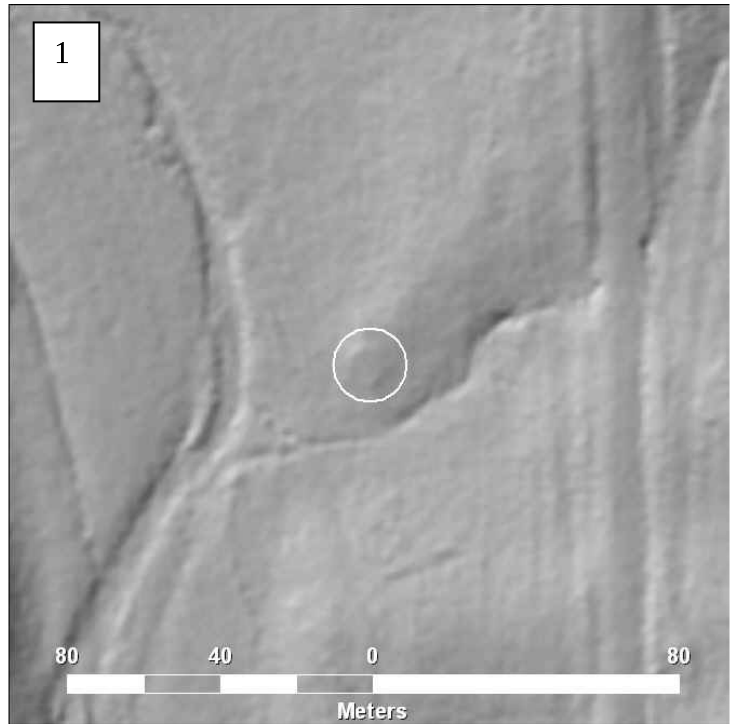

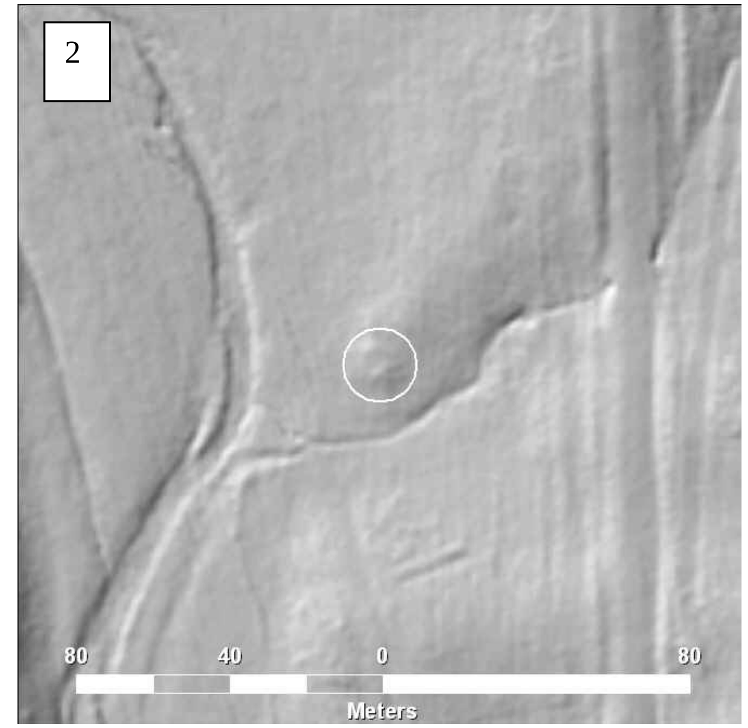

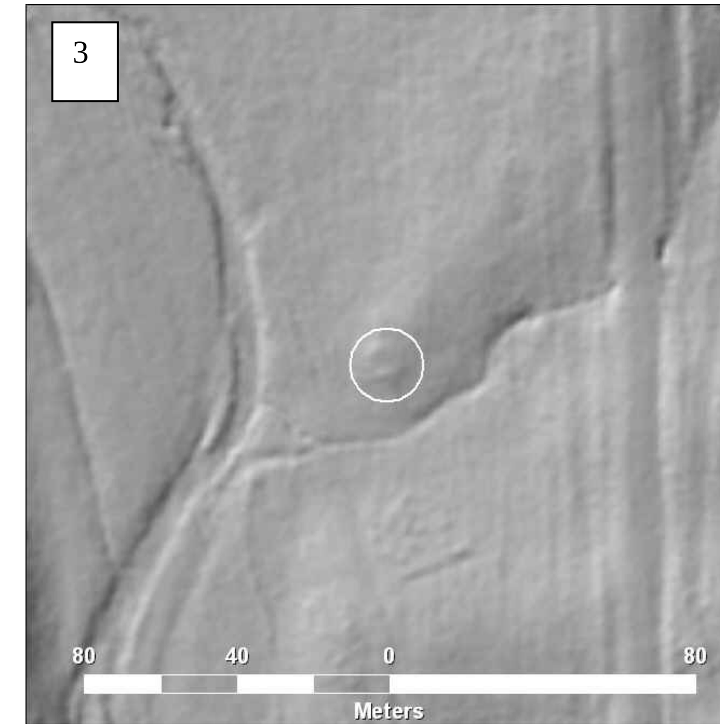

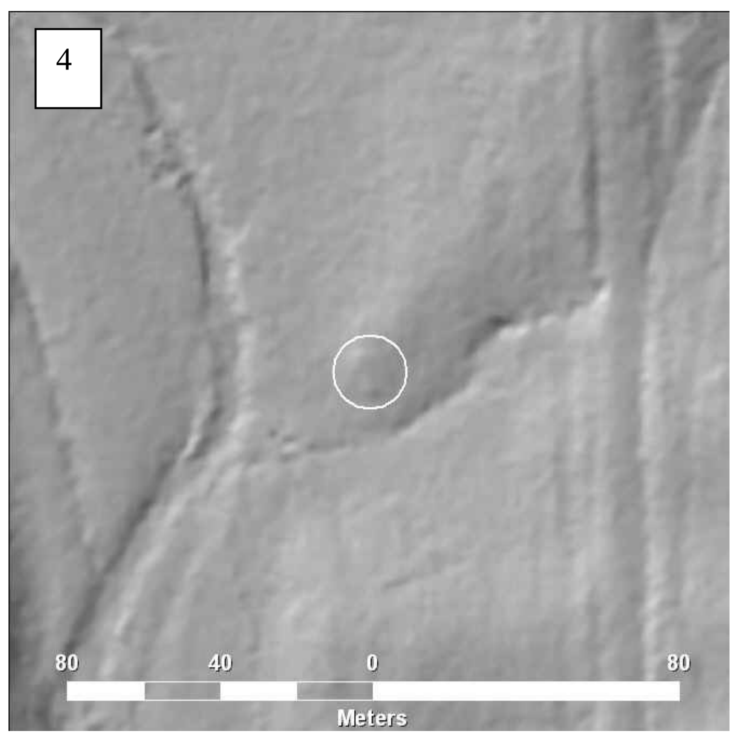

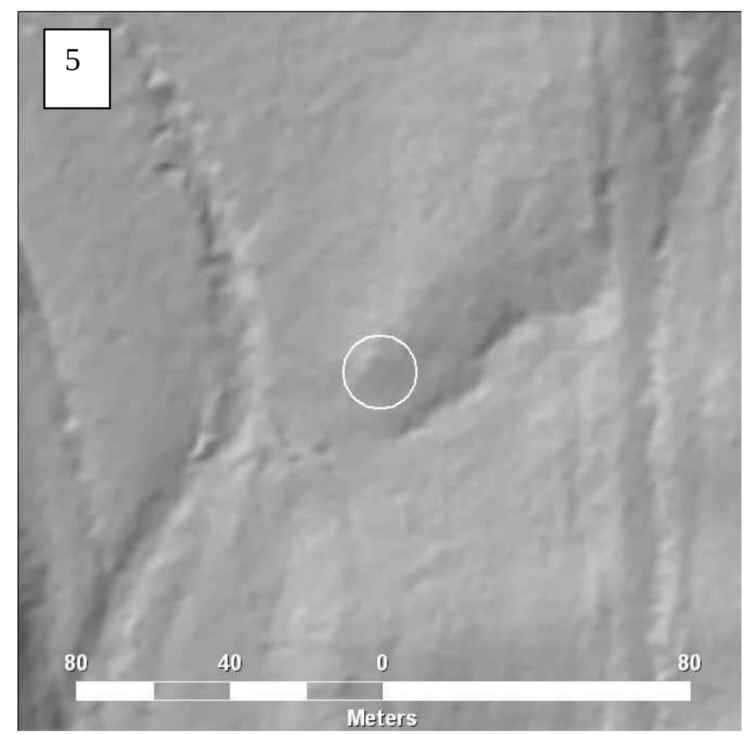

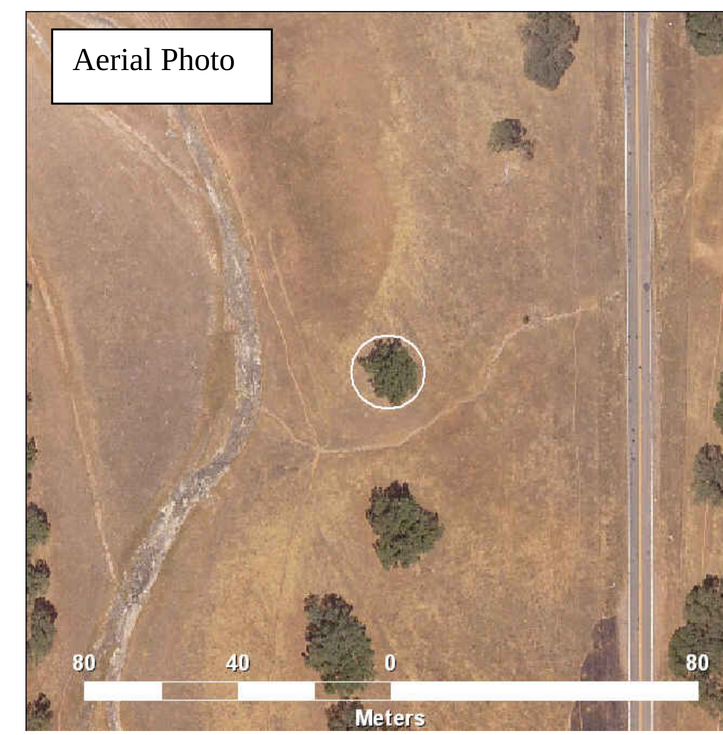

Plot # 6

Feature size: 4.6 m
Vegetation Density: 47.76 %
Lidar block reference number: 4086

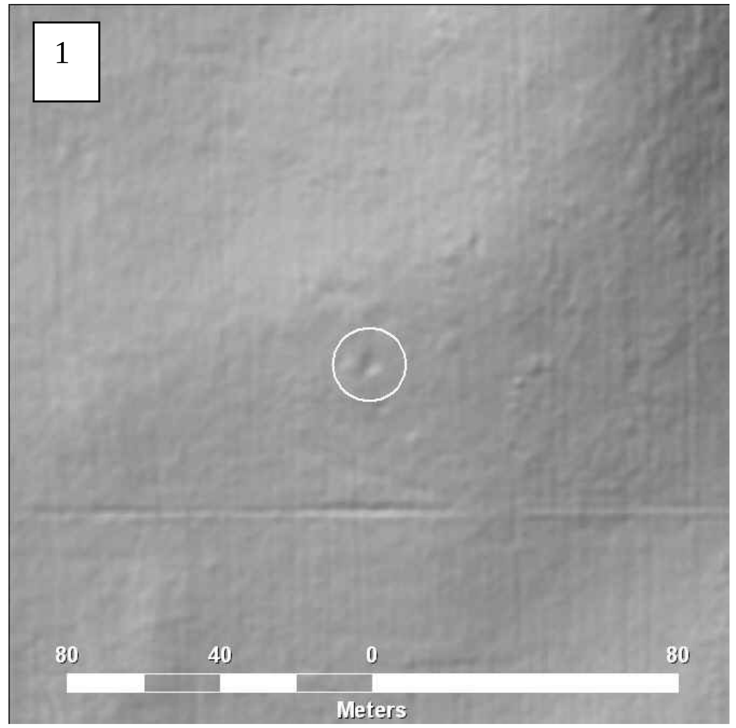

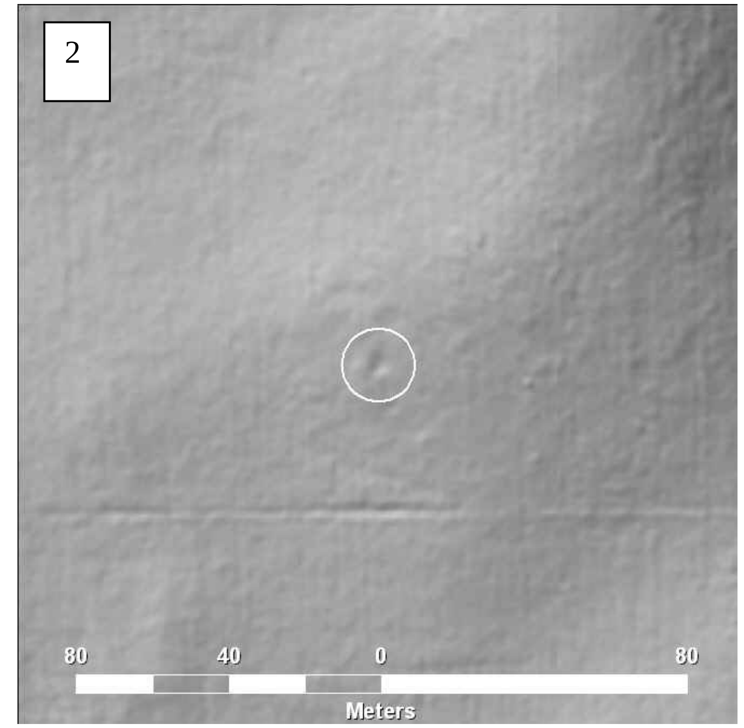

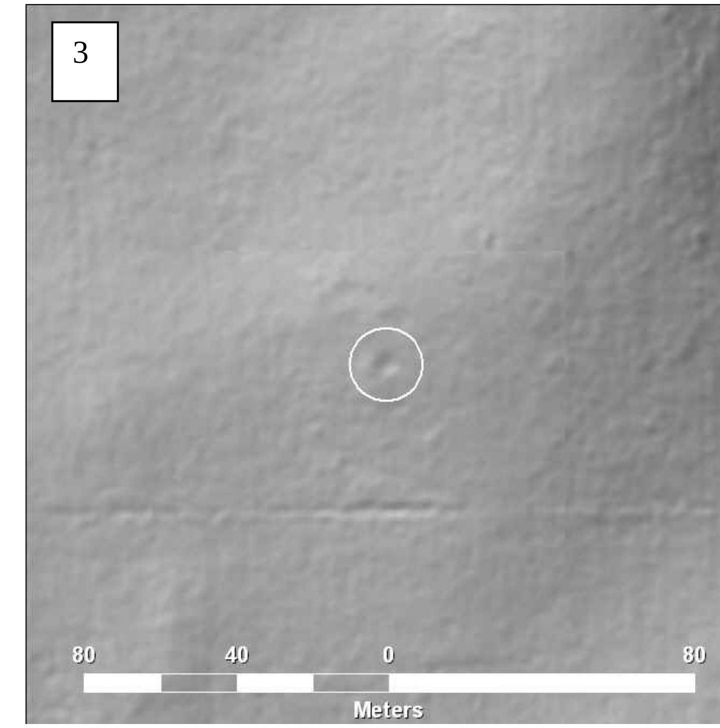

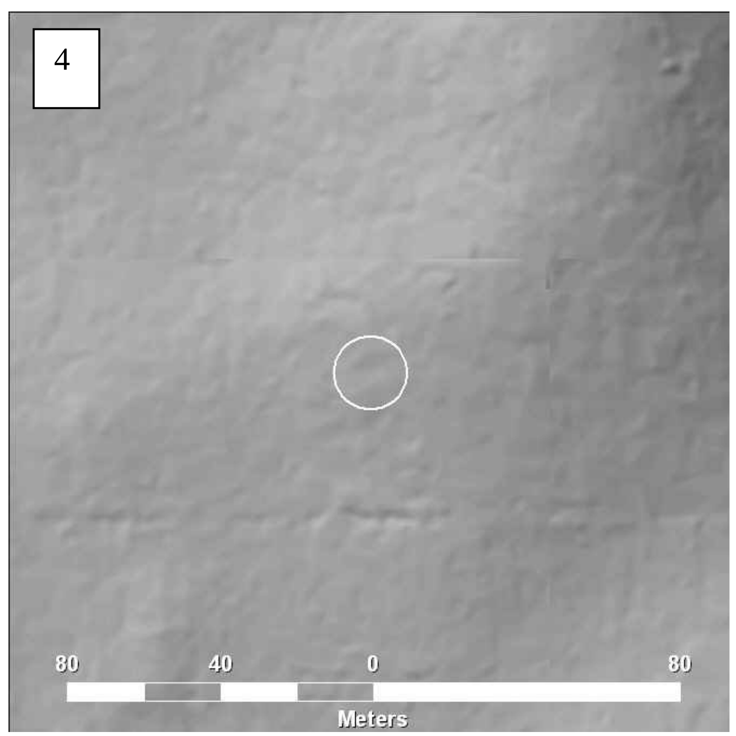

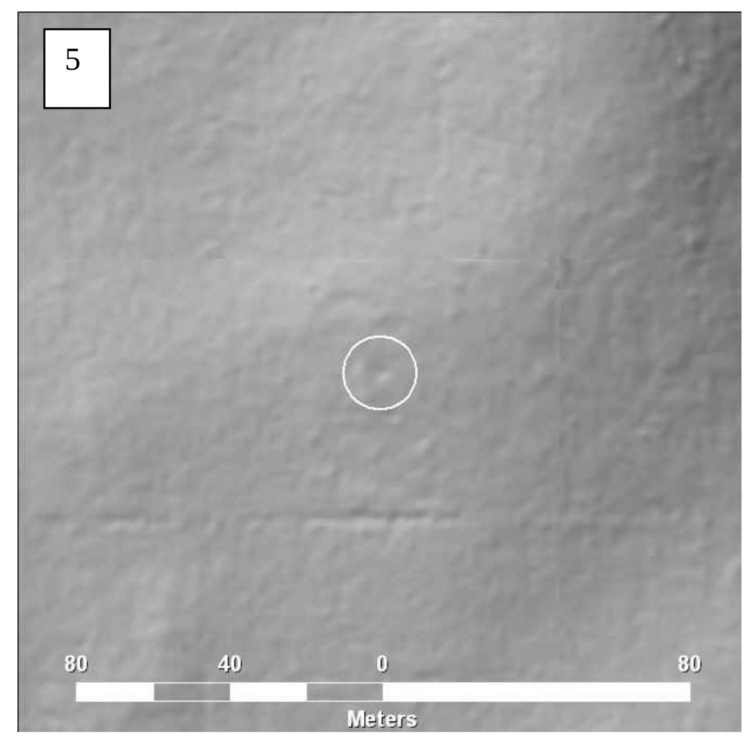

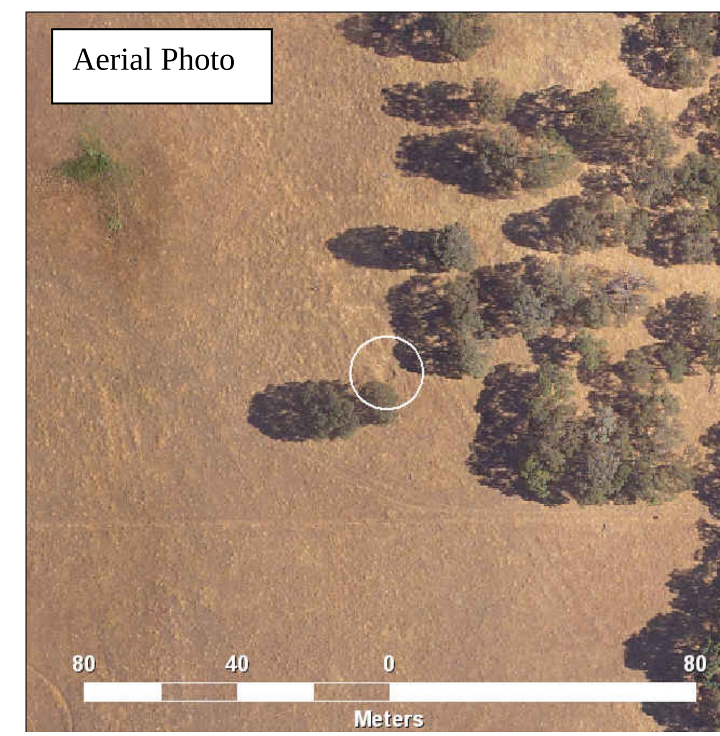

Plot # 7

Feature size: 3.8 m
Vegetation Density: 36.31 %
Lidar block reference number: 5466

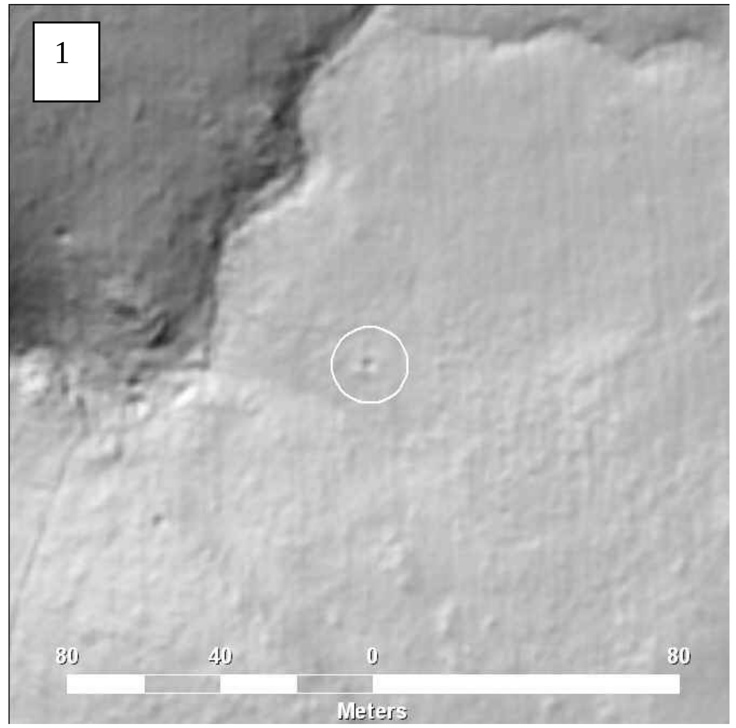

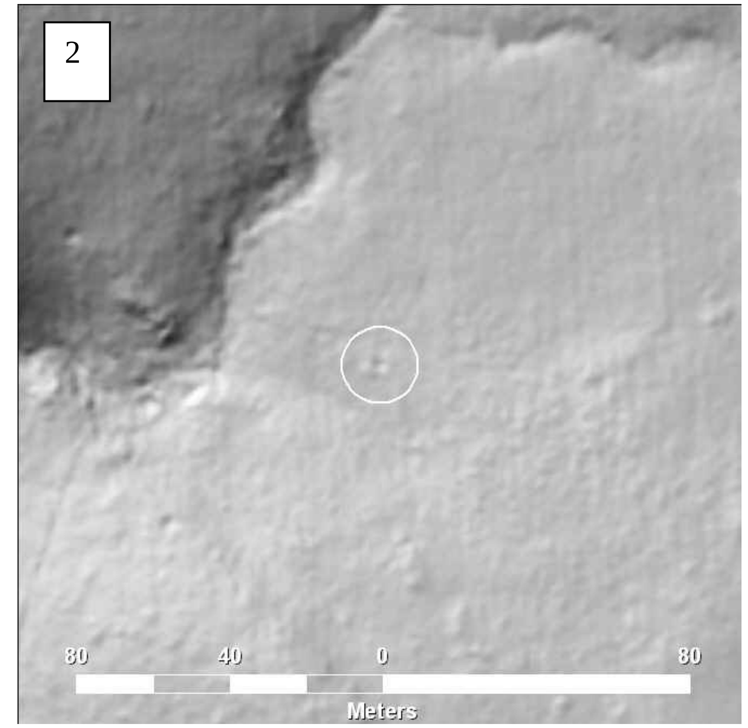

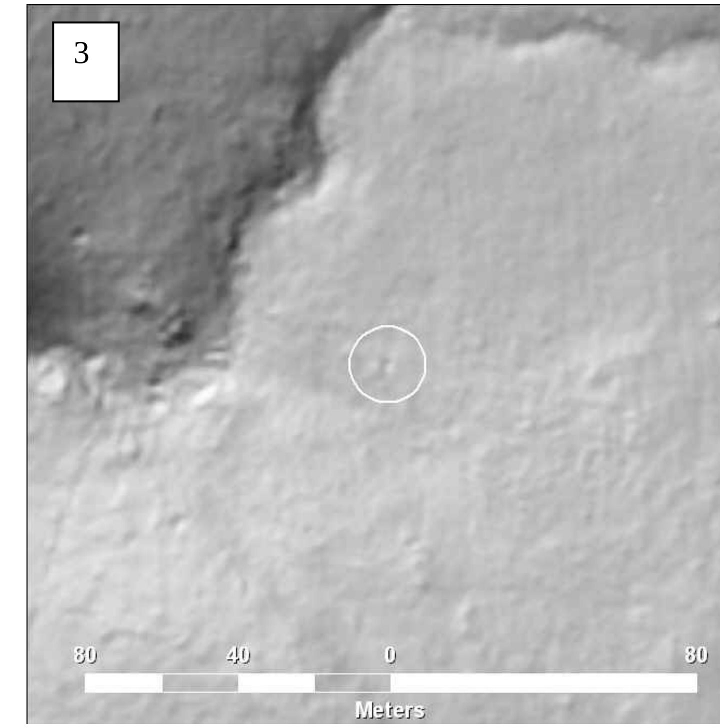

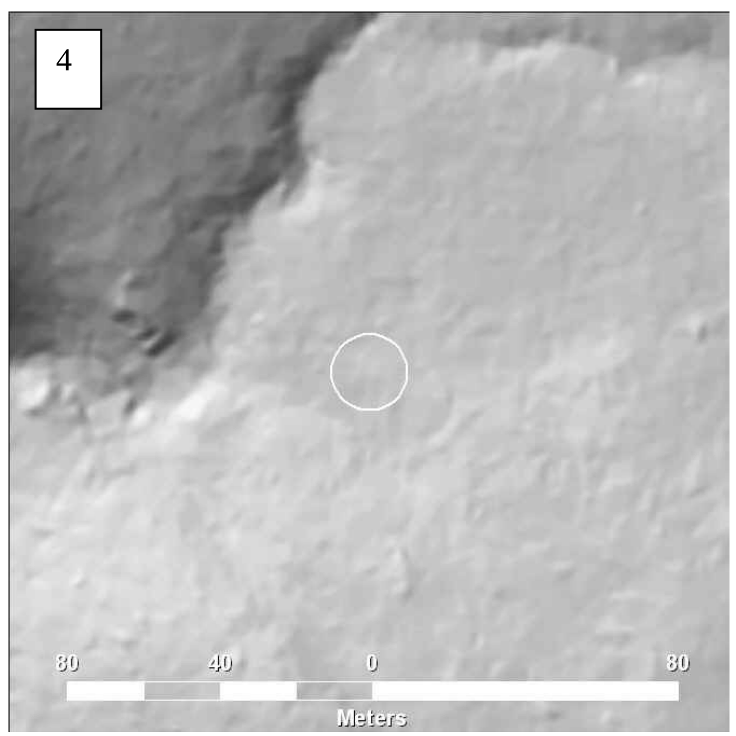

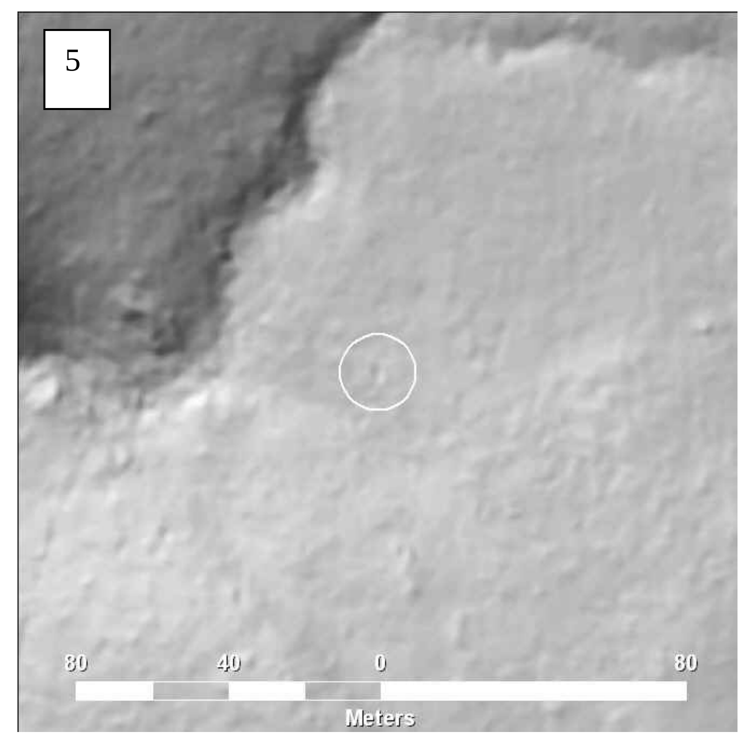

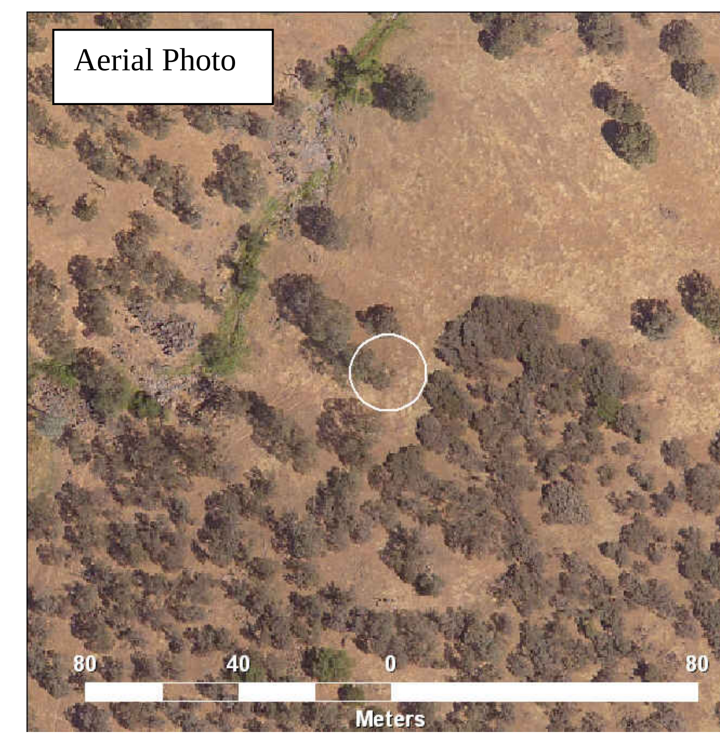

Plot # 8

Feature size: 3.8 m
Vegetation Density: 43.82 %
Lidar block reference number: 5580

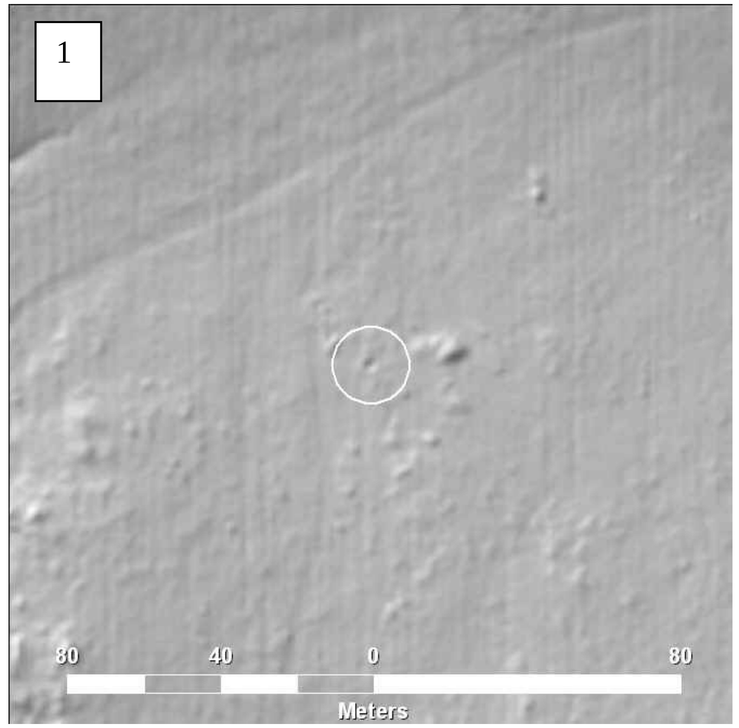

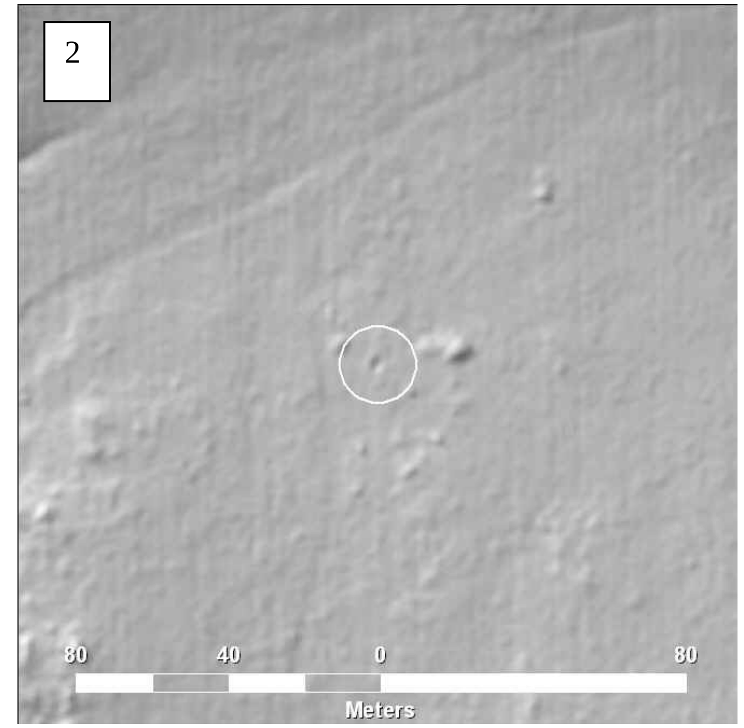

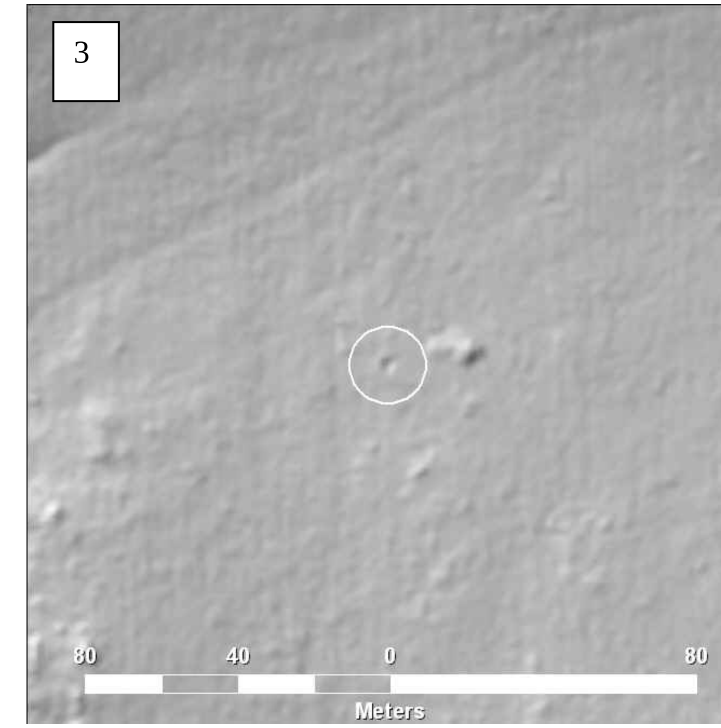

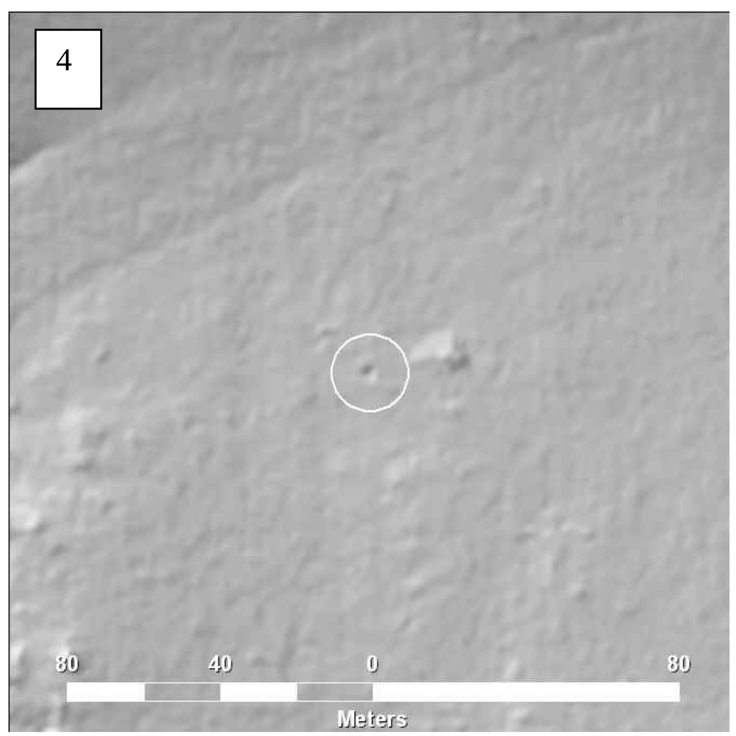

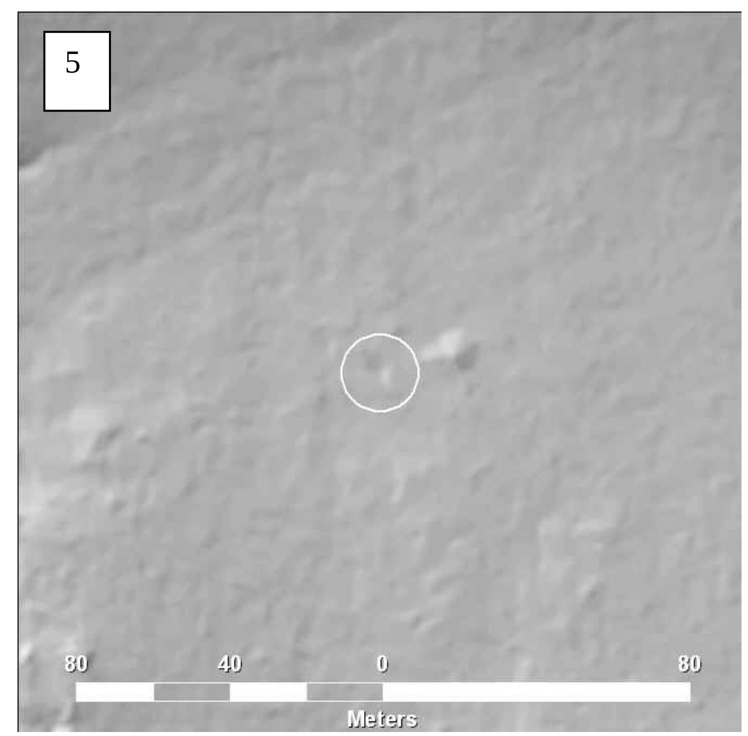

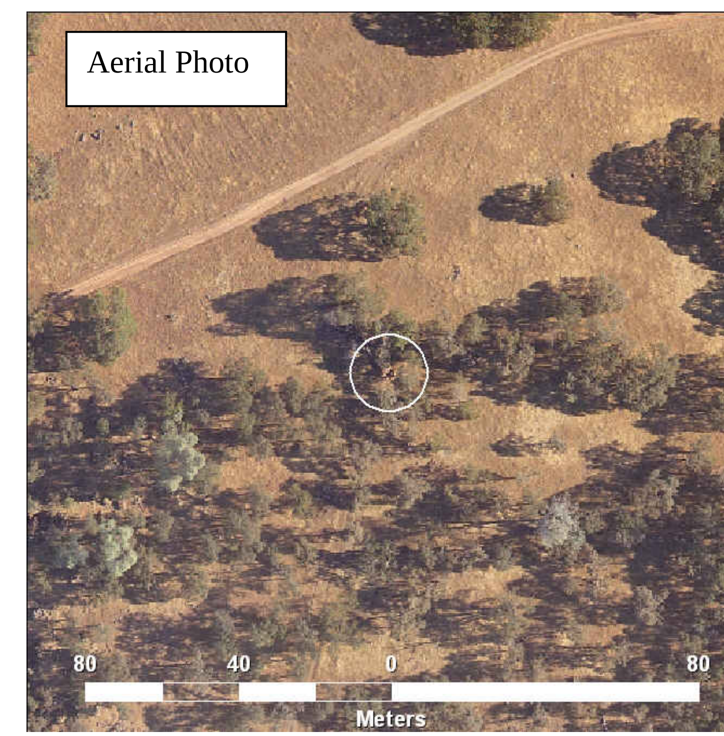

Plot # 9

Feature size: 4.8 m
Vegetation Density: 42.75 %
Lidar block reference number: 5743

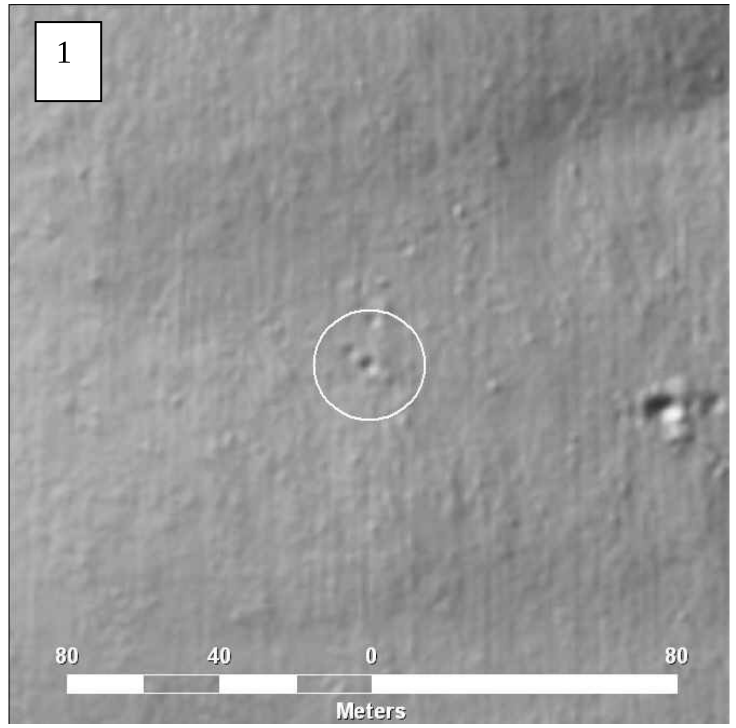

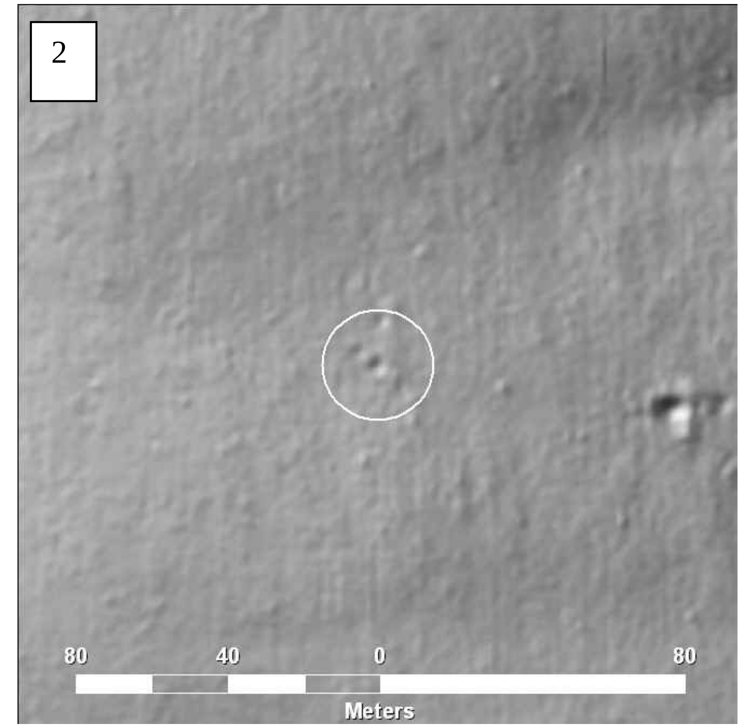

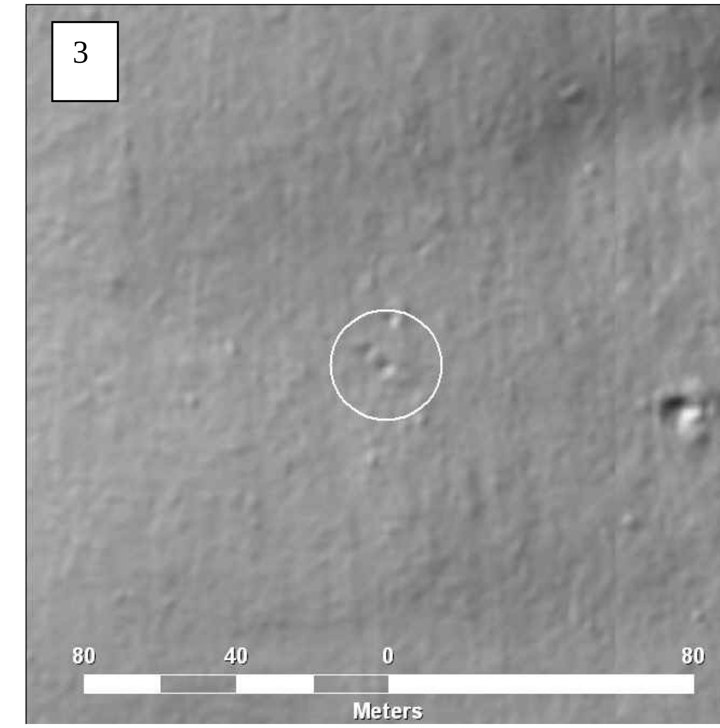

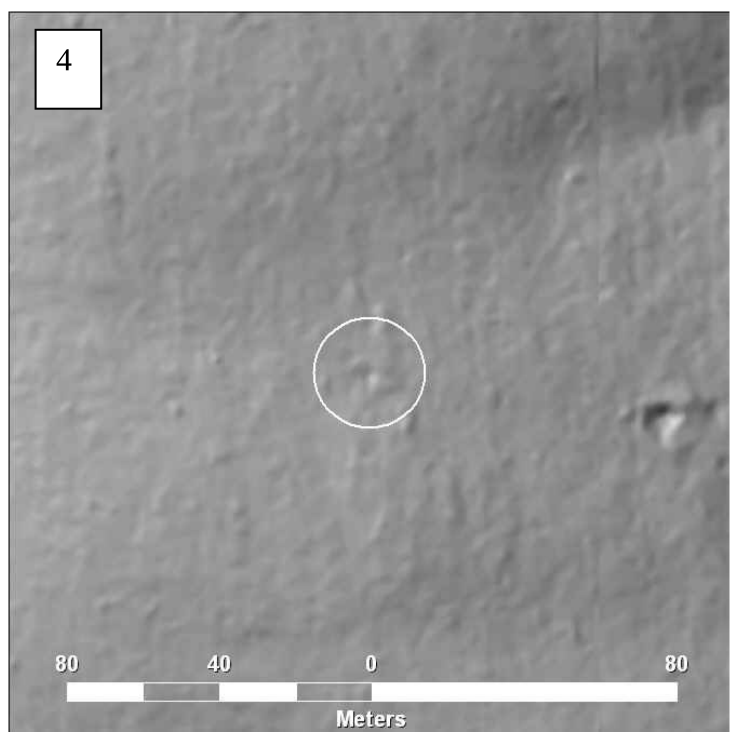

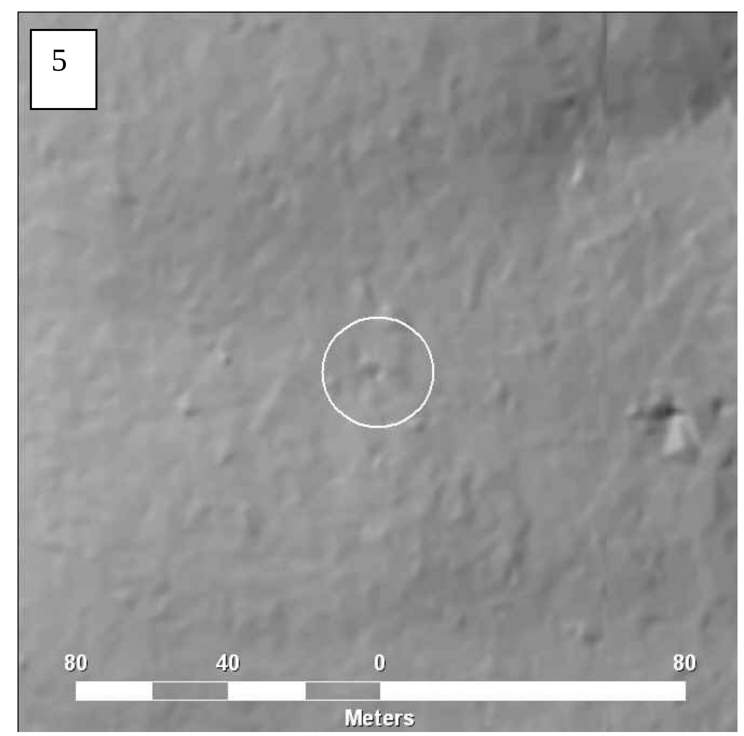

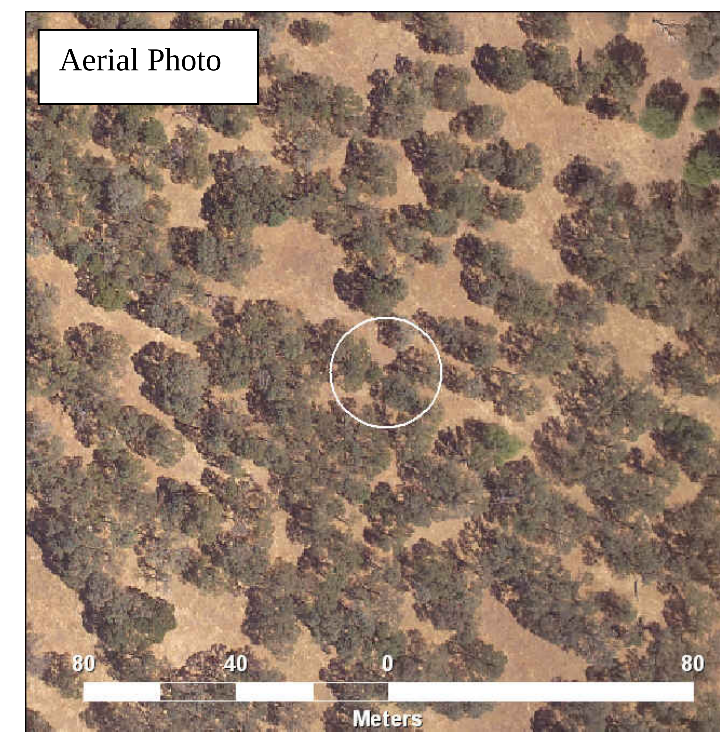

Plot # 10

Feature size: no feature visible
Vegetation Density: 48.74 %
Lidar block reference number: 4078

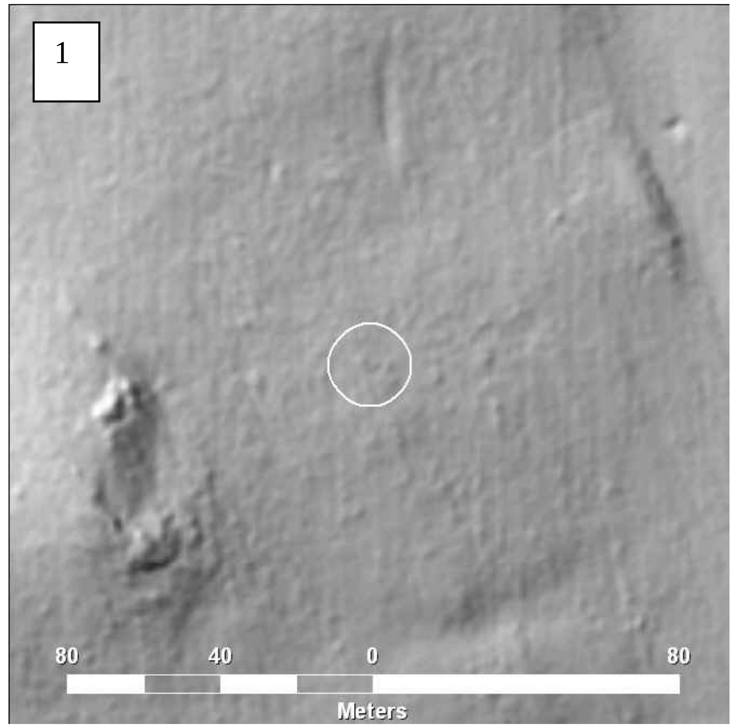

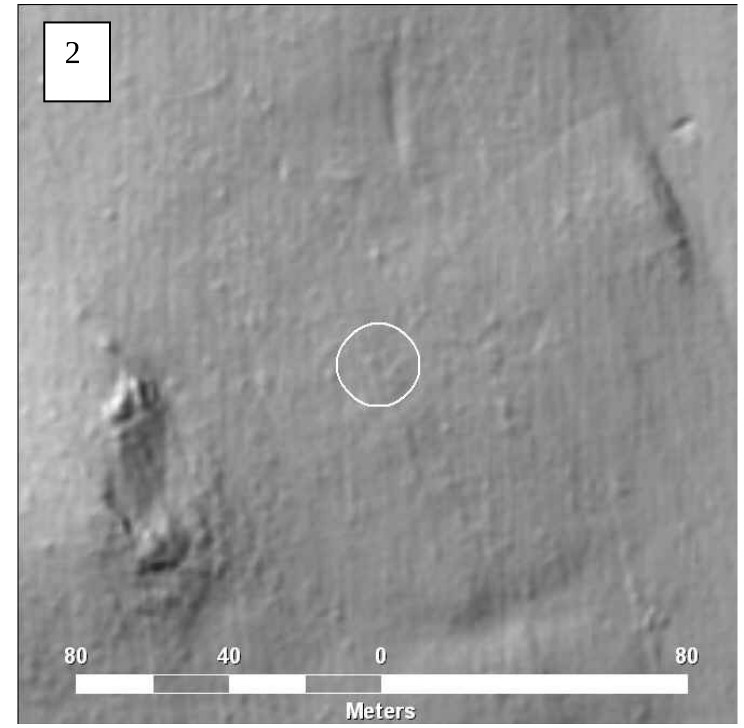

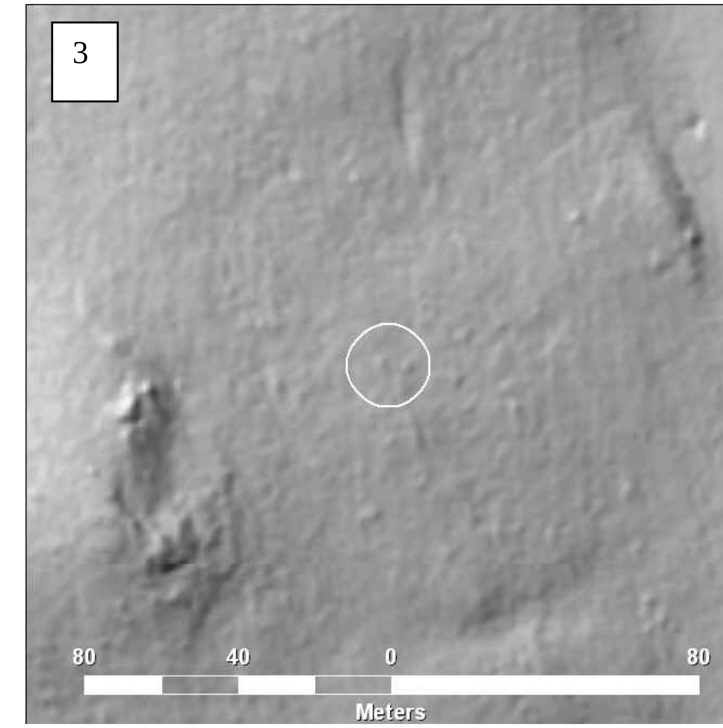

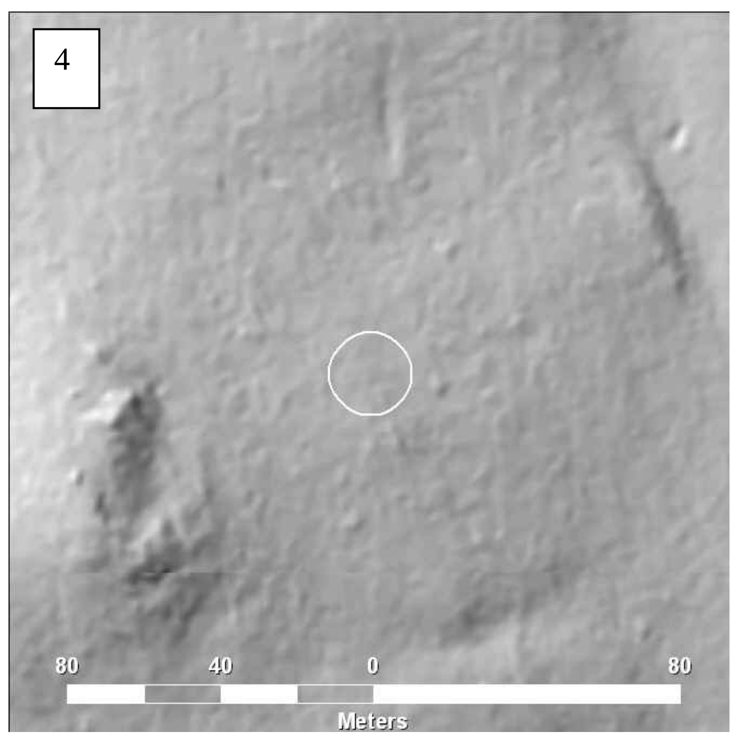

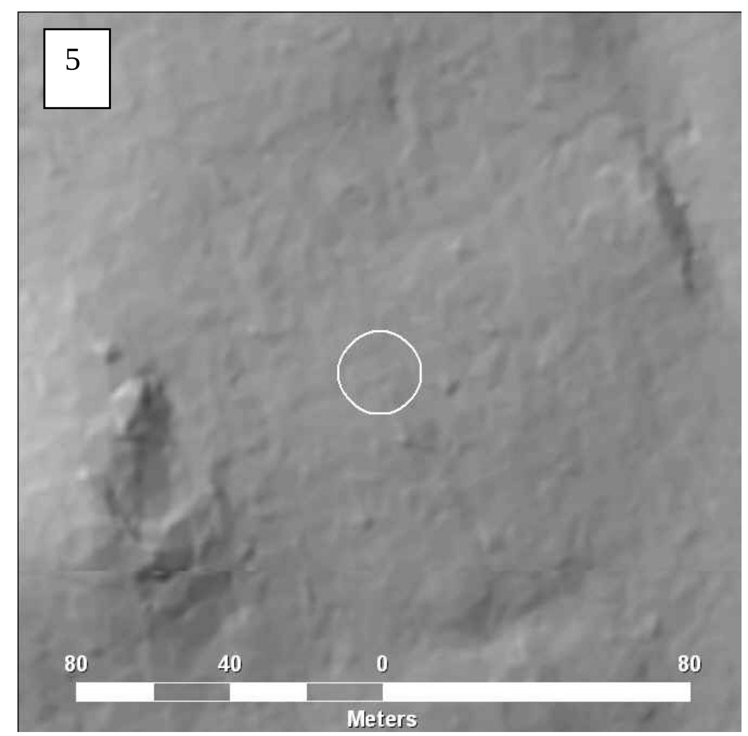

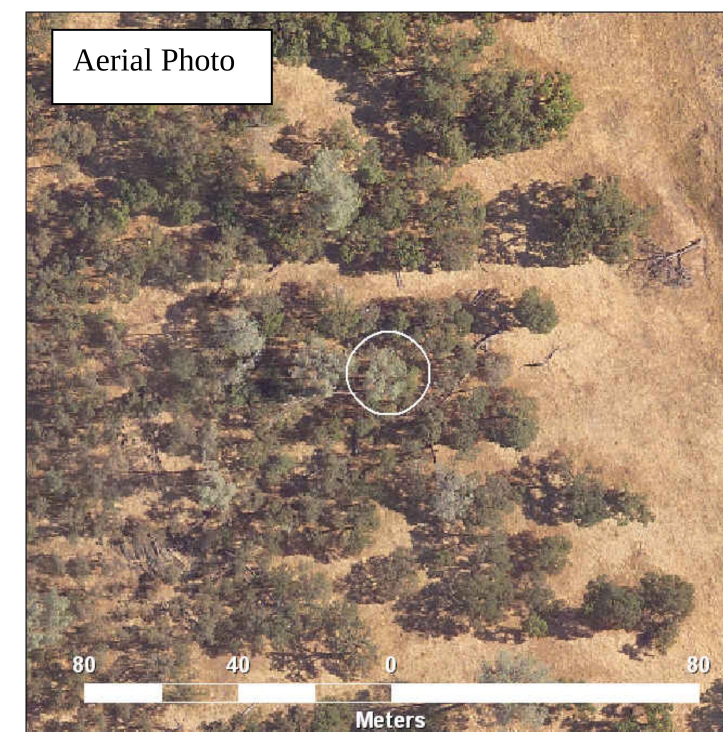

Plot # 11

Feature size: no feature visible
Vegetation Density: 30 %
Lidar block reference number: 5645

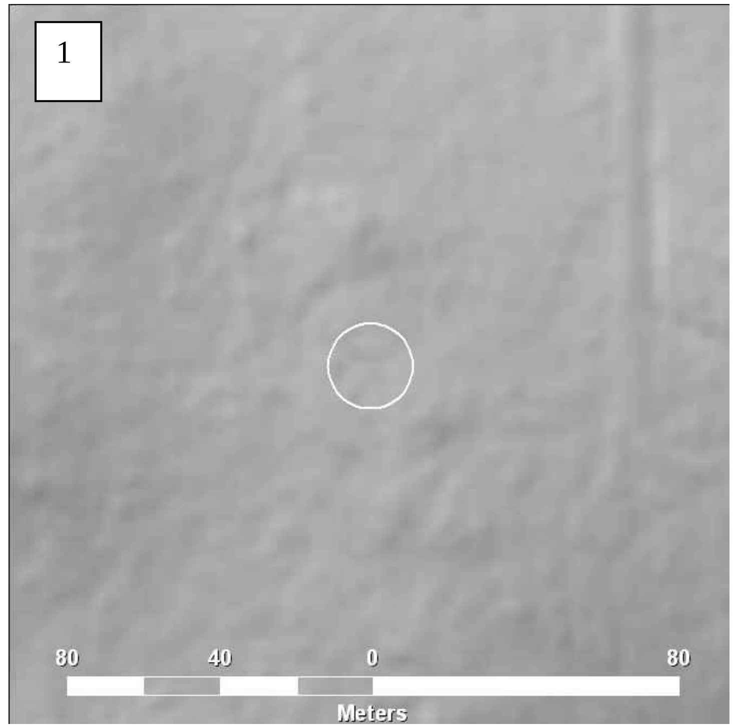

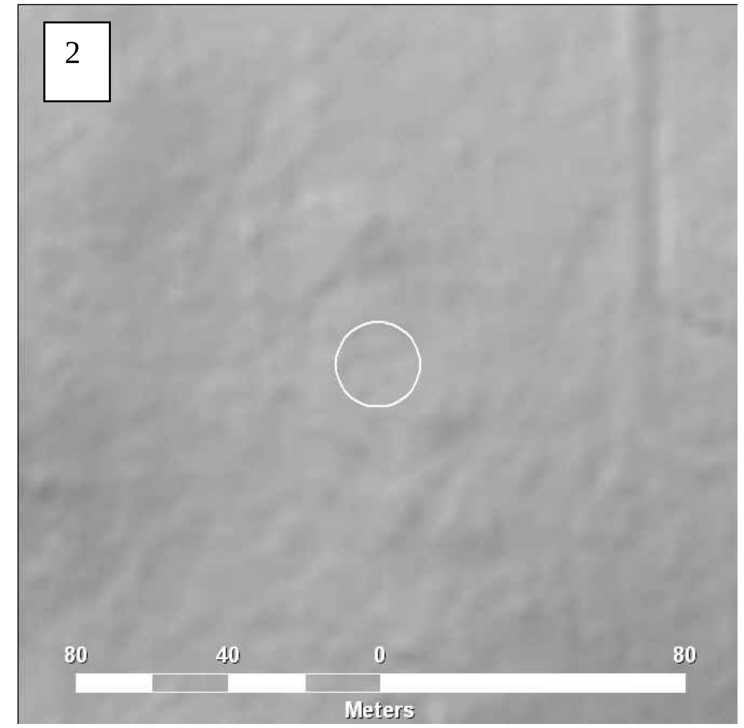

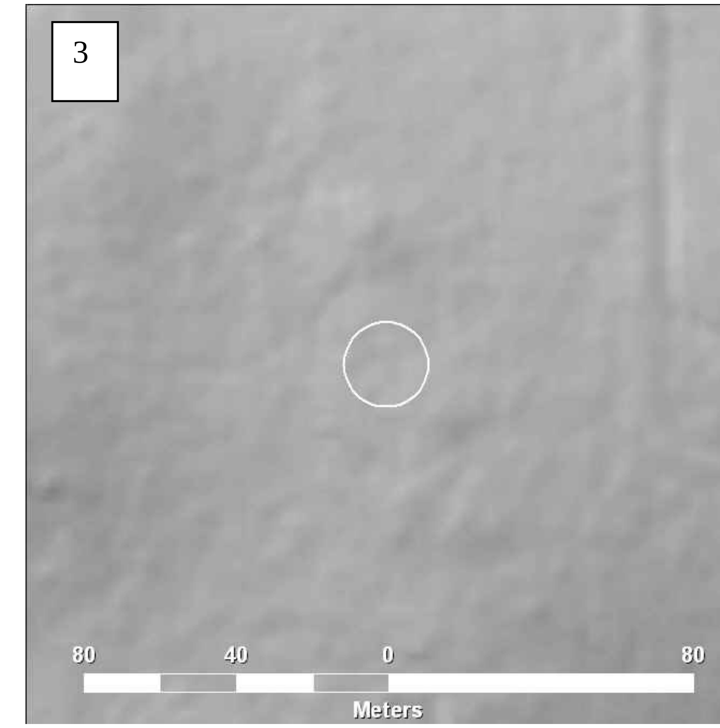

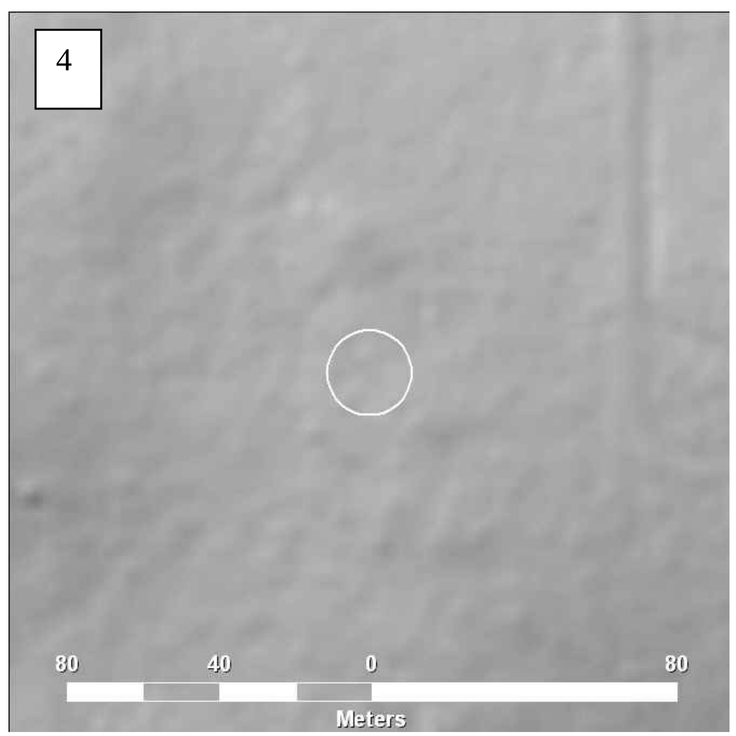

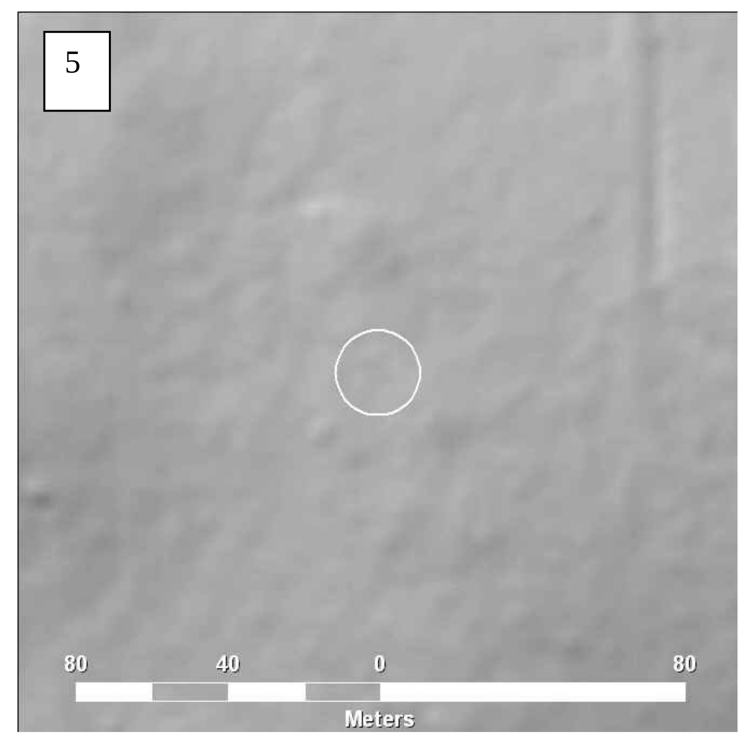

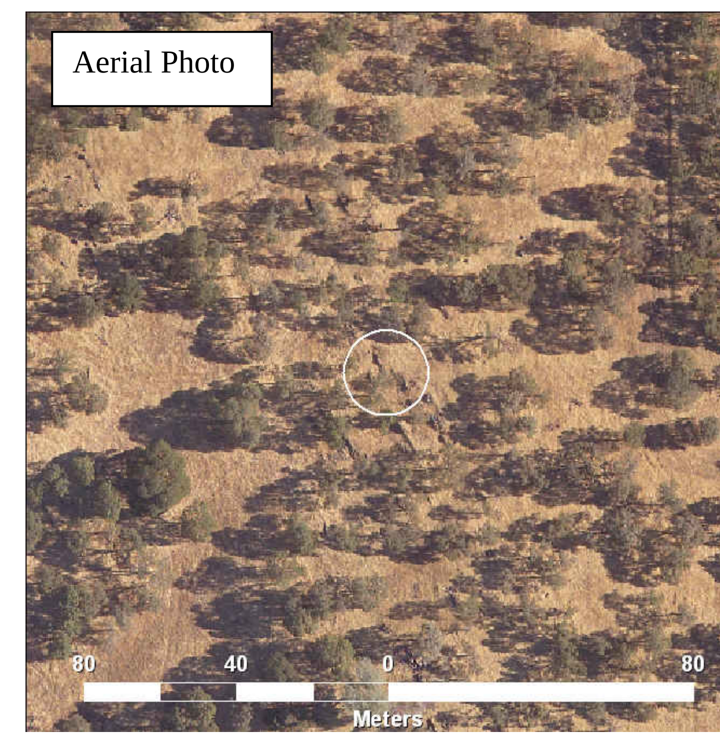

Plot # 12

Feature size: 1.5 m
Vegetation Density: 50.78 %
Lidar block reference number: 5822

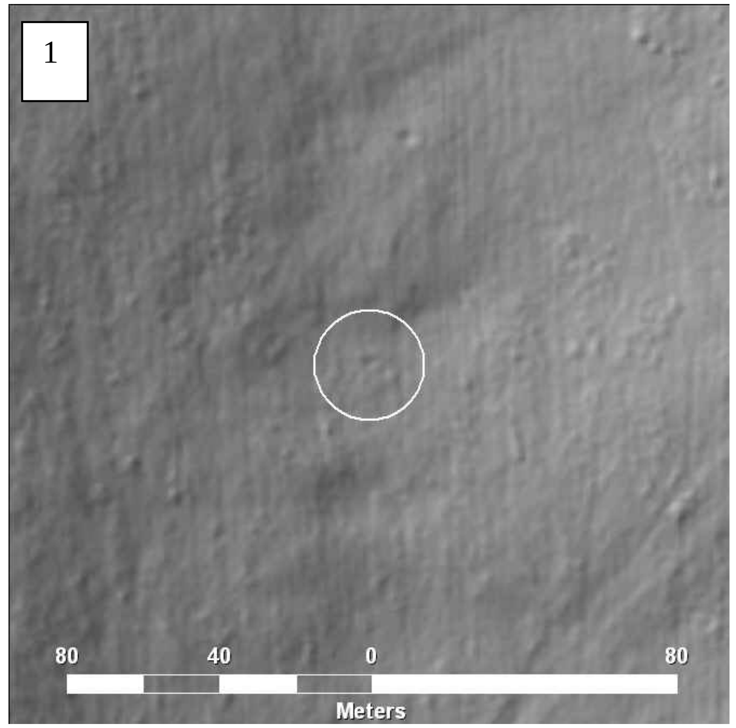

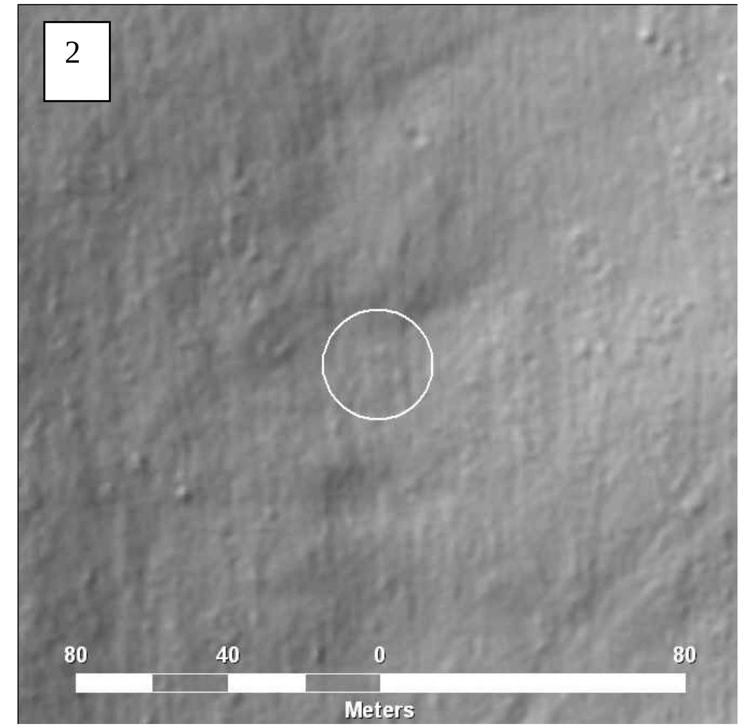

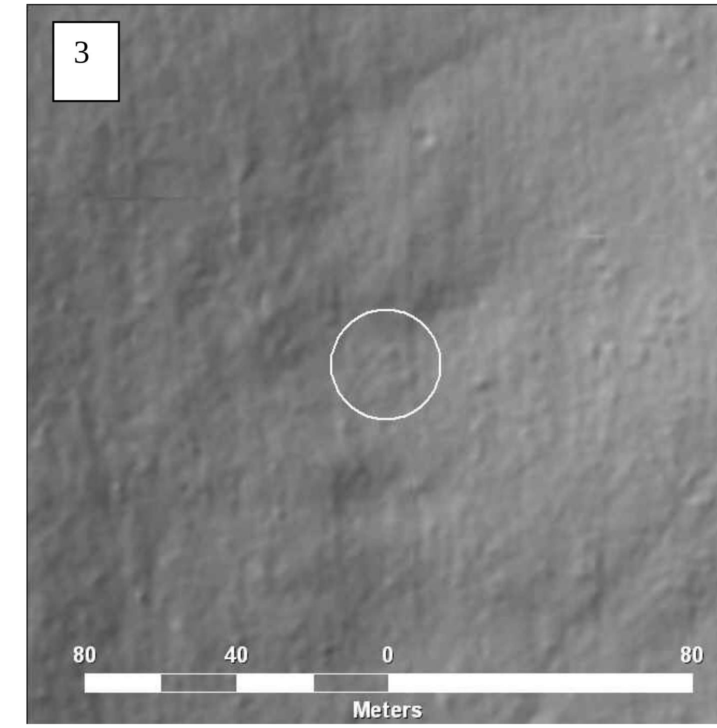

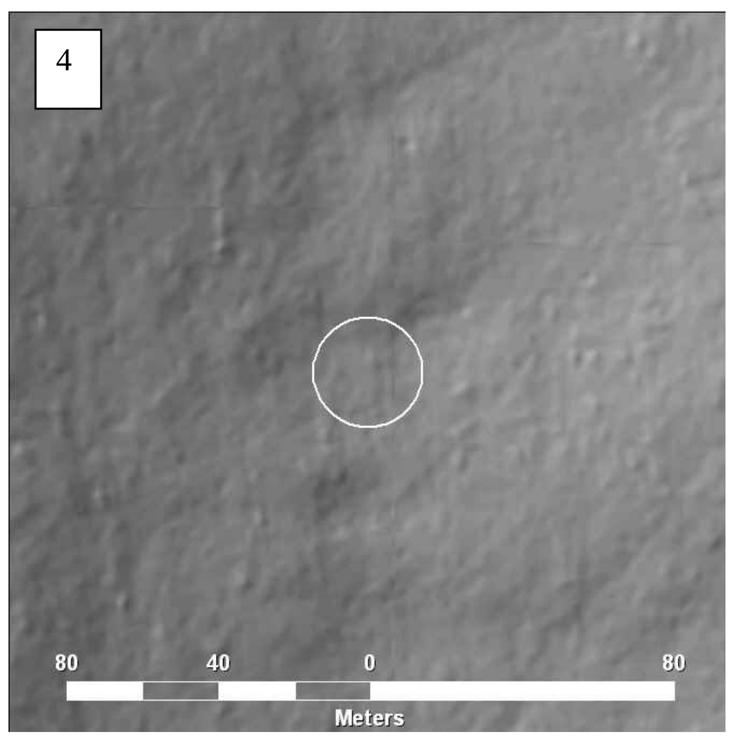

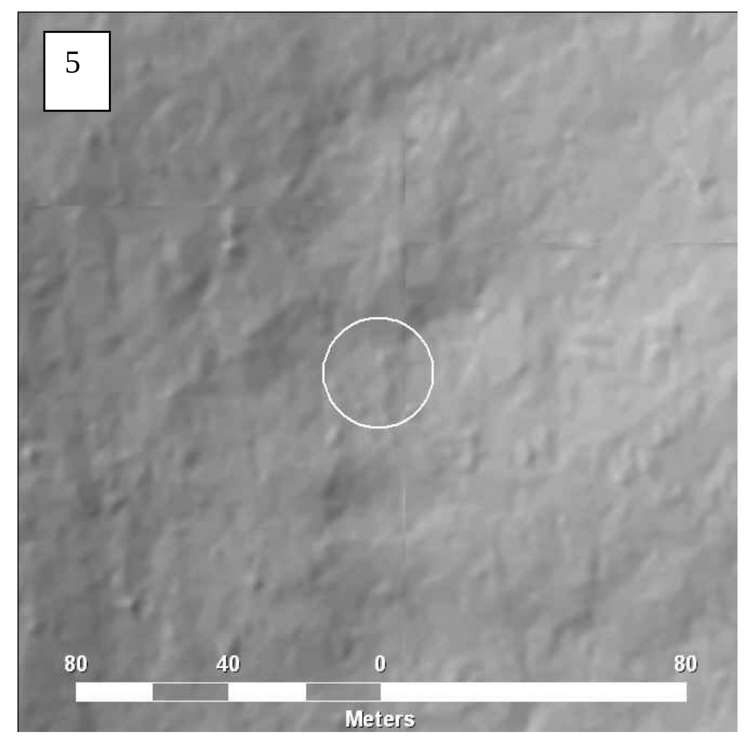

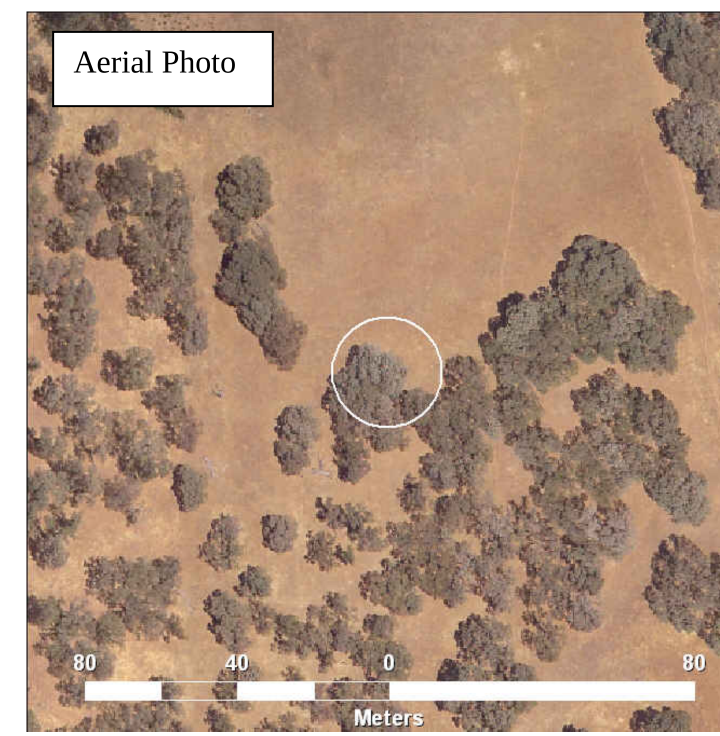

Plot # 13

Feature size: 2.6 m
Vegetation Density: 0 %
Lidar block reference number: 3978

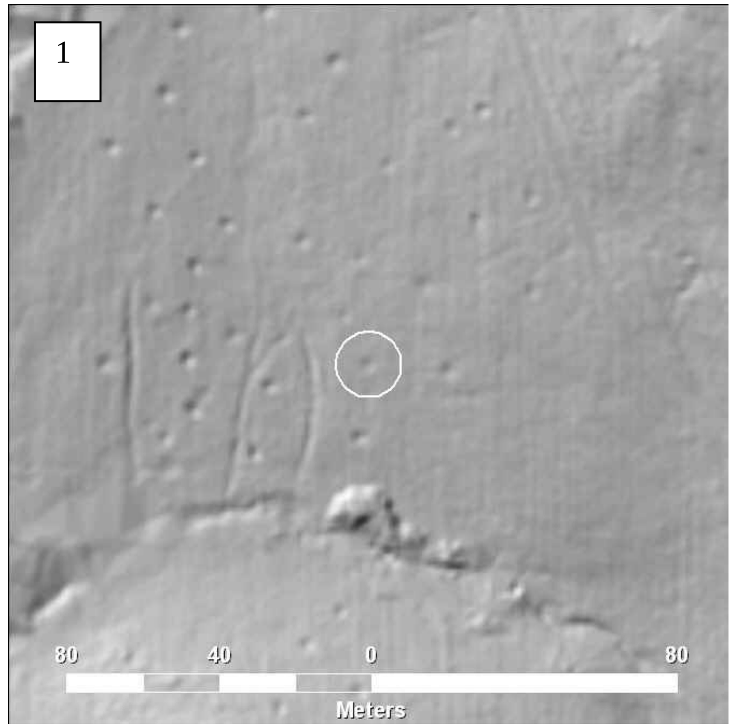

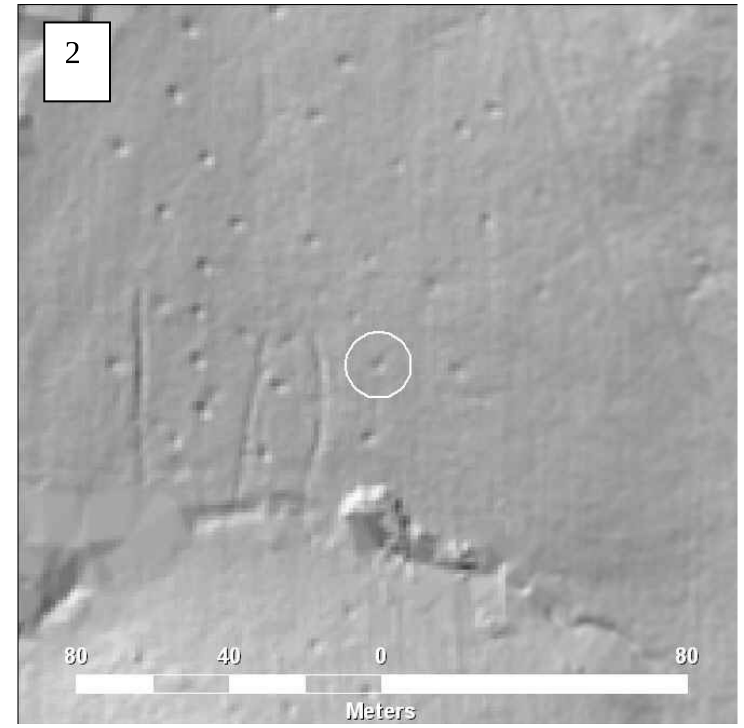

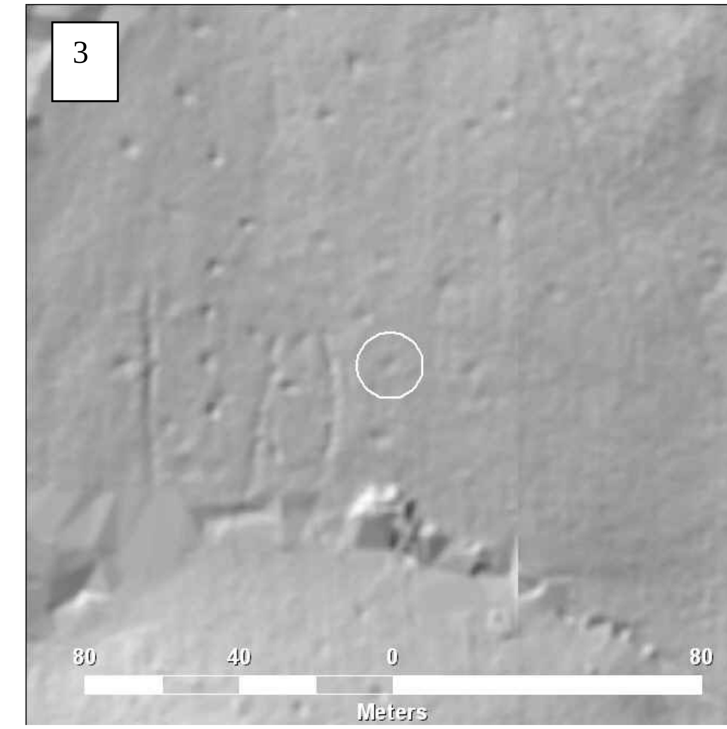

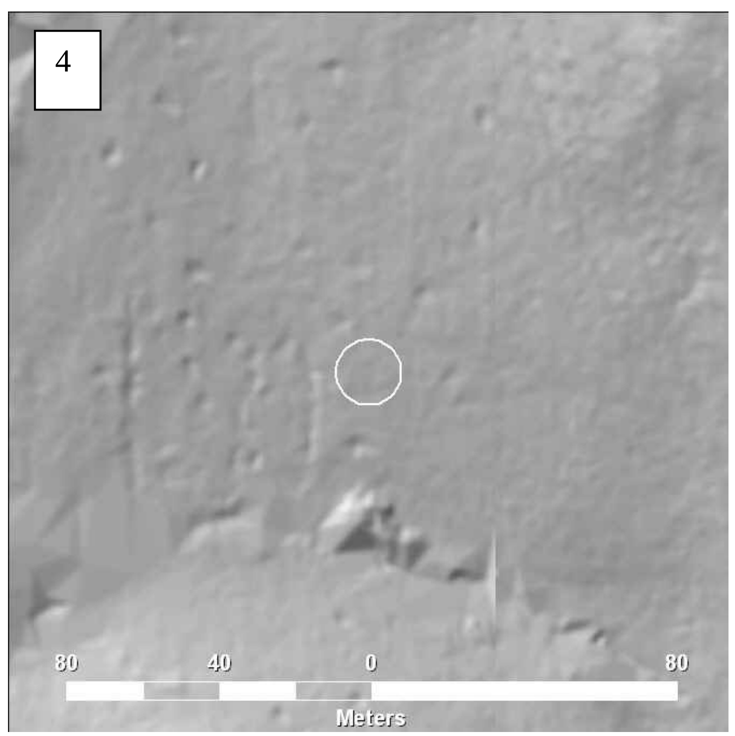

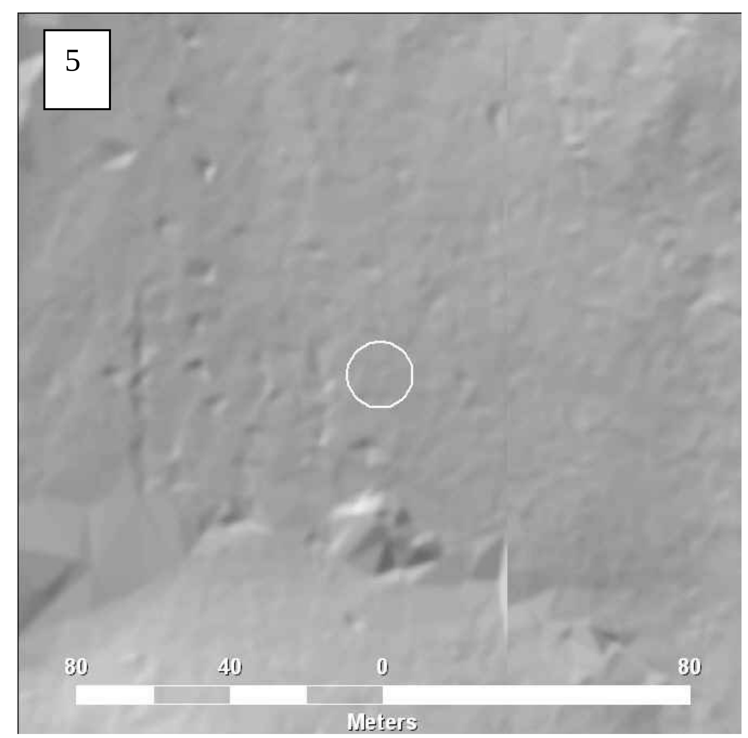

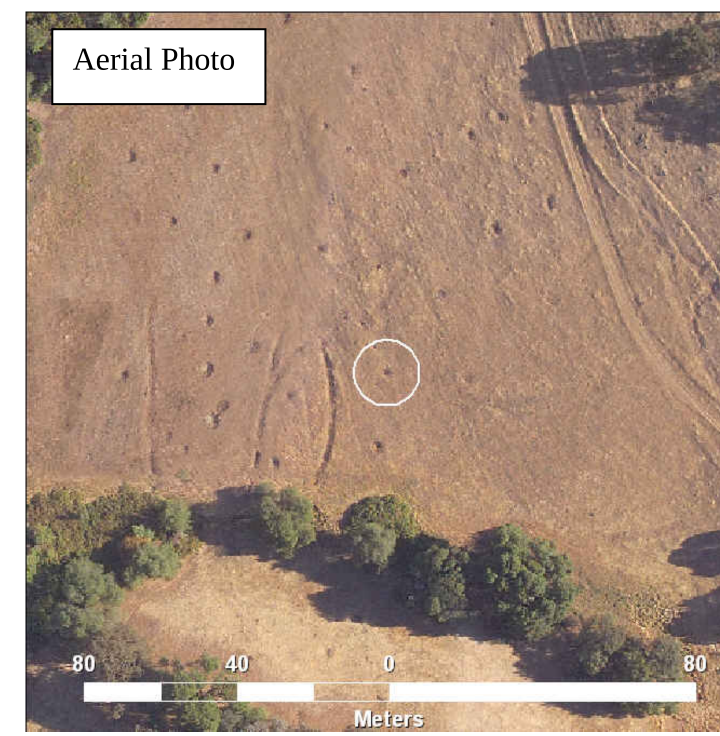

Plot # 14

Feature size: 2.7 m
Vegetation Density: 11.36 %
Lidar block reference number: 3991

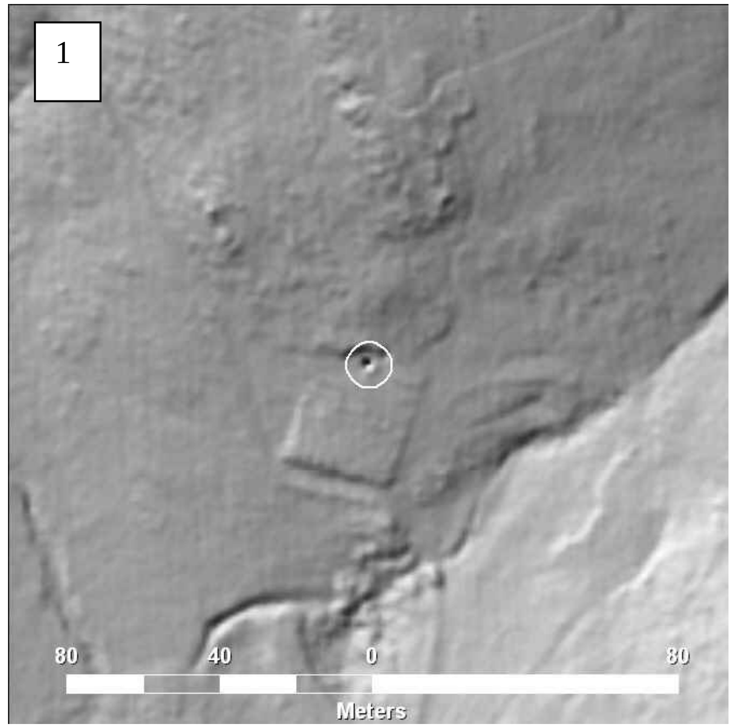

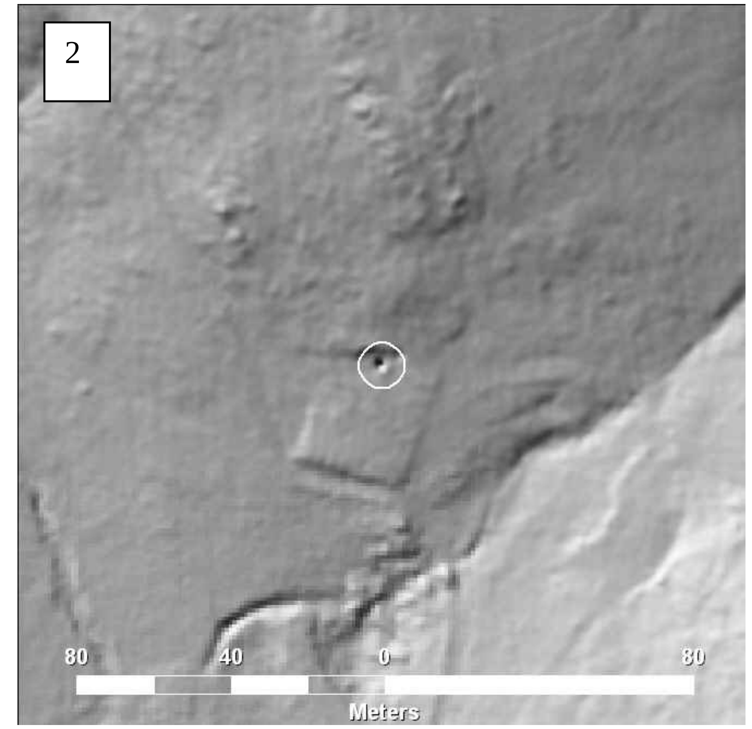

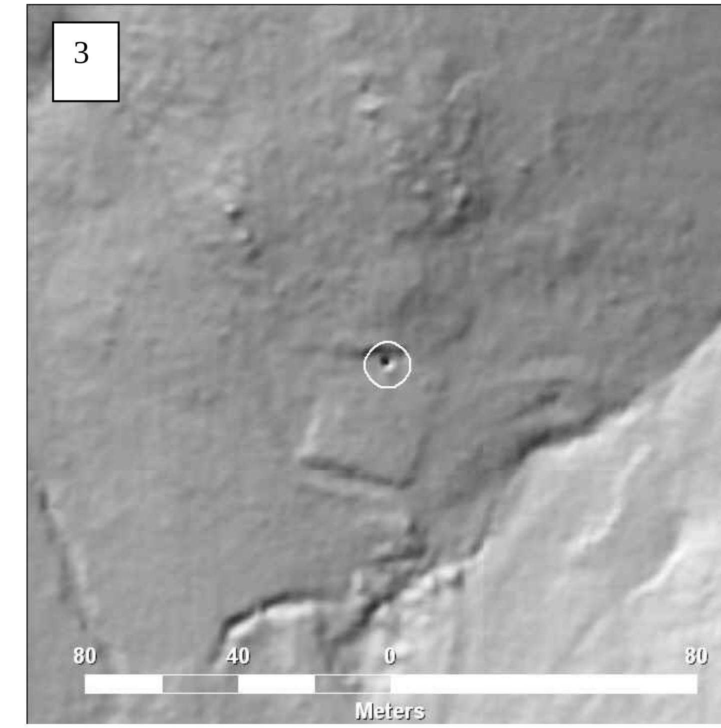

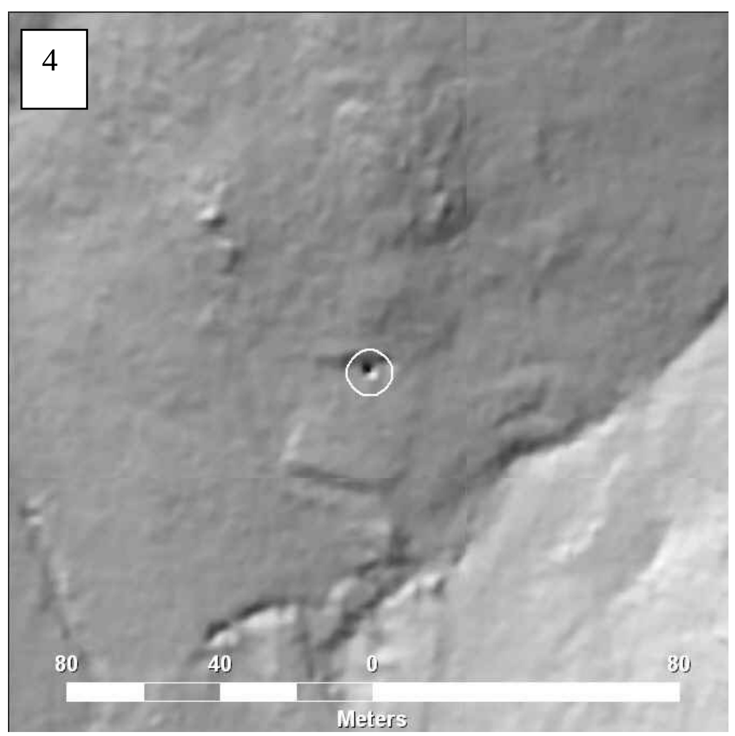

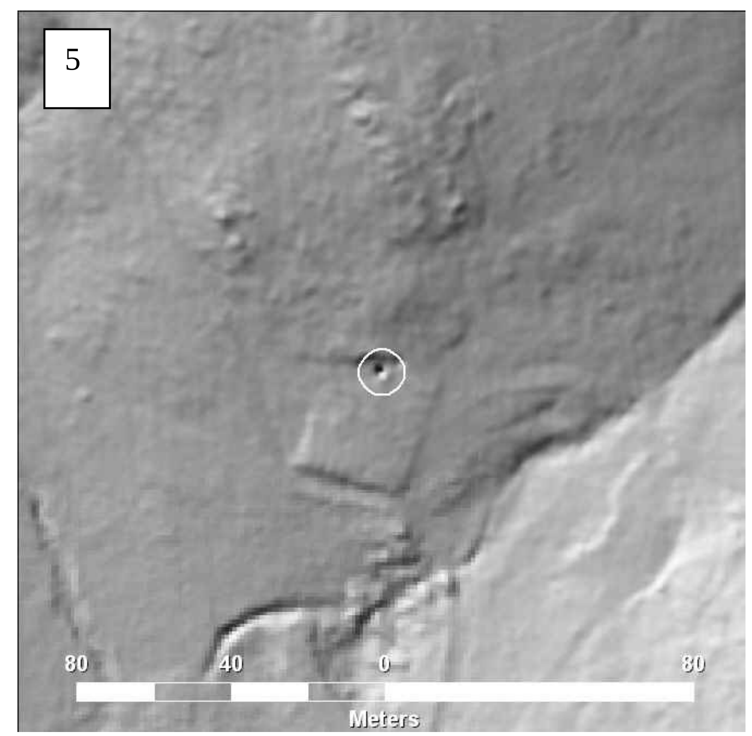

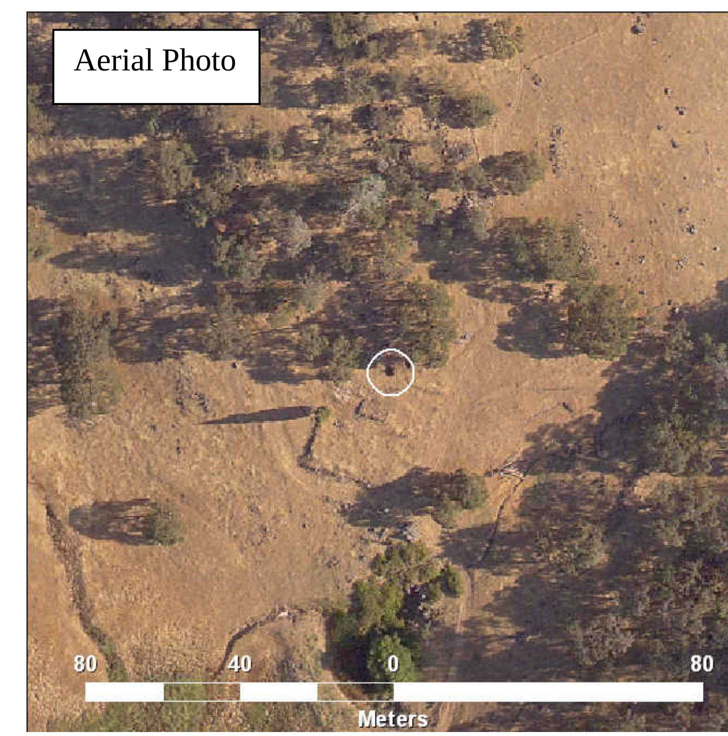

Plot # 15

Feature size: 2.9 m wide
3.7 m long
Vegetation Density: 53.25 %
Lidar block reference number: 5351

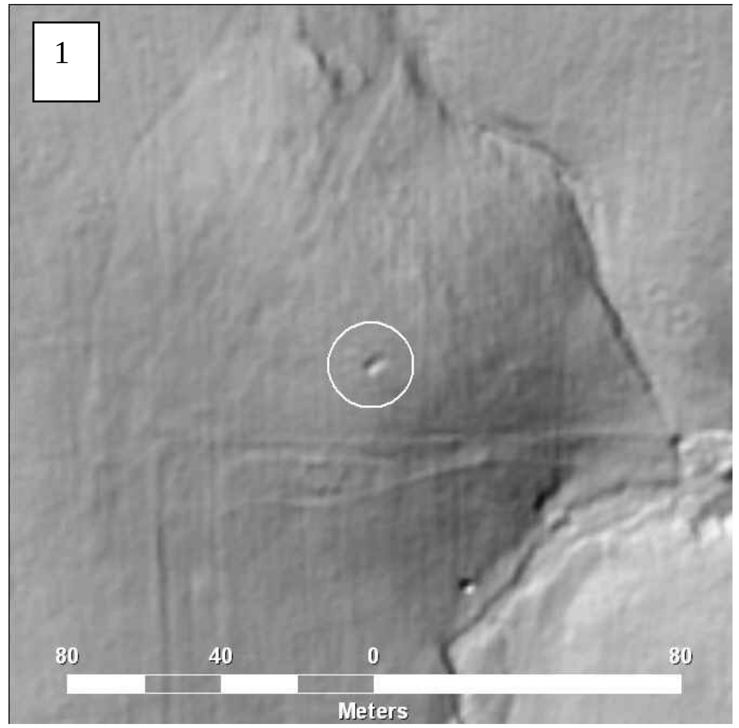

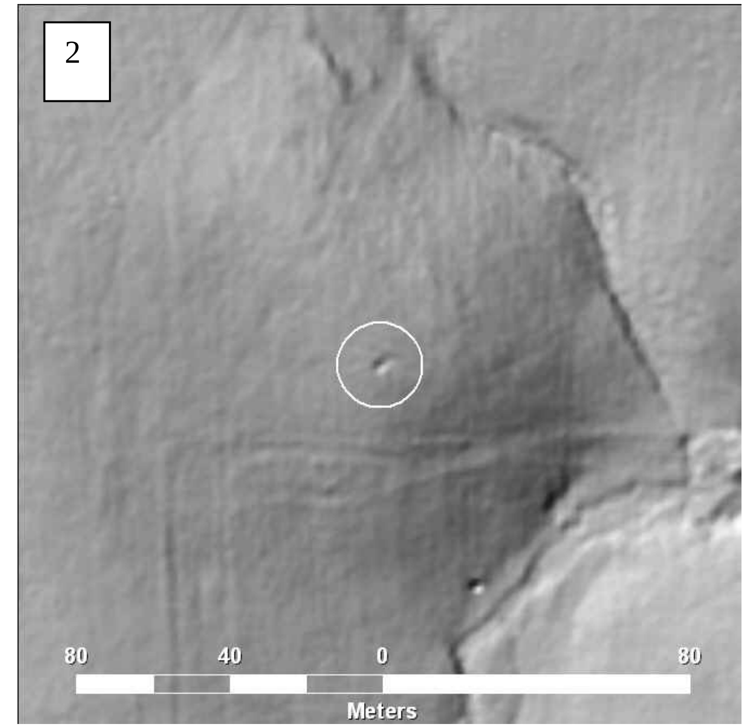

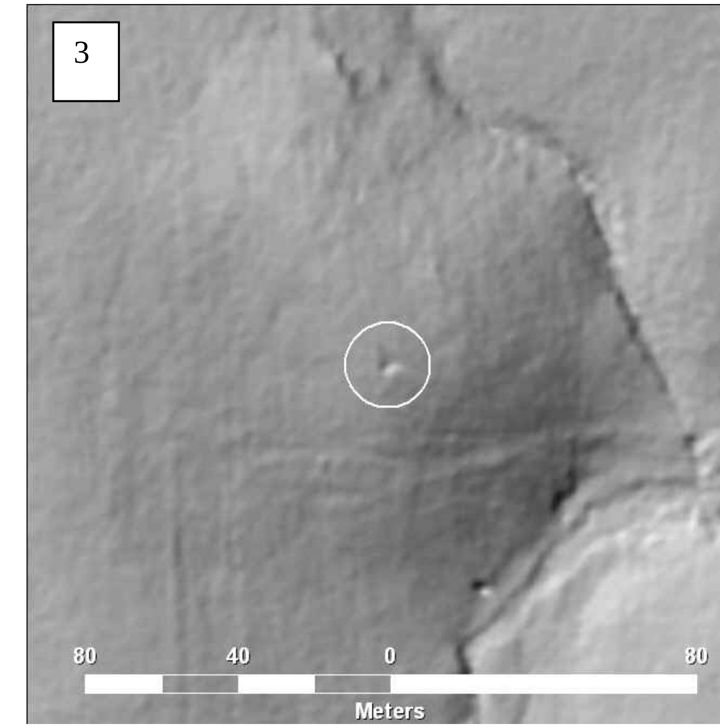

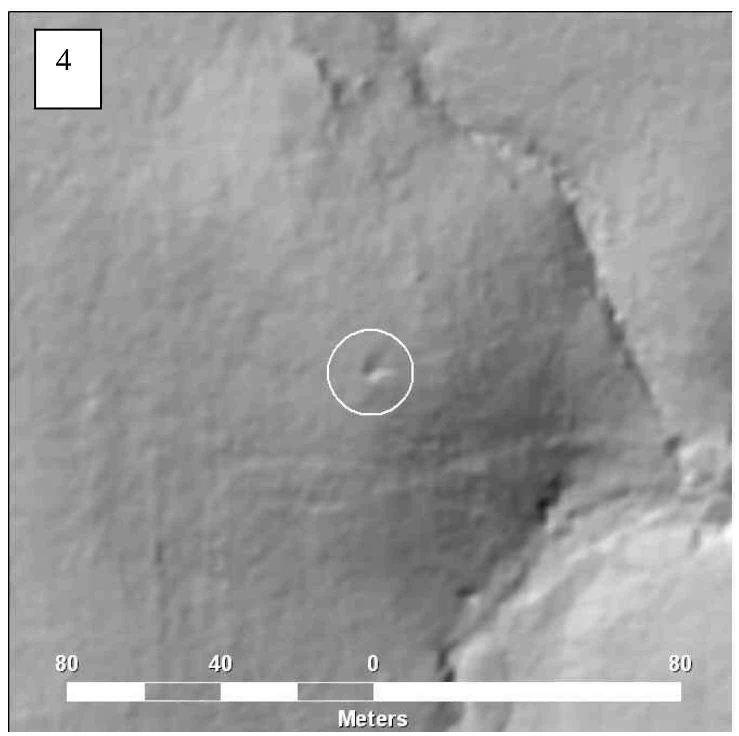

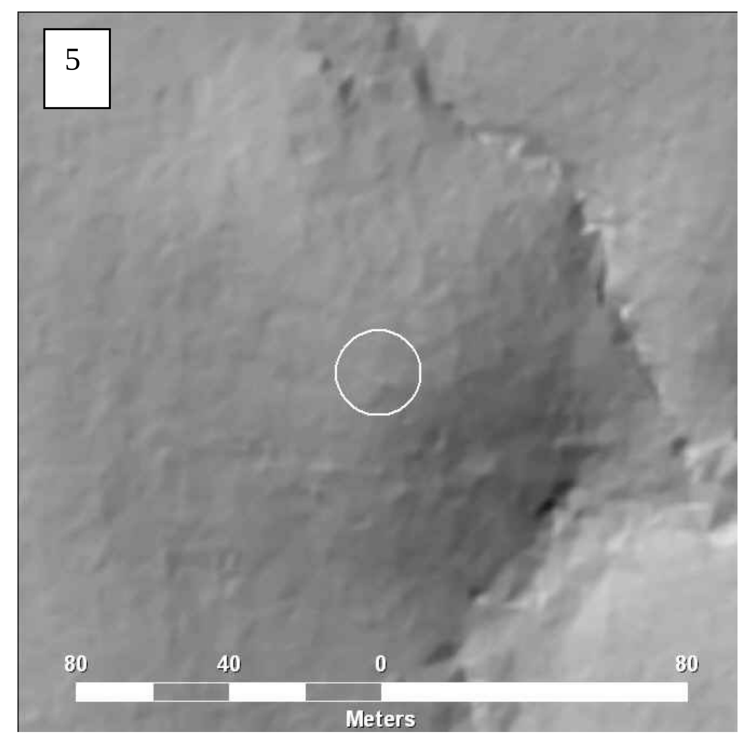

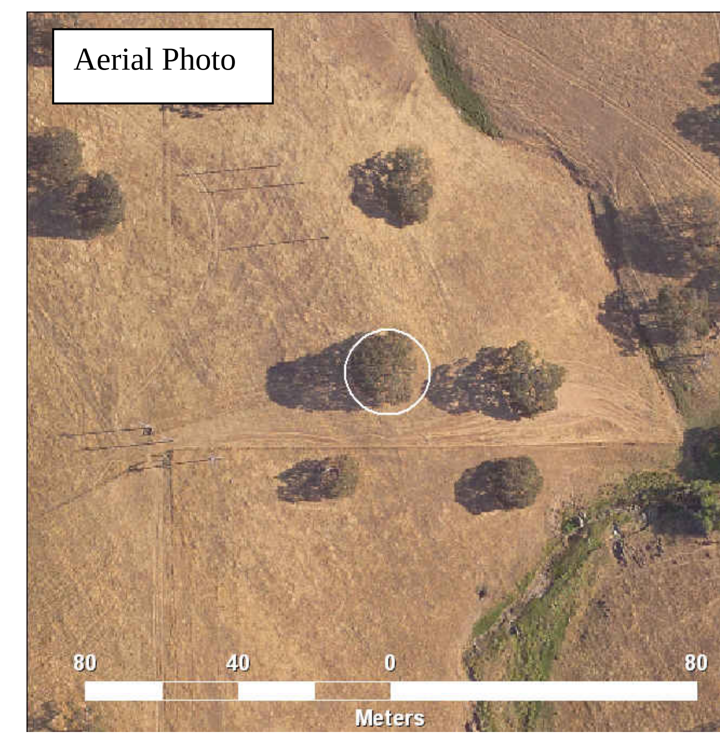

Plot # 16

Feature Size: 2.9 meters
Vegetation Density: 55.7%
Lidar block reference number: 3953

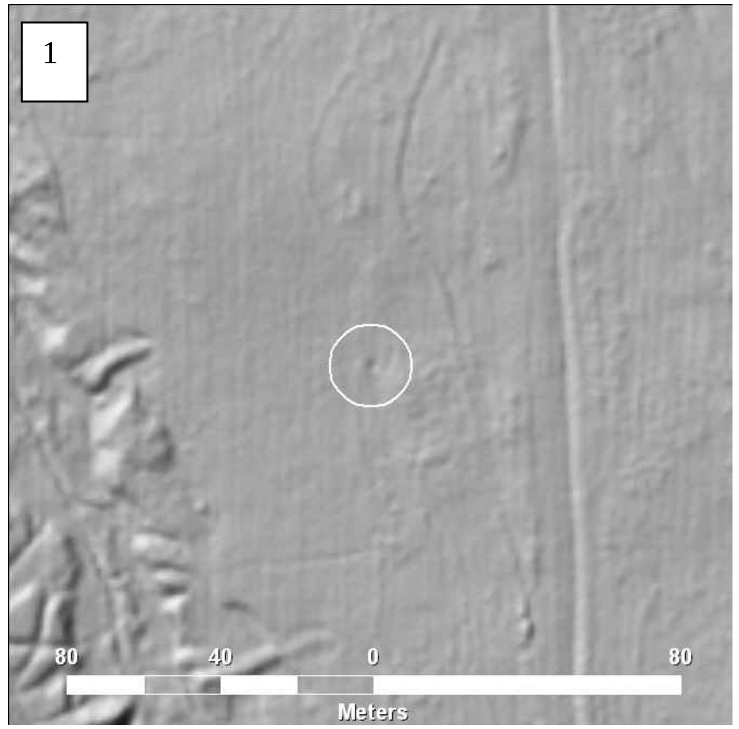

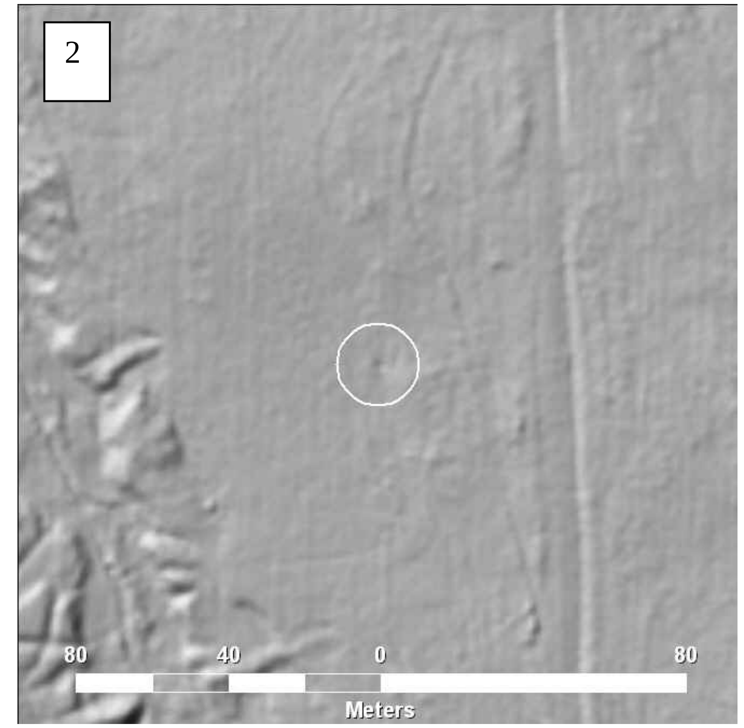

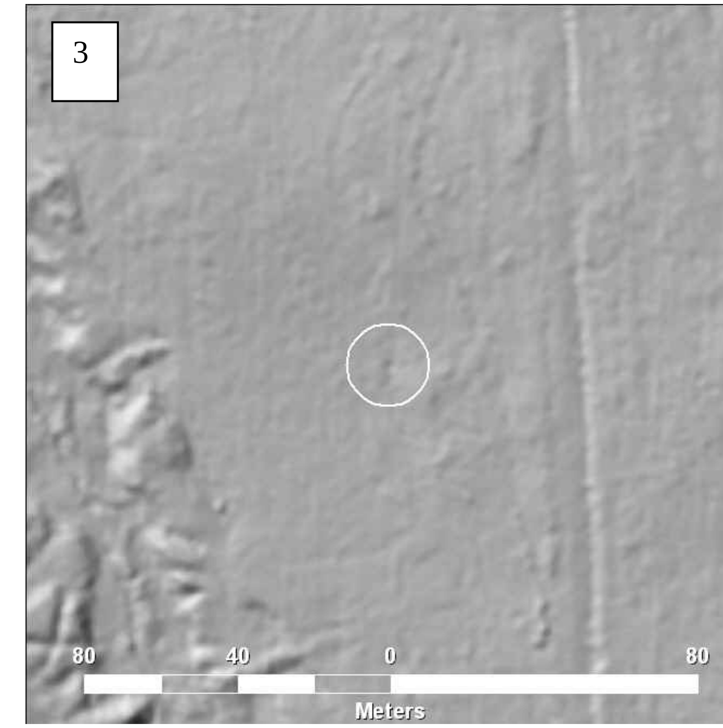

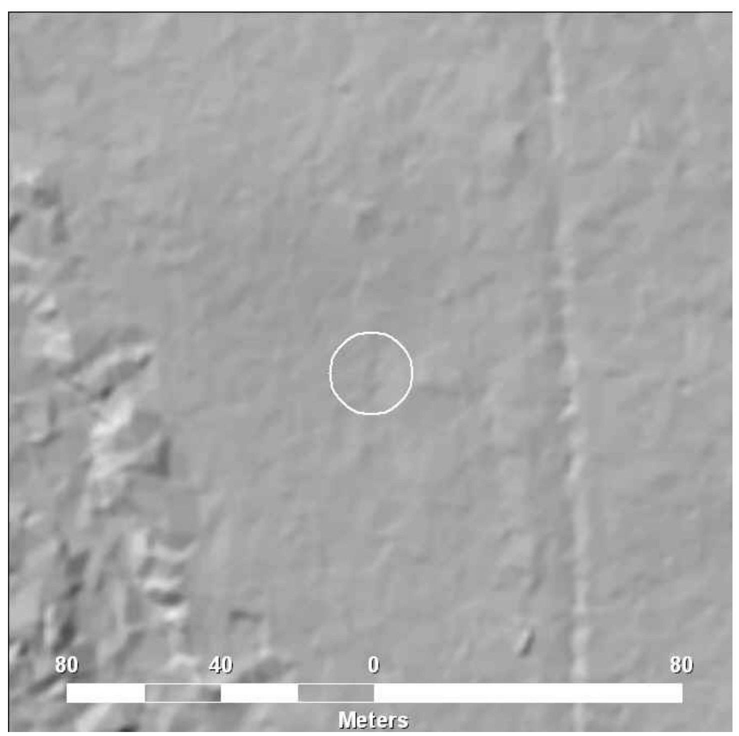

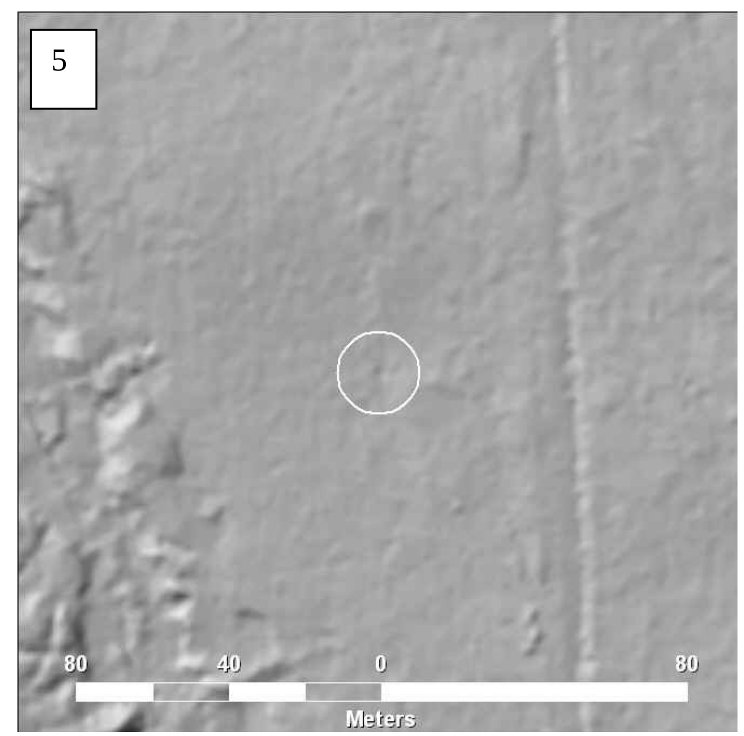

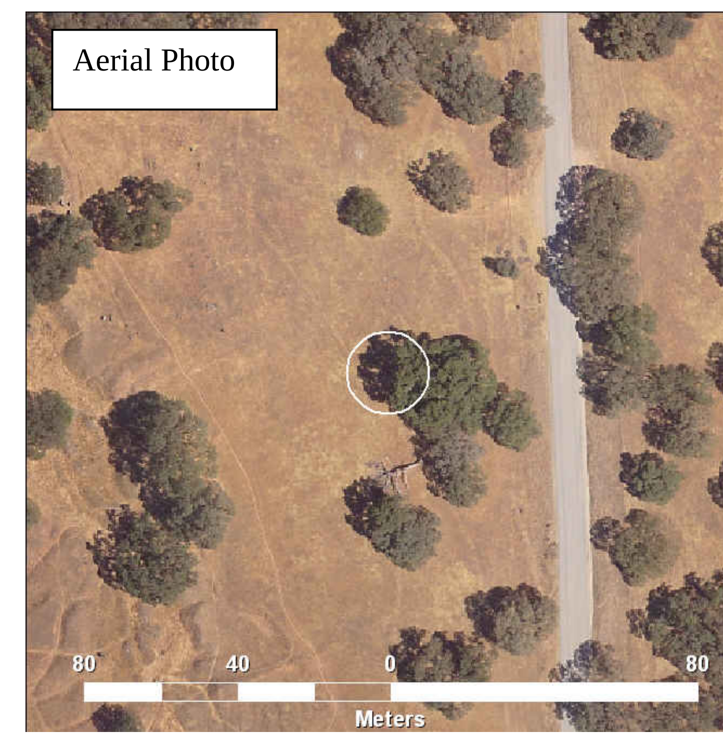

Plot # 17

Feature size: 3.1 m
Vegetation Density: 42.46 %
Lidar block reference number: 5823

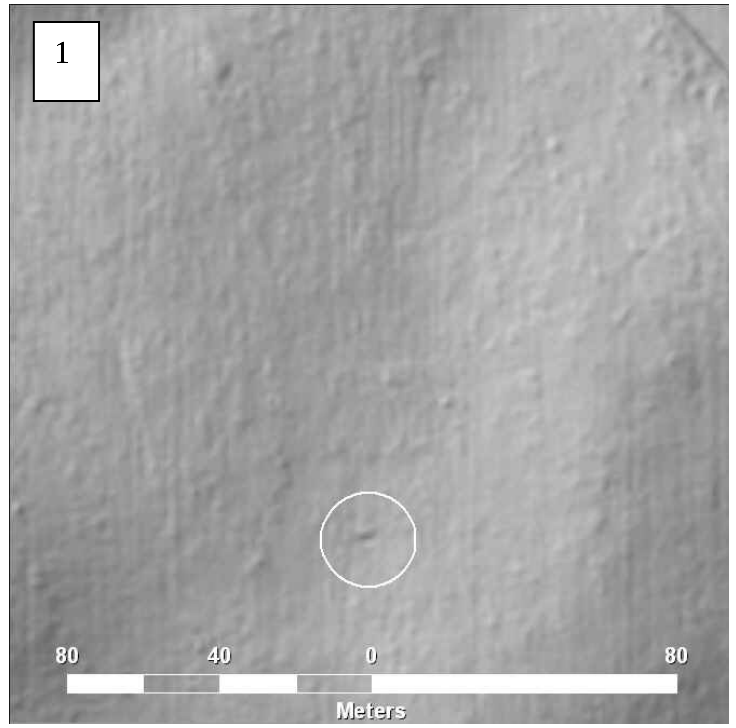

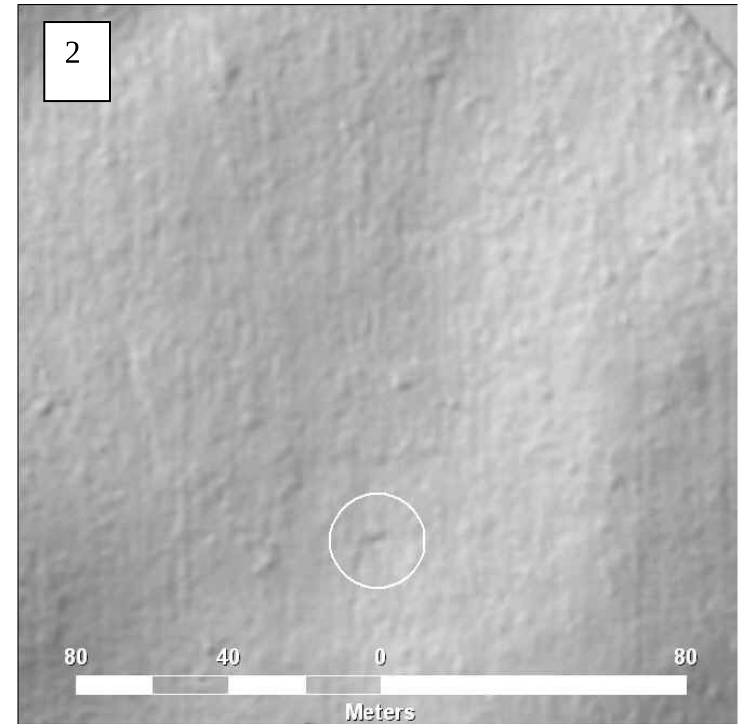

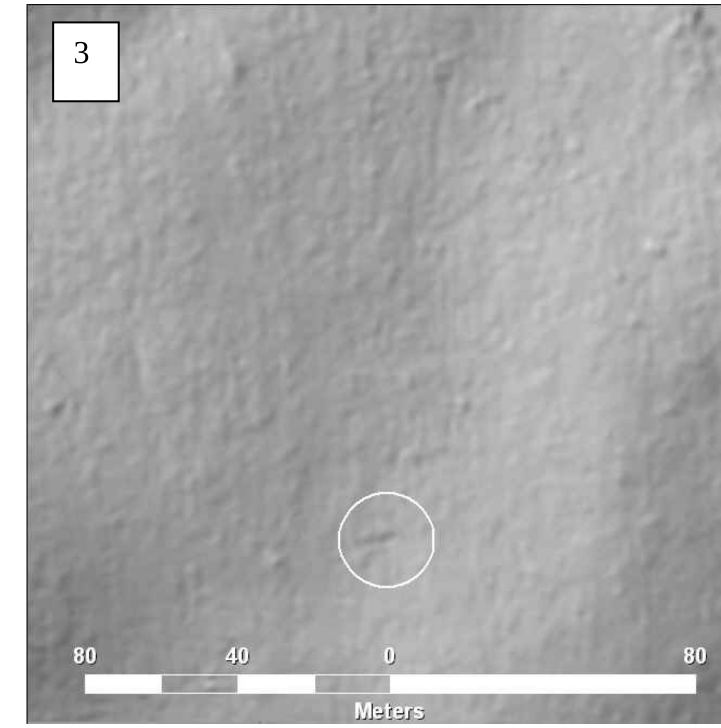

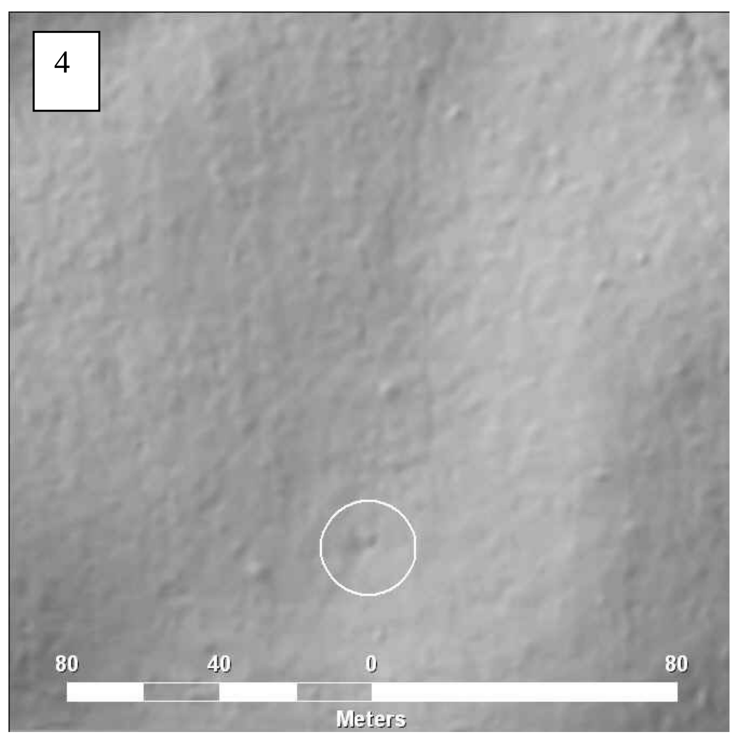

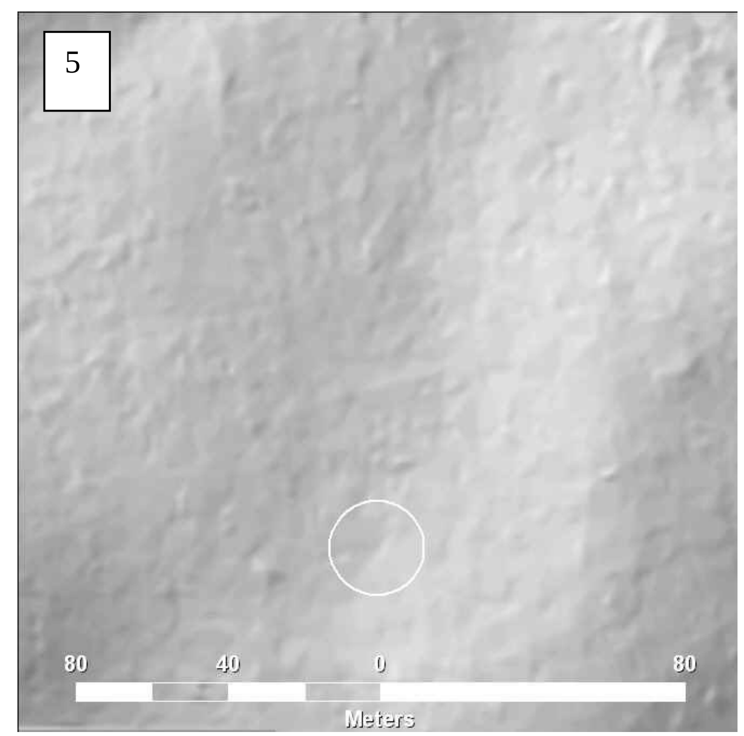

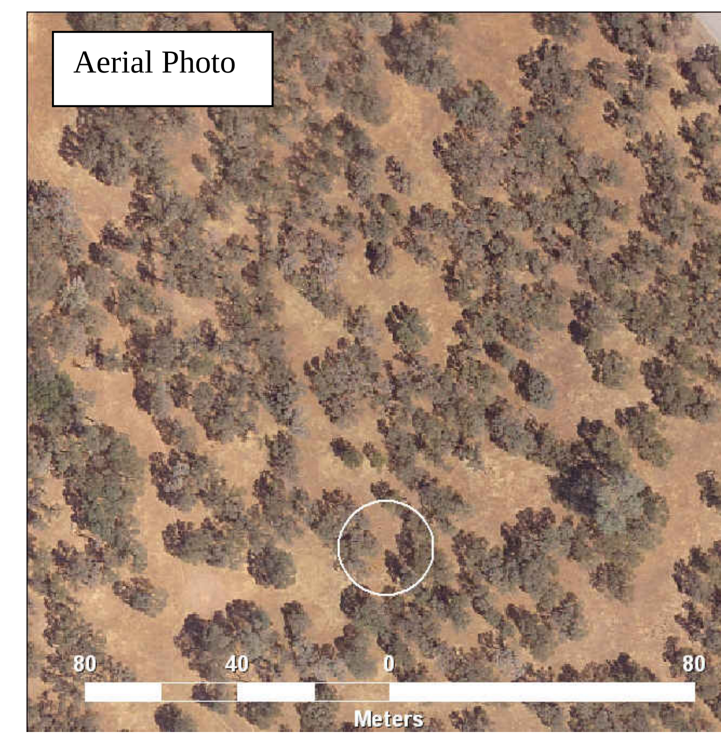

Plot # 18 Feature size: 3.1 m Vegetation Density: 33.72 % Lidar block reference number: 5718	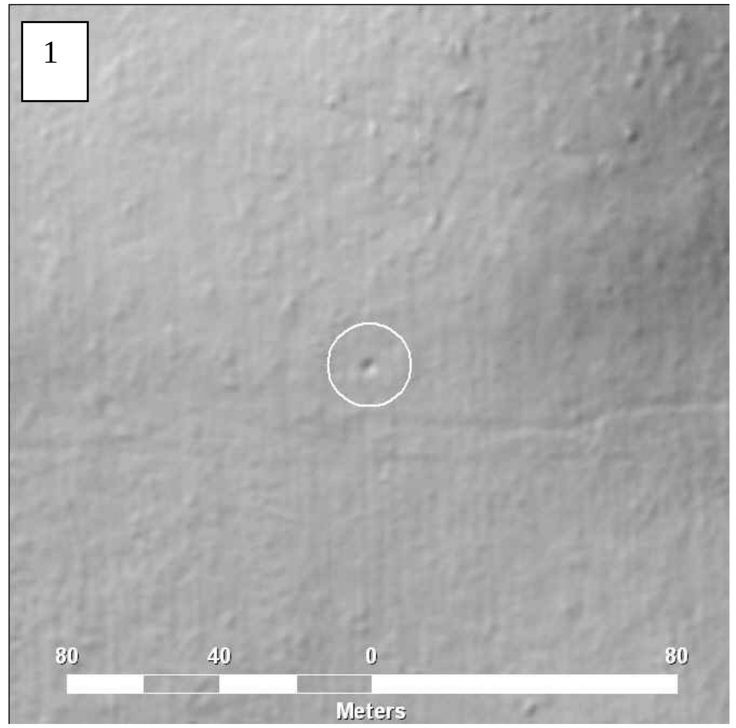	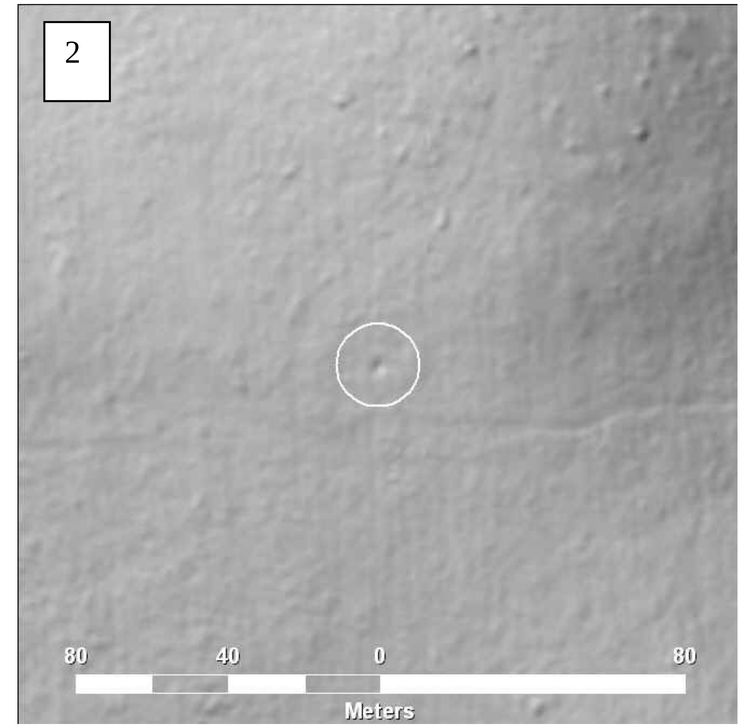	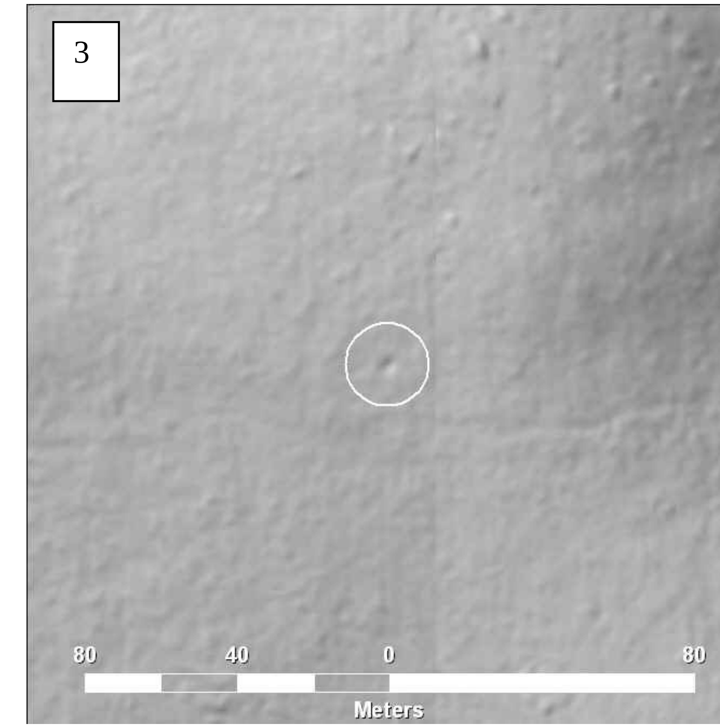
	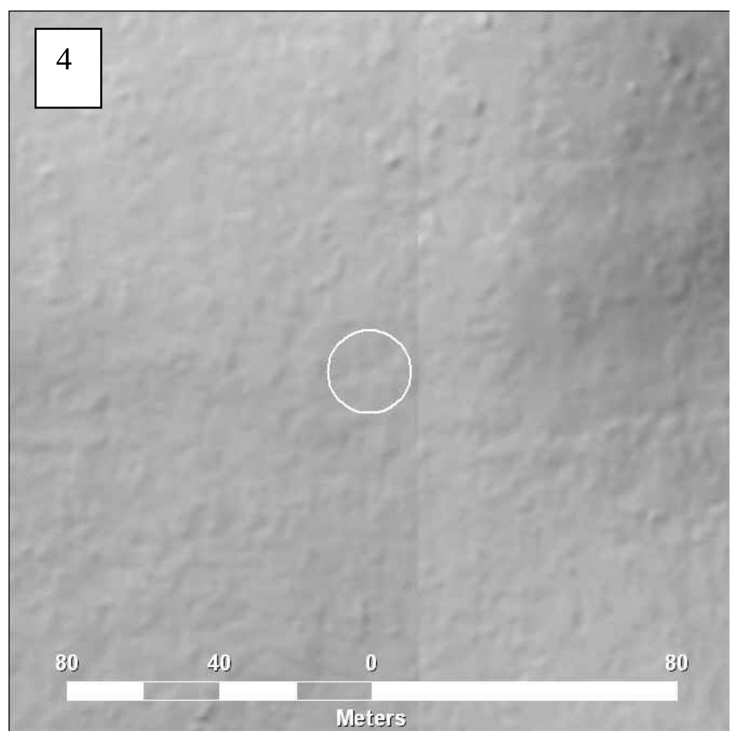	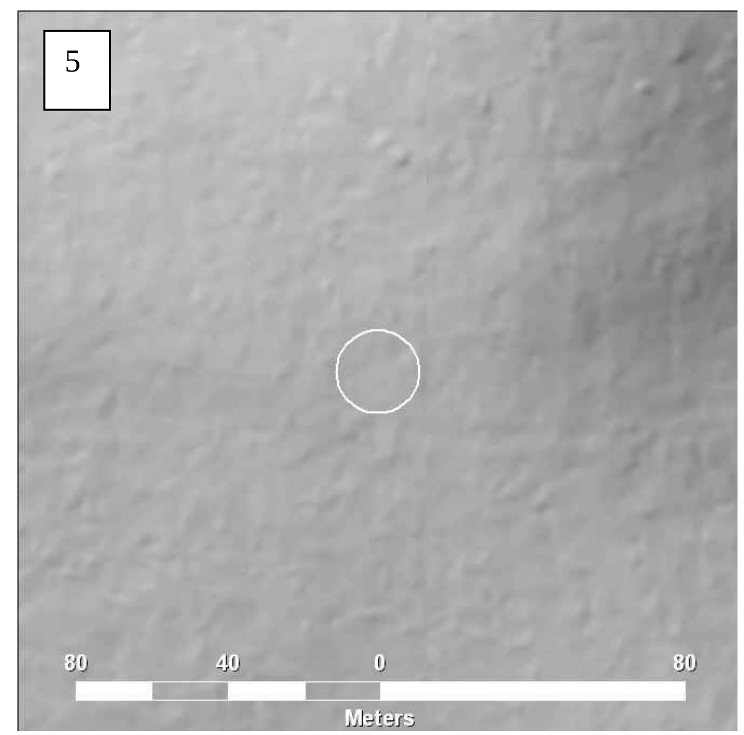	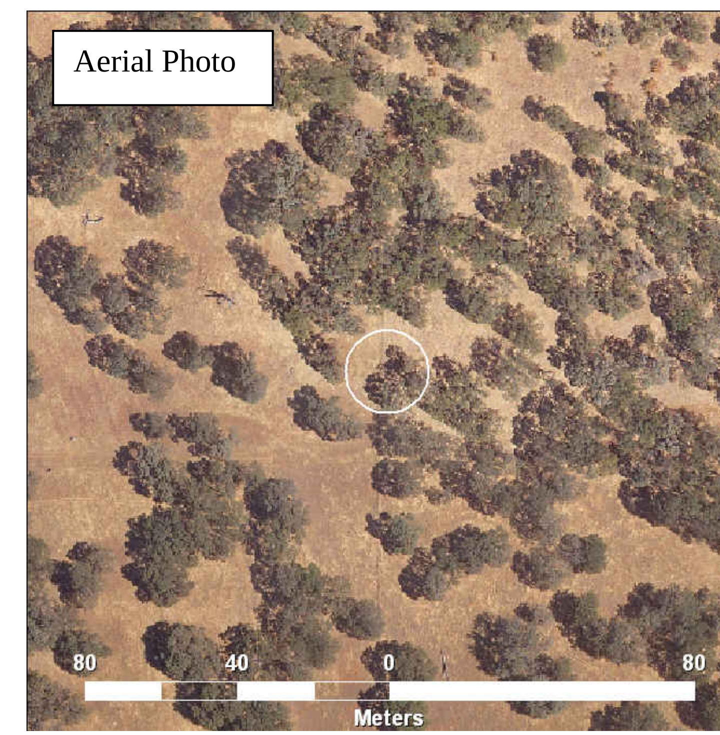

Plot # 19

Feature size: 3.1 m
Vegetation Density: 34.95 %
Lidar block reference number: 5461

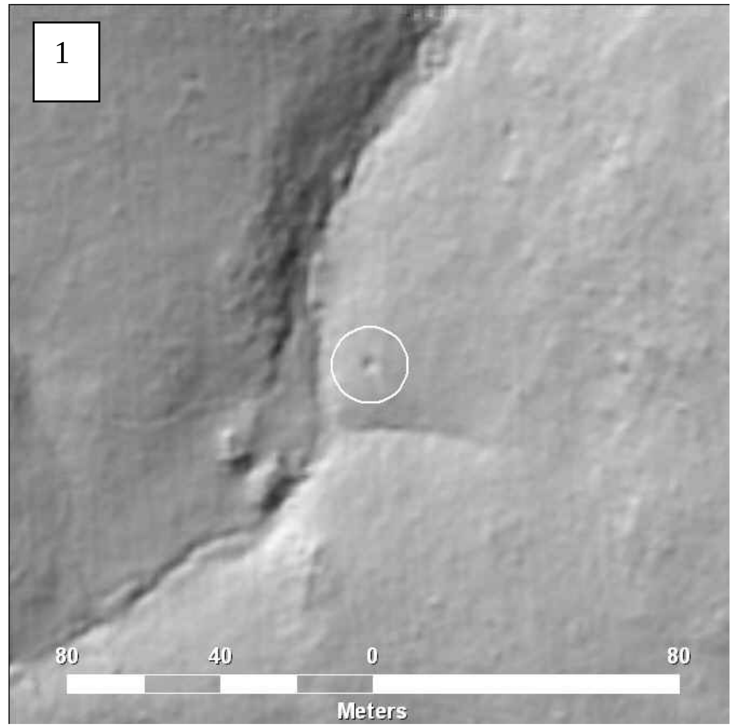

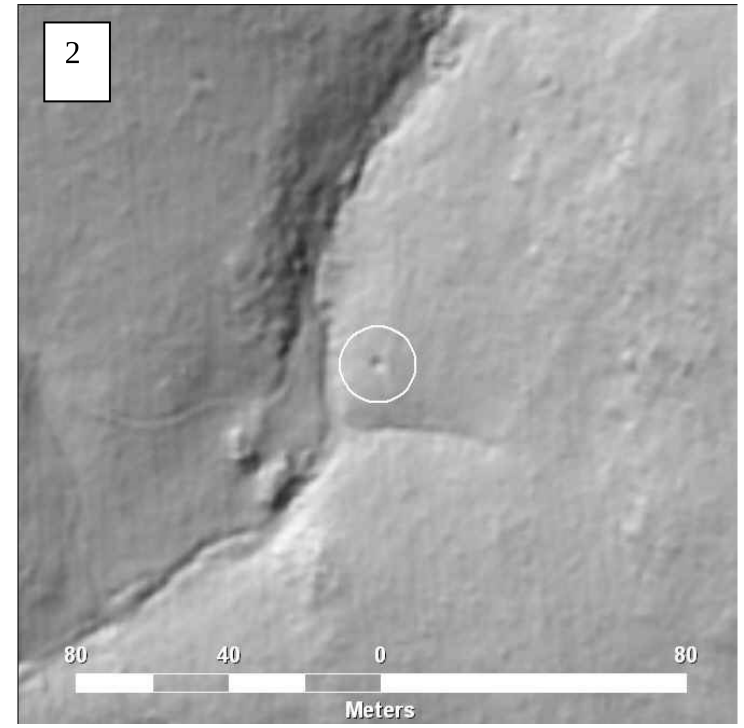

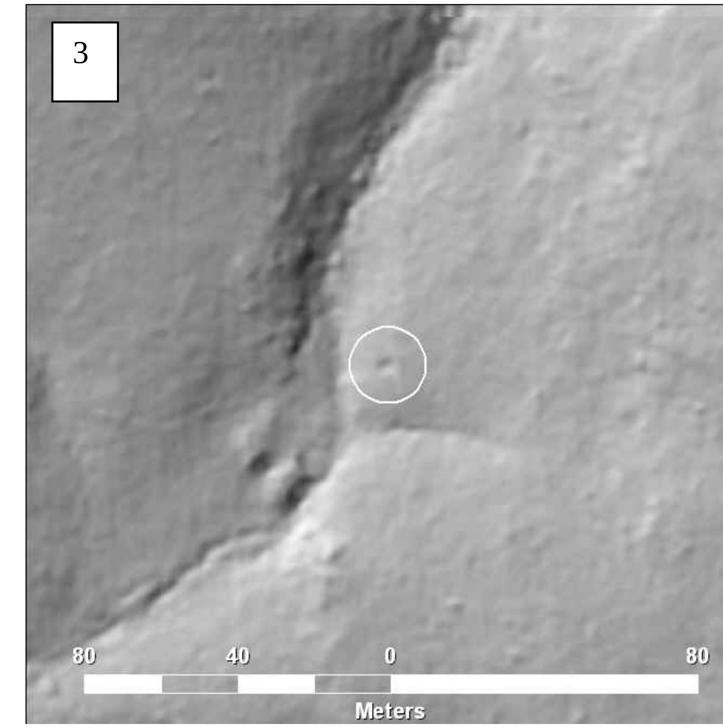

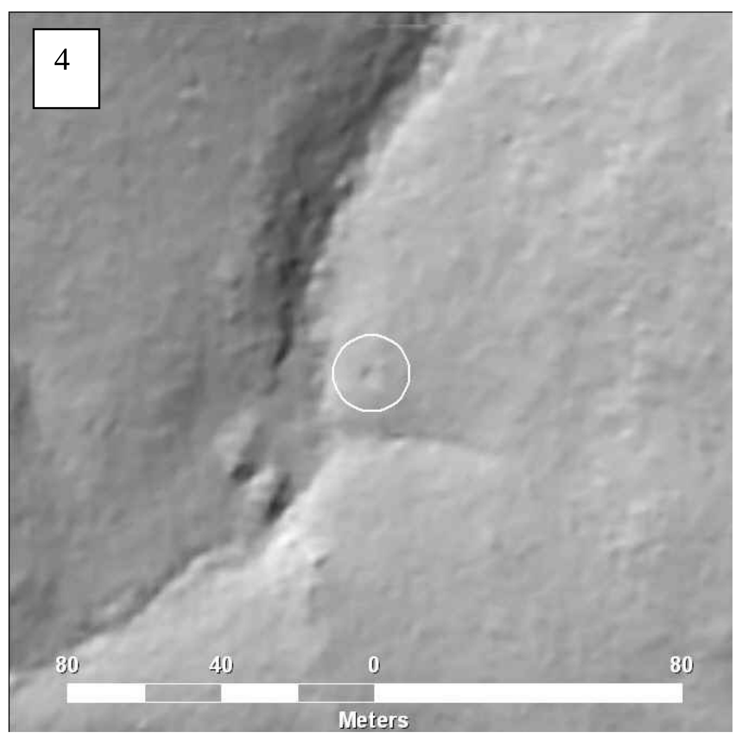

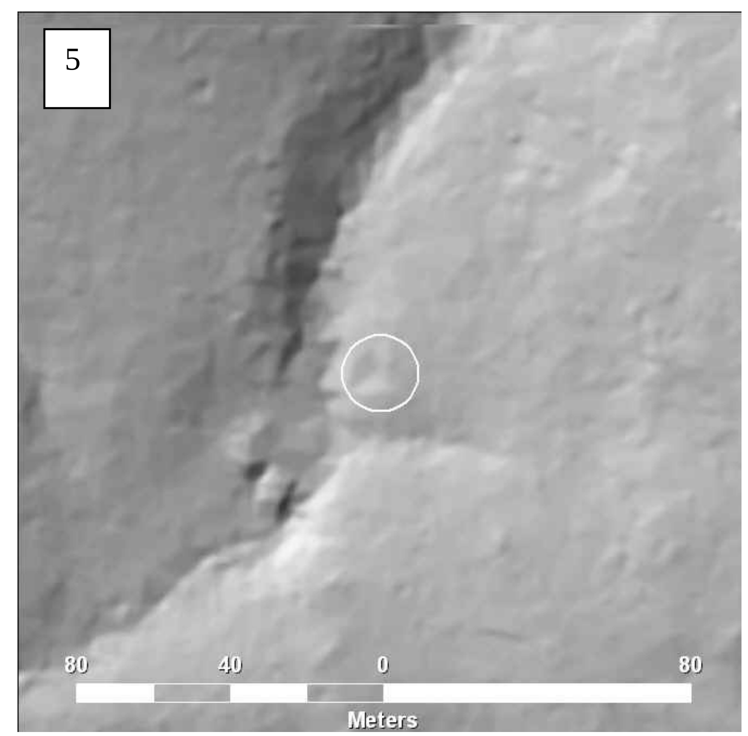

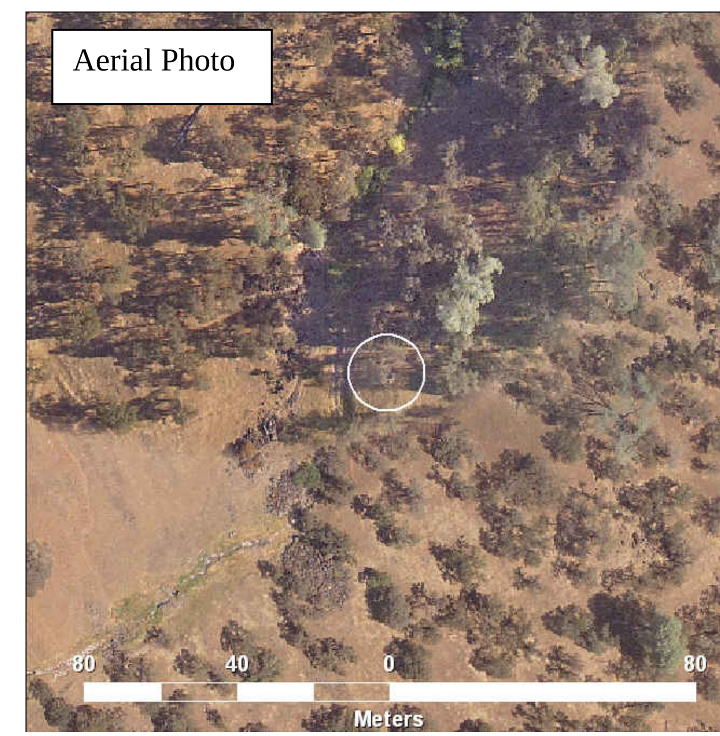

Plot # 20

Feature size: 3.25 m
Vegetation Density: 28.67 %
Lidar block reference number: 5924

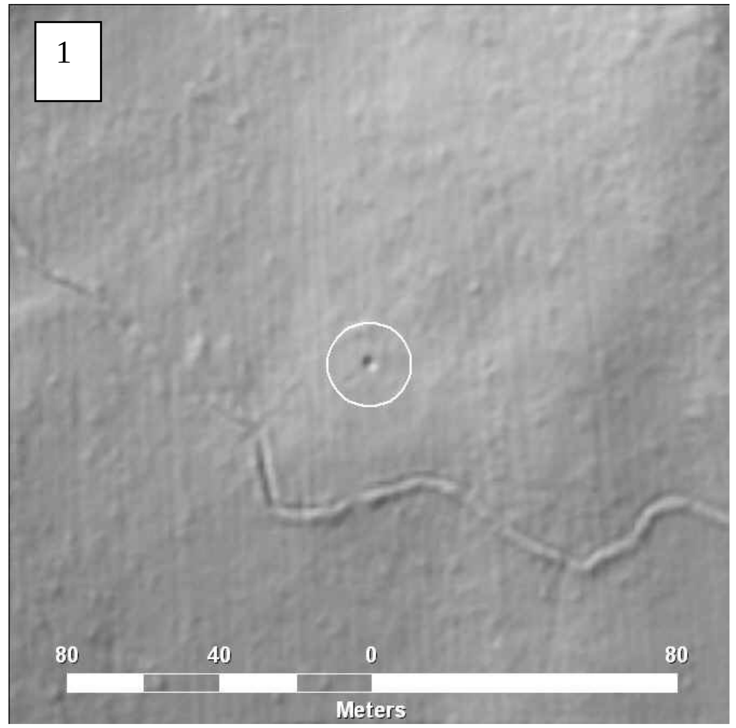

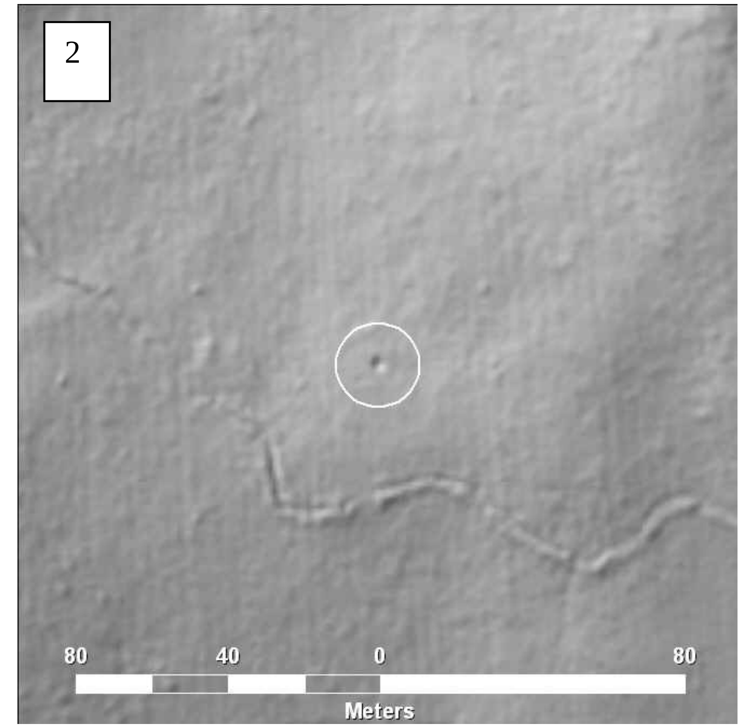

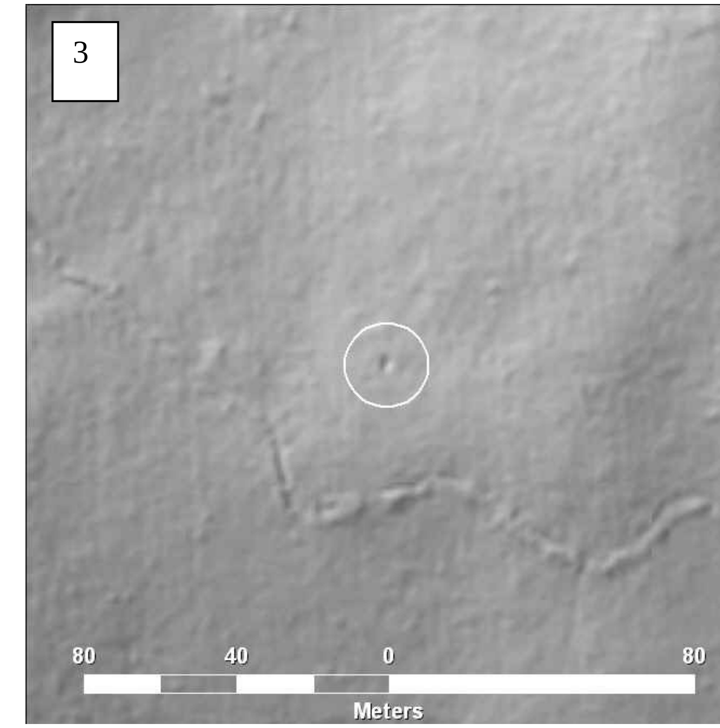

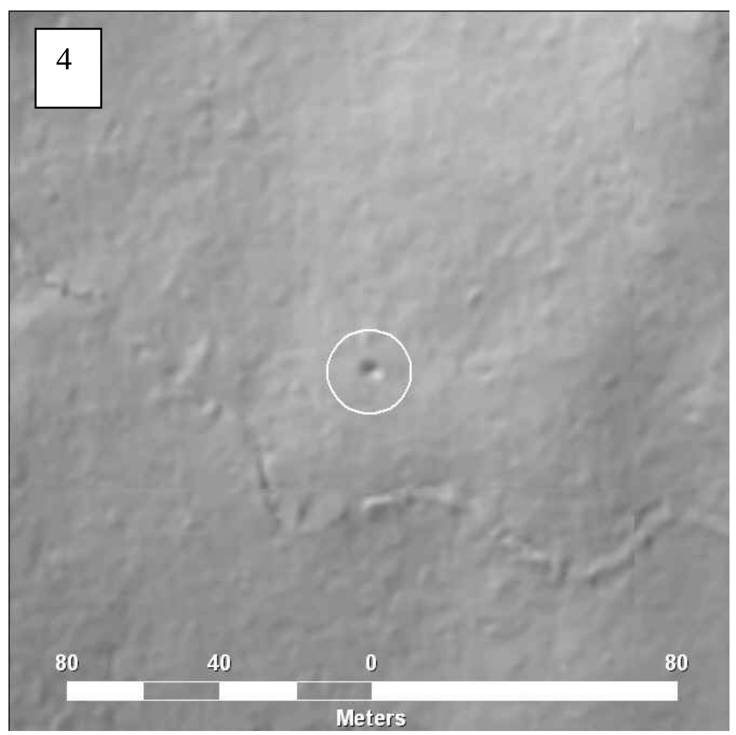

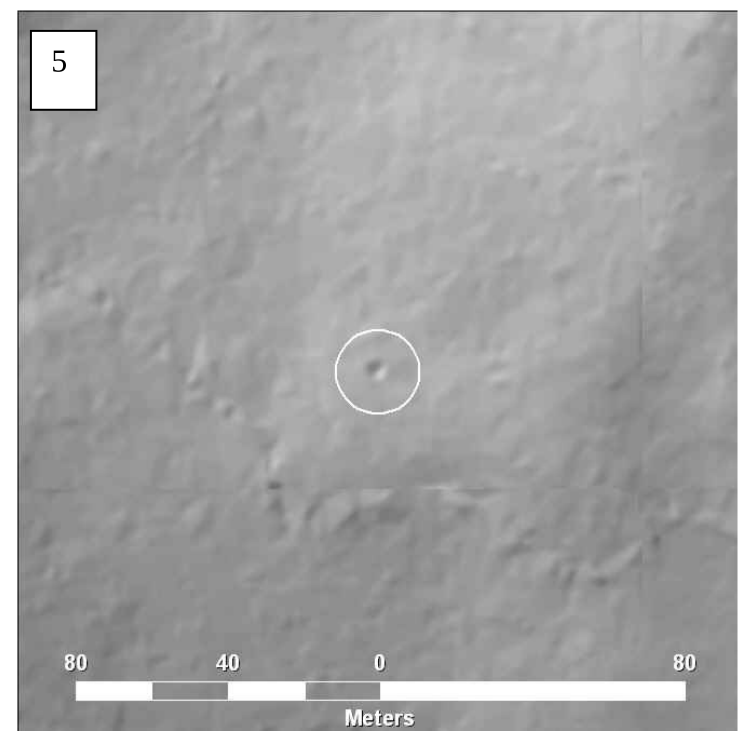

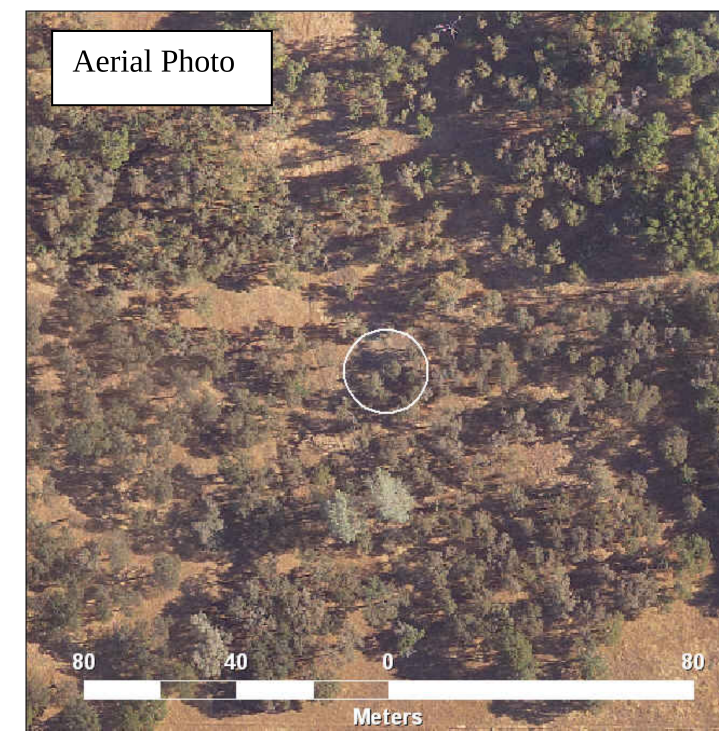

Plot # 21

Feature size: 3.25 m
Vegetation Density: 42.06 %
Lidar block reference number: 4089

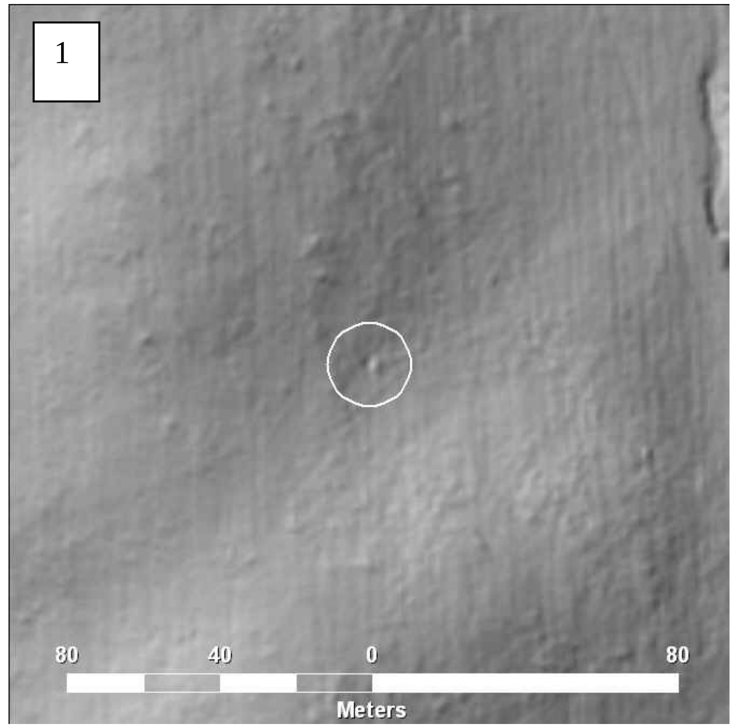

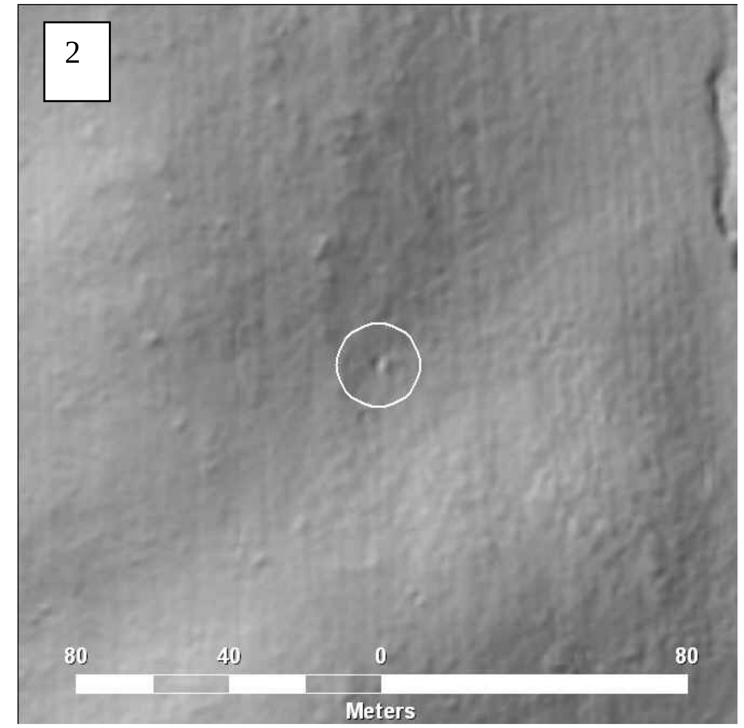

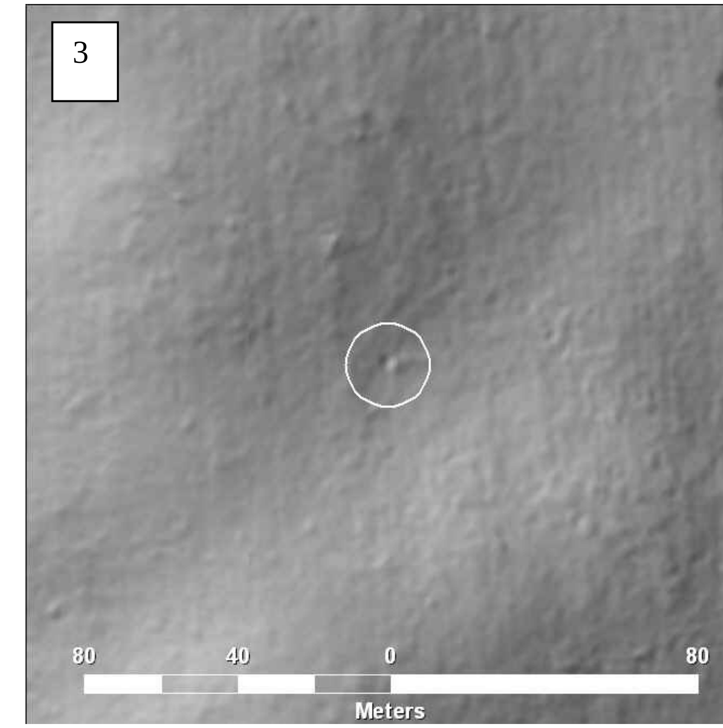

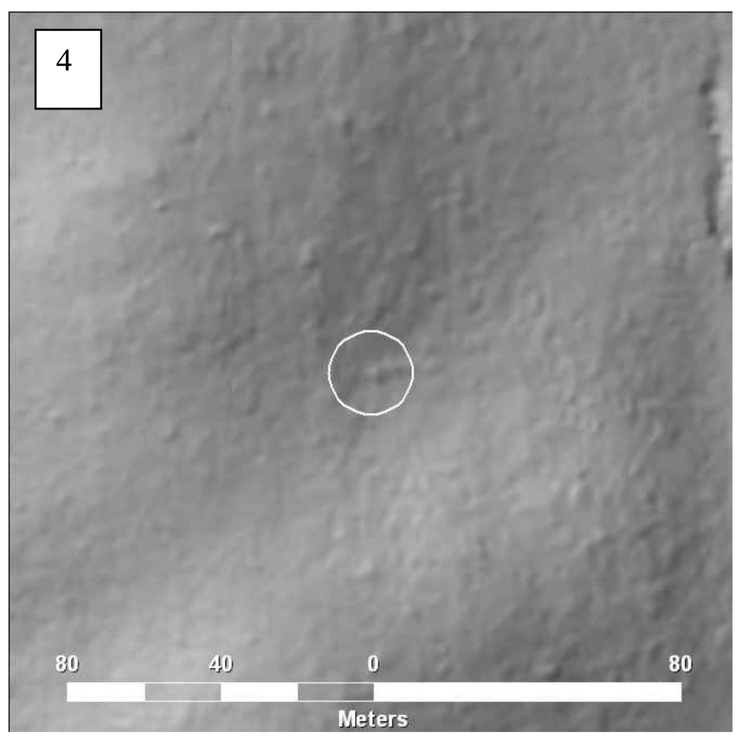

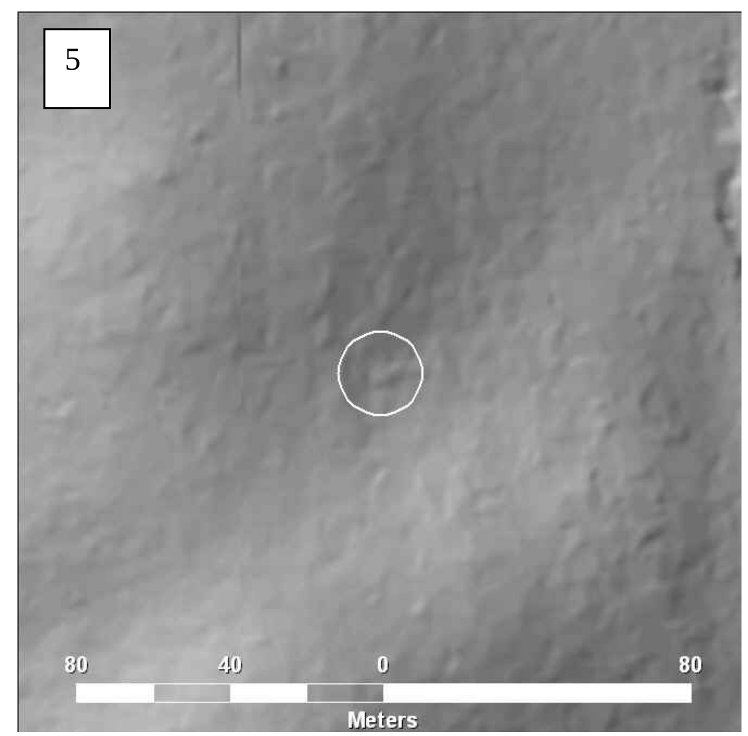

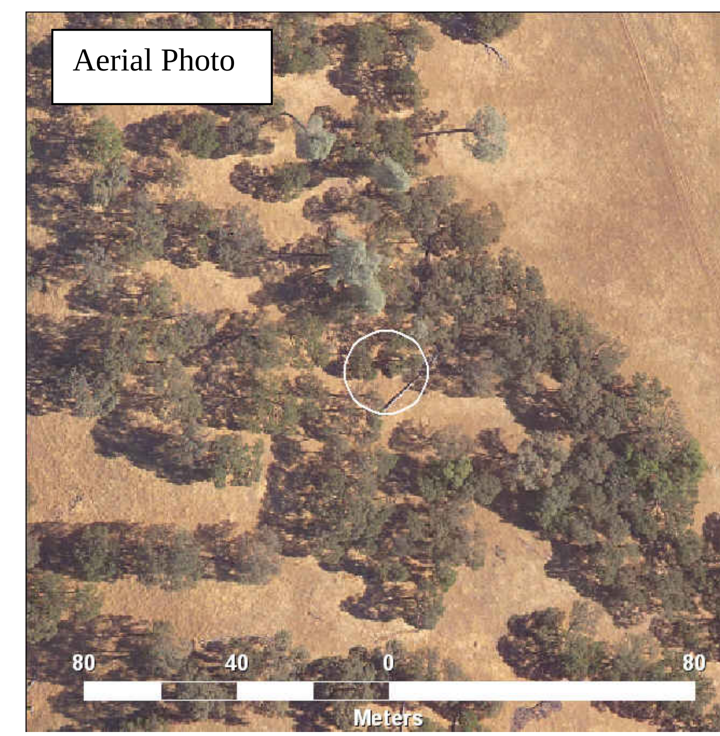

Plot # 22			
Plot # 22 Feature size: 3.5 m Vegetation Density: 57.7 % Lidar block reference number: 5738	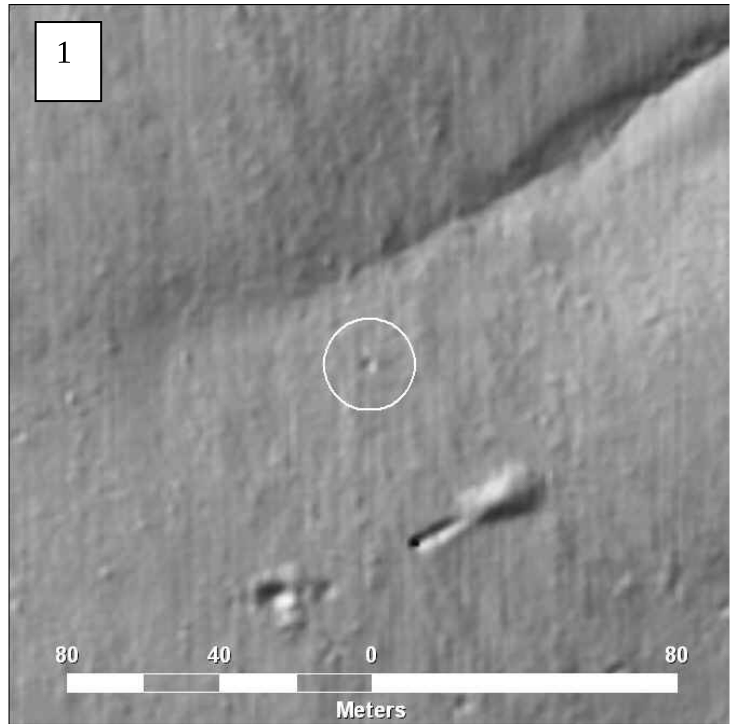	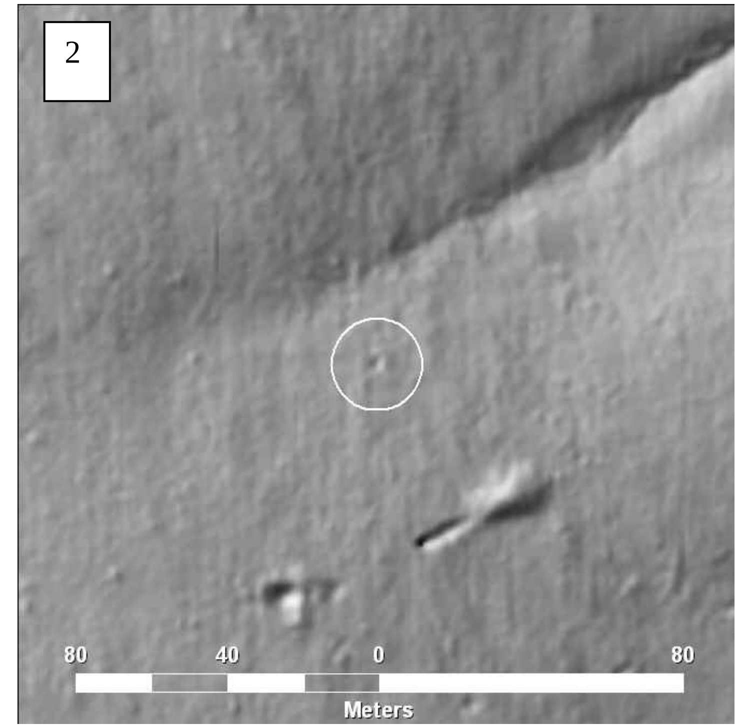	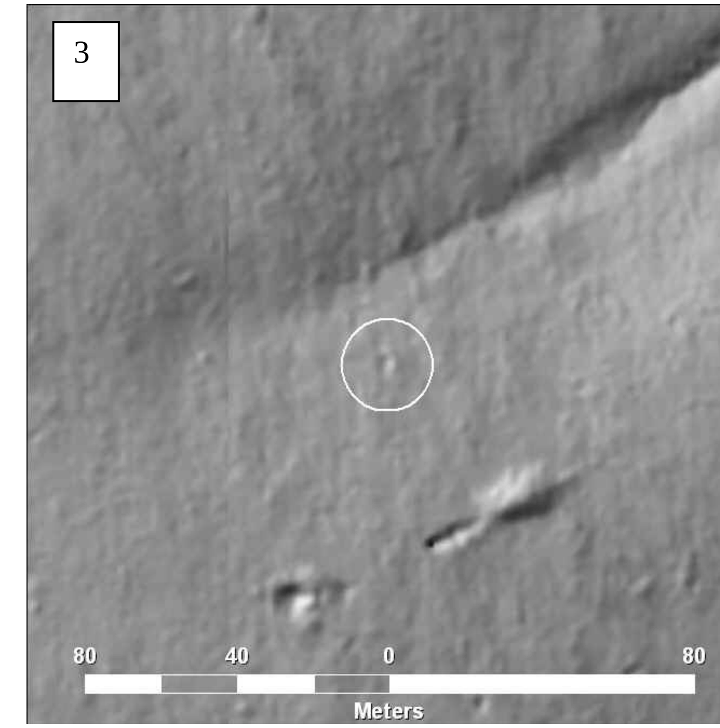
	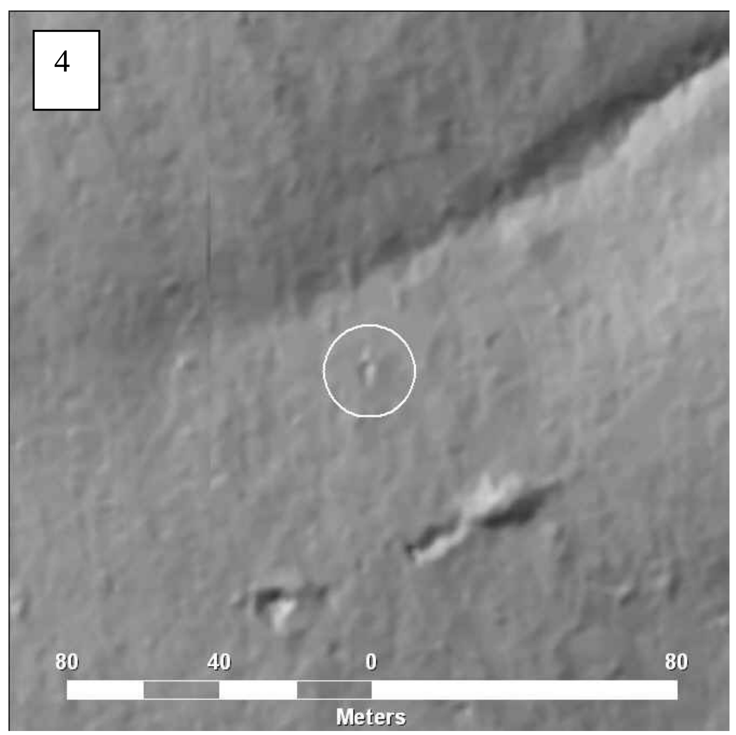	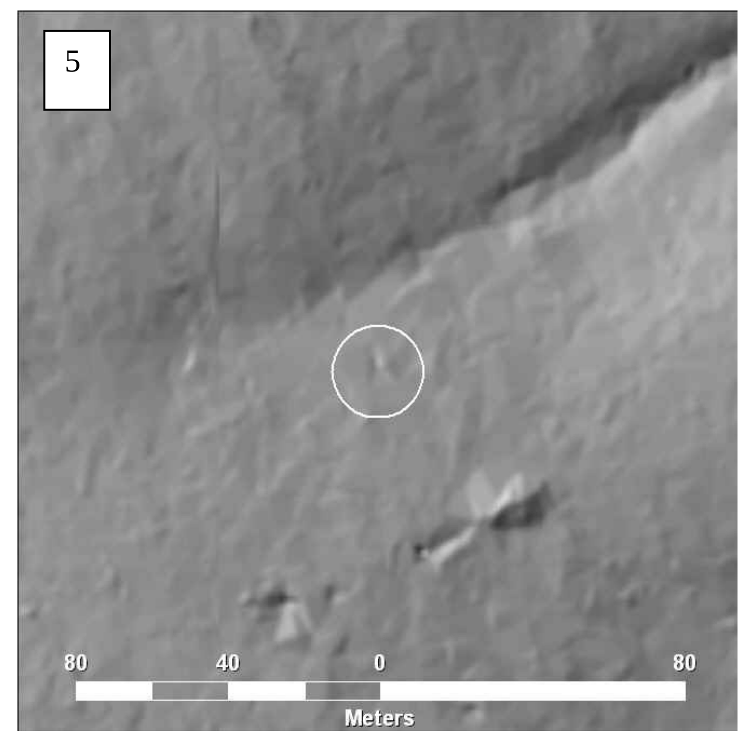	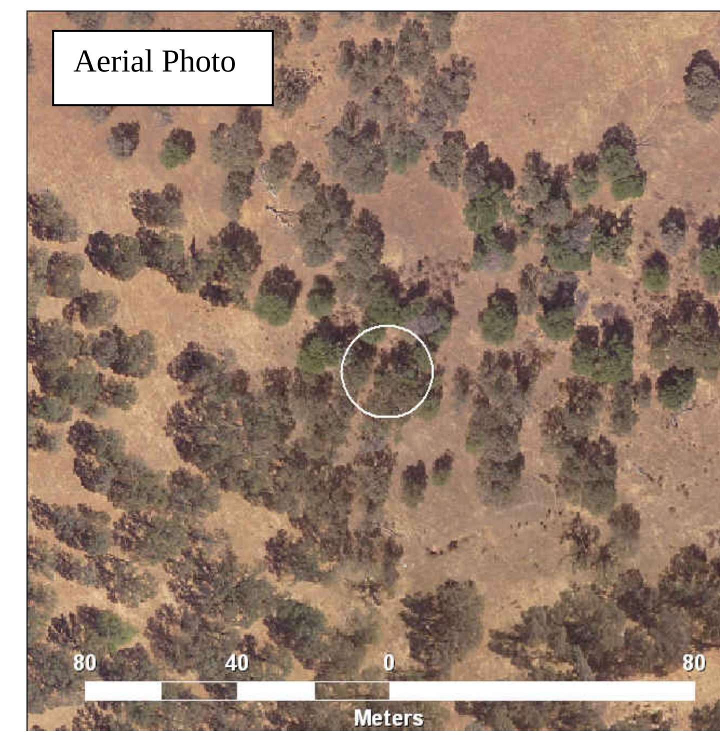

Plot # 23

Feature size: 3.7 m
Vegetation Density: 45.43 %
Lidar block reference number: 5512

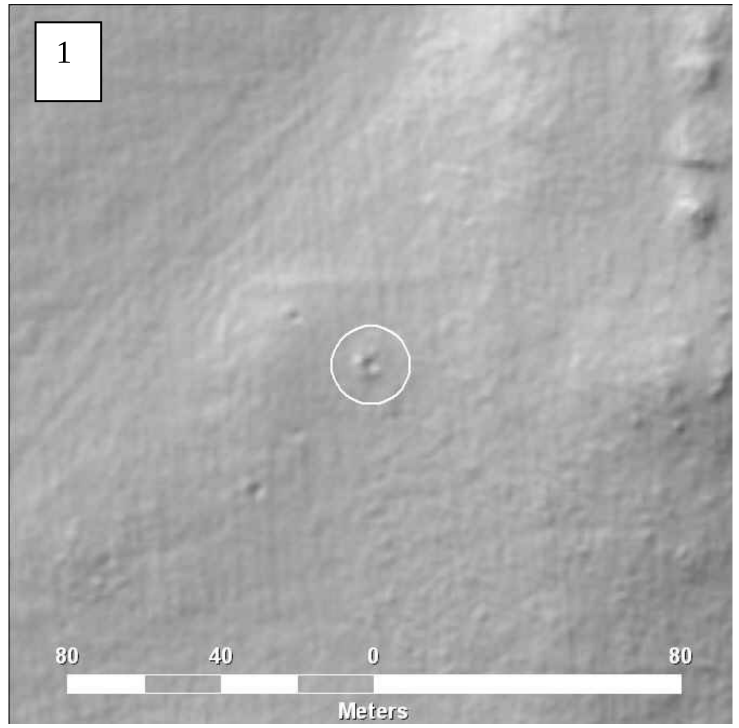

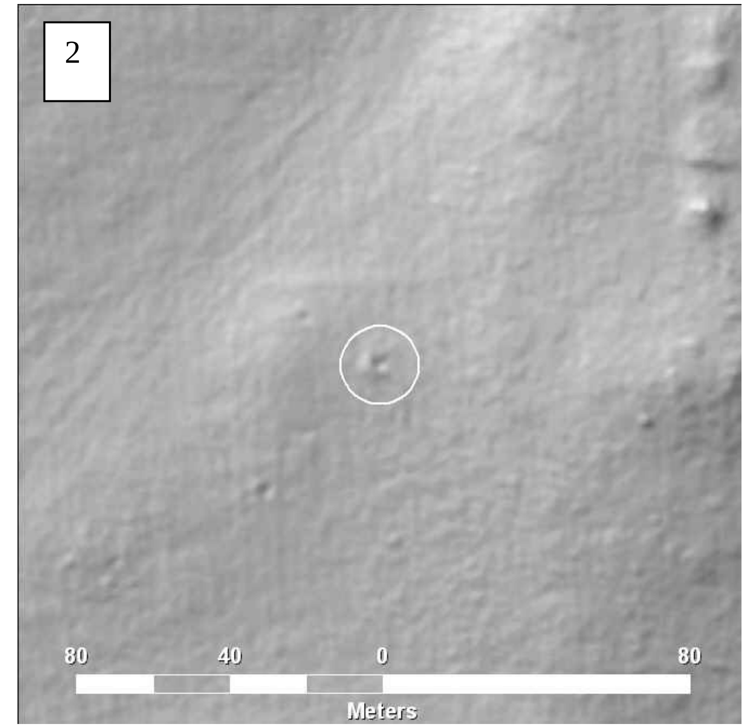

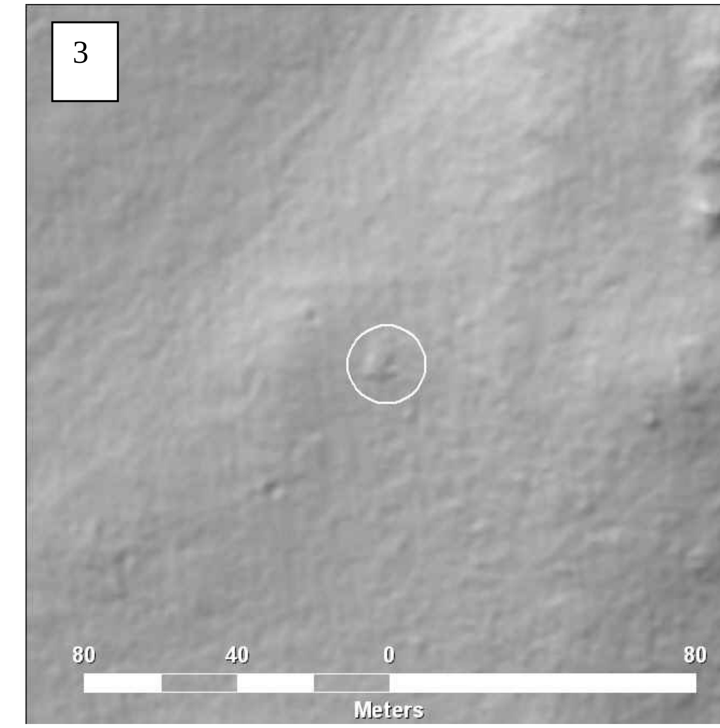

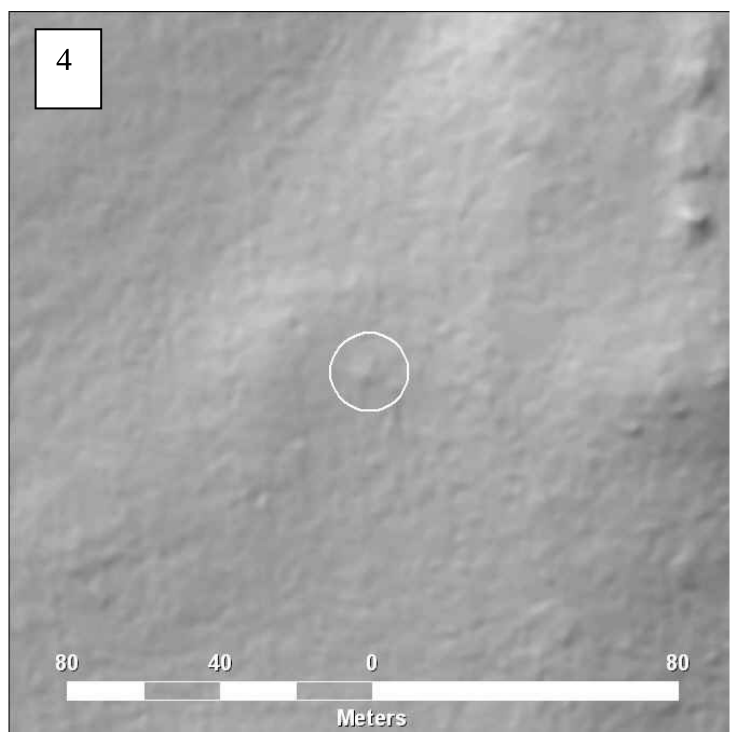

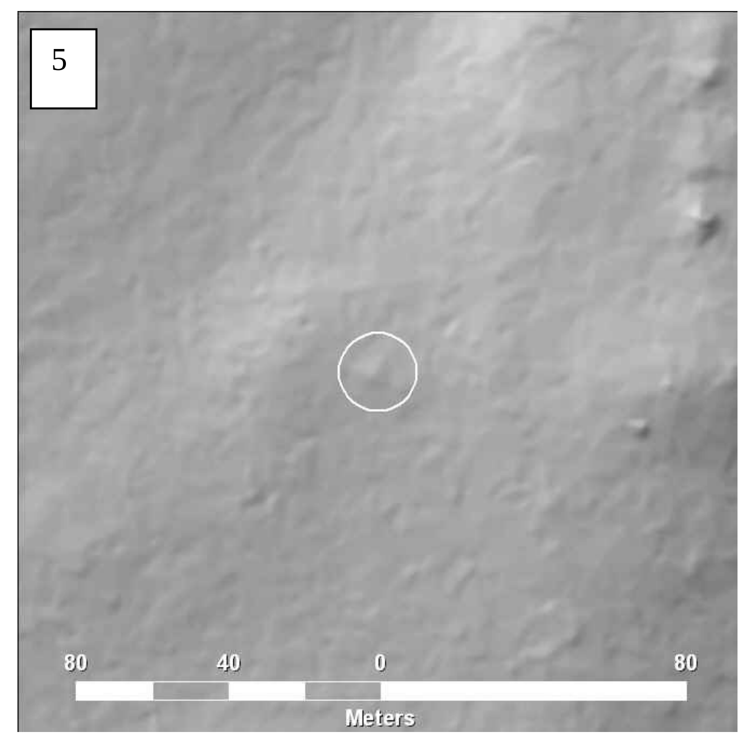

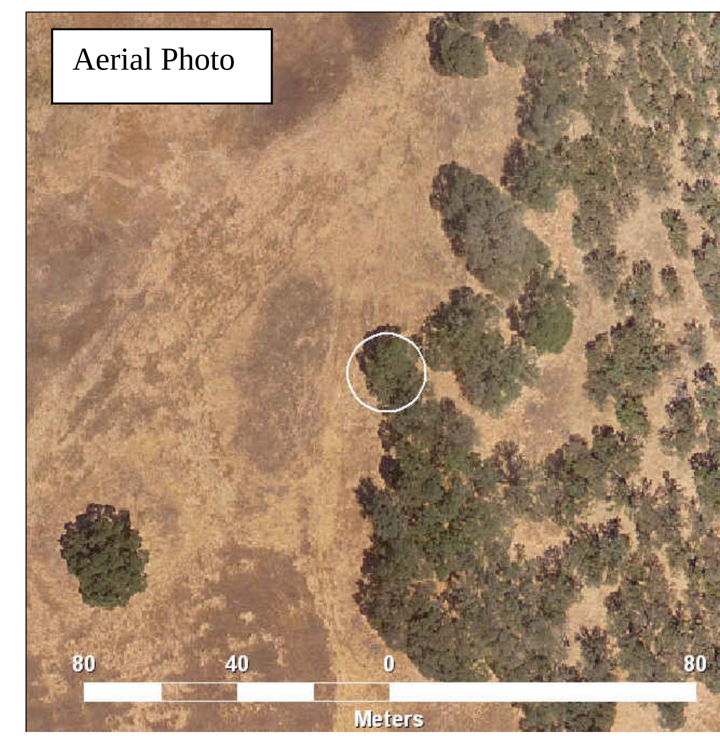

Plot # 24

Feature size: 3.8 m
Vegetation Density: 48.33 %
Lidar block reference number: 5463

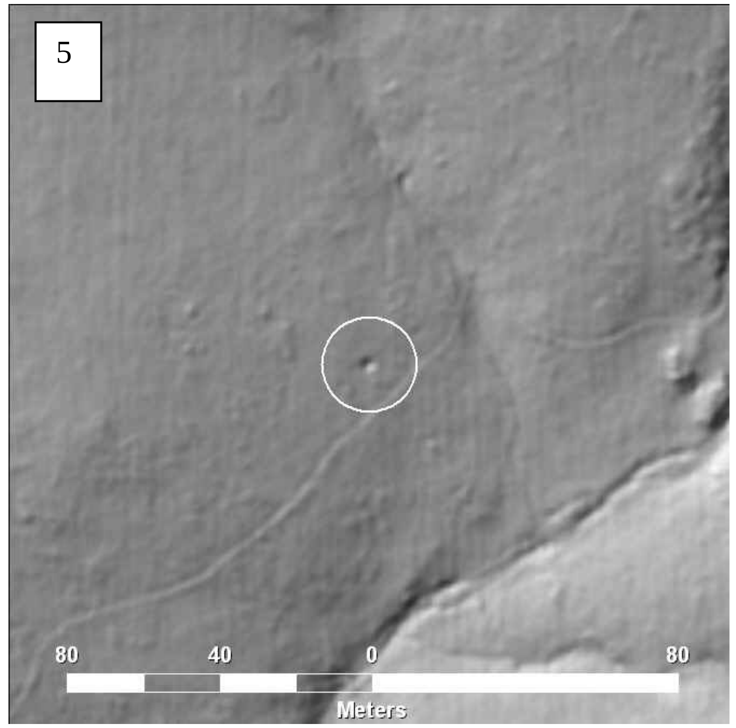

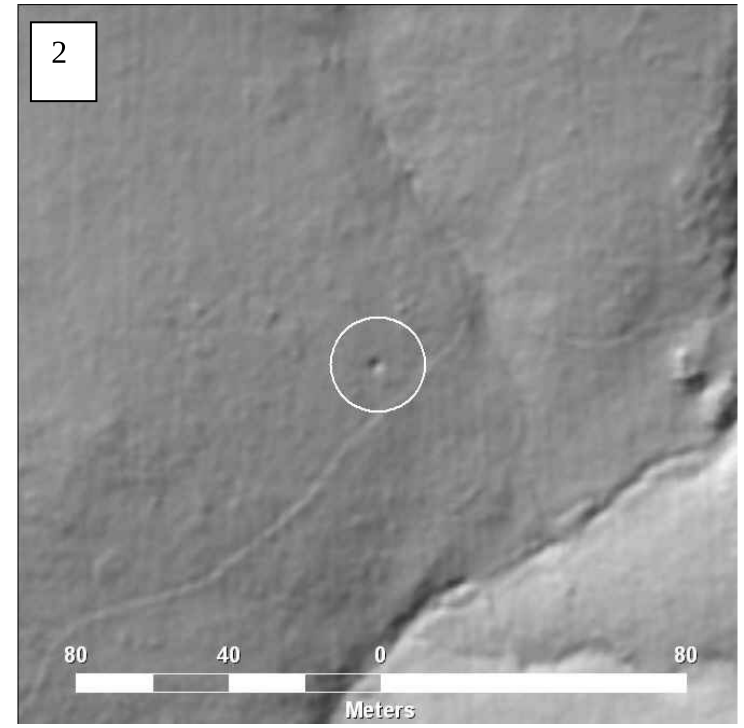

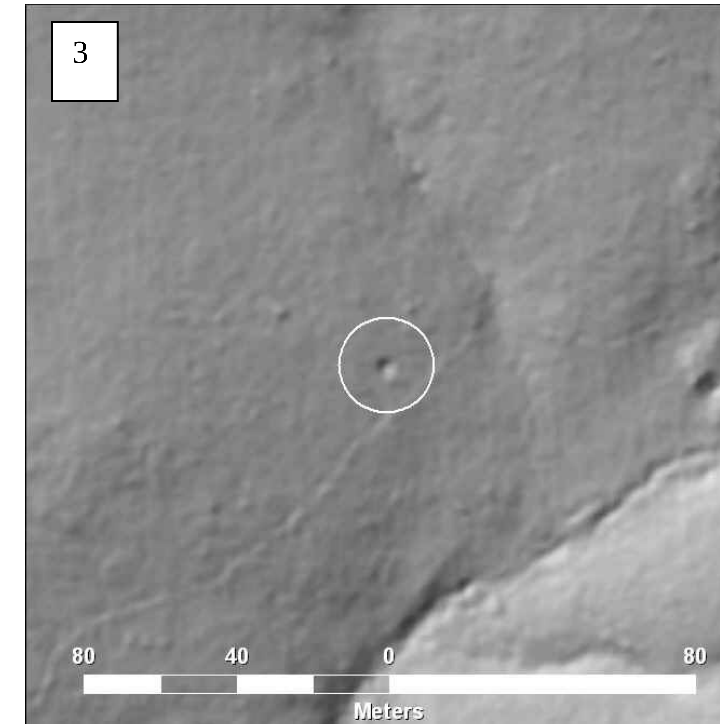

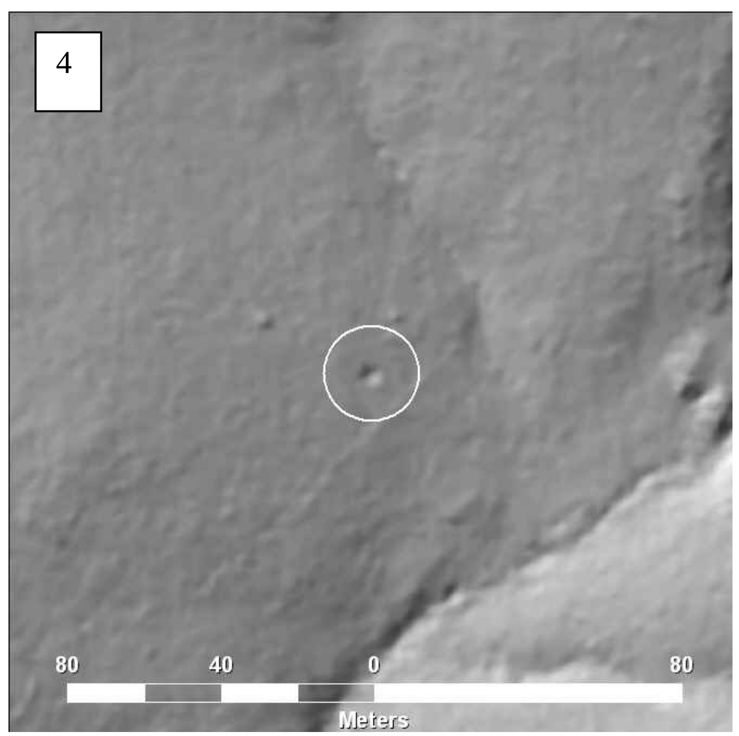

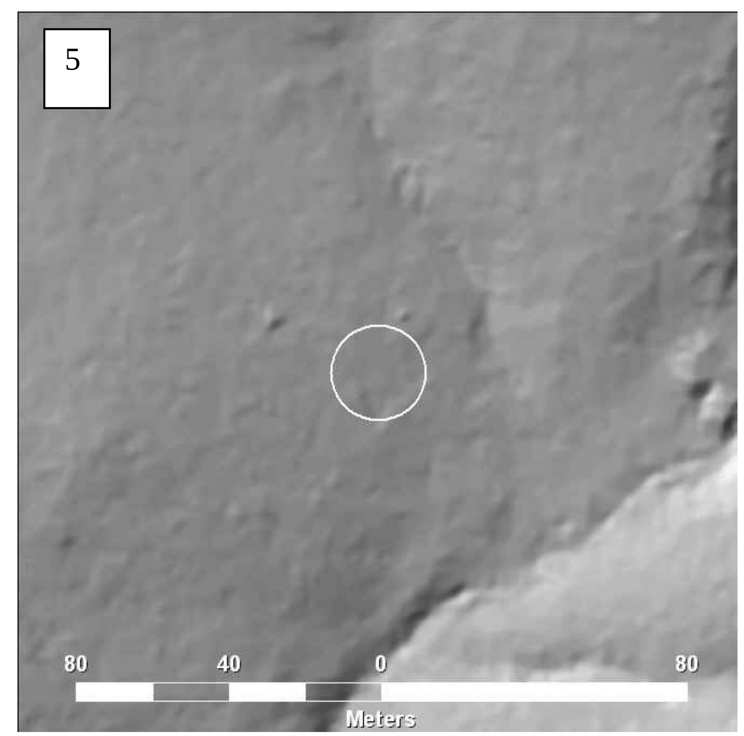

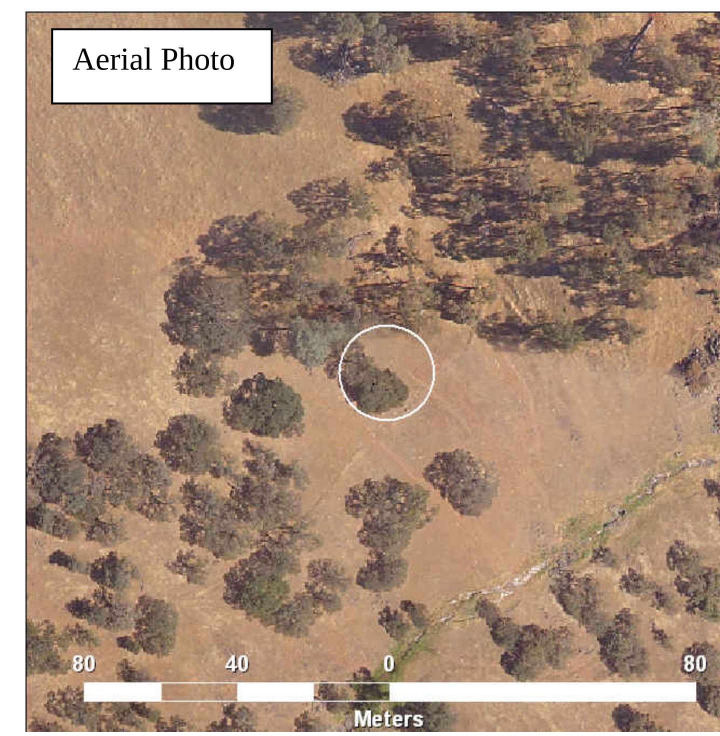

Plot # 25

Feature size: 3.8 m wide
23.25 m long
Vegetation Density: 61.5 %
Lidar block reference number: 5719

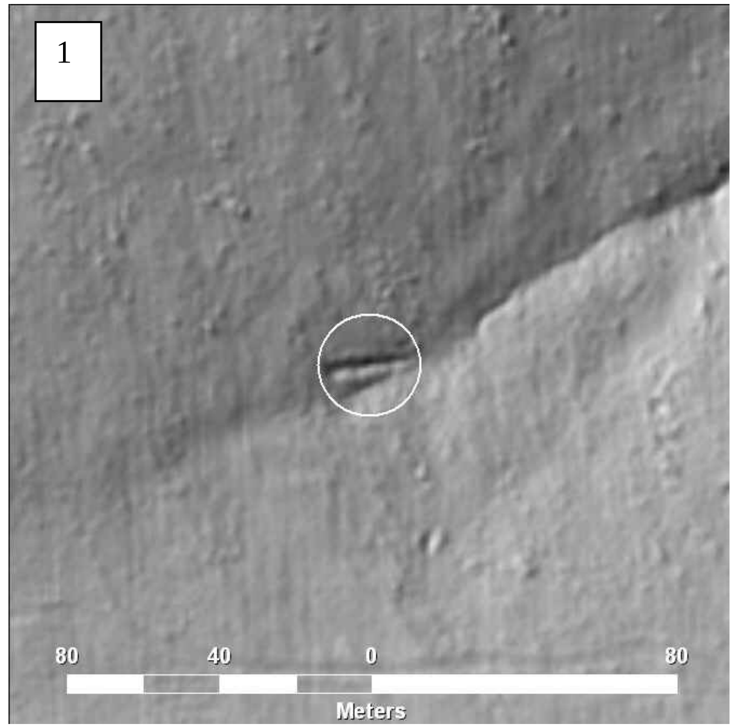

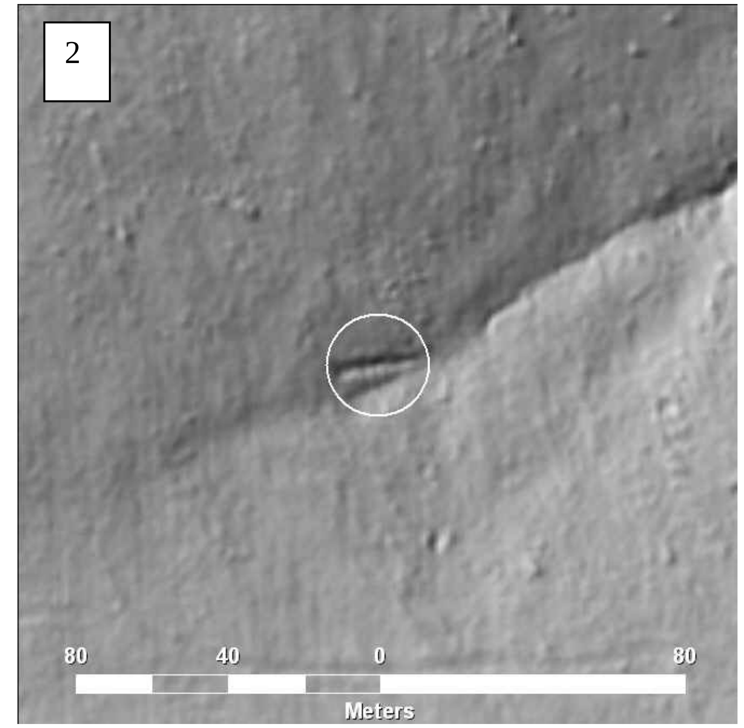

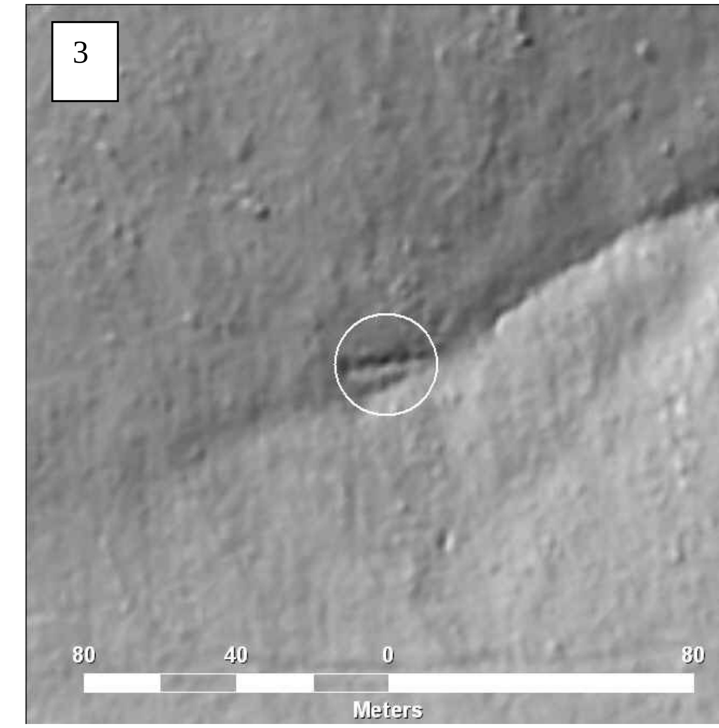

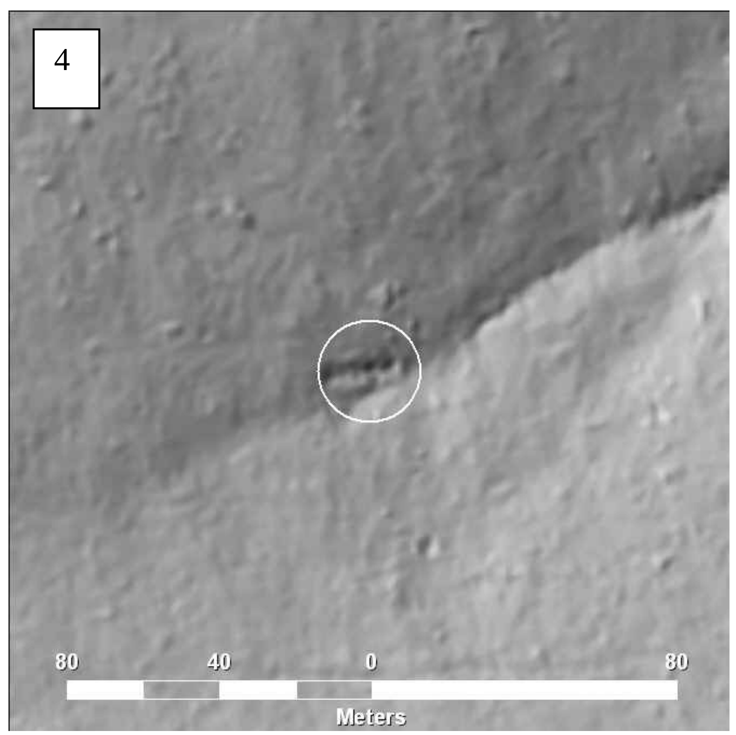

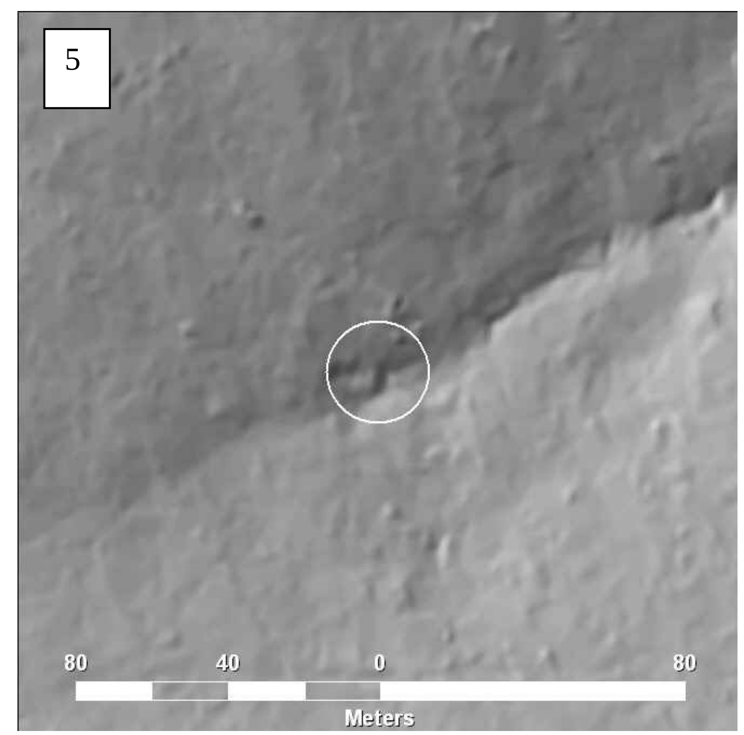

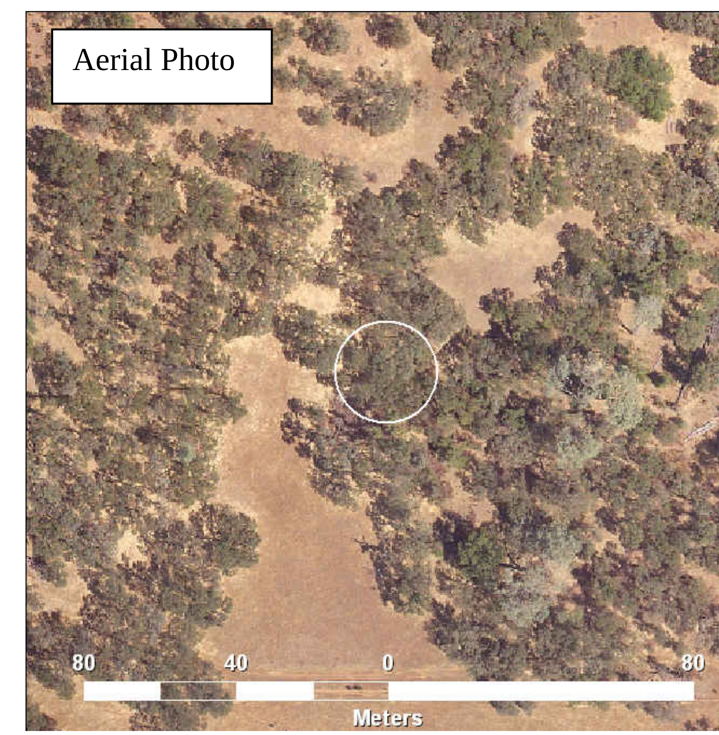

Plot # 26

Feature size: 3.9 m
Vegetation Density: 38.58 %
Lidar block reference number: 5465

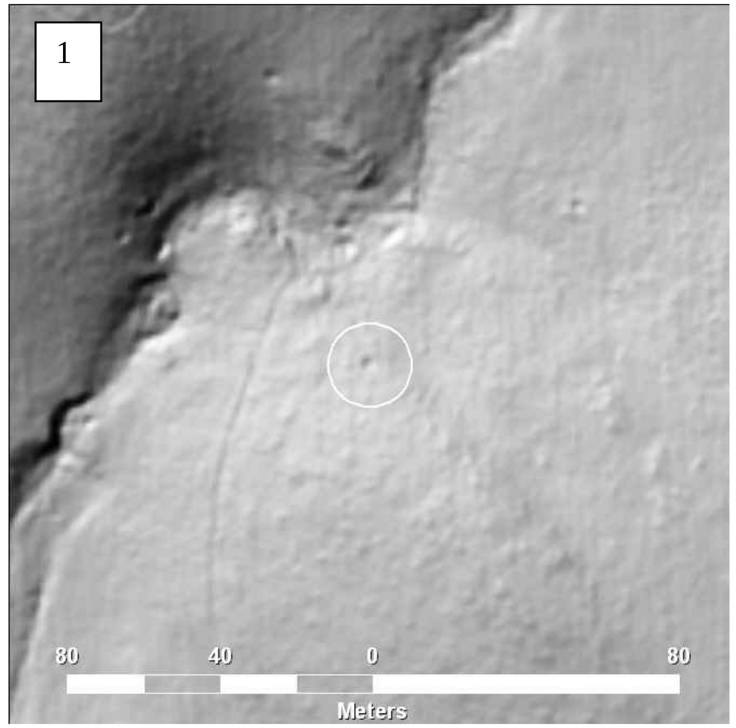

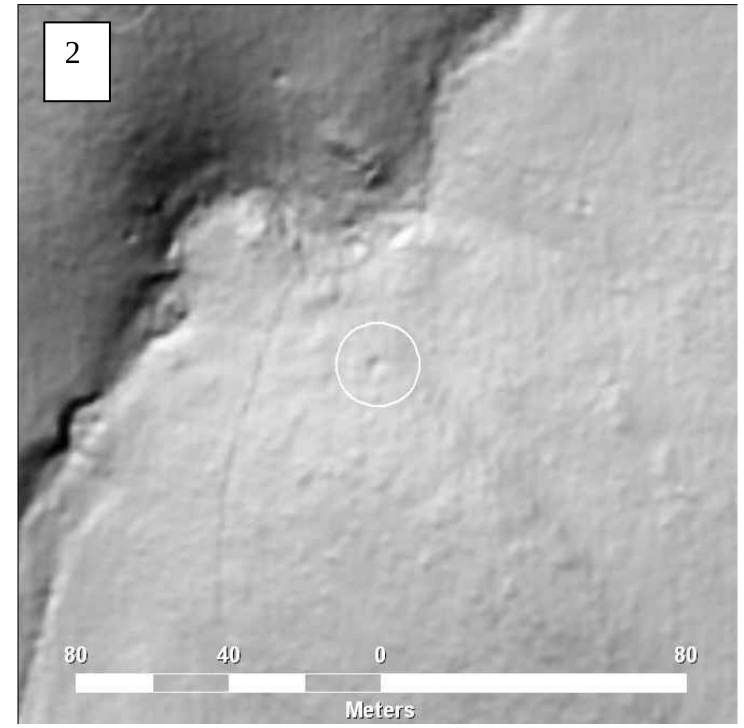

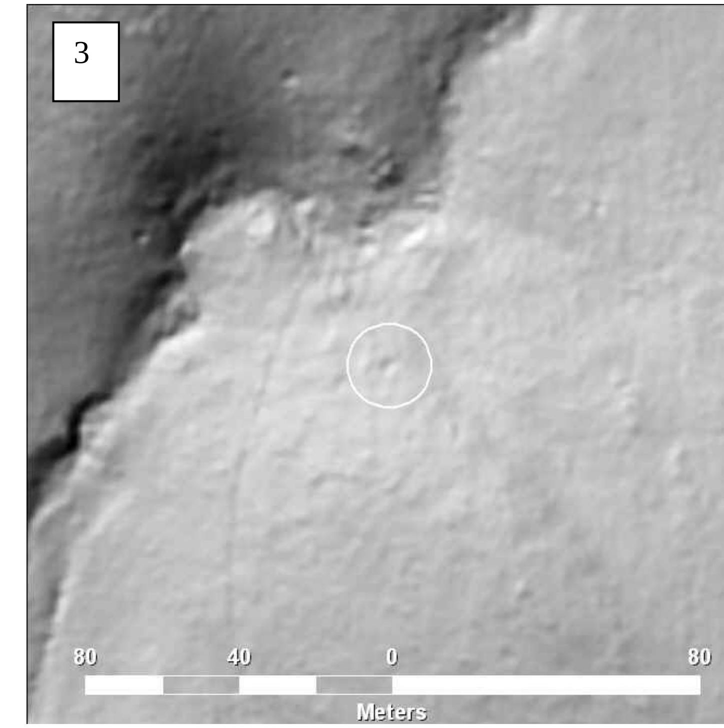

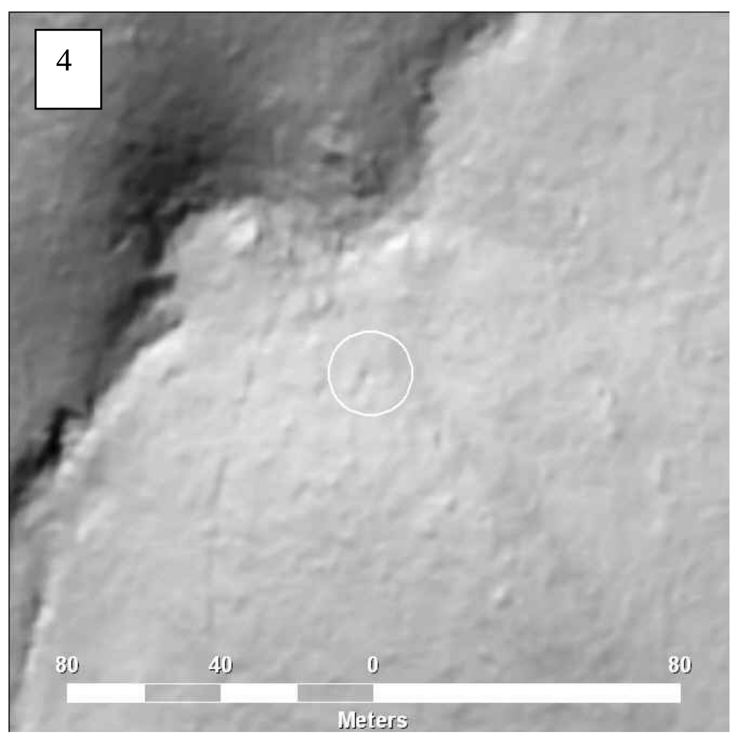

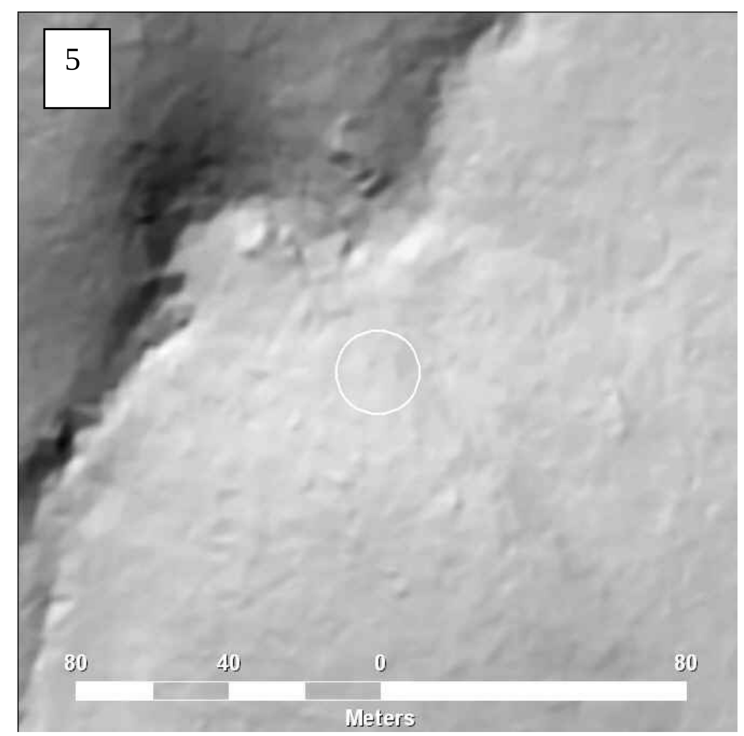

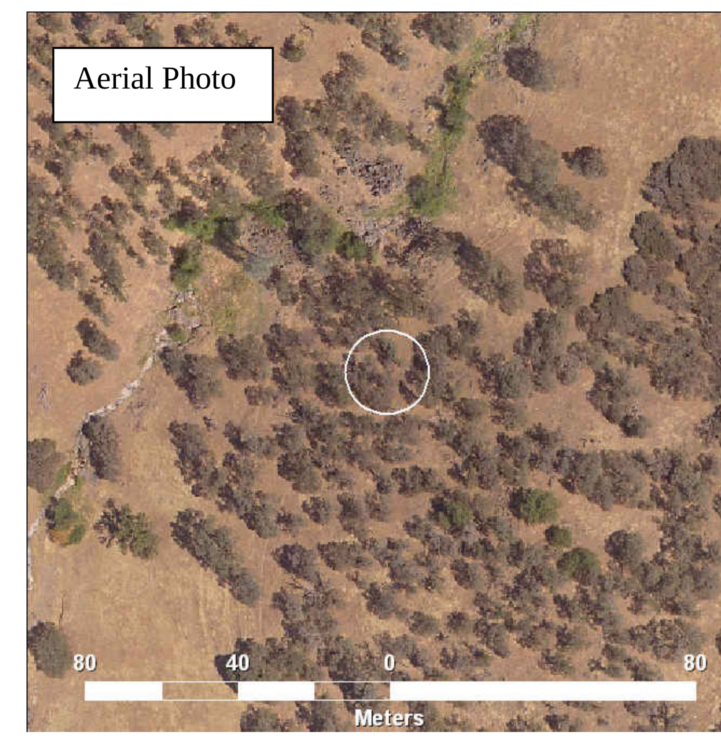

Plot # 27

Feature size: 4 m
Vegetation Density: 38.97 %
Lidar block reference number: 5740

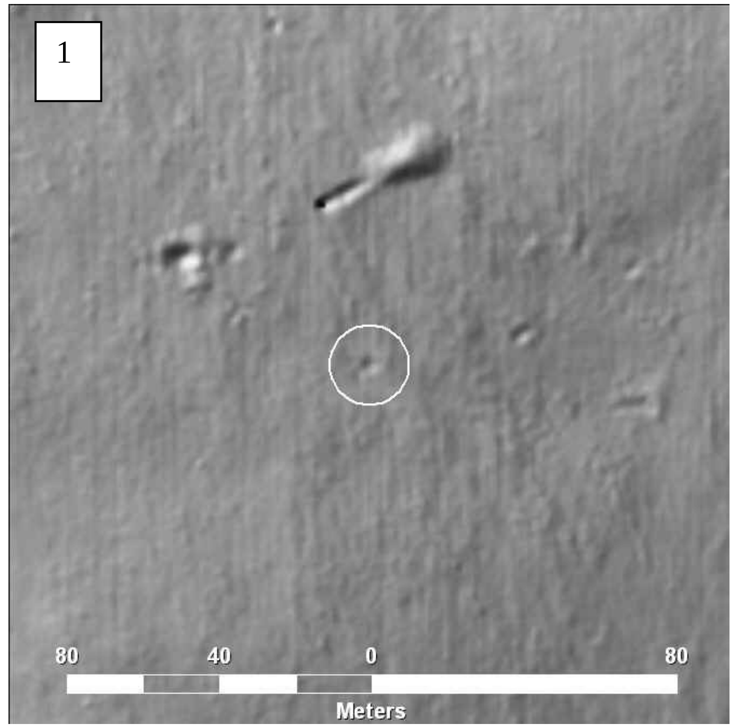

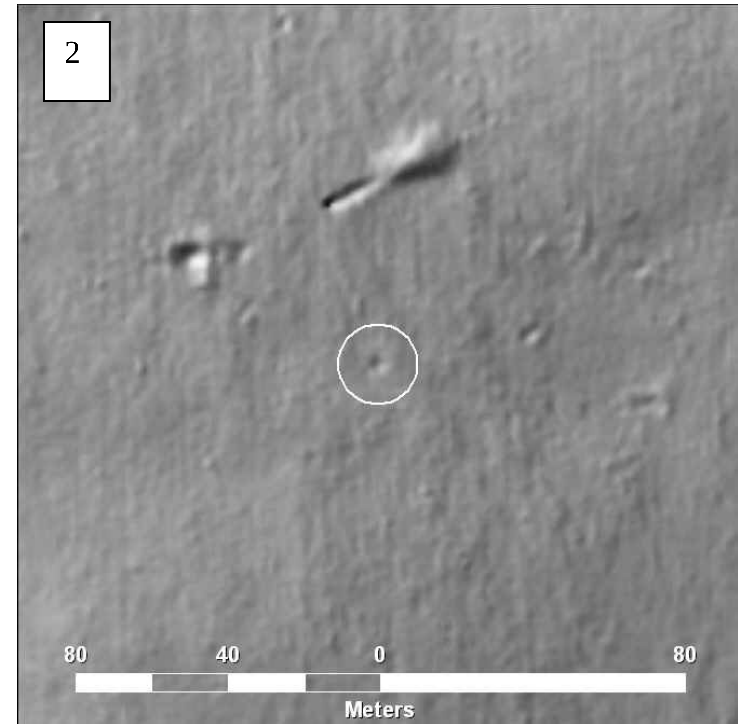

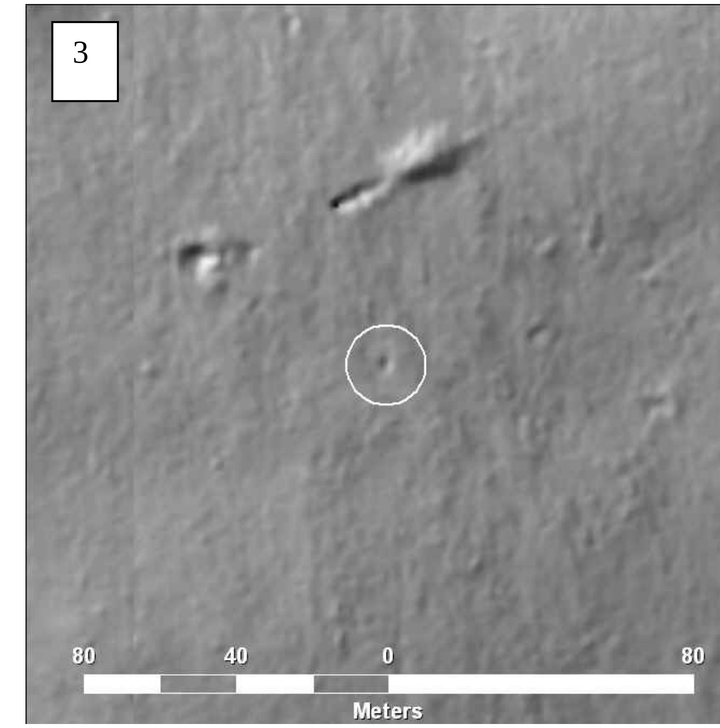

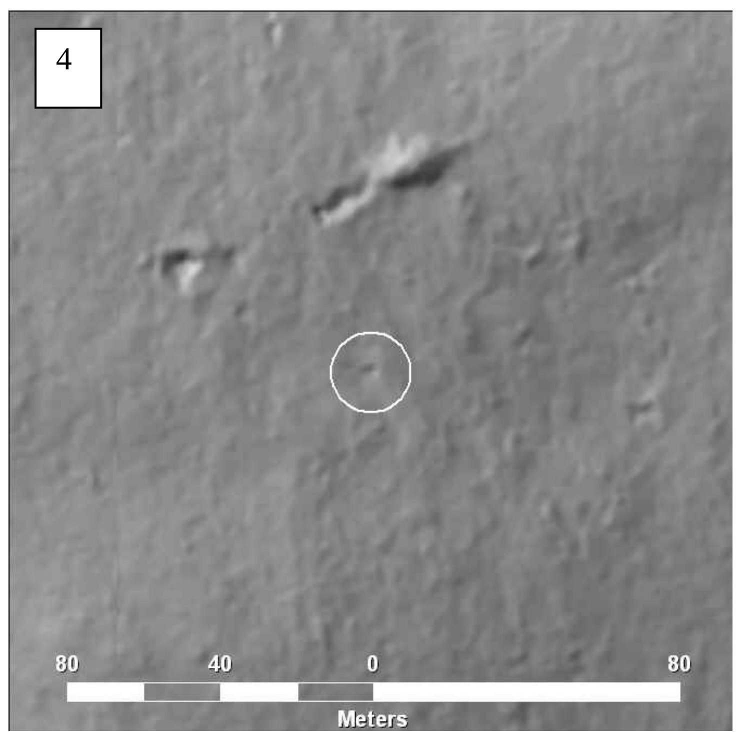

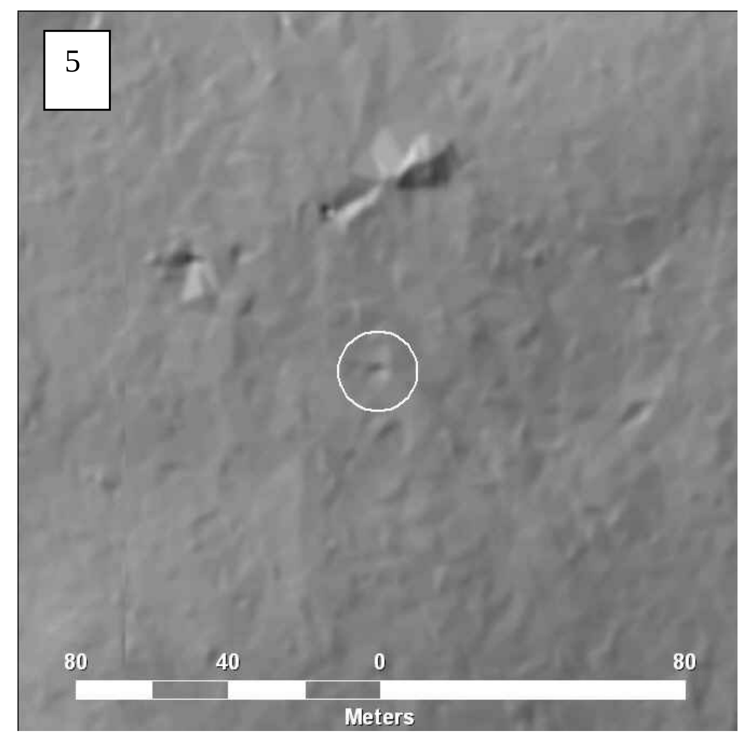

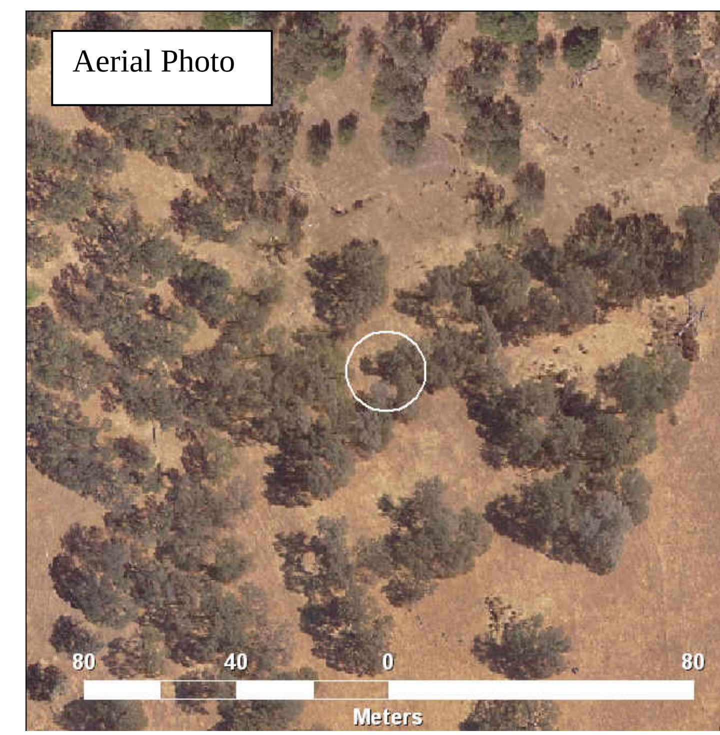

Plot # 28

Feature size: 4.1 m
Vegetation Density: 57.2 %
Lidar block reference number: 5641

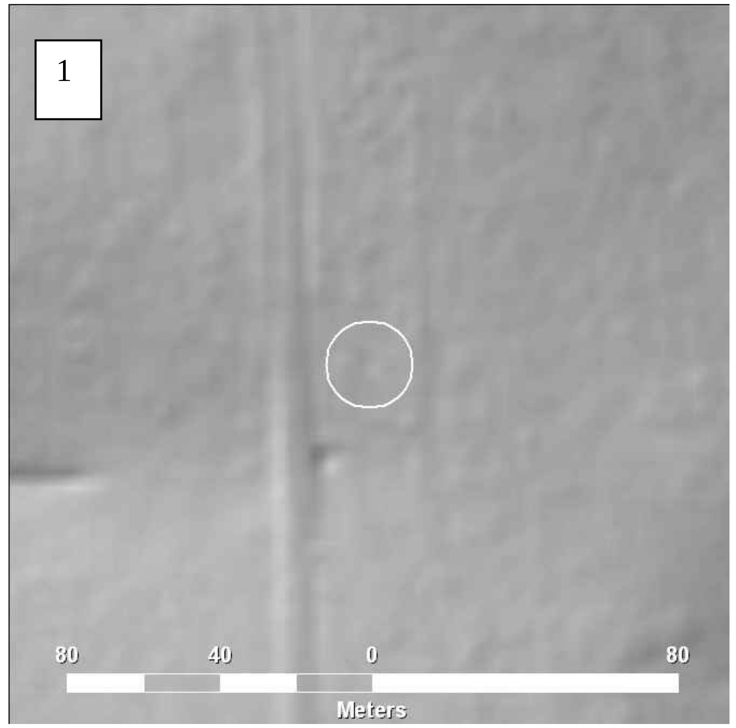

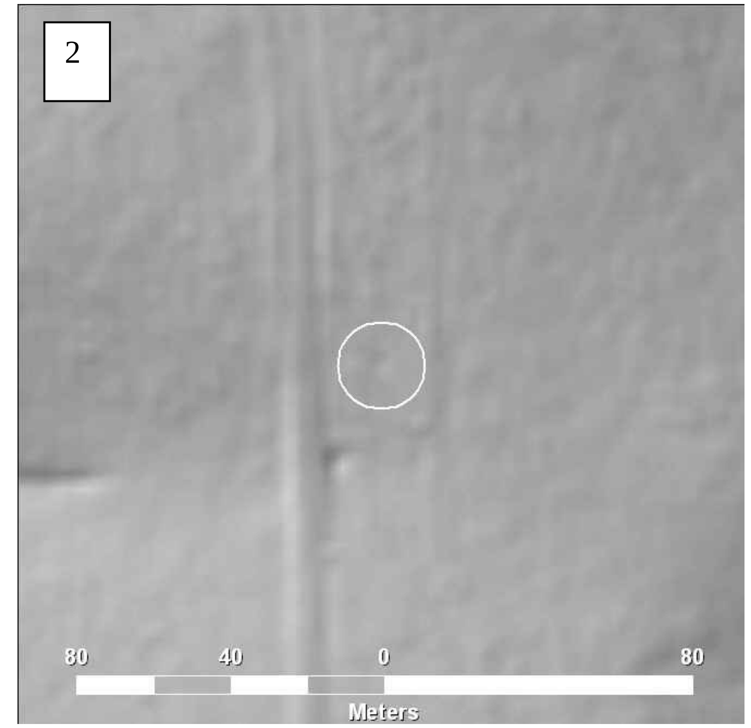

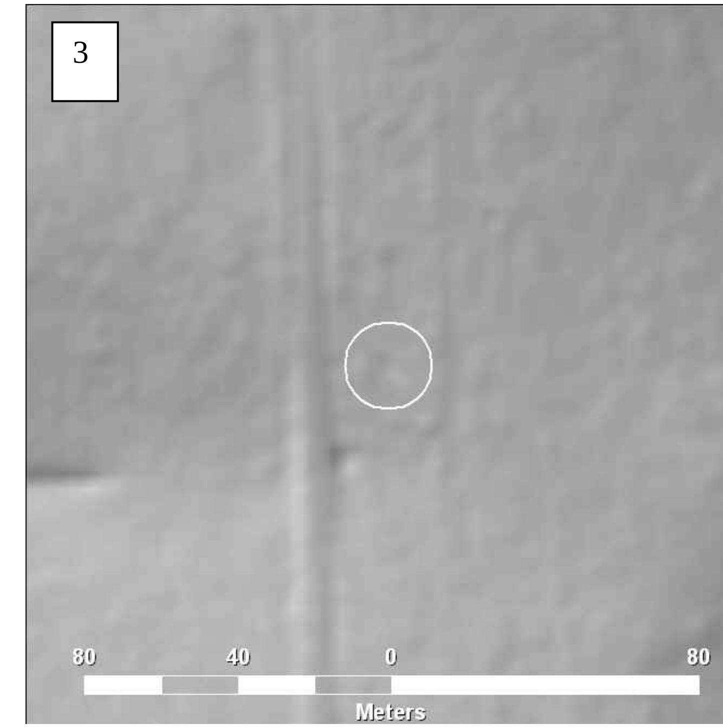

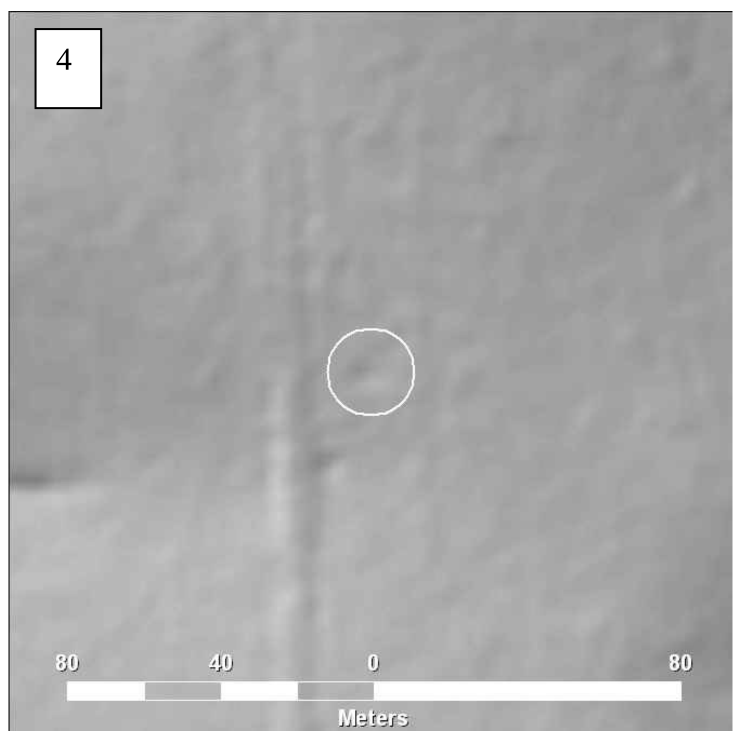

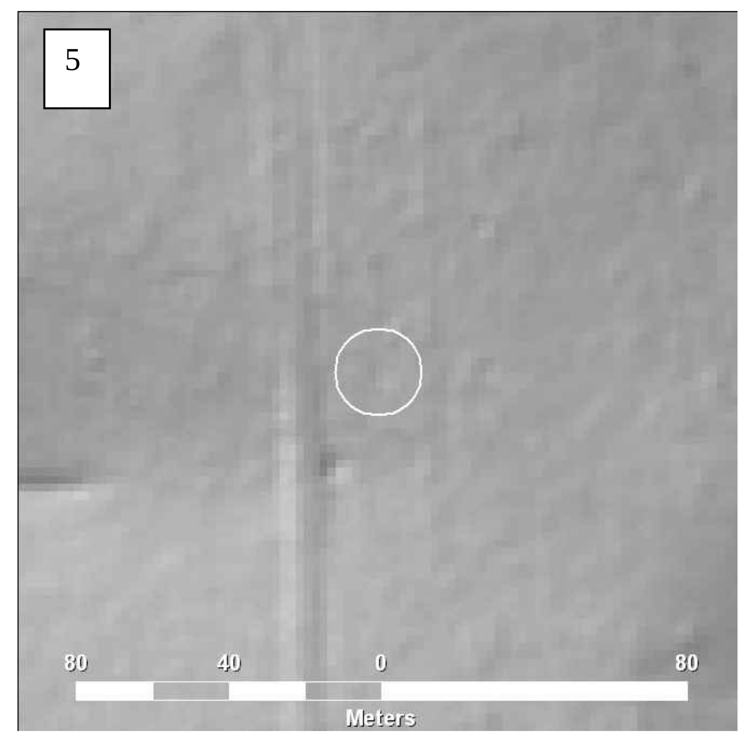

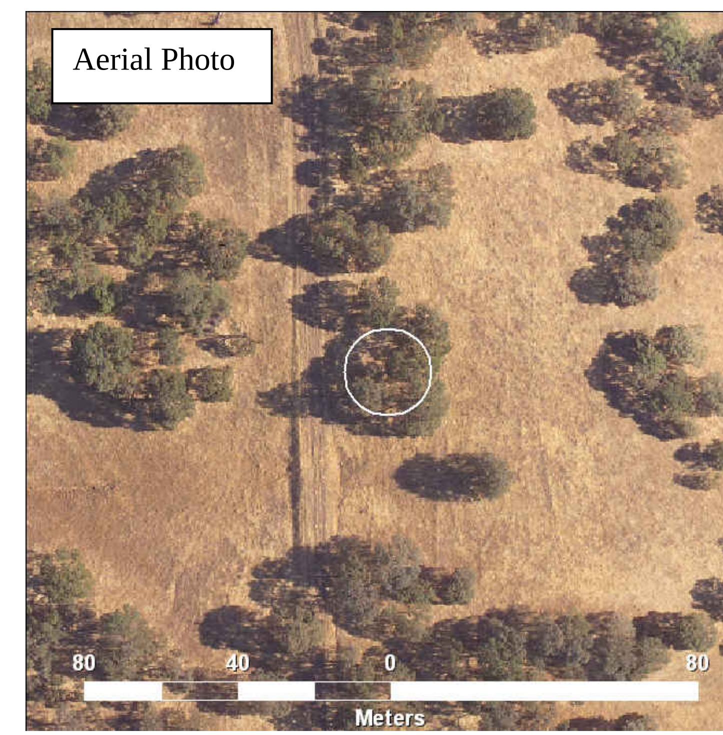

Plot # 29

Feature size: 4.25 m
Vegetation Density: 52.9 %
Lidar block reference number: 5615

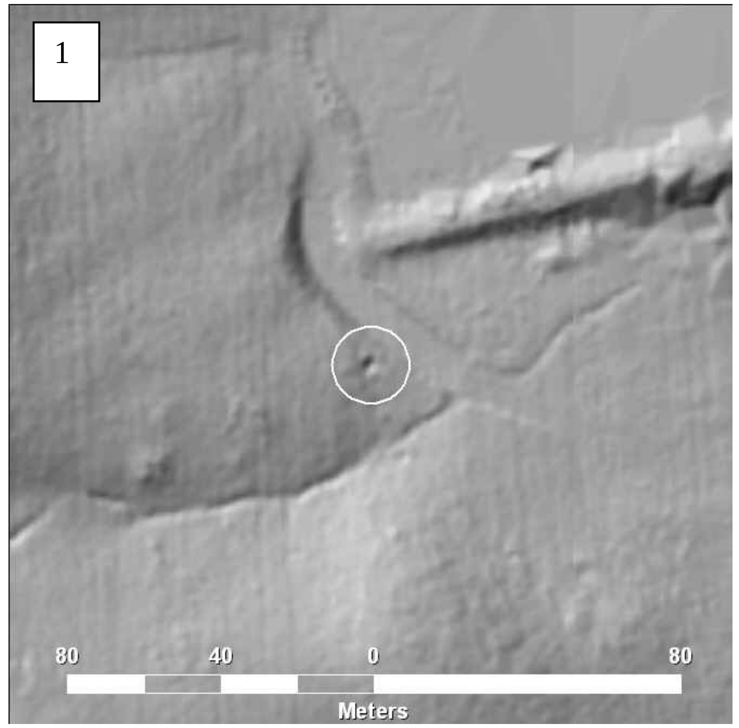

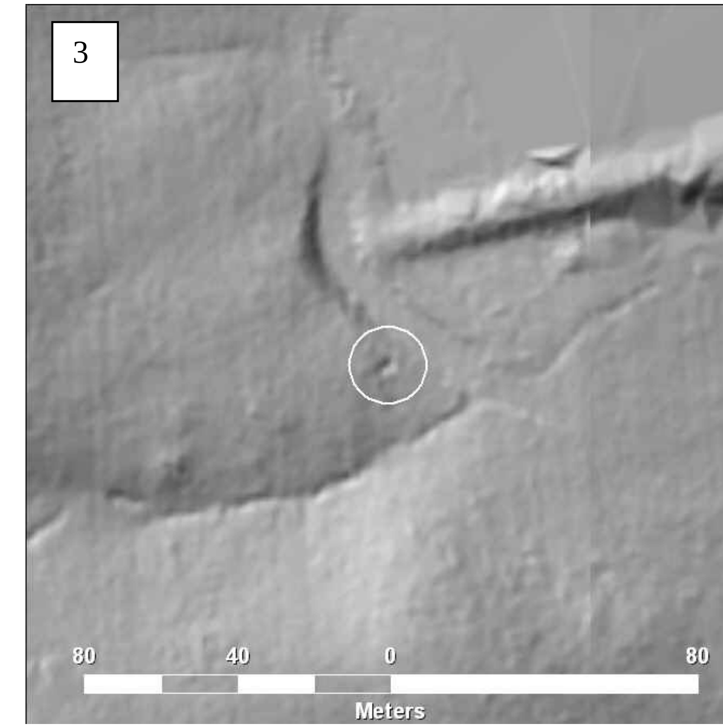

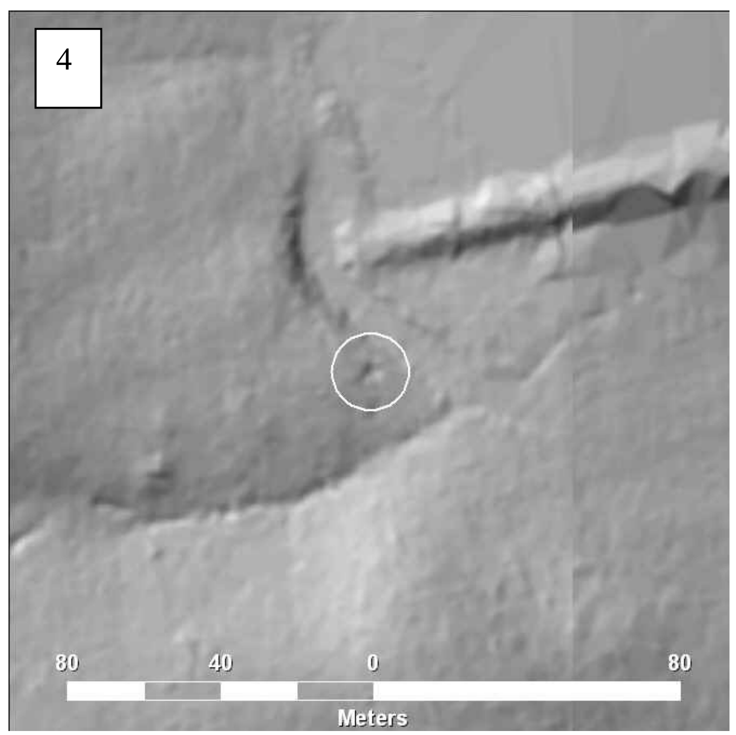

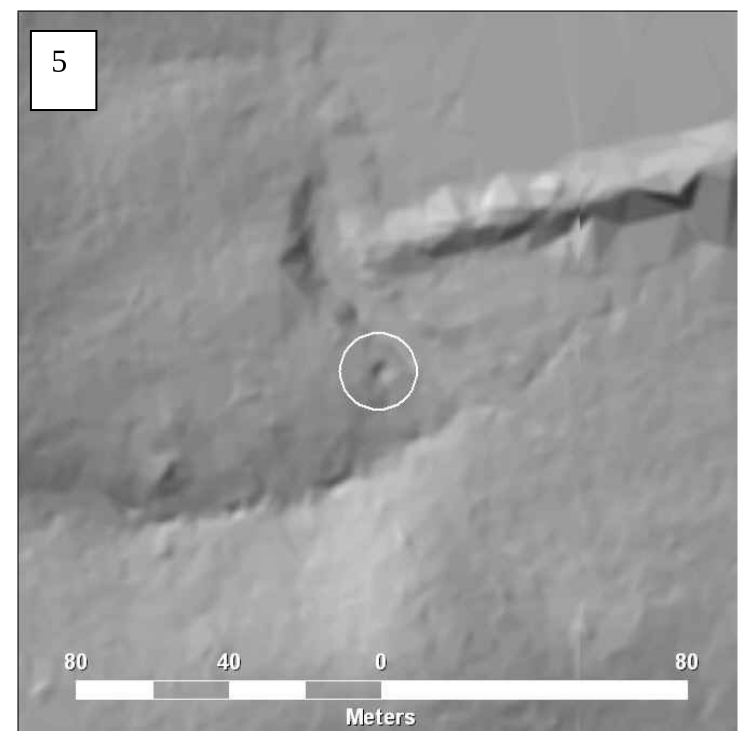

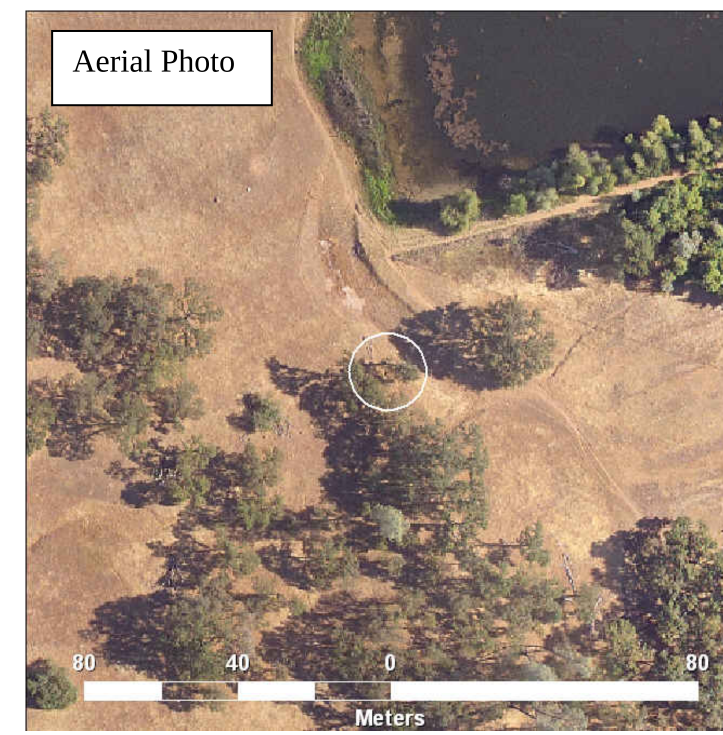

Plot # 30

Feature size: 4.3 m
Vegetation Density: 73.79 %
Lidar block reference number: 4077

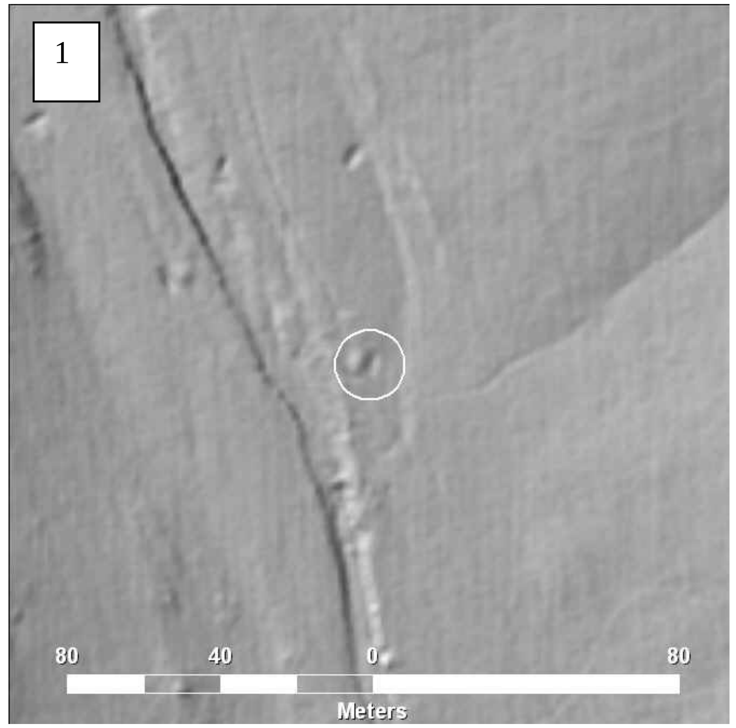

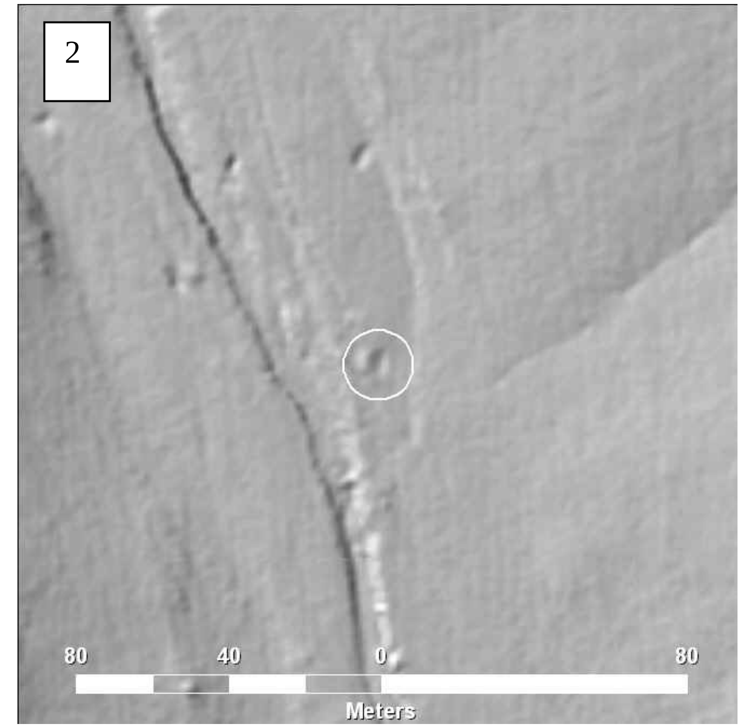

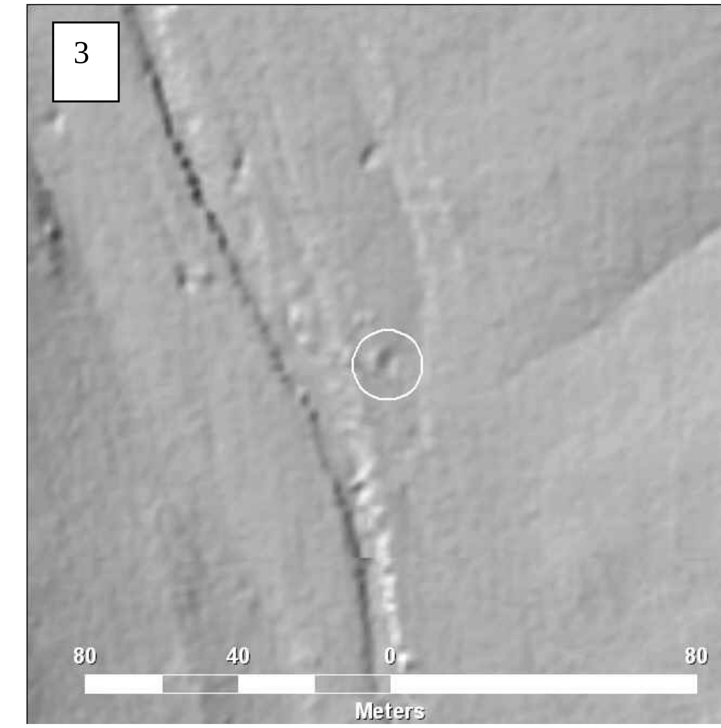

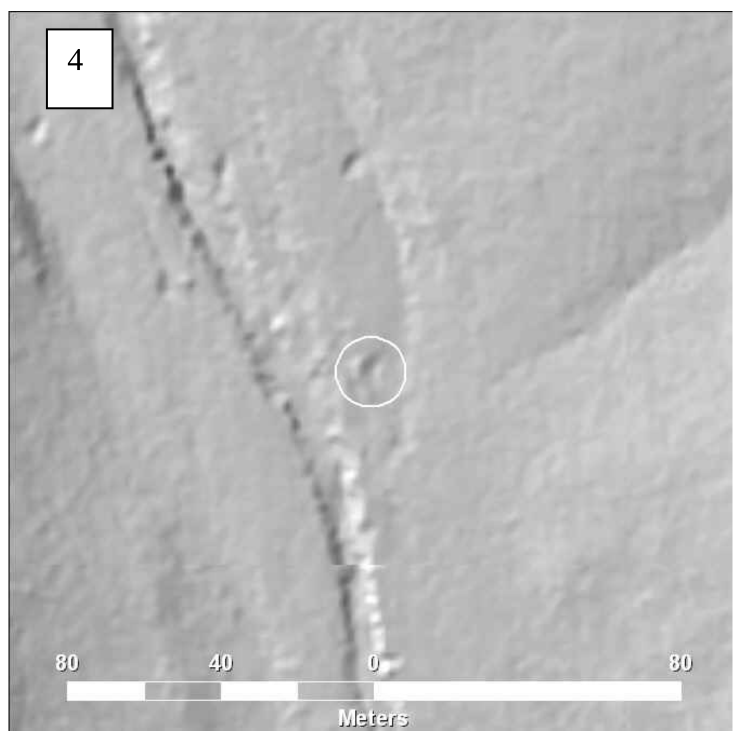

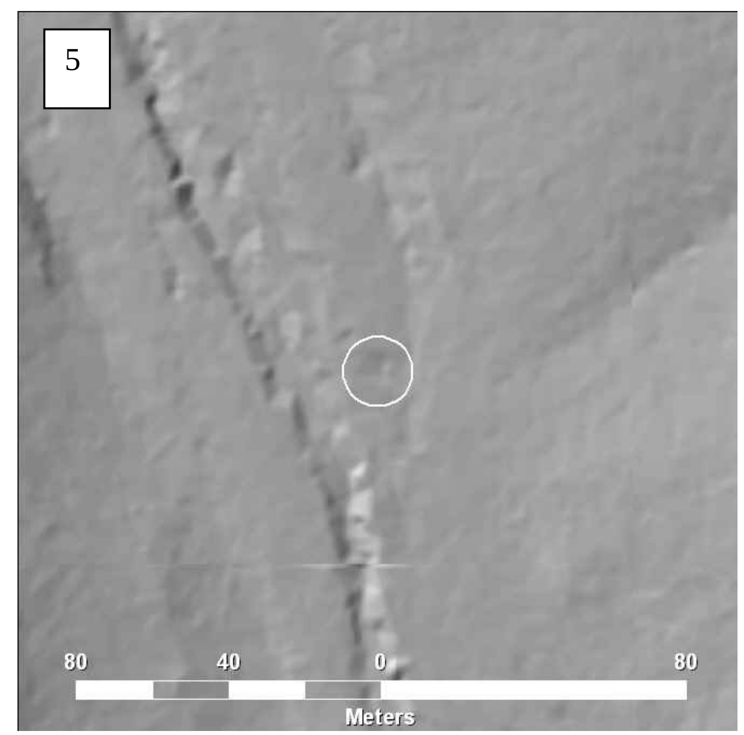

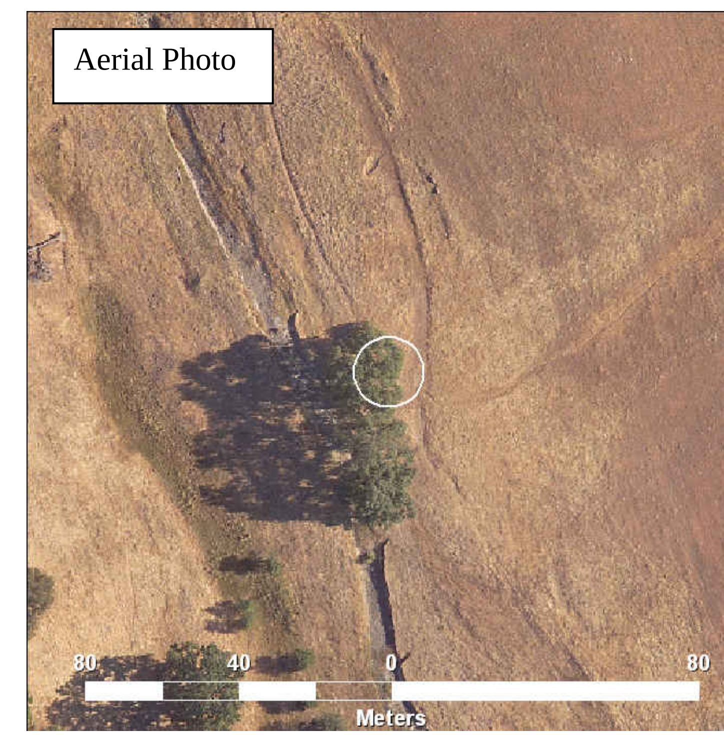

Plot # 31 Feature size: 4.5 m Vegetation Density: 38.5 % Lidar block reference number: 4001	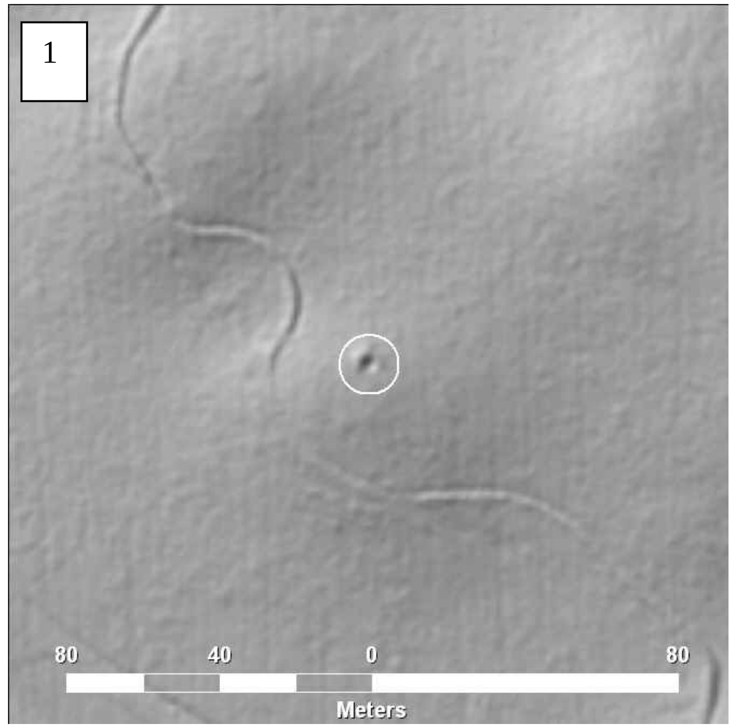	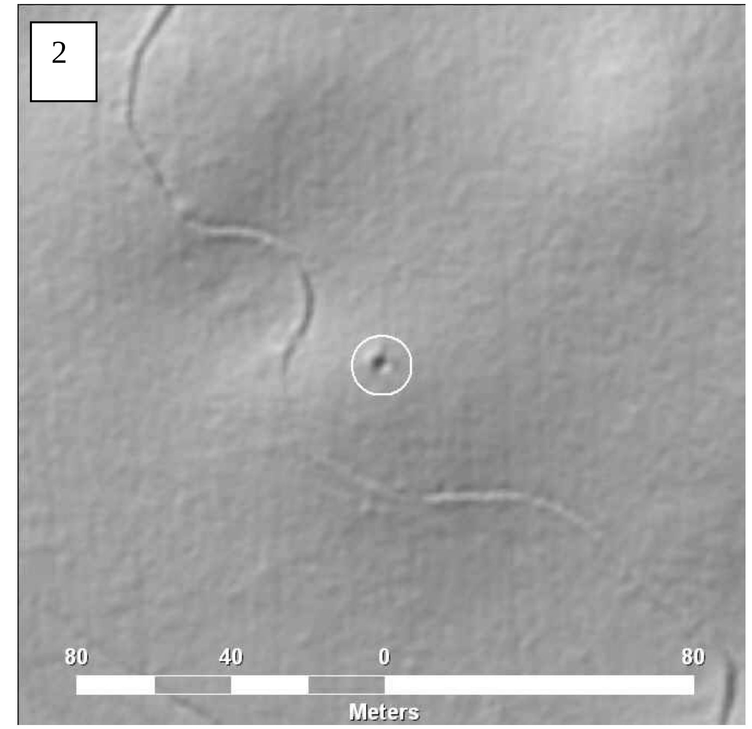	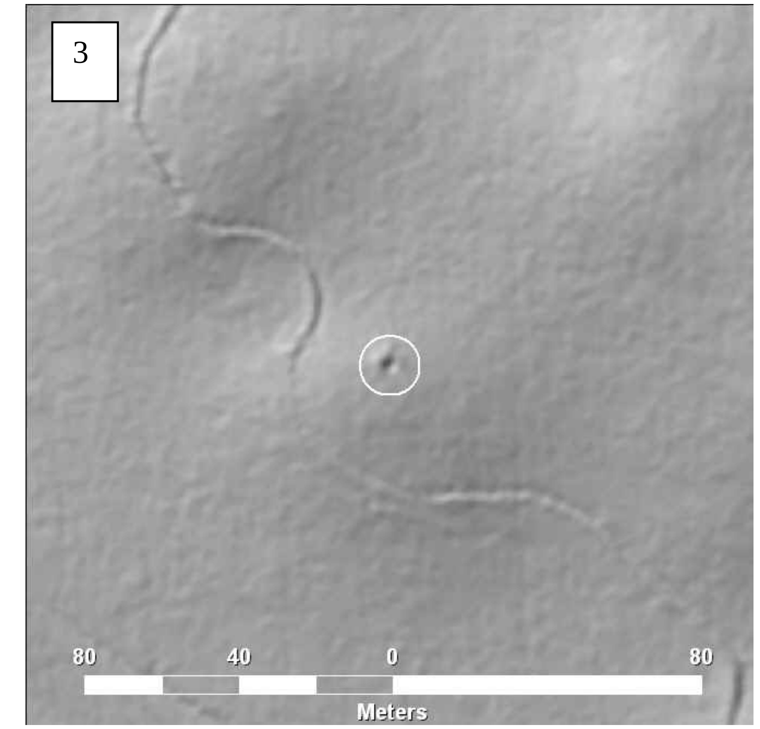
	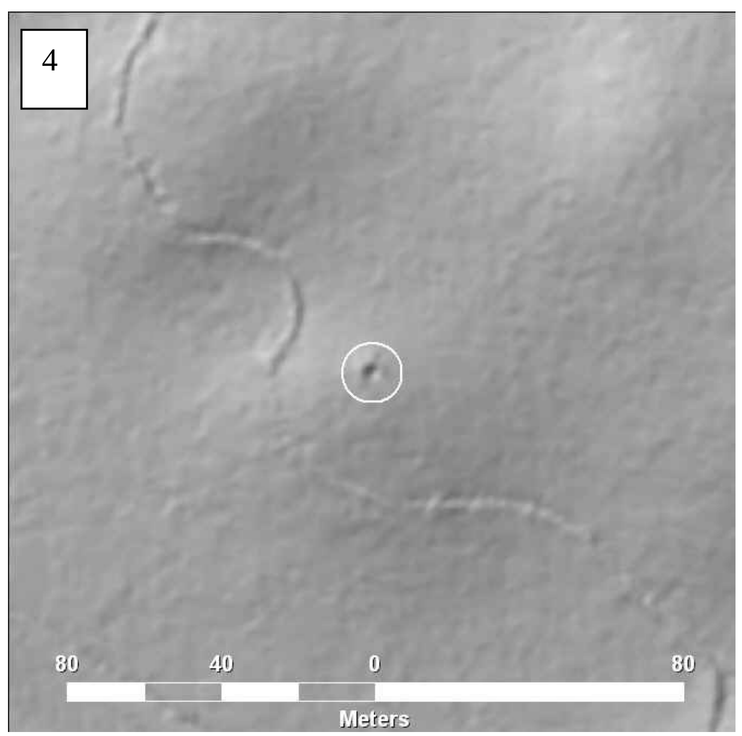	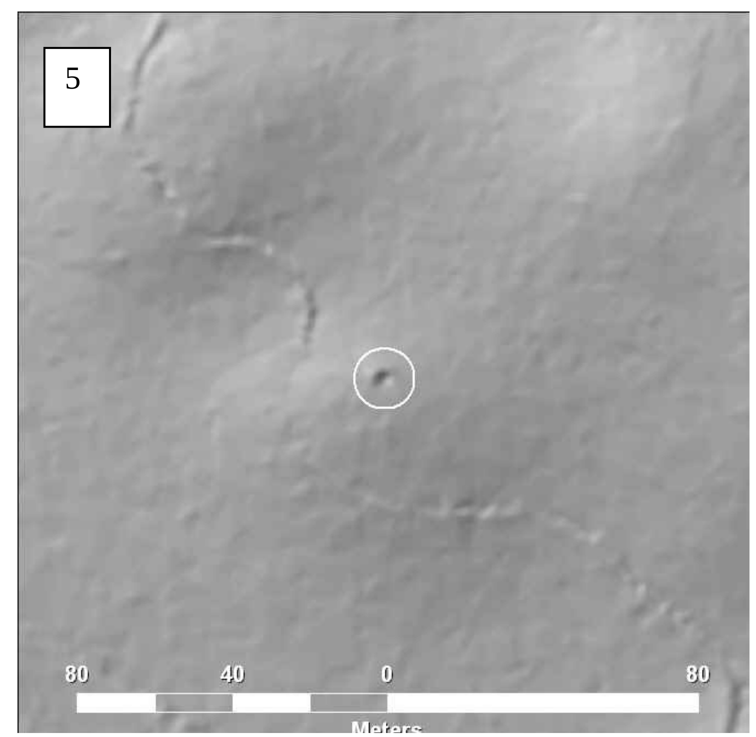	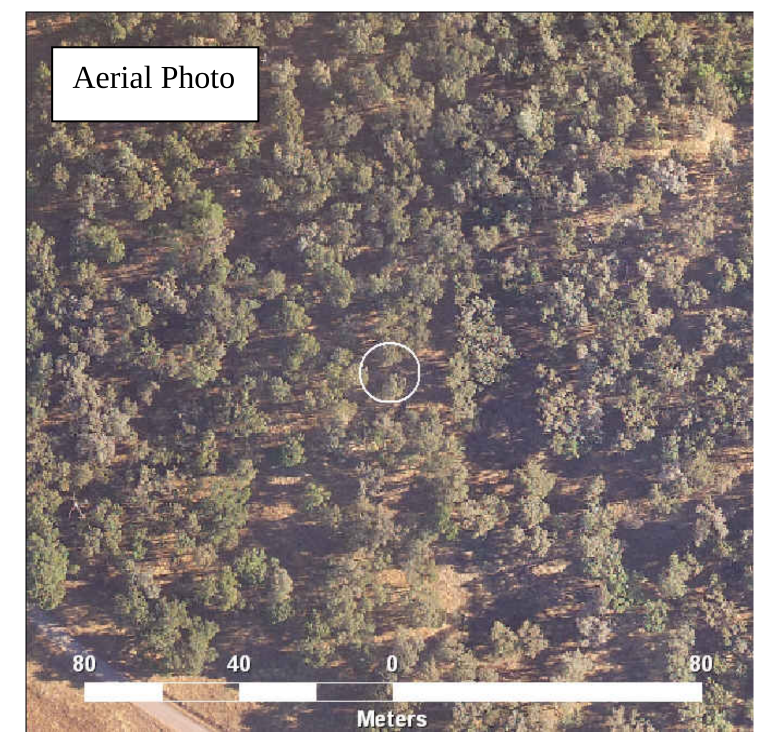

Plot # 32

Feature size: 4.5 m
Vegetation Density: 63.38 %
Lidar block reference number: 5468

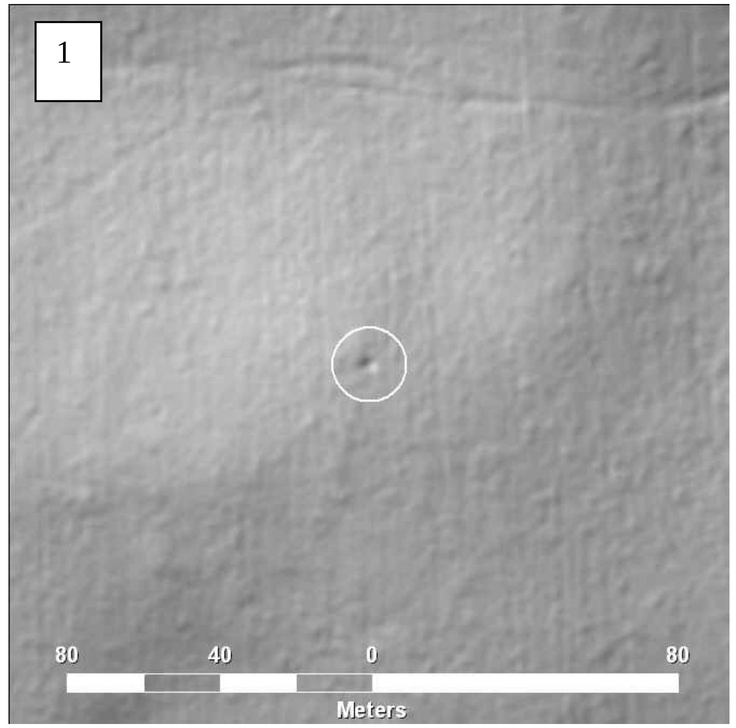

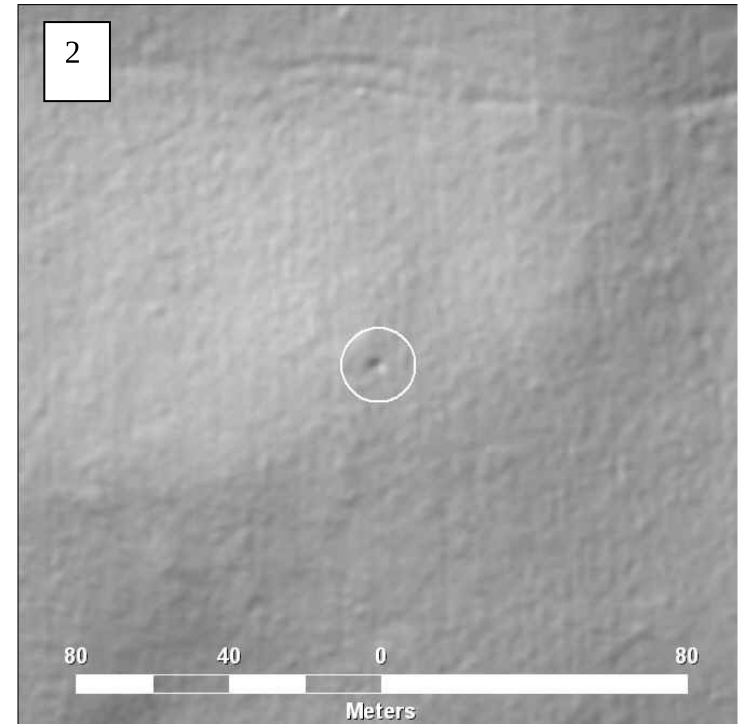

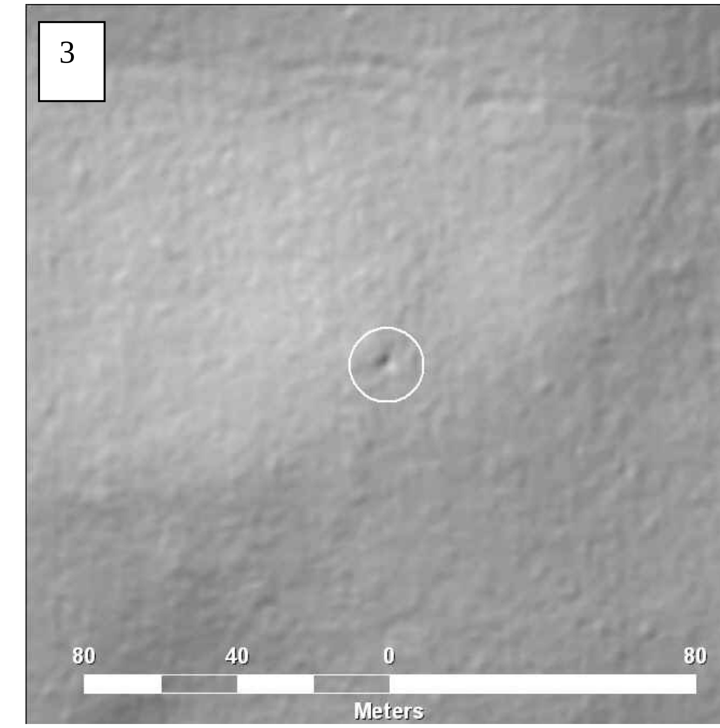

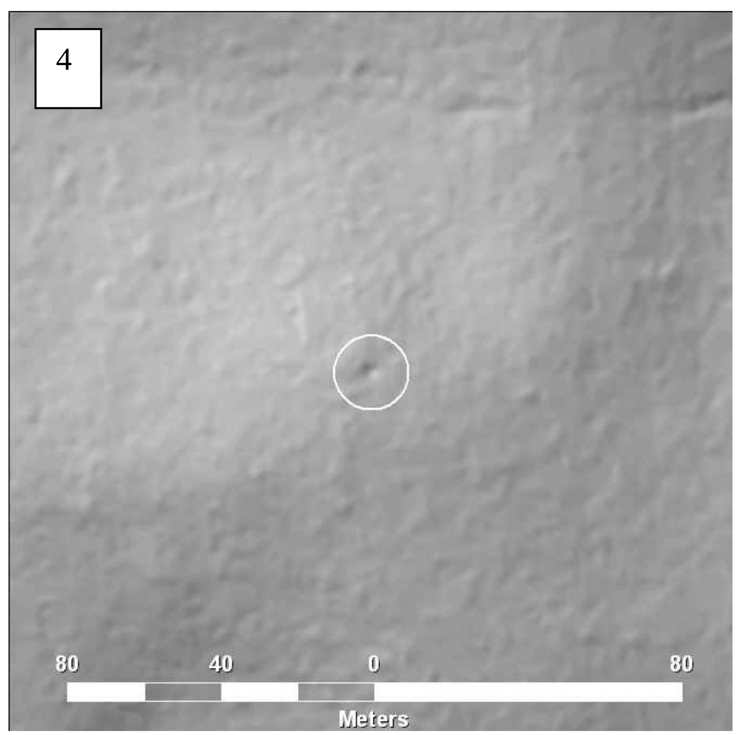

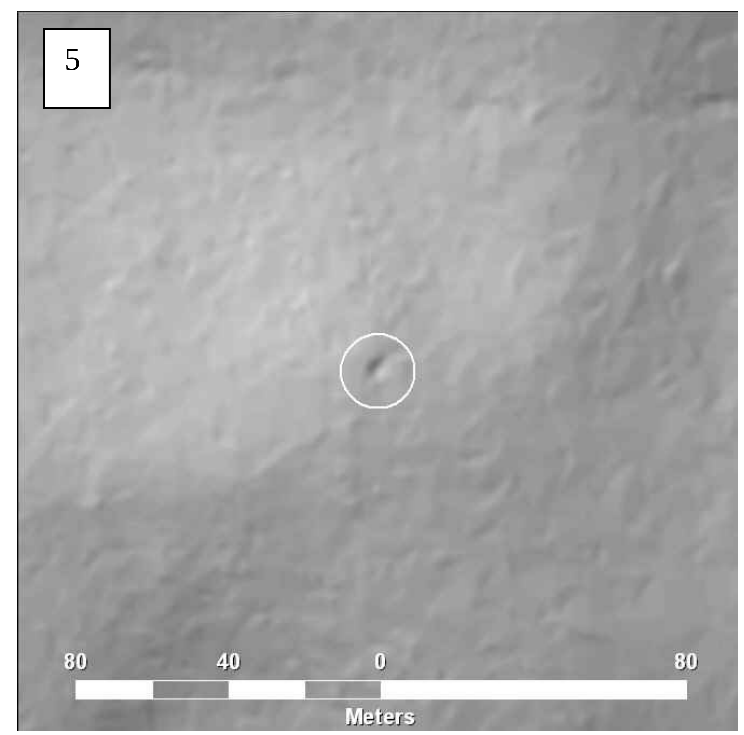

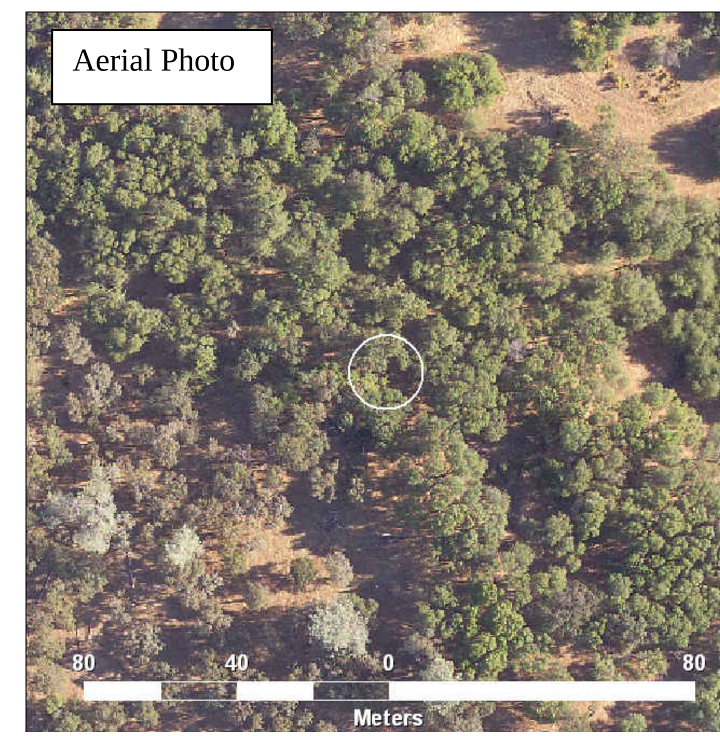

Plot # 33

Feature size: 4.7 m
Vegetation Density: 47.67 %
Lidar block reference number: 4014

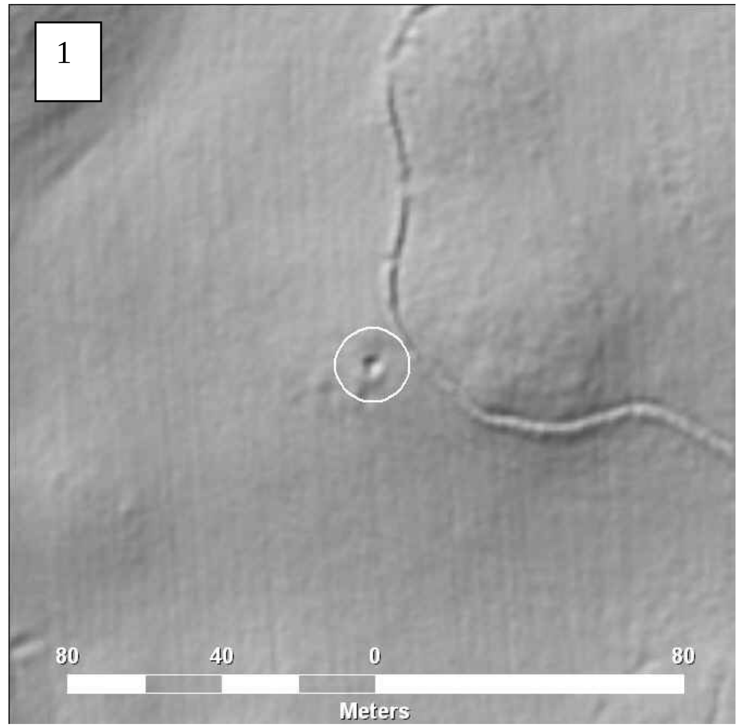

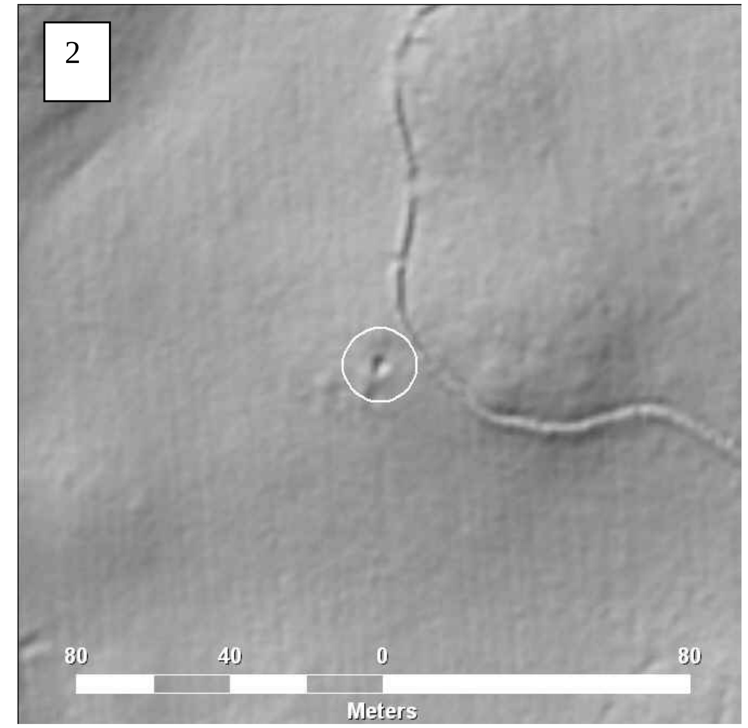

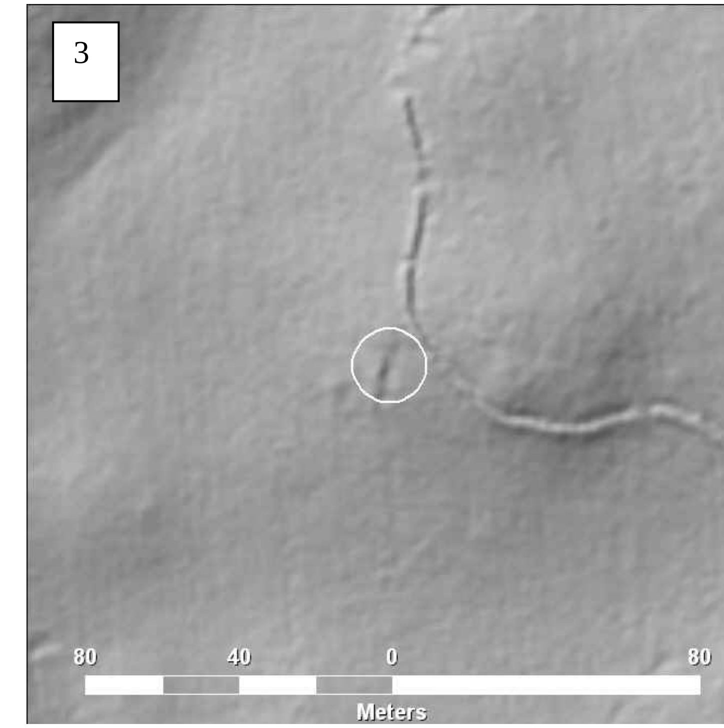

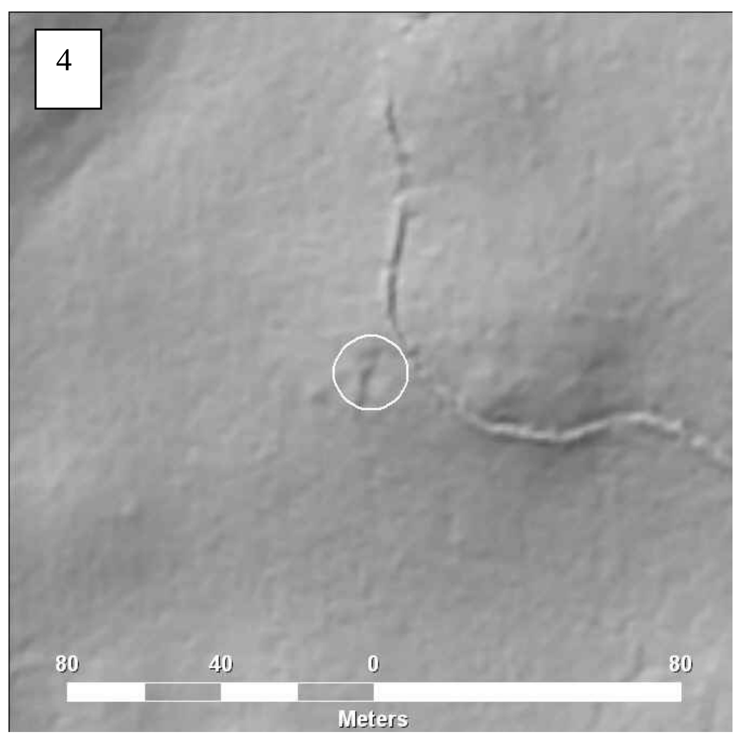

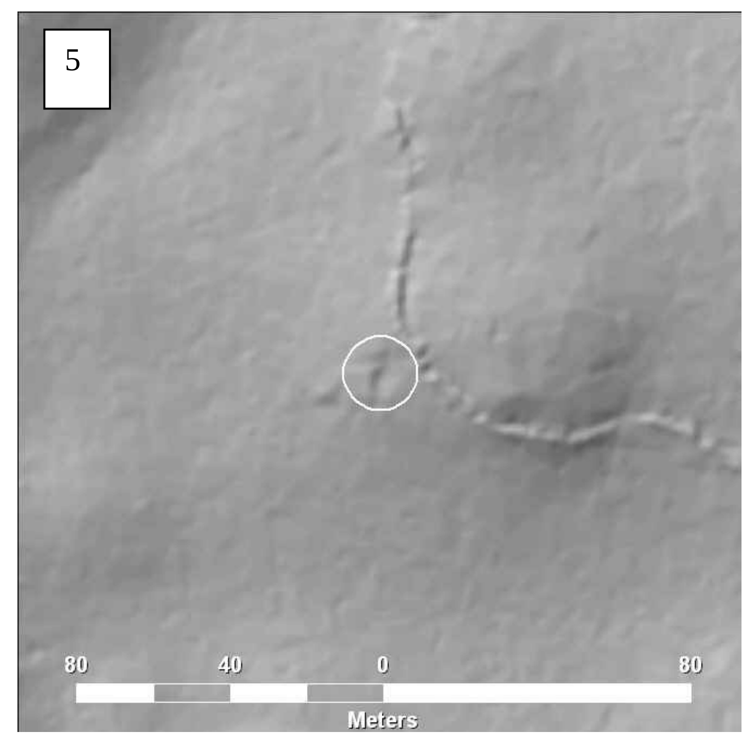

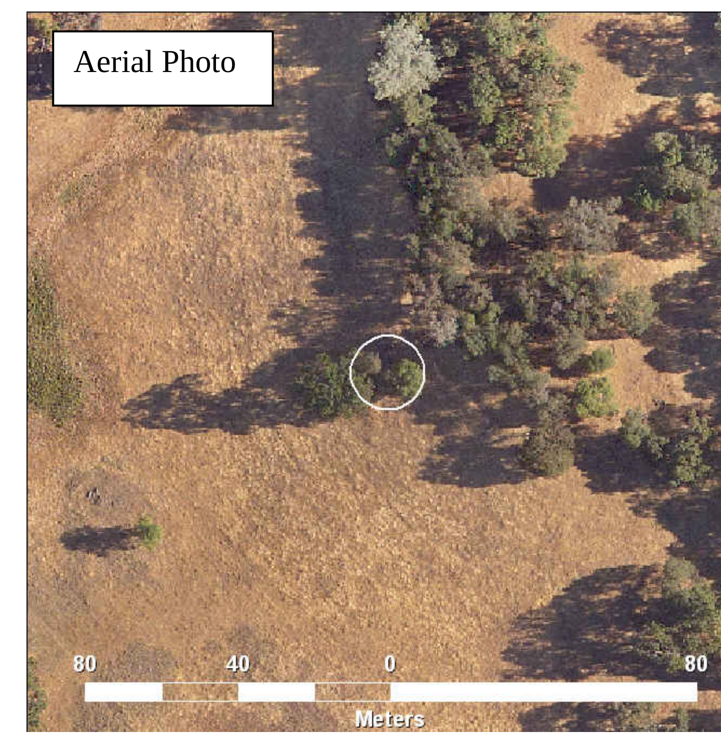

Plot # 34

Feature size: 4.8 m
Vegetation Density: 50.17 %
Lidar block reference number: 5521

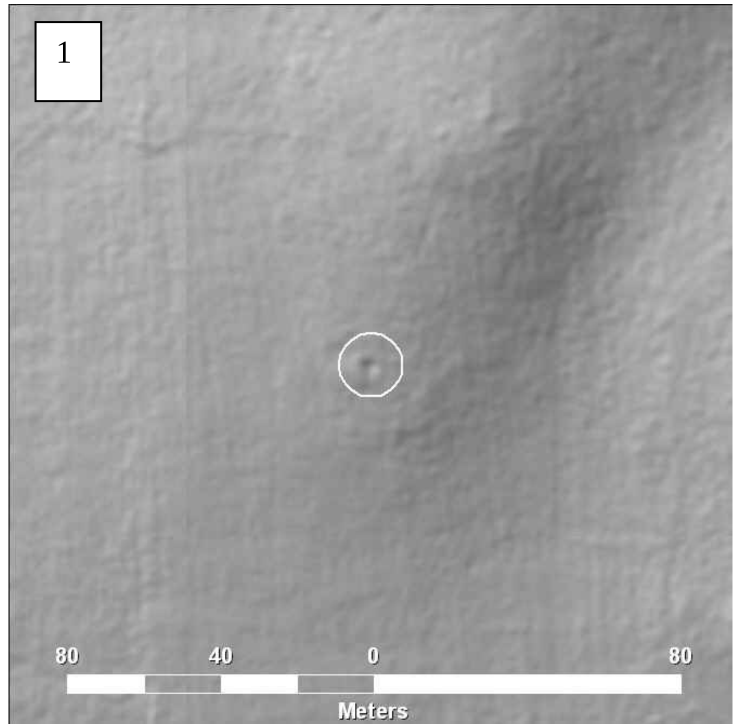

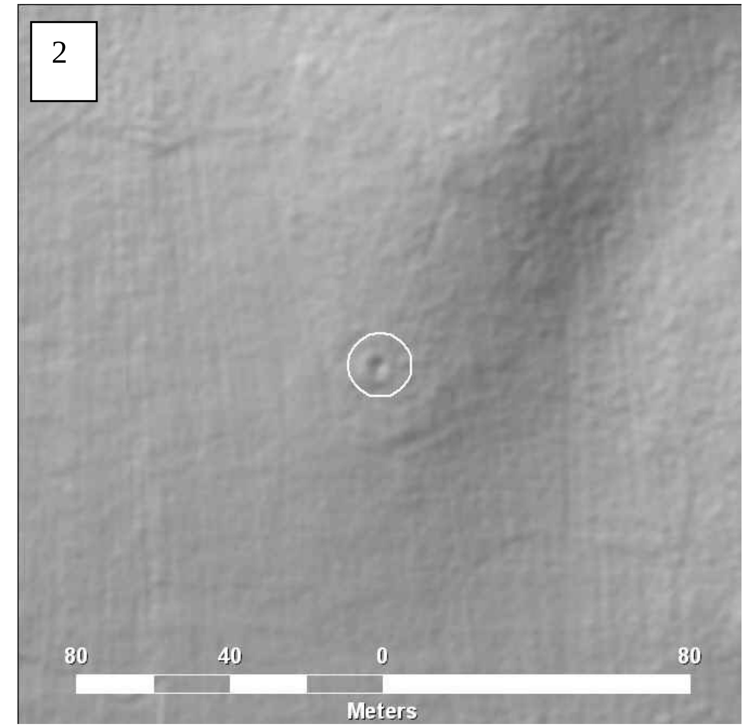

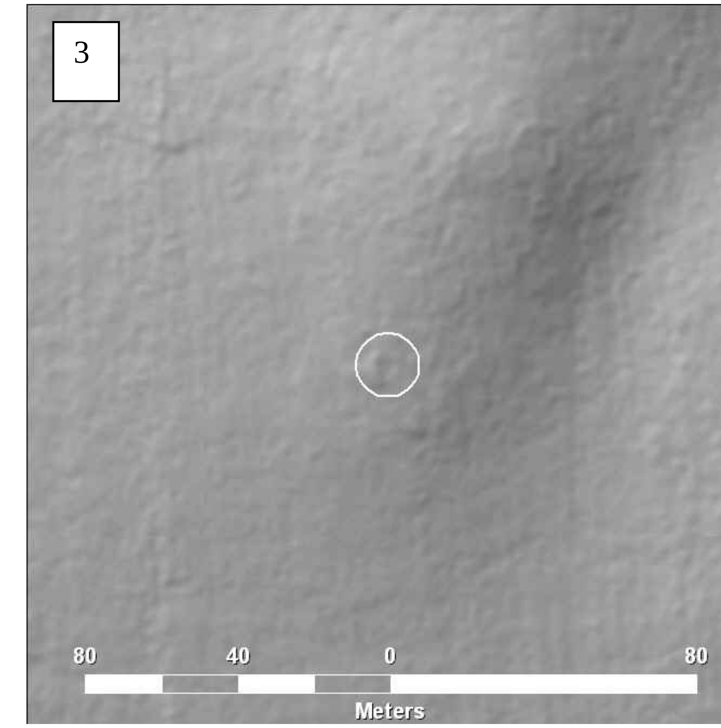

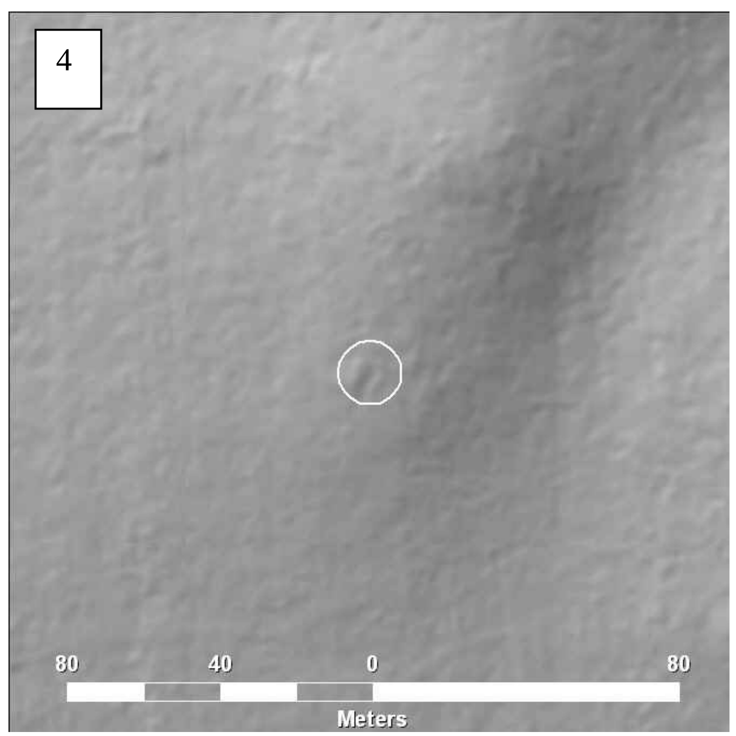

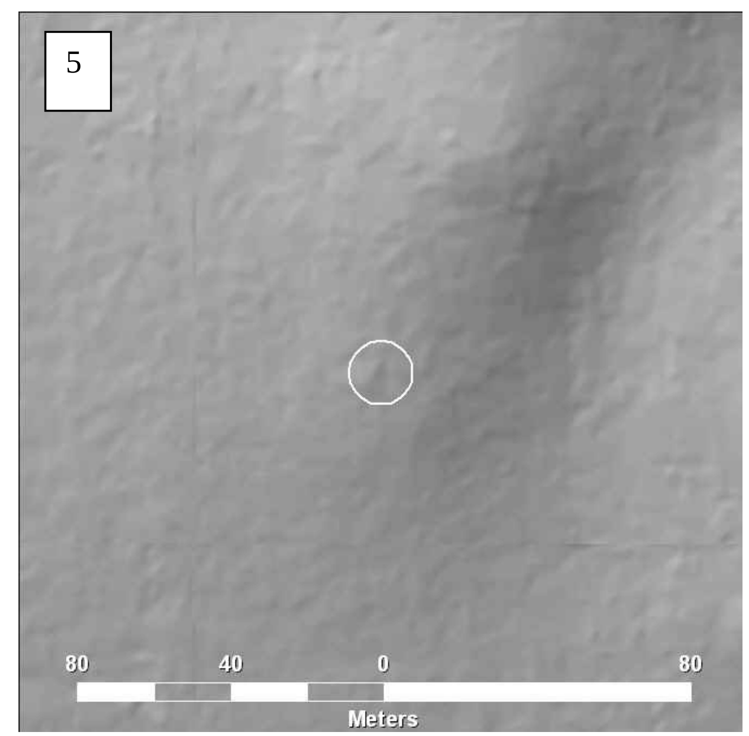

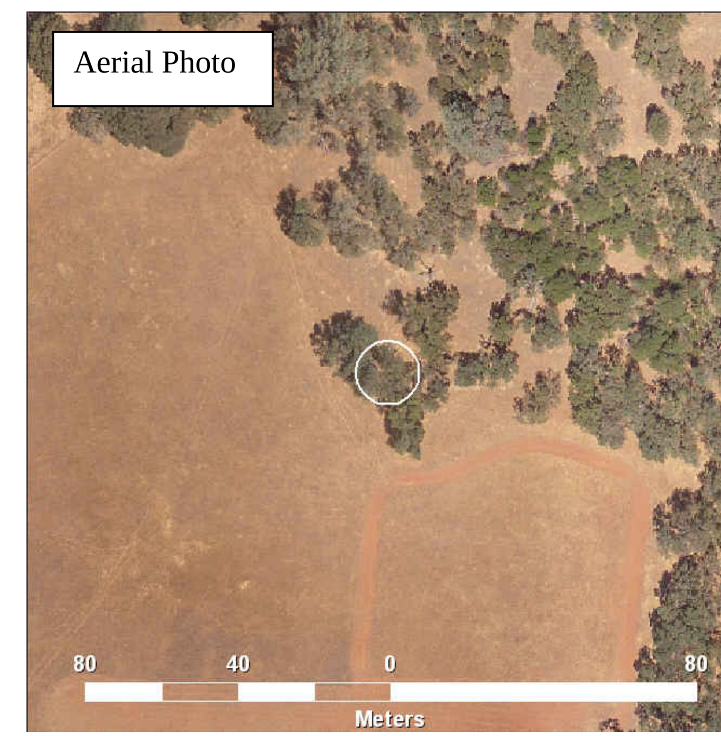

Plot # 35

Feature size: 5.1 m
Vegetation Density: 53.5 %
Lidar block reference number: 5569

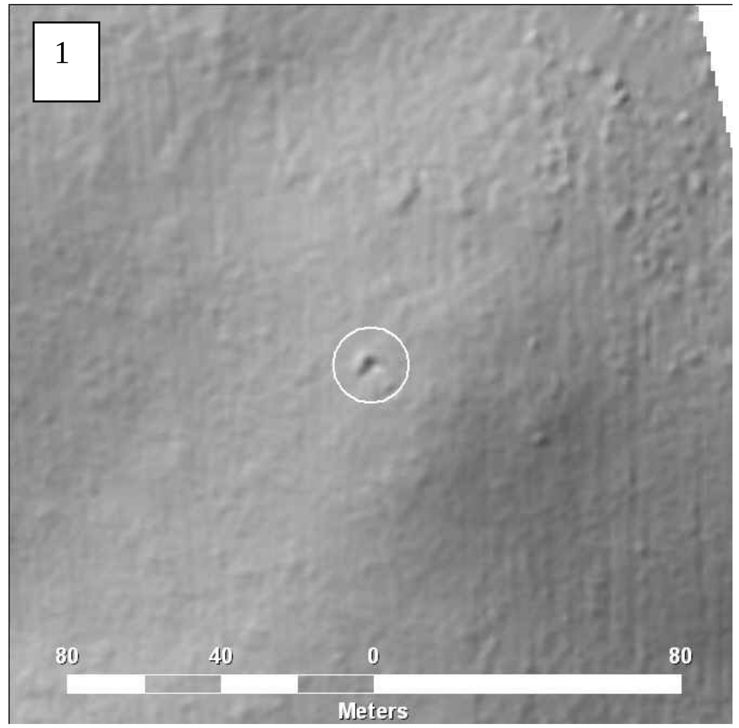

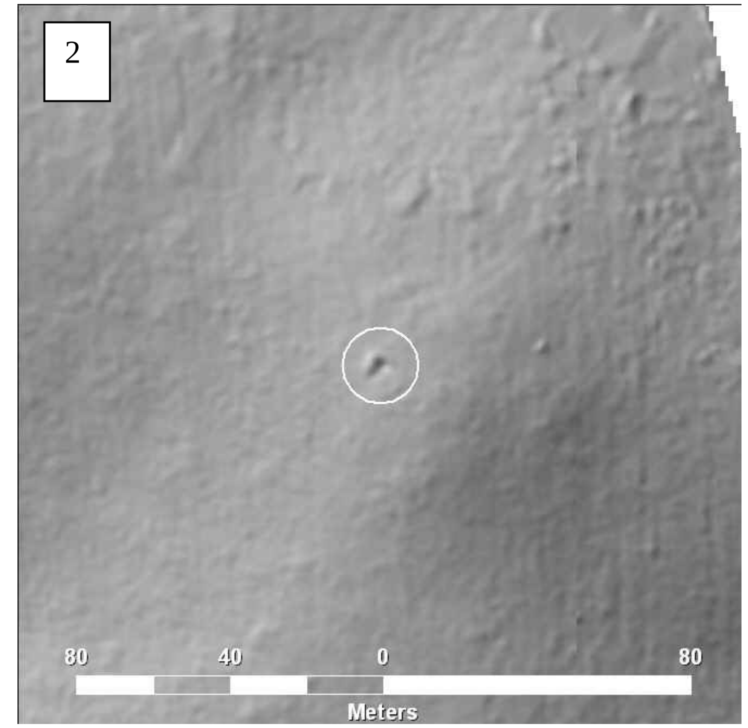

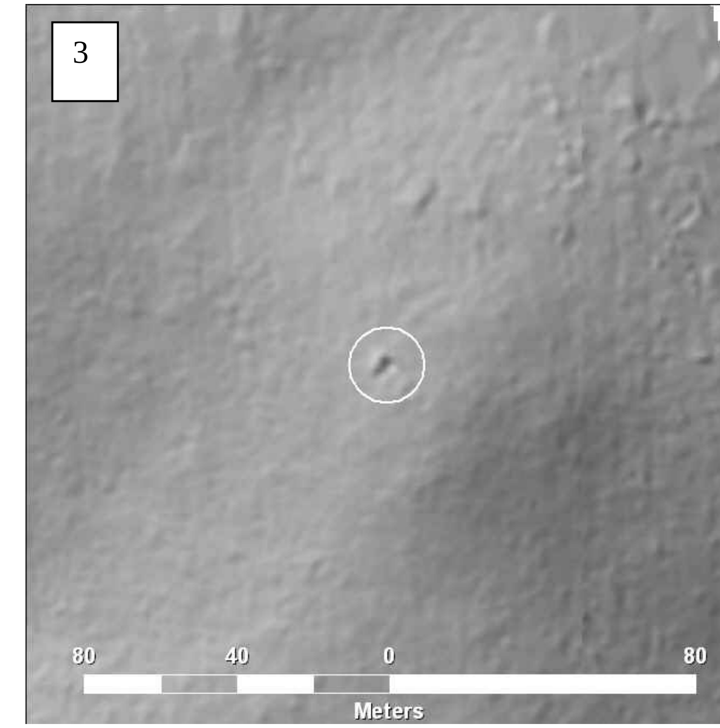

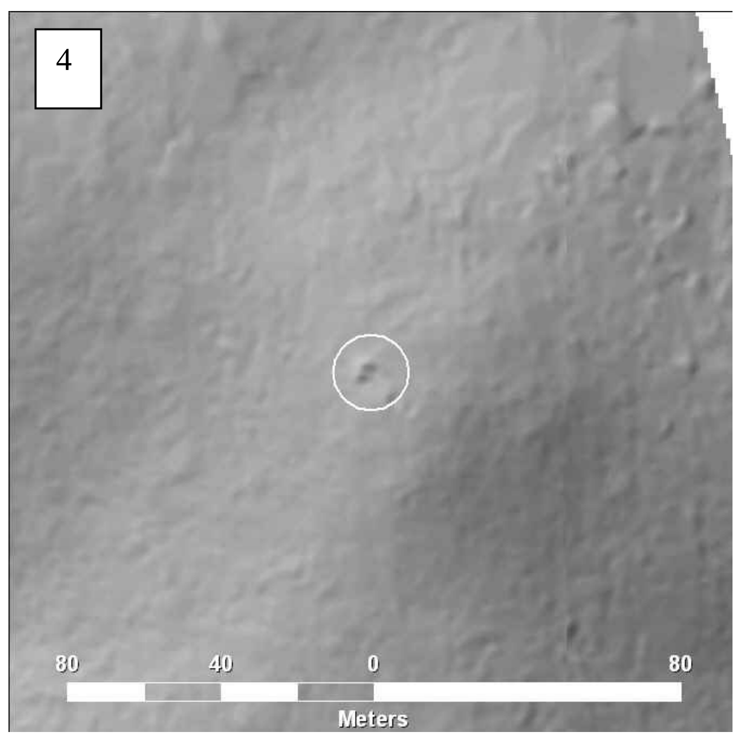

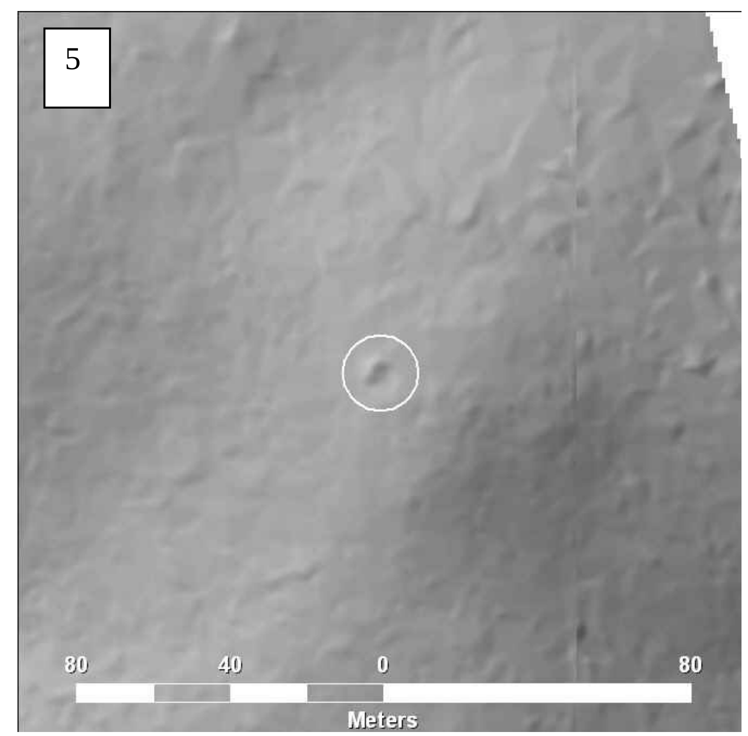

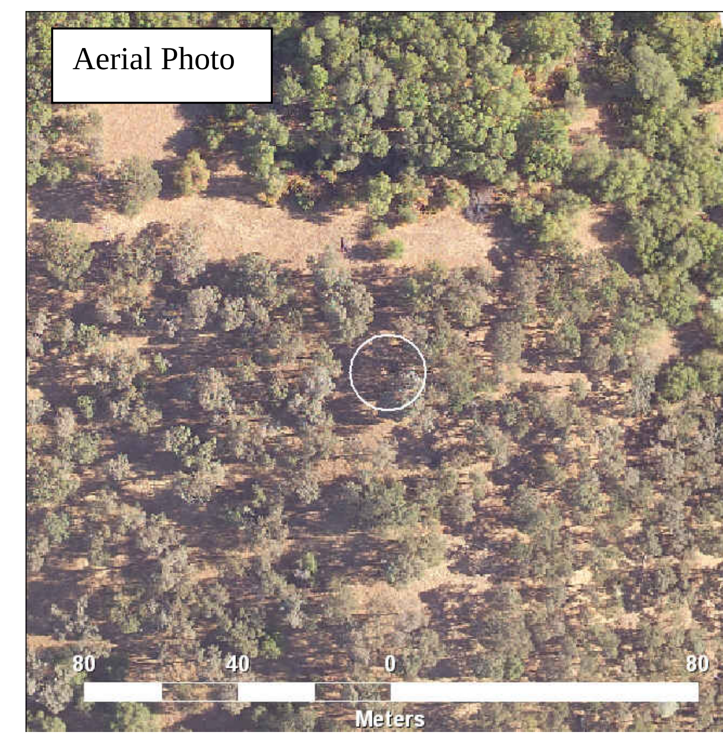

Plot # 36 Feature size: 5.2 m Vegetation Density: 38.94 % Lidar block reference number: 5736	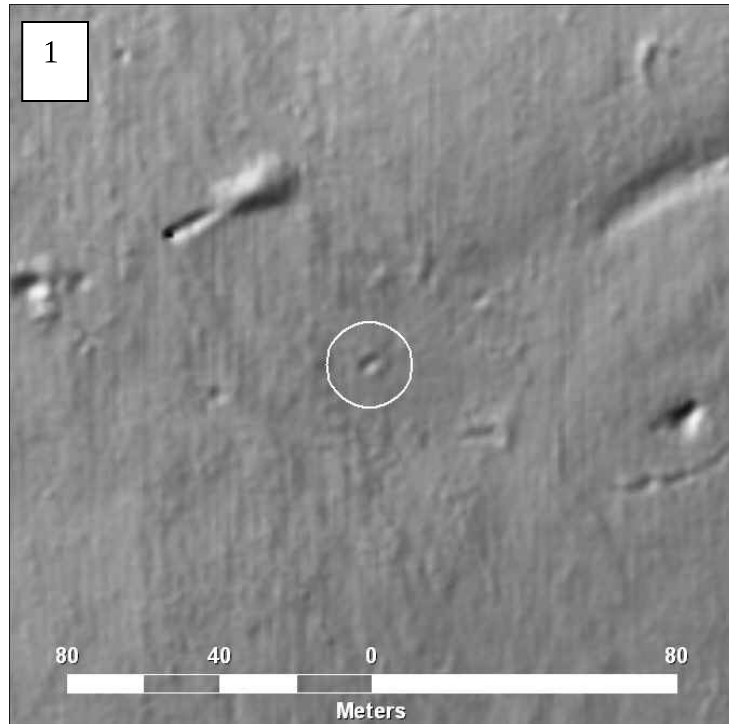	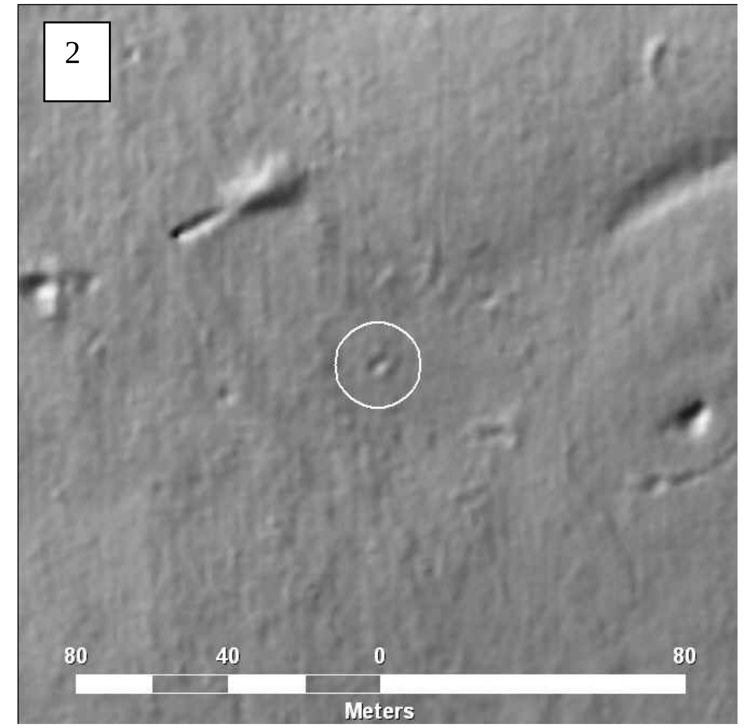	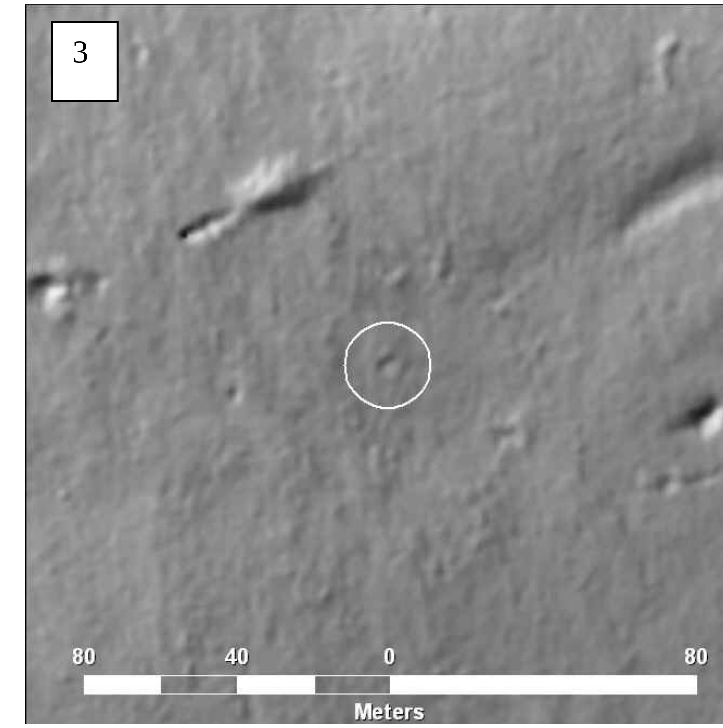
	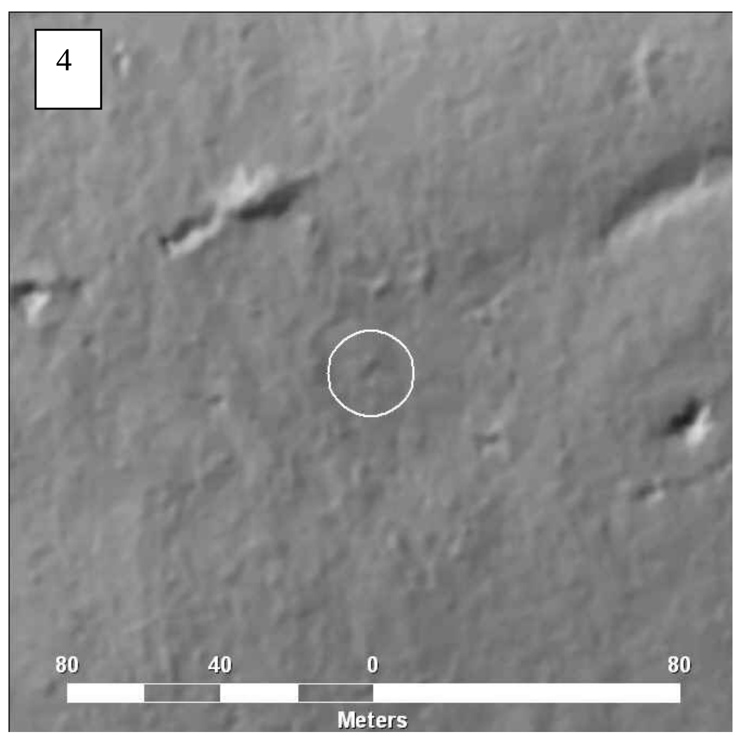	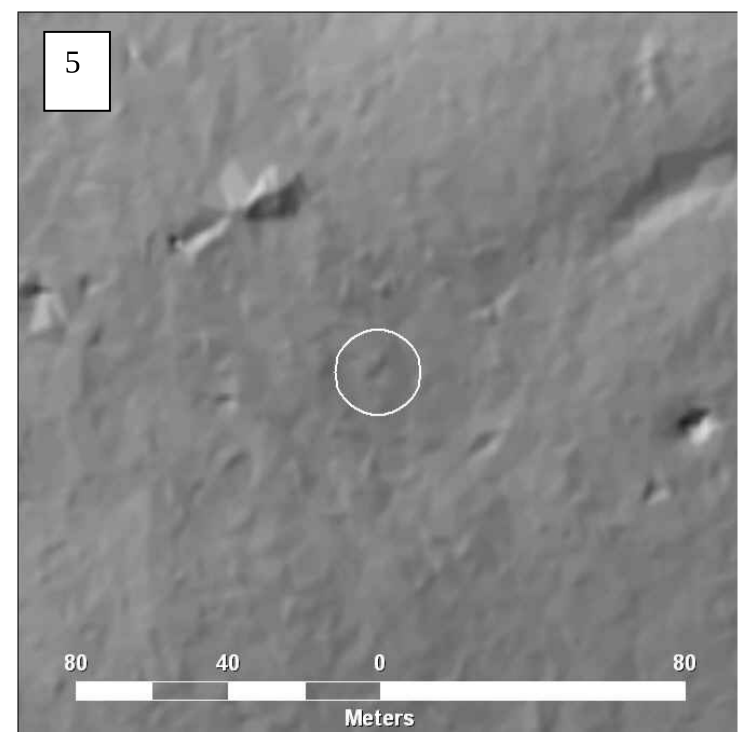	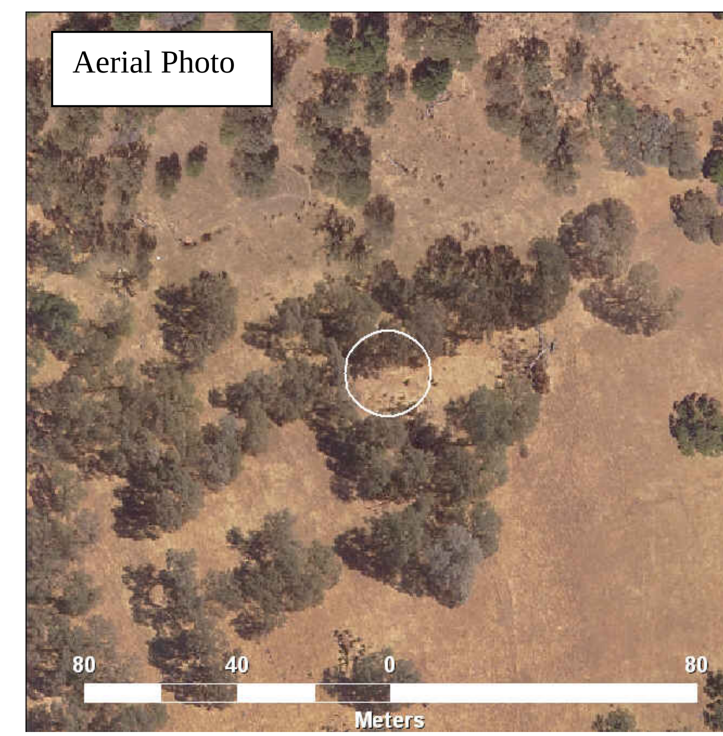

Plot # 37

Feature size: 5.2 m wide
10 m long
Vegetation Density: 43.17 %
Lidar block reference number: 3965

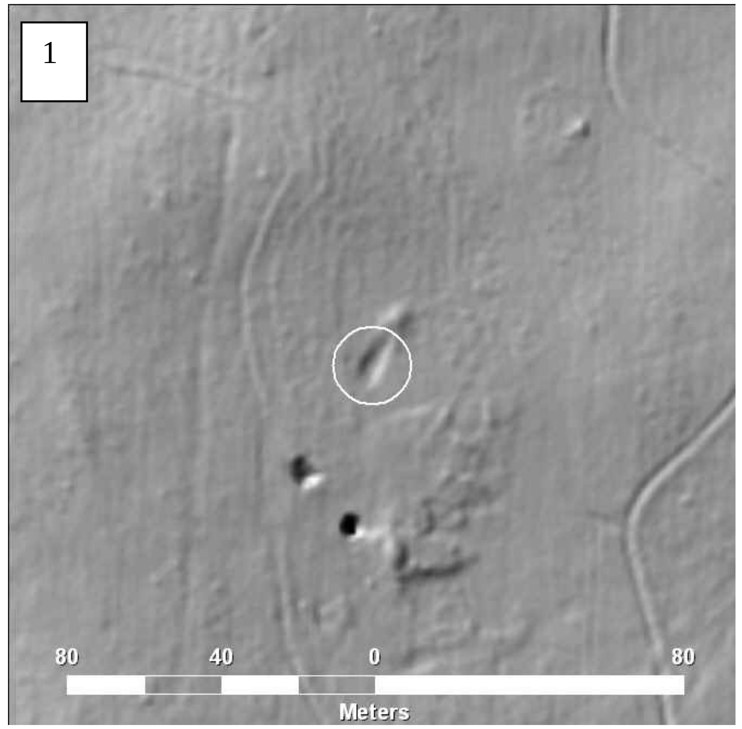

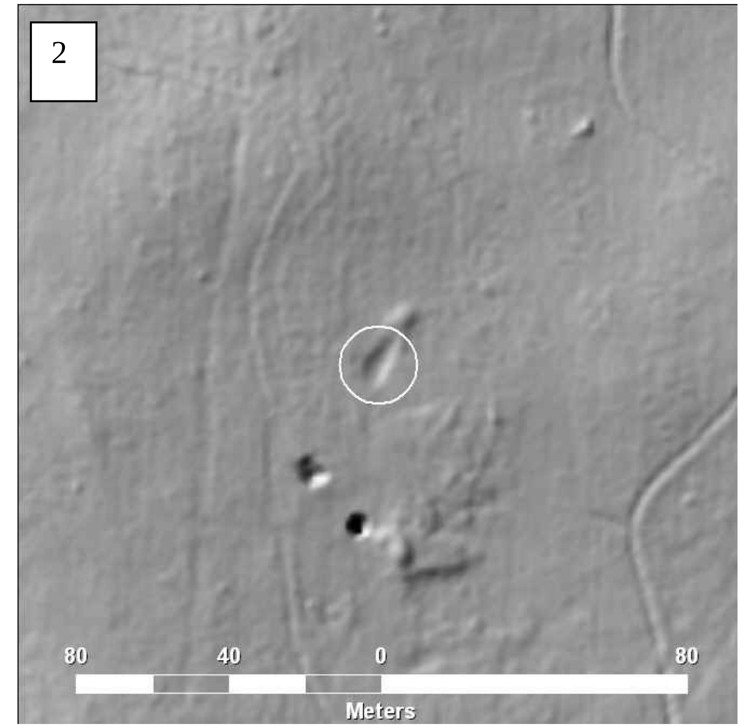

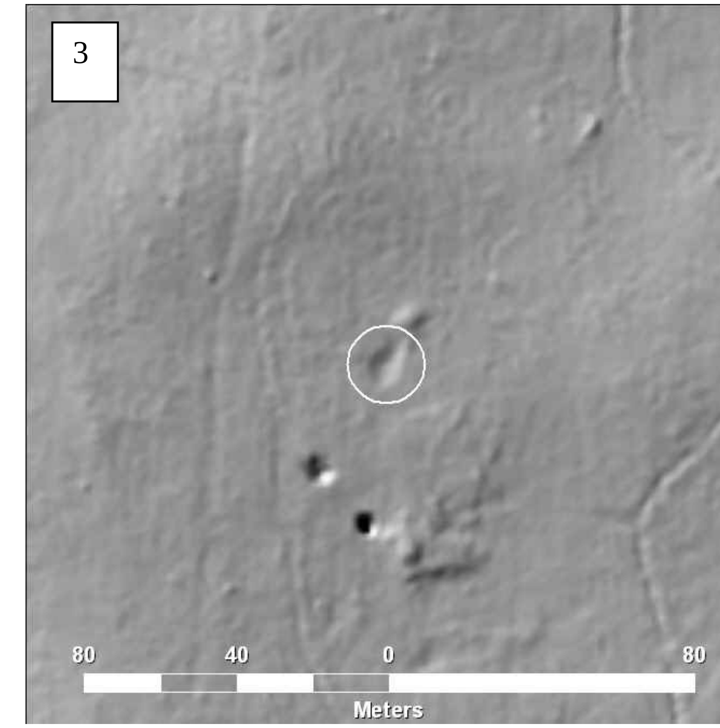

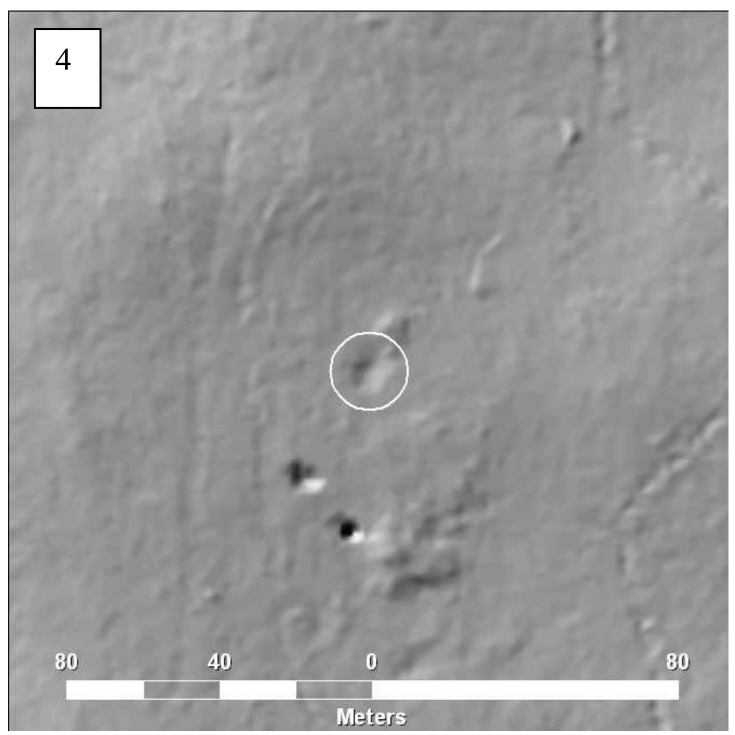

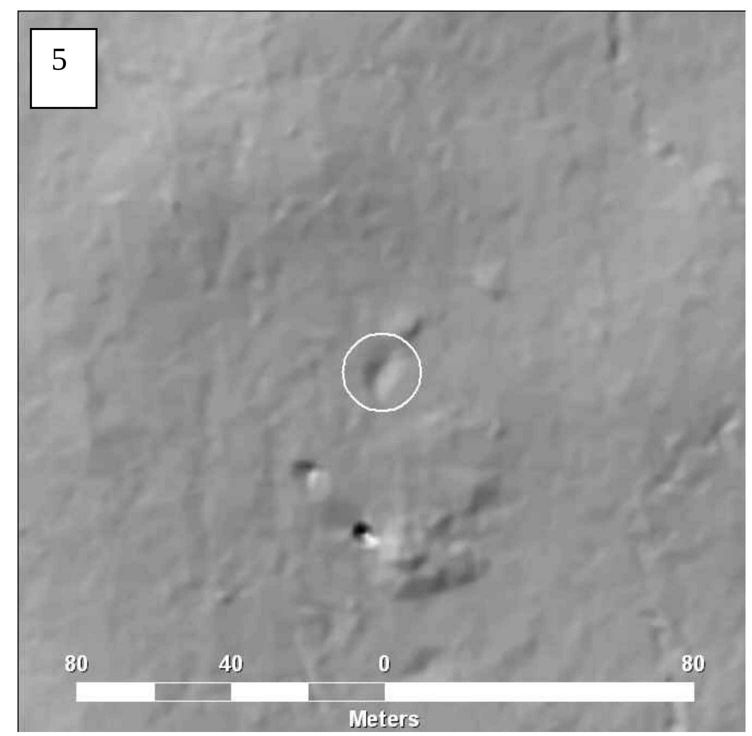

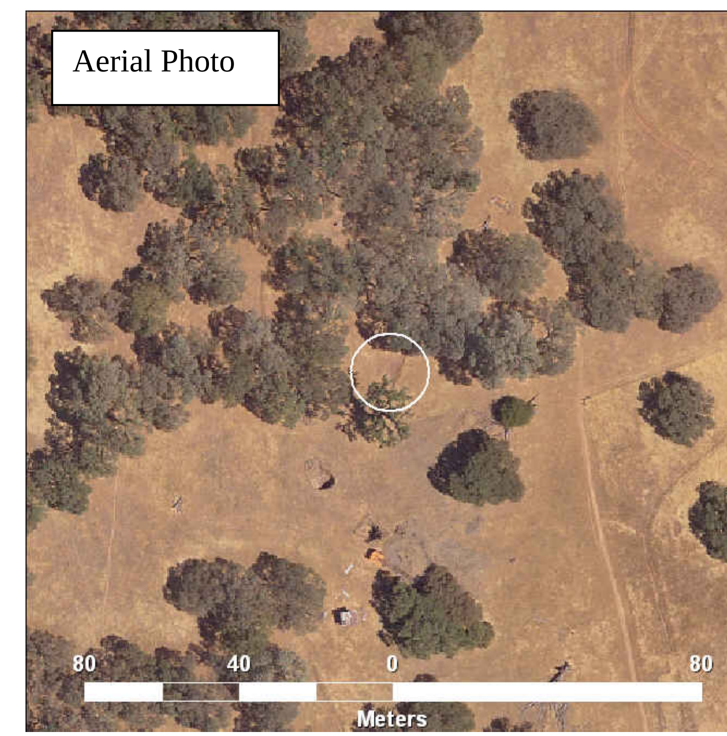

Plot # 38

Feature size: 5.3 m wide
Vegetation Density: 52.97 %
Lidar block reference number: 5644

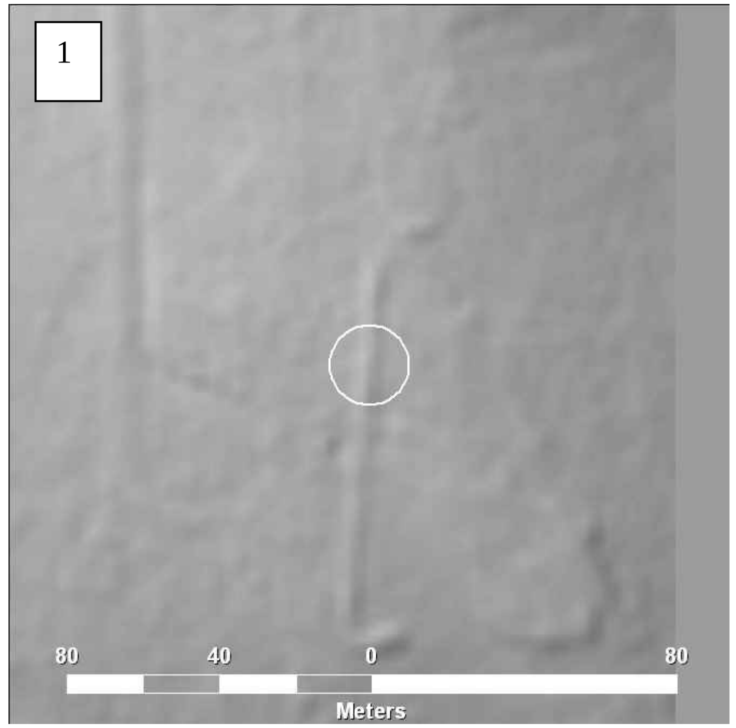

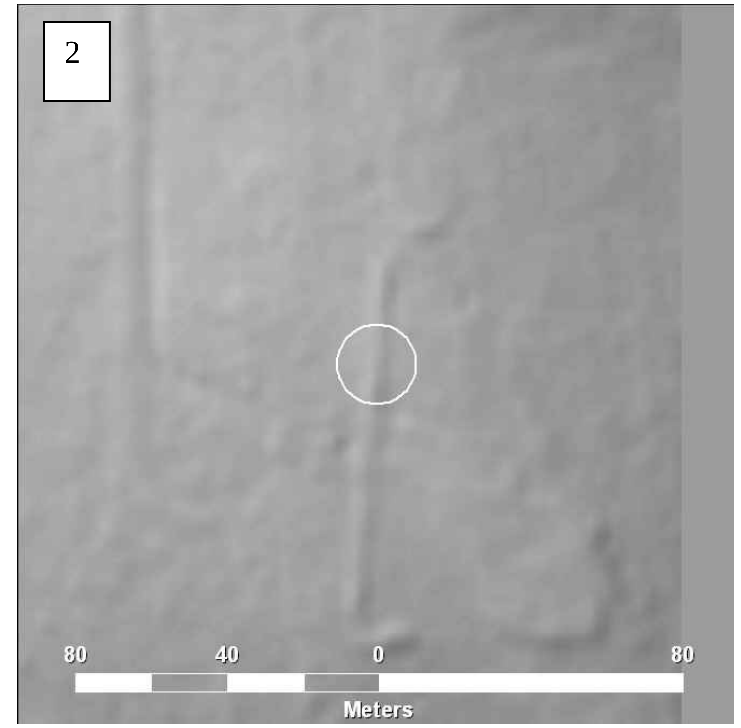

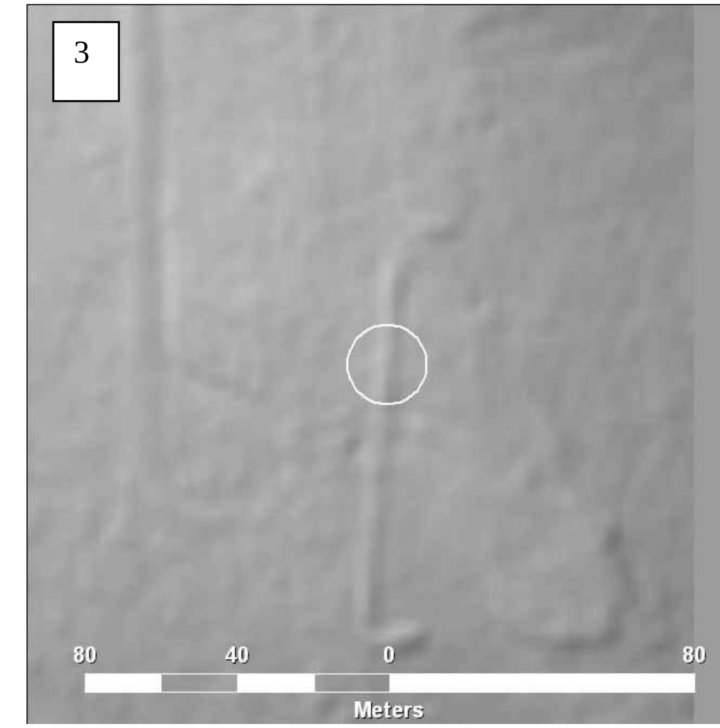

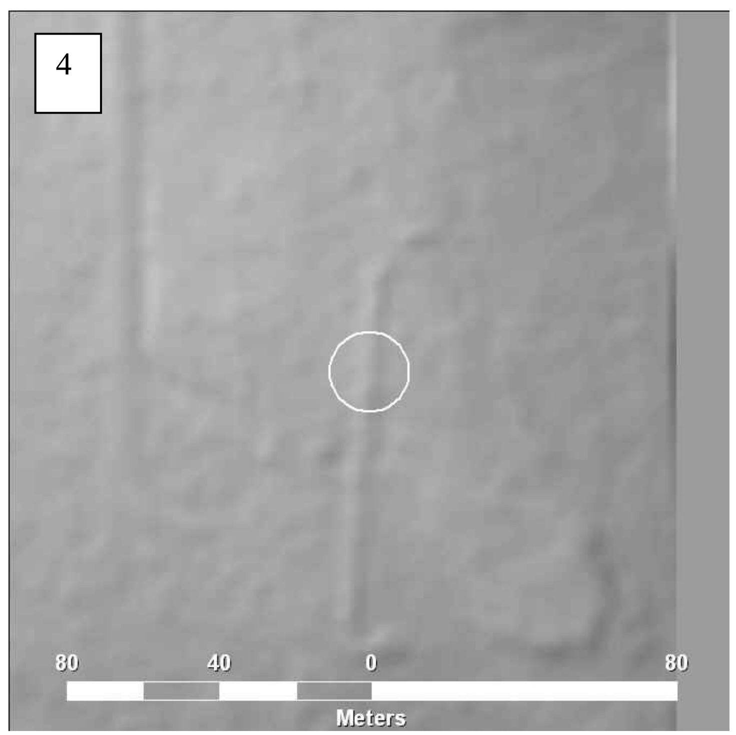

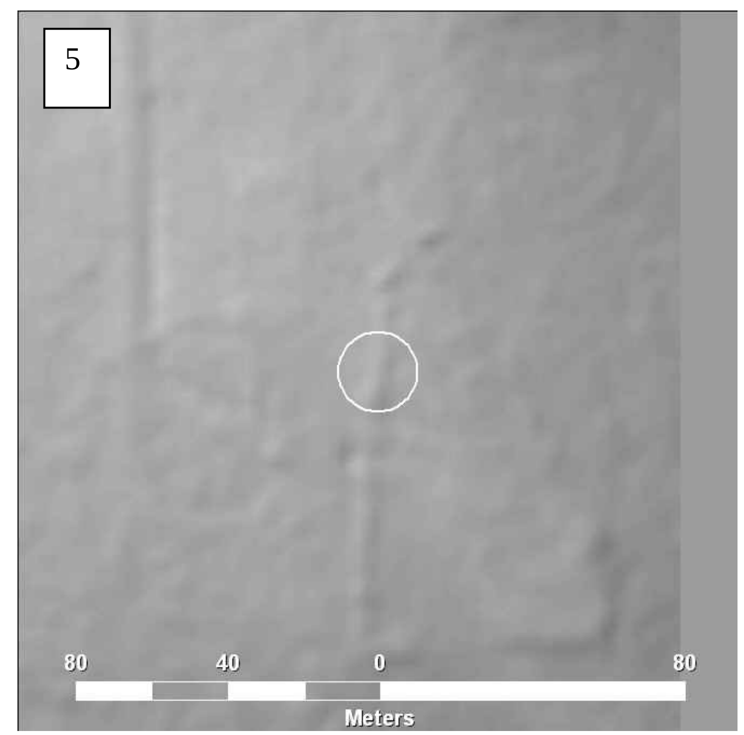

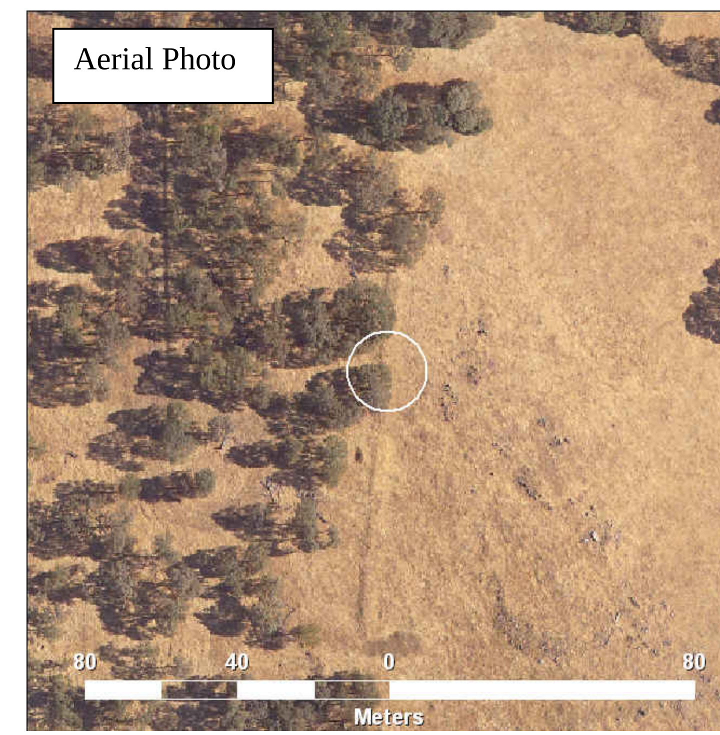

Plot # 39 Feature size: 5.3 m Vegetation Density: 51.68 % Lidar block reference number: 5675	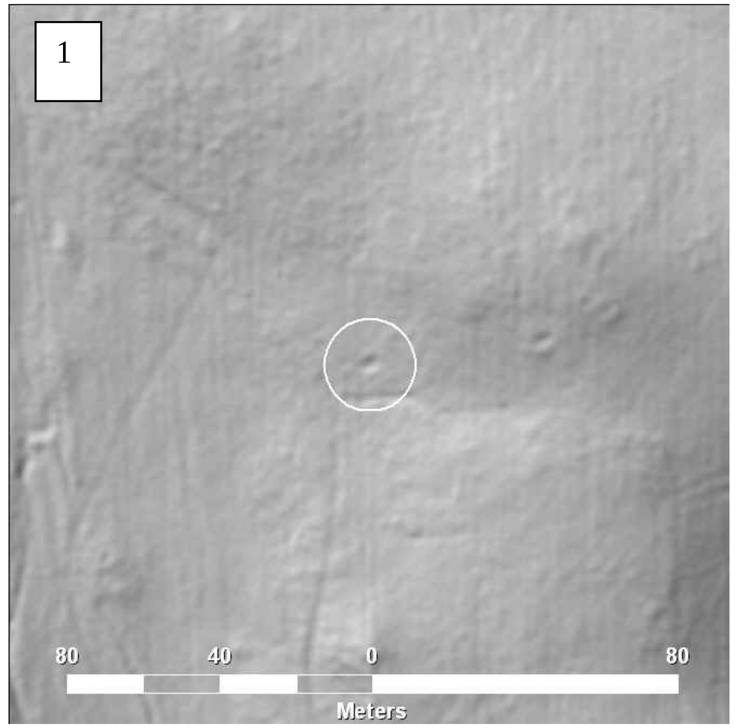	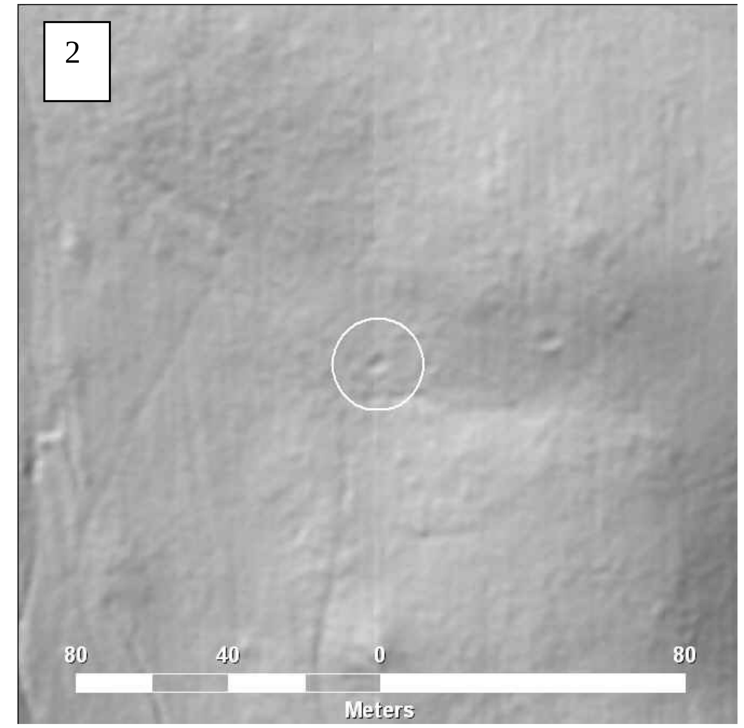	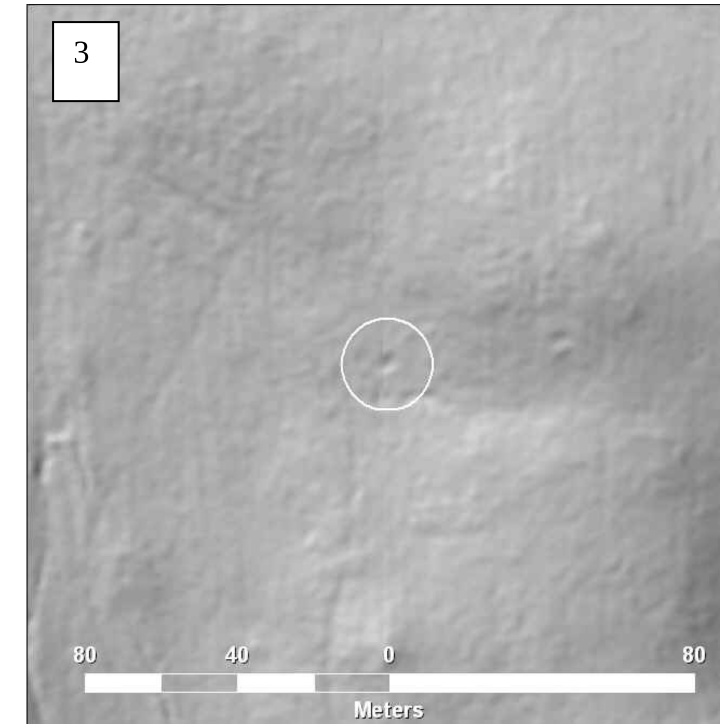
	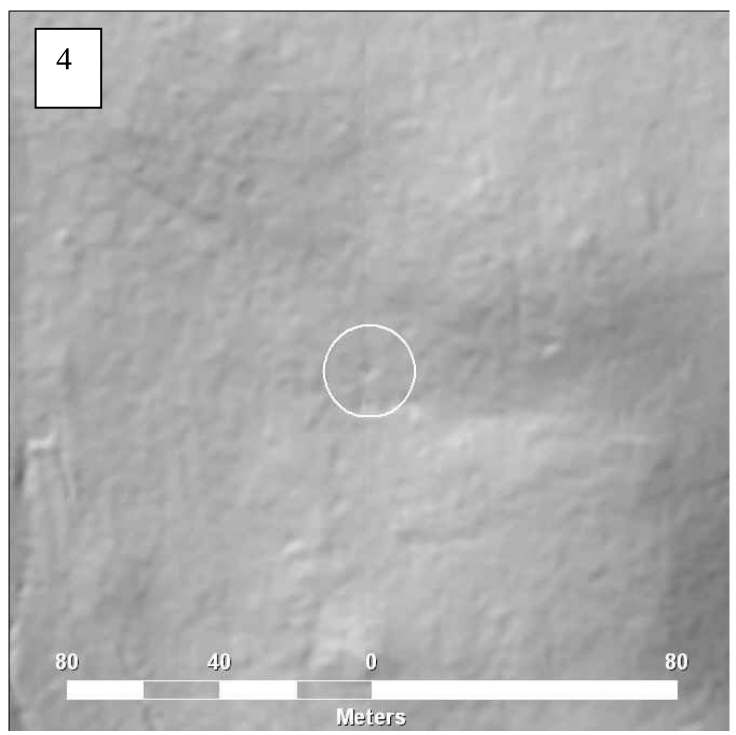	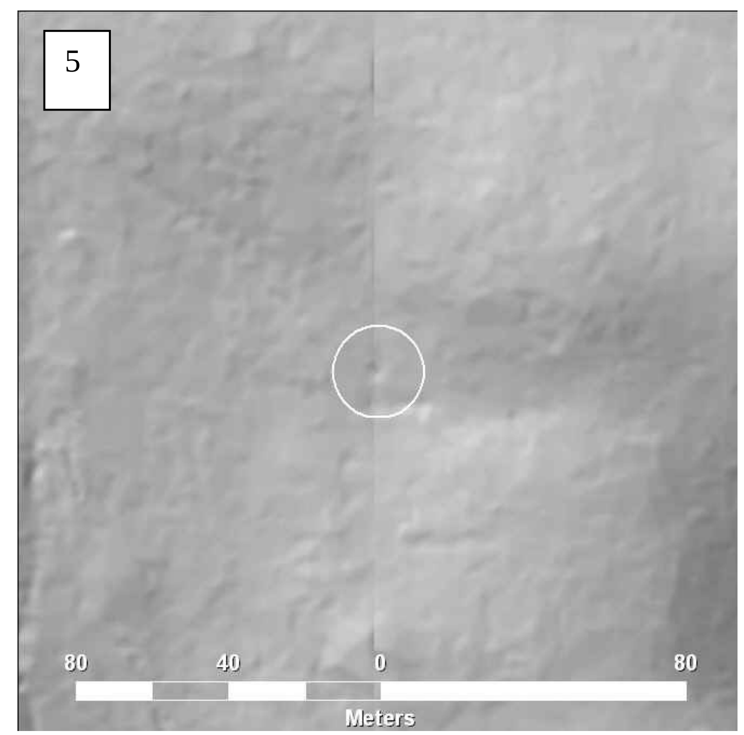	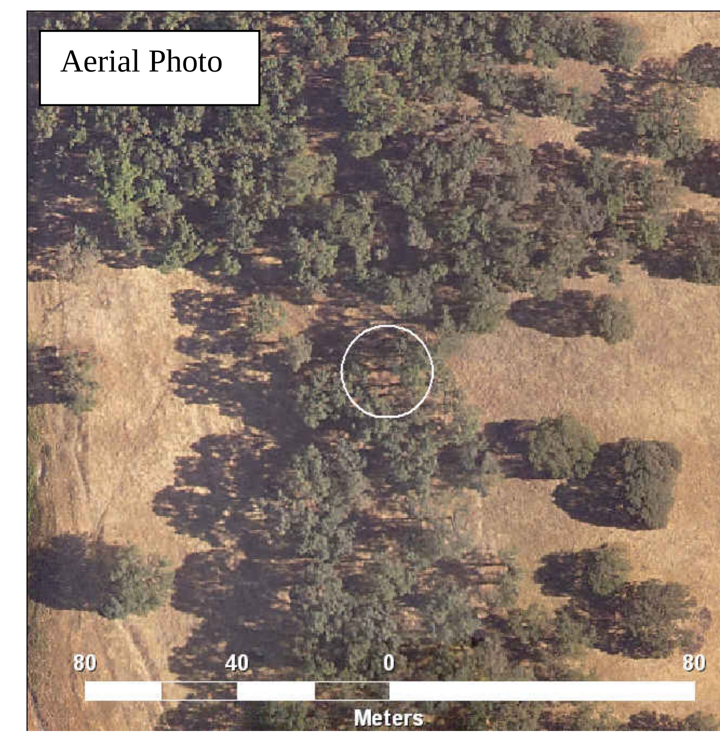

Plot # 40 Feature size: 5.6 m wide 32.1 m 14.6 m Vegetation Density: 54.89 % Lidar block reference number: 5715	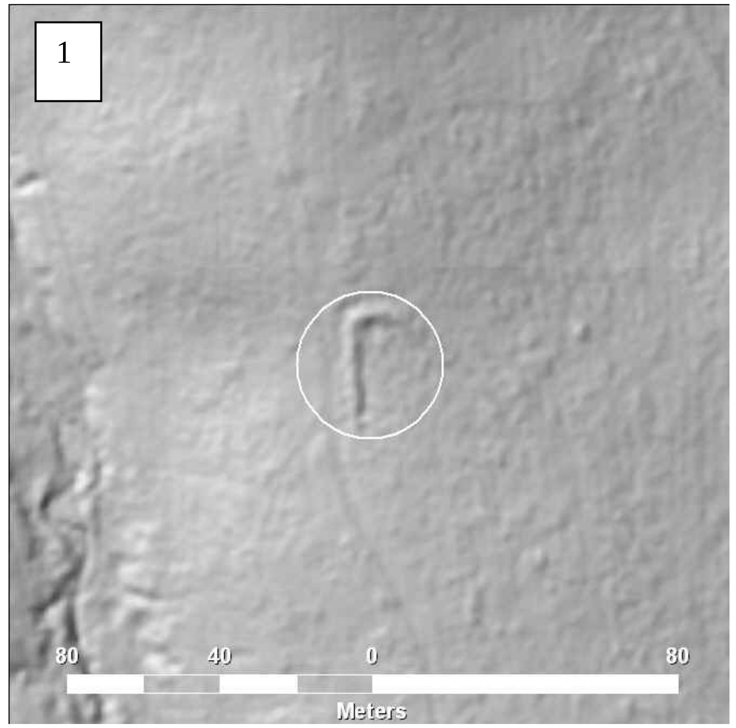	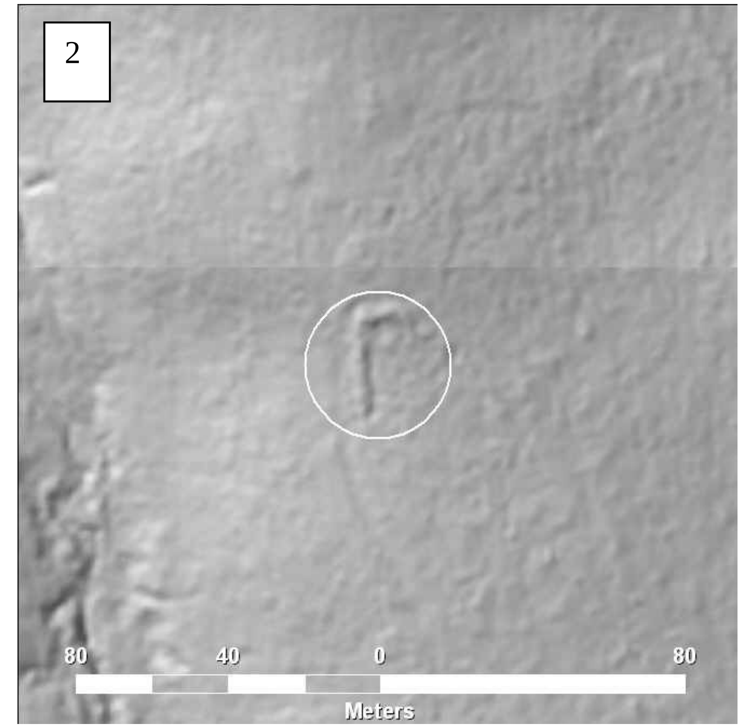	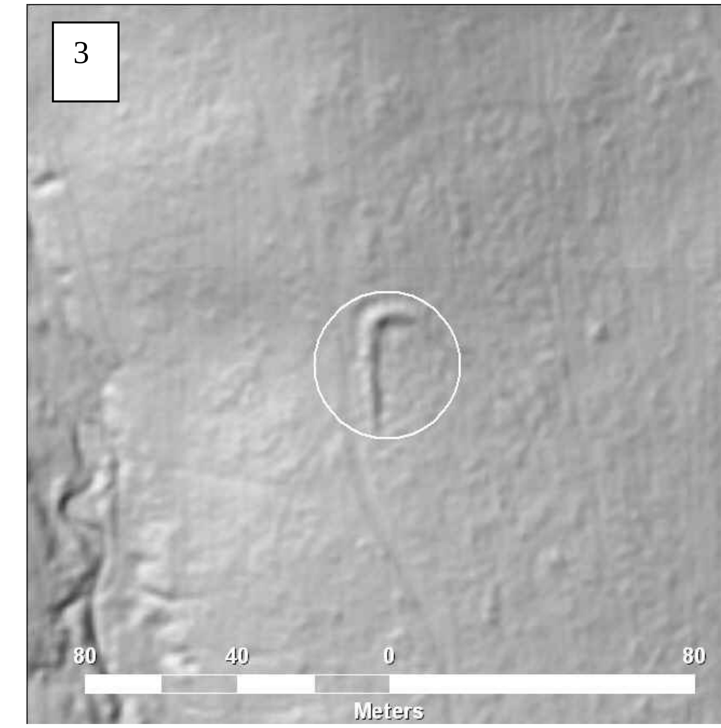
	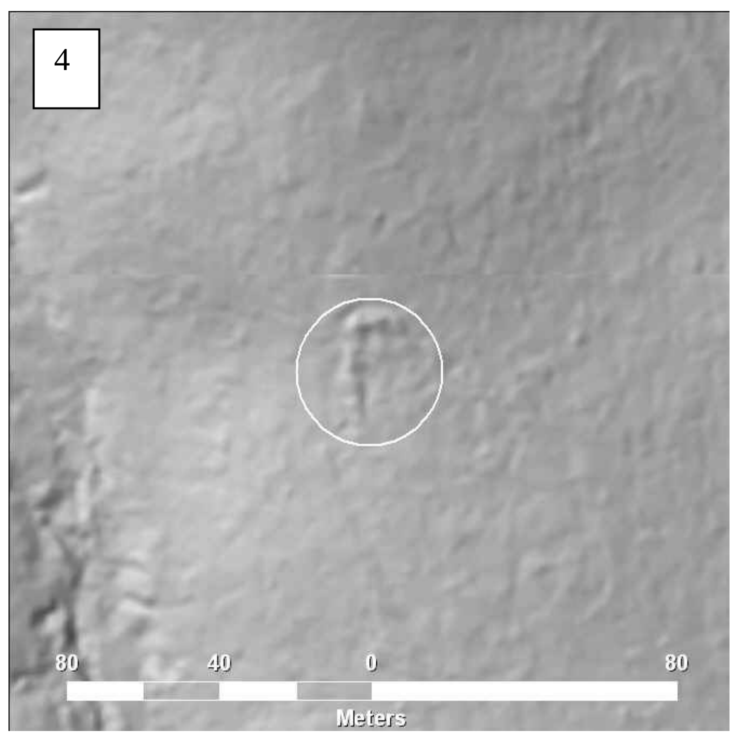	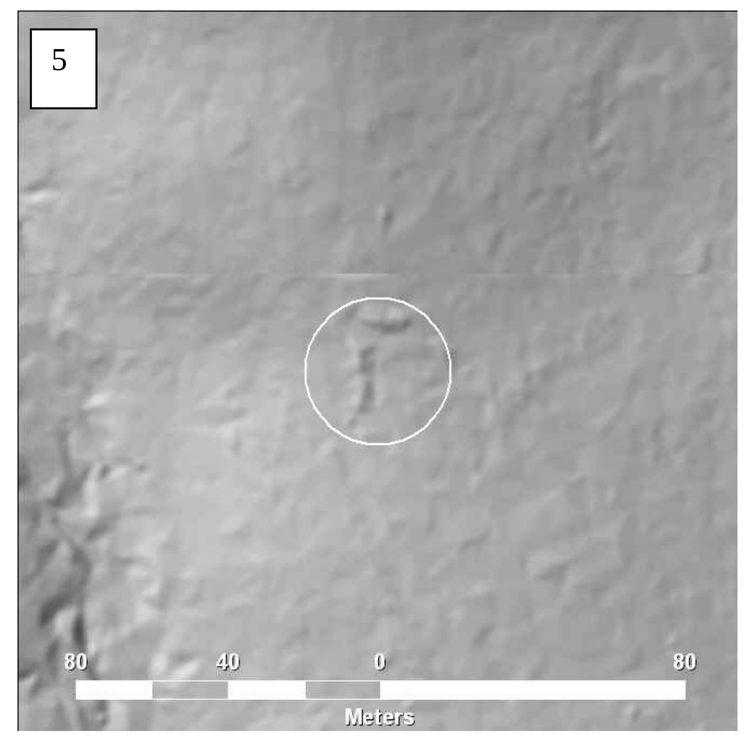	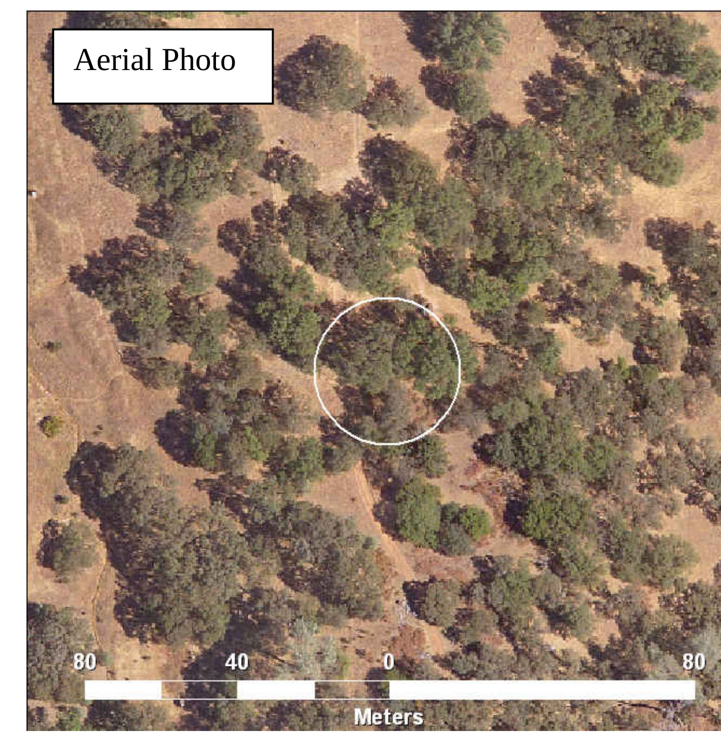

Plot # 41 Feature size: 5.8 m Vegetation Density: 37.38 % Lidar block reference number: 4033	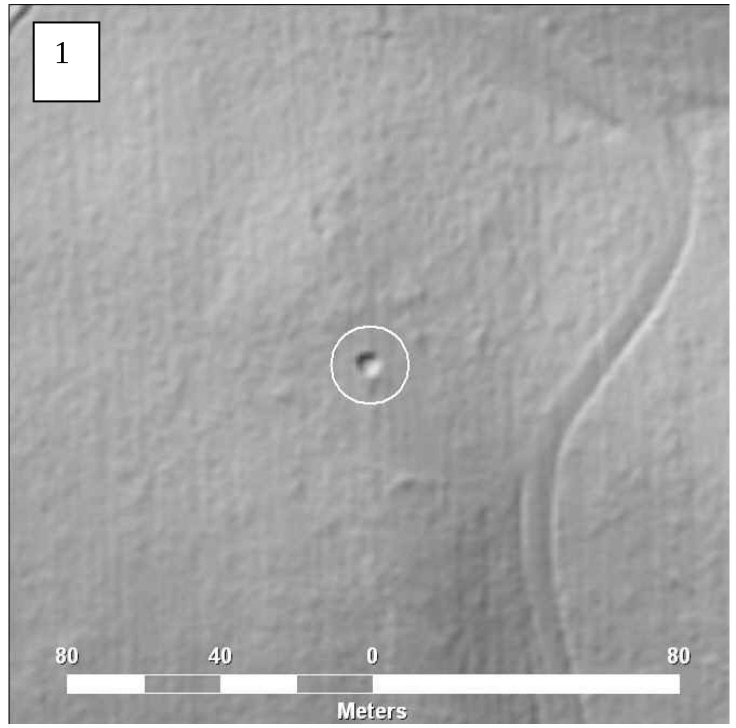	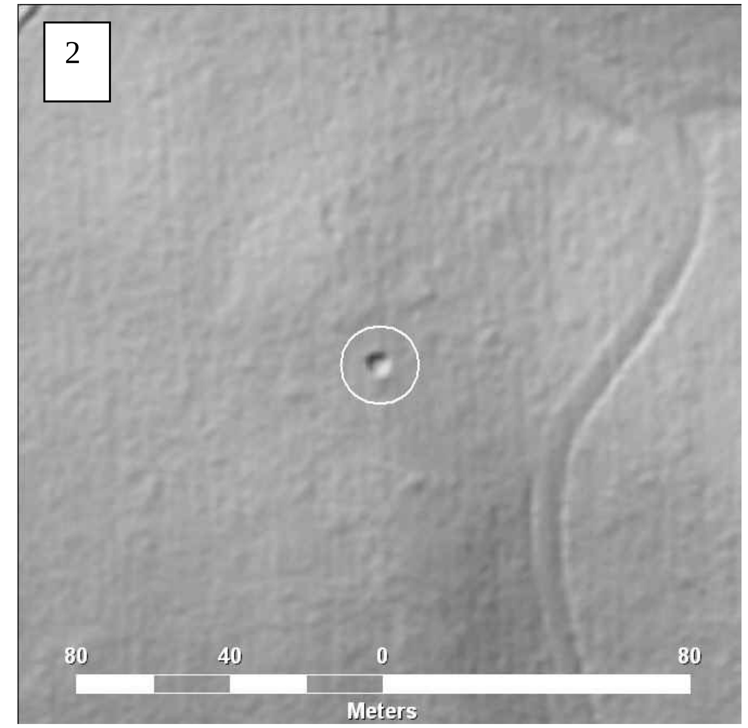	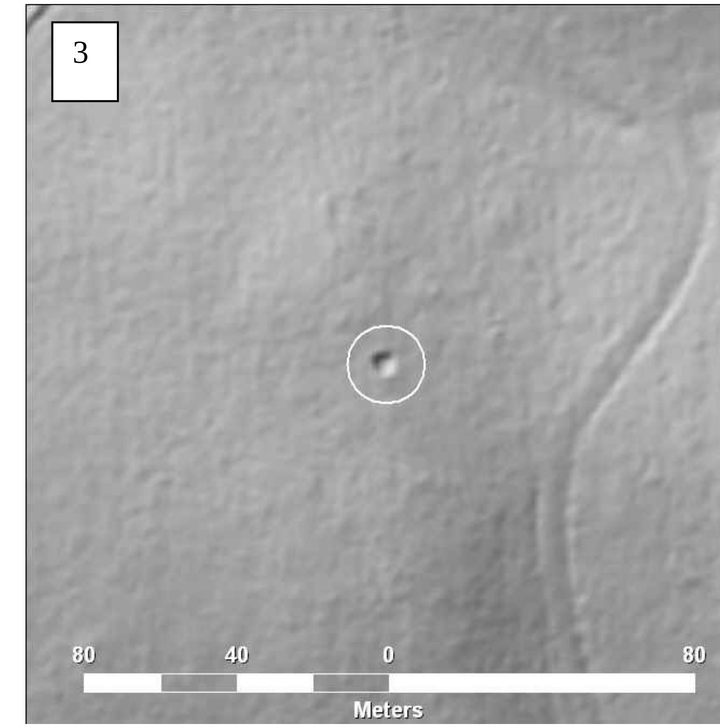
	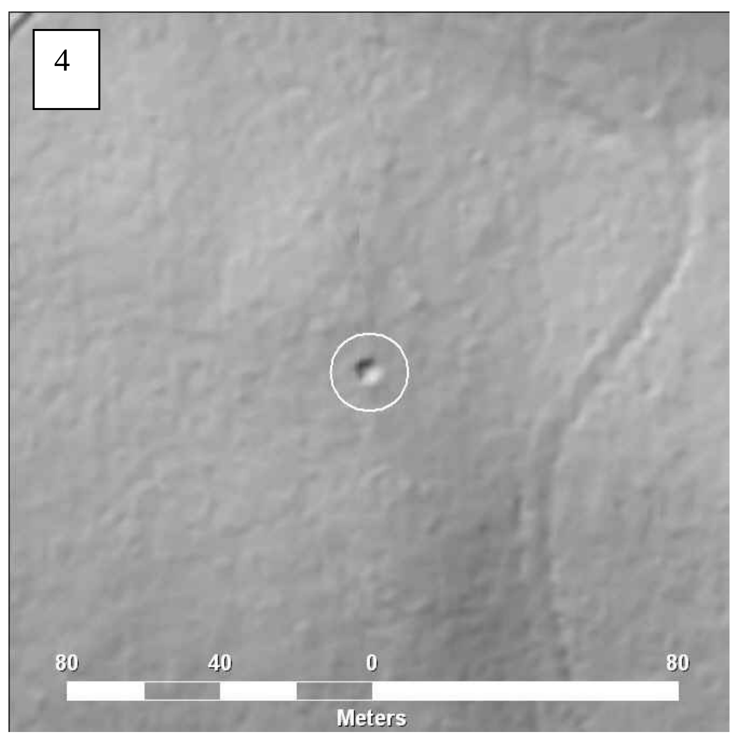	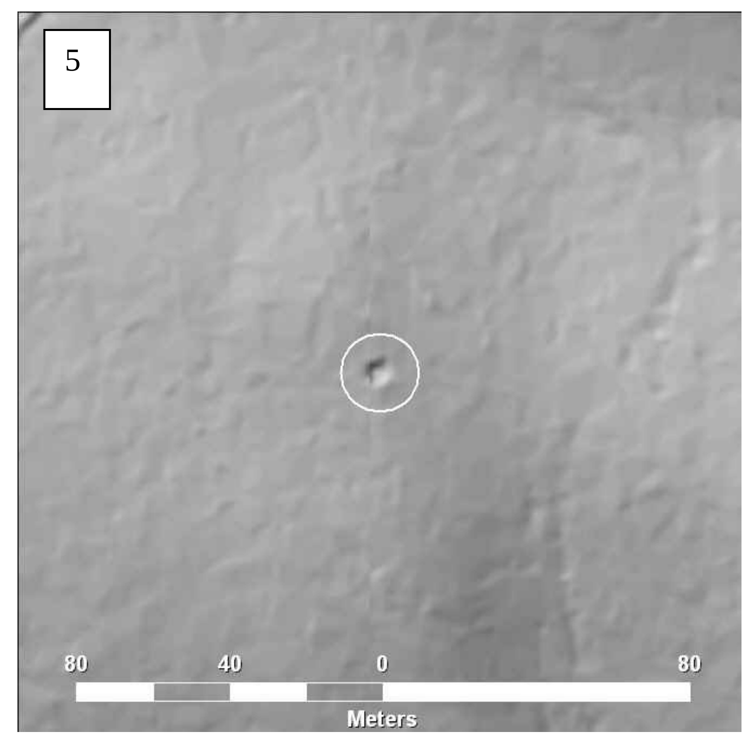	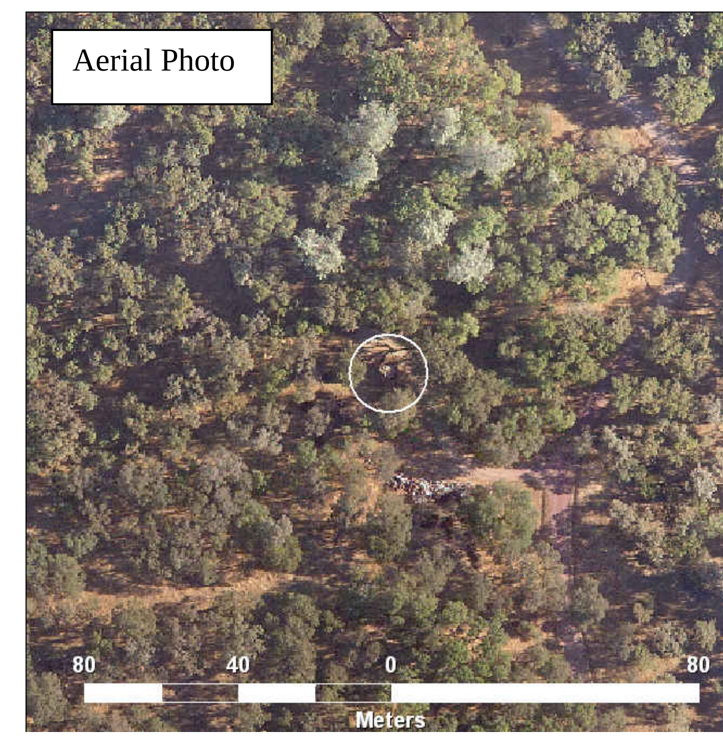

Plot # 42

Feature size: 5.8 m
Vegetation Density: 47.04 %
Lidar block reference number: 5717

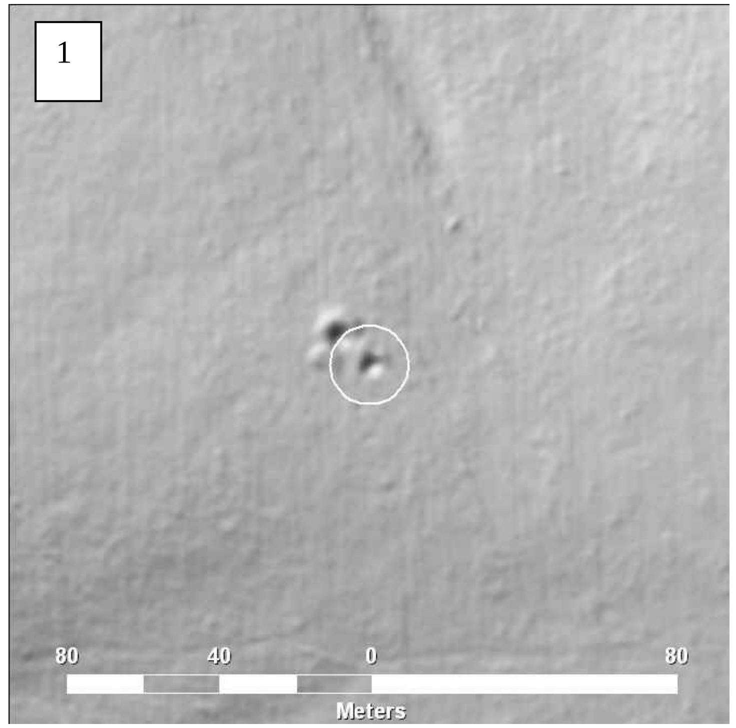

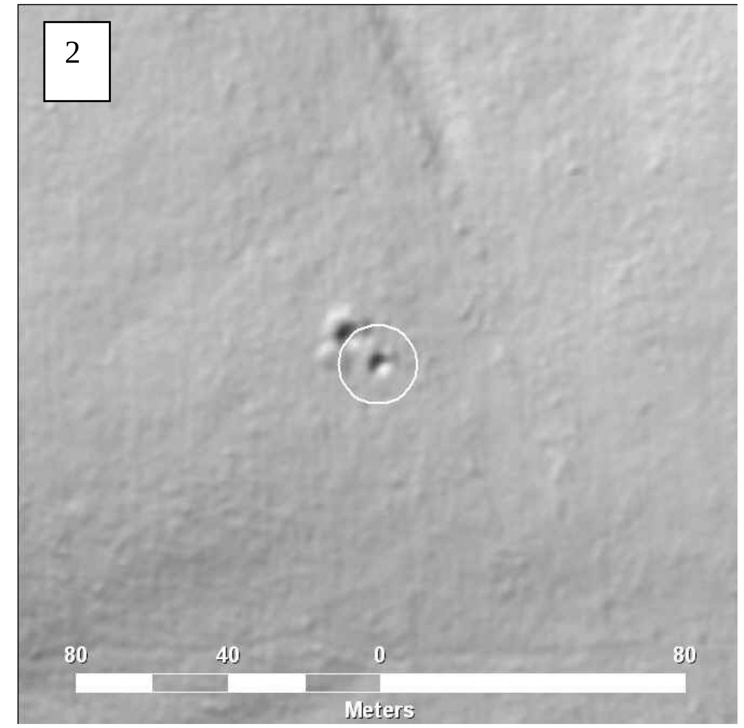

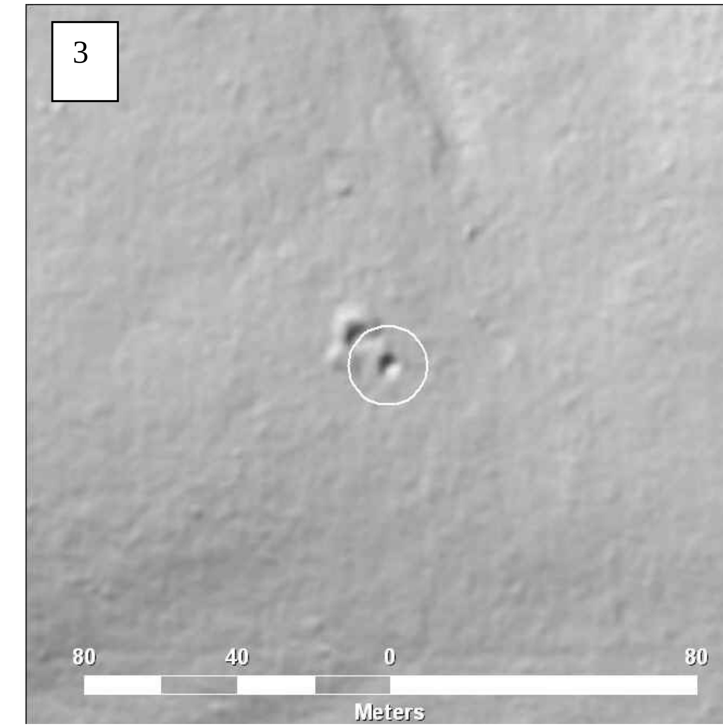

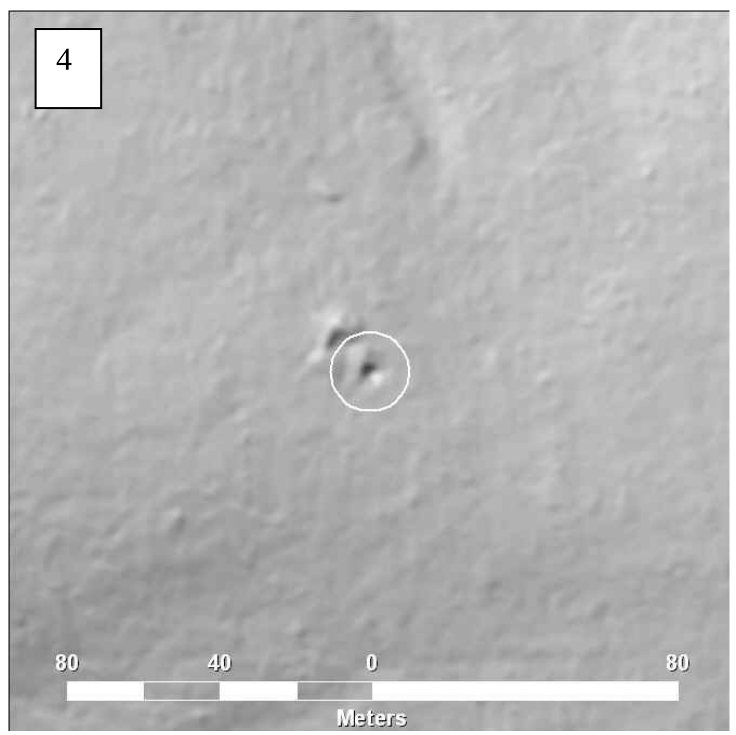

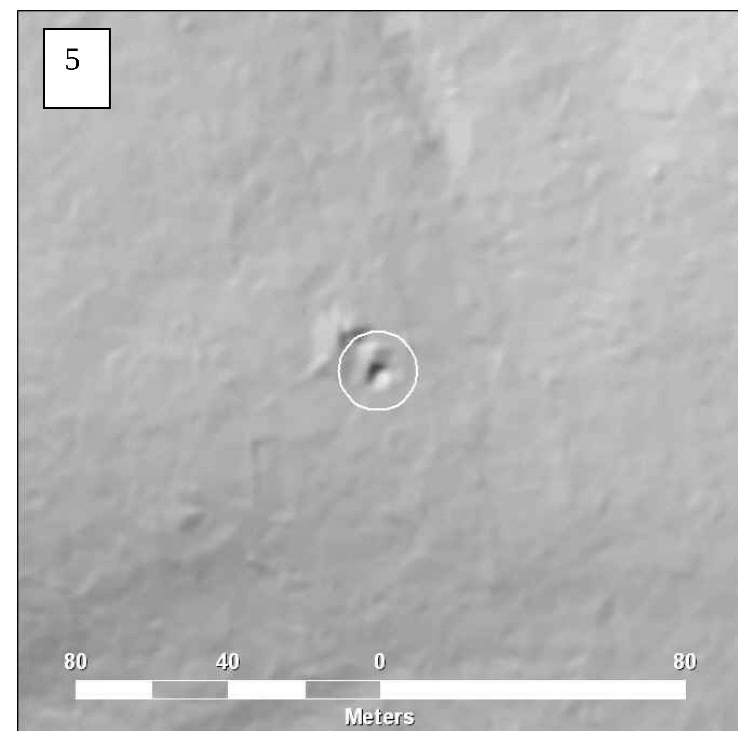

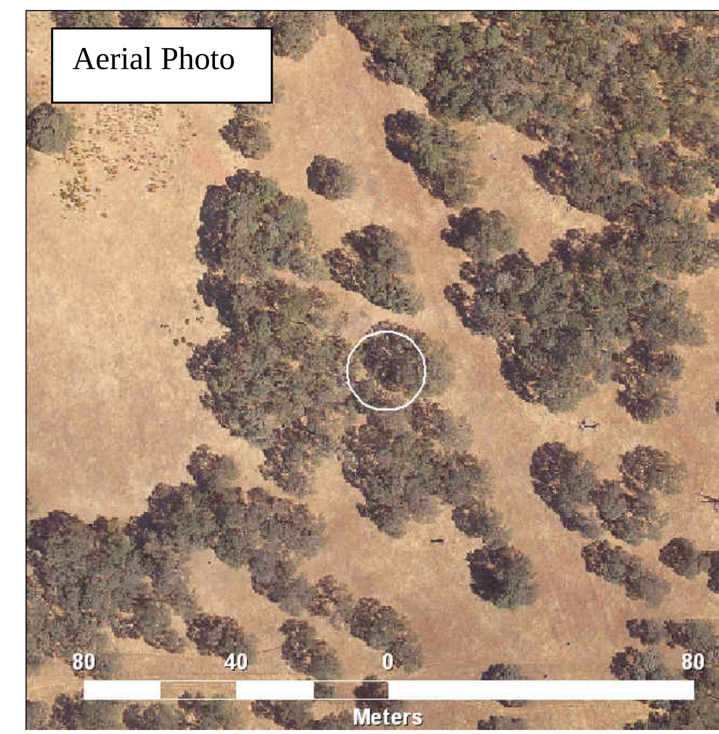

Plot # 43

Feature size: 6.2 m
Vegetation Density: 51.12 %
Lidar block reference number: 5613

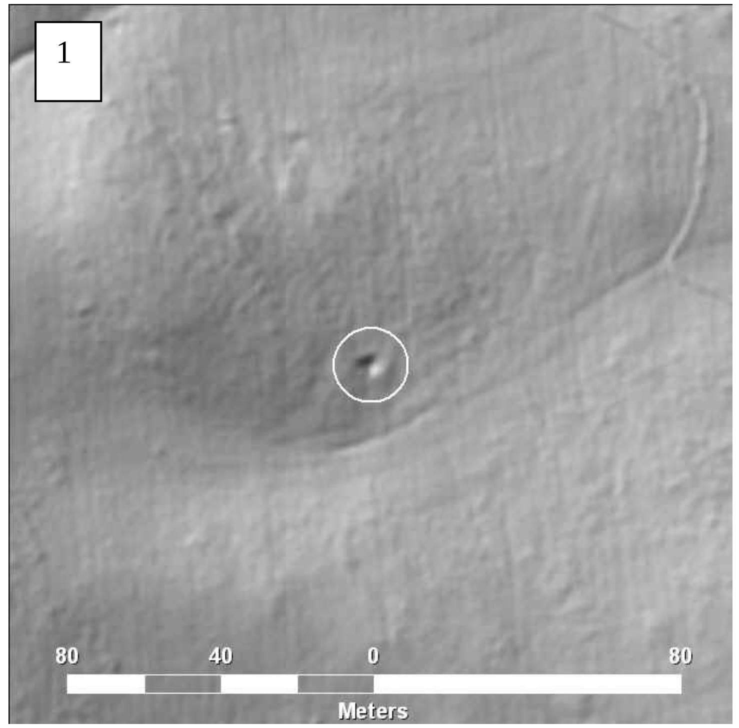

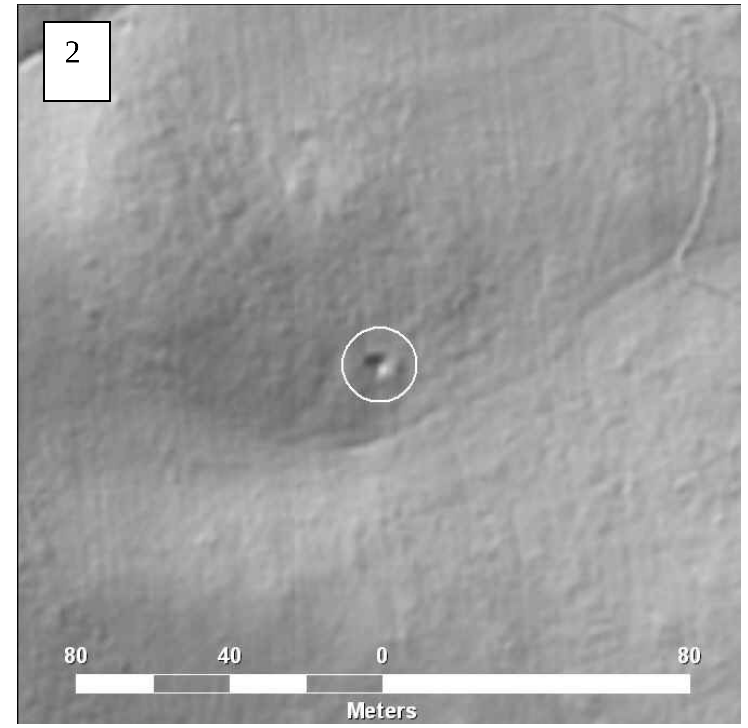

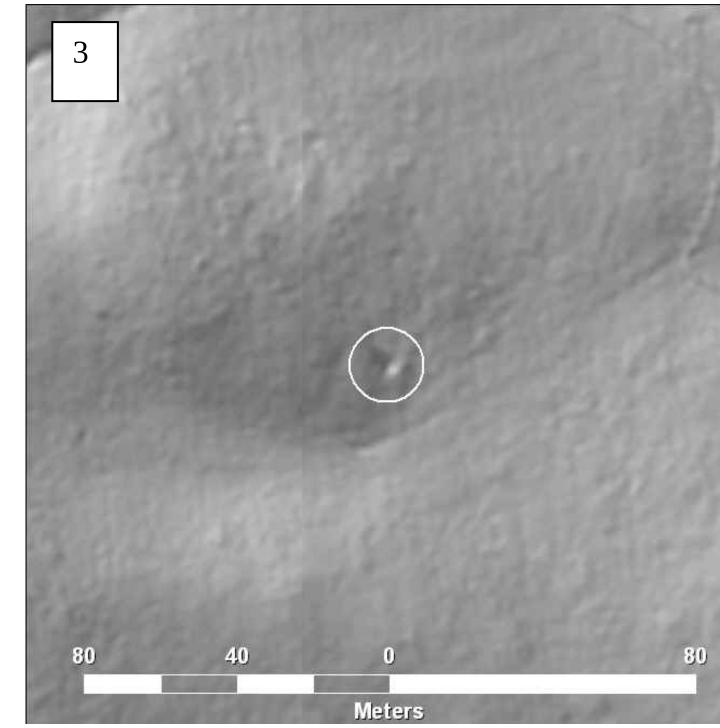

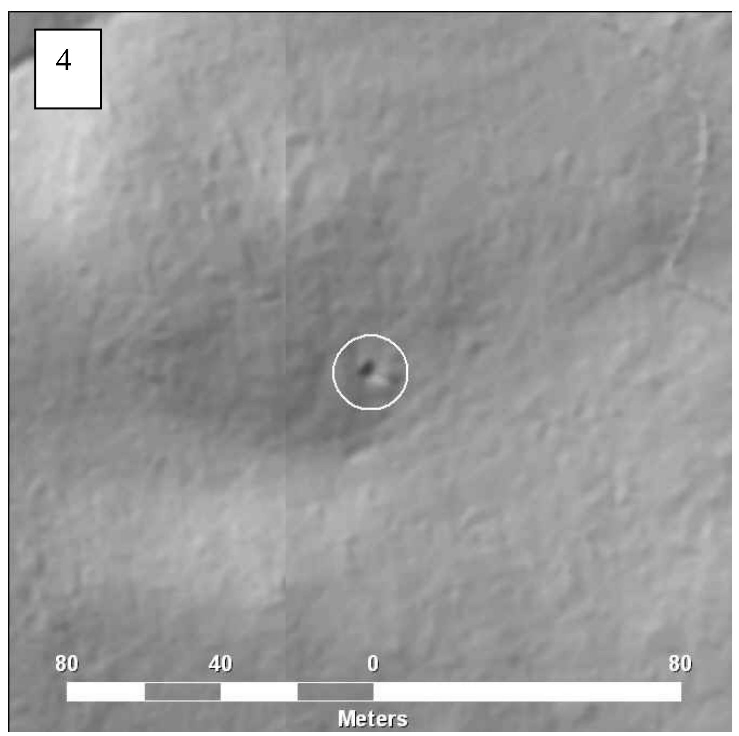

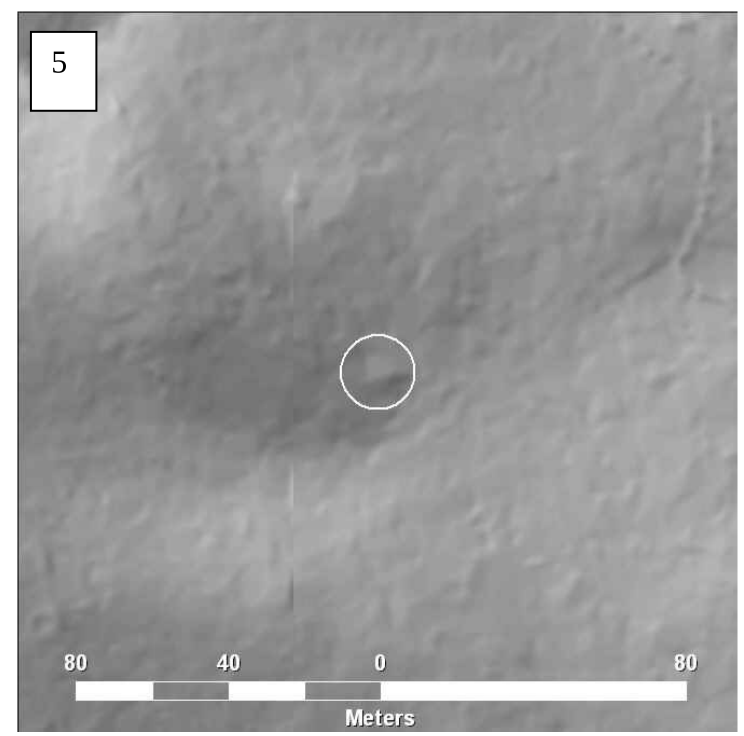

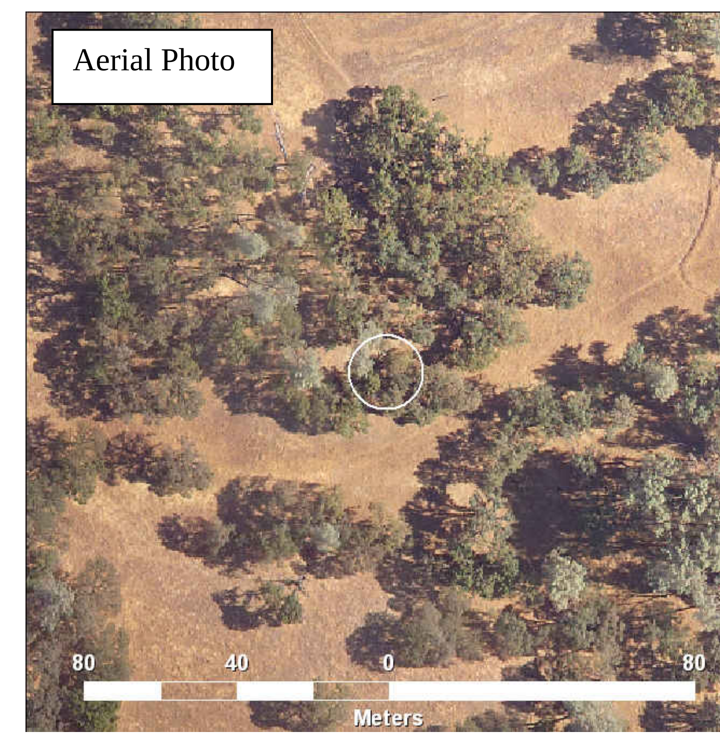

Plot # 44

Feature size: 6.3 m
4.3 m
Vegetation Density: 67.05 %
Lidar block reference number: 5350

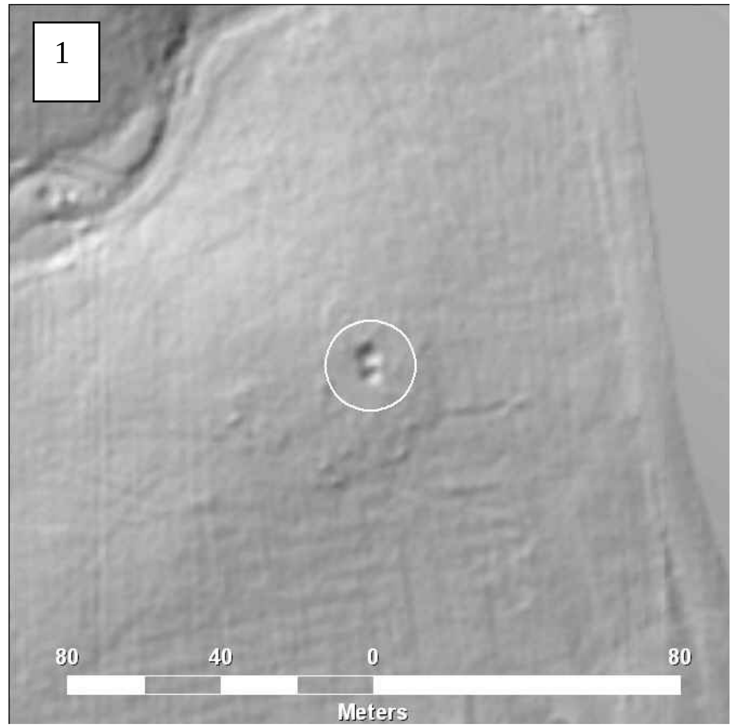

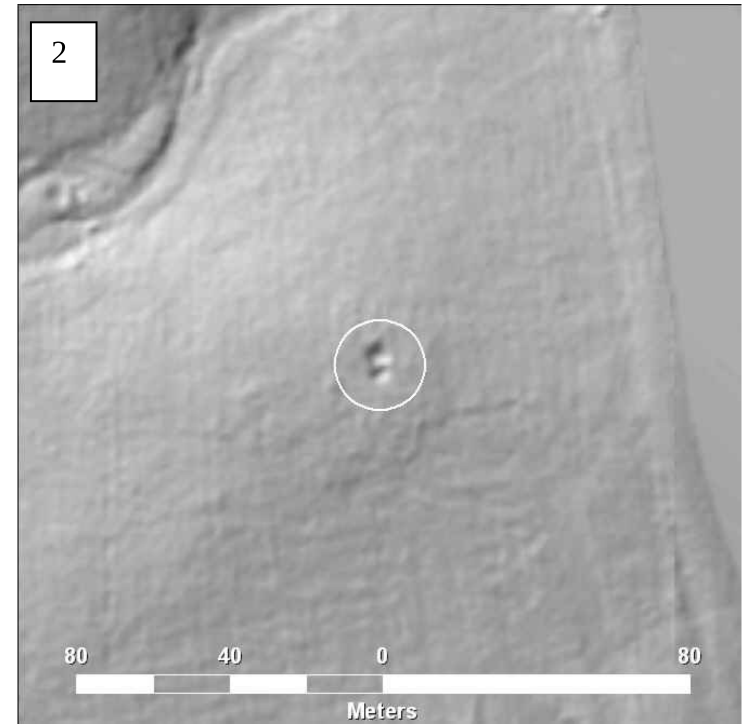

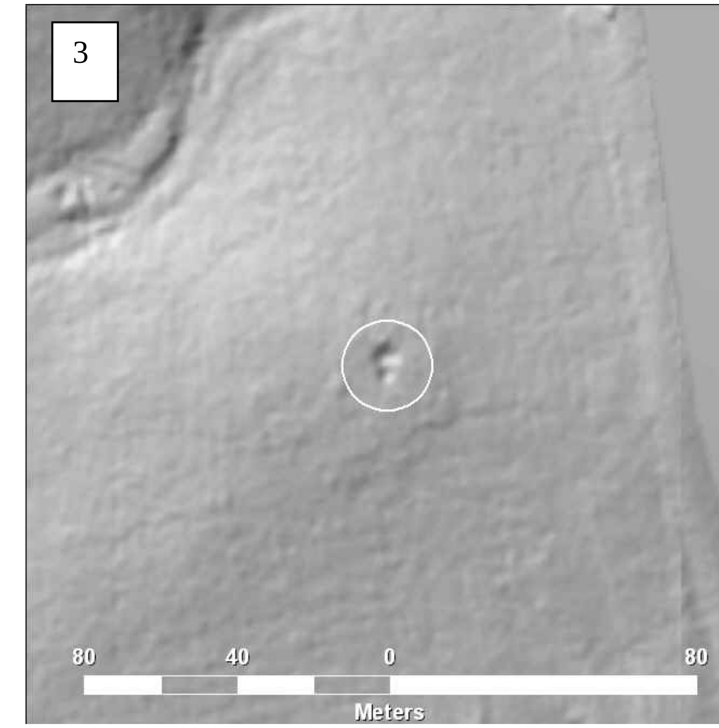

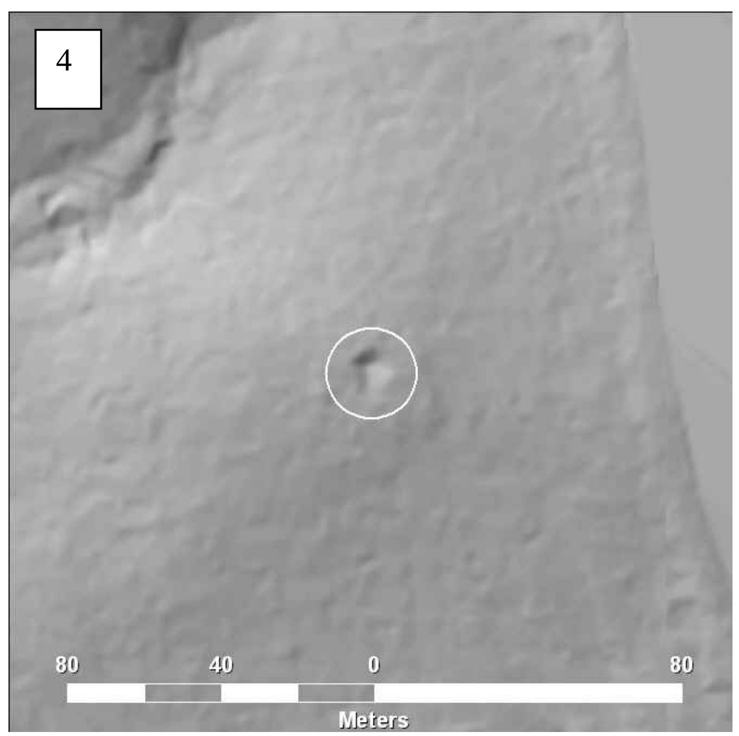

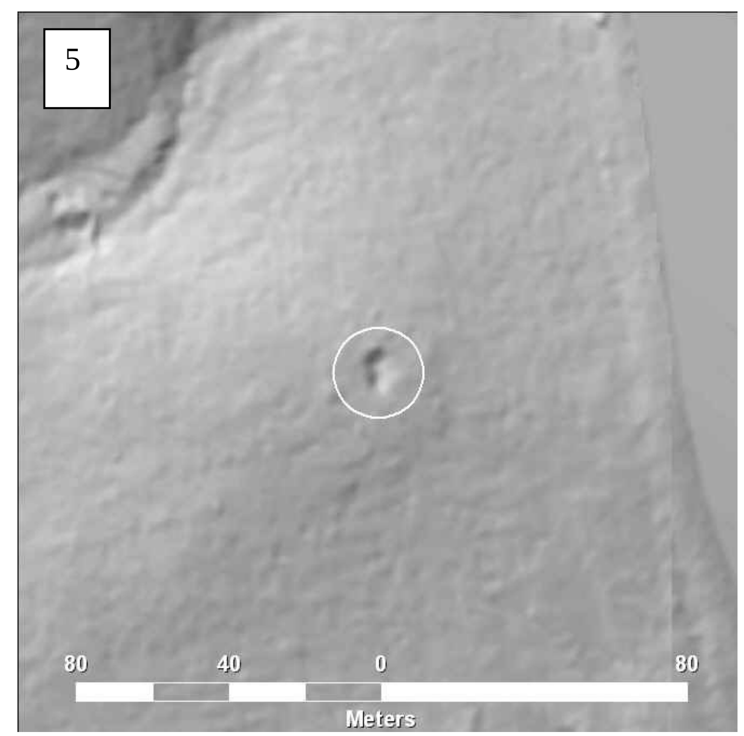

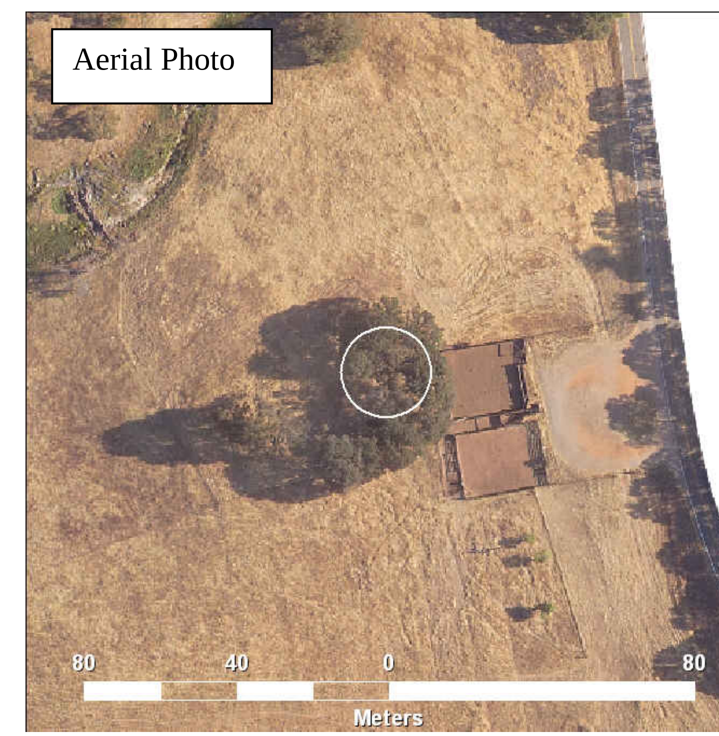

Plot # 45

Feature size: 12 m
6.5 m
Vegetation Density: 47.48 %
Lidar block reference number: 5678

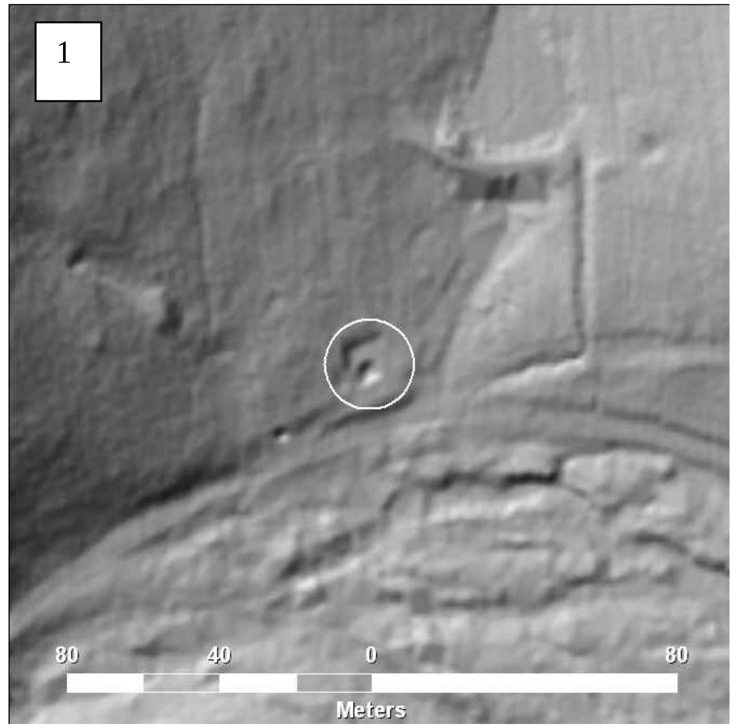

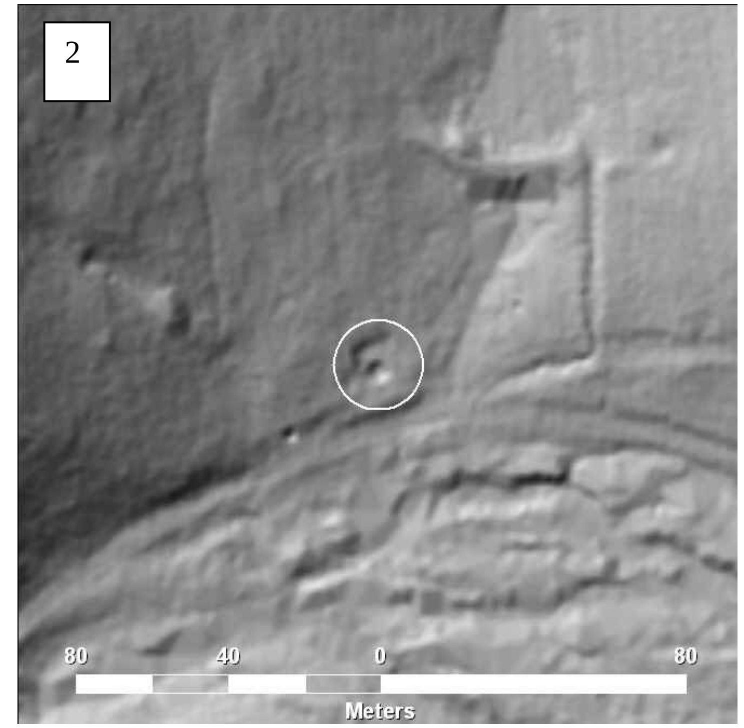

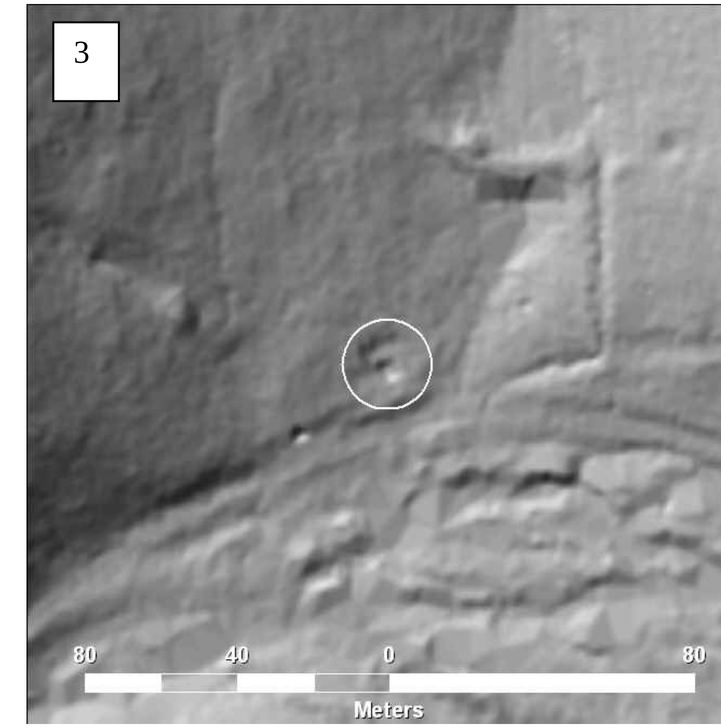

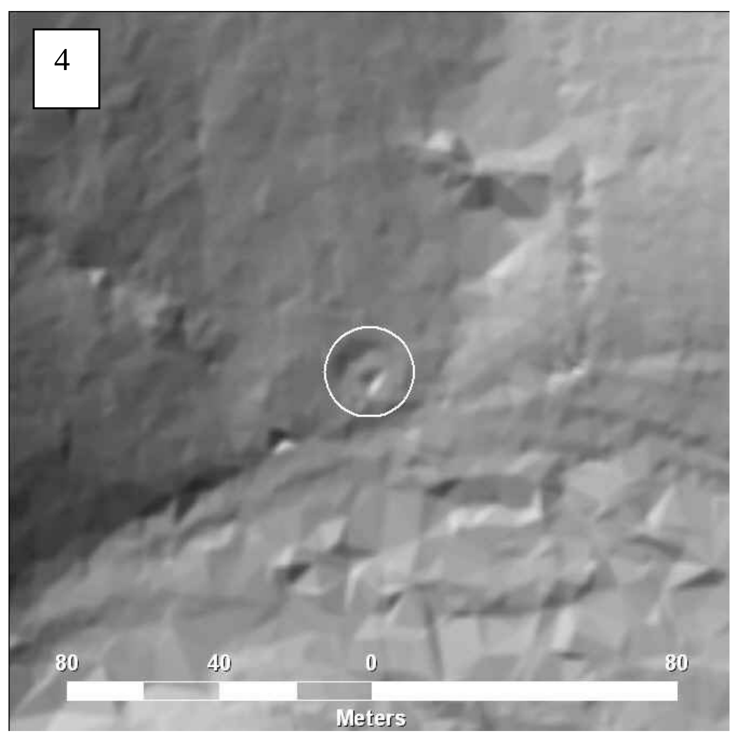

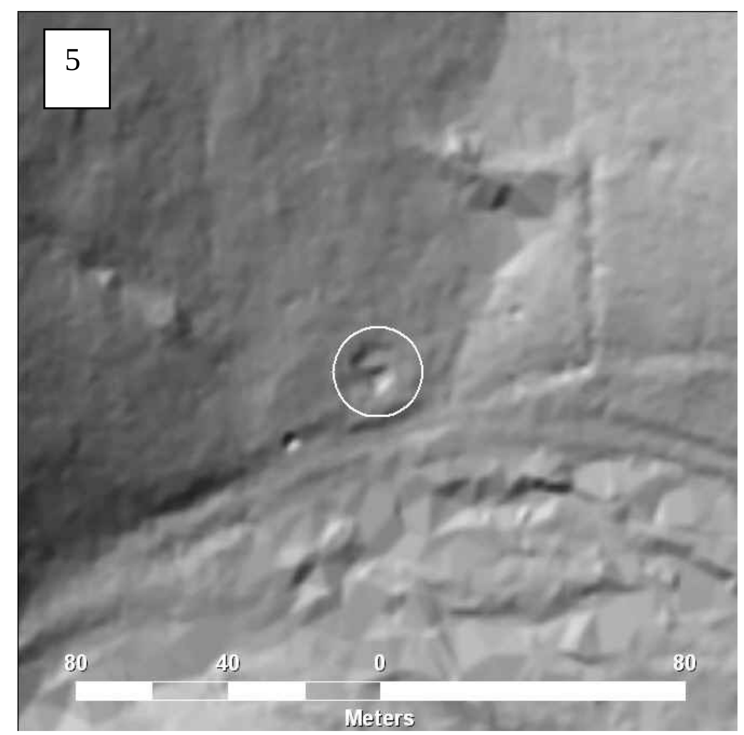

Plot # 46

Feature size: 7.1 m
Vegetation Density: 44.58 %
Lidar block reference number: 3975

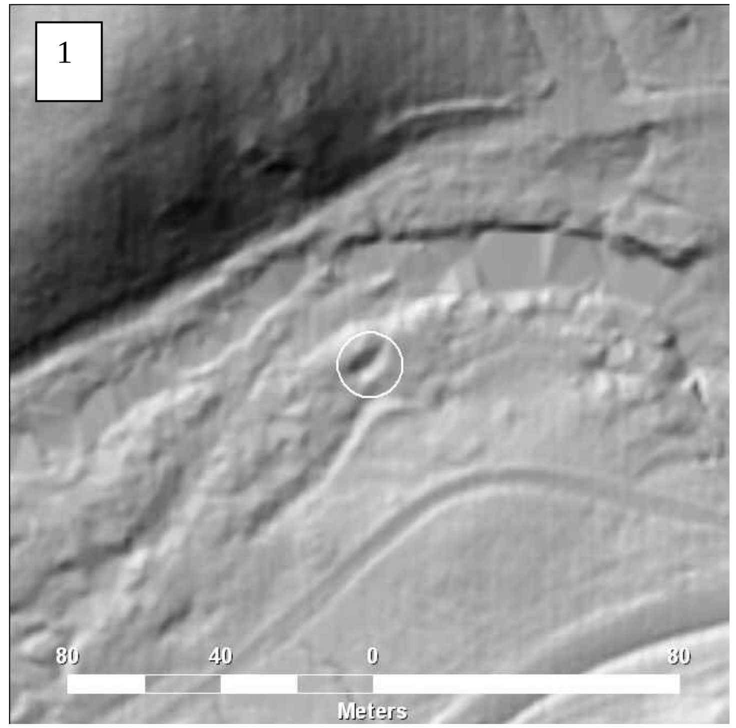

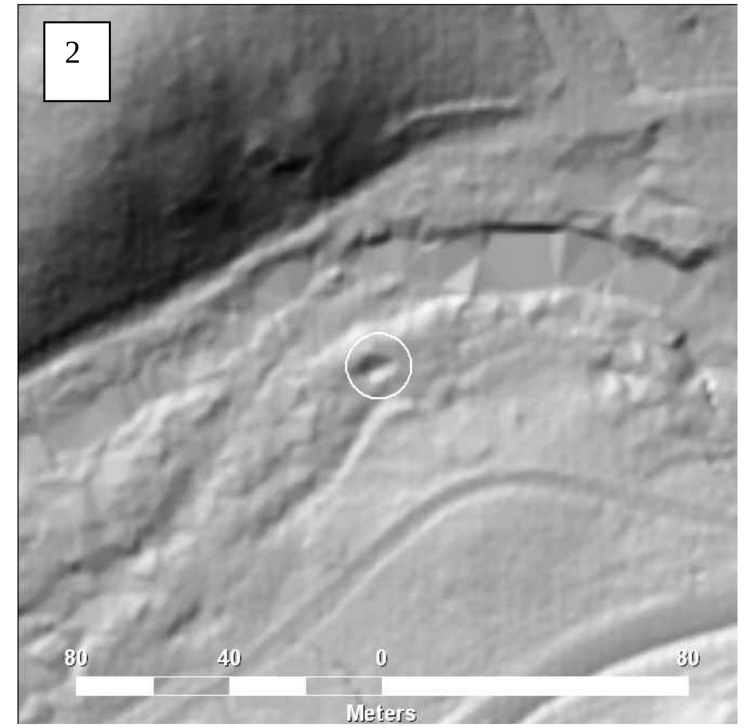

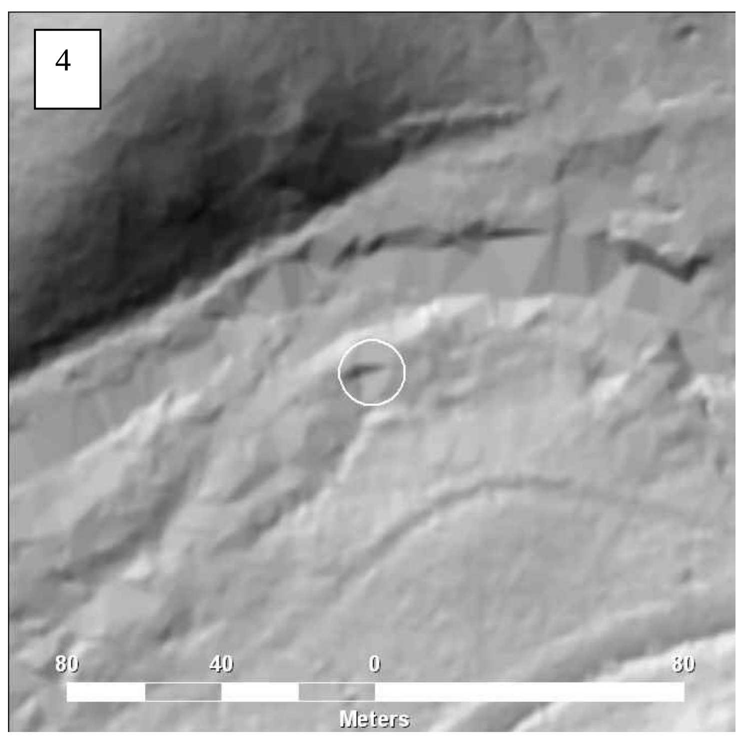

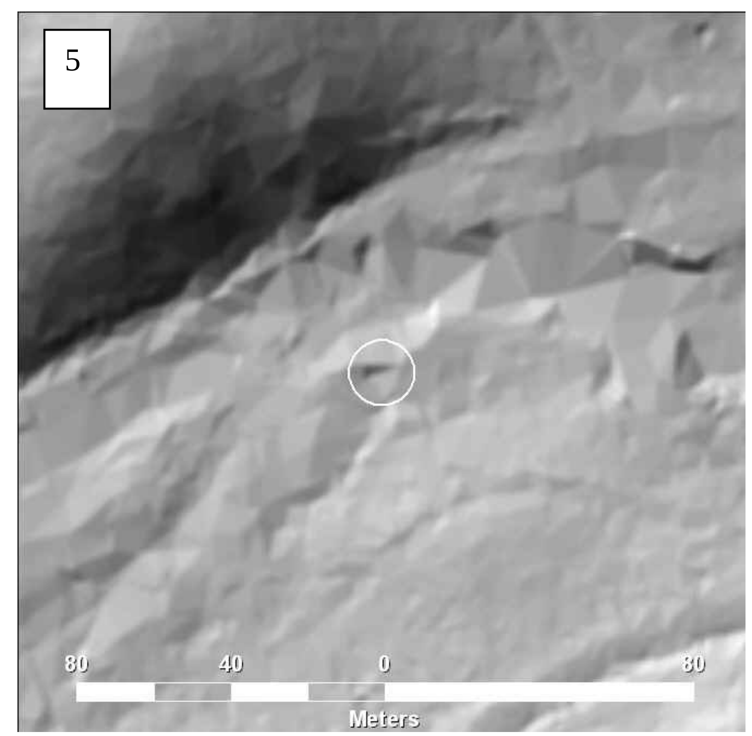

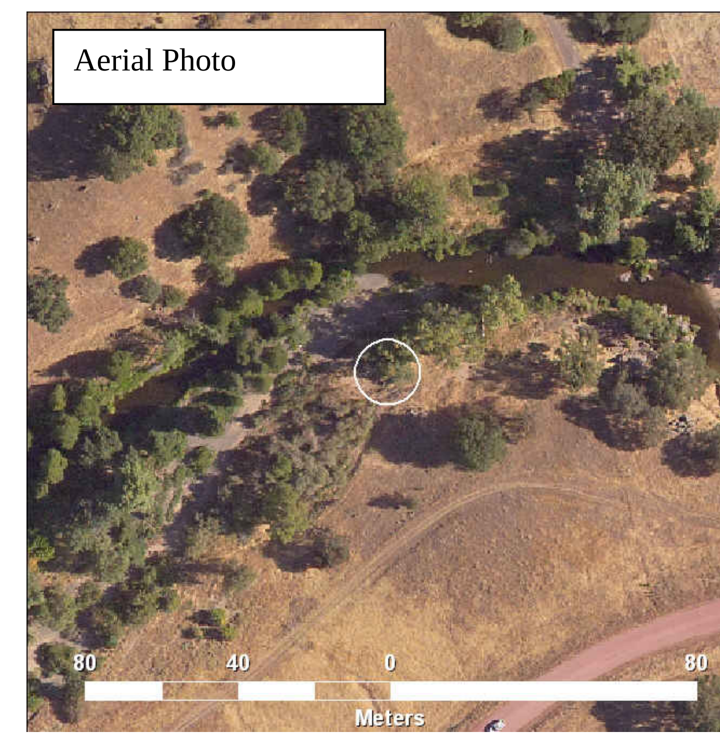

Plot # 47

Feature size: 8 m wide
52 m long
Vegetation Density: 62.79 %
Lidar block reference number: 5609

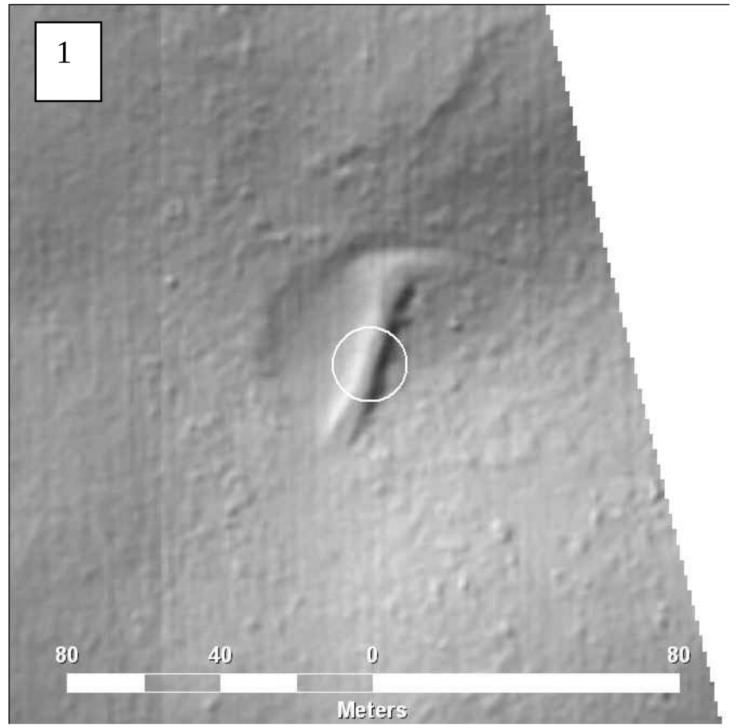

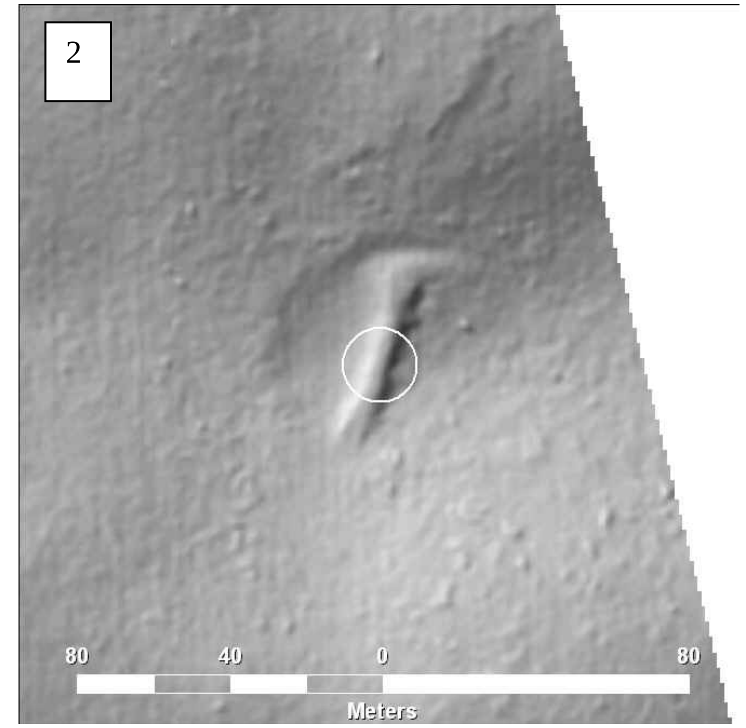

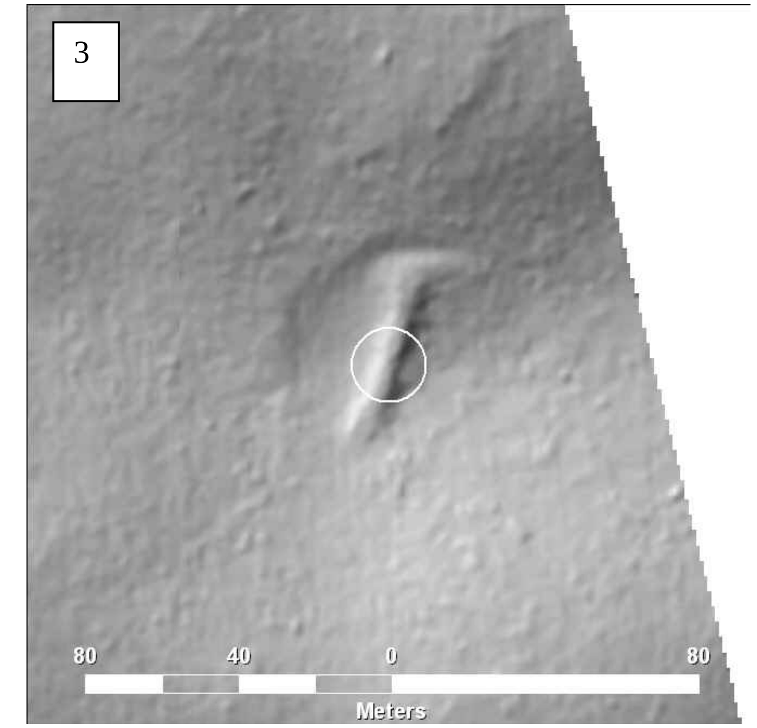

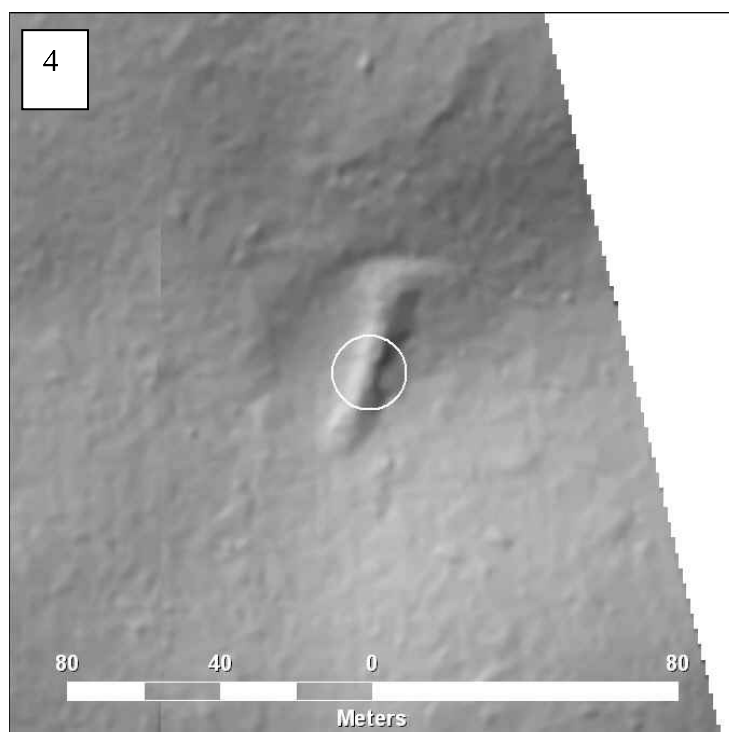

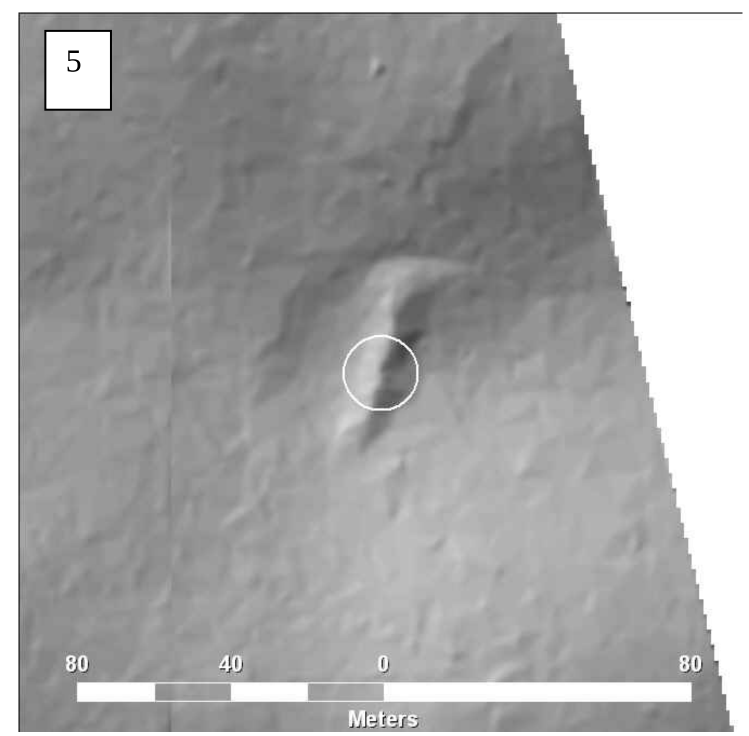

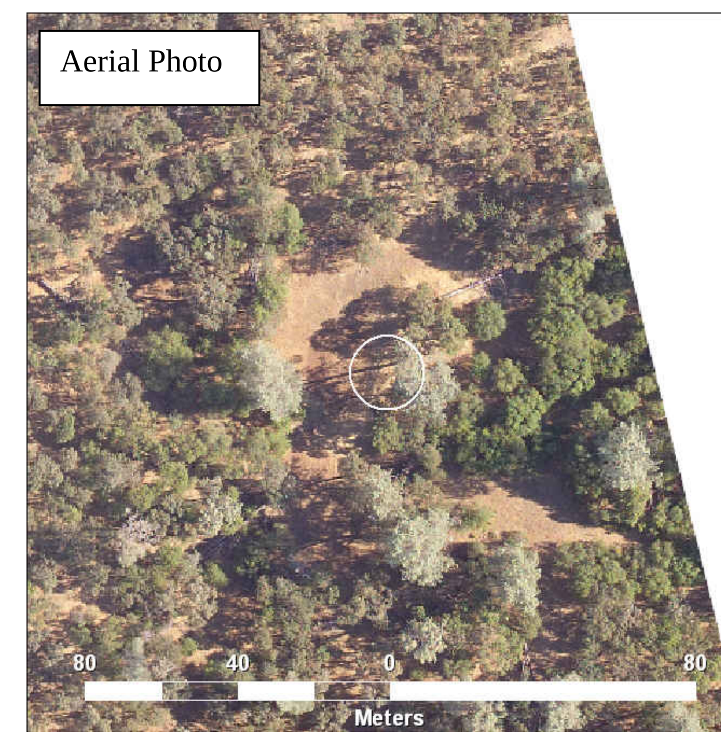

Plot # 48

Feature size: 8.2 m
Vegetation Density: 46.96 %
Lidar block reference number: 5921

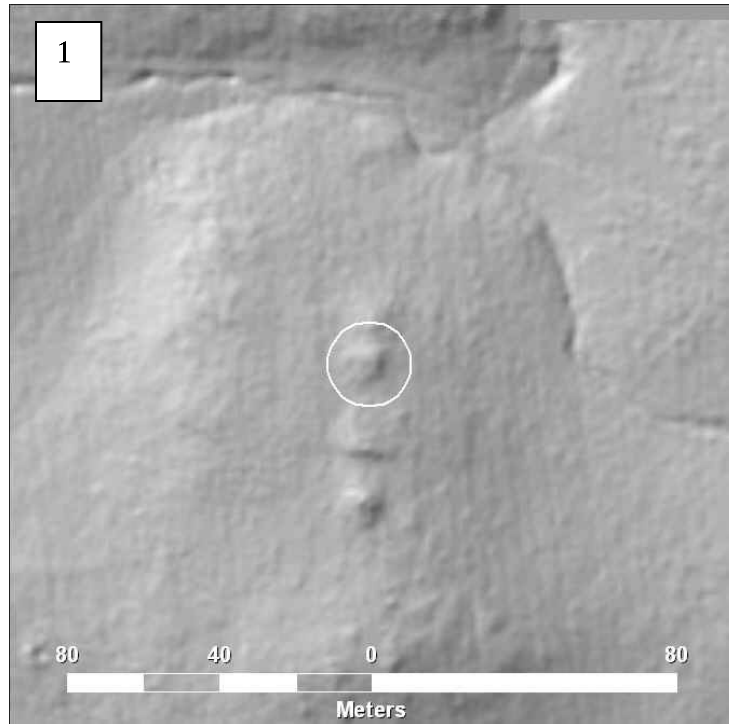

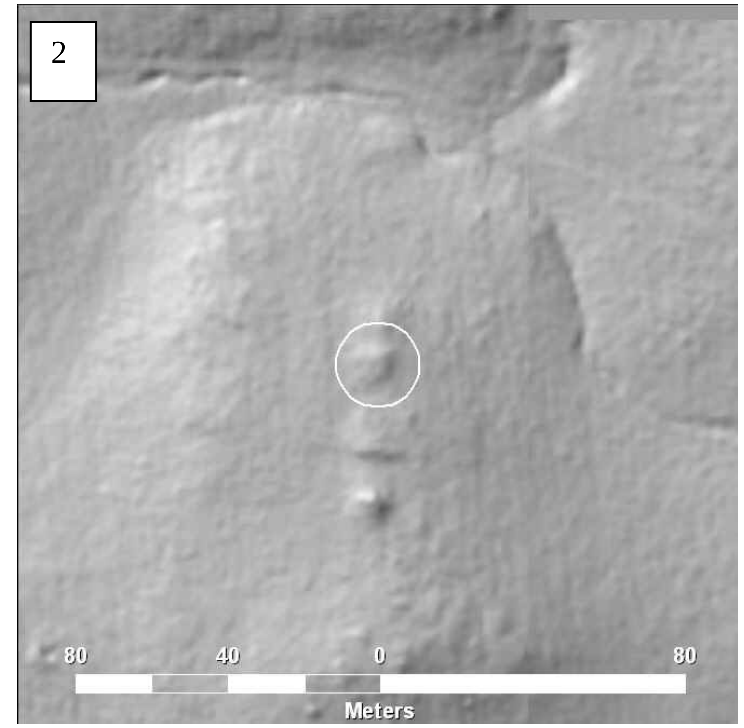

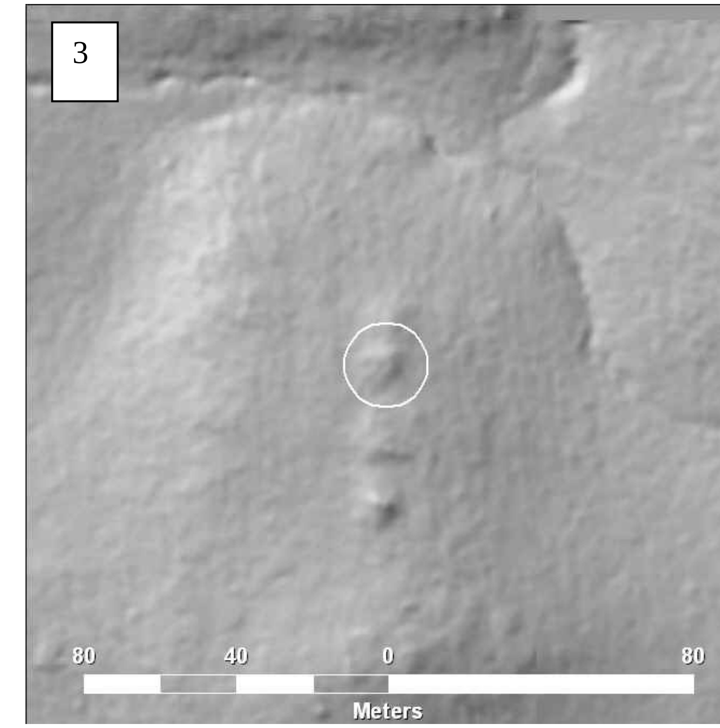

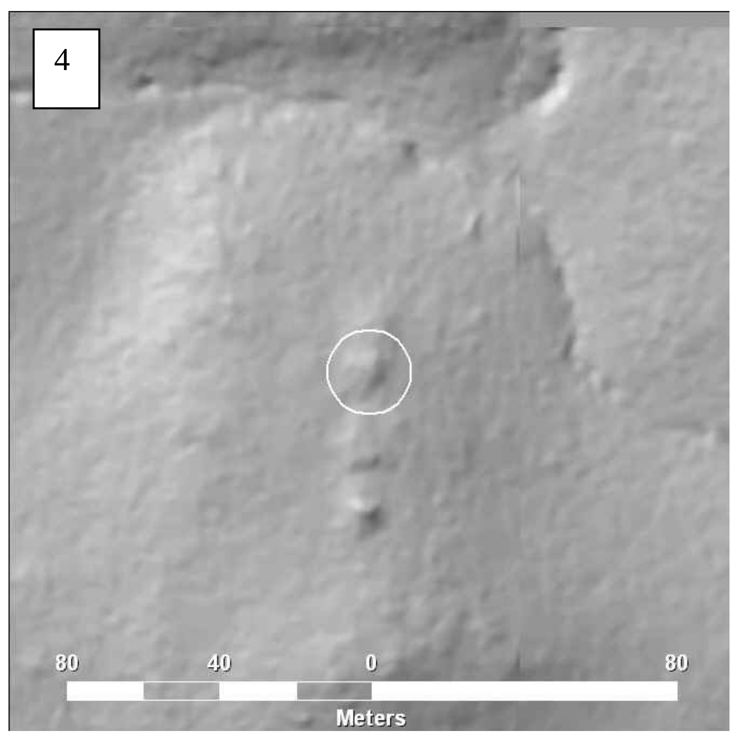

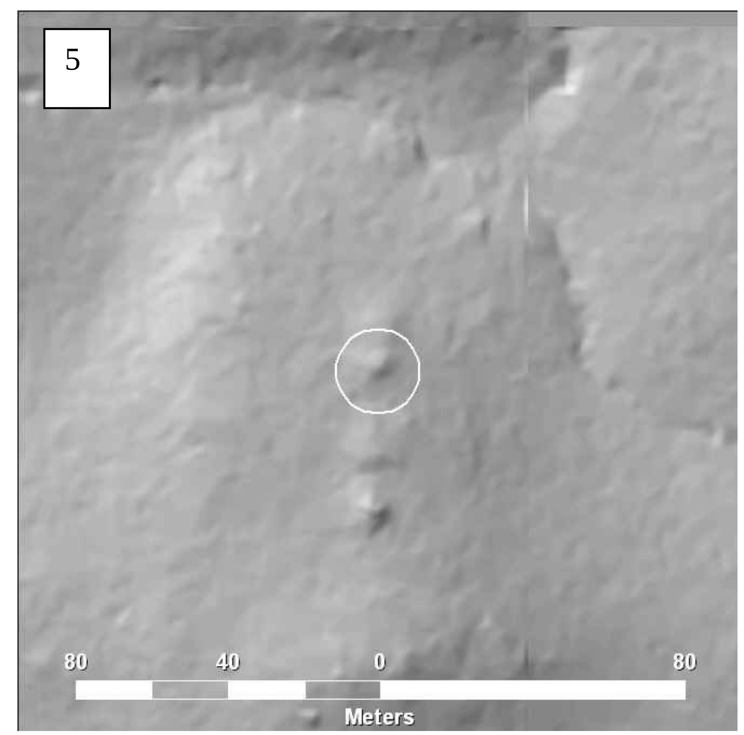

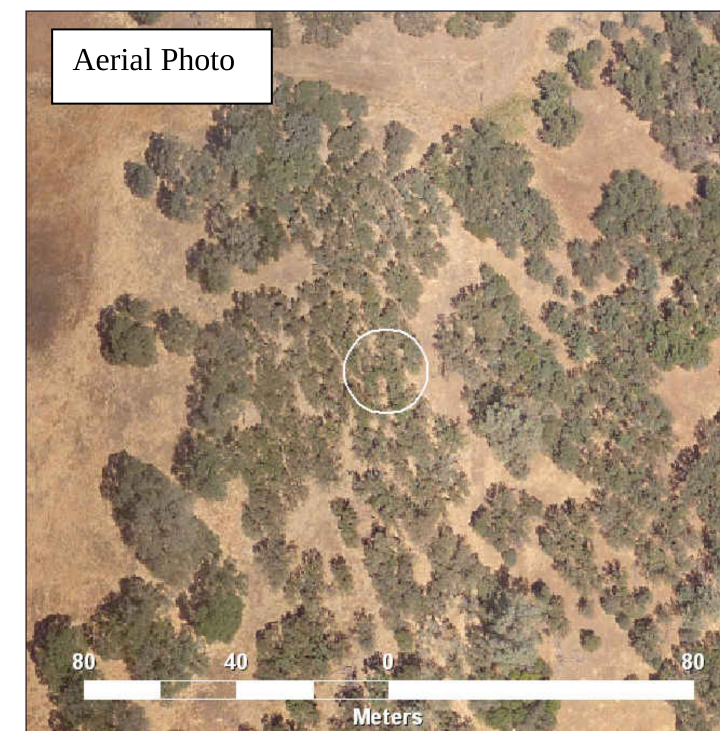

Plot # 49

Feature size: 8.2 m
Vegetation Density: 51.24 %
Lidar block reference number: 4029

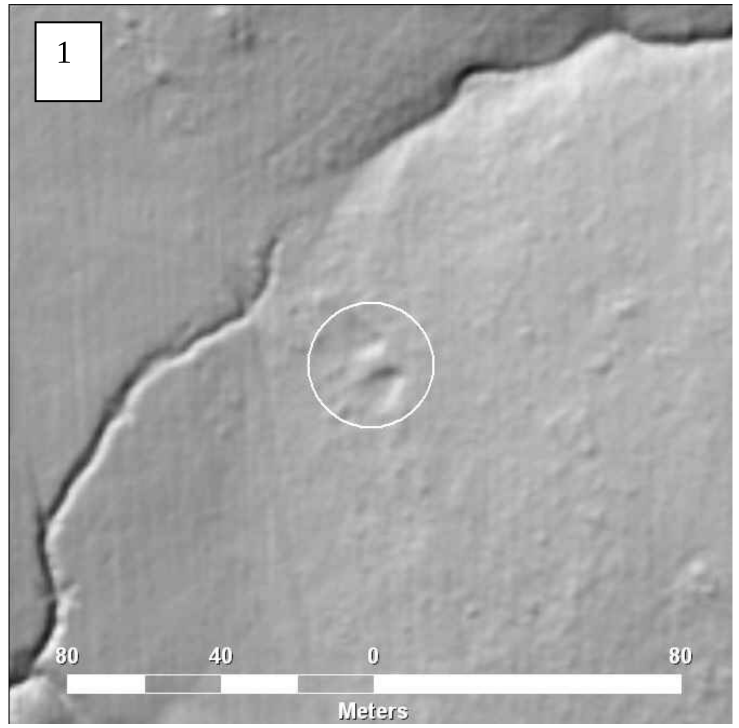

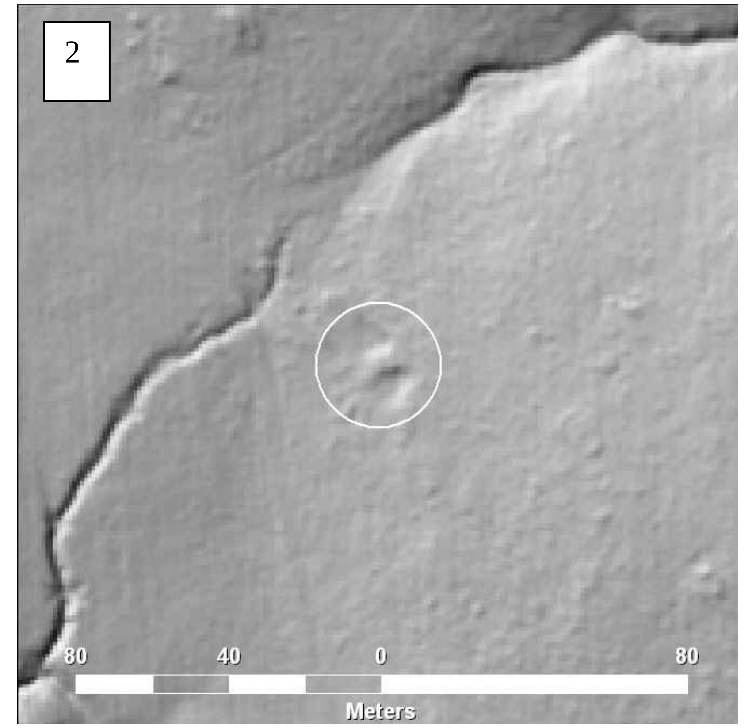

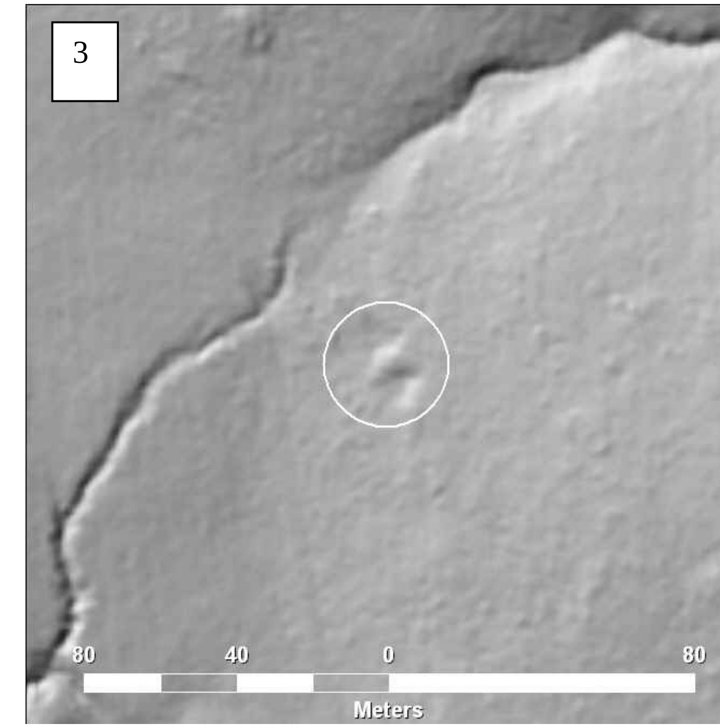

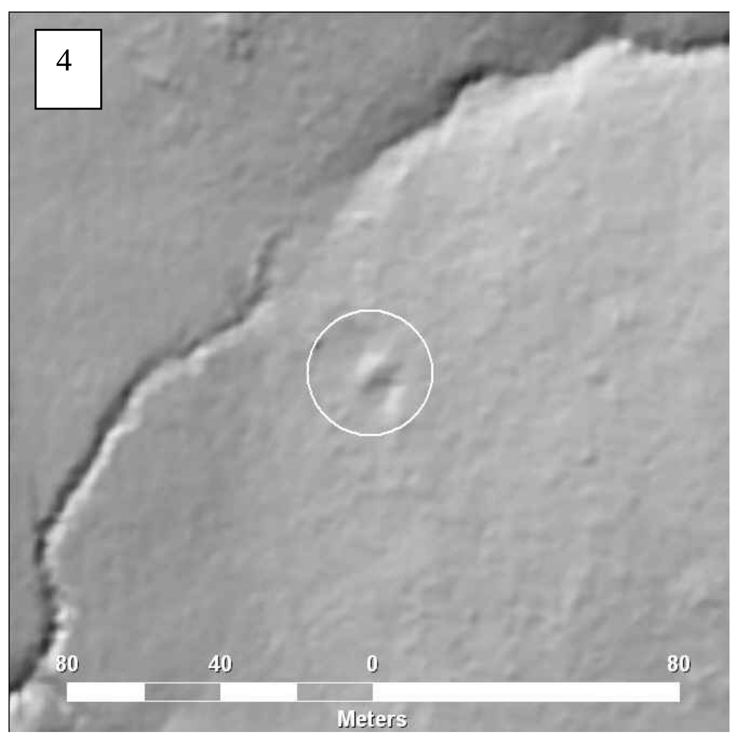

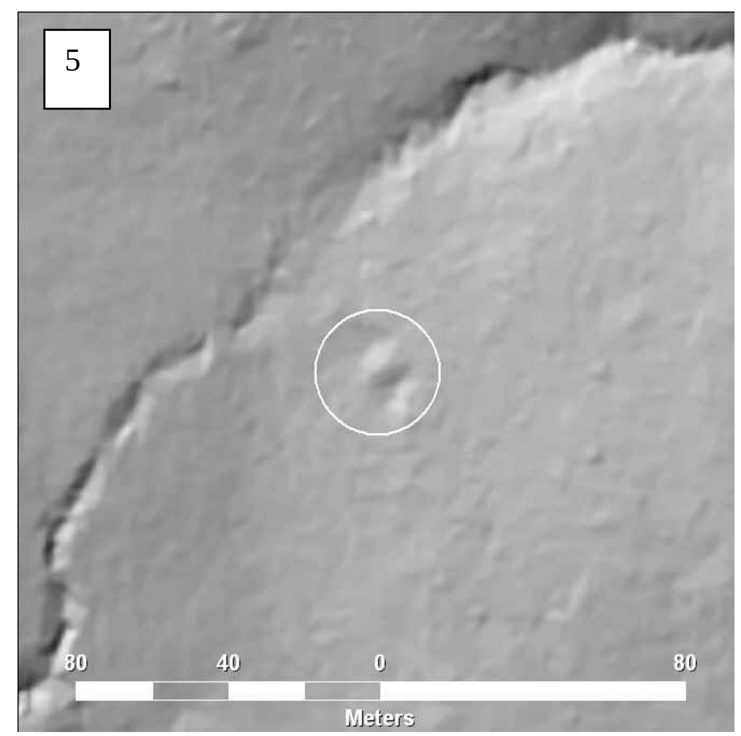

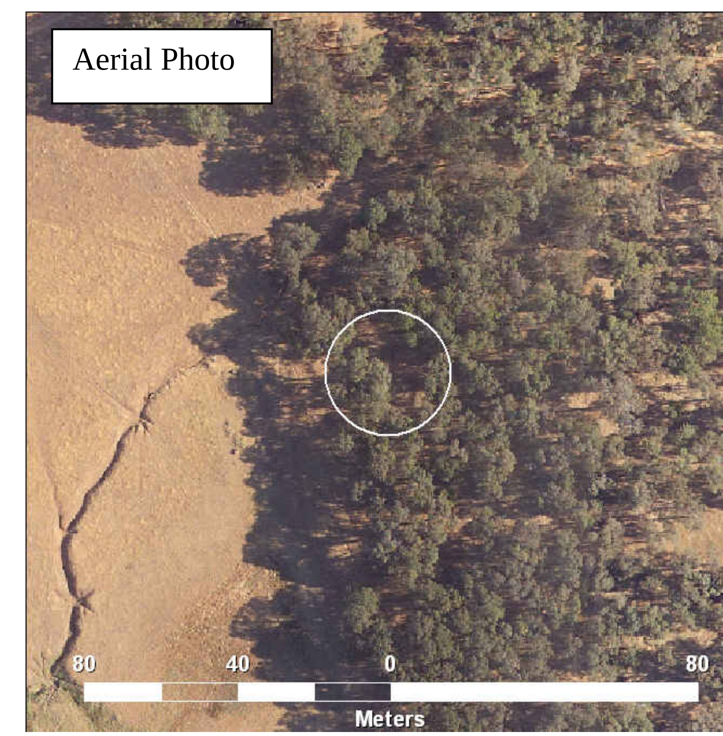

Plot # 50 Feature size: 8.6 m Vegetation Density: 51.46 % Lidar block reference number: 5735	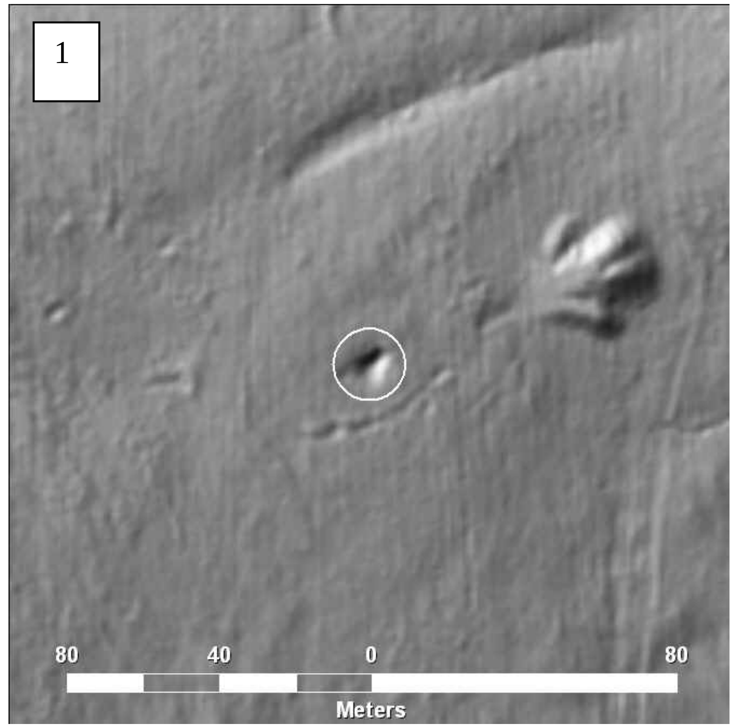	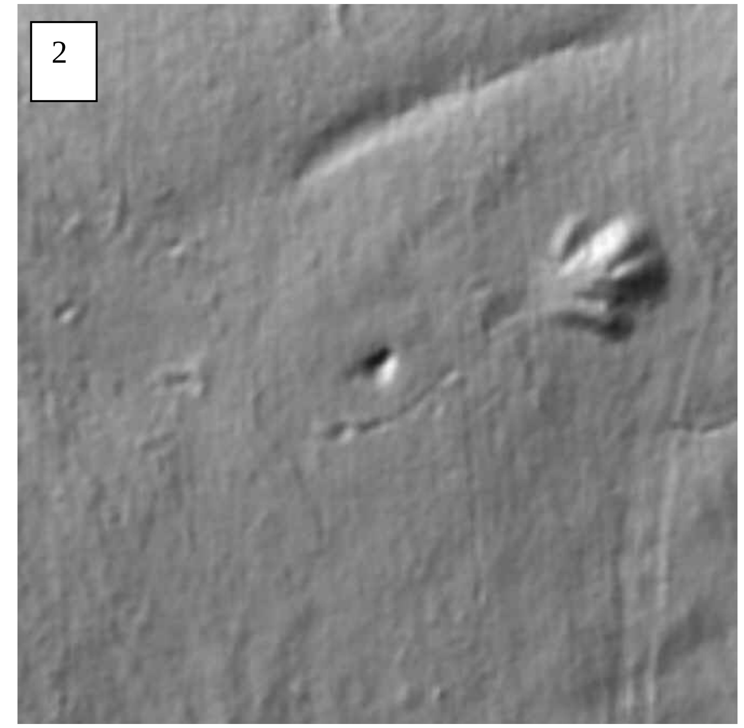	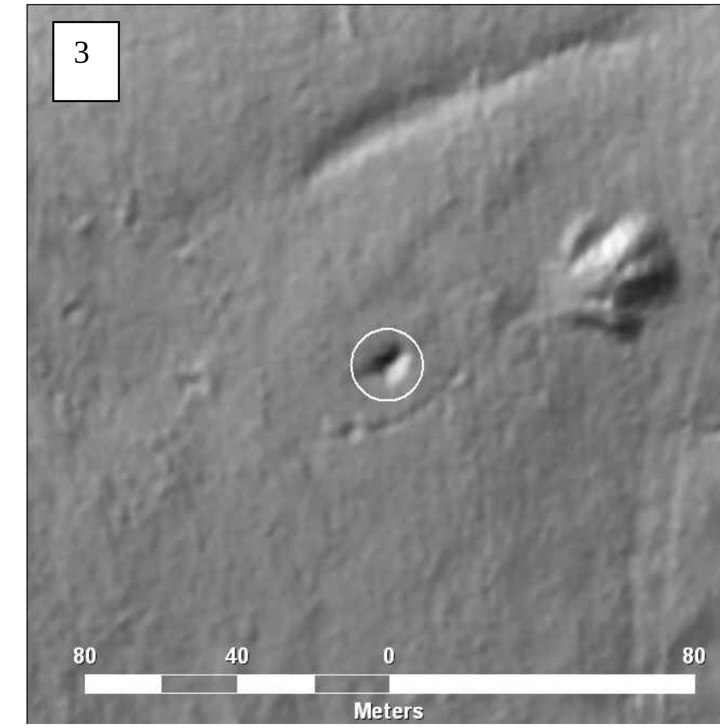
	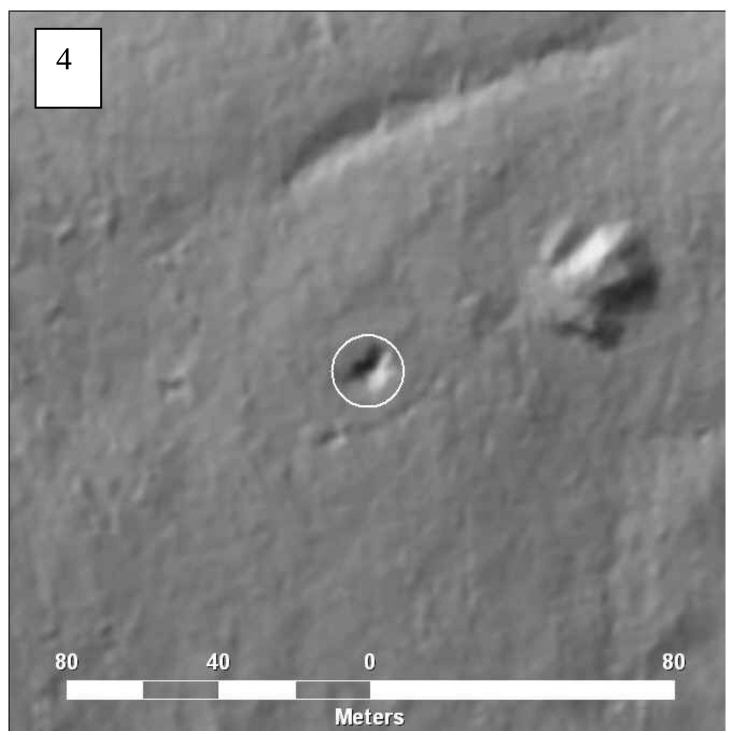	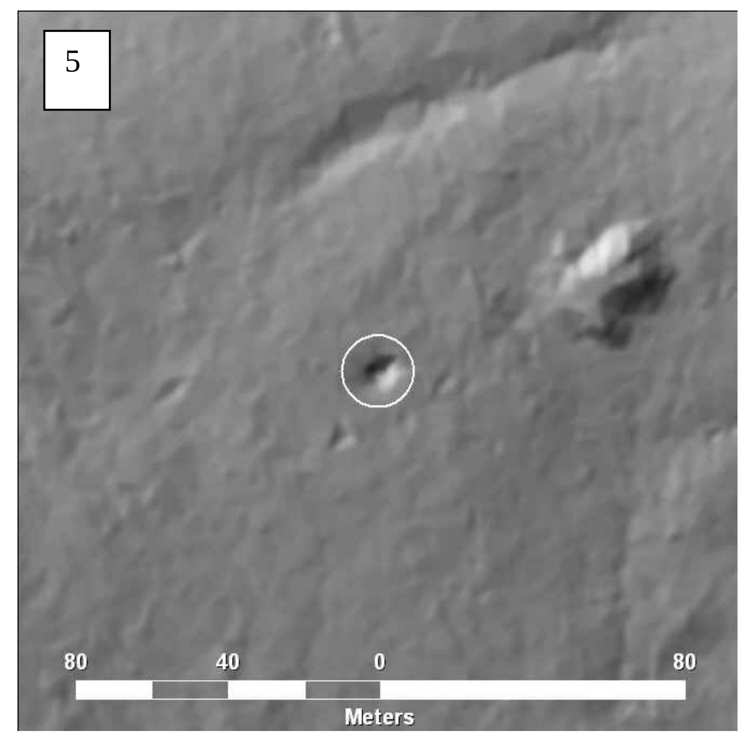	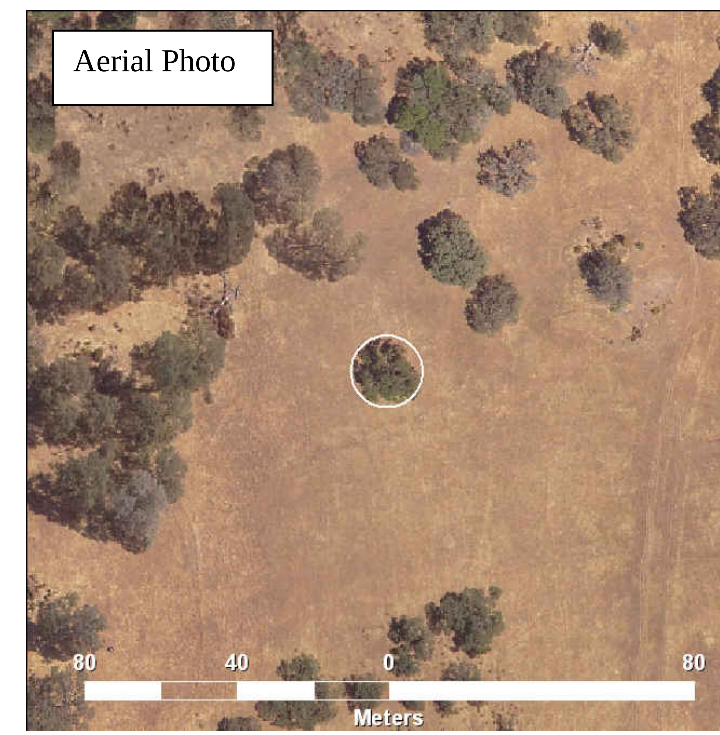

Plot # 51

Feature size: 8.7 m wide
12.6 m long
Vegetation Density: 55.53 %
Lidar block reference number: 5679

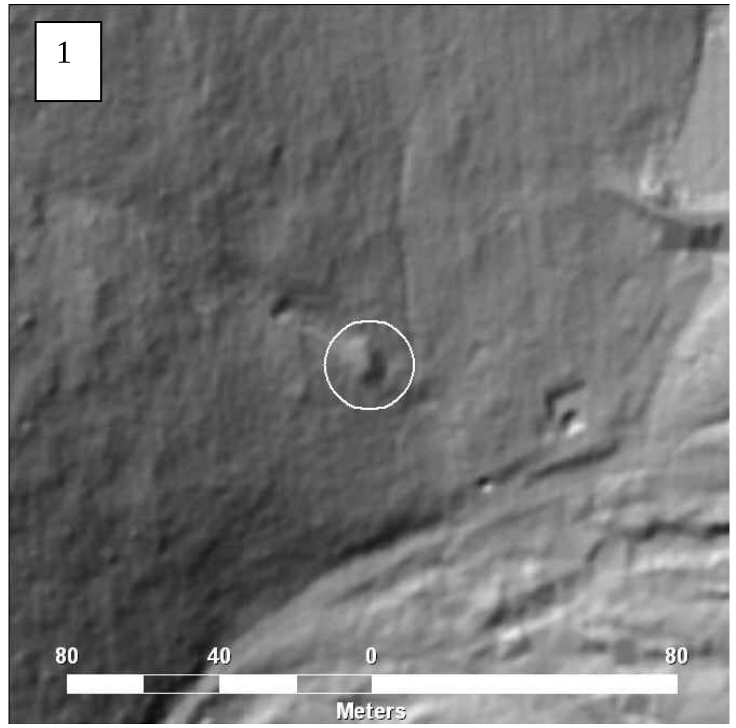

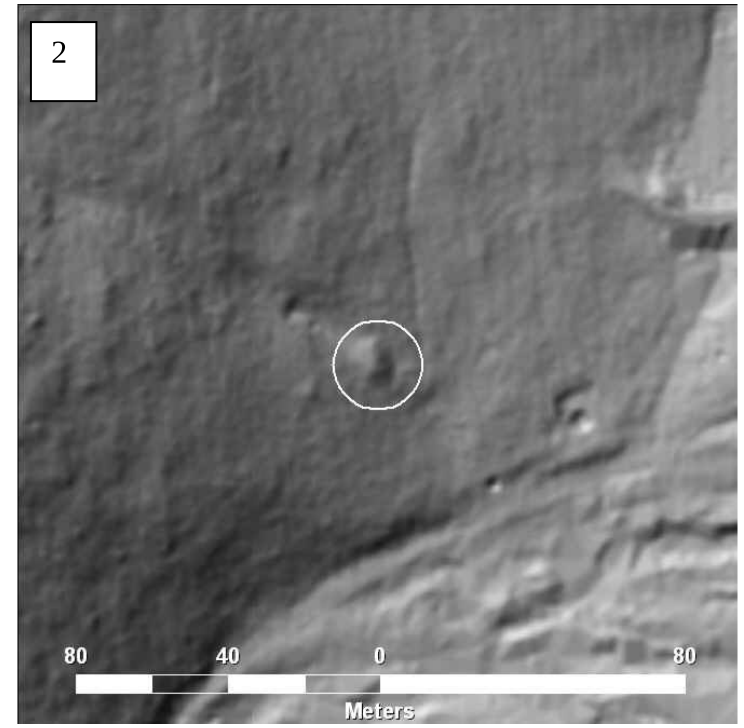

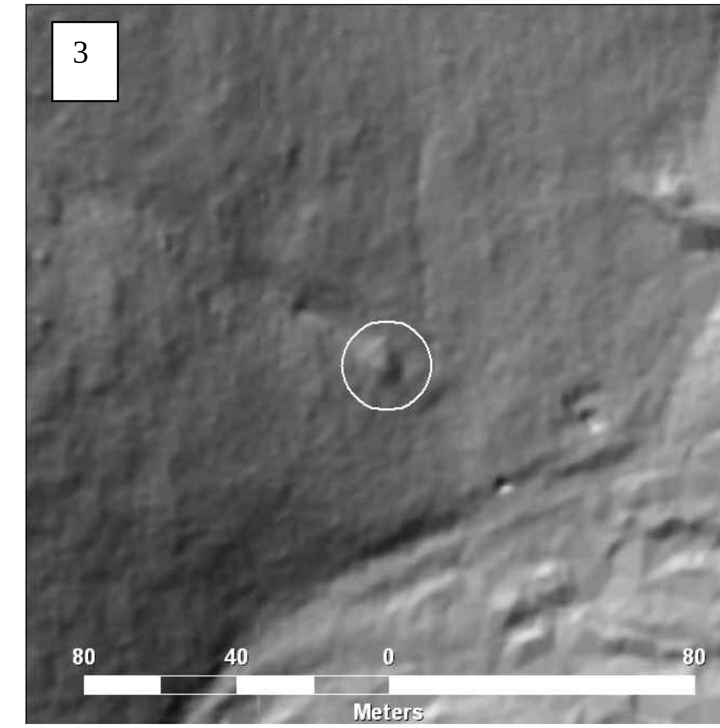

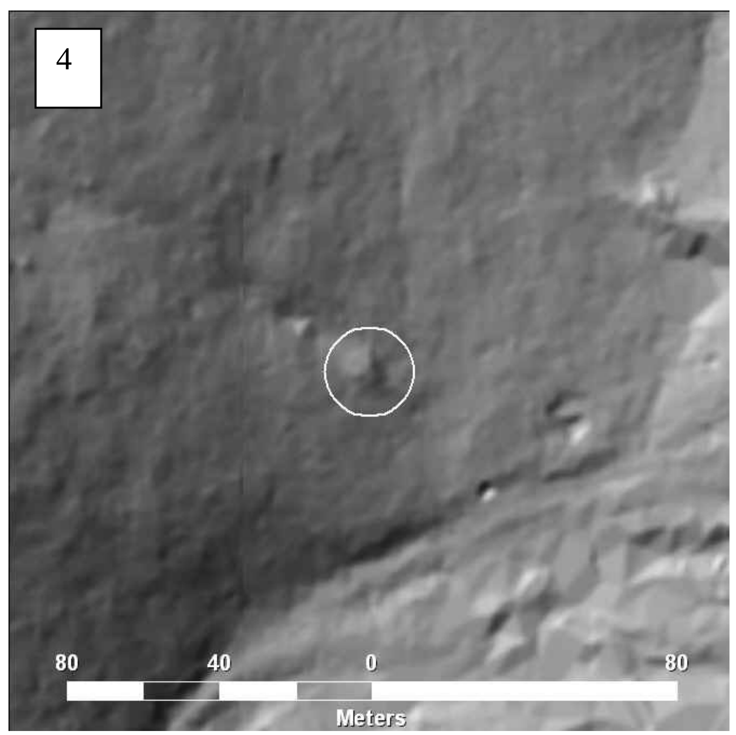

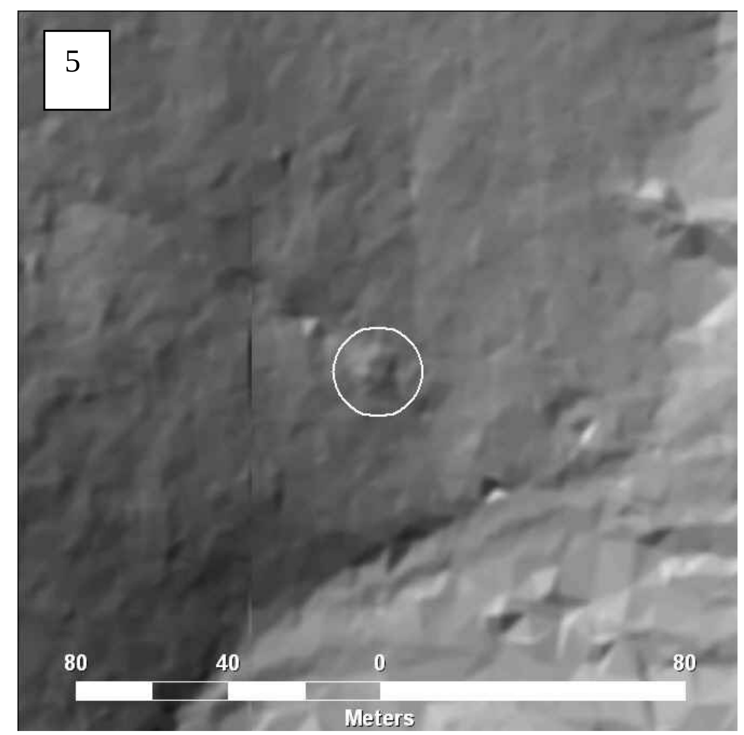

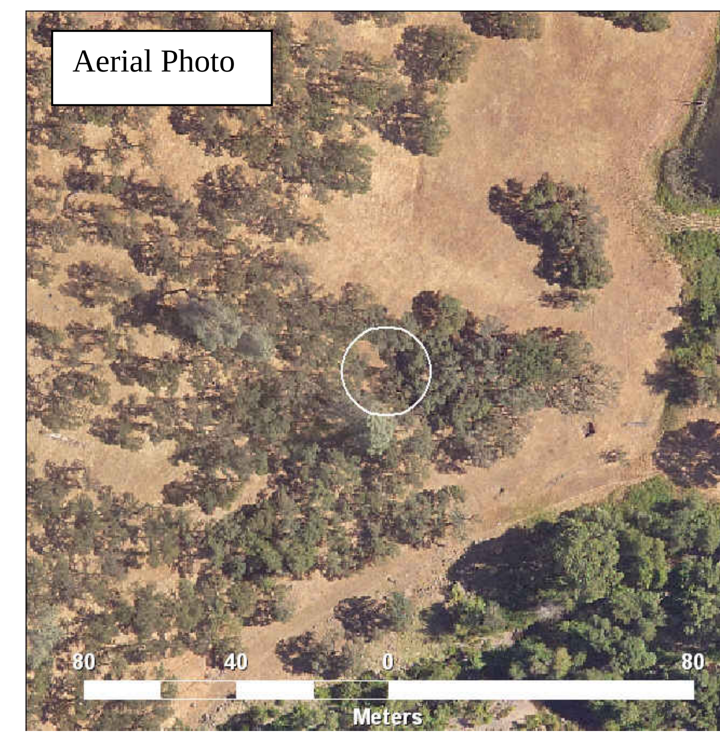

Plot # 52

Feature size: 8.8 m
Vegetation Density: 40.96 %
Lidar block reference number: 4030

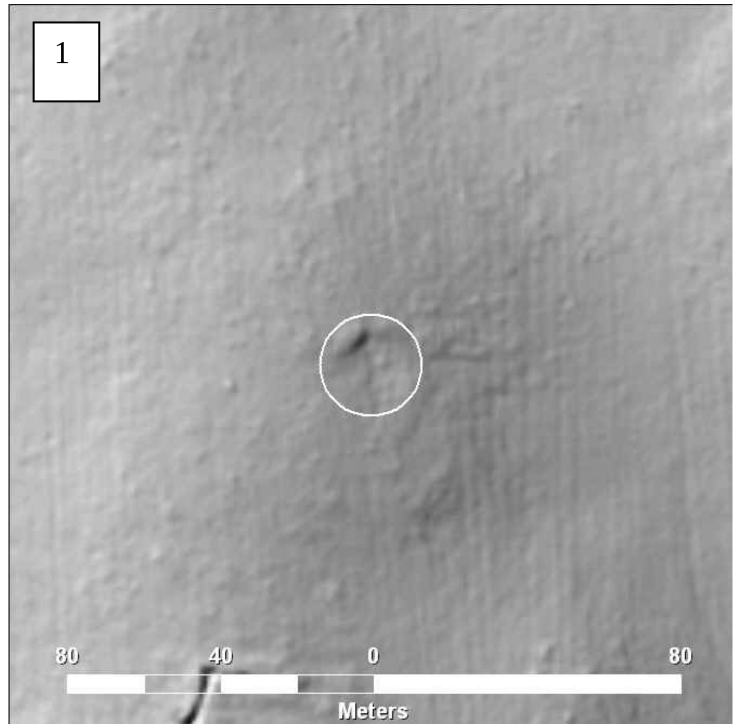

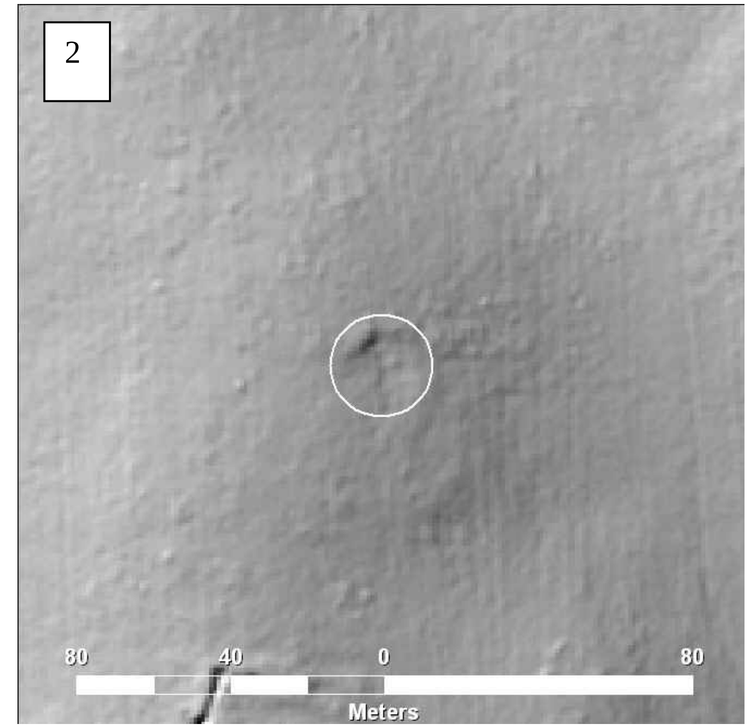

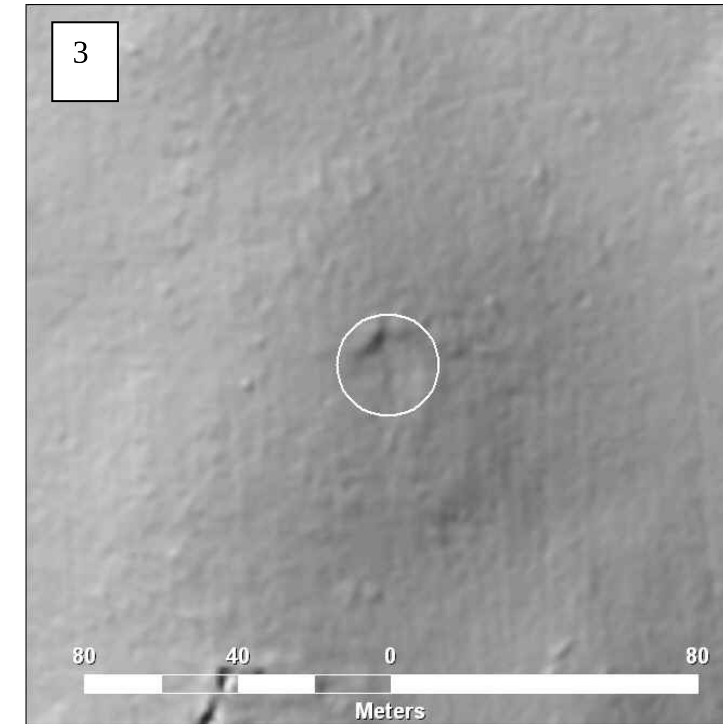

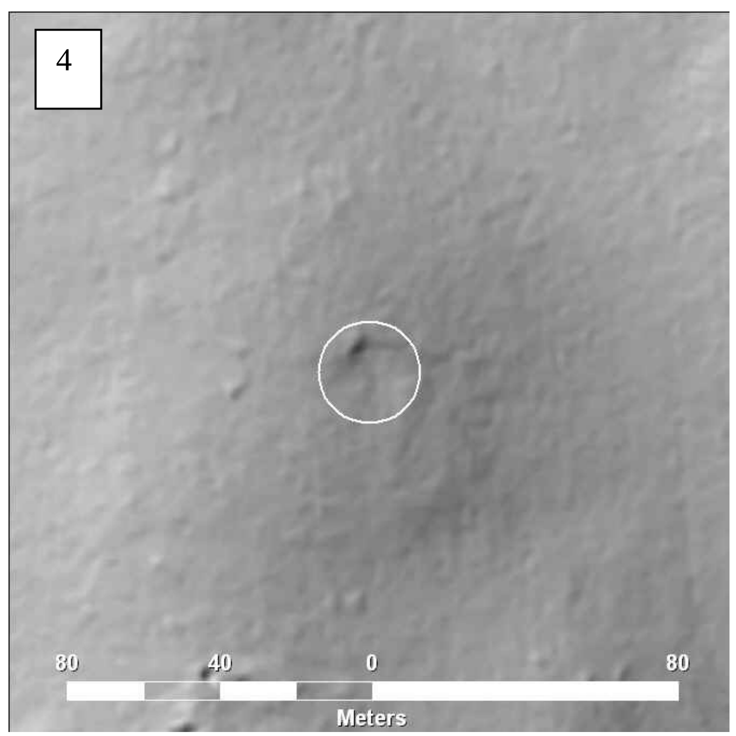

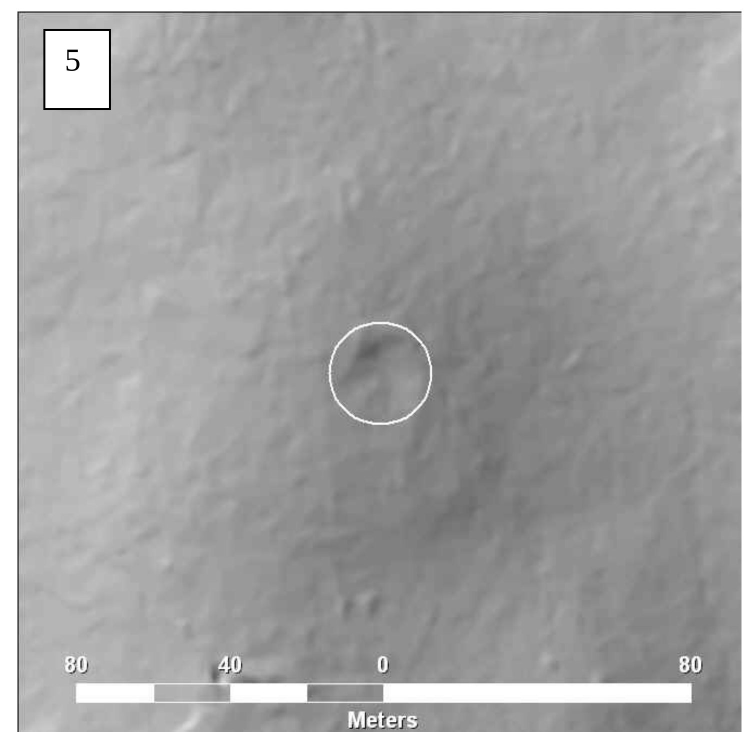

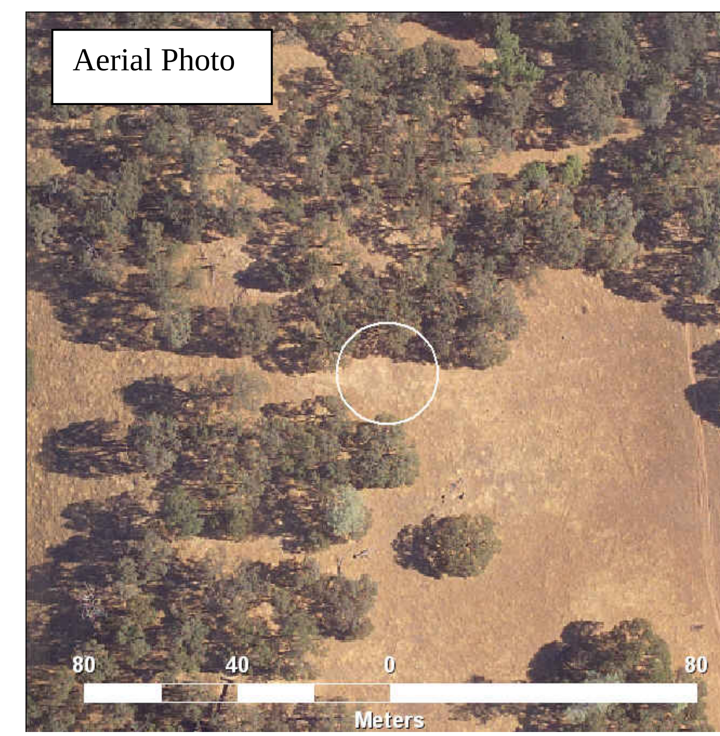

Plot # 53

Feature size: 10.3 m
Vegetation Density: 46.88 %
Lidar block reference number: 5739

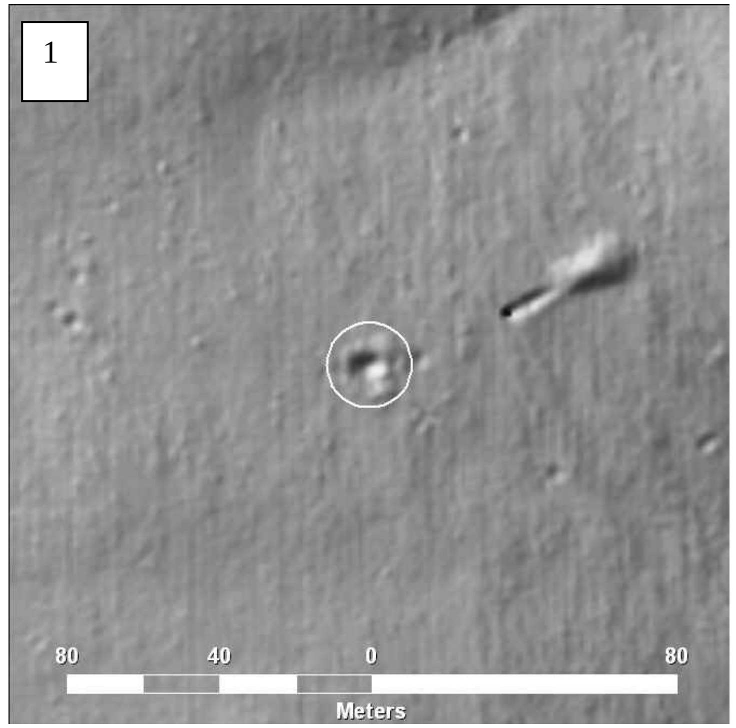

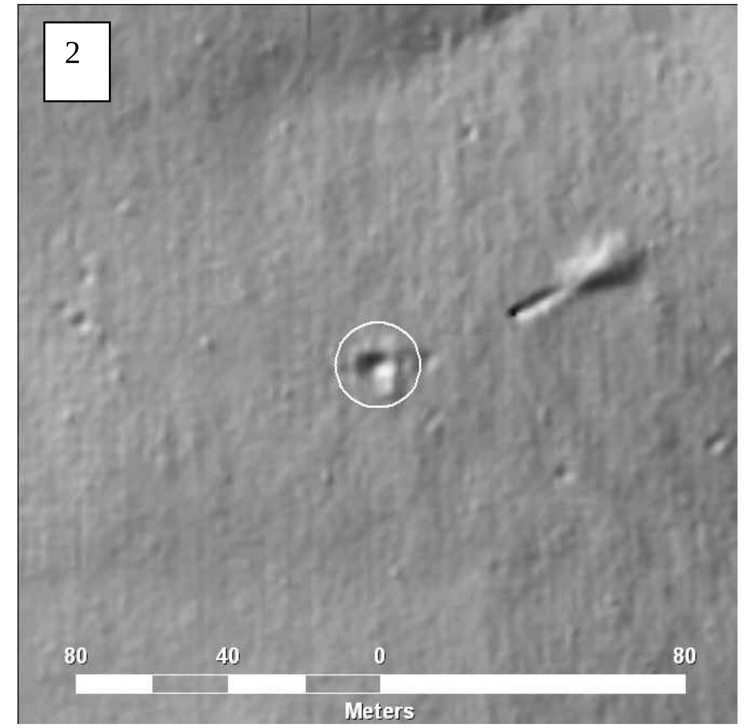

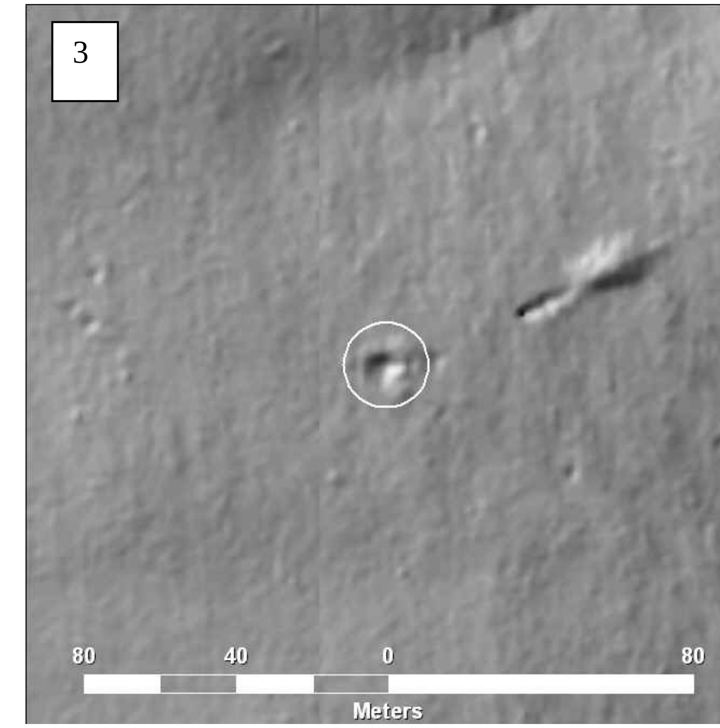

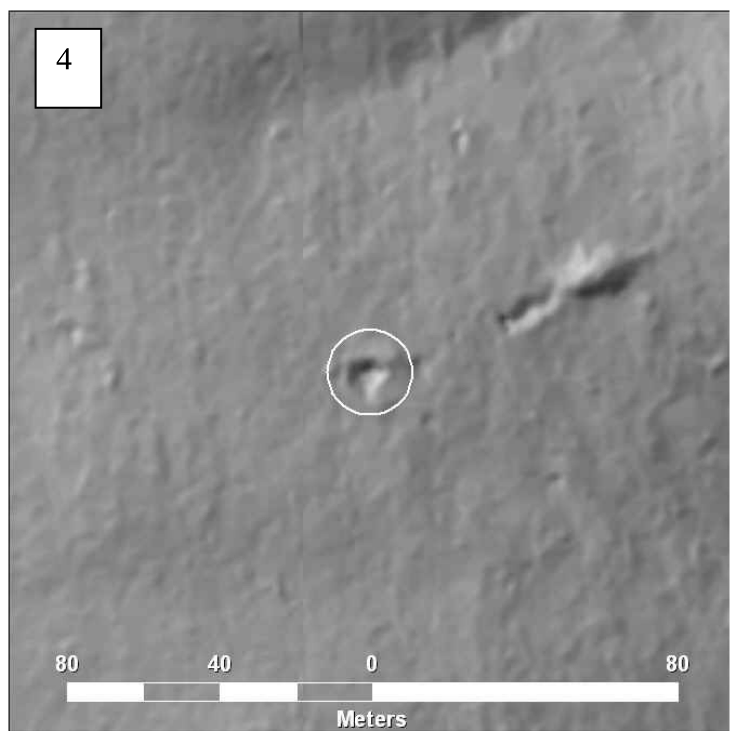

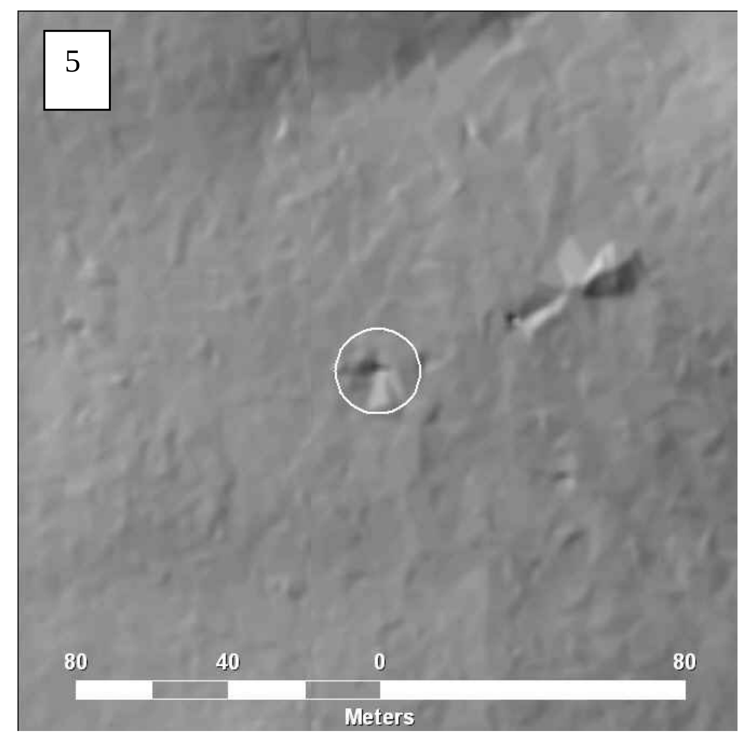

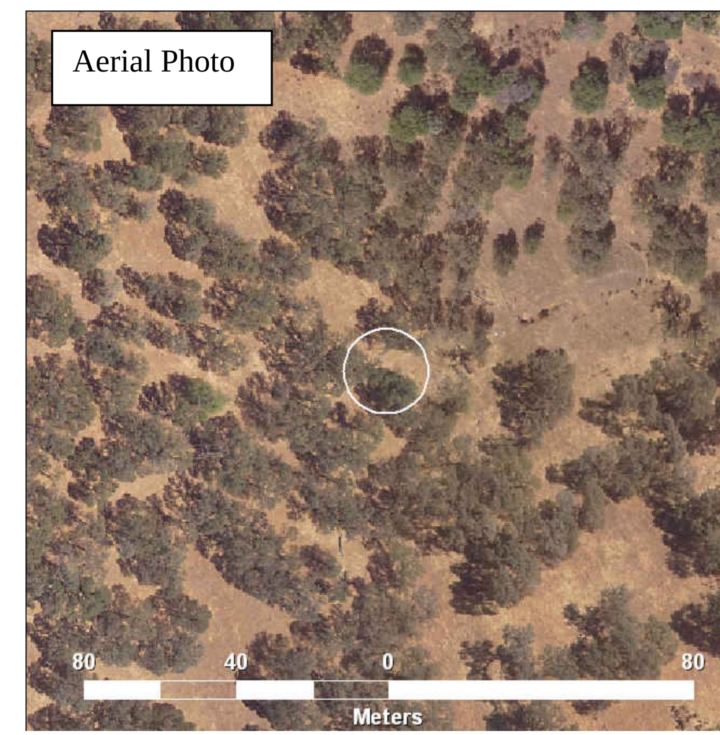

Plot # 54

Feature size: 10.4 m
Vegetation Density: 60.17 %
Lidar block reference number: 5913

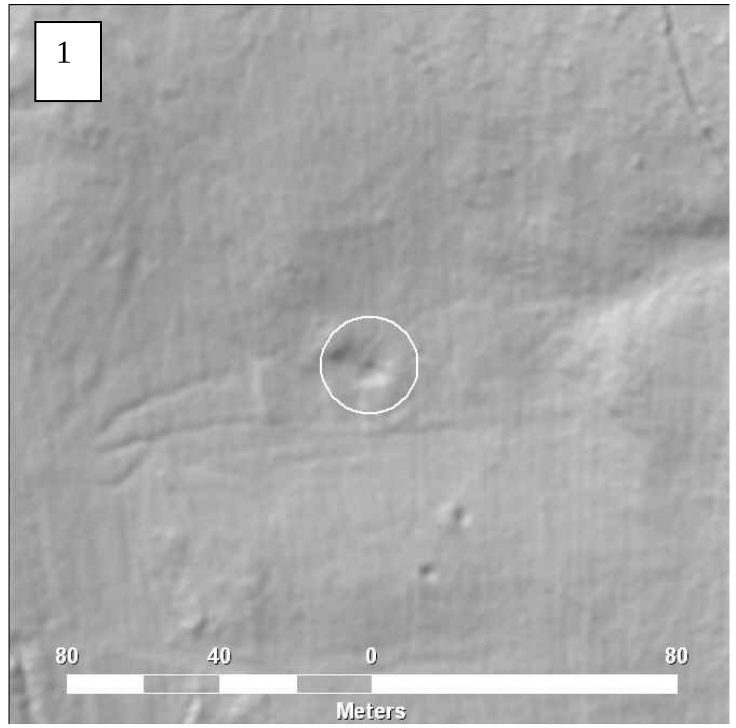

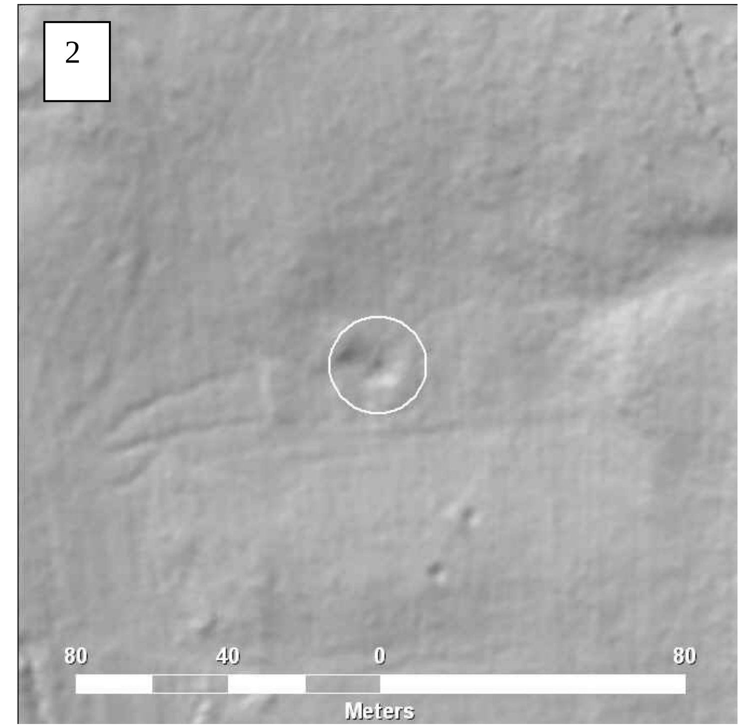

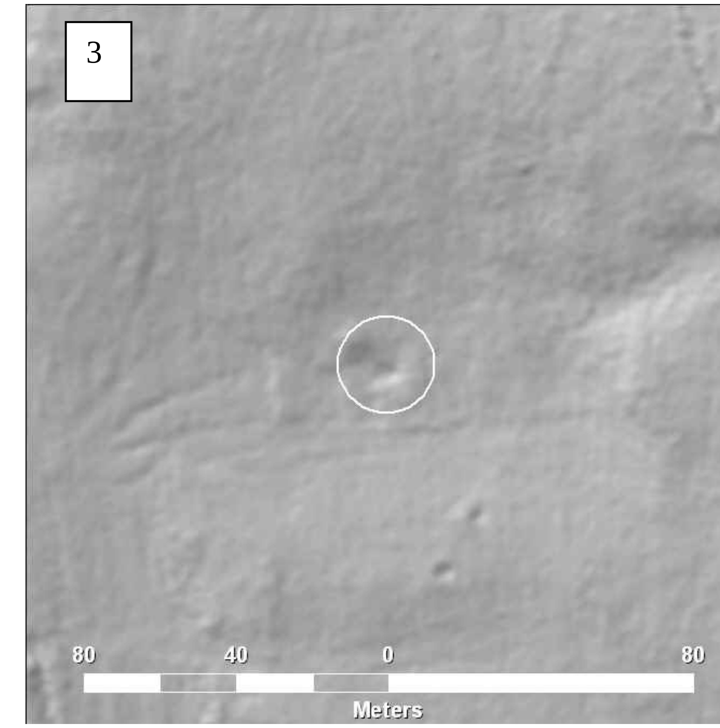

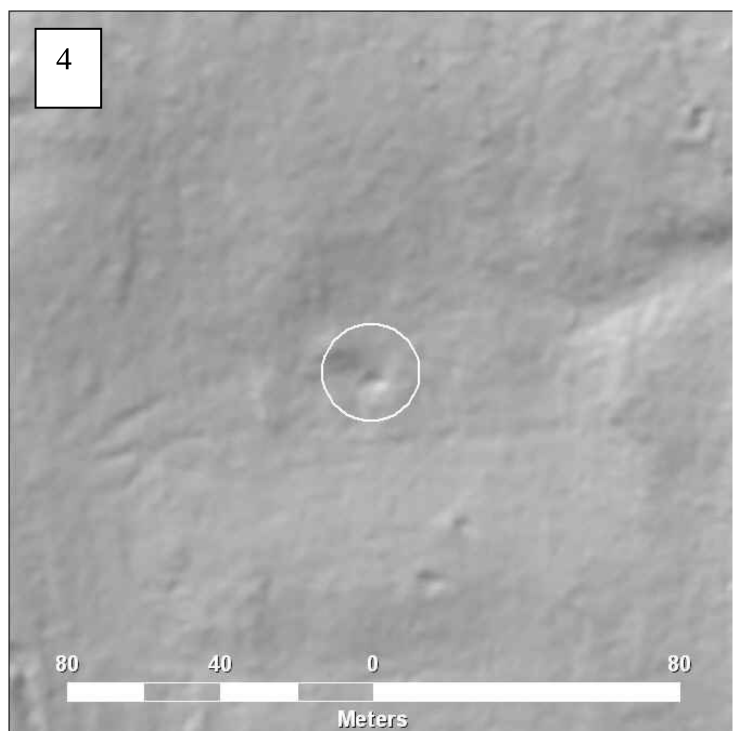

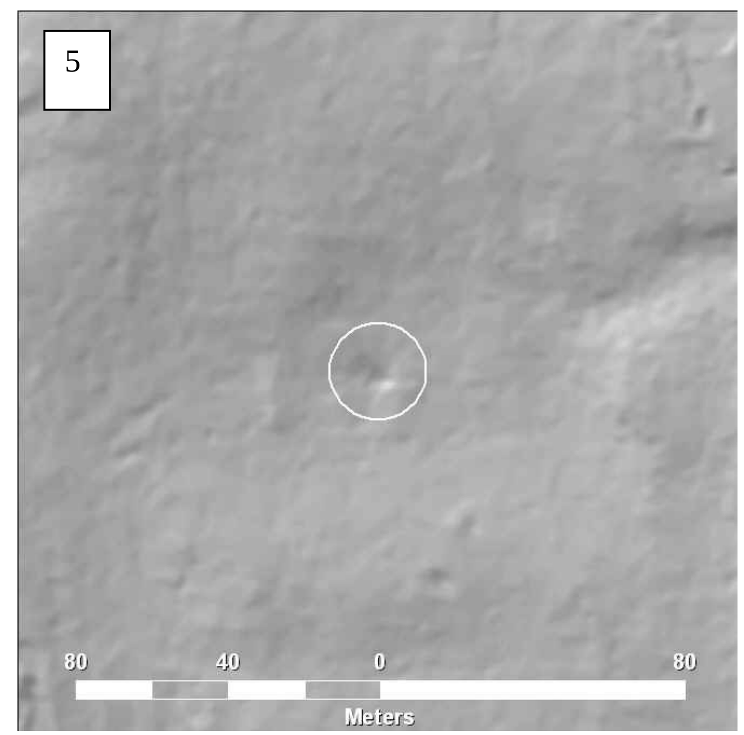

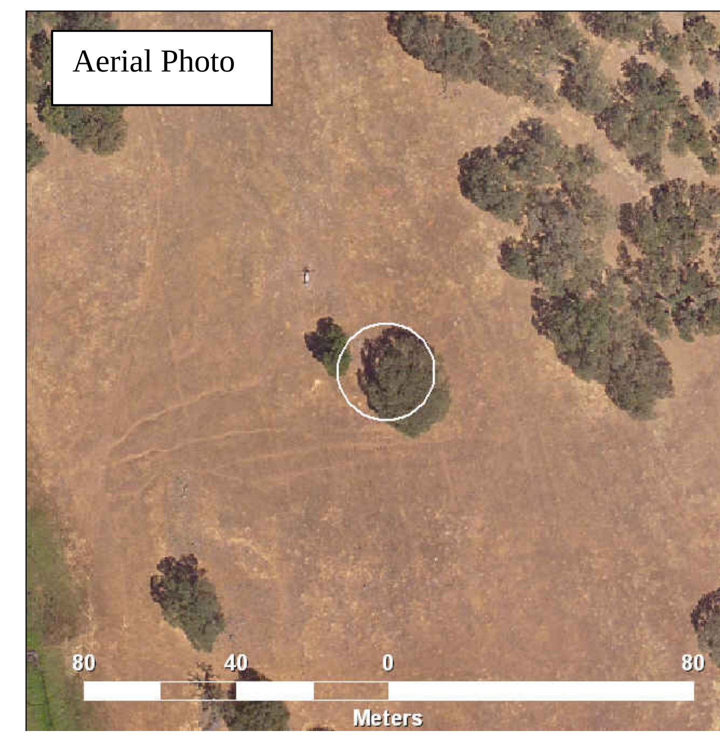

Plot # 55

Feature size: 11.3 m
Vegetation Density: 36.49 %
Lidar block reference number: 5923

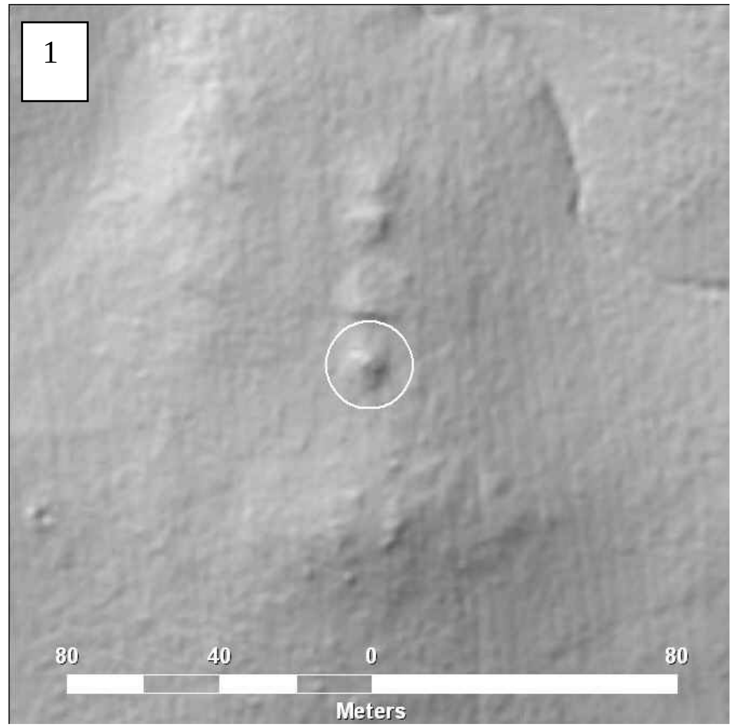

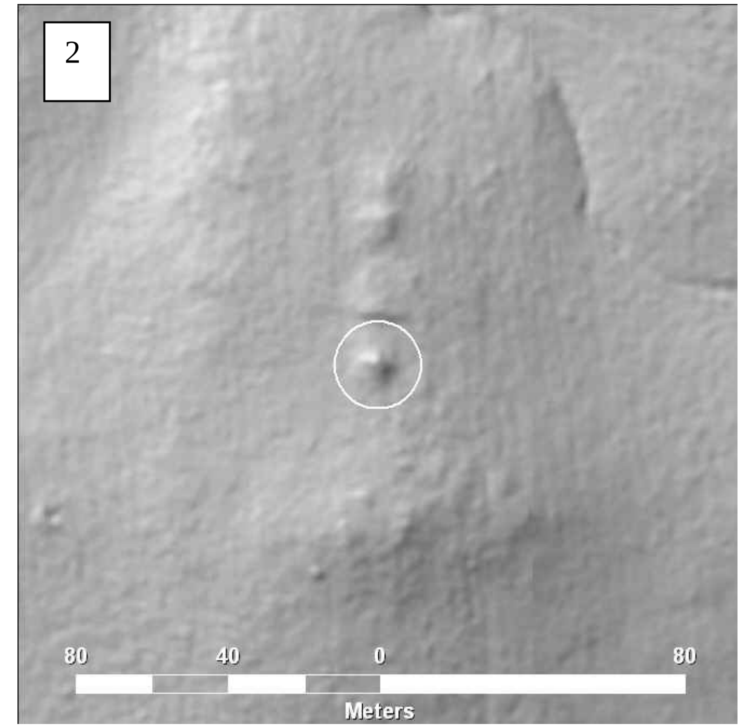

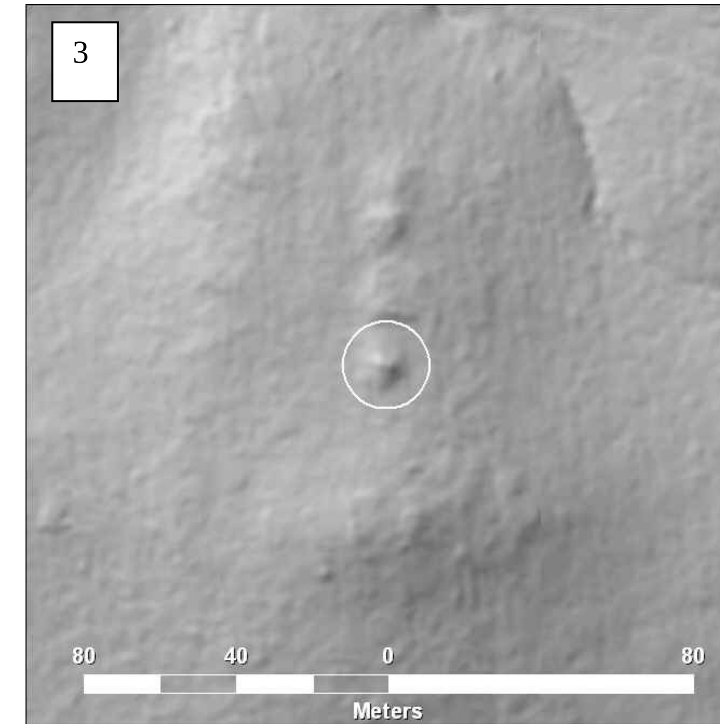

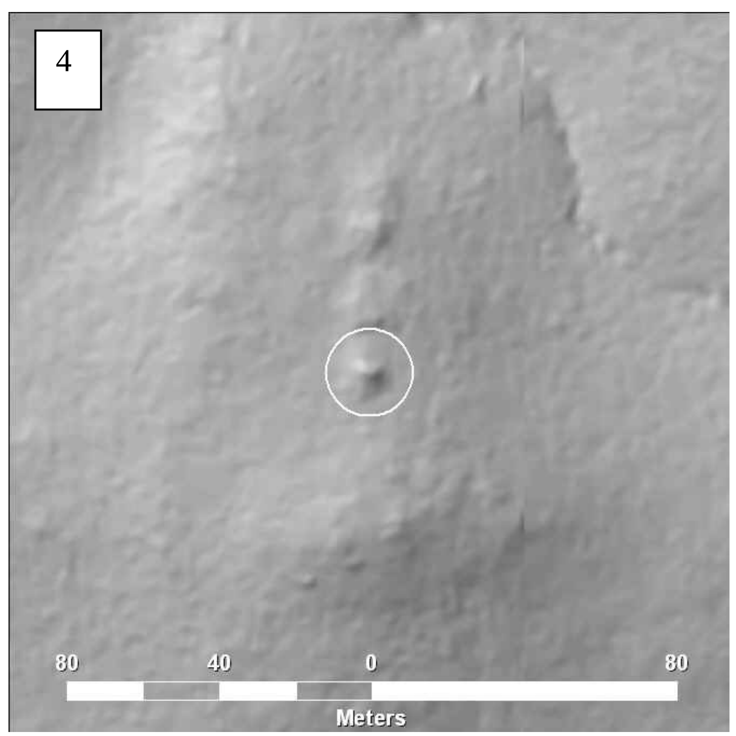

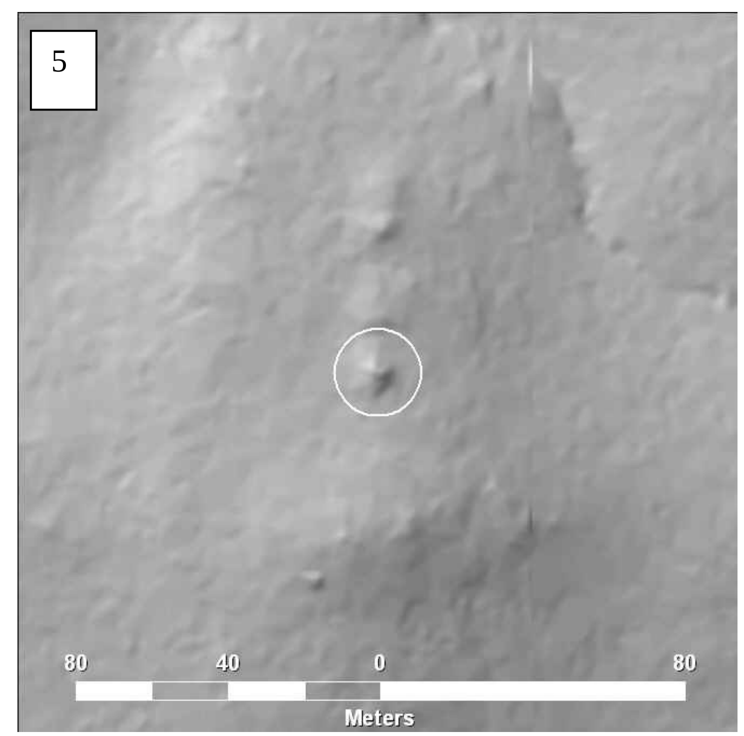

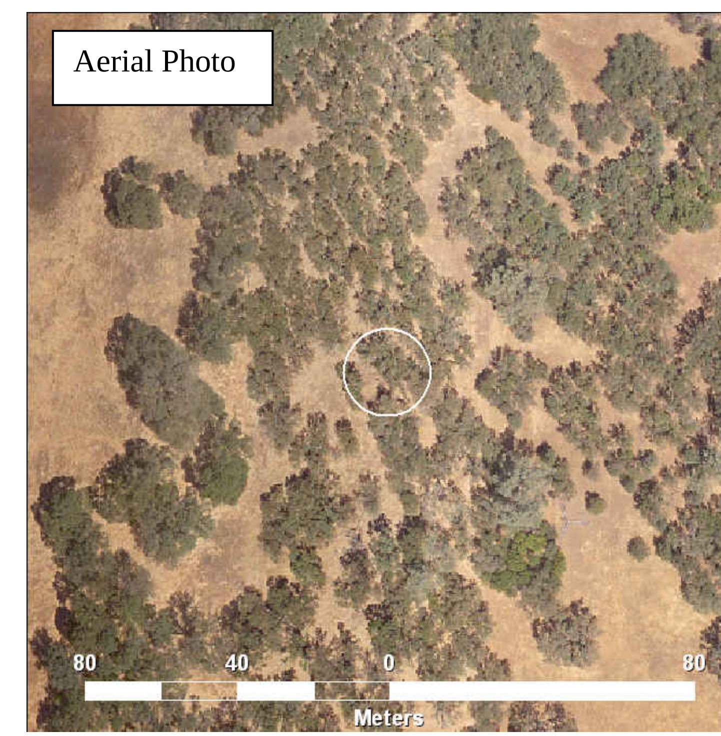

Plot # 56

Feature size: 12.2 m
Vegetation Density: 43.21 %
Lidar block reference number: 5583

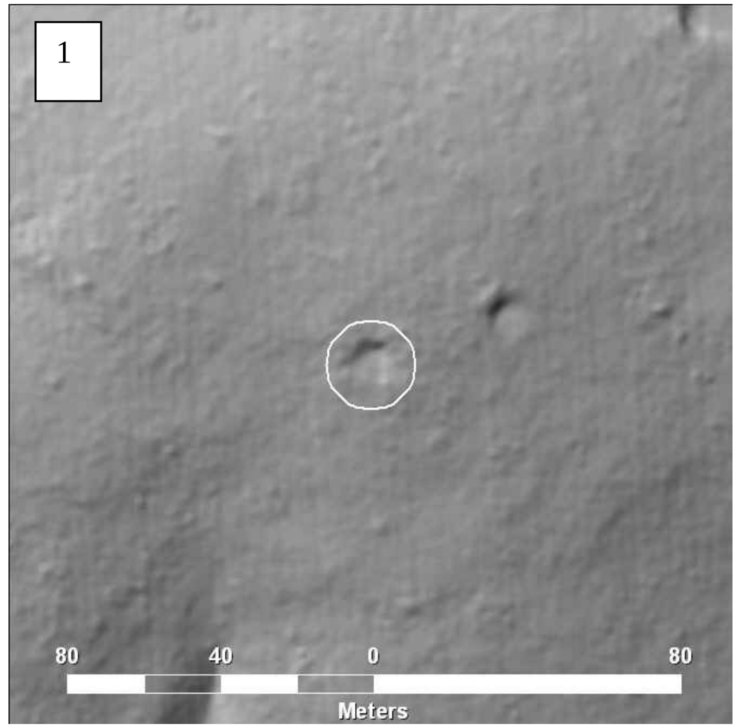

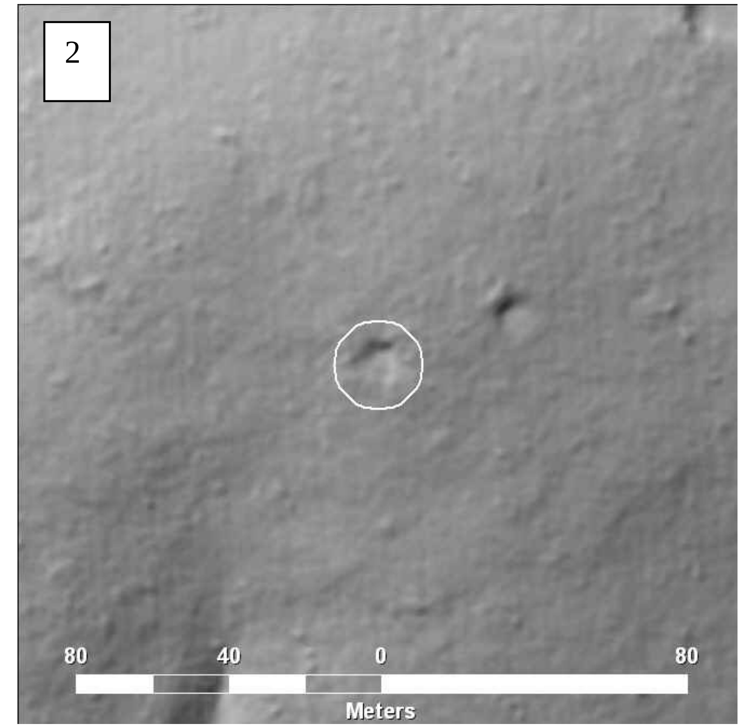

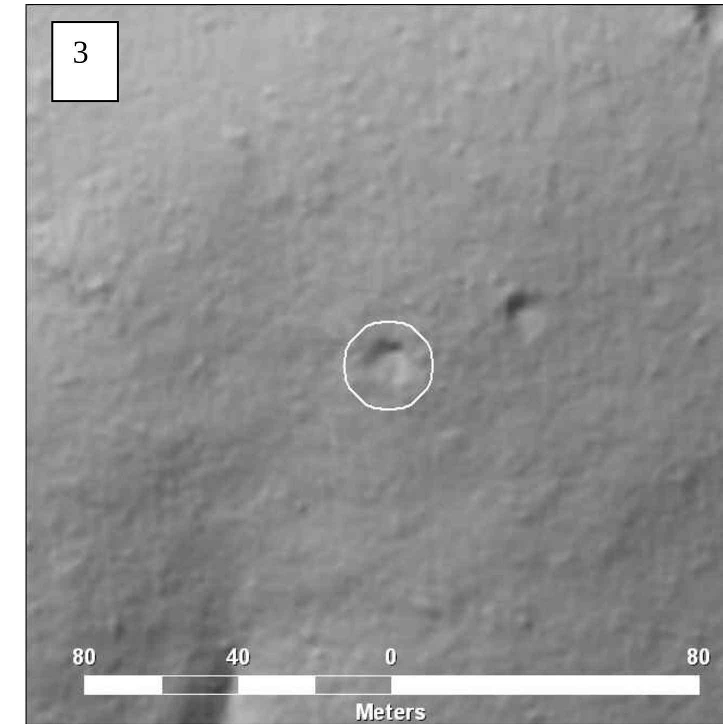

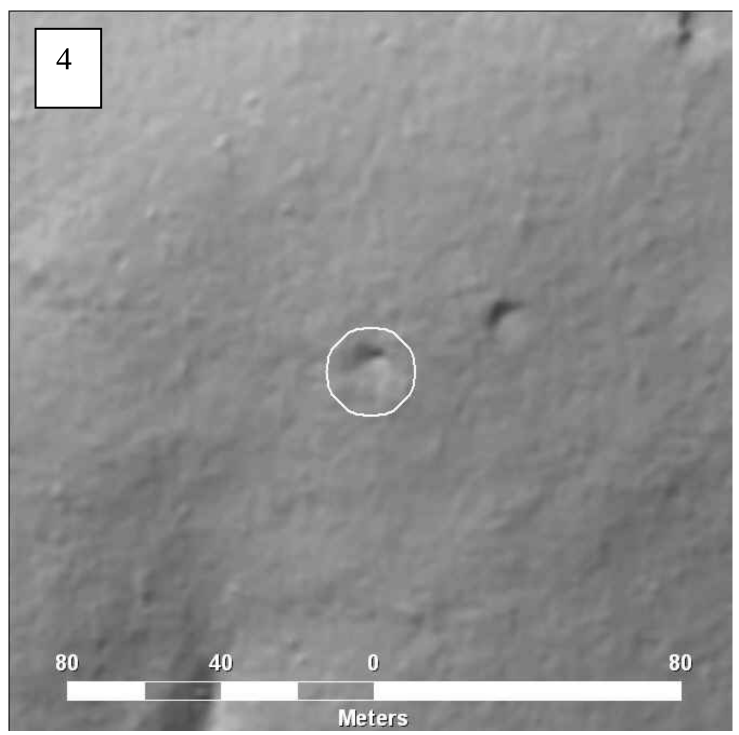

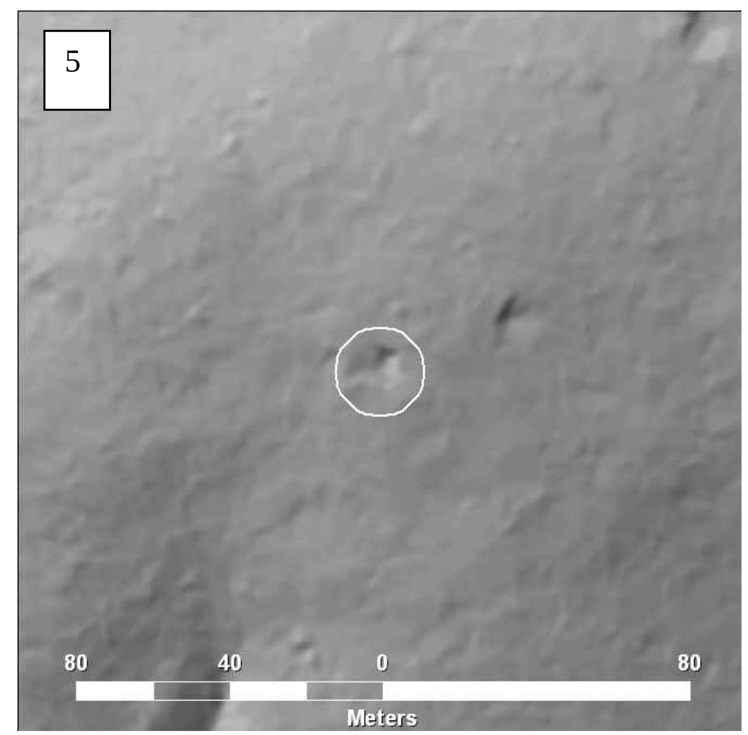

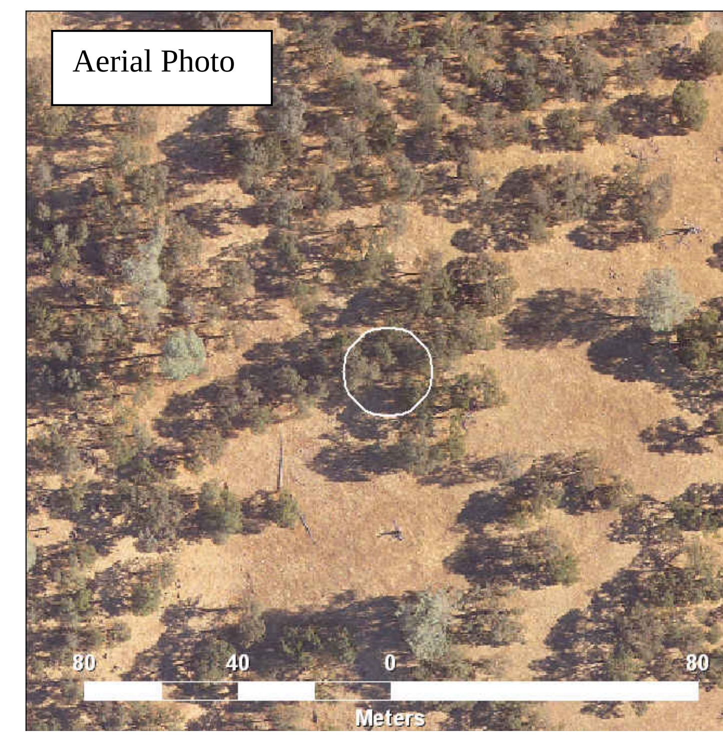

Plot # 57

Feature size: 14.3 m wide
28.4 m long
Vegetation Density: 46.03 %
Lidar block reference number: 4035

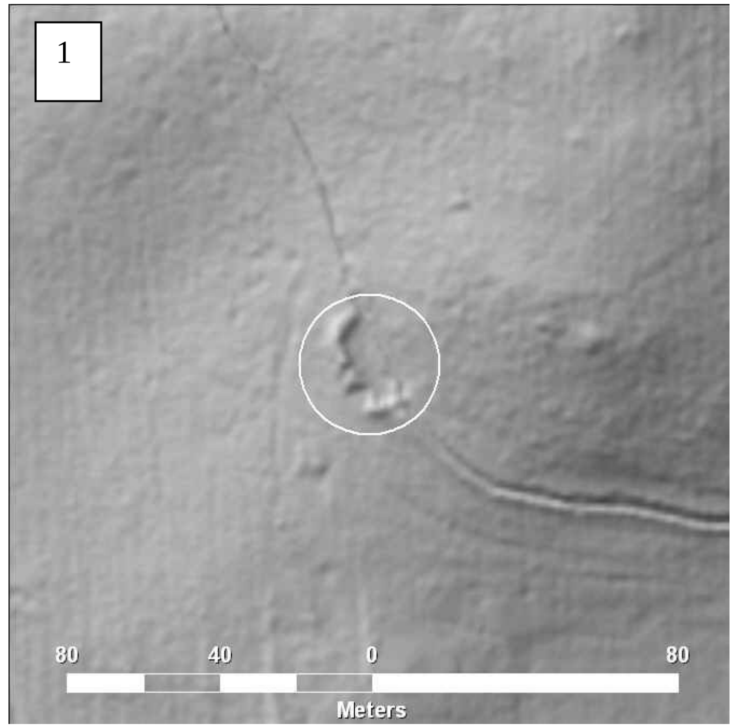

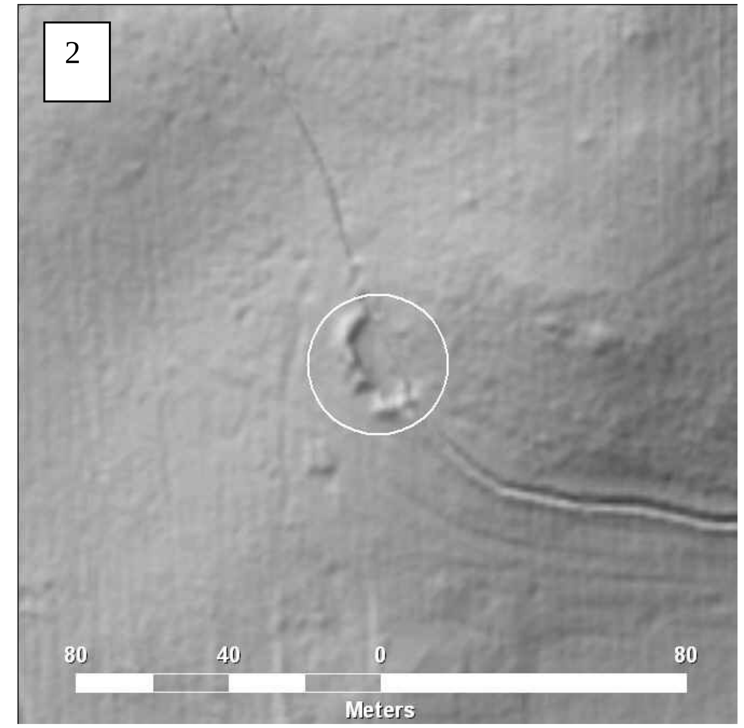

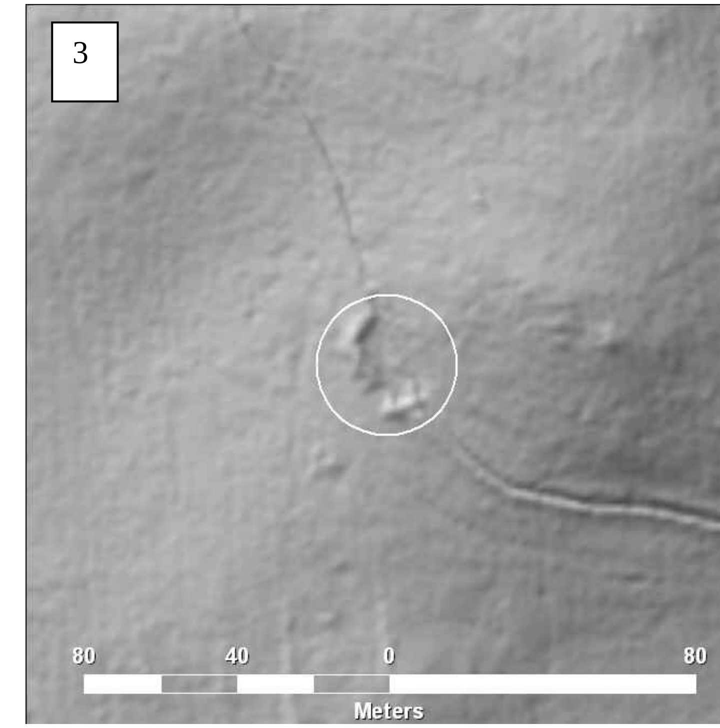

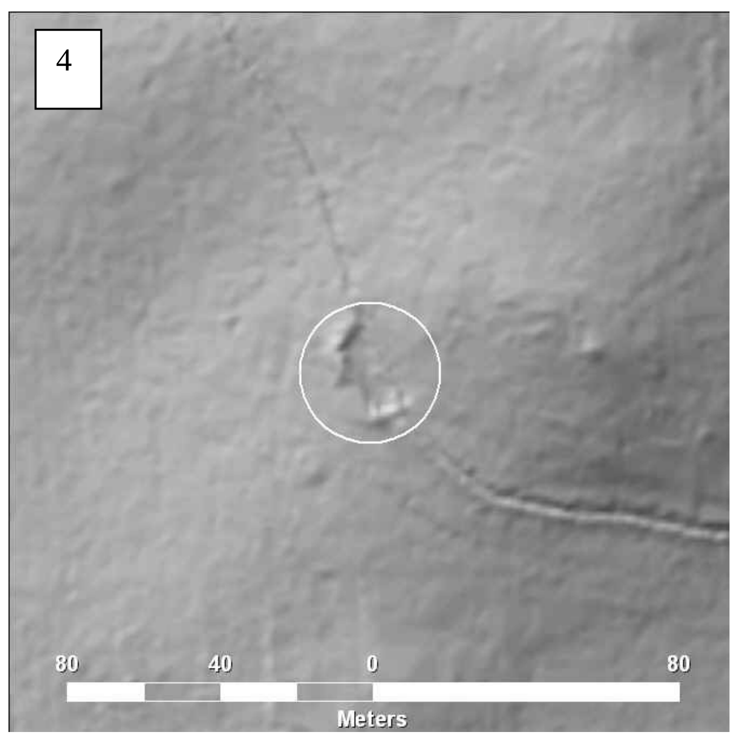

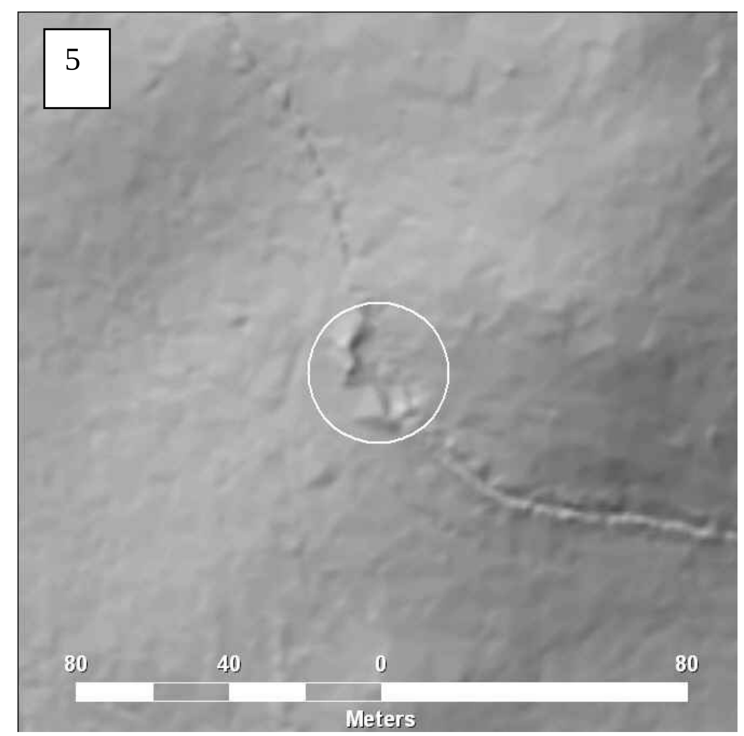

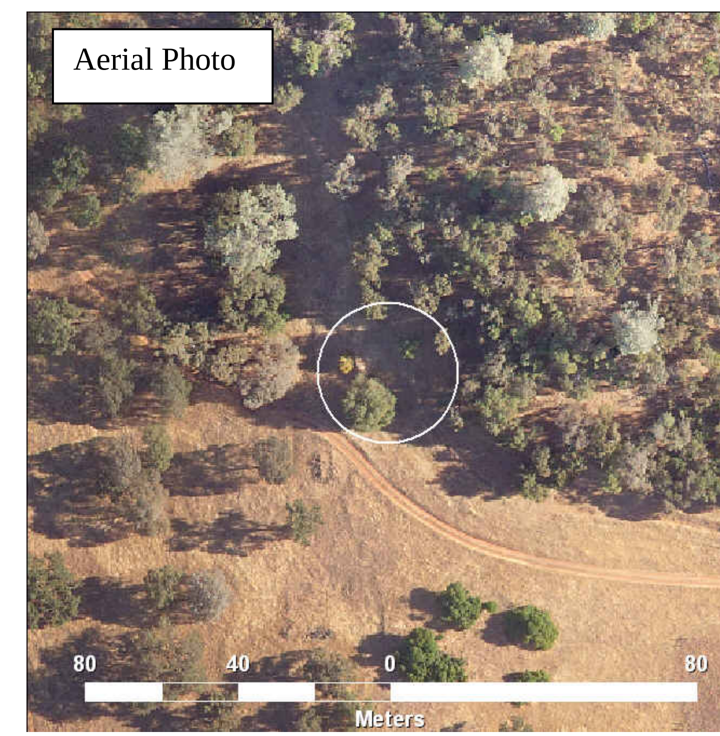

Plot # 58

Feature size: no feature visible
Vegetation Density: 48.85 %
Lidar block reference number: 3987

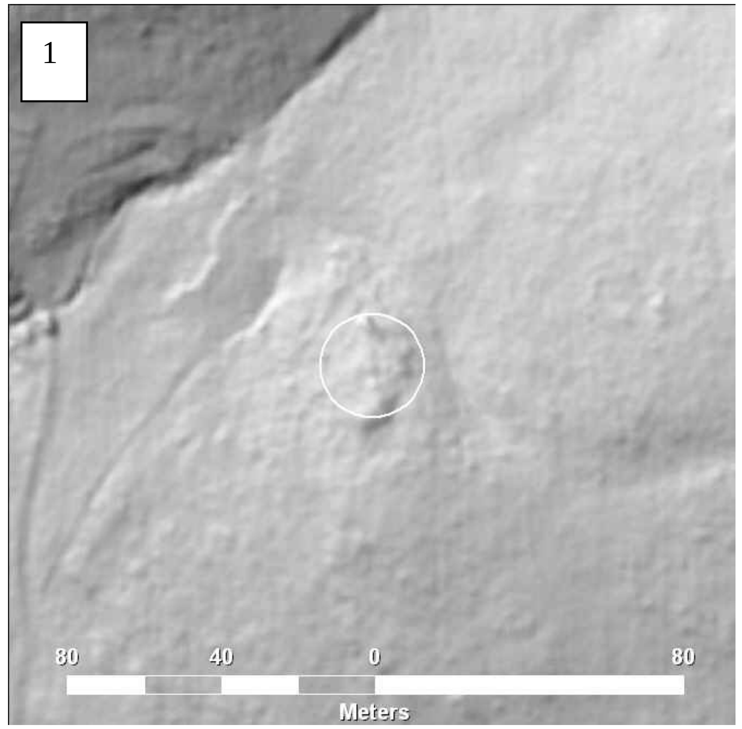

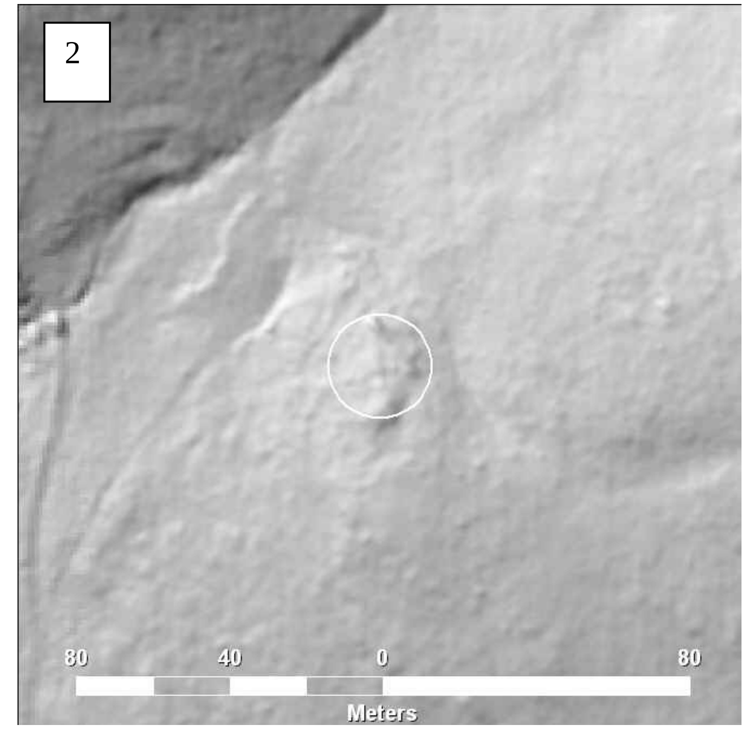

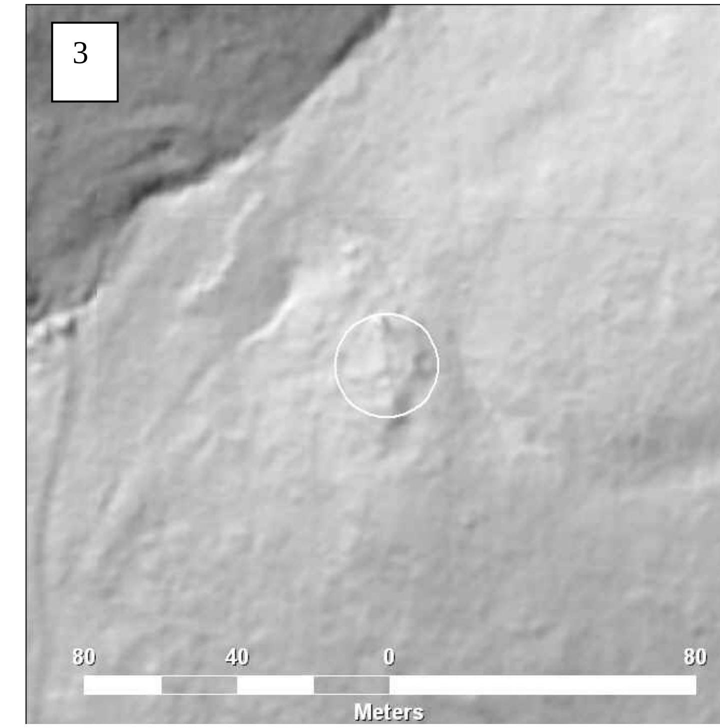

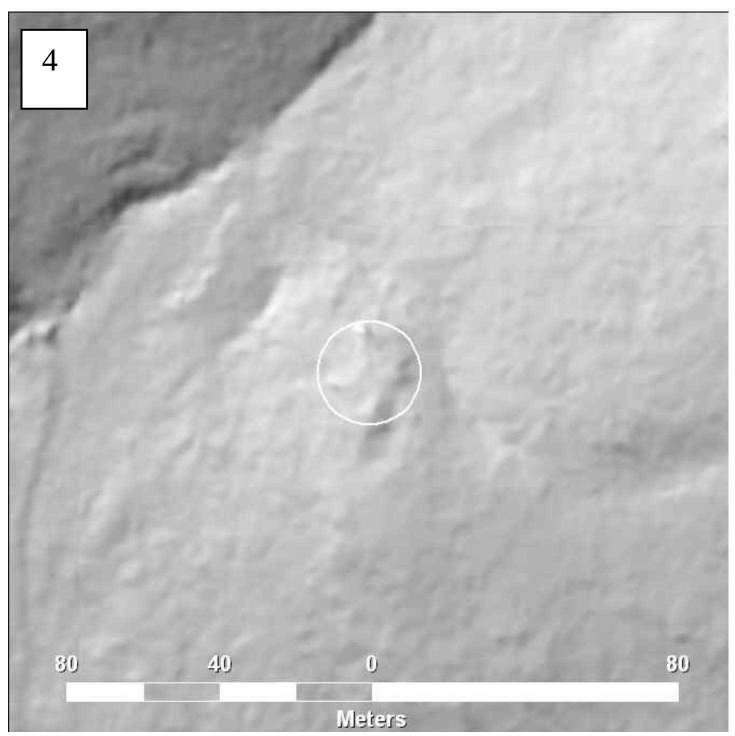

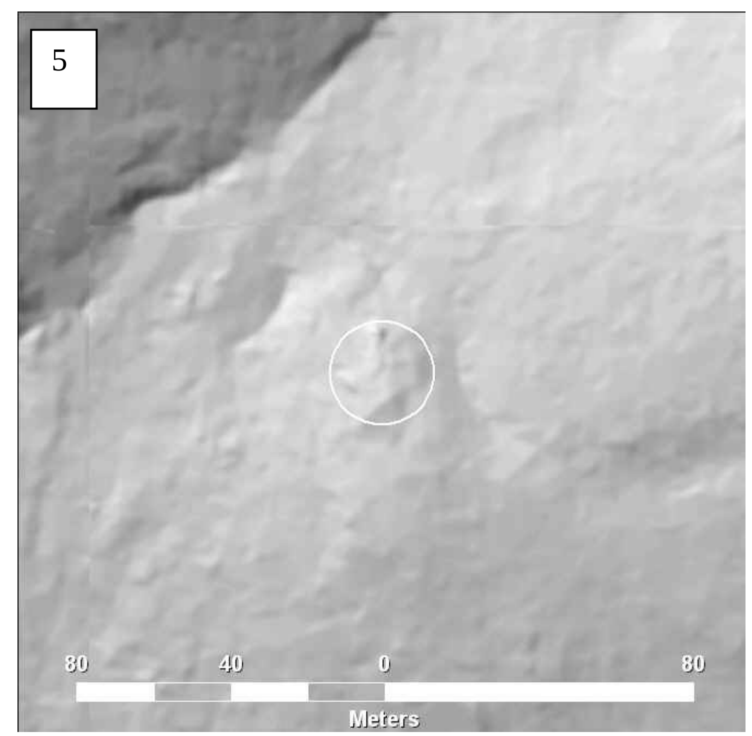

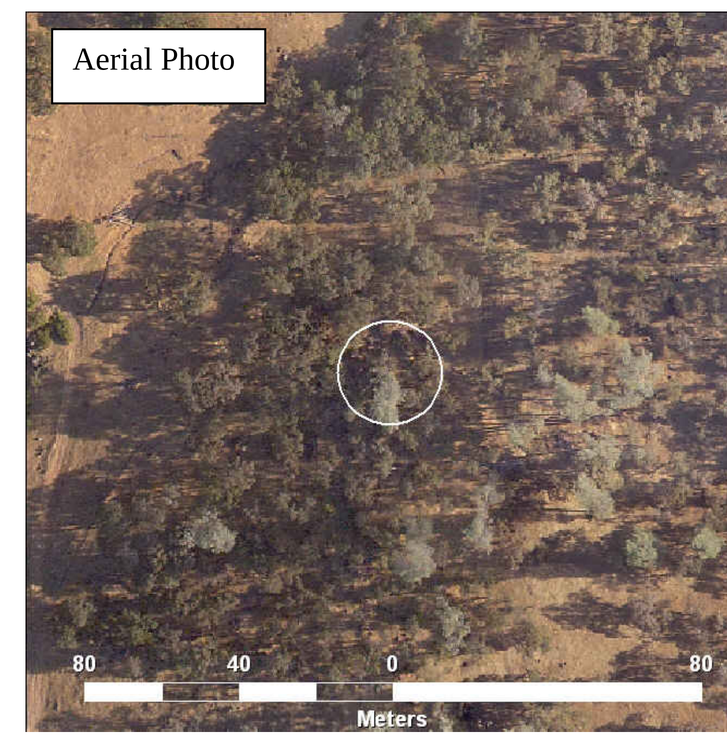

Plot # 59 Feature size: Vegetation Density: 63.28 % Lidar block reference number: 4068	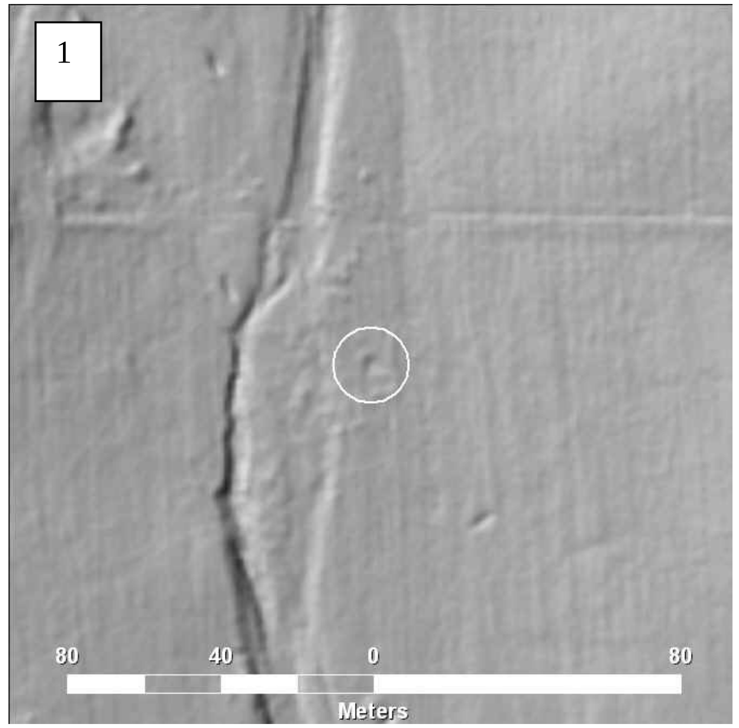	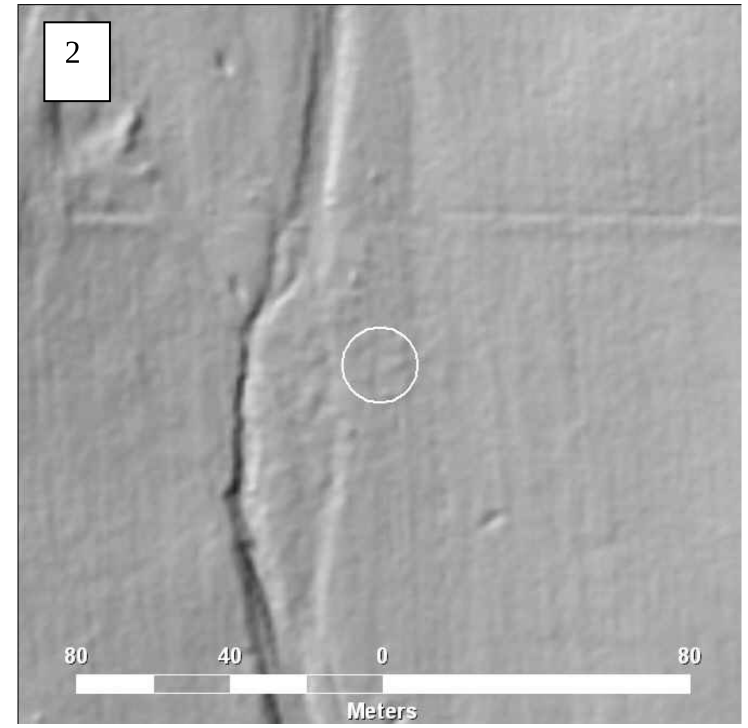	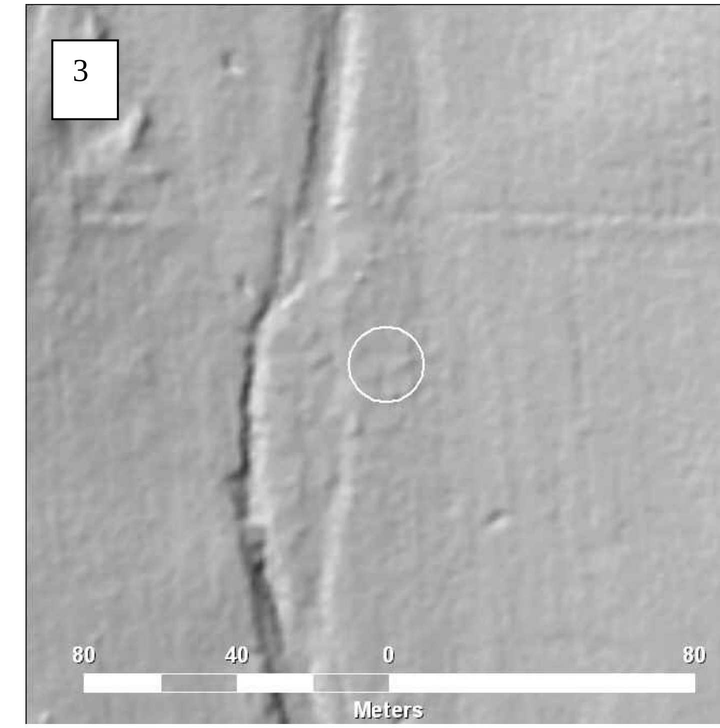
	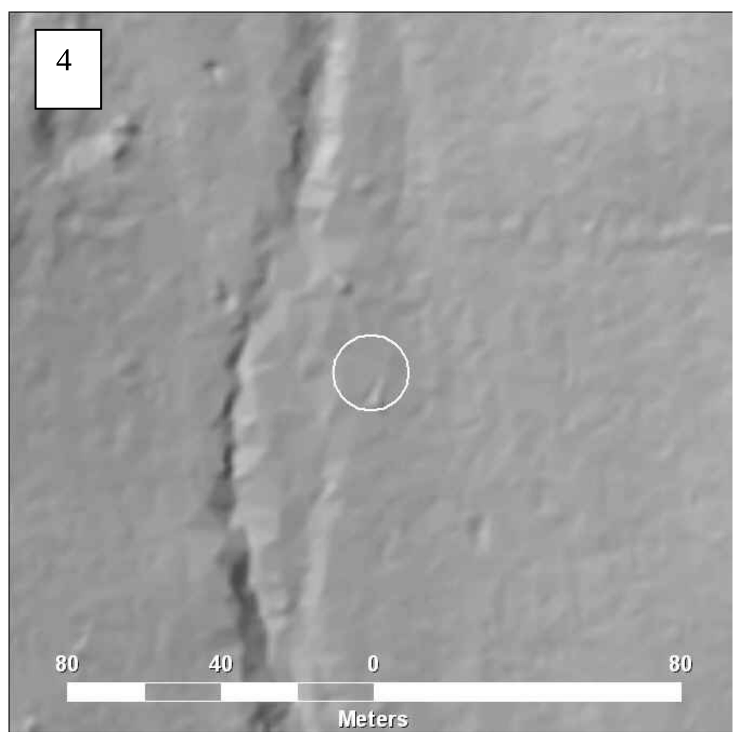	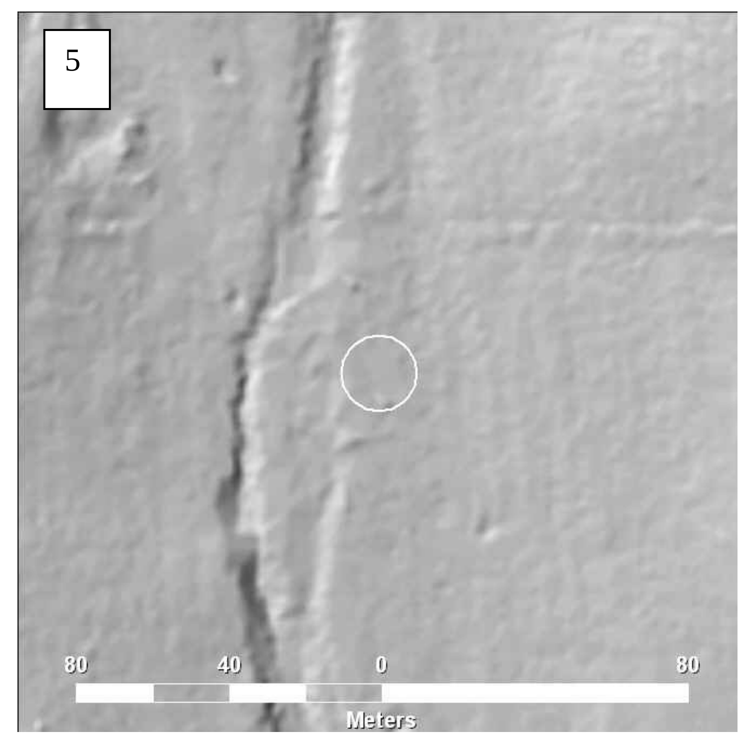	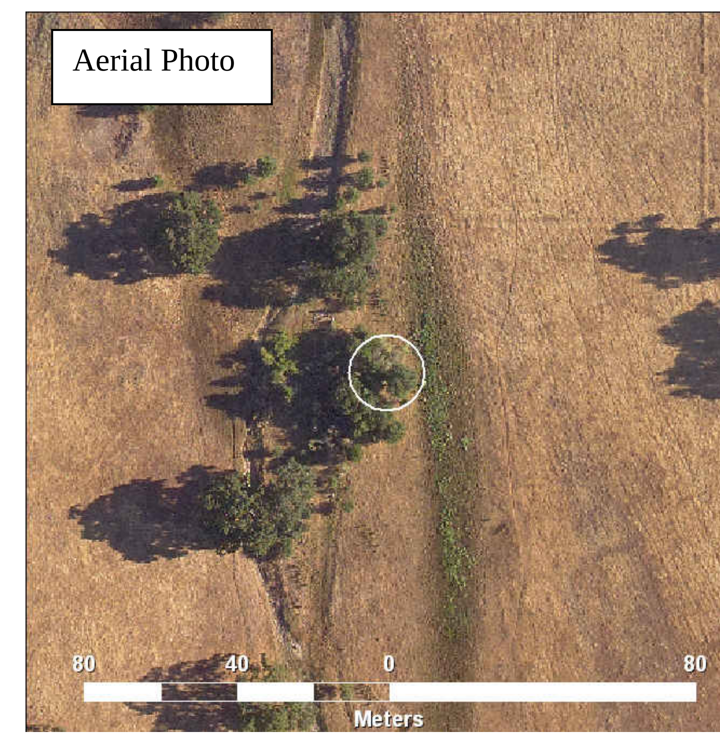

APPENDIX F
FEATURE DETECTION AND POINT DECIMATION – SURFACE MODEL RESULTS

Plot # 1

Feature size: 3.2 m
Vegetation density: 0%
Surface method: TIN
DEM cell size: 1 m
Lidar block reference number: 3977

Additional features visible: possible
Existing features more clearly visible: yes

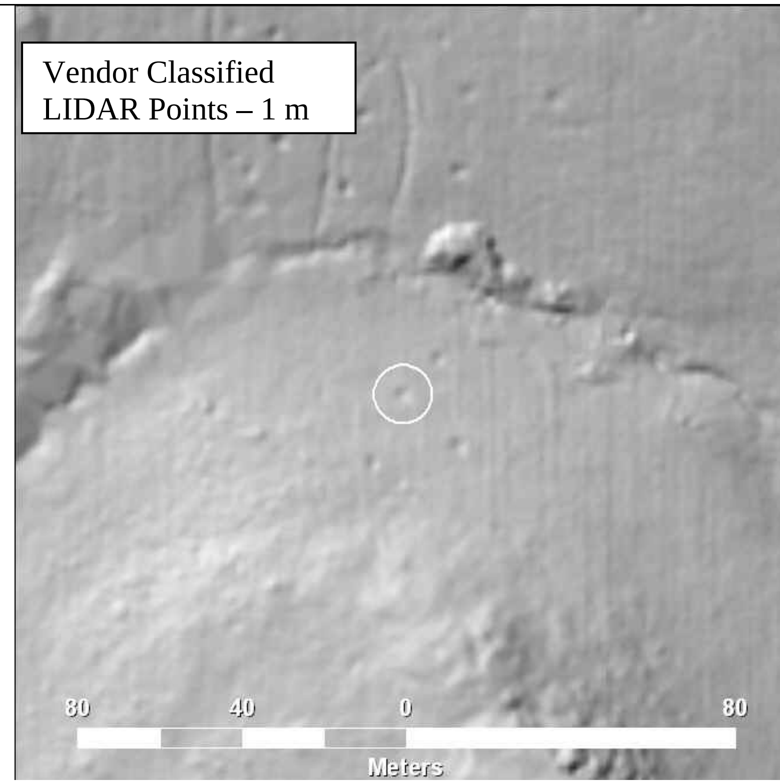

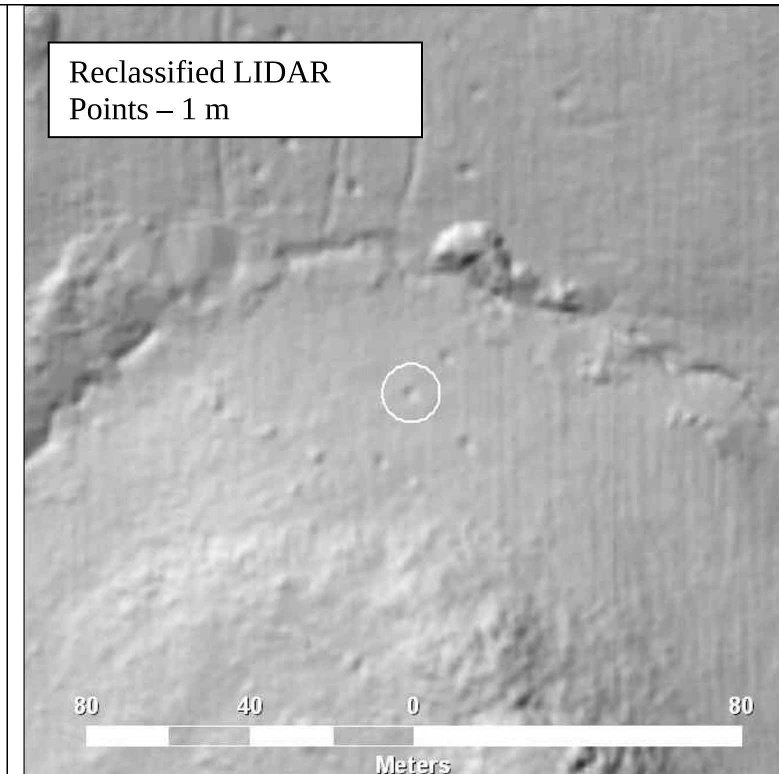

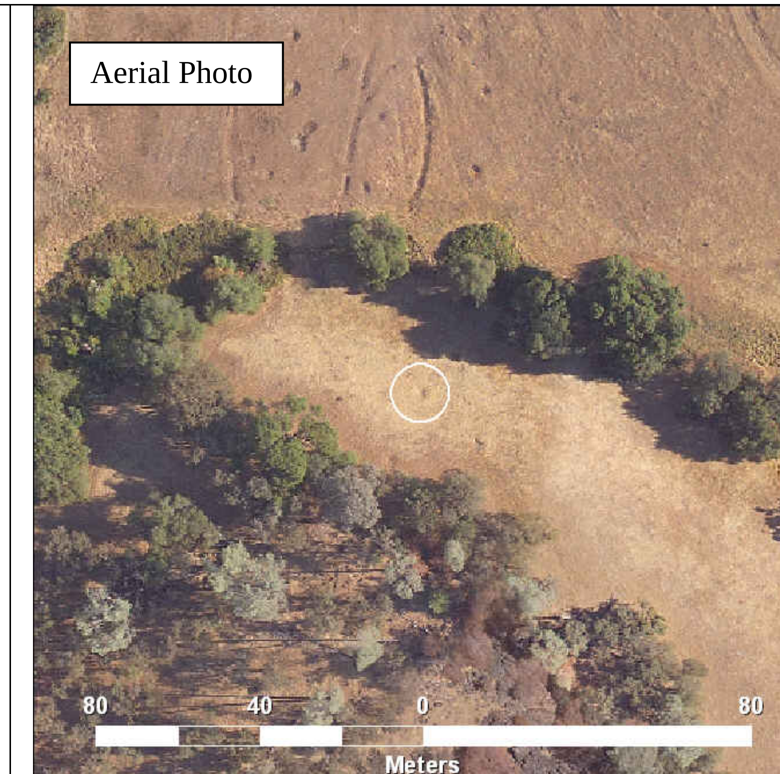

Plot # 1

Feature size: 3.2 m
Vegetation density: 0%
Surface method: TIN
DEM cell size: 0.3 m
Lidar block reference number: 3977

Additional features visible: possible
Existing features more clearly visible: yes

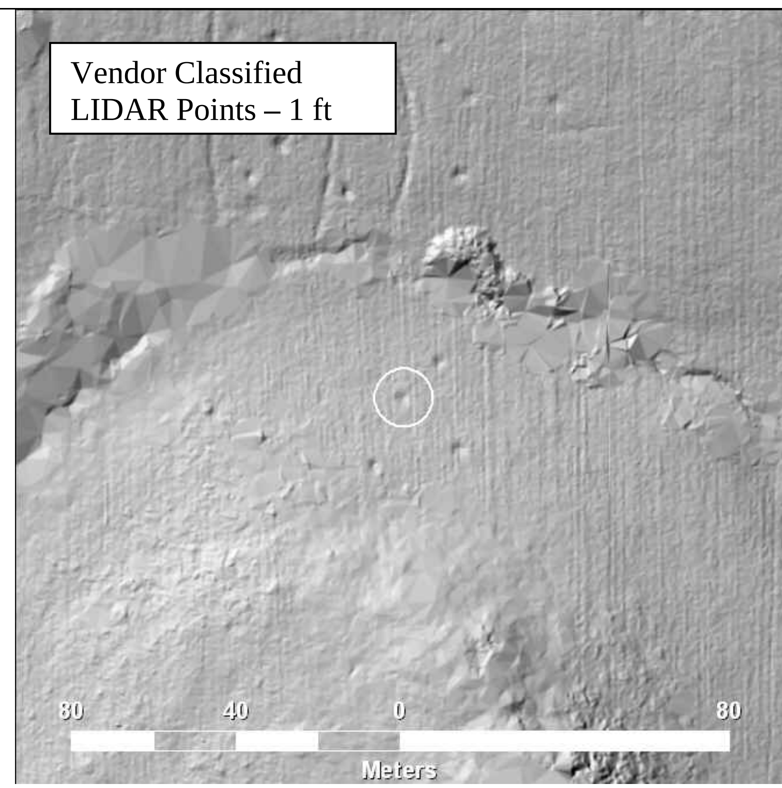

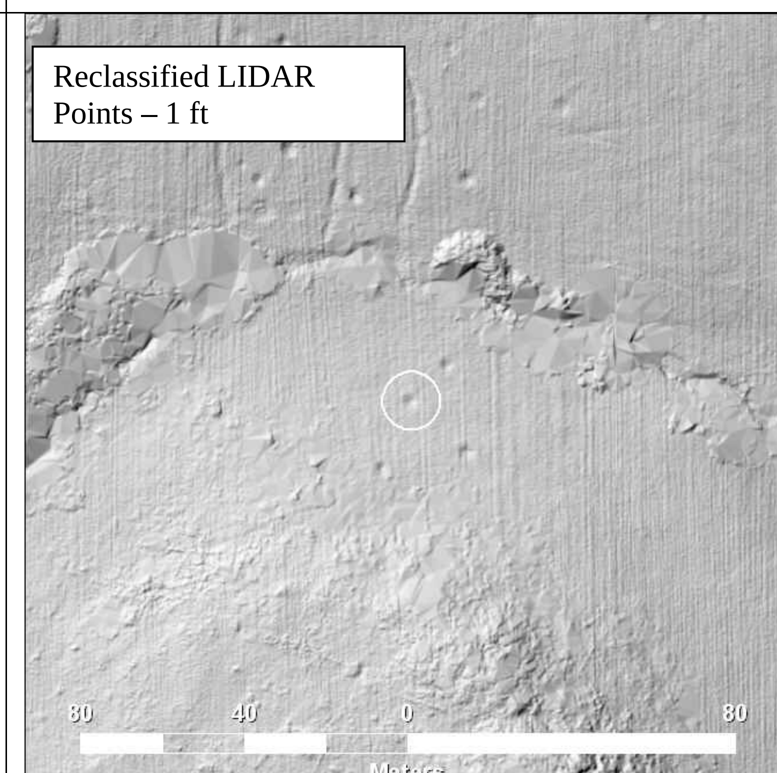

Plot # 1 Feature size: 3.2 m Vegetation density: 0% Surface method: IDW DEM cell size: 1 m Lidar block reference number: 3977 Additional features visible: possible Existing features more clearly visible: yes Interpolated surface shows additional features, and gives a different view of features, than TIN-derived surface.	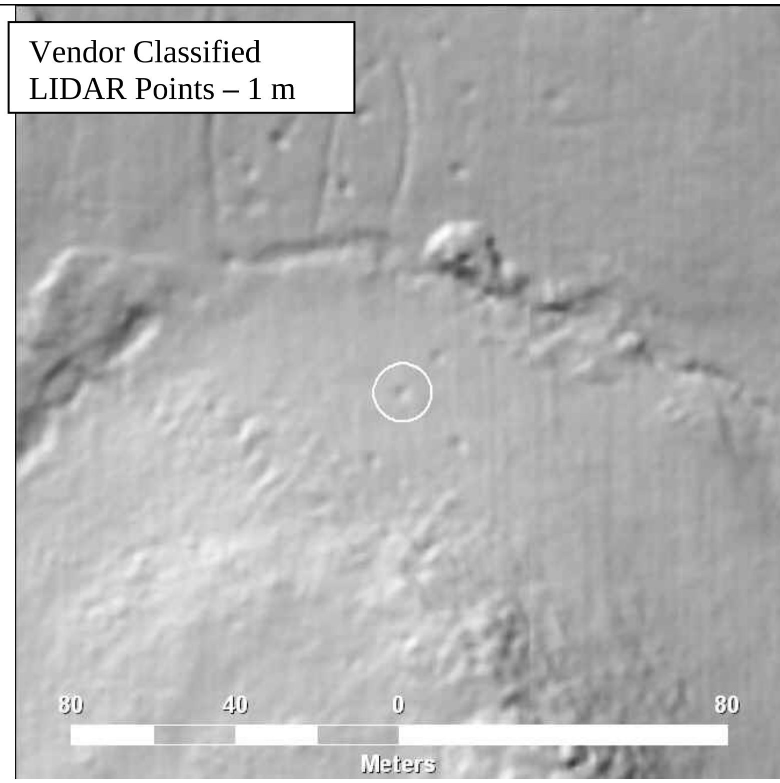	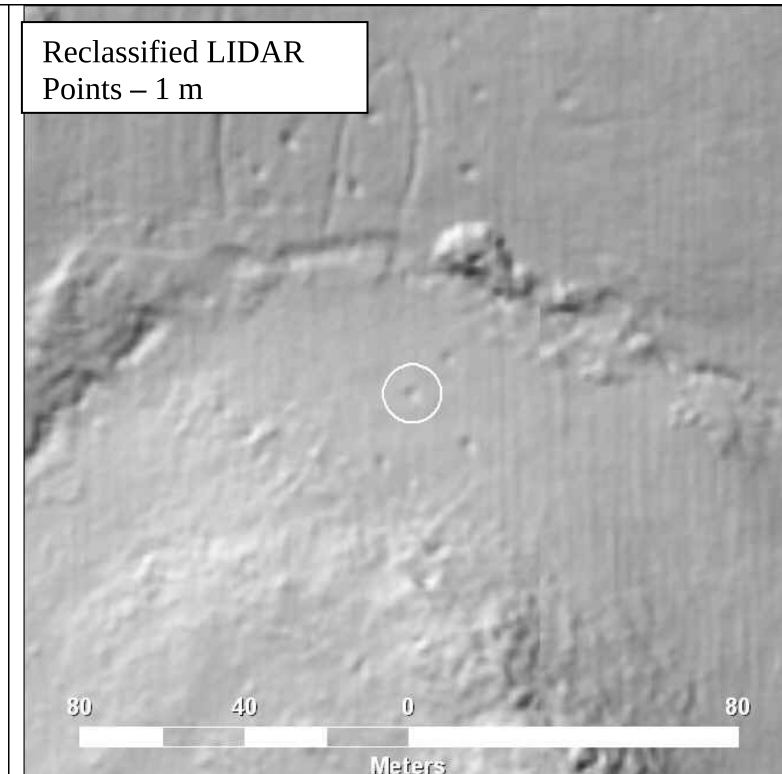	
Plot # 1 Feature size: 3.2 m Vegetation density: 0% Surface method: IDW DEM cell size: 0.3 m Lidar block reference number: 3977 Additional features visible: possible Existing features more clearly visible: yes Interpolated surface shows additional features, and gives a different view of features, than TIN-derived surface.	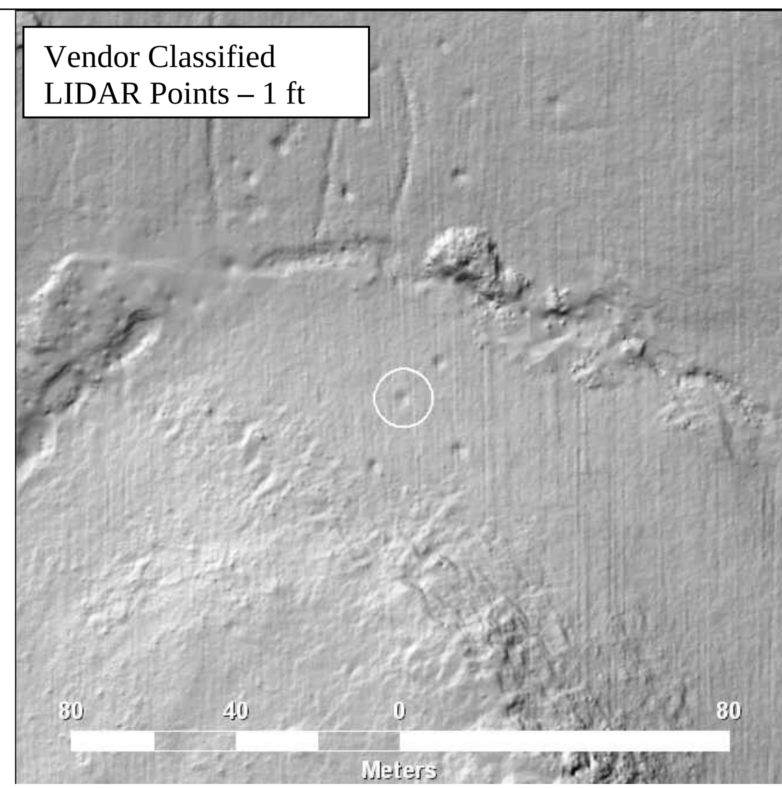	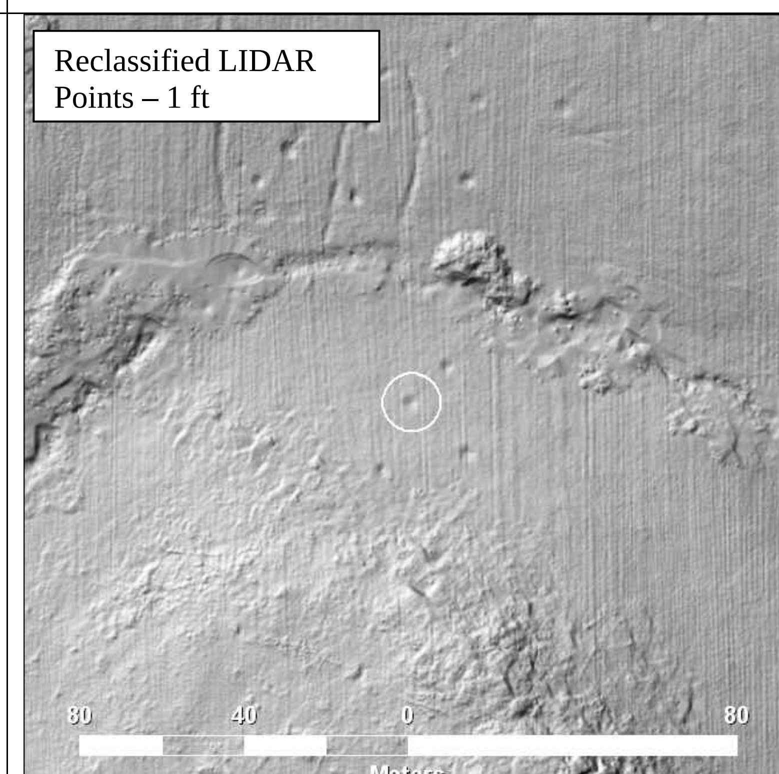	

Plot # 2

Feature size: 1.9 m
Vegetation density: 0%
Surface method: TIN
DEM cell size: 1 m
Lidar block reference number: 4004

Additional features visible: no
Existing features more clearly visible: possible

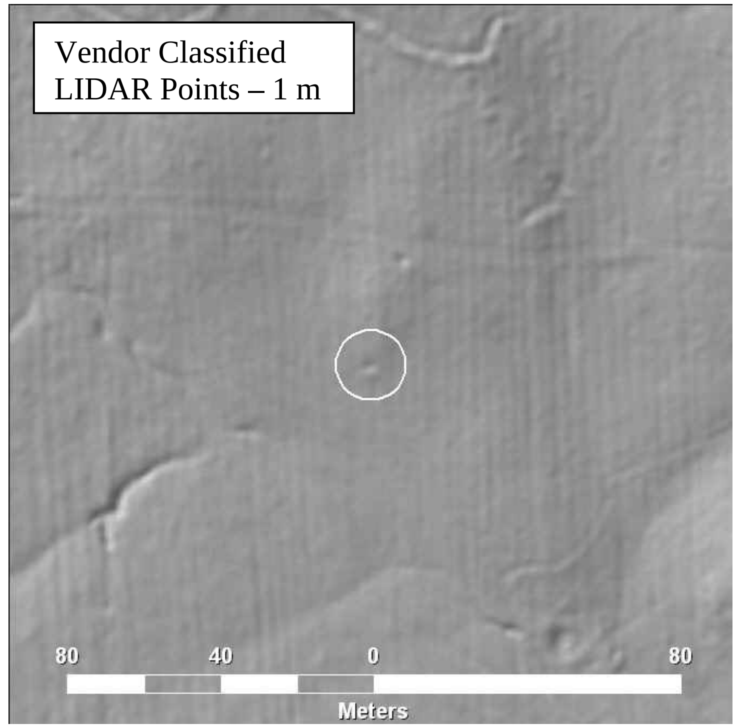

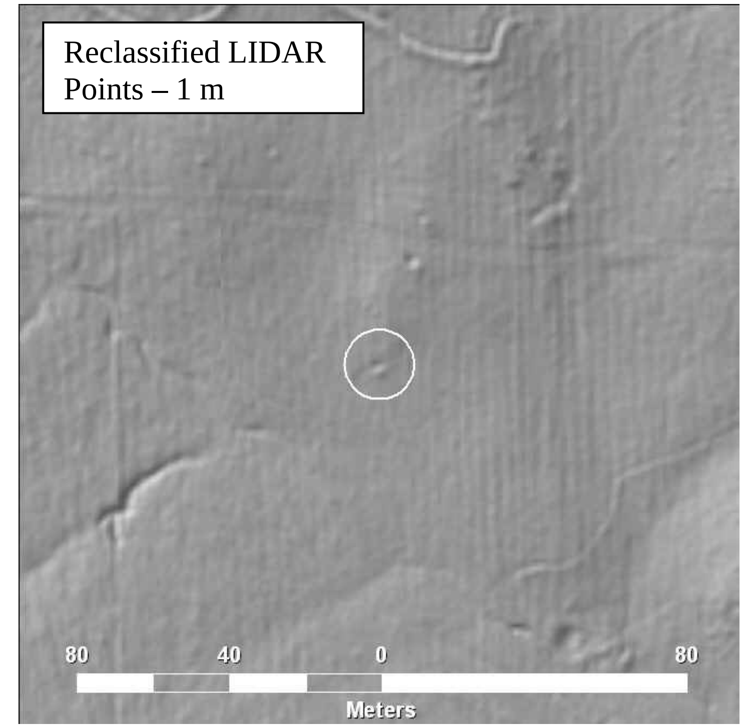

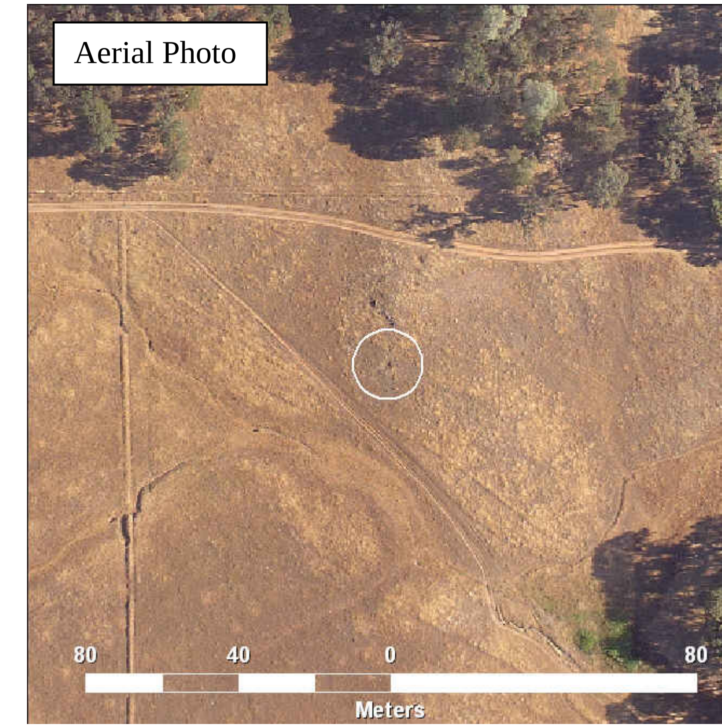

Plot # 2

Feature size: 1.9 m
Vegetation density: 0%
Surface method: TIN
DEM cell size: 0.3 m
Lidar block reference number: 4004

Additional features visible: possible
Existing features more clearly visible: possible

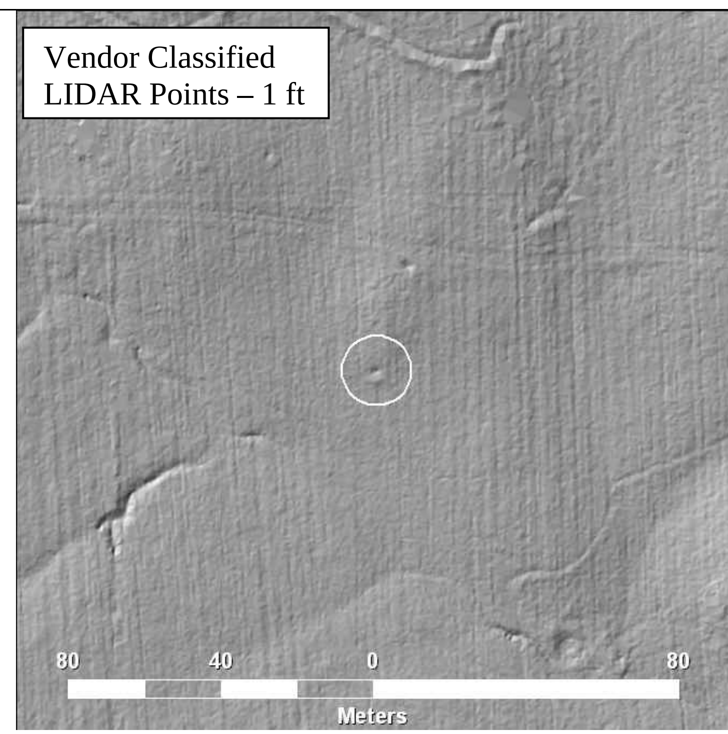

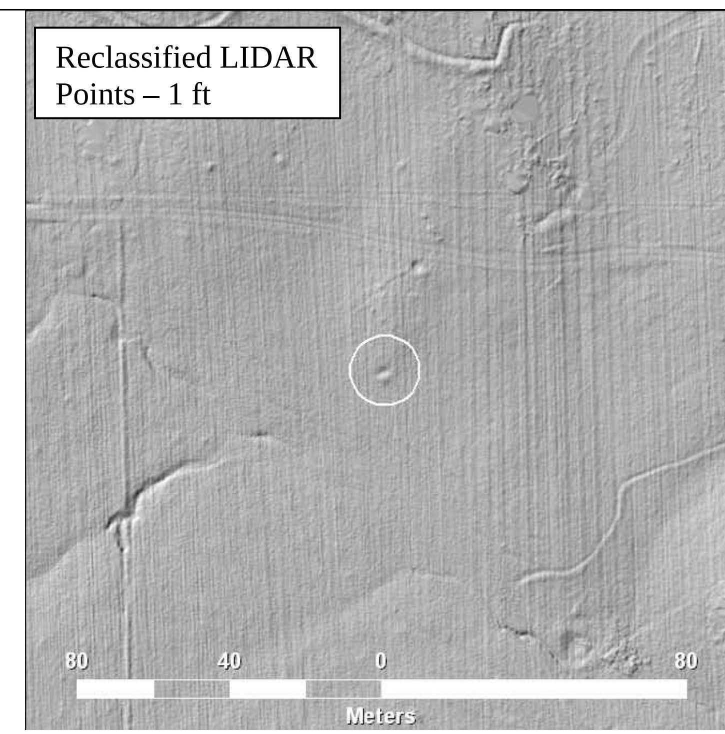

<table>
<tr>
<td>Plot # 2

Feature size: 1.9 m
Vegetation density: 0%
Surface method: IDW
DEM cell size: 1 m
Lidar block reference number: 4004

Additional features visible: no
Existing features more clearly visible: possible

Interpolated surface is generally similar to TIN-derived surface.</td>
<td>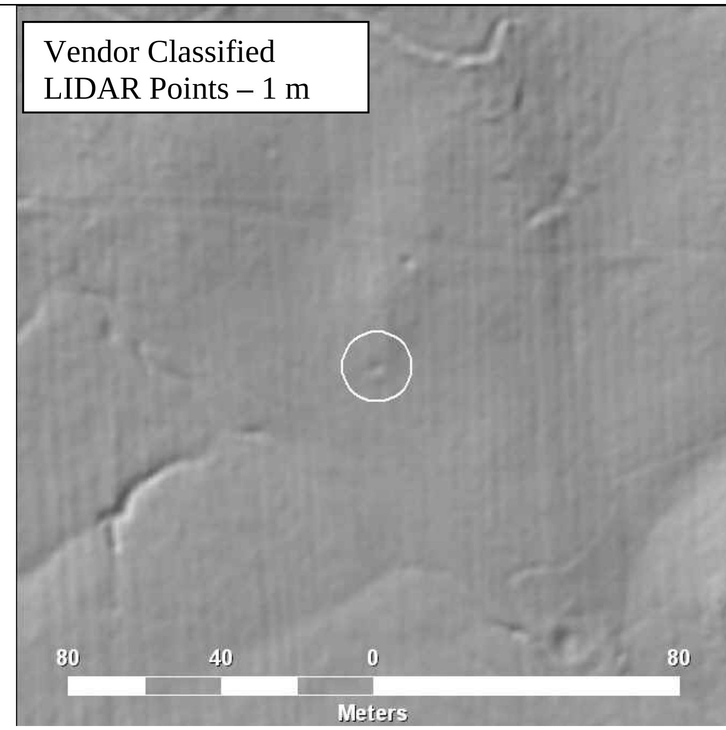
</td>
<td>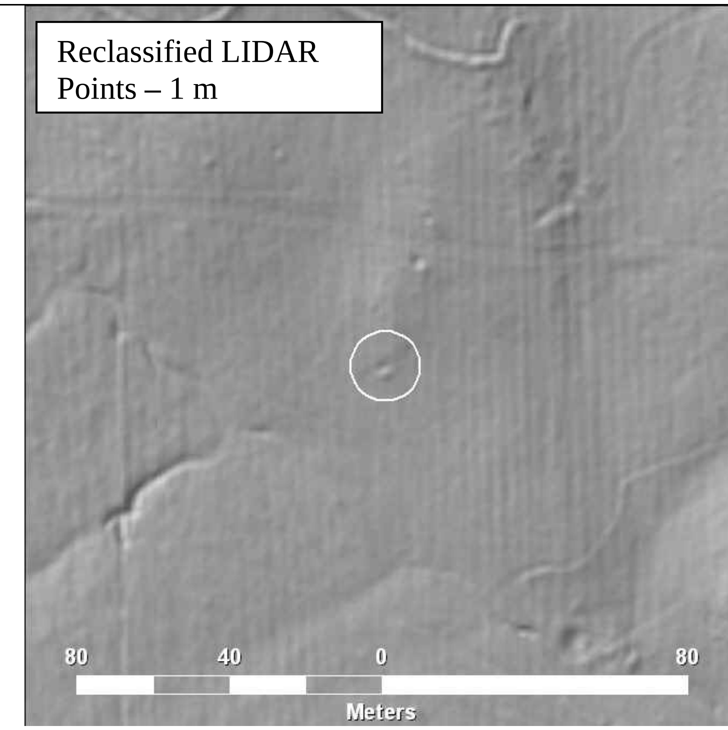
</td>
<td></td>
</tr>
<tr>
<td>Plot # 2

Feature size: 1.9 m
Vegetation density: 0%
Surface method: IDW
DEM cell size: 0.3 m
Lidar block reference number: 4004

Additional features visible: no
Existing features more clearly visible: yes

Interpolated surface is generally similar to TIN-derived surface.</td>
<td>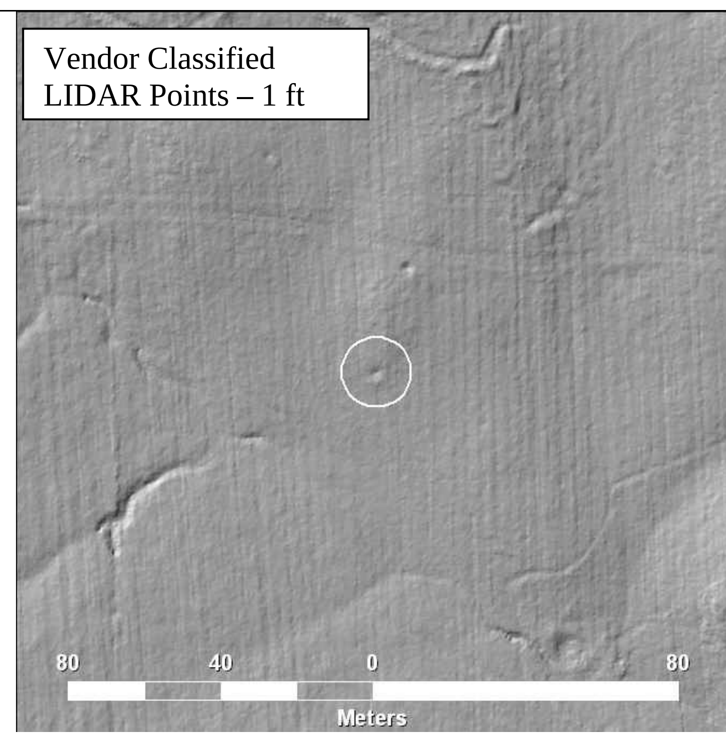
</td>
<td>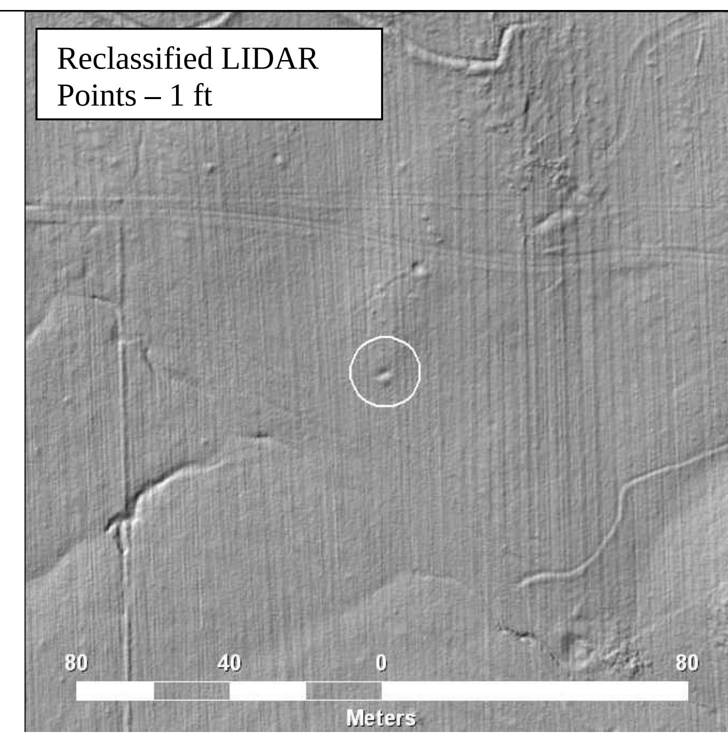
</td>
<td></td>
</tr>
</table>

Plot # 3

Feature size: 4.2 m
Vegetation density: 46.35%
Surface method: TIN
DEM cell size: 1 m
Lidar block reference number: 4088

Additional features visible: possible
Existing features more clearly visible: possible

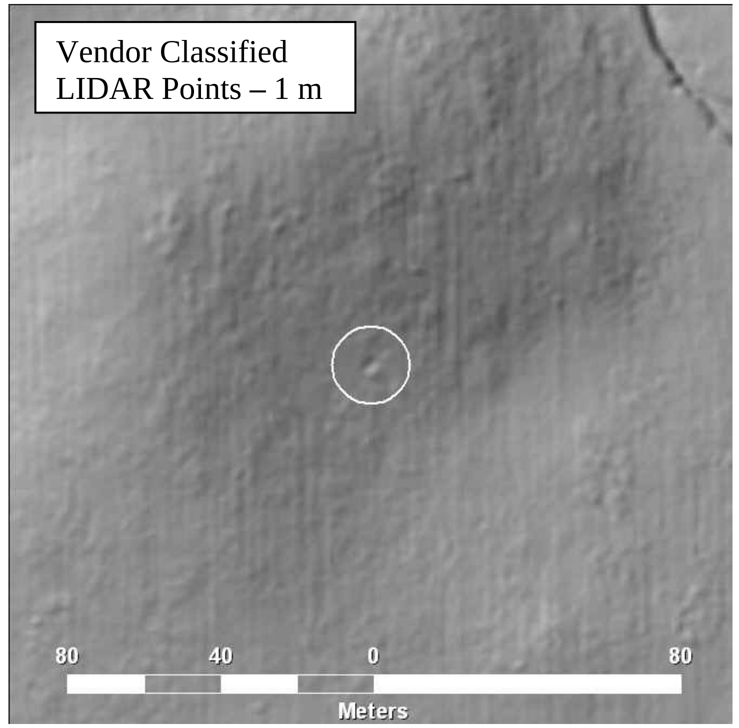

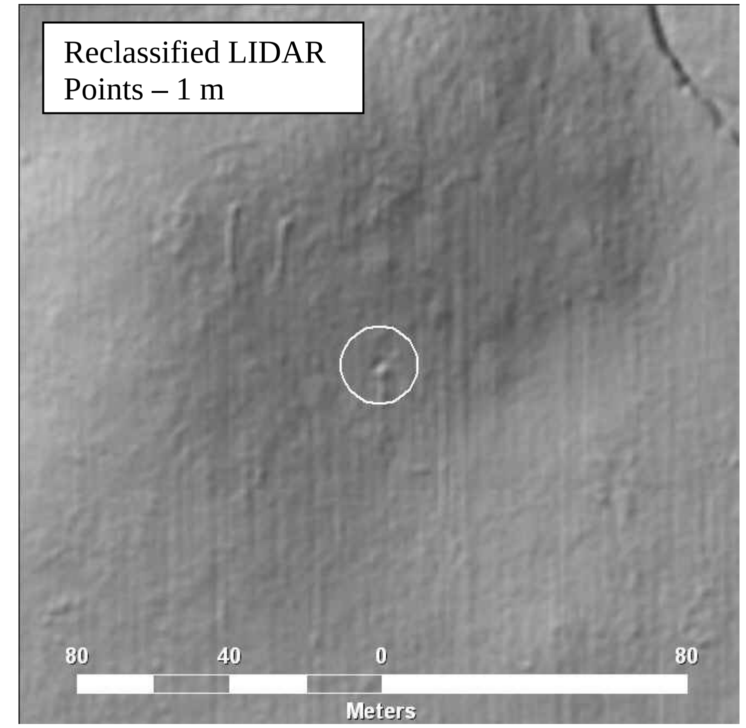

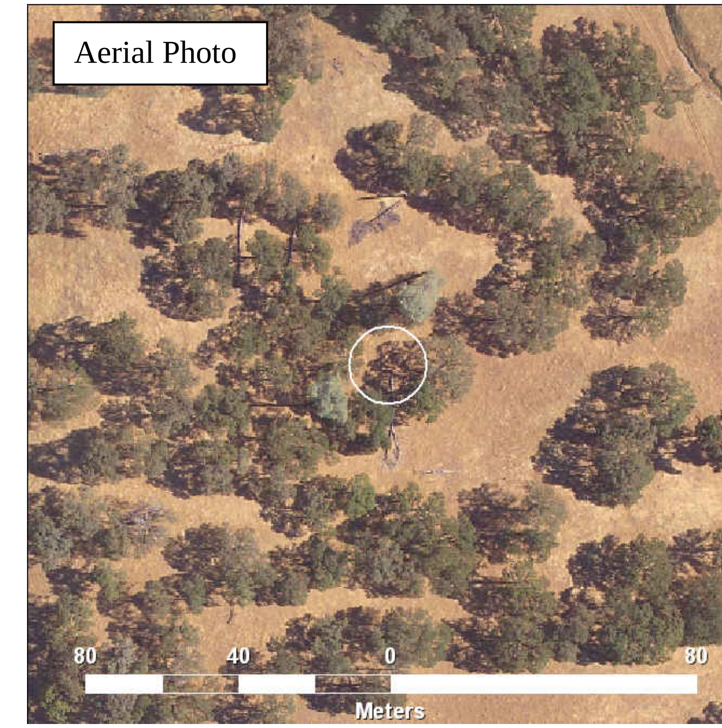

Plot # 3

Feature size: 4.2 m
Vegetation density: 46.35%
Surface method: TIN
DEM cell size: 0.3 m
Lidar block reference number: 4088

Additional features visible: possible
Existing features more clearly visible: possible

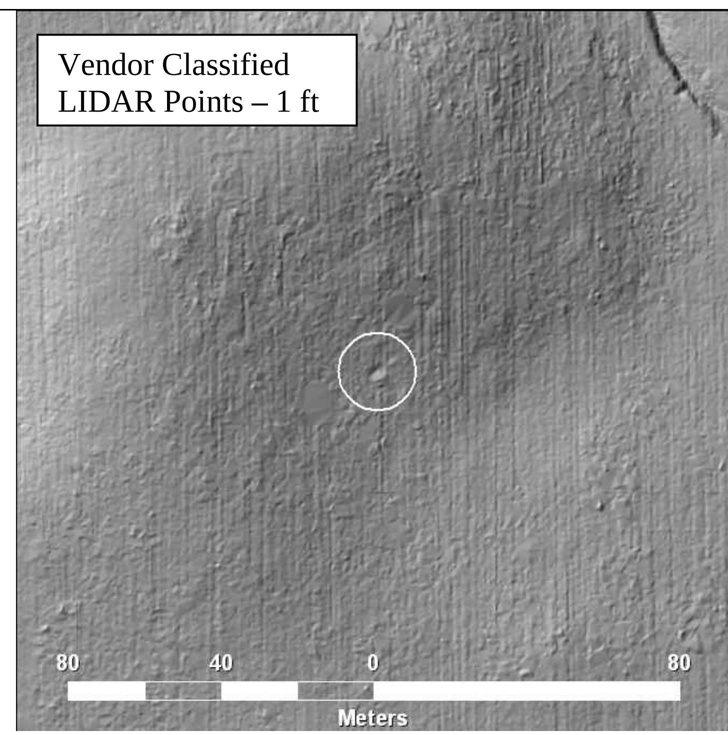

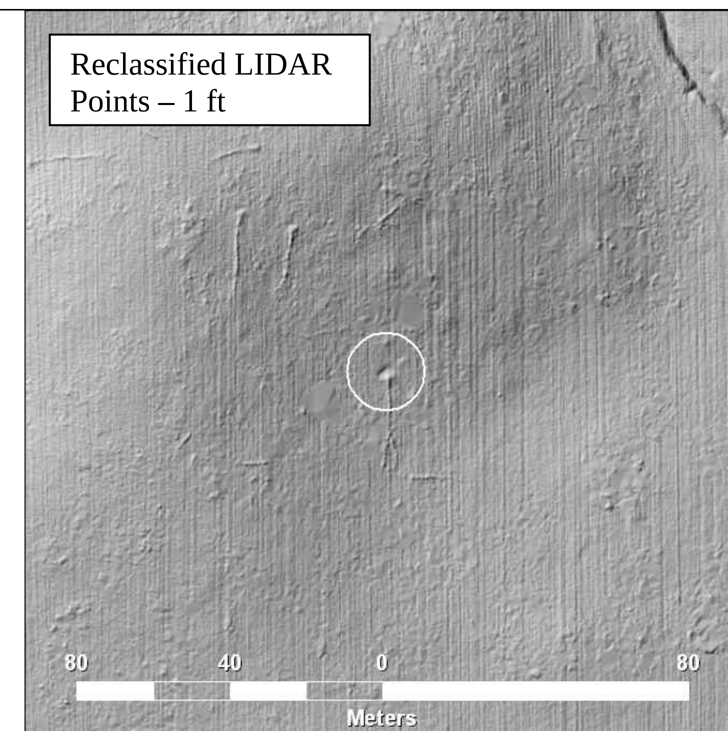

Plot # 3 Feature size: 4.2 m Vegetation density: 46.35% Surface method: IDW DEM cell size: 1 m Lidar block reference number: 4088 Additional features visible: possible Existing features more clearly visible: possible Interpolated surface shows additional features than TIN-derived surface.	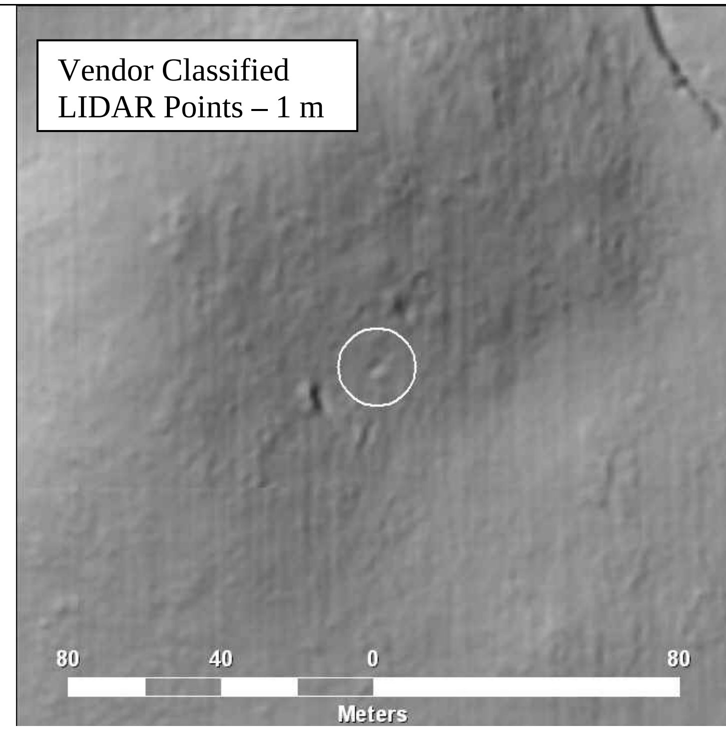	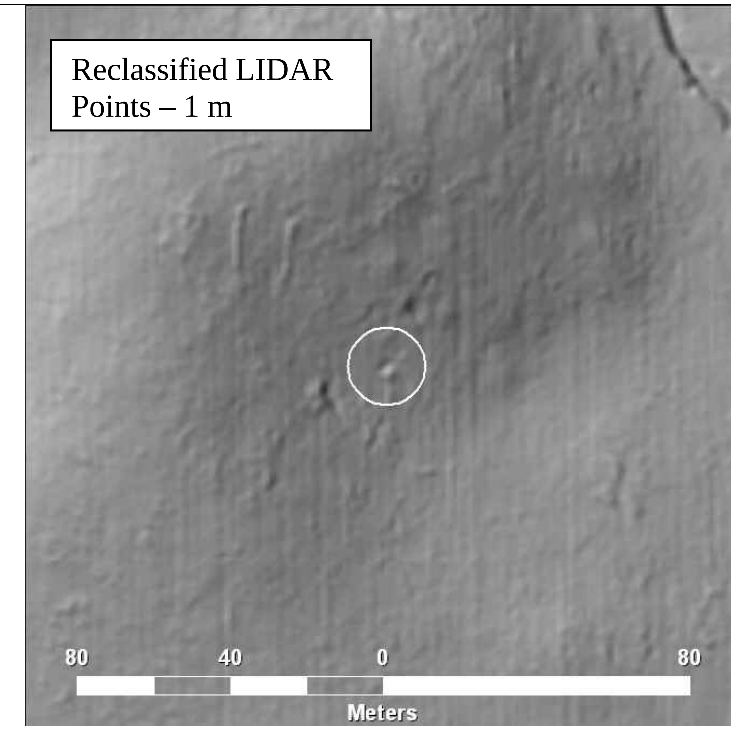	
Plot # 3 Feature size: 4.2 m Vegetation density: 46.35% Surface method: IDW DEM cell size: 0.3 m Lidar block reference number: 4088 Additional features visible: possible Existing features more clearly visible: possible Interpolated surface shows additional features than TIN-derived surface.	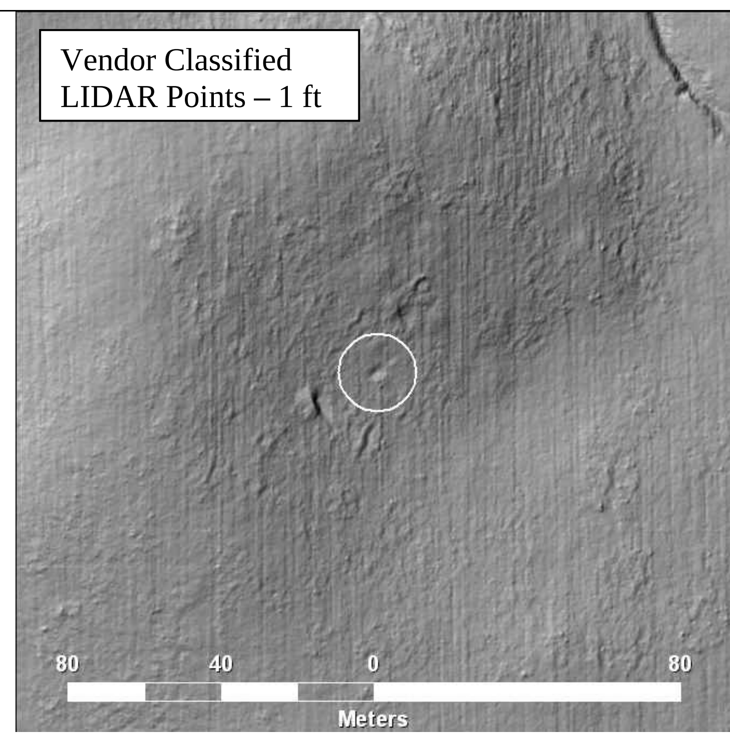	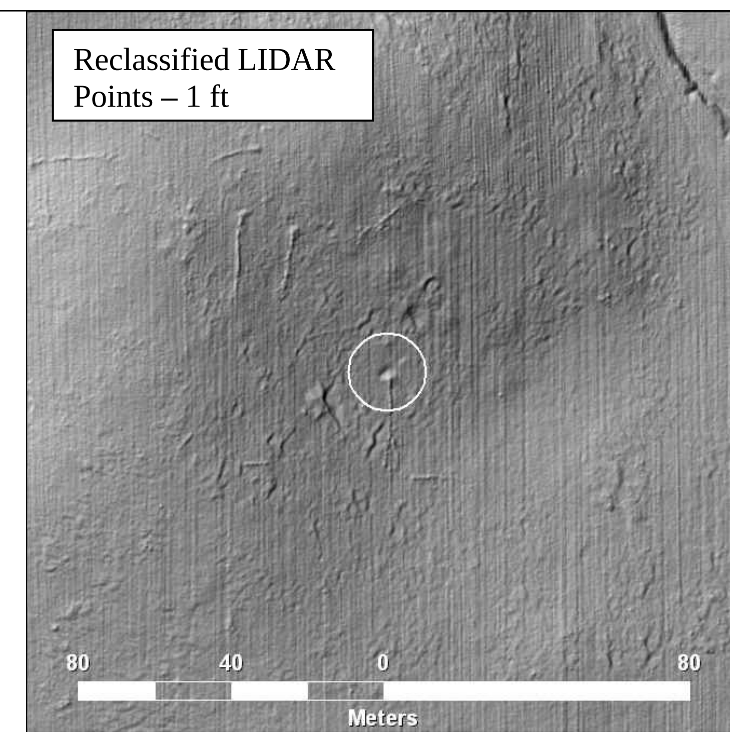	

<table>
<tr>
<td>Plot # 4

Feature size: 2.9 m
Vegetation density: 34.16%
Surface method: TIN
DEM cell size: 1 m
Lidar block reference number: 4007

Additional features visible: no
Existing features more clearly visible: possible</td>
<td>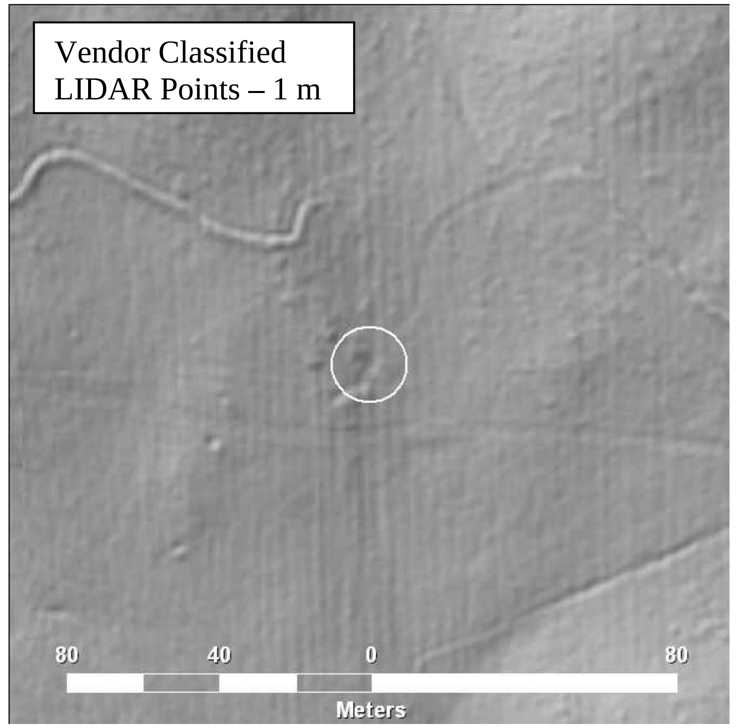
</td>
<td>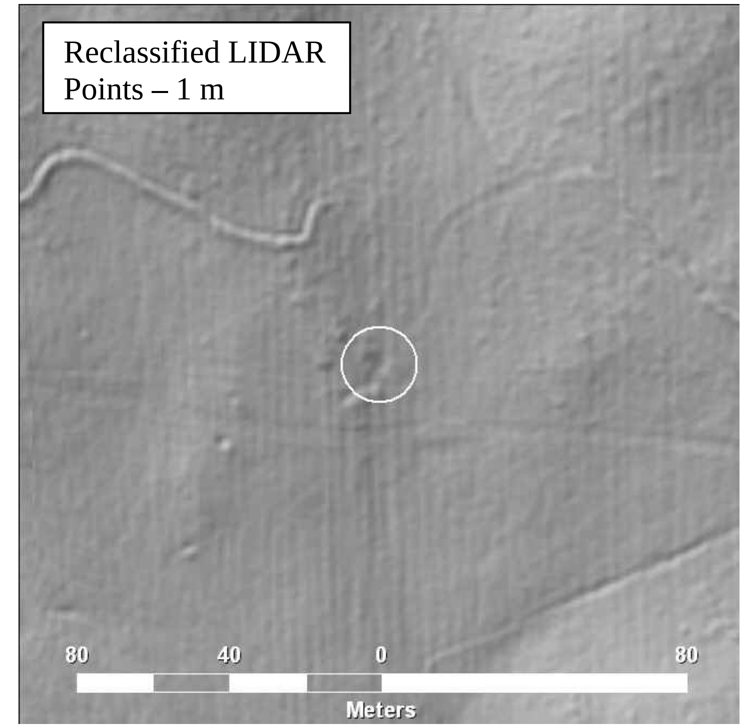
</td>
<td>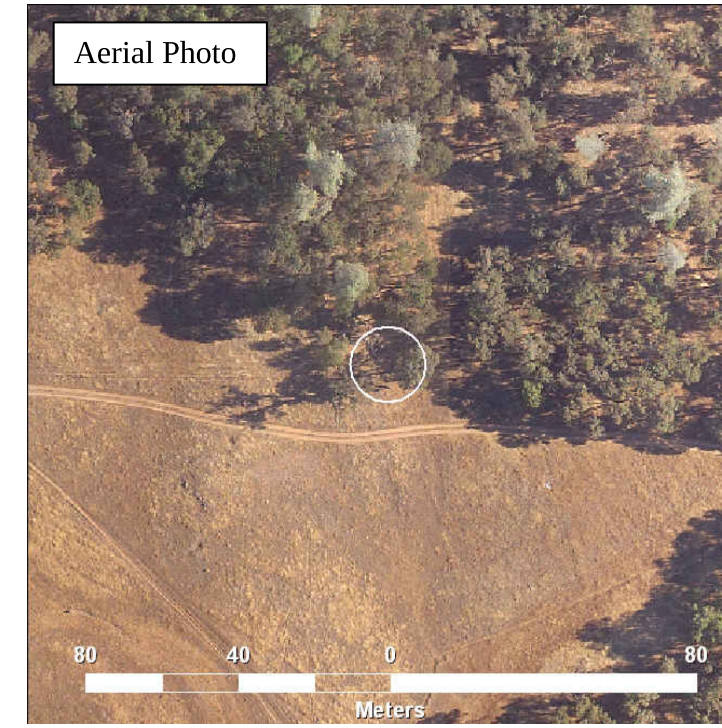
</td>
</tr>
<tr>
<td>Plot # 4

Feature size: 2.9 m
Vegetation density: 34.16%
Surface method: TIN
DEM cell size: 0.3 m
Lidar block reference number: 4007

Additional features visible: no
Existing features more clearly visible: possible</td>
<td>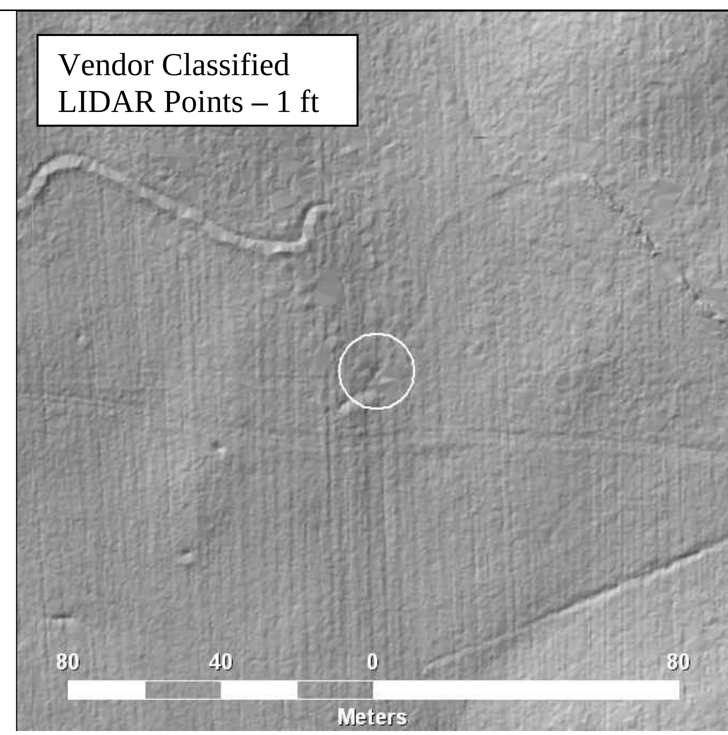
</td>
<td>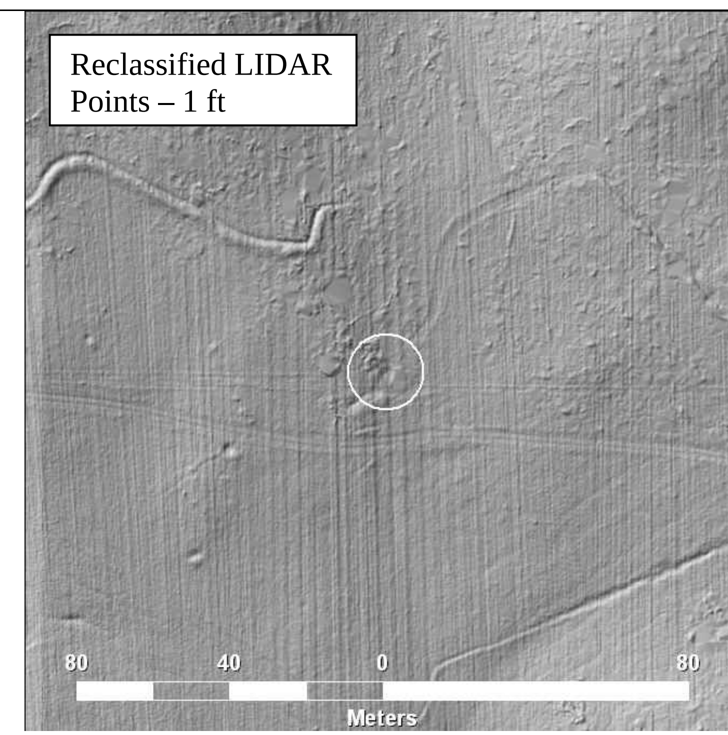
</td>
<td></td>
</tr>
</table>

Plot # 5 Feature size: 4 m Vegetation density: 47.44% Surface method: TIN DEM cell size: 1 m Lidar block reference number: 4065 Additional features visible: no Existing features more clearly visible: possible	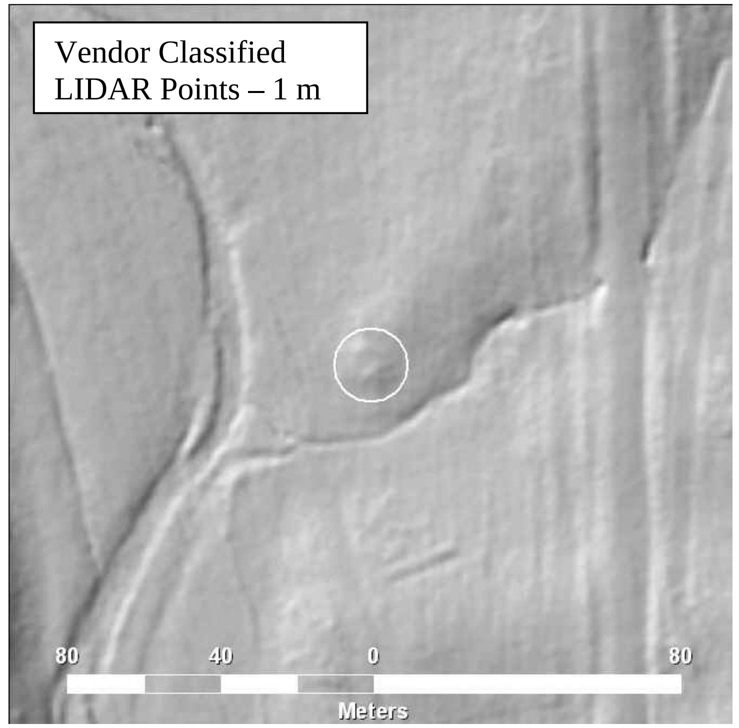	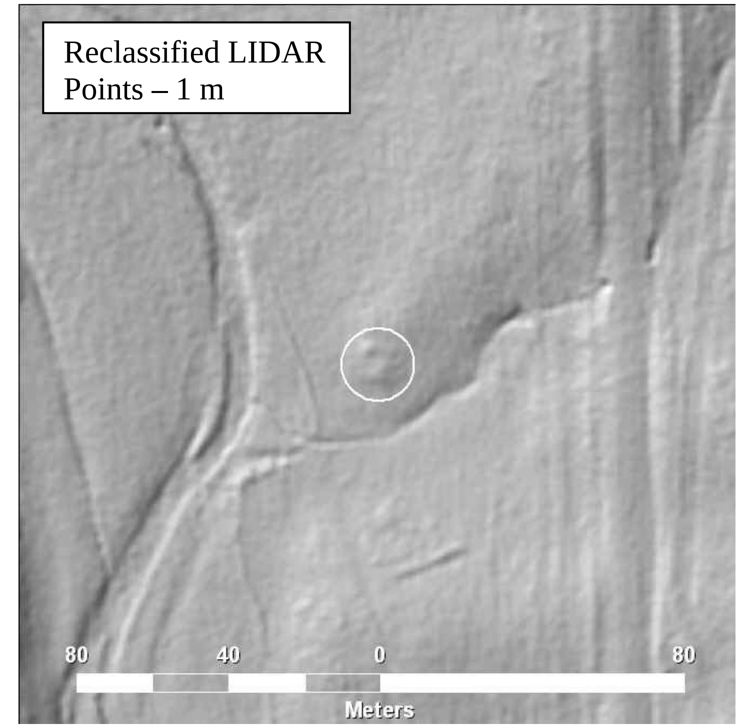	
Plot # 5 Feature size: 4 m Vegetation density: 47.44% Surface method: TIN DEM cell size: 0.3 m Lidar block reference number: 4065 Additional features visible: no Existing features more clearly visible: possible	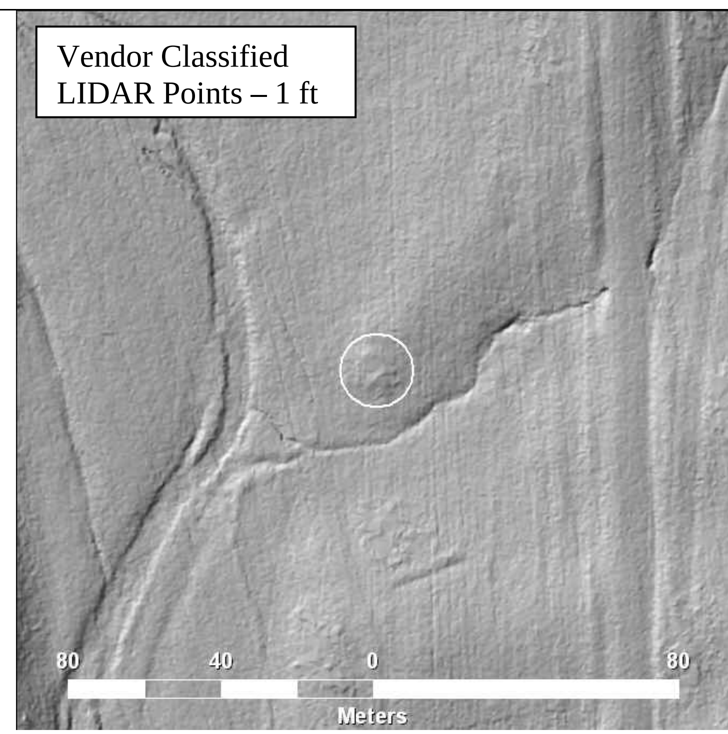	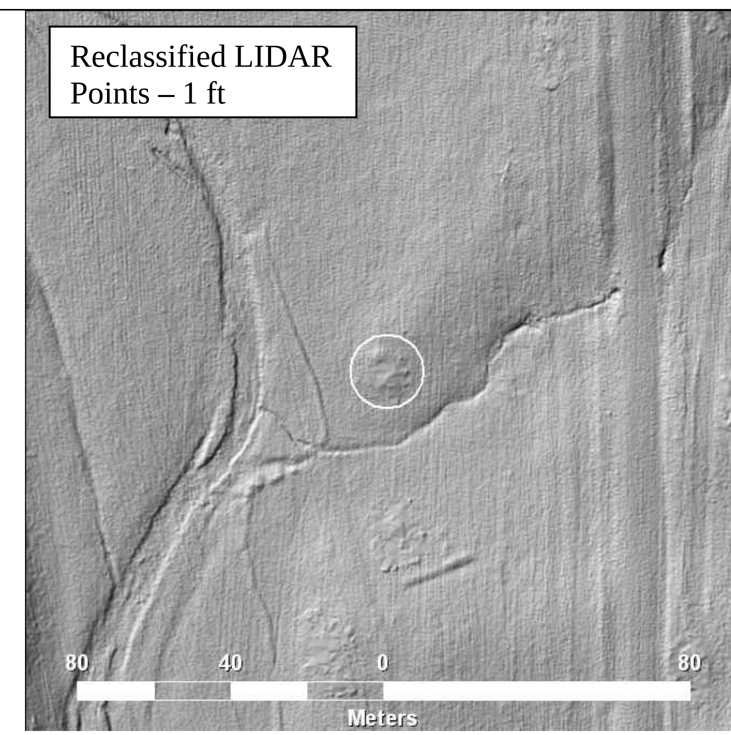	

Plot # 6 Feature size: 4.6 m Vegetation density: 47.76% Surface method: TIN DEM cell size: 1 m Lidar block reference number: 4086 Additional features visible: no Existing features more clearly visible: possible	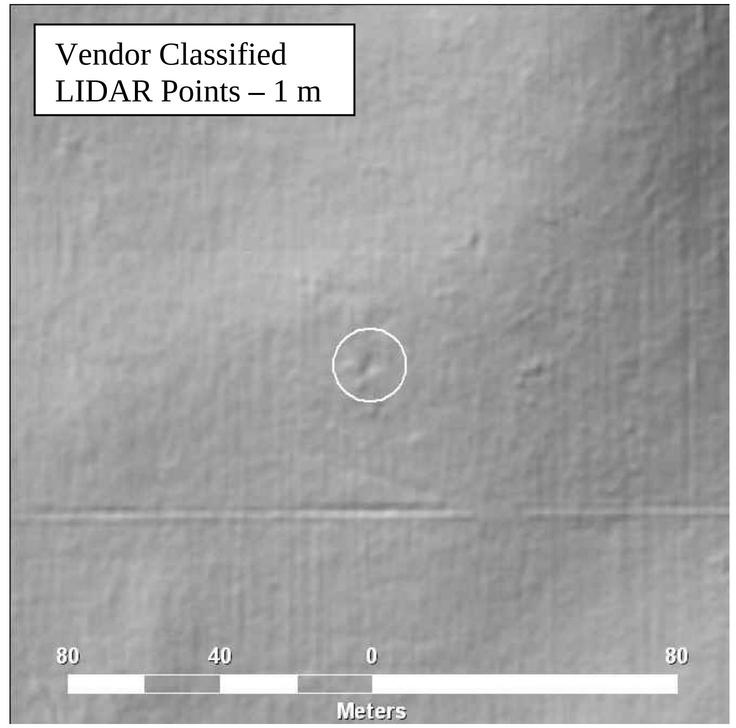 	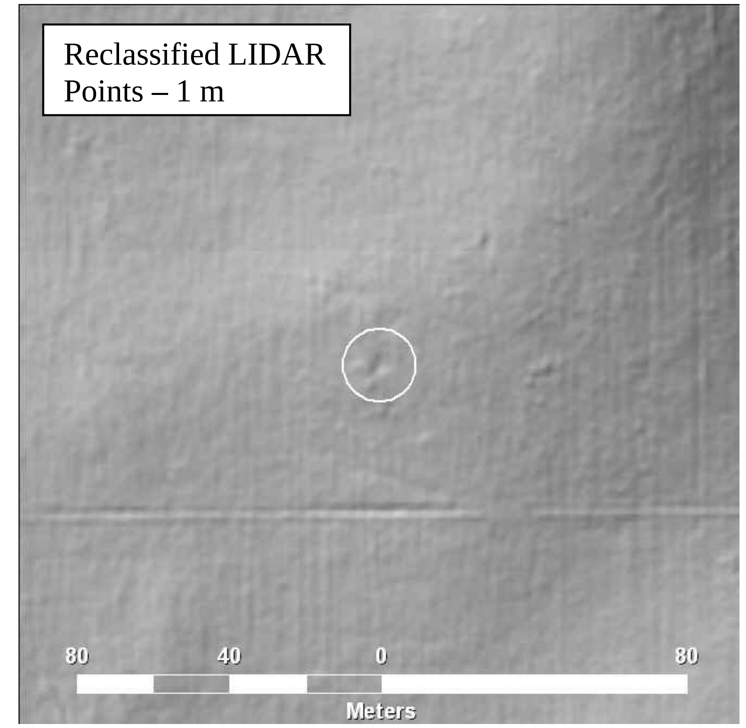 	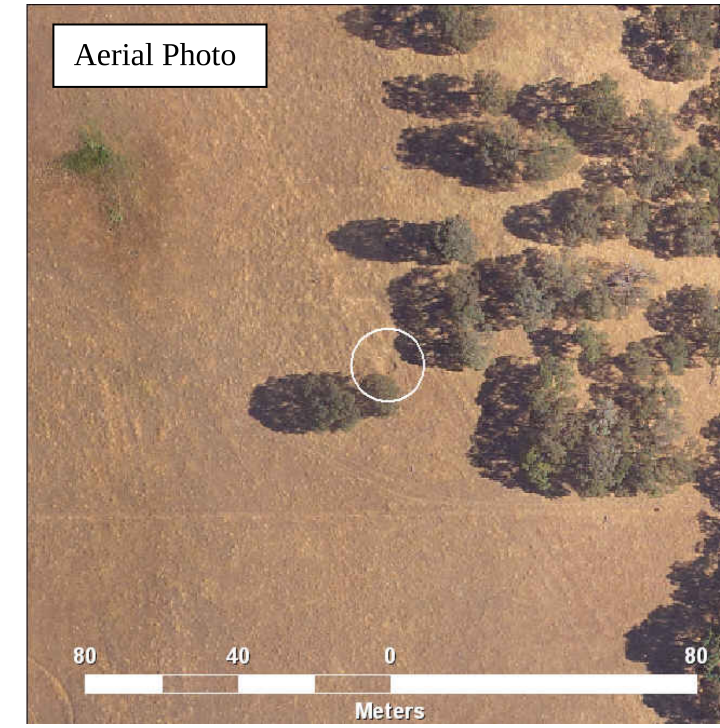
Plot # 6 Feature size: 4.6 m Vegetation density: 47.76% Surface method: TIN DEM cell size: 0.3 m Lidar block reference number: 4086 Additional features visible: no Existing features more clearly visible: no	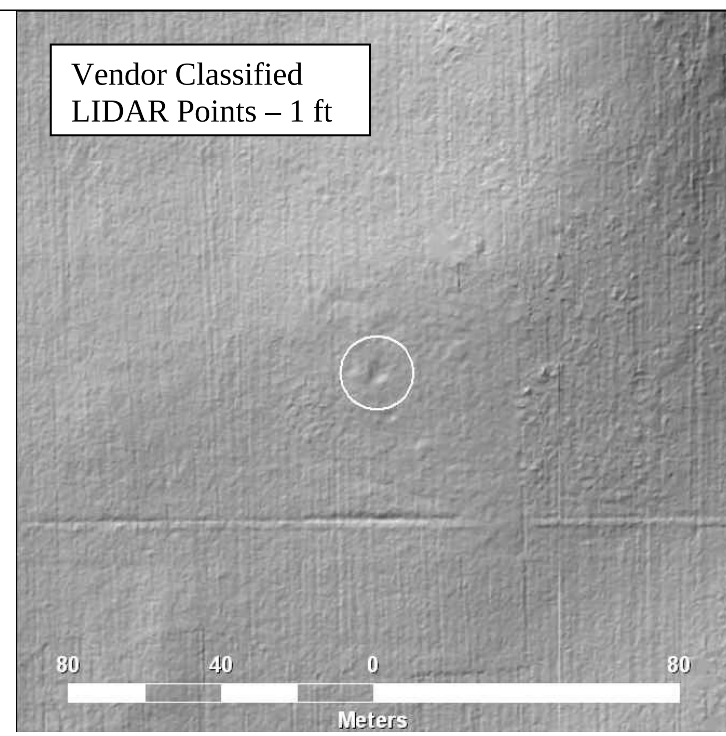 	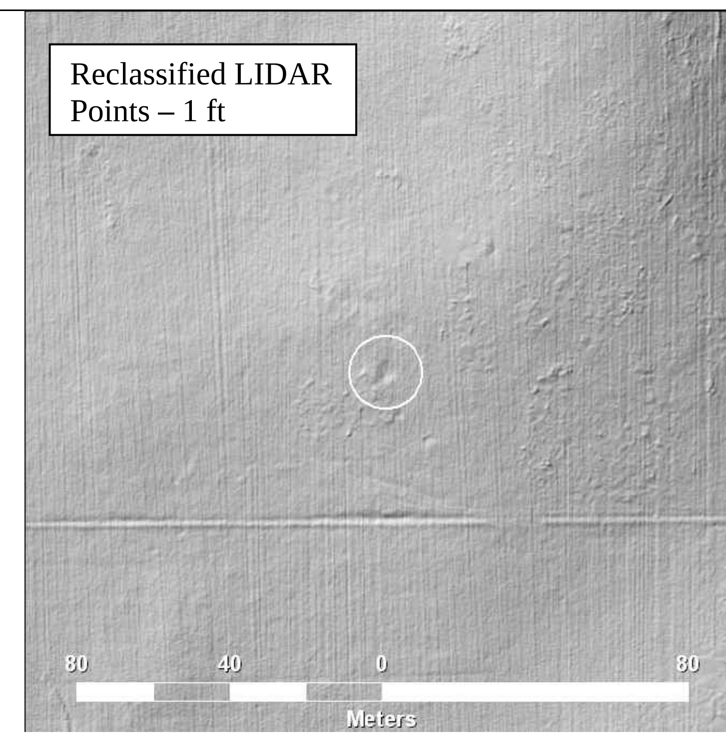 	

Plot # 7

Feature size: 3.8 m
Vegetation density: 36.31%
Surface method: TIN
DEM cell size: 1 m
Lidar block reference number: 5466

Additional features visible: no
Existing features more clearly visible: possible

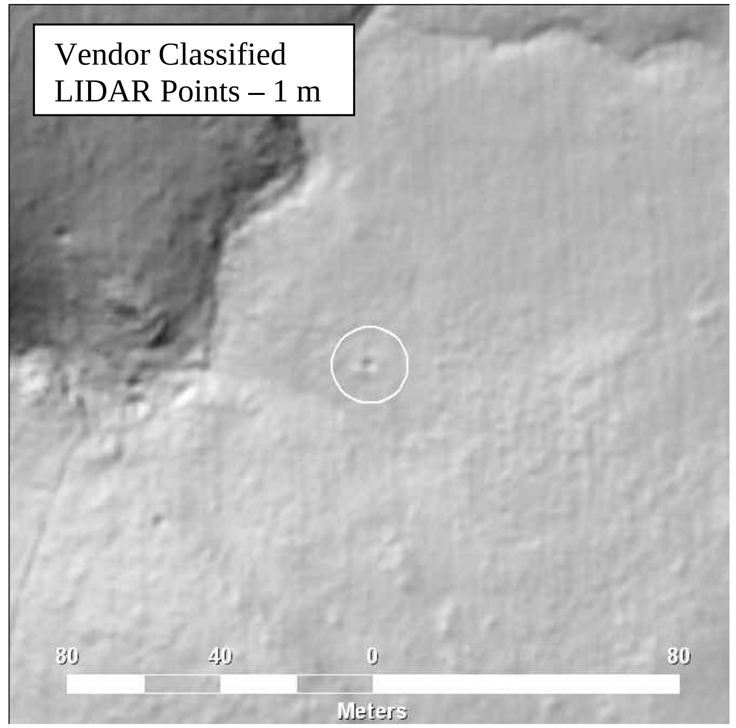

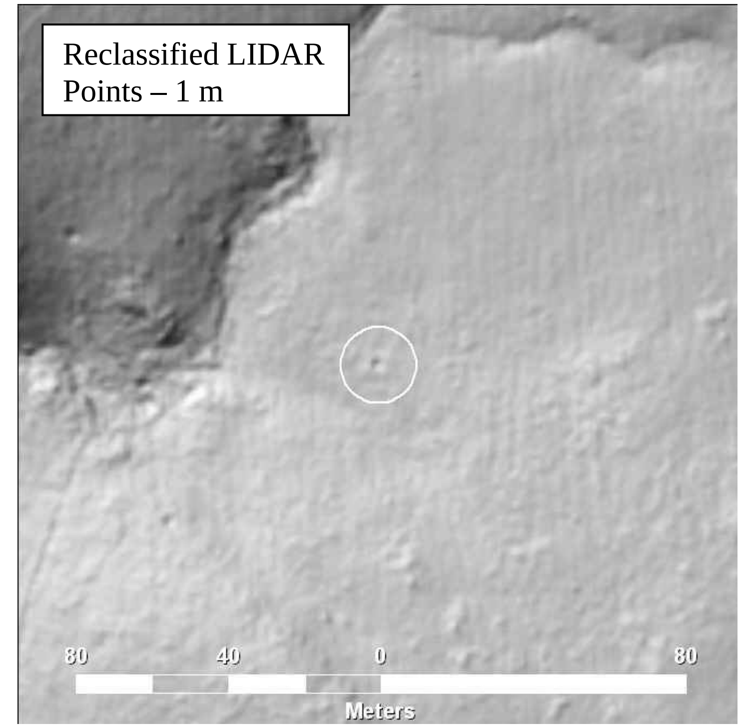

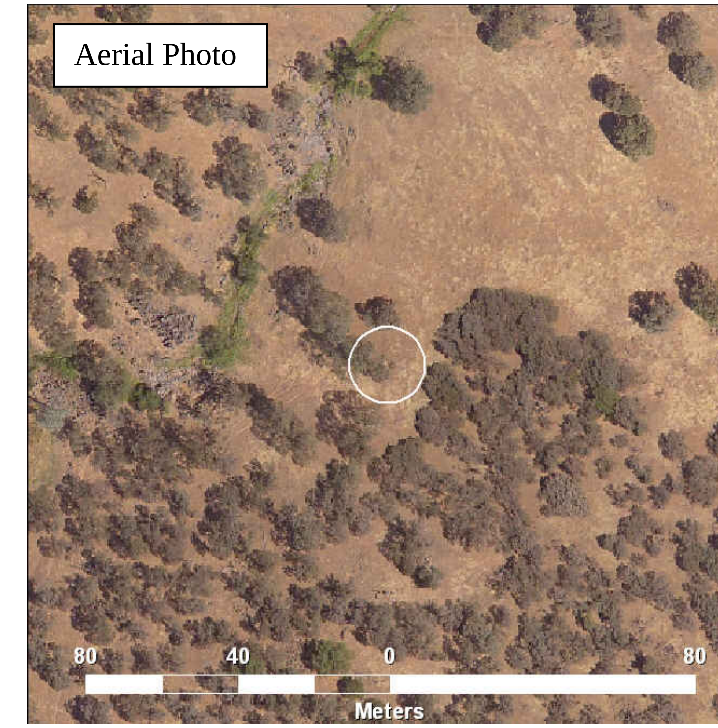

Plot # 7

Feature size: 3.8 m
Vegetation density: 36.31%
Surface method: TIN
DEM cell size: 0.3 m
Lidar block reference number: 5466

Additional features visible: no
Existing features more clearly visible: possible

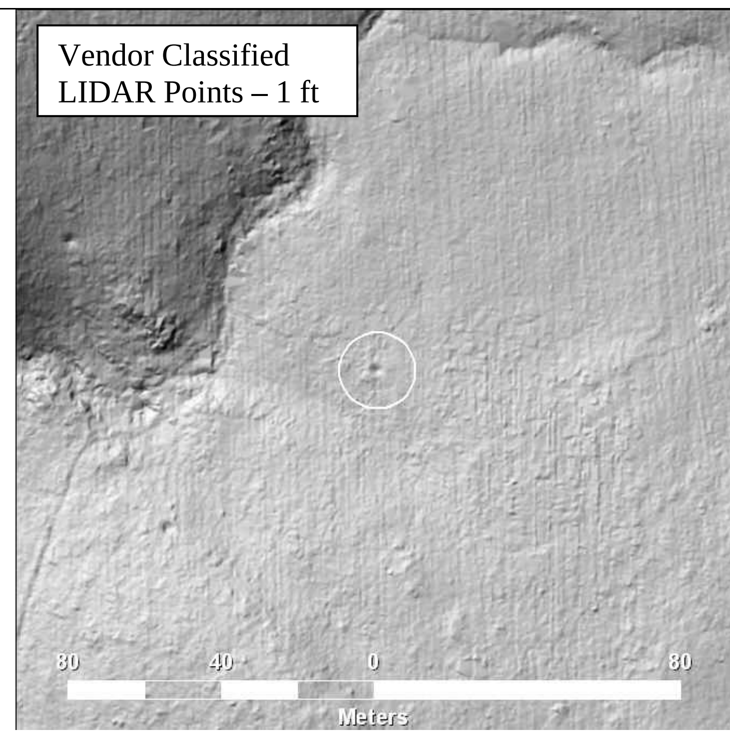

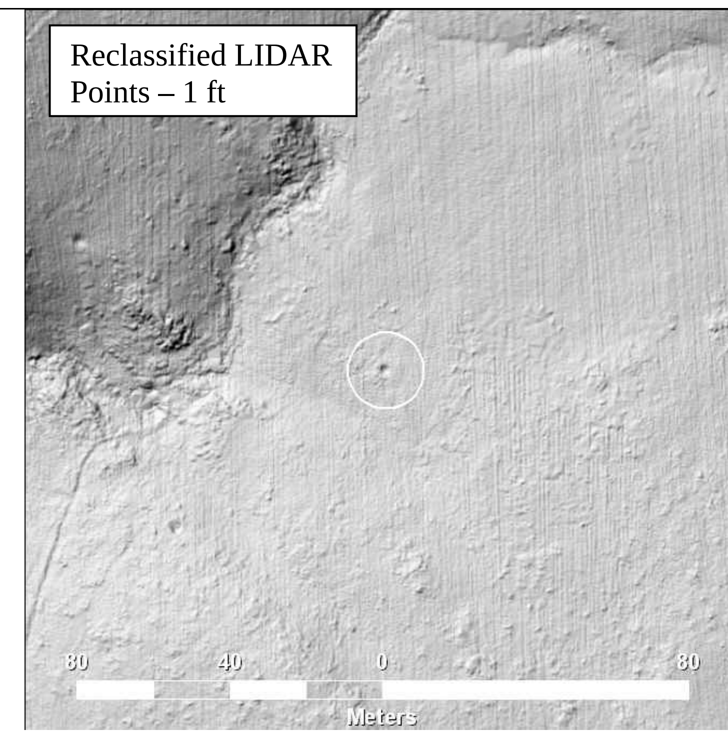

<table>
<tr>
<td>

Plot # 8

Feature size: 3.8 m
Vegetation density: 43.82%
Surface method: TIN
DEM cell size: 1 m
Lidar block reference number: 5580

Additional features visible: possible
Existing features more clearly visible: possible

</td>
<td>

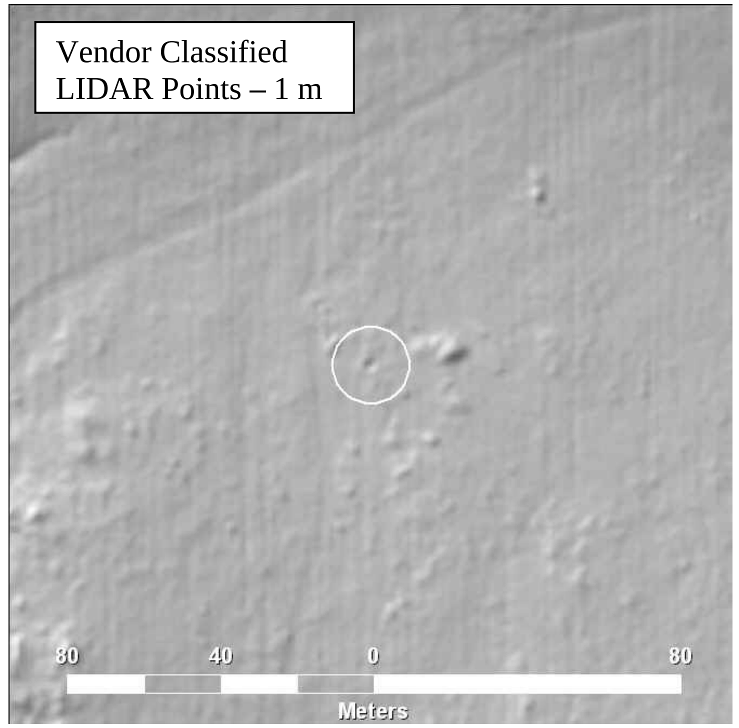

</td>
<td>

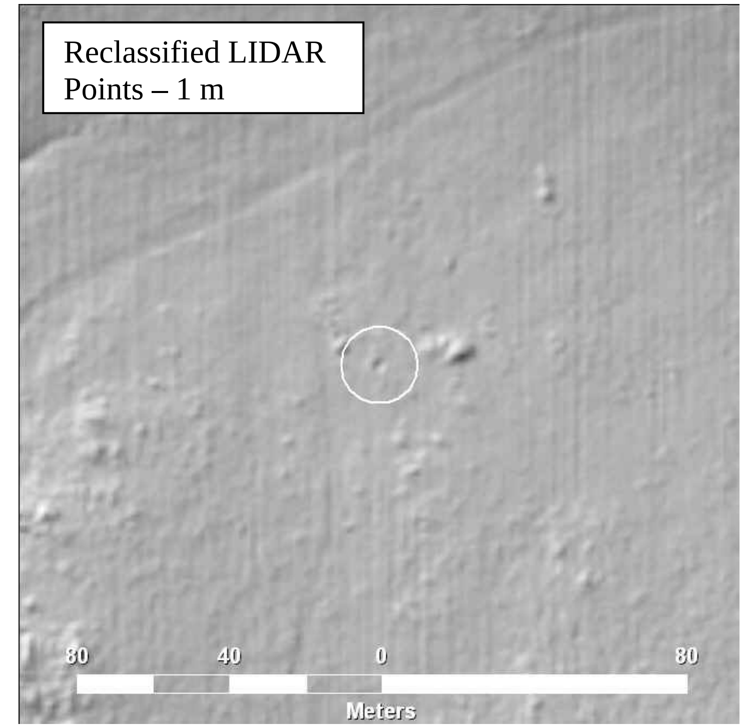

</td>
<td>

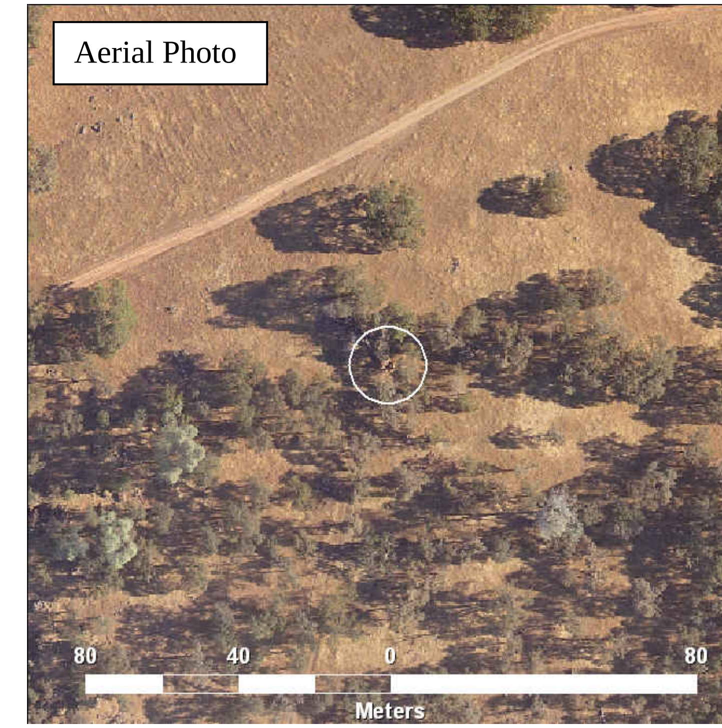

</td>
</tr>
<tr>
<td>

Plot # 8

Feature size: 3.8 m
Vegetation density: 43.82%
Surface method: TIN
DEM cell size: 0.3 m
Lidar block reference number: 5580

Additional features visible: no
Existing features more clearly visible: possible

</td>
<td>

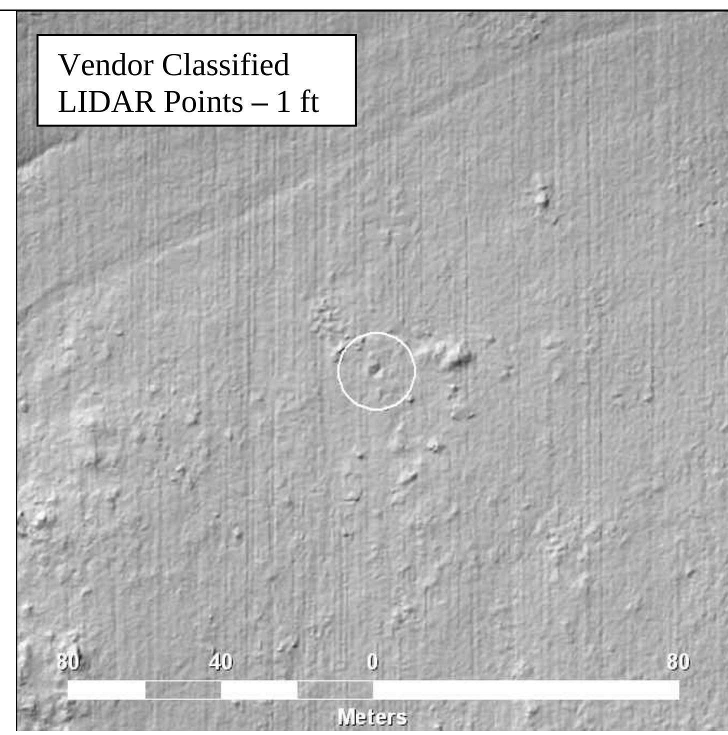

</td>
<td>

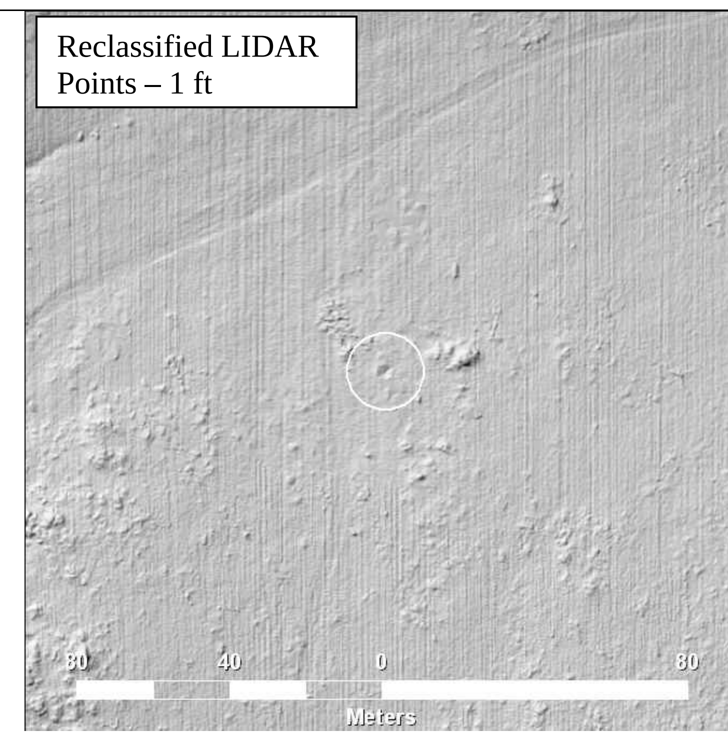

</td>
<td></td>
</tr>
</table>

Plot # 9

Feature size: 4.8 m
Vegetation density: 42.75%
Surface method: TIN
DEM cell size: 1 m
Lidar block reference number: 5743

Additional features visible: no
Existing features more clearly visible: possible

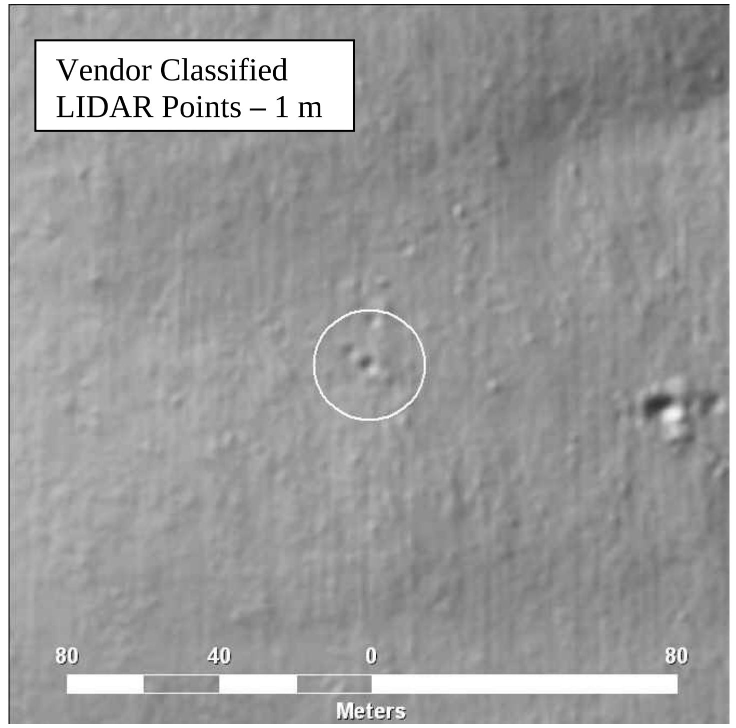

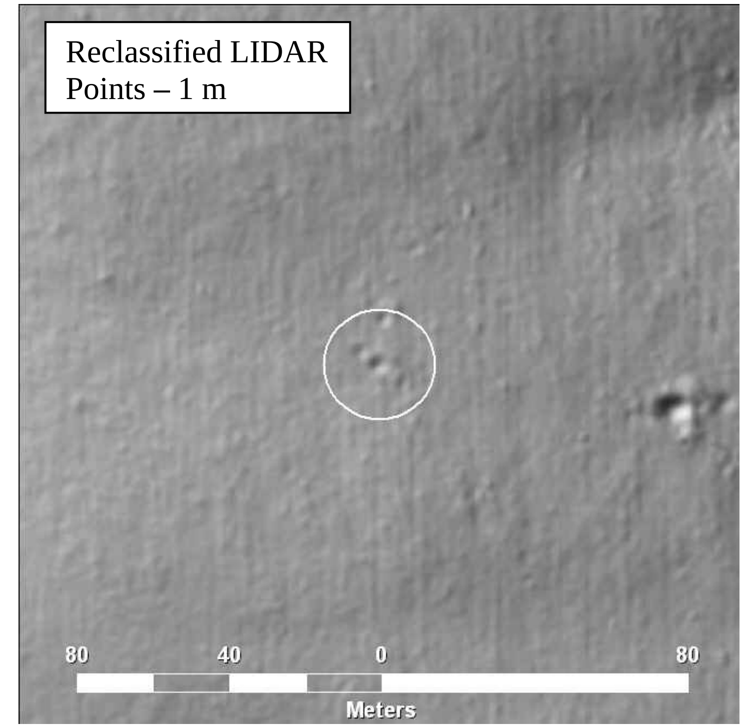

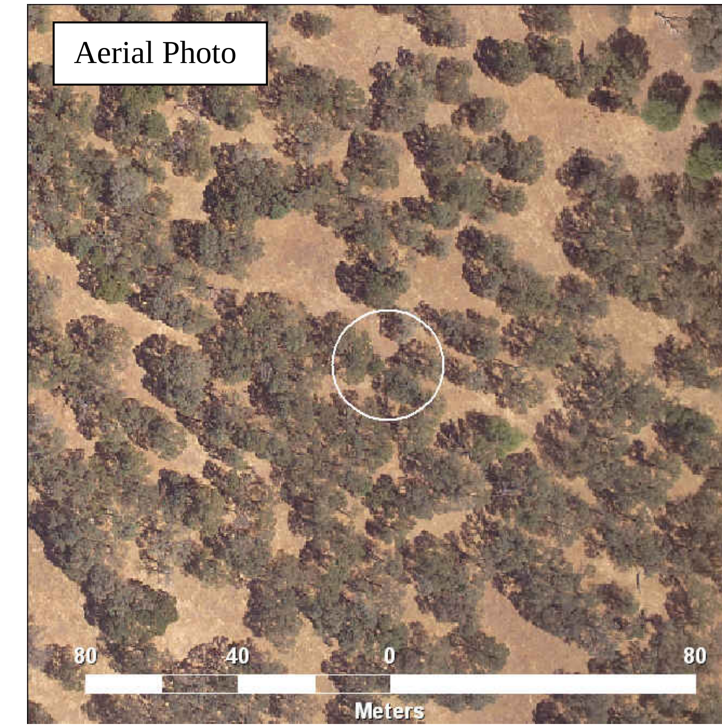

Plot # 9

Feature size: 4.8 m
Vegetation density: 42.75%
Surface method: TIN
DEM cell size: 0.3 m
Lidar block reference number: 5743

Additional features visible: no
Existing features more clearly visible: possible

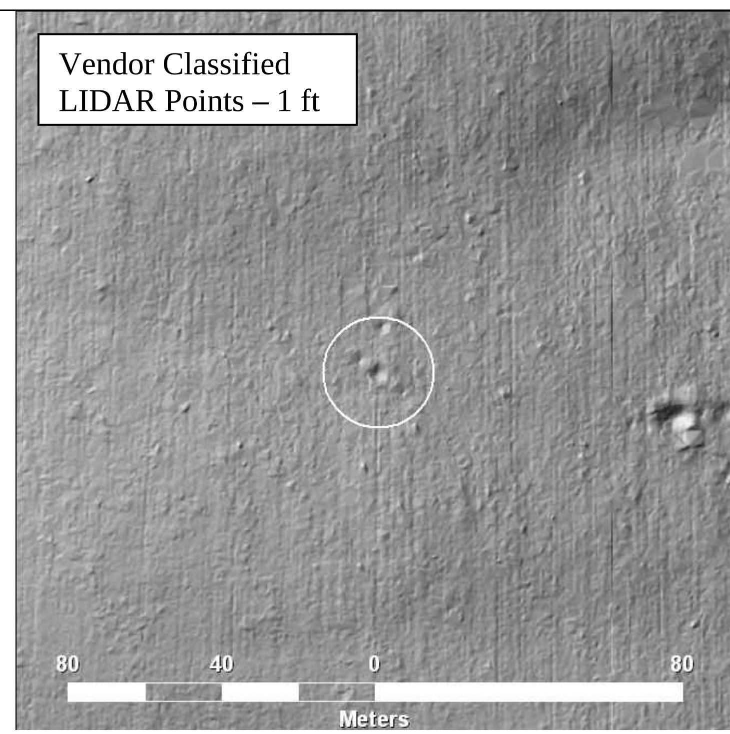

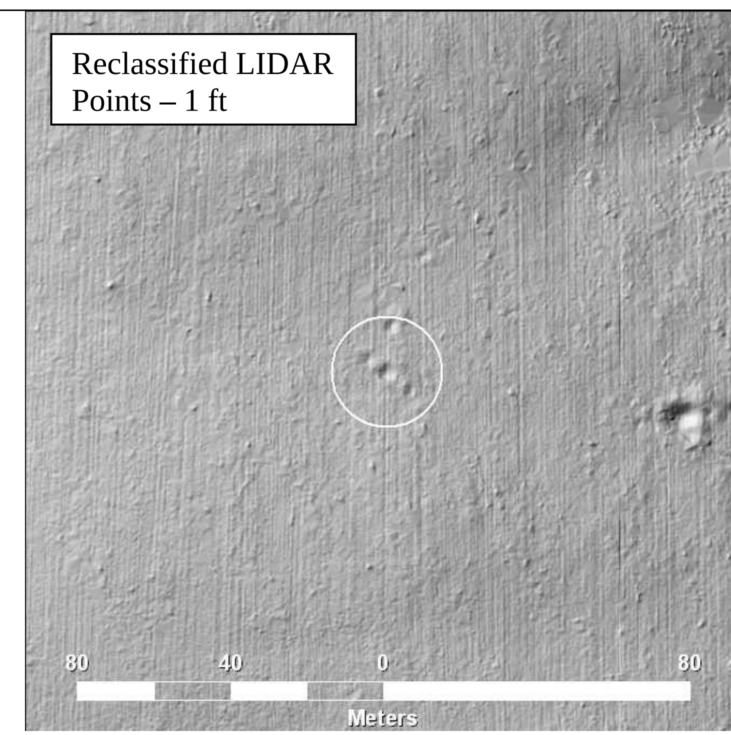

Plot # 10

Feature size: no feature visible
Vegetation density: 48.74%
Surface method: TIN
DEM cell size: 1 m
Lidar block reference number: 4078

Additional features visible: possible
Existing features more clearly visible: possible

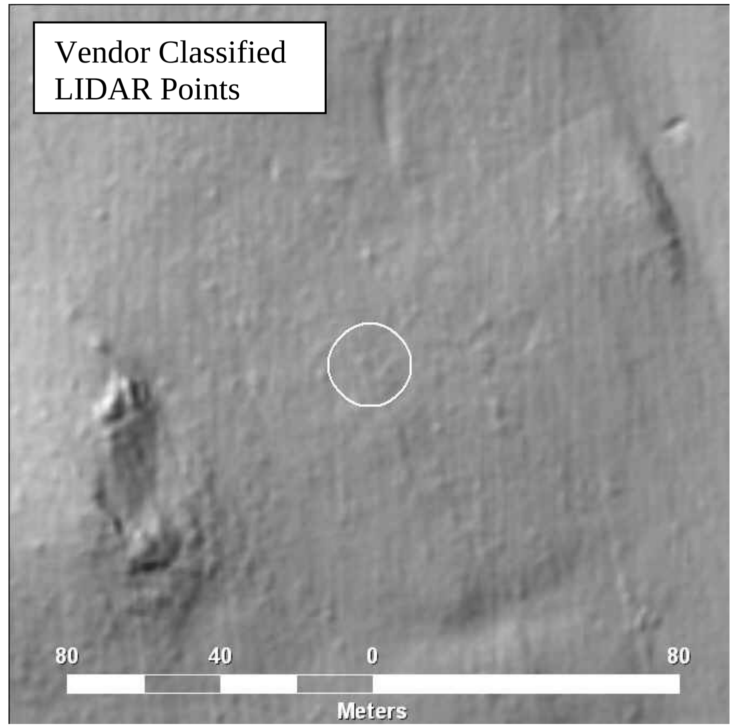

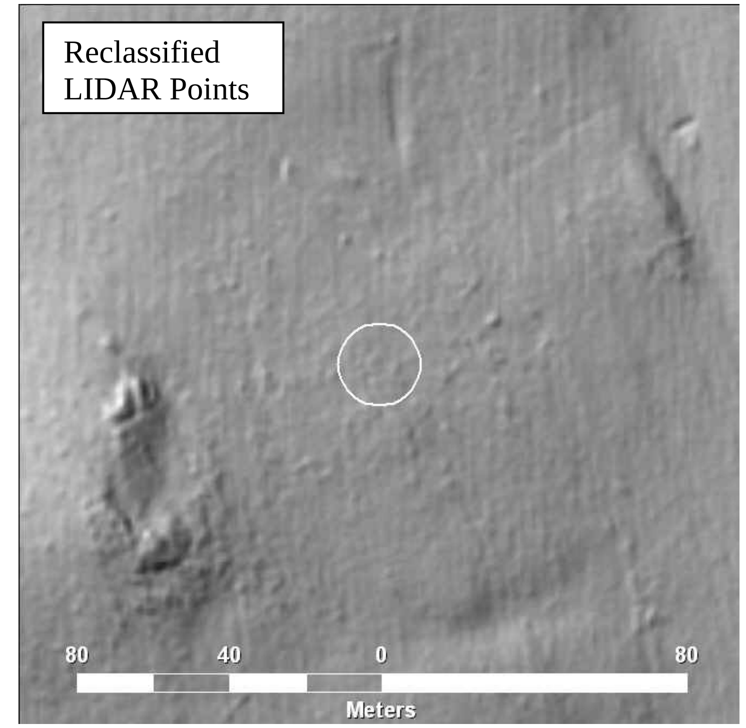

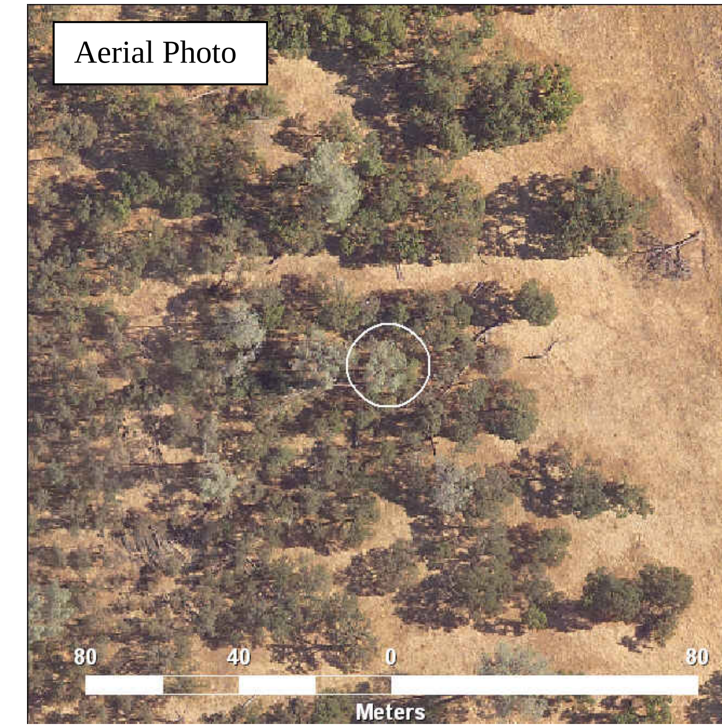

Plot # 11

Feature size: no feature visible
Vegetation density: 30.0%
Surface method: TIN
DEM cell size: 1 m
Lidar block reference number: 5645

Additional features visible: no
Existing features more clearly visible: possible

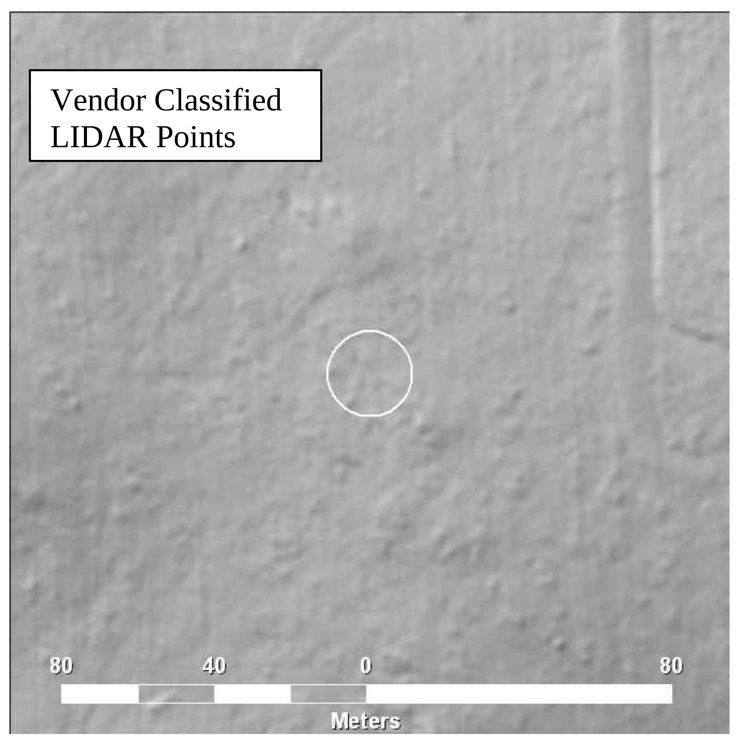

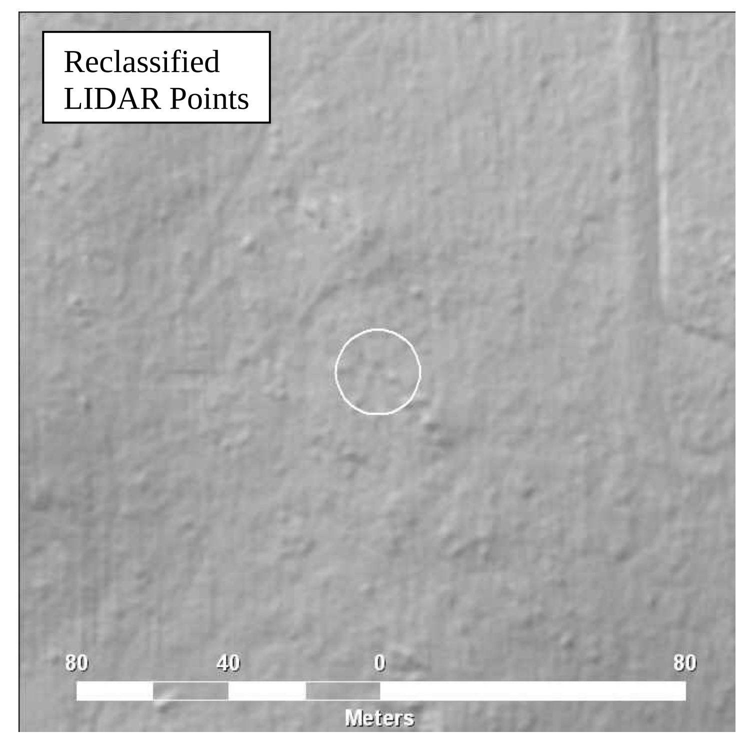

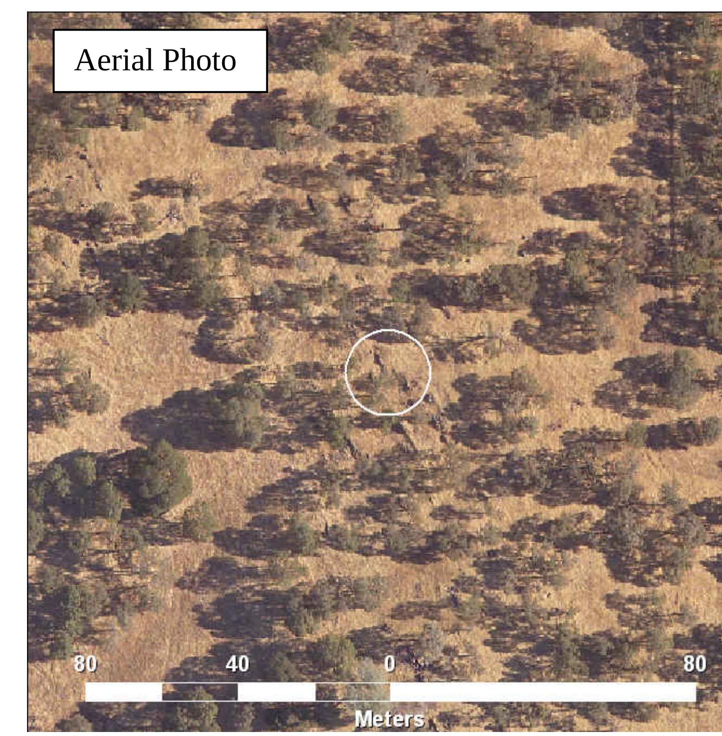

Plot # 12 Feature size: 1.5 m Vegetation density: 50.78% Surface method: TIN DEM cell size: 1 m Lidar block reference number: 5822 Additional features visible: no Existing features more clearly visible: possible	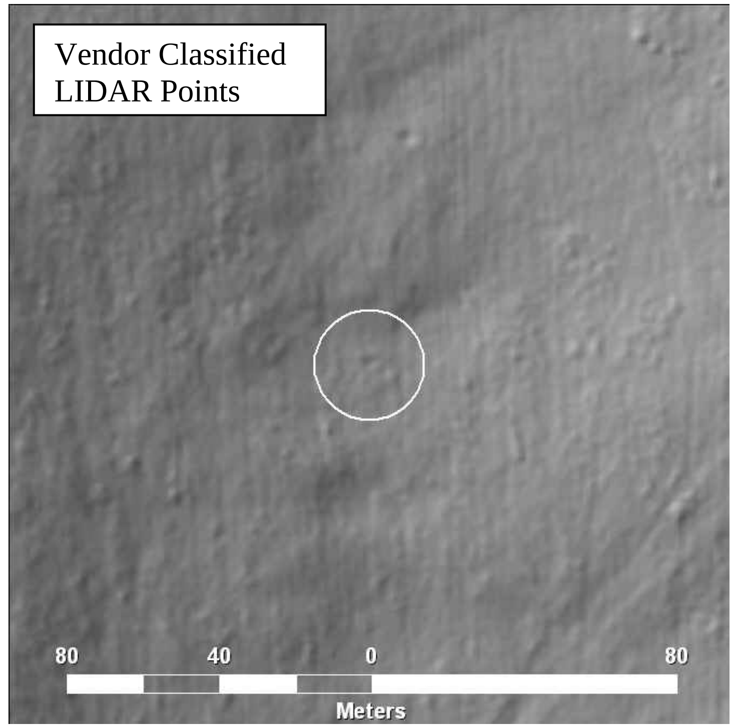	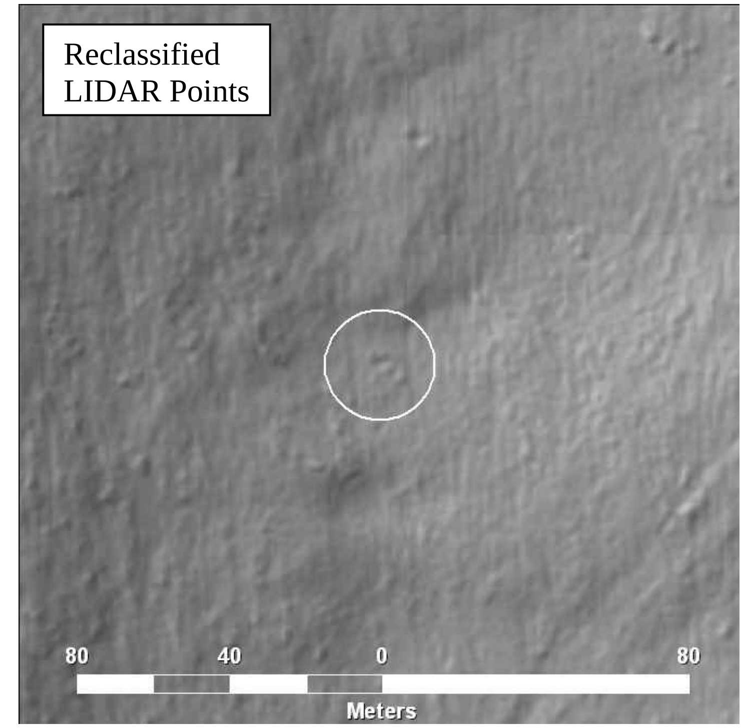	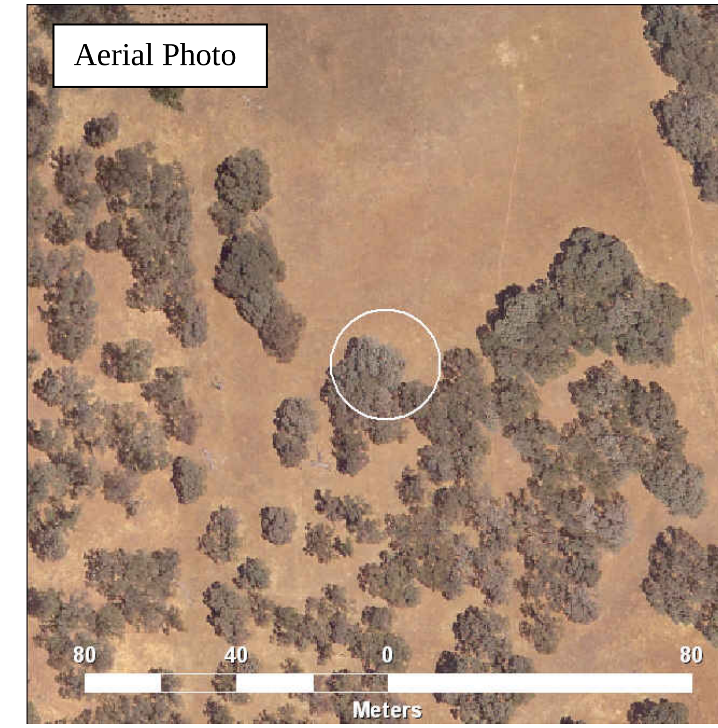
Plot # 13 Feature size: 2.6 m Vegetation density: 0% Surface method: TIN DEM cell size: 1 m Lidar block reference number: 3978 Additional features visible: no Existing features more clearly visible: yes	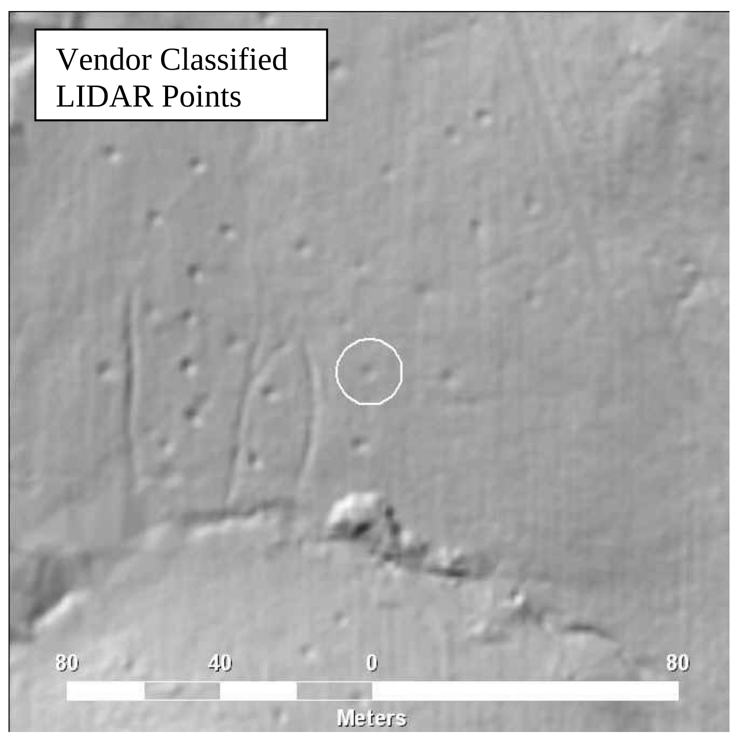	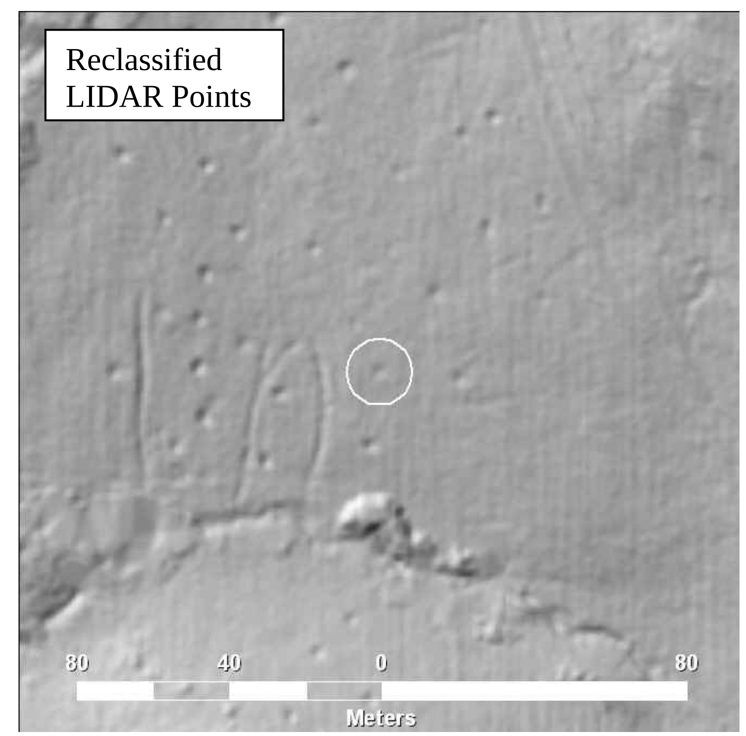	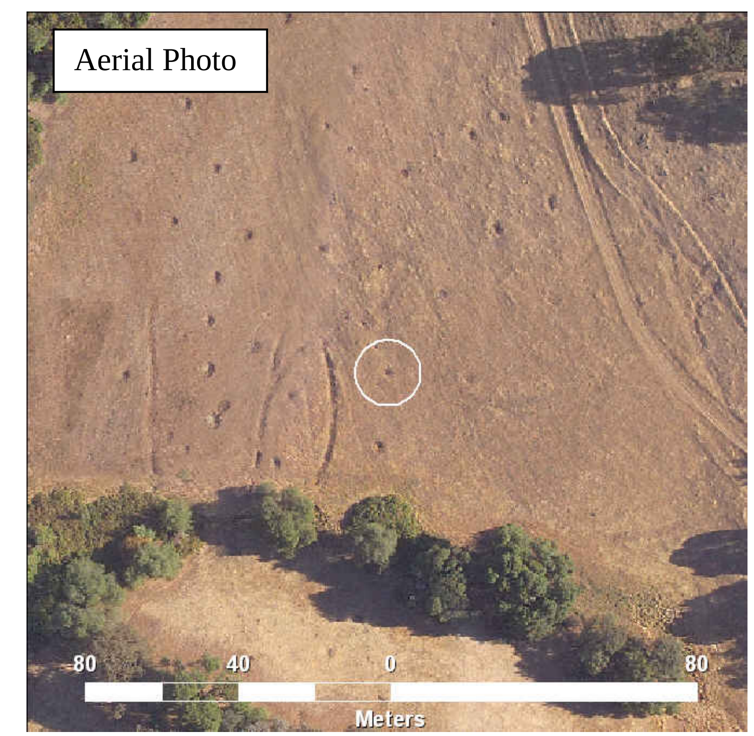

Plot # 14 Feature size: 2.7 m Vegetation density: 11.36% Surface method: TIN DEM cell size: 1 m Lidar block reference number: 3991 Additional features visible: possible Existing features more clearly visible: yes	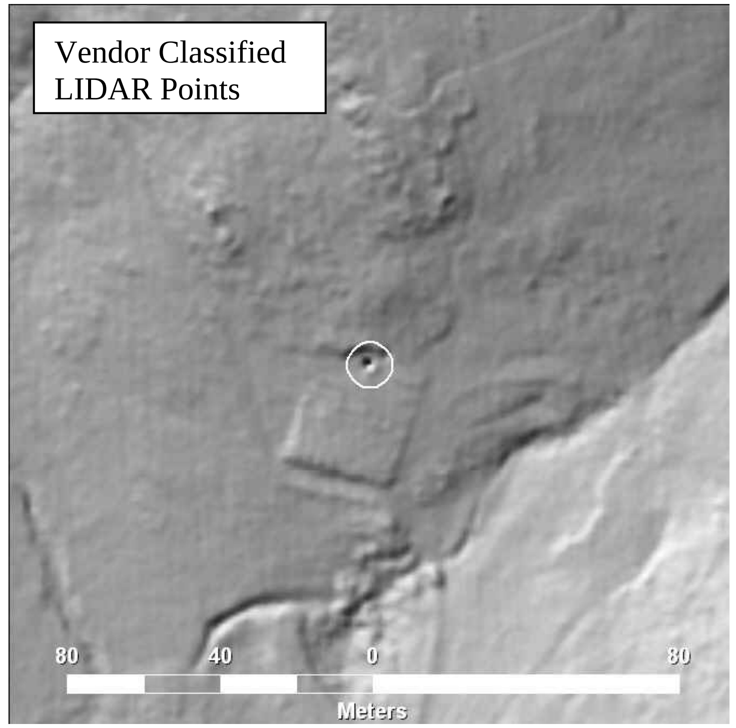	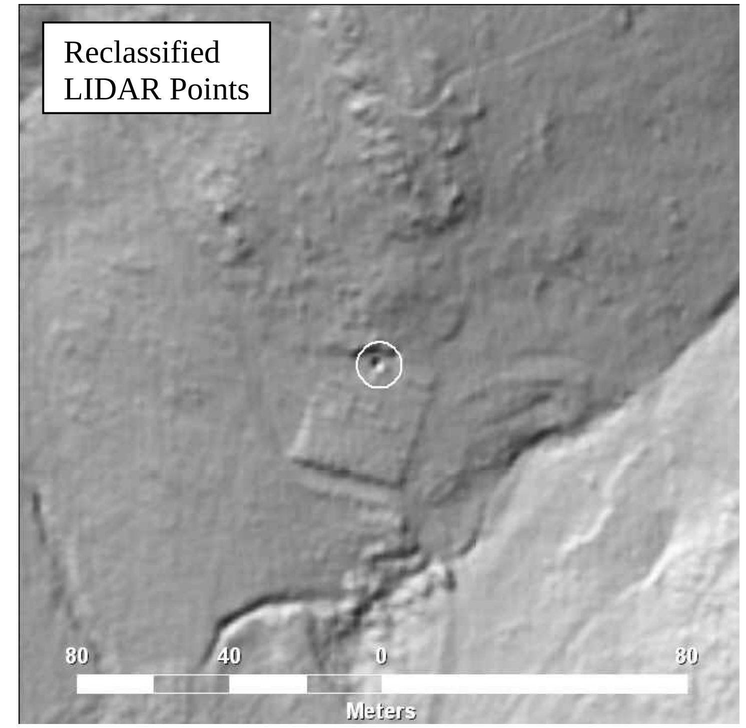	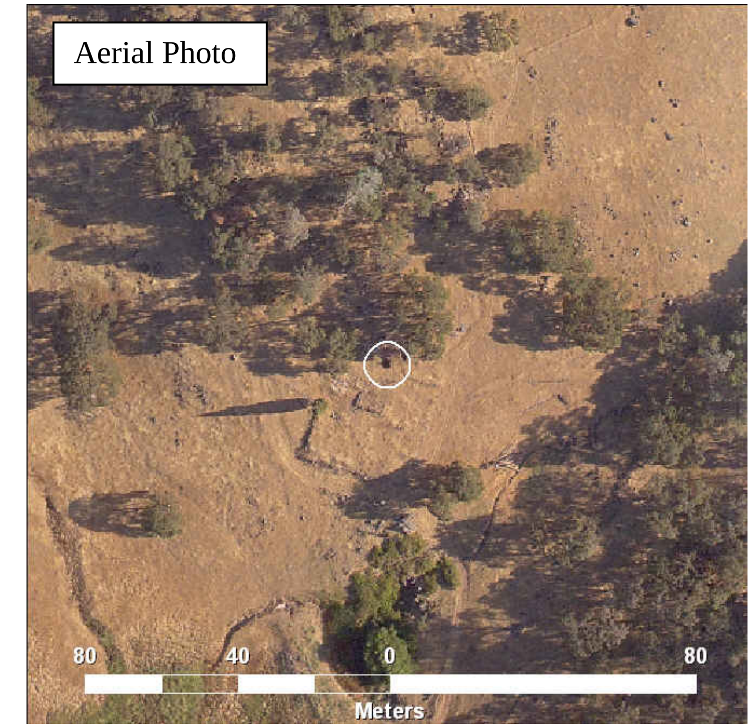
Plot # 15 Feature size: 2.9 m wide, 3.7 m long Vegetation density: 53.25% Surface method: TIN DEM cell size: 1 m Lidar block reference number: 5351 Additional features visible: no Existing features more clearly visible: possible	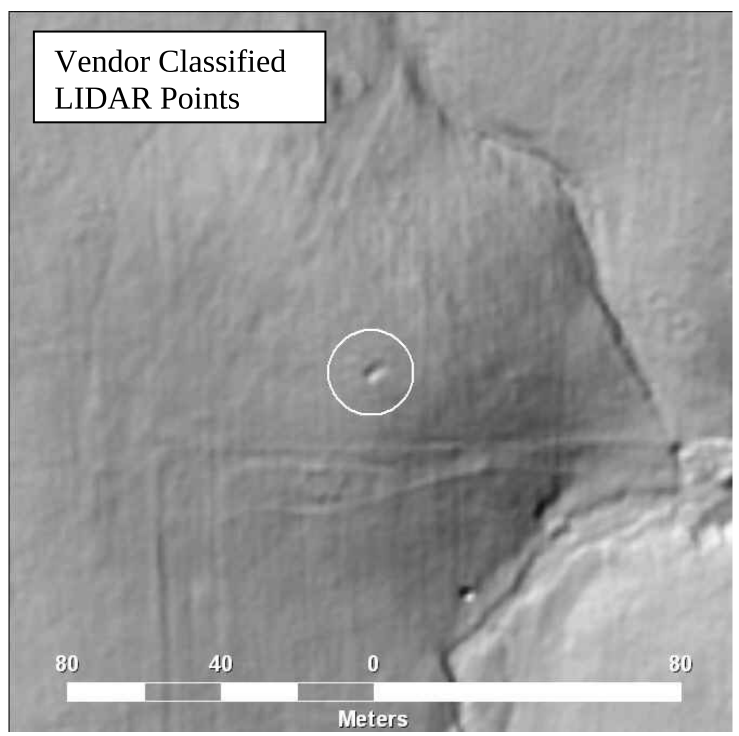	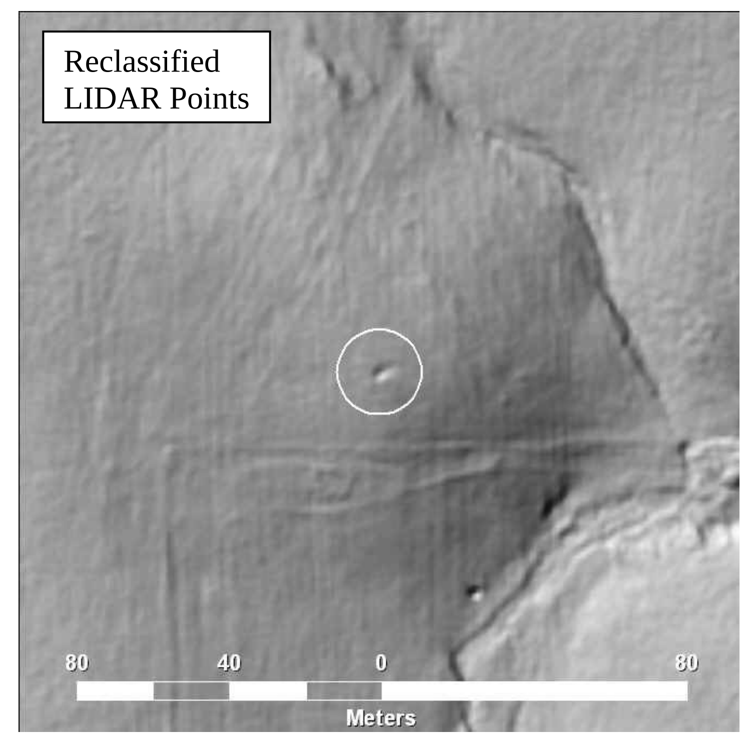	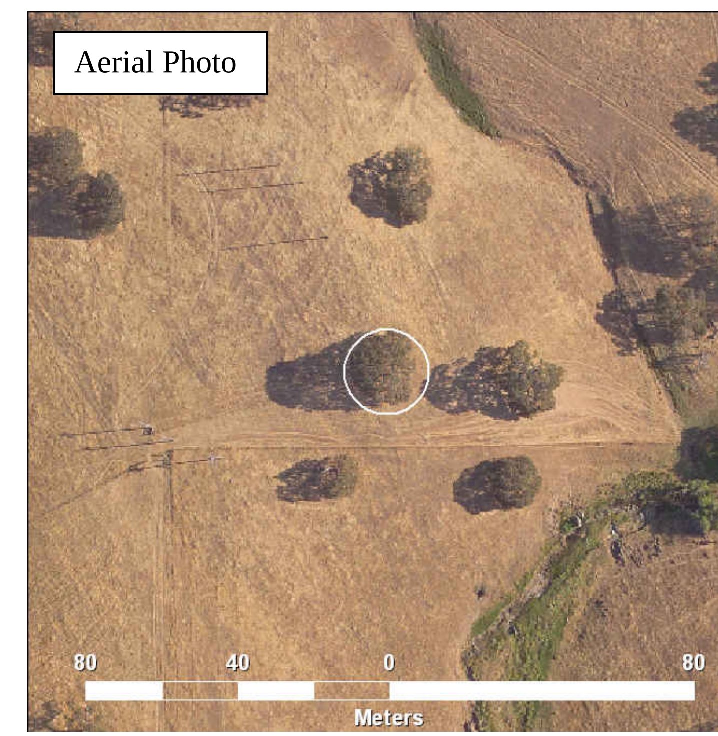

Plot # 16 Feature size: 2.9 meters Vegetation density: 55.7% Surface method: TIN DEM cell size: 1 m Lidar block reference number: 3953 Additional features visible: no Existing features more clearly visible: yes	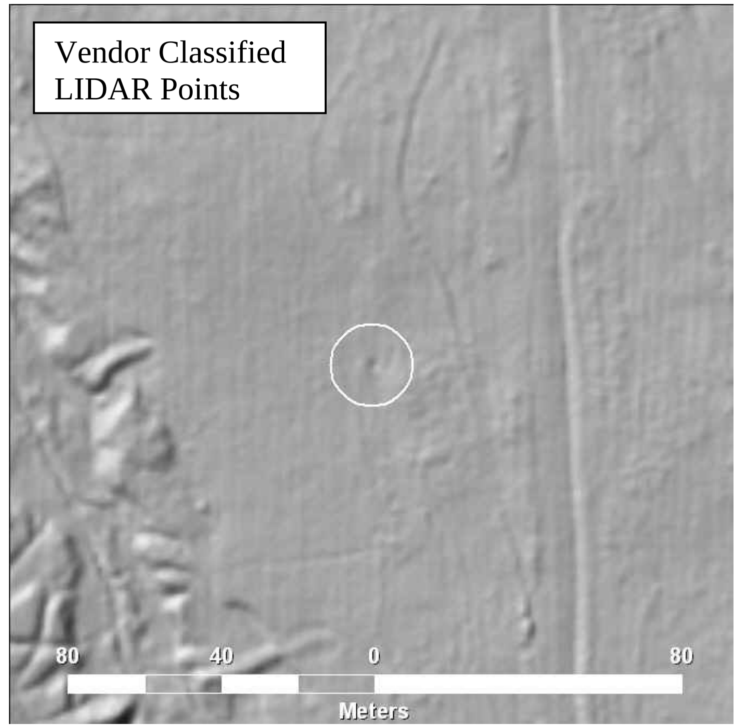	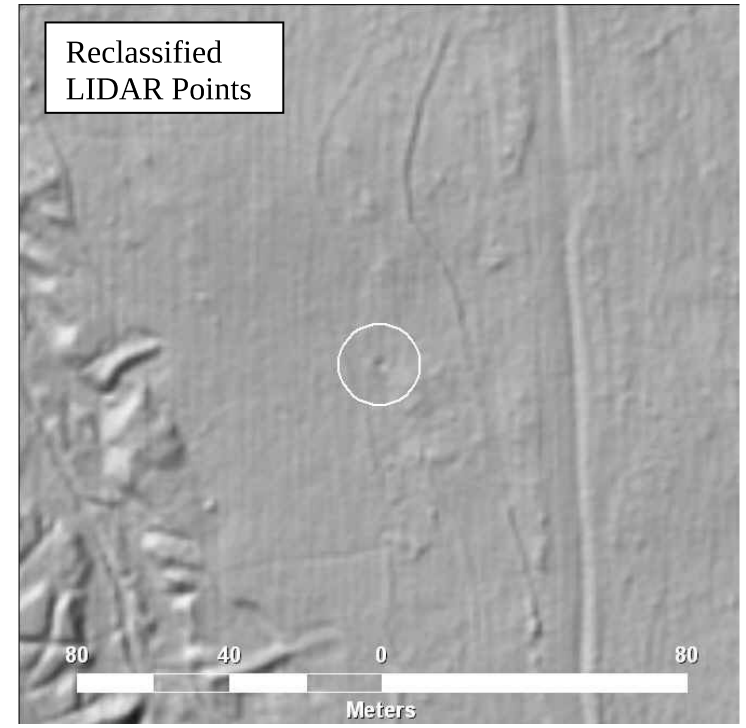	
Plot # 17 Feature size: 3.1 m Vegetation density: 42.46% Surface method: TIN DEM cell size: 1 m Lidar block reference number: 5823 Additional features visible: no Existing features more clearly visible: possible	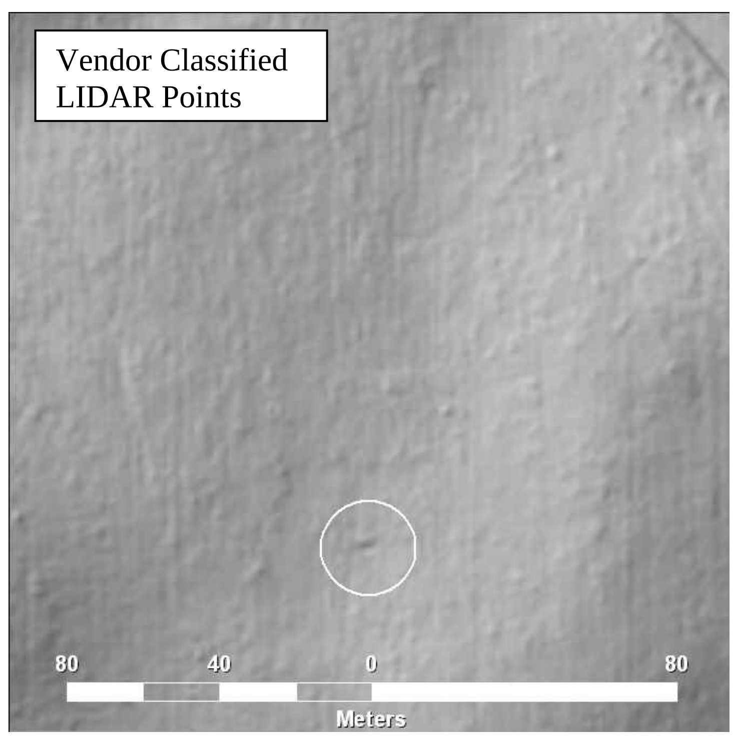	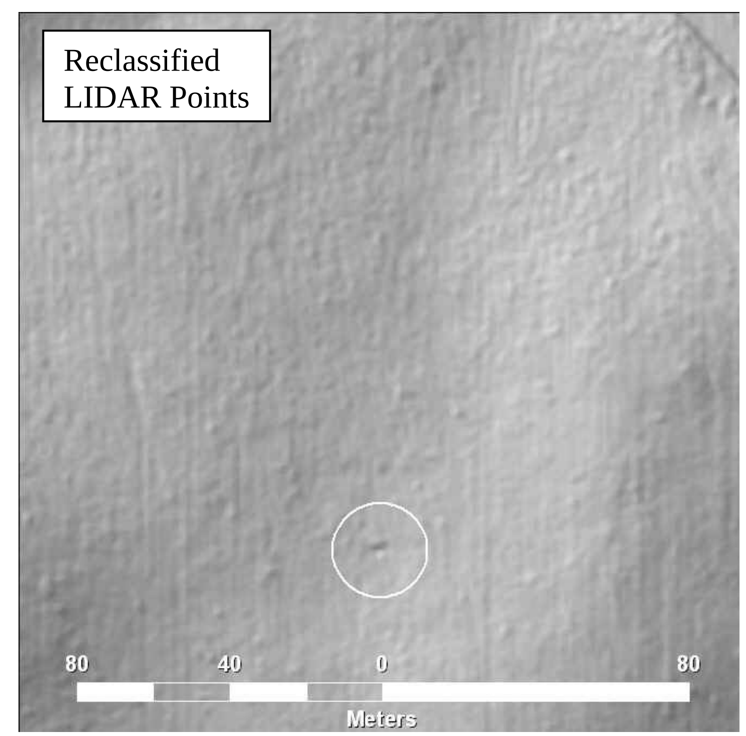	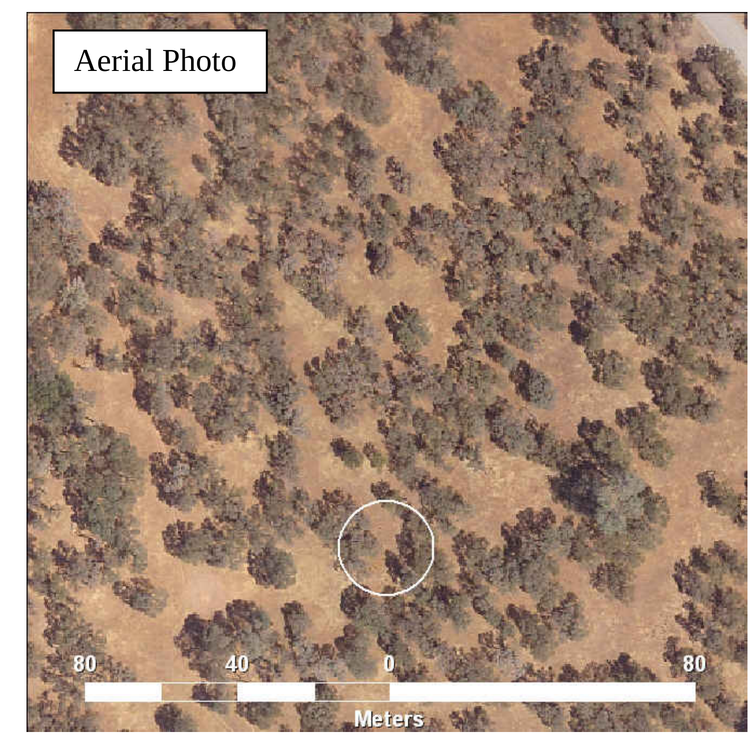

Plot # 18 Feature size: 3.1 m Vegetation density: 33.72% Surface method: TIN DEM cell size: 1 m Lidar block reference number: 5718 Additional features visible: possible Existing features more clearly visible: possible	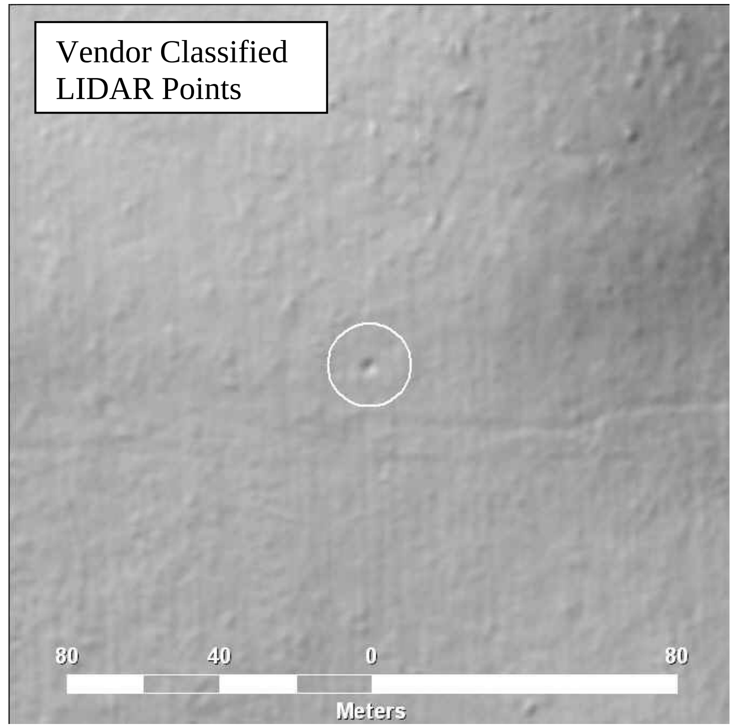	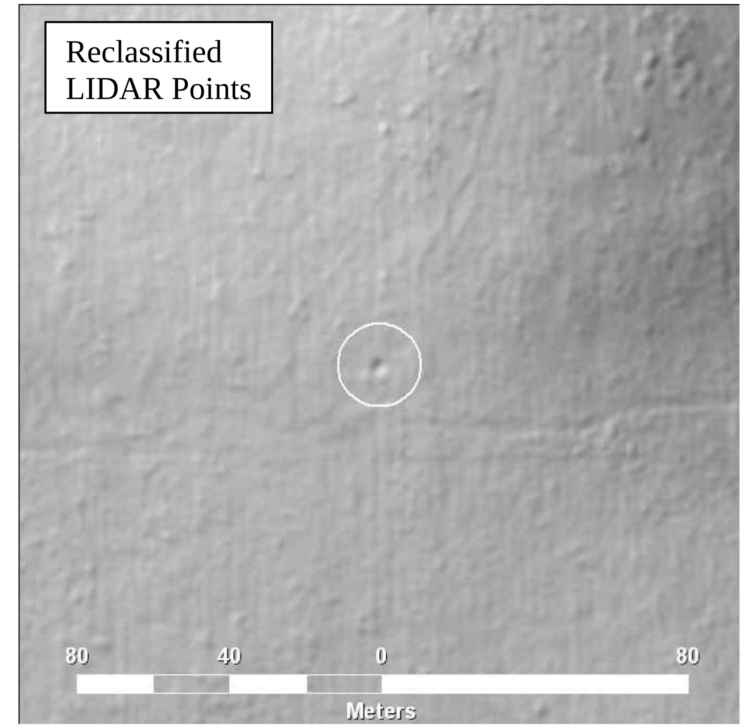	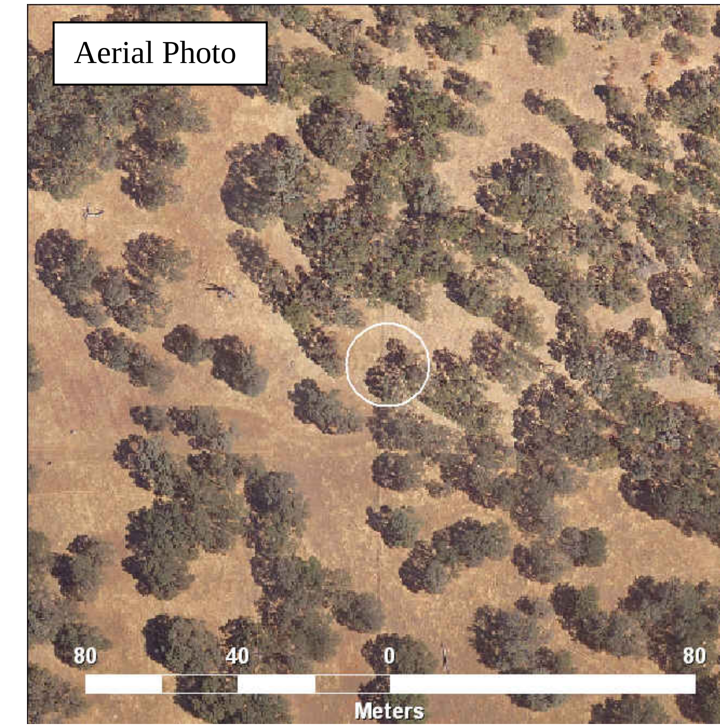
Plot # 19 Feature size: 3.1 m Vegetation density: 34.95% Surface method: TIN DEM cell size: 1 m Lidar block reference number: 5461 Additional features visible: possible Existing features more clearly visible: possible	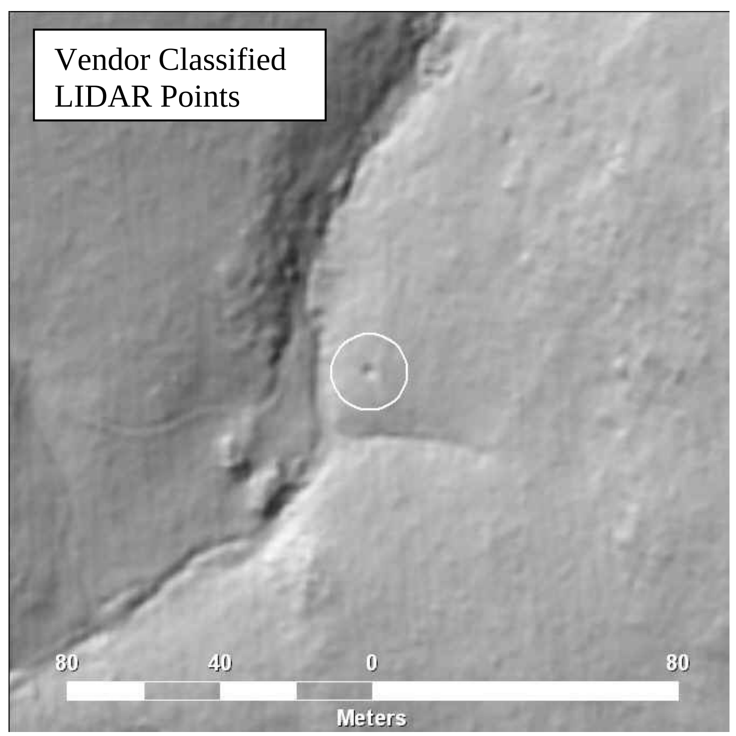	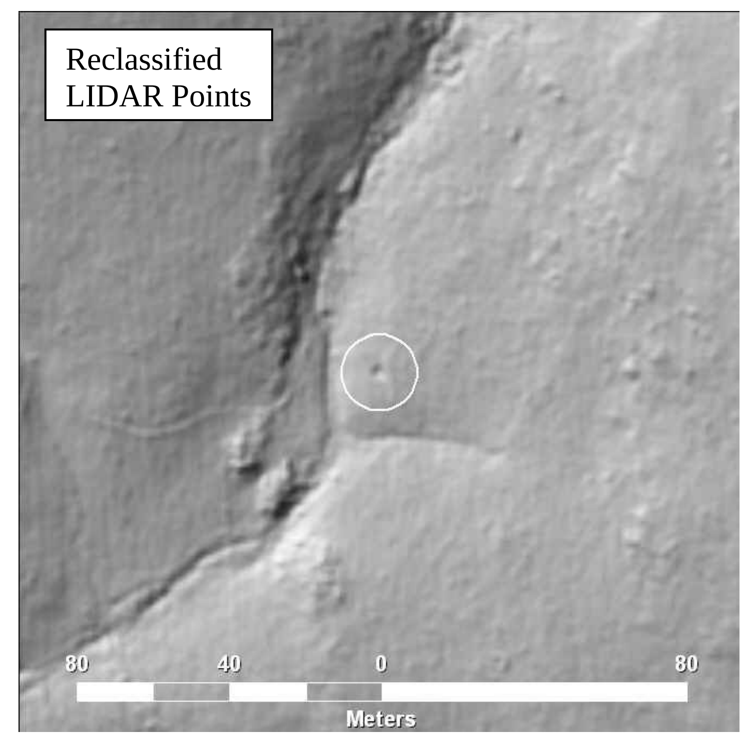	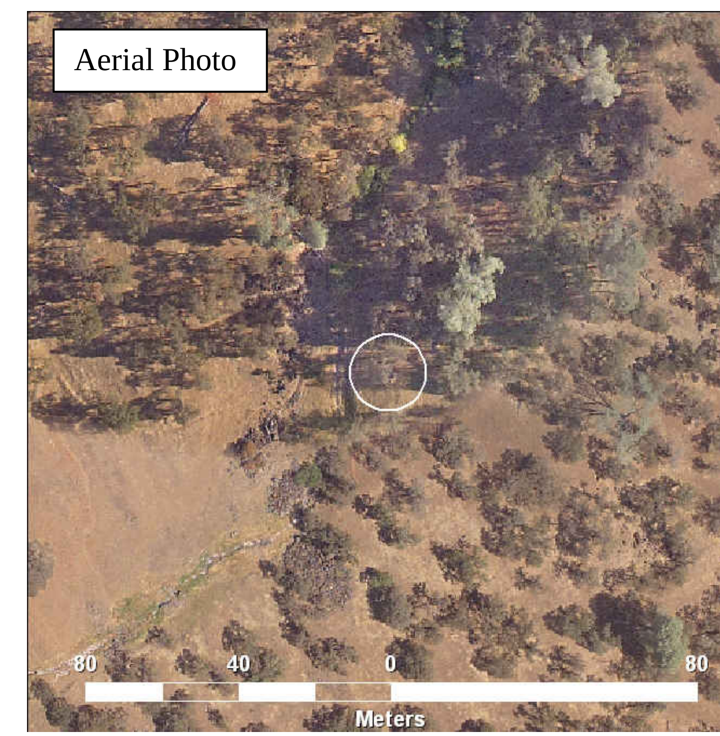

Plot # 20

Feature size: 3.25 m
Vegetation density: 28.67%
Surface method: TIN
DEM cell size: 1 m
Lidar block reference number: 5924

Additional features visible: no
Existing features more clearly visible: possible

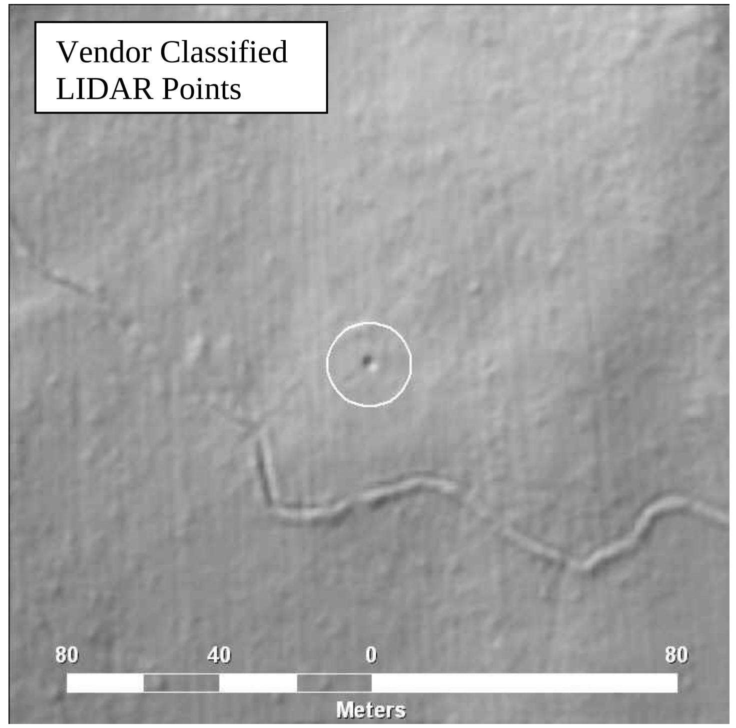

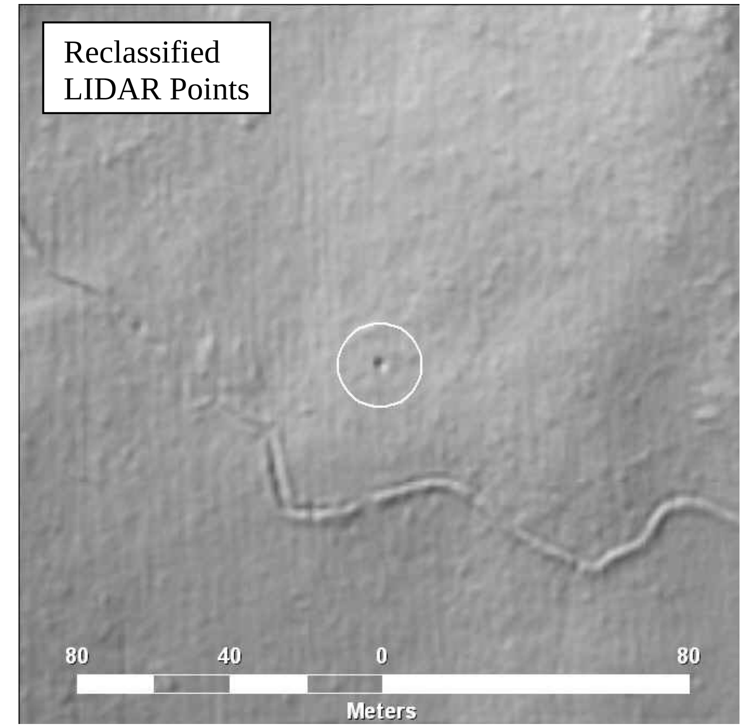

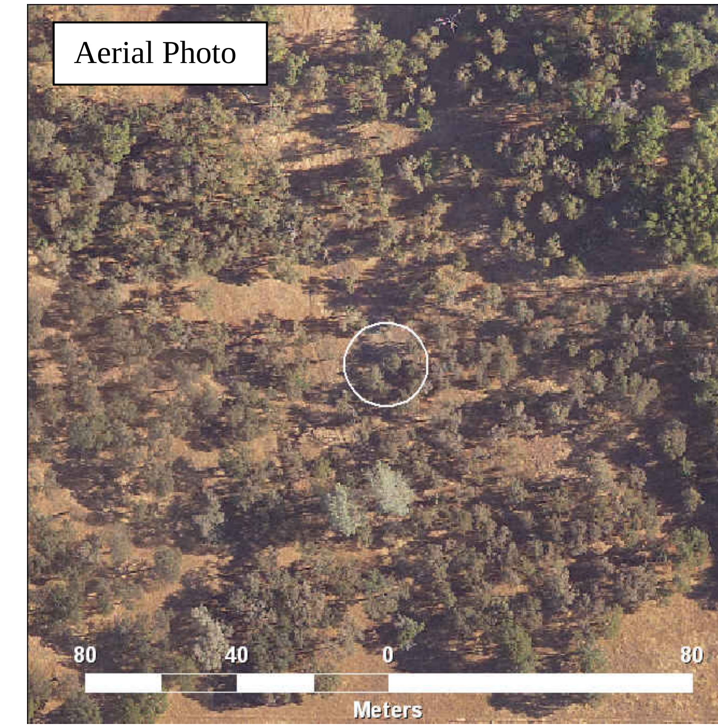

Plot # 21

Feature size: 3.25 m
Vegetation density: 42.06%
Surface method: TIN
DEM cell size: 1 m
Lidar block reference number: 4089

Additional features visible: no
Existing features more clearly visible: possible

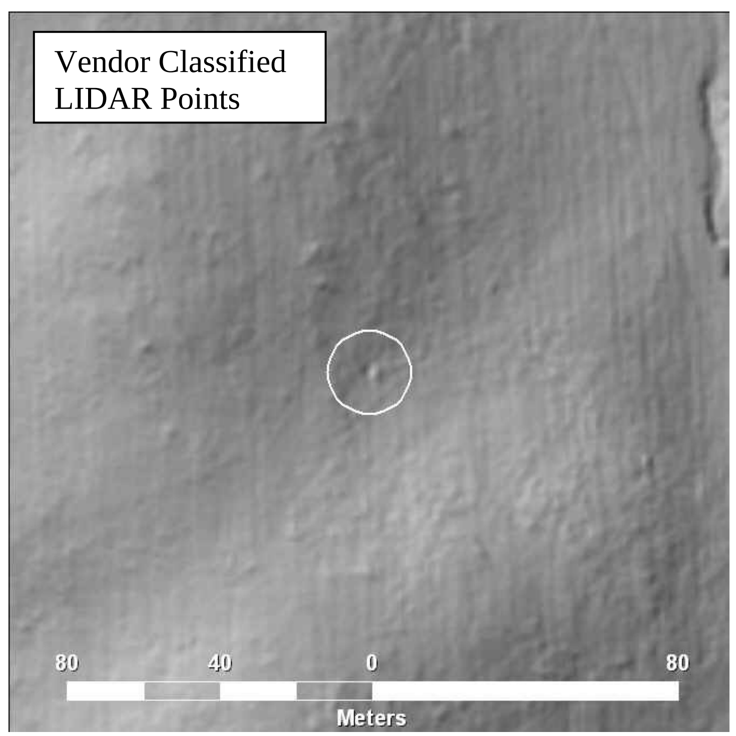

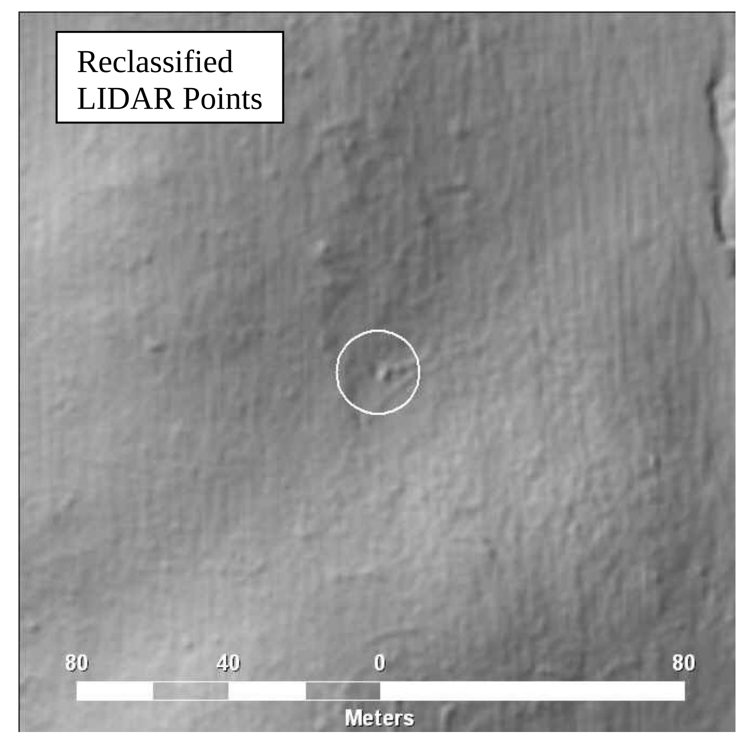

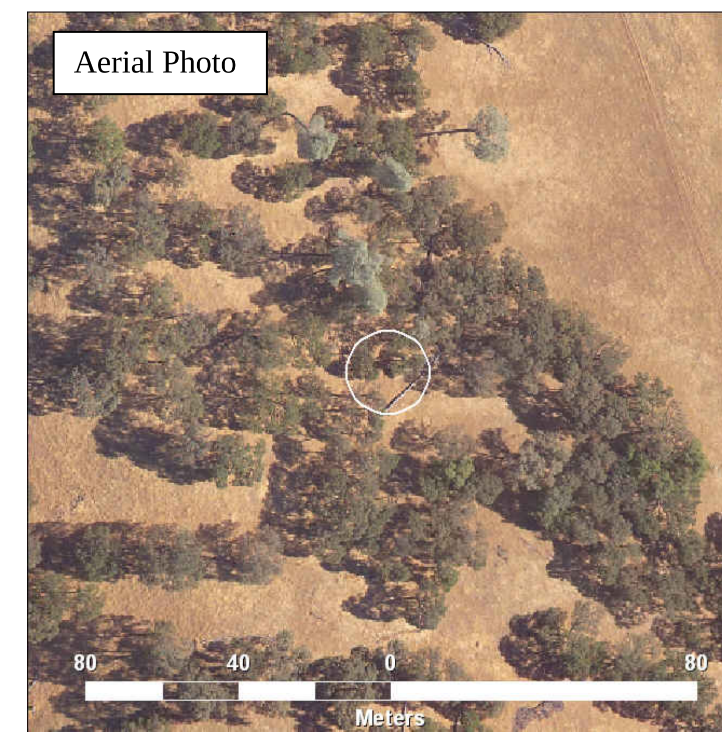

Plot # 22 Feature size: 3.5 m Vegetation density: 57.70% Surface method: TIN DEM cell size: 1 m Lidar block reference number: 5738 Additional features visible: no Existing features more clearly visible: possible	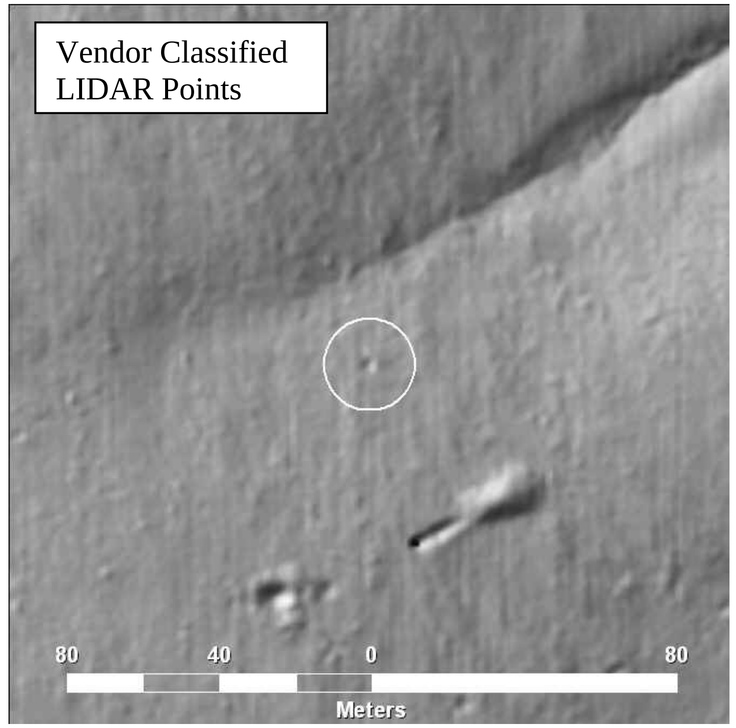	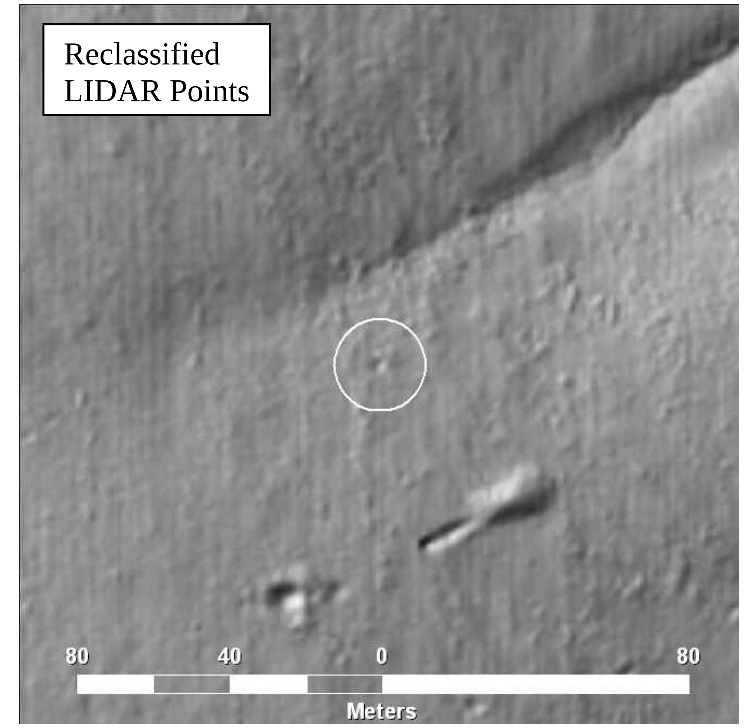	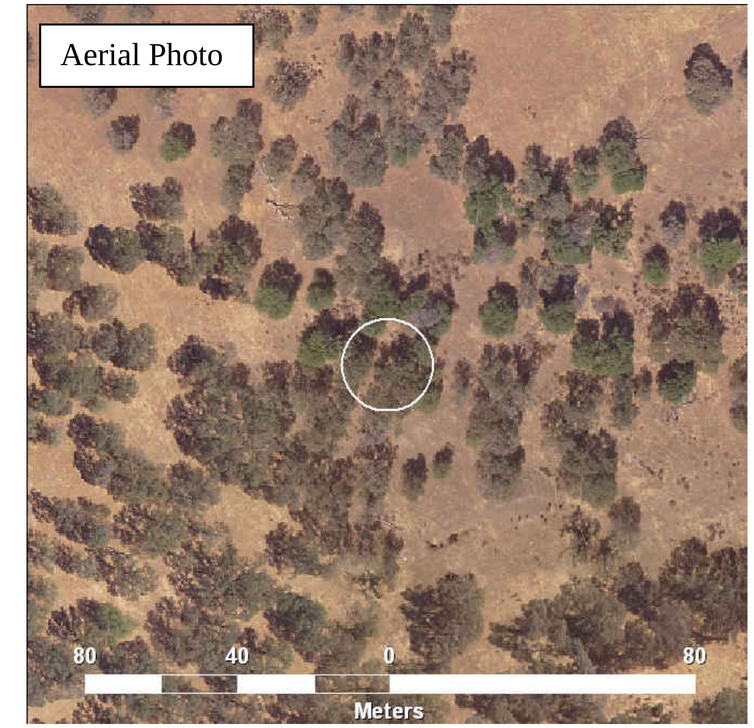
Plot # 23 Feature size: 3.7 m Vegetation density: 45.43% Surface method: TIN DEM cell size: 1 m Lidar block reference number: 5512 Additional features visible: no Existing features more clearly visible: possible	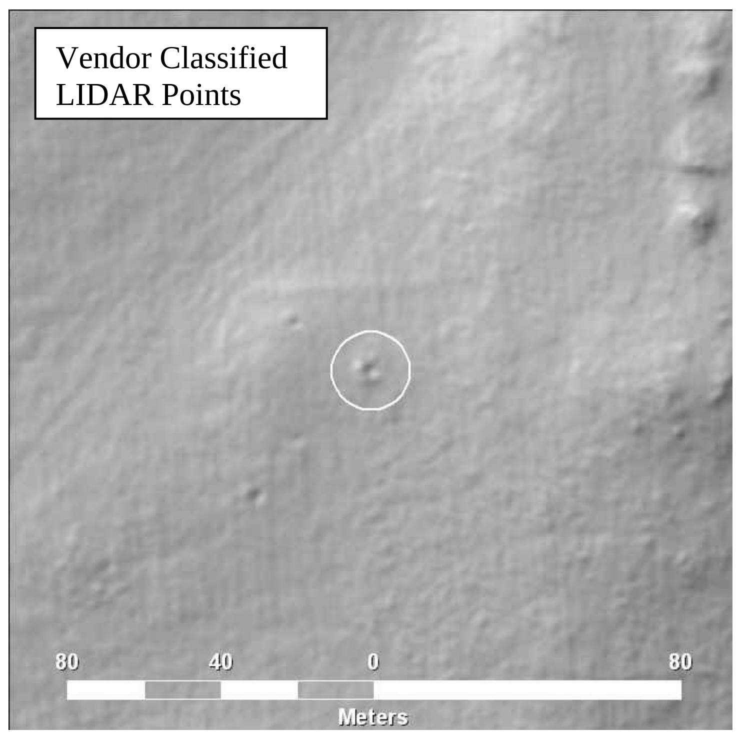	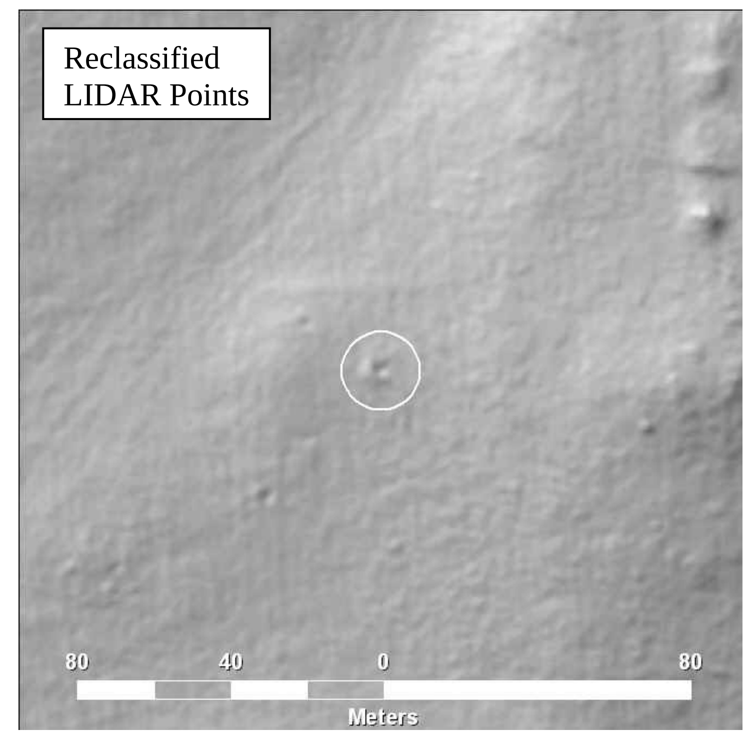	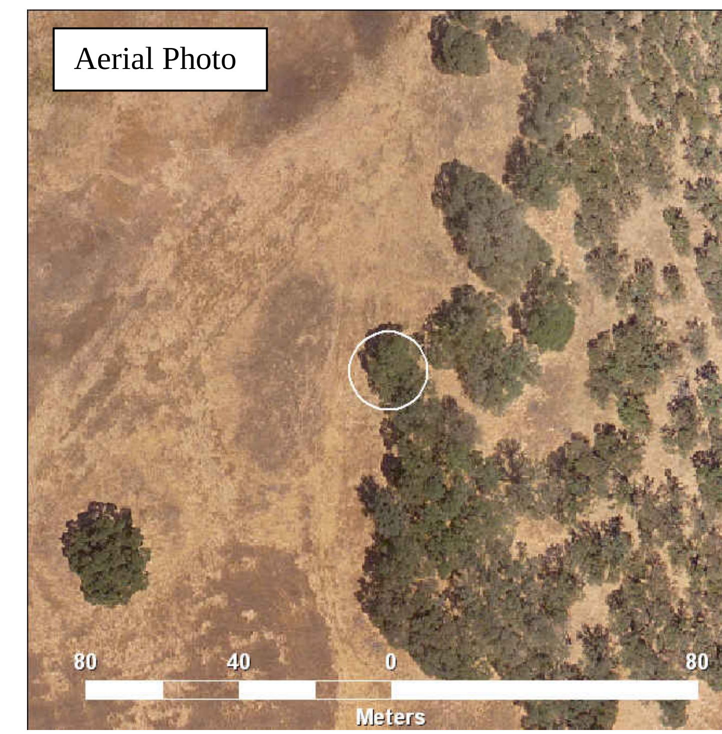

<table>
<tr>
<td>

Plot # 24

Feature size: 3.8 m
Vegetation density: 48.33%
Surface method: TIN
DEM cell size: 1 m
Lidar block reference number: 5463

Additional features visible: possible
Existing features more clearly visible: possible

</td>
<td>

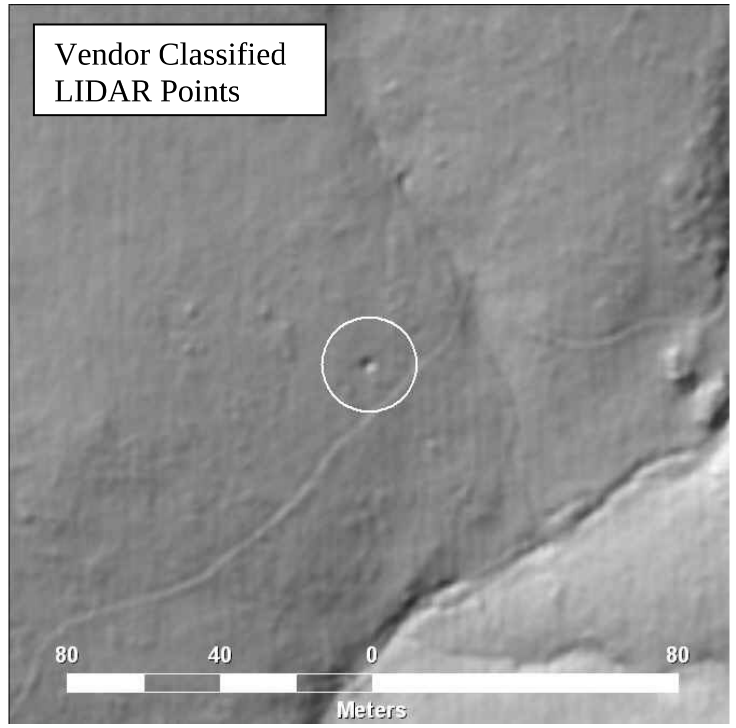

</td>
<td>

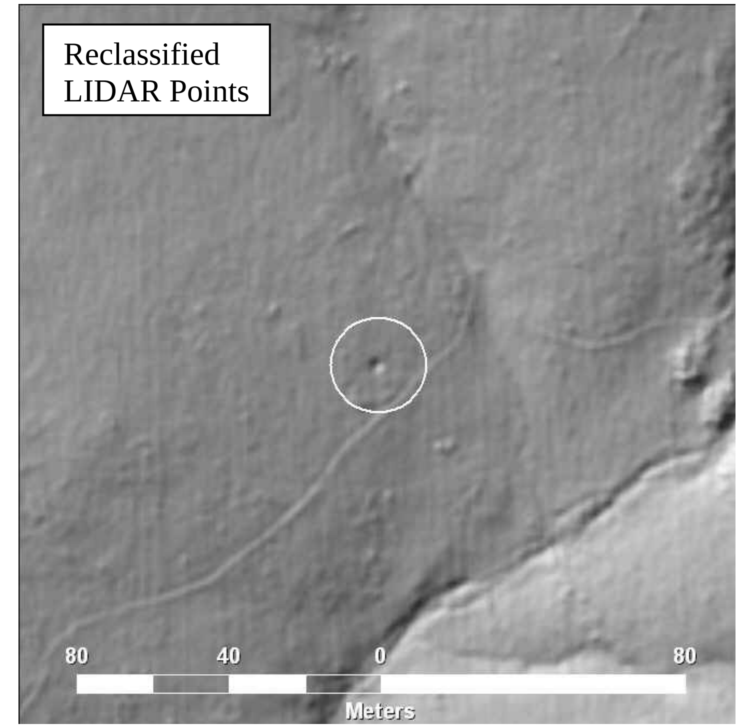

</td>
<td>

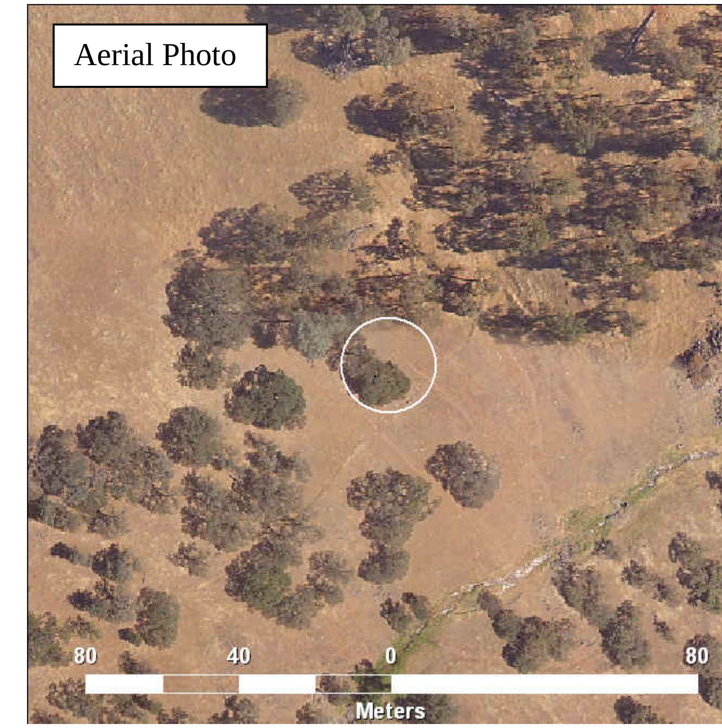

</td>
</tr>
<tr>
<td>

Plot # 25

Feature size: 3.8 m wide, 23.2 m long
Vegetation density: 61.50%
Surface method: TIN
DEM cell size: 1 m
Lidar block reference number: 5719

Additional features visible: no
Existing features more clearly visible: possible

</td>
<td>

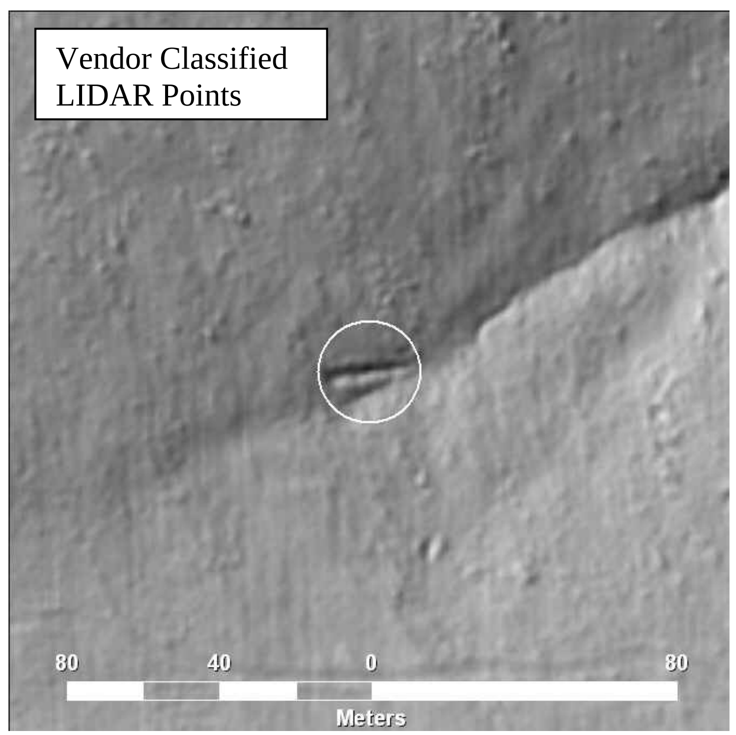

</td>
<td>

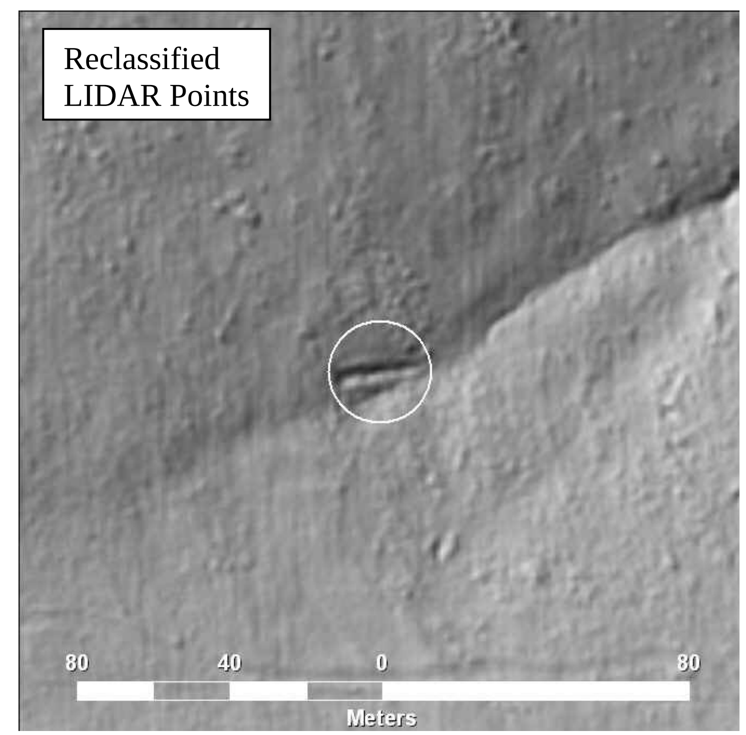

</td>
<td>

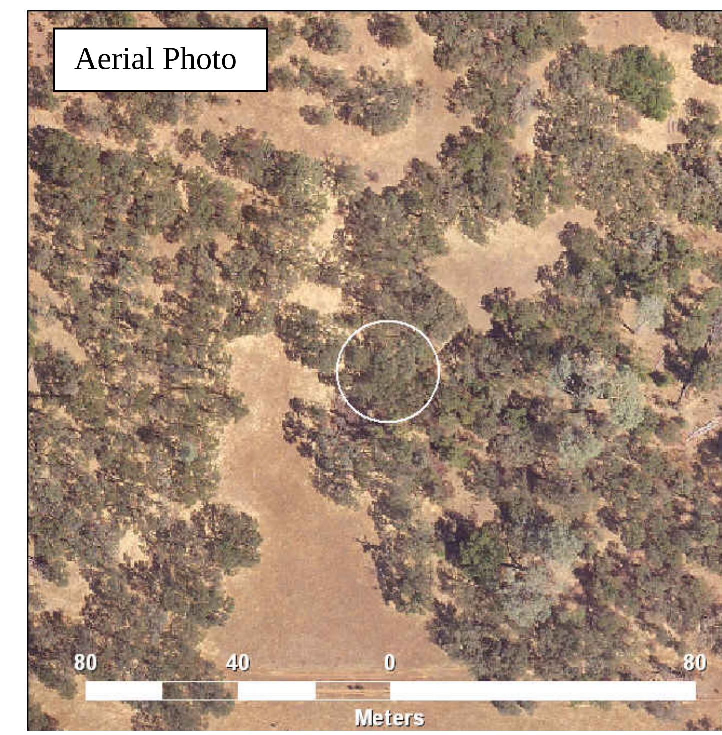

</td>
</tr>
</table>

Plot # 26 Feature size: 3.9 m Vegetation density: 38.58% Surface method: TIN DEM cell size: 1 m Lidar block reference number: 5465 Additional features visible: no Existing features more clearly visible: possible	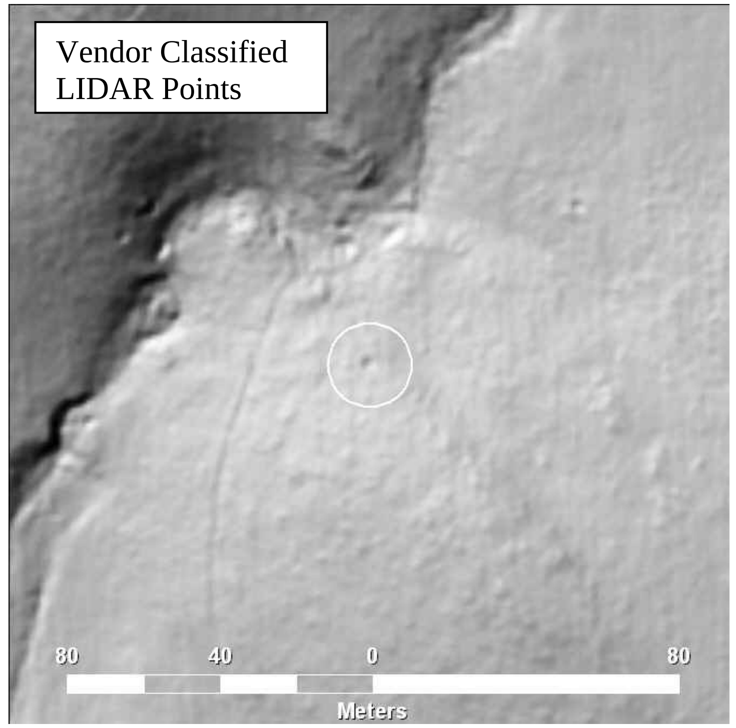	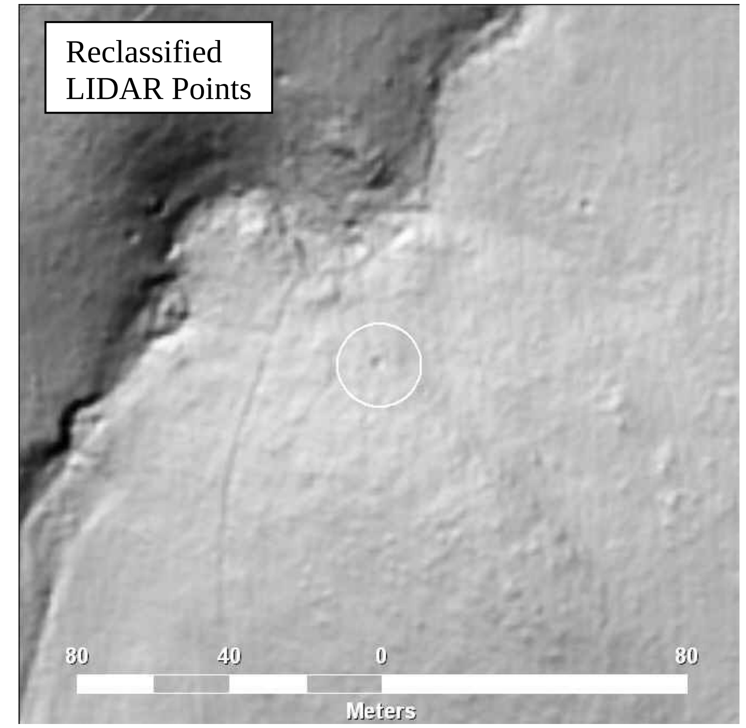	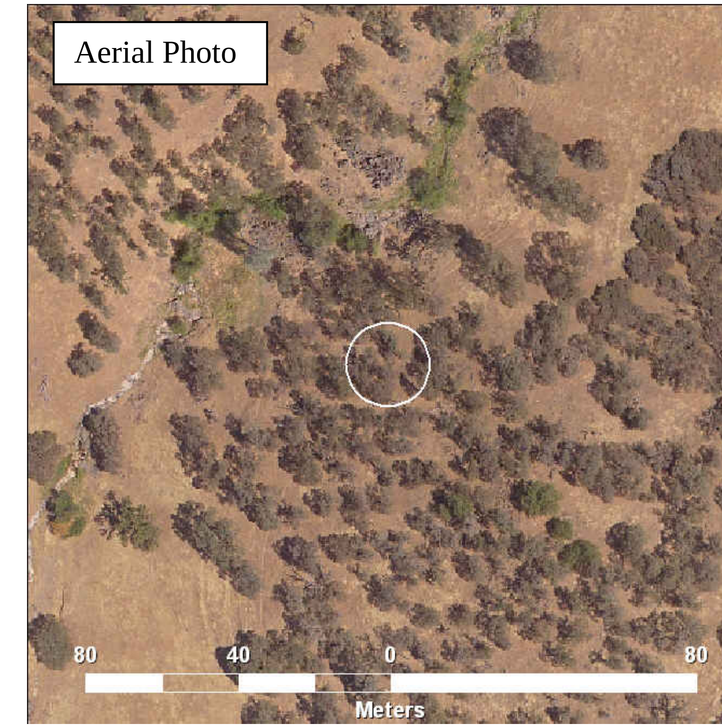
Plot # 27 Feature size: 4.0 m Vegetation density: 38.97% Surface method: TIN DEM cell size: 1 m Lidar block reference number: 5740 Additional features visible: possible Existing features more clearly visible: possible	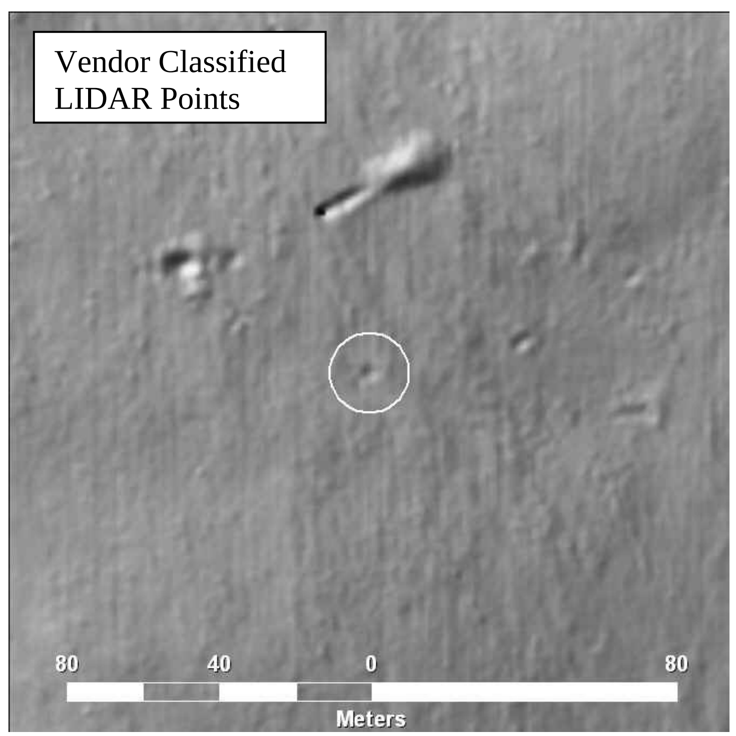	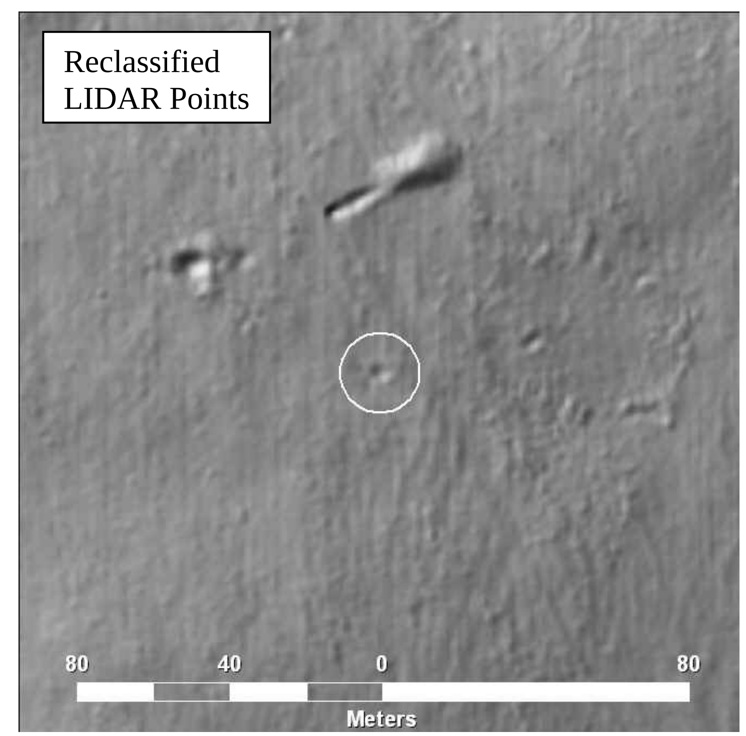	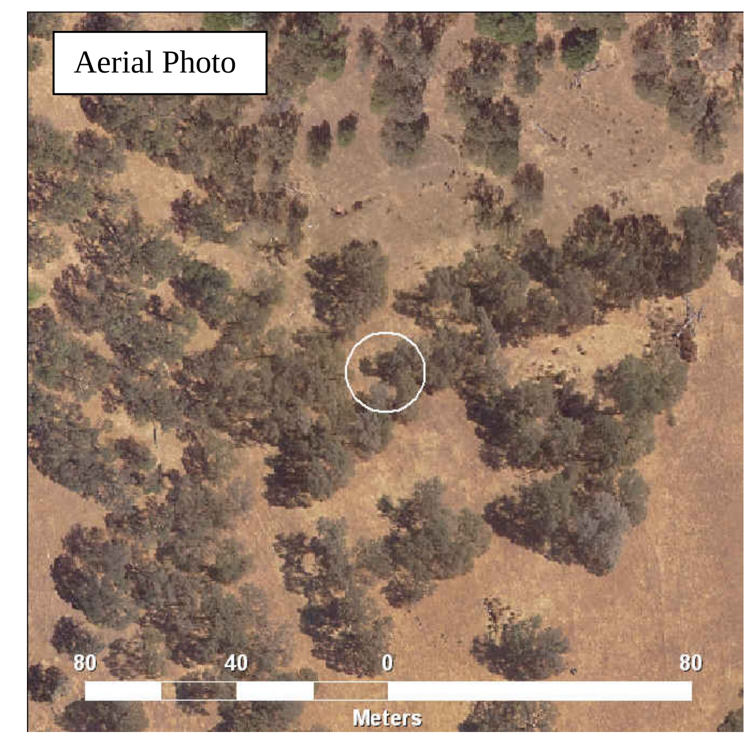

Plot # 28 Feature size: 4.1 m Vegetation density: 57.20% Surface method: TIN DEM cell size: 1 m Lidar block reference number: 5641 Additional features visible: no Existing features more clearly visible: possible	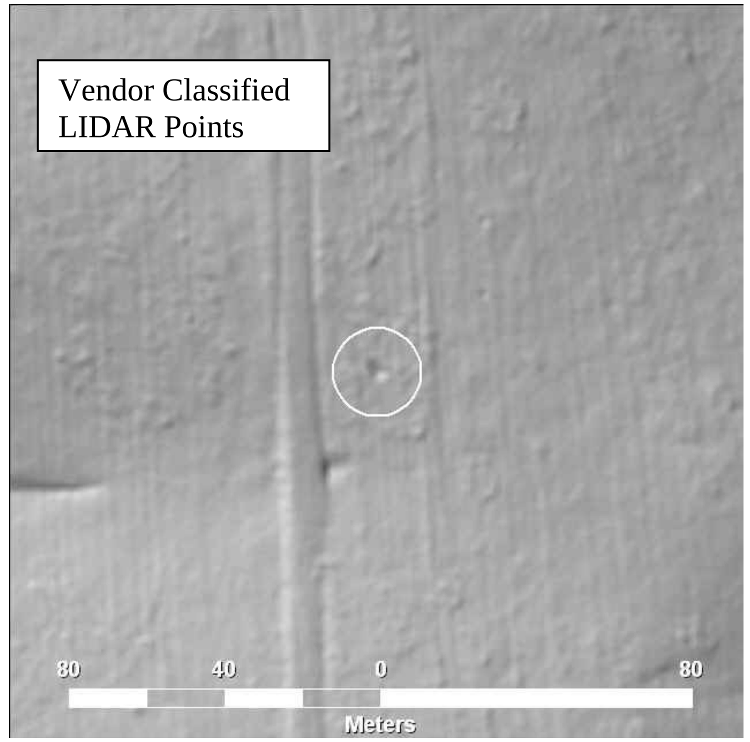	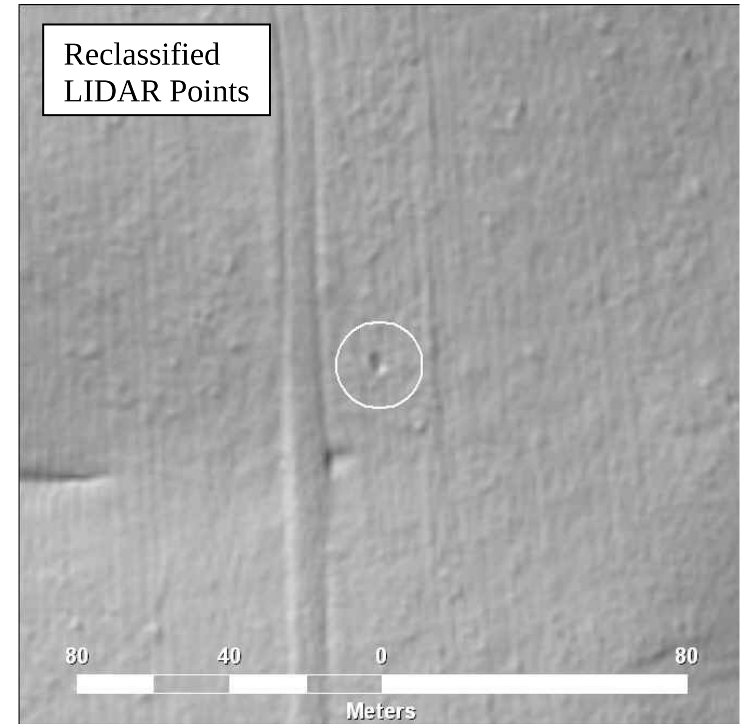	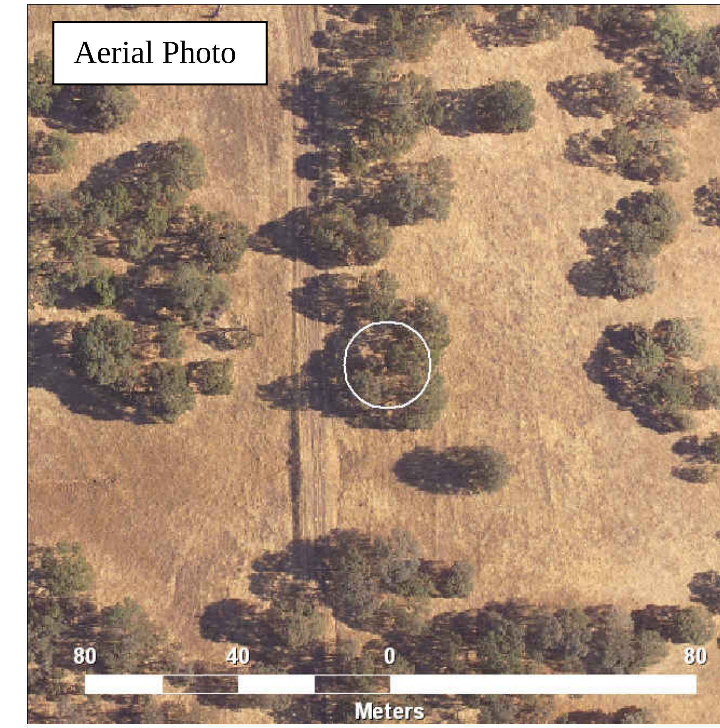
Plot # 29 Feature size: 4.25 m Vegetation density: 52.90% Surface method: TIN DEM cell size: 1 m Lidar block reference number: 5615 Additional features visible: no Existing features more clearly visible: possible	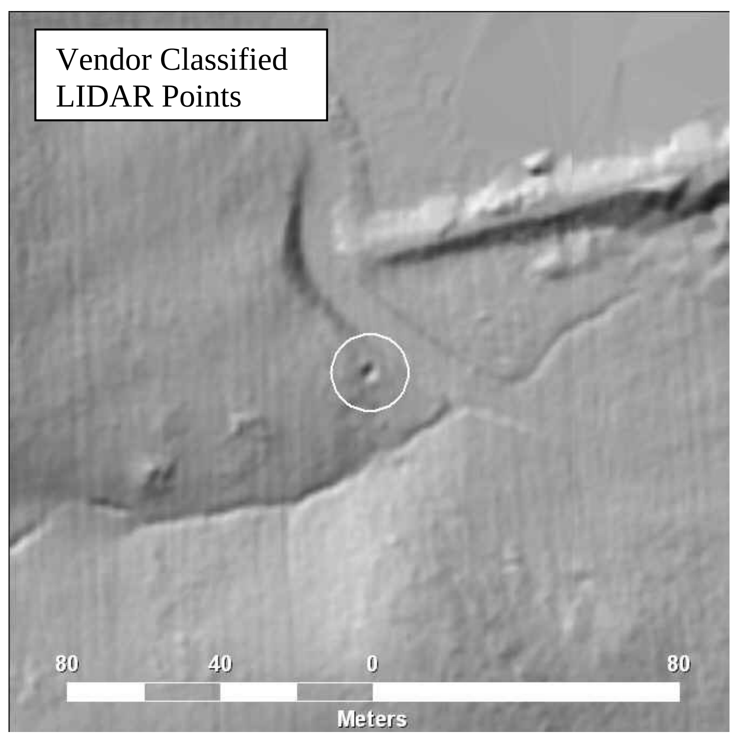	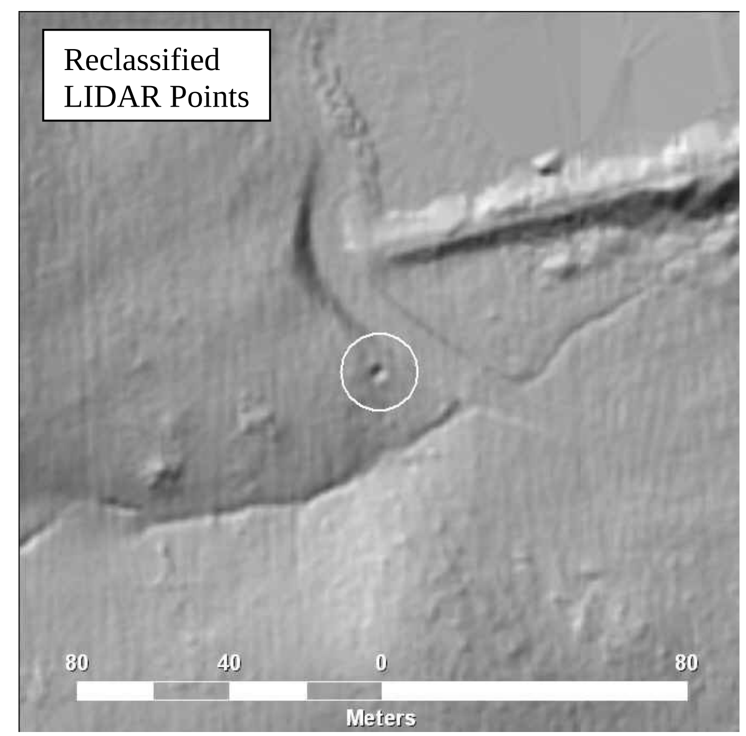	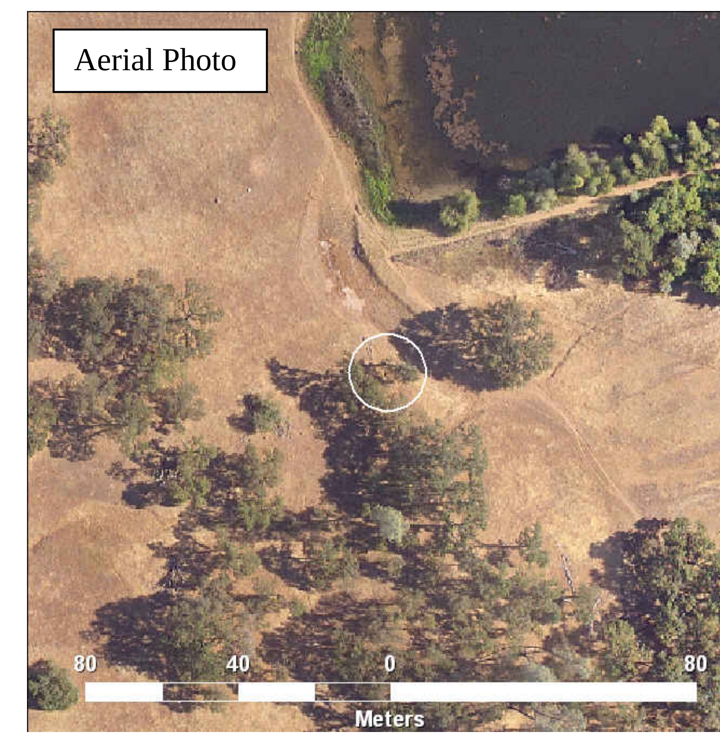

Plot # 30 Feature size: 4.3 m Vegetation density: 73.79% Surface method: TIN DEM cell size: 1 m Lidar block reference number: 4077 Additional features visible: no Existing features more clearly visible: possible	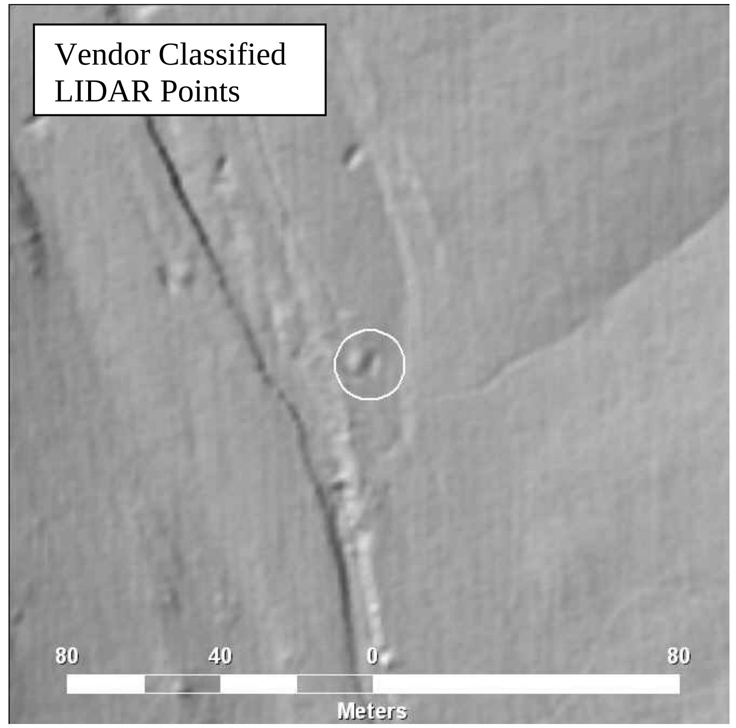	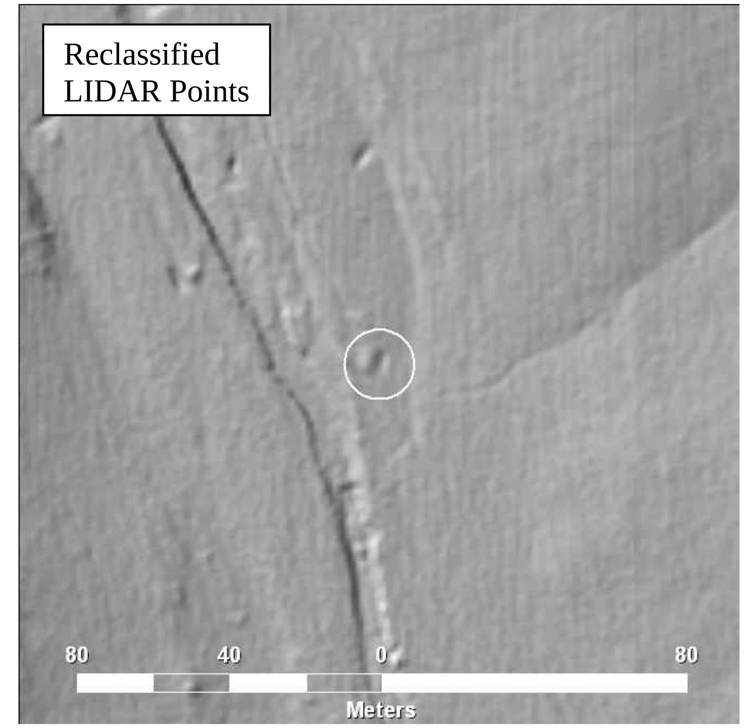	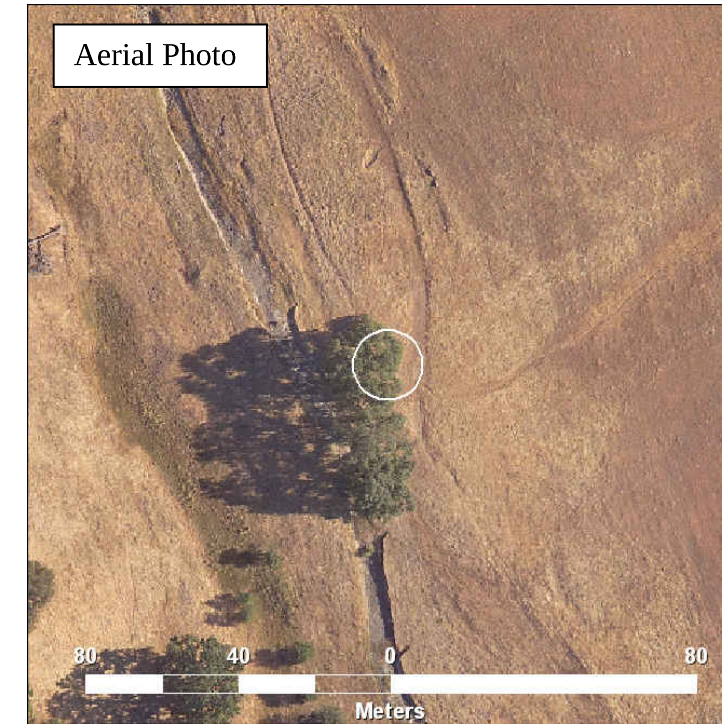
Plot # 31 Feature size: 4.5 m Vegetation density: 48.85% Surface method: TIN DEM cell size: 1 m Lidar block reference number: 4001 Additional features visible: possible Existing features more clearly visible: no	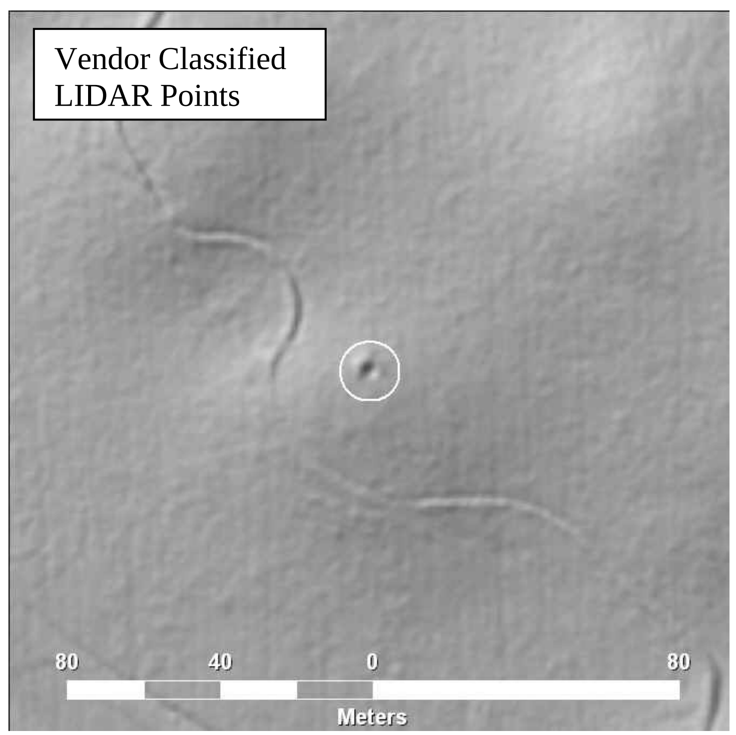	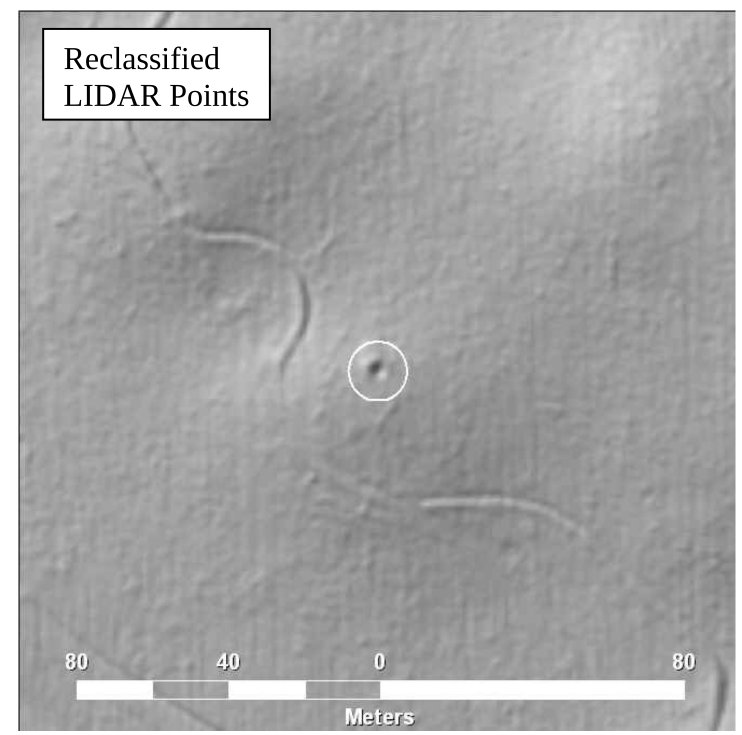	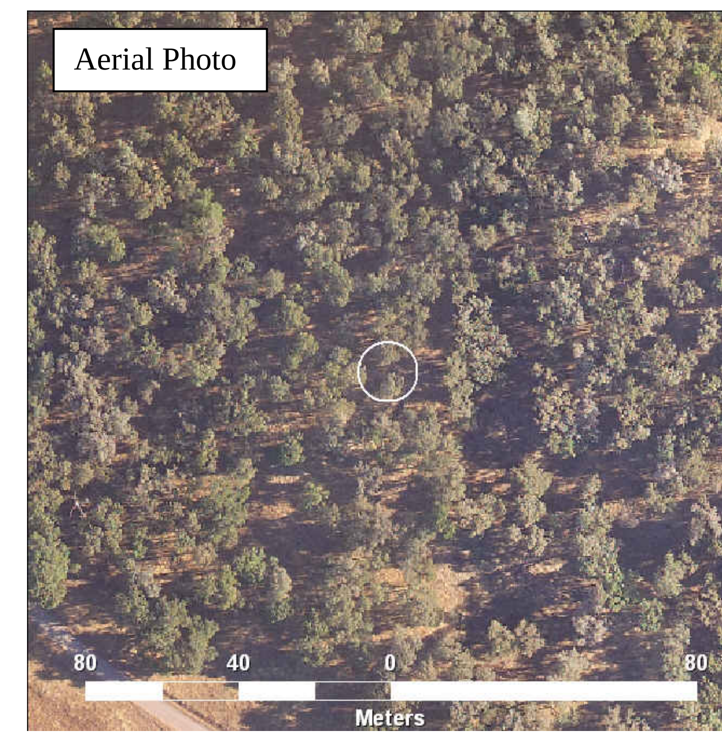

Plot # 32

Feature size: 4.5 m
Vegetation density: 63.38%
Surface method: TIN
DEM cell size: 1 m
Lidar block reference number: 5468

Additional features visible: possible
Existing features more clearly visible: possible

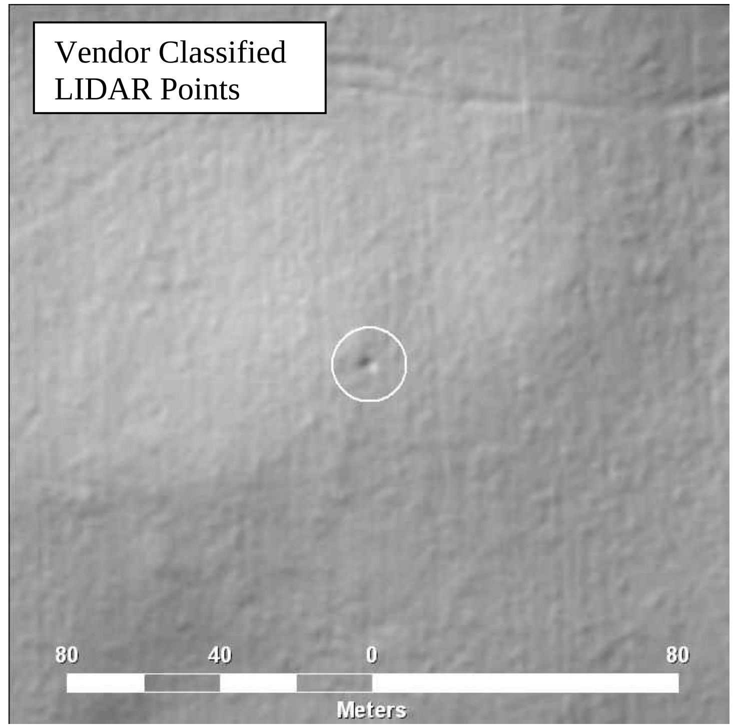

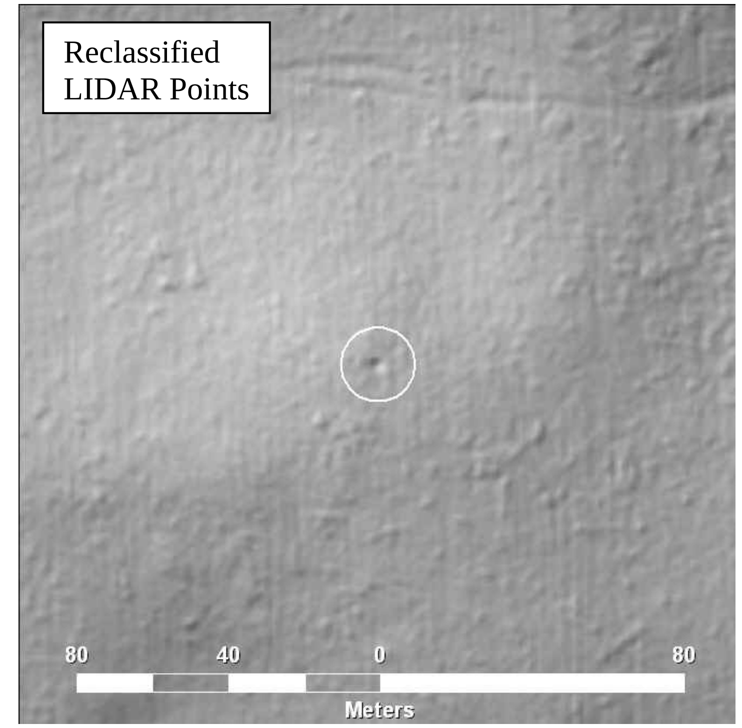

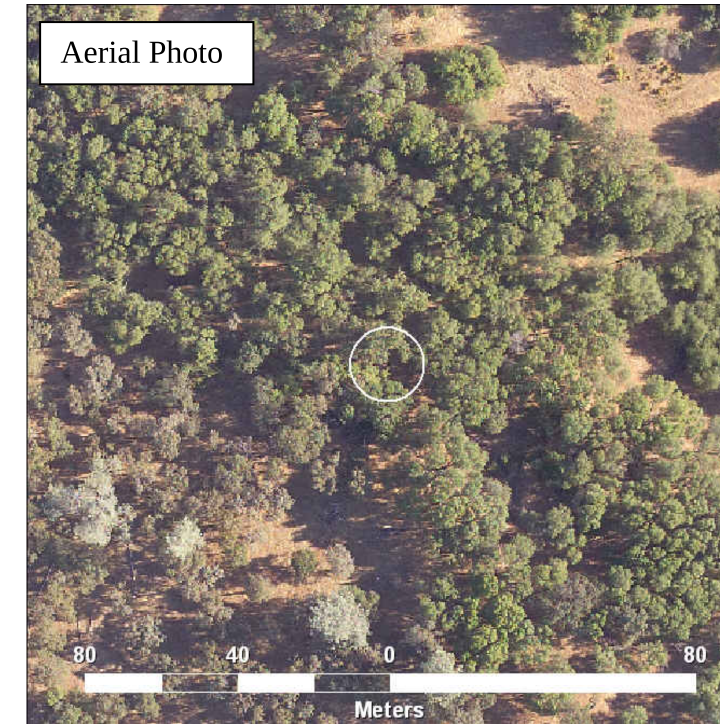

Plot # 33

Feature size: 4.7 m
Vegetation density: 47.67%
Surface method: TIN
DEM cell size: 1 m
Lidar block reference number: 4014

Additional features visible: no
Existing features more clearly visible: possible

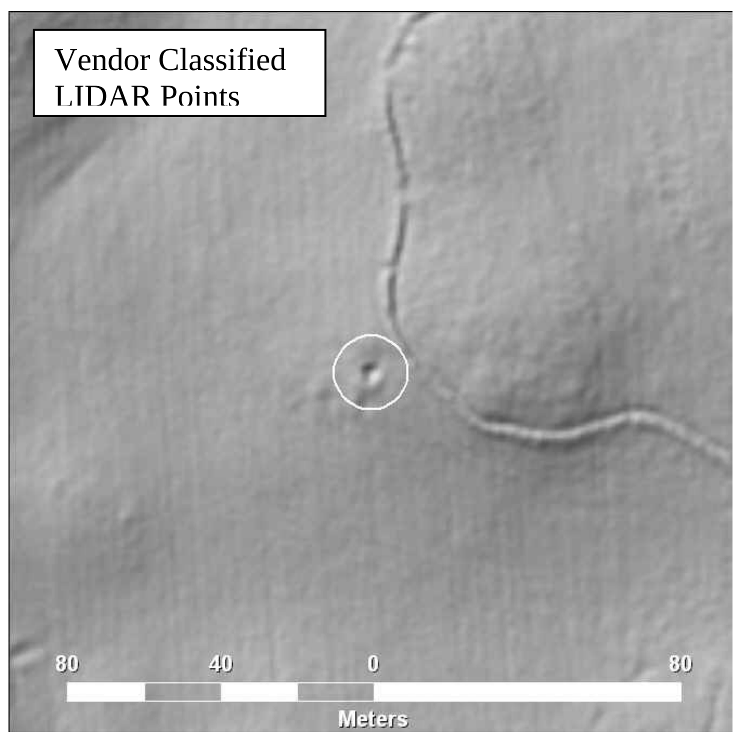

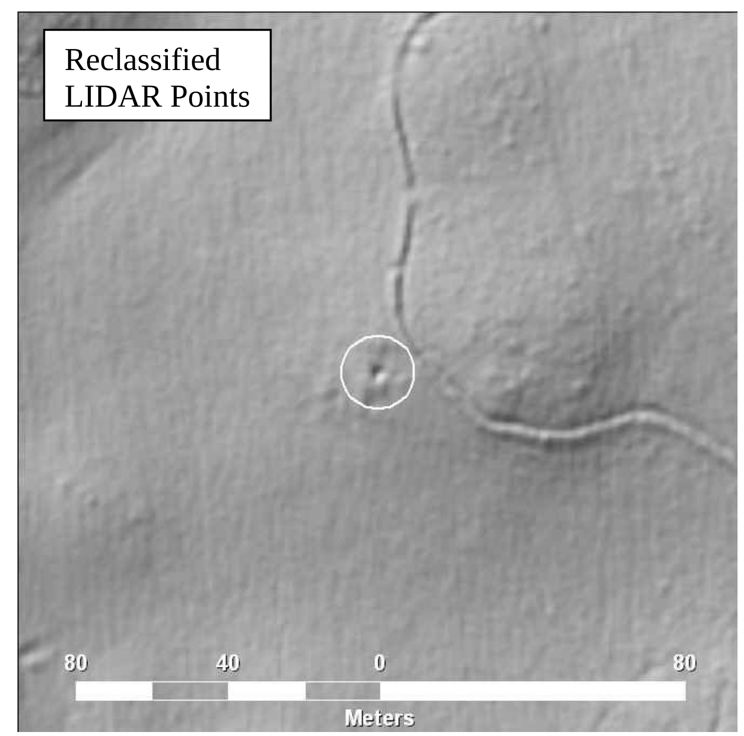

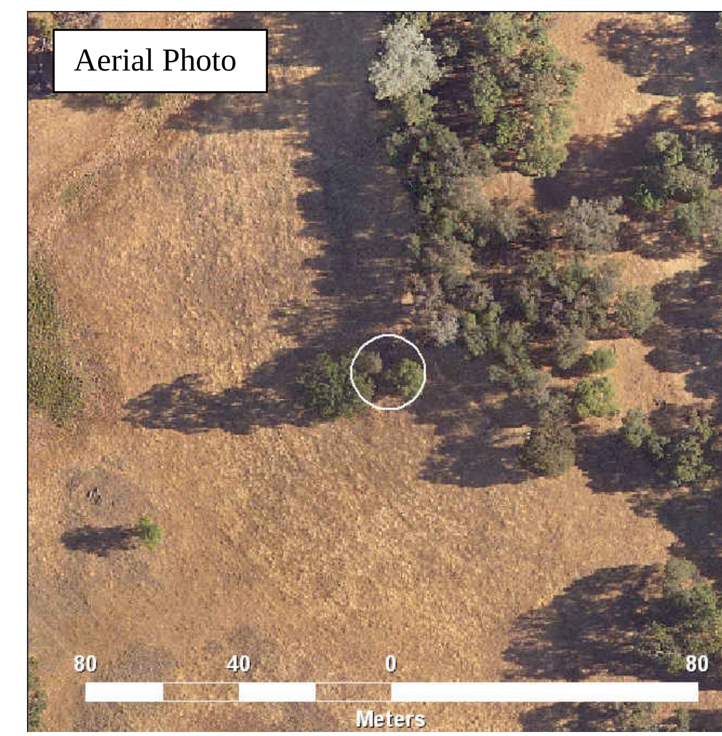

Plot # 34

Feature size: 4.8 m
Vegetation density: 50.17%
Surface method: TIN
DEM cell size: 1 m
Lidar block reference number: 5521

Additional features visible: no
Existing features more clearly visible: possible

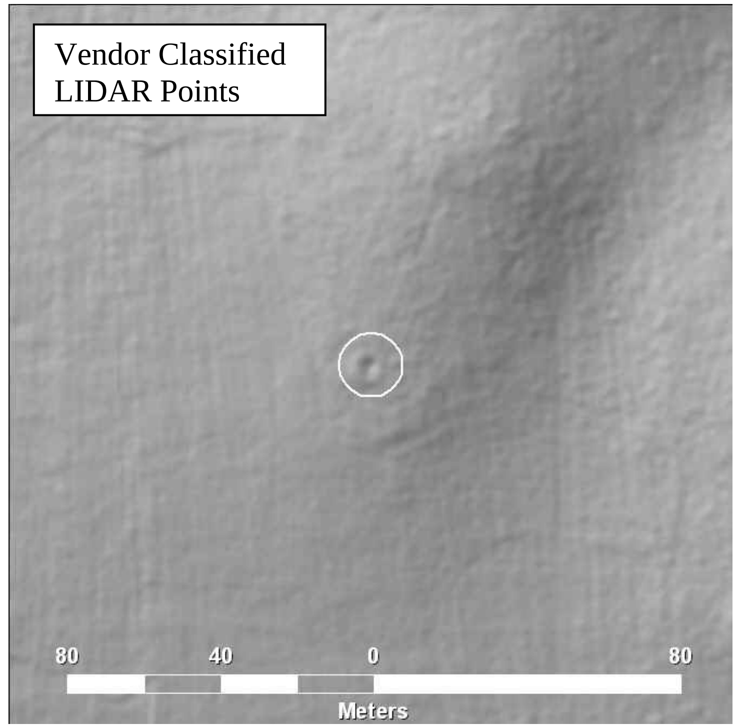

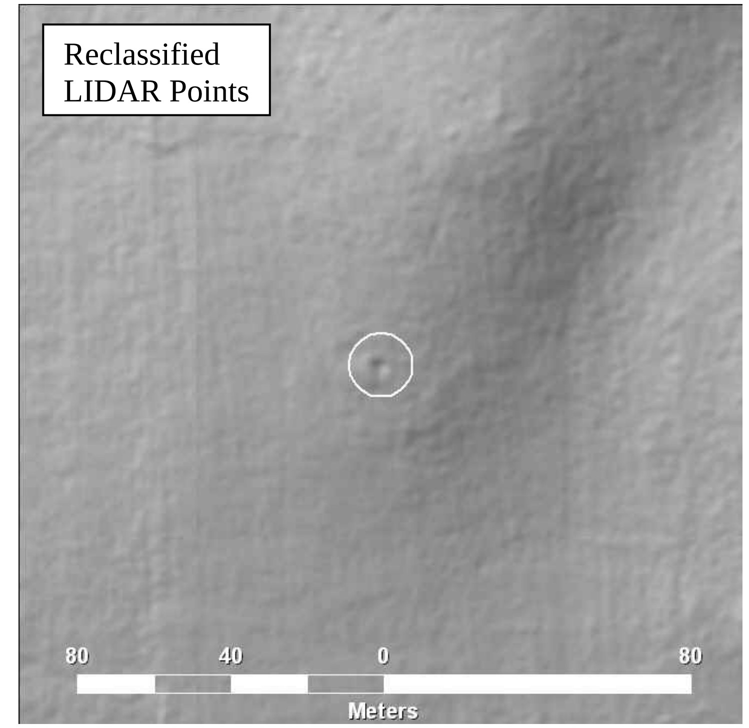

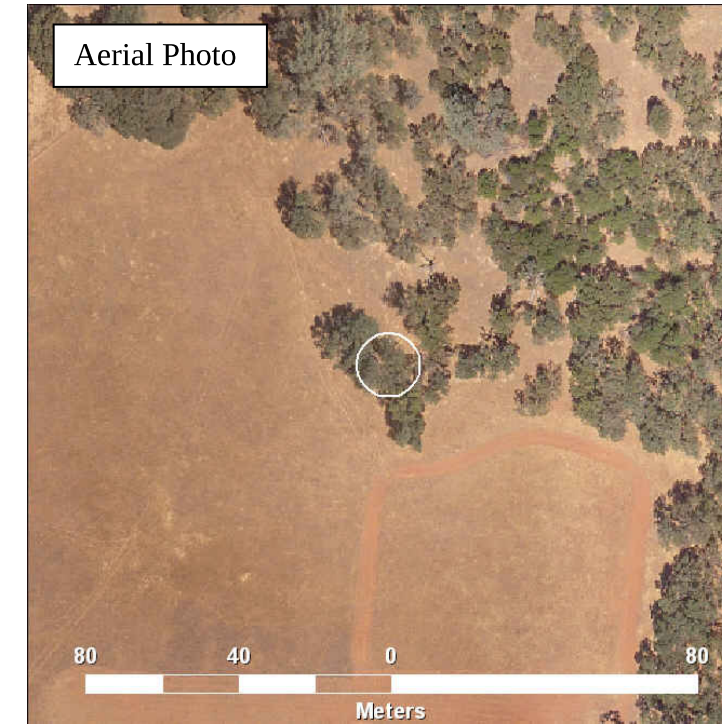

Plot # 35

Feature size: 5.1 m
Vegetation density: 53.50%
Surface method: TIN
DEM cell size: 1 m
Lidar block reference number: 5569

Additional features visible: possible
Existing features more clearly visible: possible

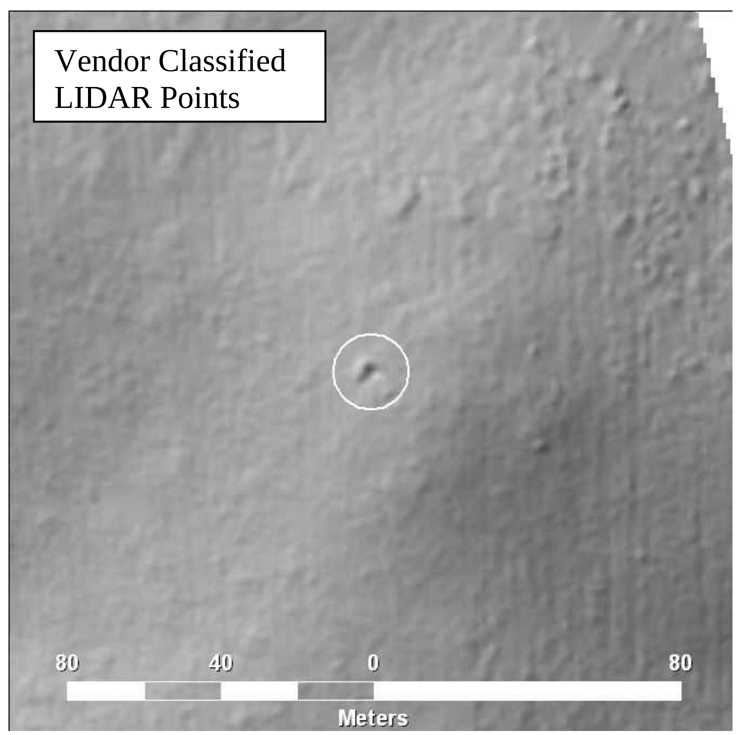

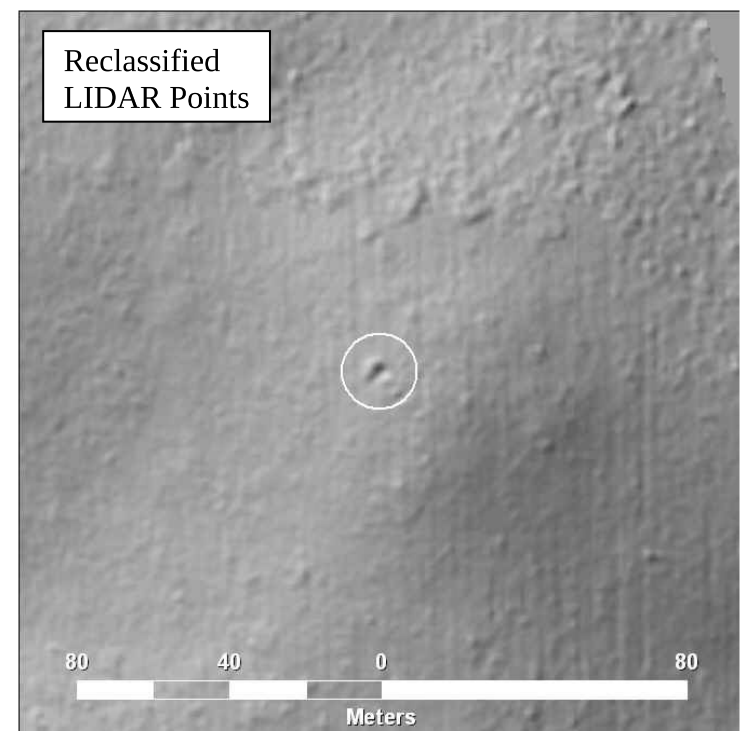

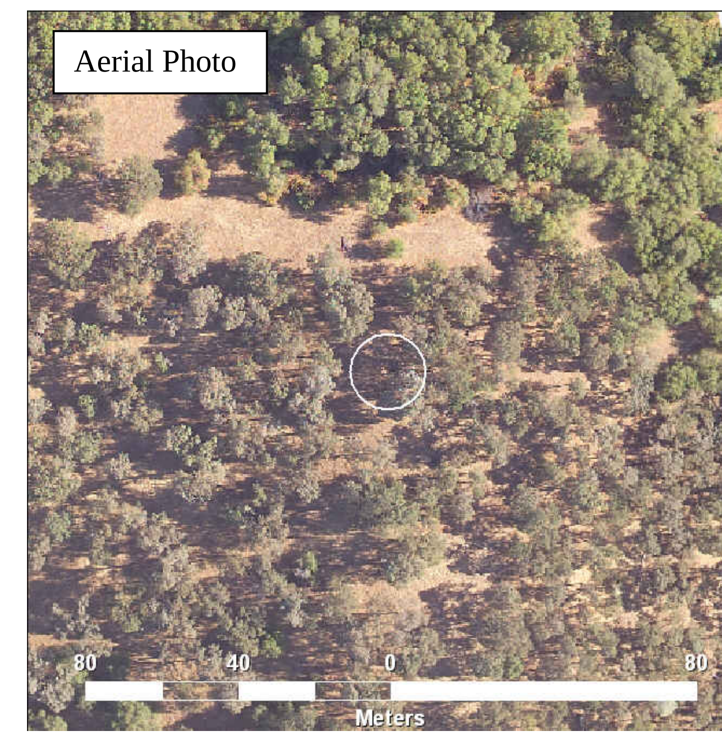

<table>
<tr>
<td>

Plot # 36

Feature size: 5.2 m
Vegetation density: 38.94%
Surface method: TIN
DEM cell size: 1 m
Lidar block reference number: 5736

Additional features visible: no
Existing features more clearly visible: possible

</td>
<td>
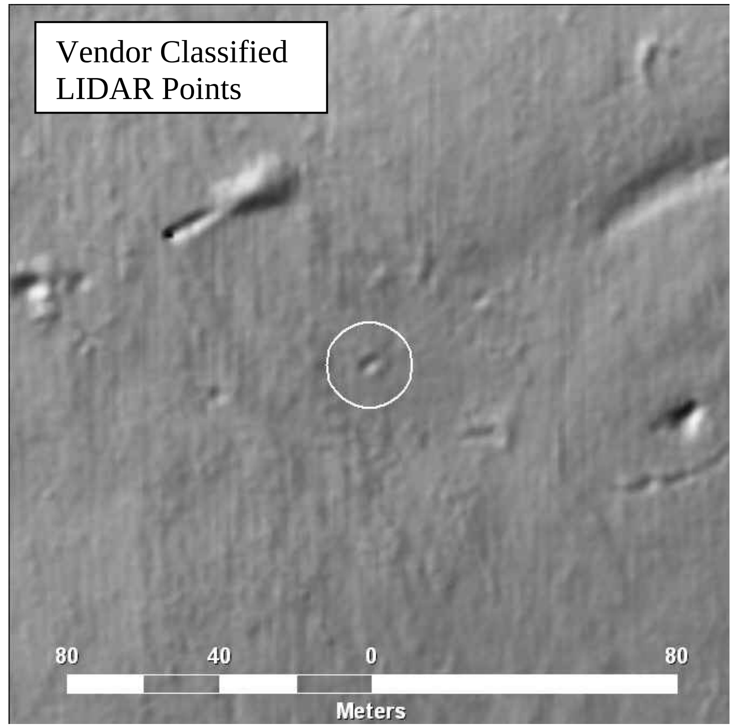

</td>
<td>
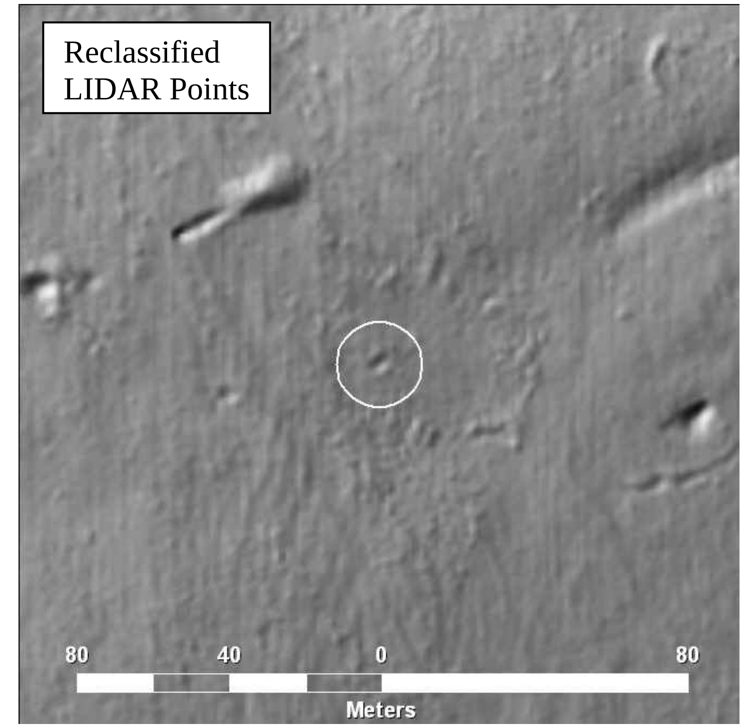

</td>
<td>
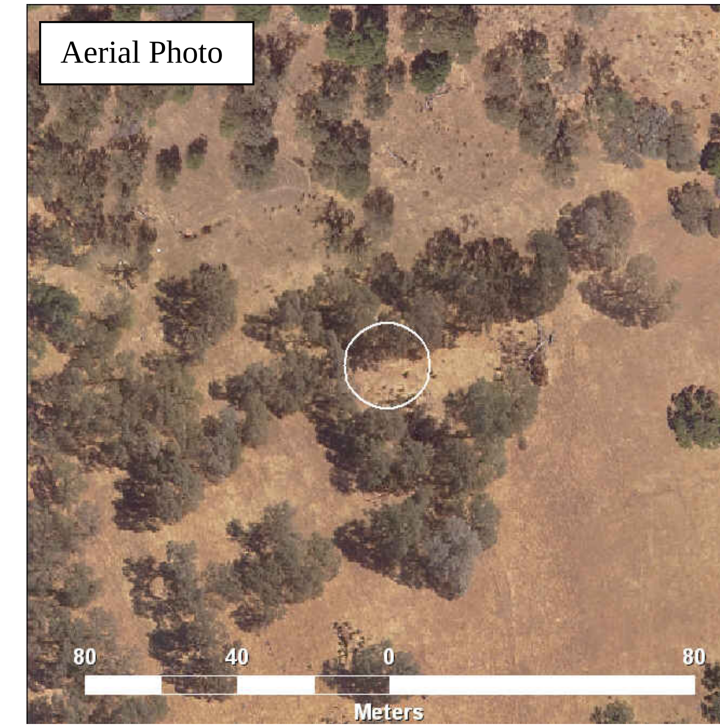

</td>
</tr>
<tr>
<td>

Plot # 37

Feature size: 5.2 m wide 10.0 m long
Vegetation density: 43.17 %
Surface method: TIN
DEM cell size: 1 m
Lidar block reference number: 3965

Additional features visible: no
Existing features more clearly visible: yes

</td>
<td>
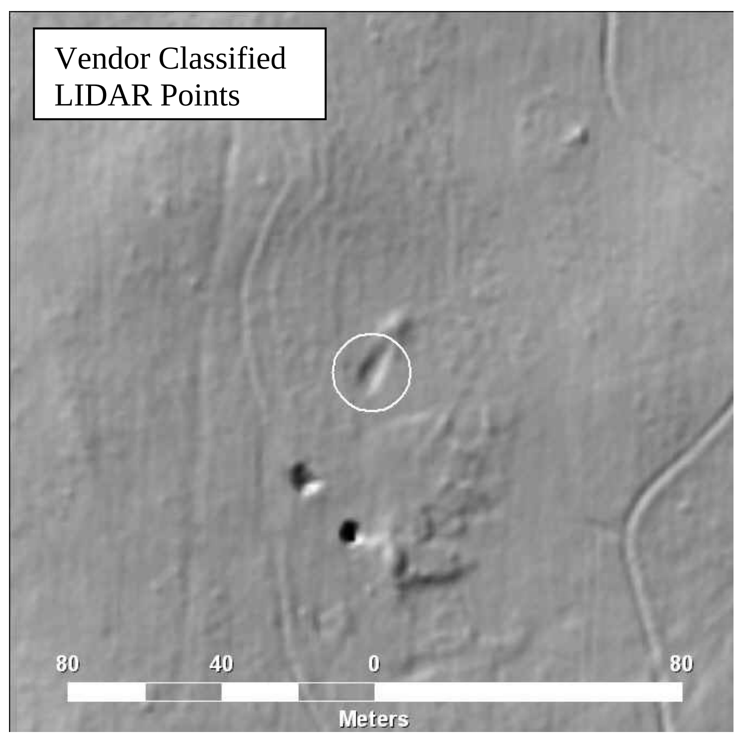

</td>
<td>
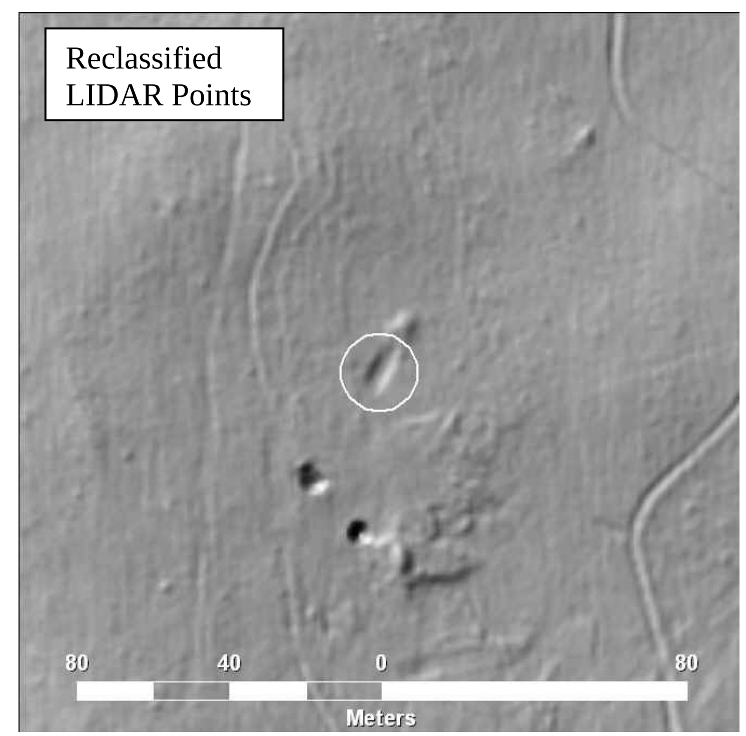

</td>
<td>
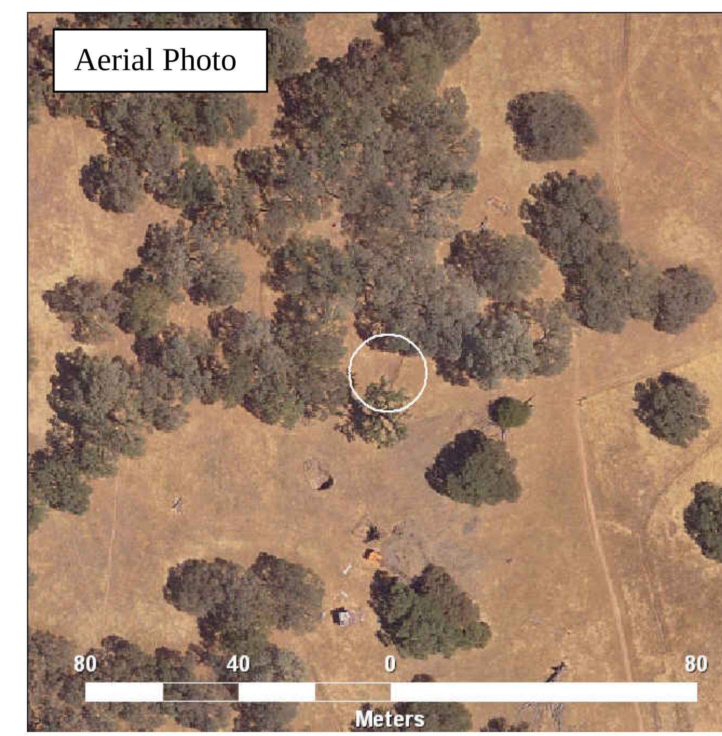

</td>
</tr>
</table>

Plot # 38

Feature size: 5.3 m
Vegetation density: 52.97%
Surface method: TIN
DEM cell size: 1 m
Lidar block reference number: 5644

Additional features visible: no
Existing features more clearly visible: possible

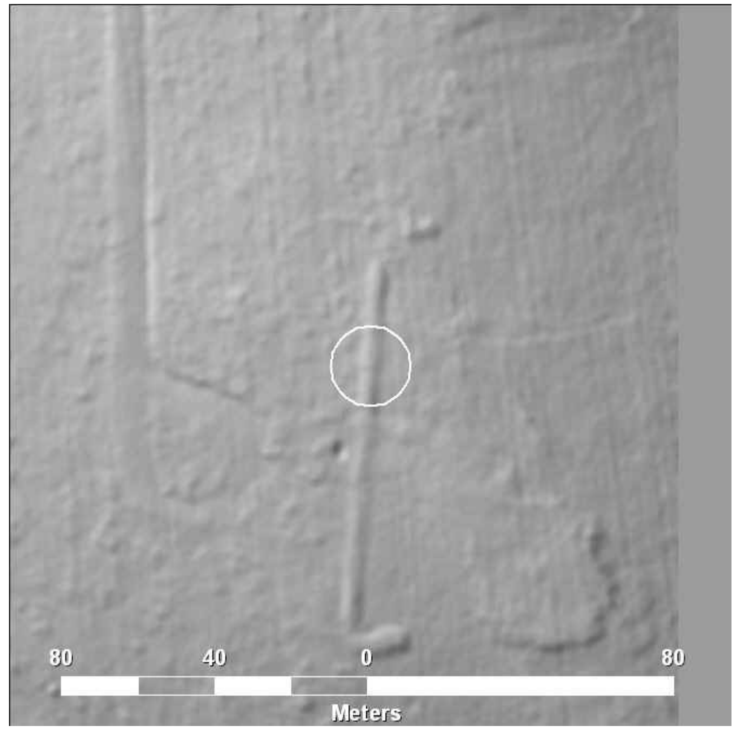

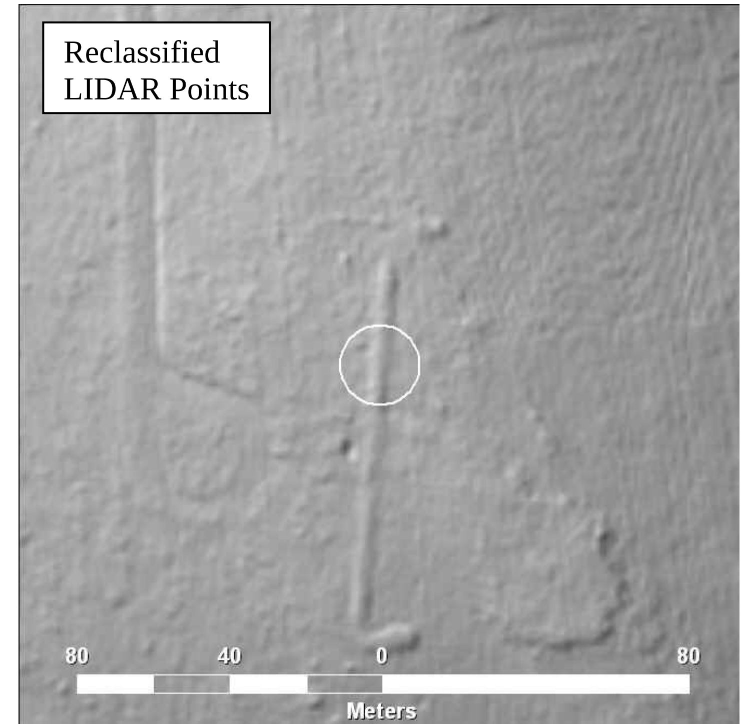

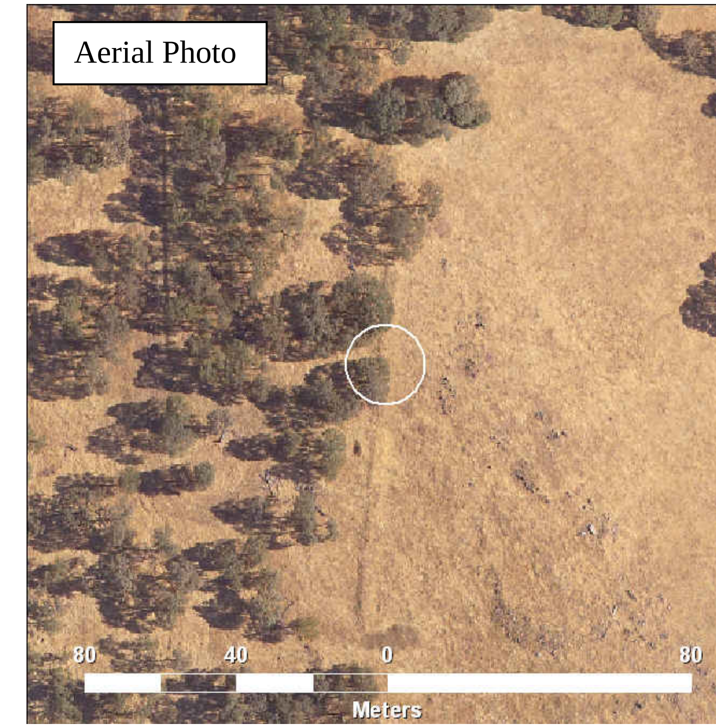

Plot # 39

Feature size: 5.3 m
Vegetation density: 51.68%
Surface method: TIN
DEM cell size: 1 m
Lidar block reference number: 5675

Additional features visible: no
Existing features more clearly visible: possible

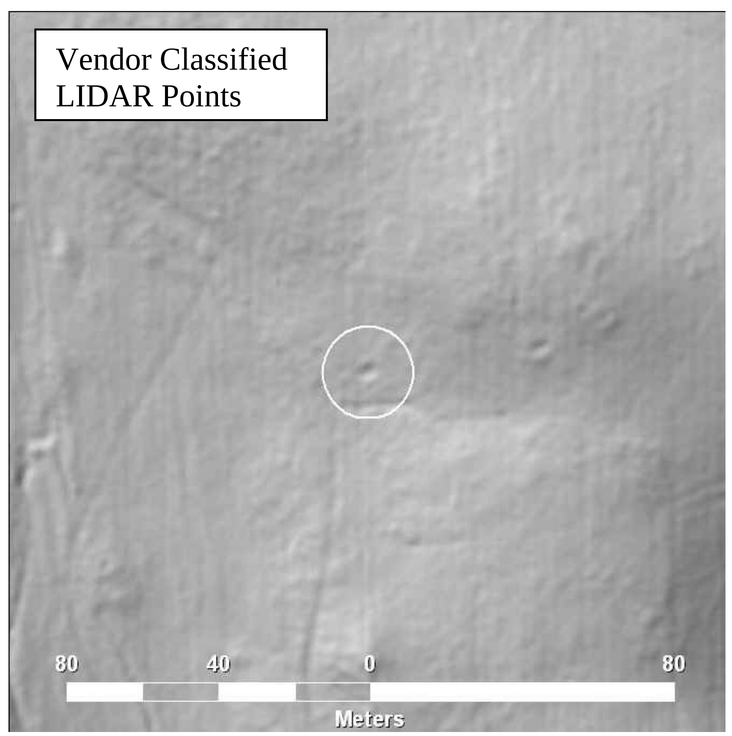

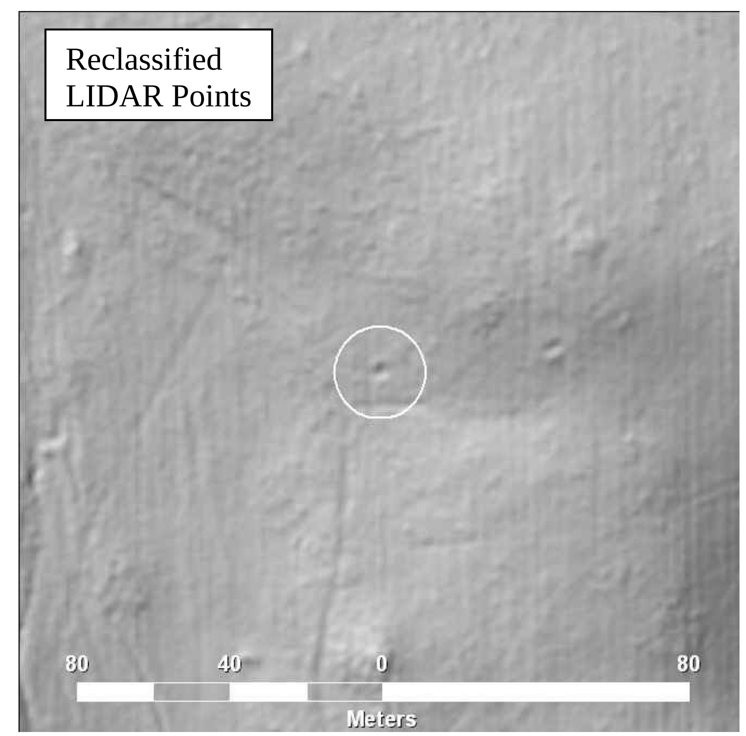

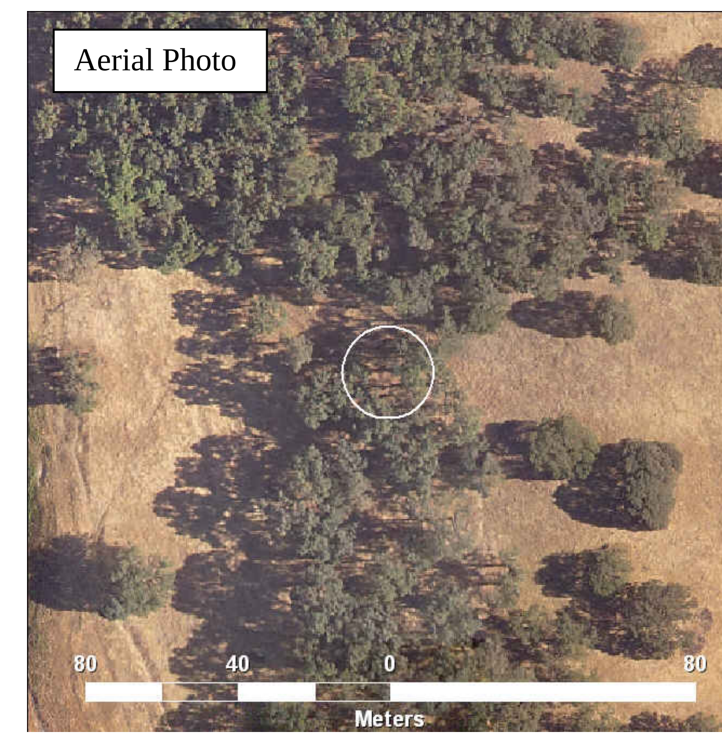

Plot # 40 Feature size: 5.6 m wide, 32.1 m long, 14.6 m long Vegetation density: 58.89% Surface method: TIN DEM cell size: 1 m Lidar block reference number: 5715 Additional features visible: possible Existing features more clearly visible: possible	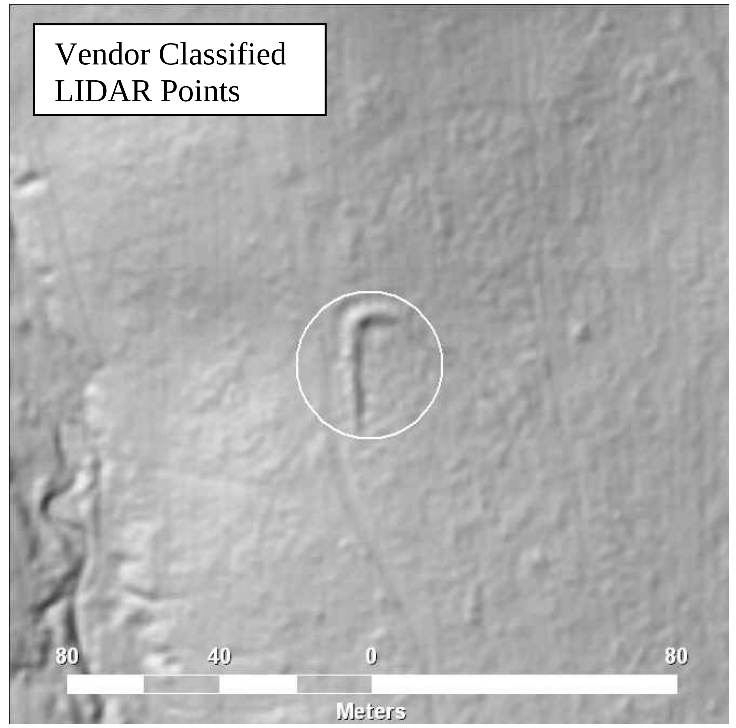	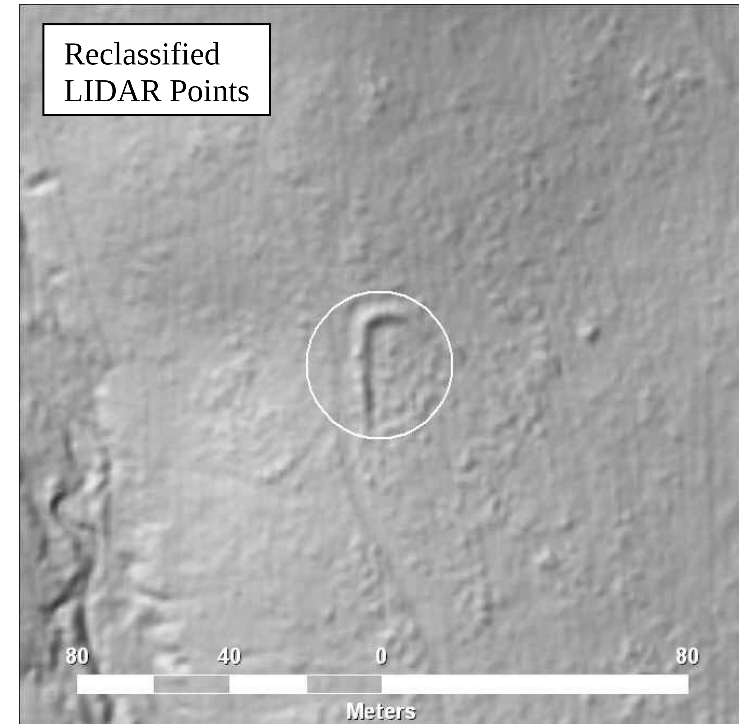	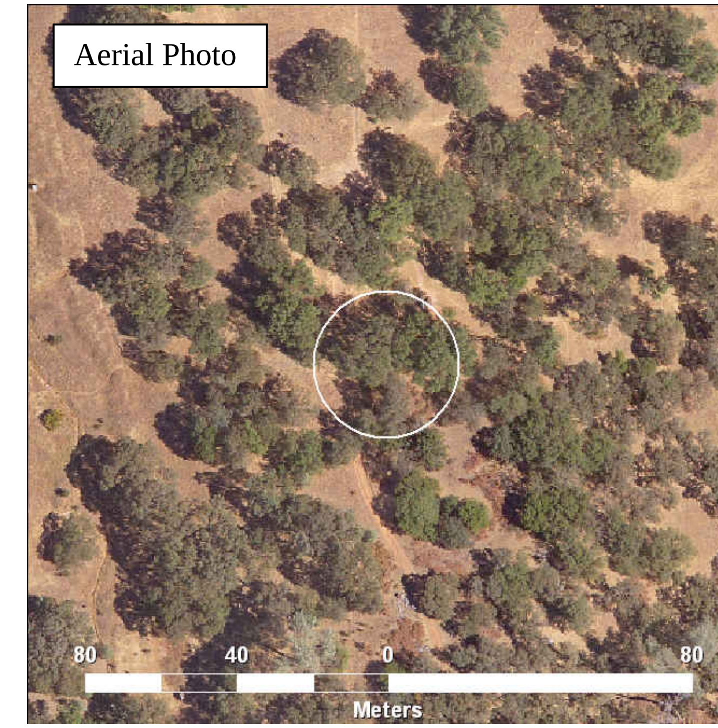
Plot # 41 Feature size: 5.8 m Vegetation density: 37.38% Surface method: TIN DEM cell size: 1 m Lidar block reference number: 4033 Additional features visible: possible Existing features more clearly visible: possible	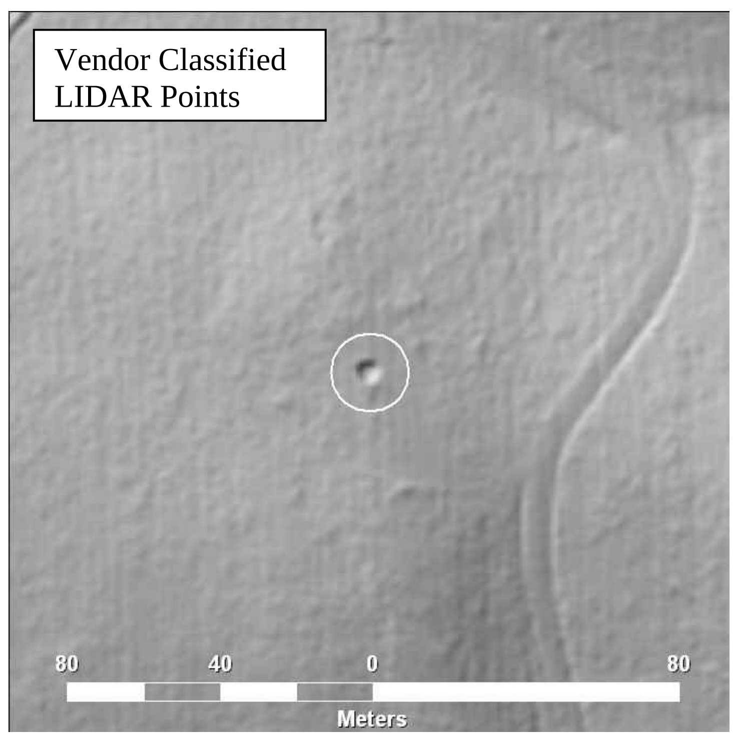	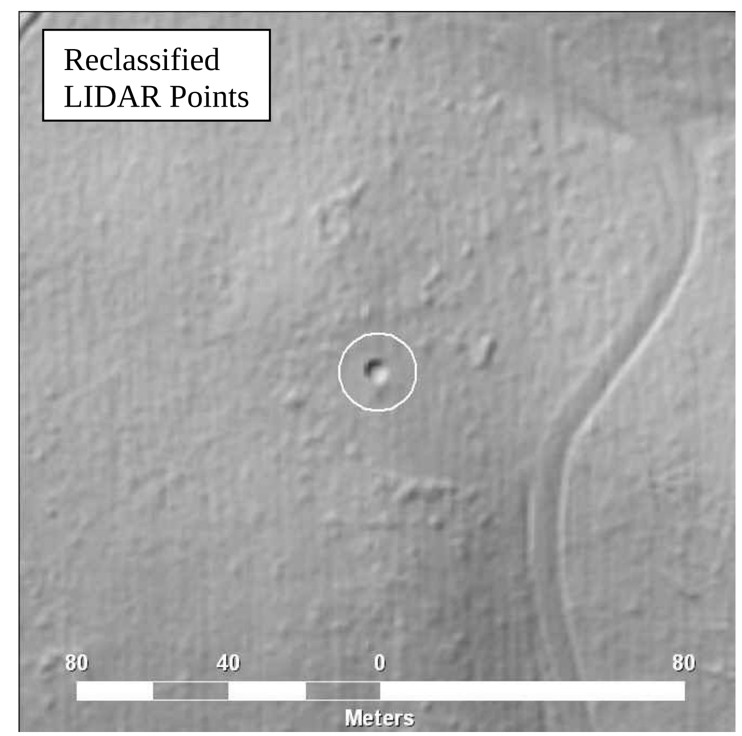	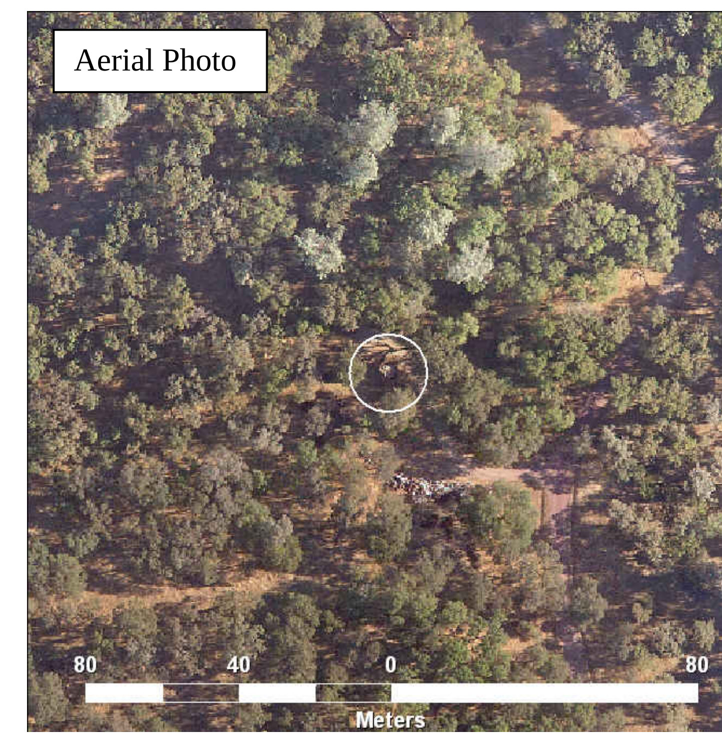

Plot # 42

Feature size: 5.8 m
Vegetation density: 47.04%
Surface method: TIN
DEM cell size: 1 m
Lidar block reference number: 5717

Additional features visible: possible
Existing features more clearly visible: possible

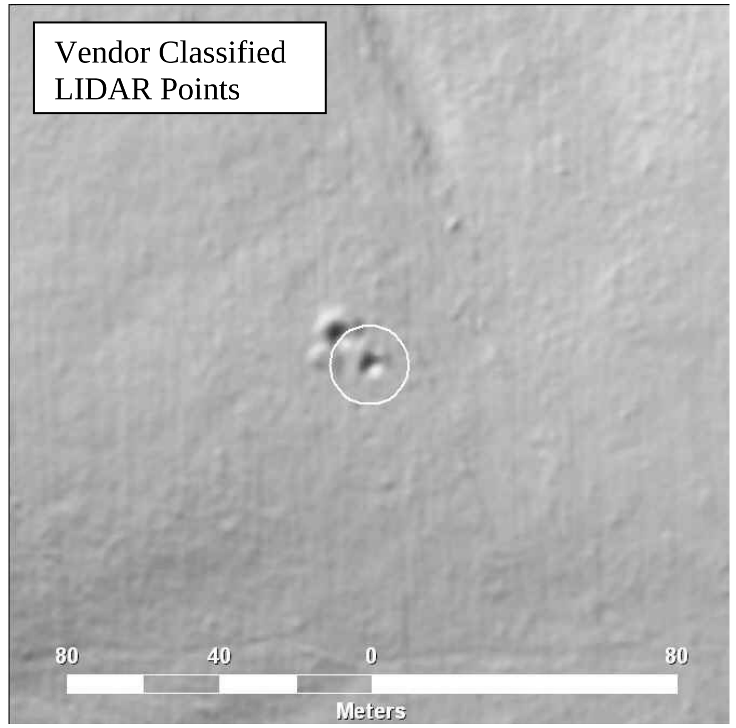

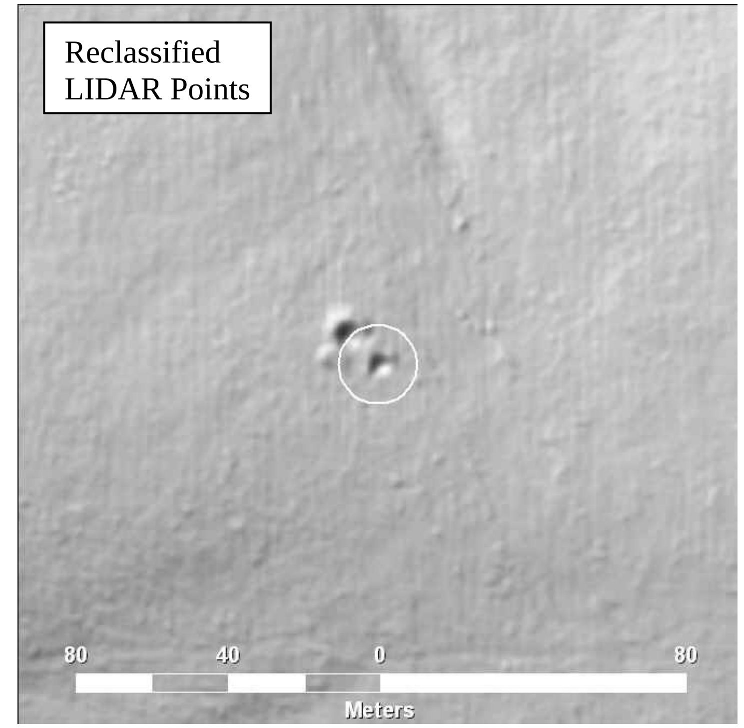

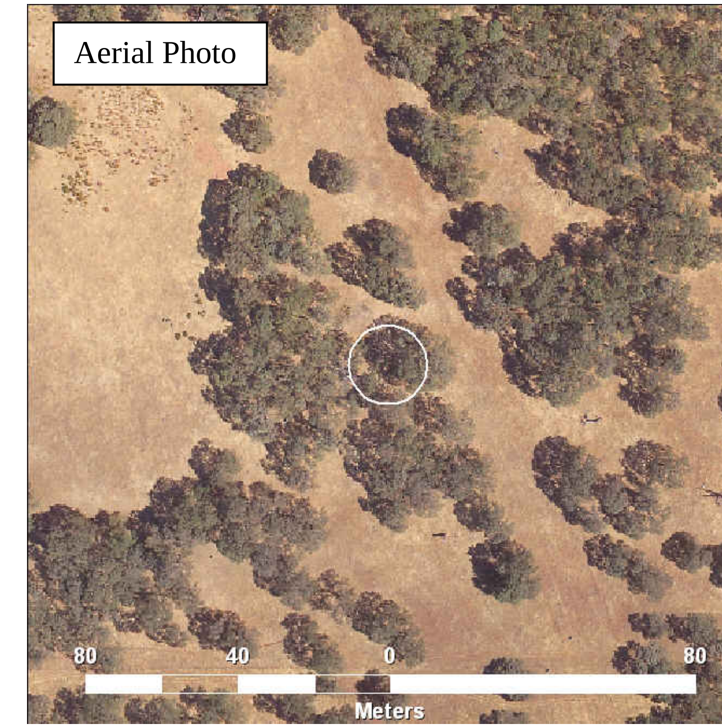

Plot # 43

Feature size: 6.2 m
Vegetation density: 51.12%
Surface method: TIN
DEM cell size: 1 m
Lidar block reference number: 5613

Additional features visible: possible
Existing features more clearly visible: possible

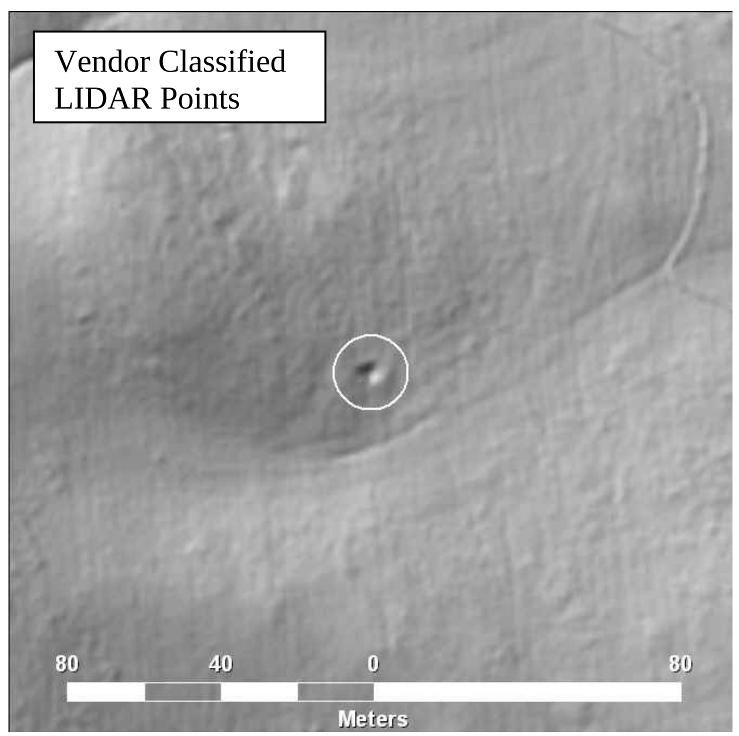

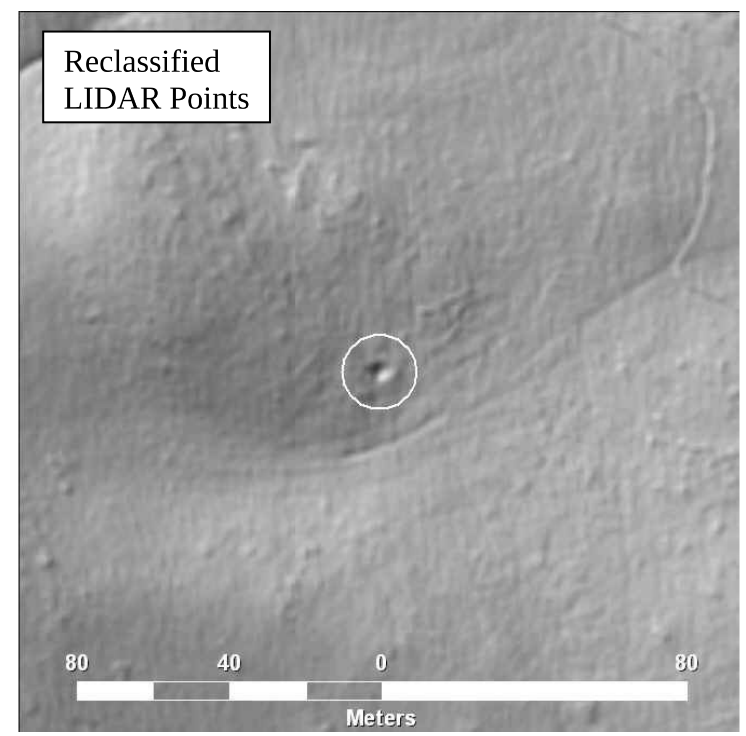

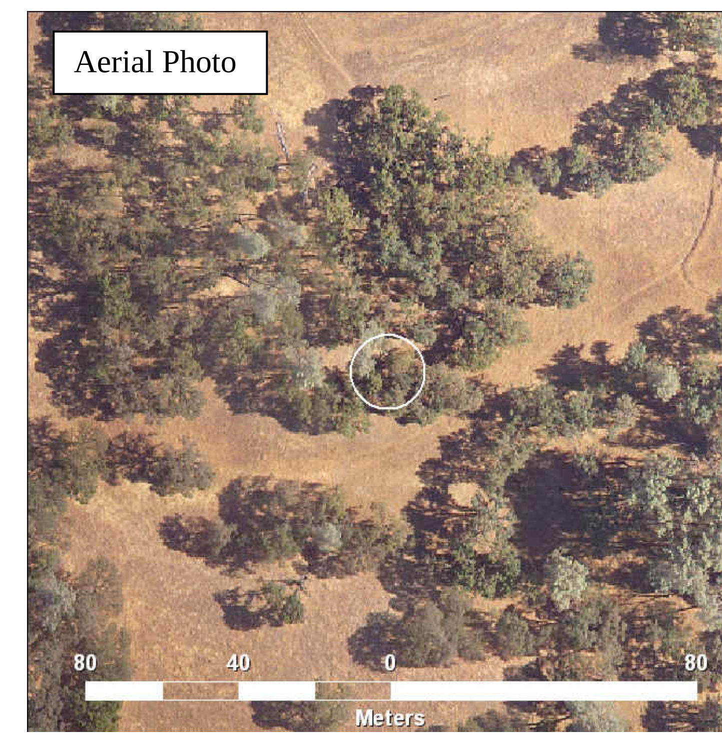

<table>
<tr>
<td>

Plot # 44

Feature size: 6.3 m, 4.3 m
Vegetation density: 67.05%
Surface method: TIN
DEM cell size: 1 m
Lidar block reference number: 5350

Additional features visible: no
Existing features more clearly visible: possible
</td>
<td>
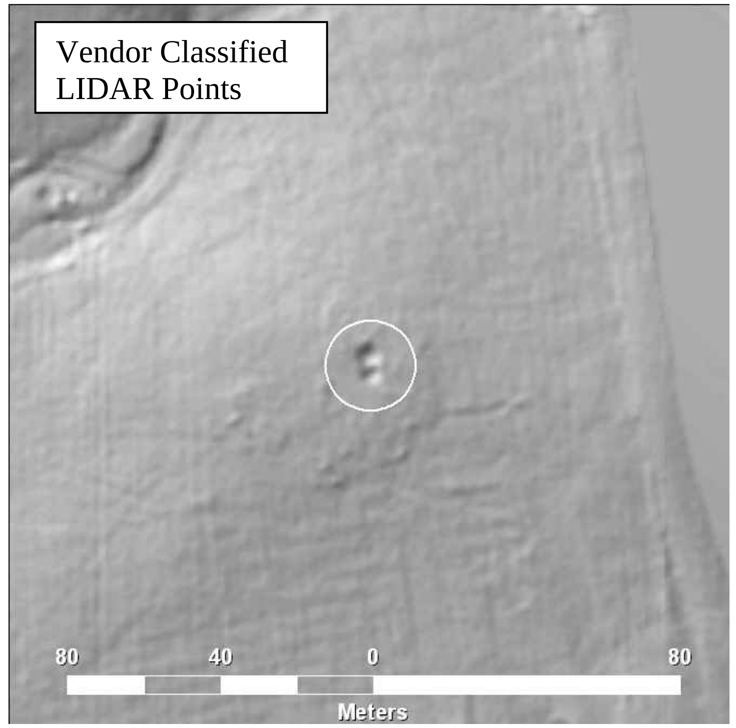

</td>
<td>
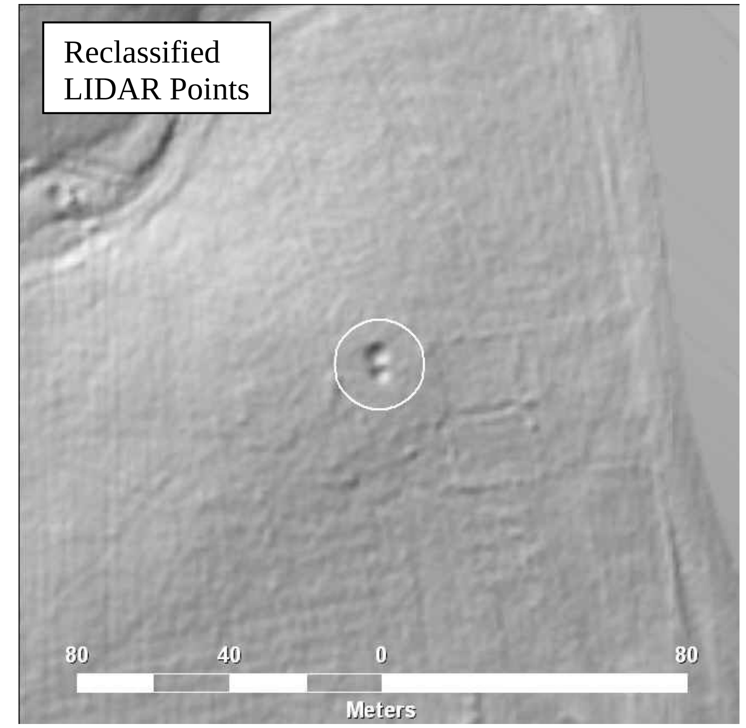

</td>
<td>
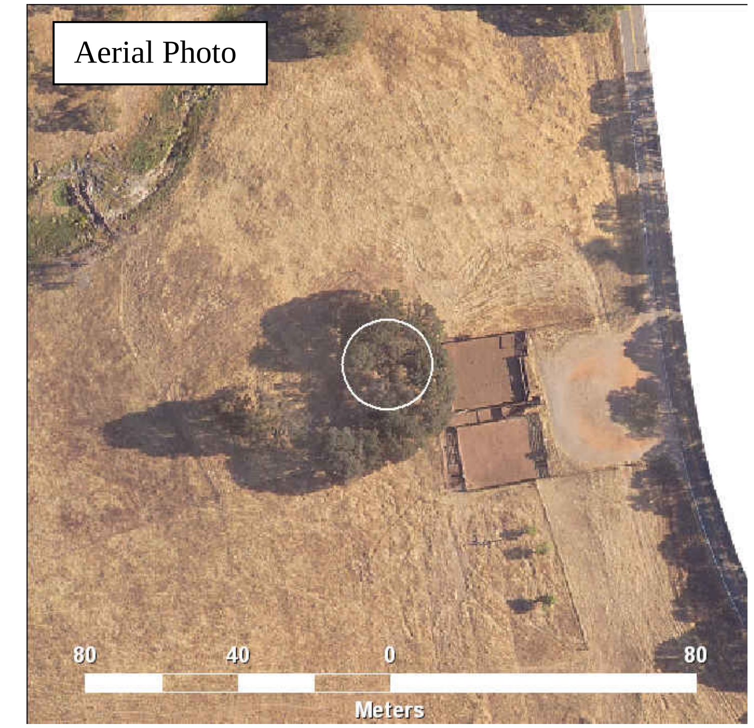

</td>
</tr>
<tr>
<td>

Plot # 45

Feature size: 6.5 m, 12 m
Vegetation density: 47.48%
Surface method: TIN
DEM cell size: 1 m
Lidar block reference number: 5678

Additional features visible: no
Existing features more clearly visible: possible
</td>
<td>
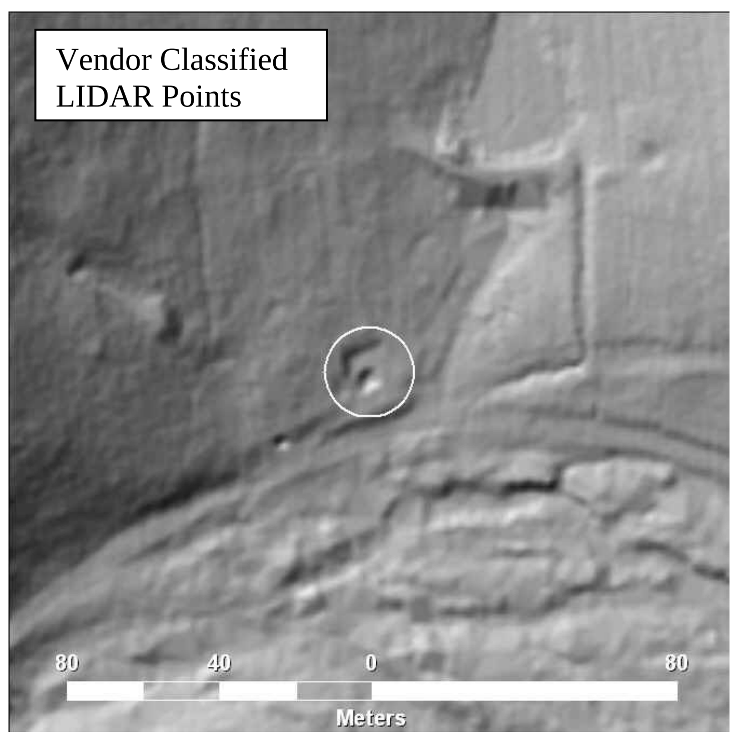

</td>
<td>
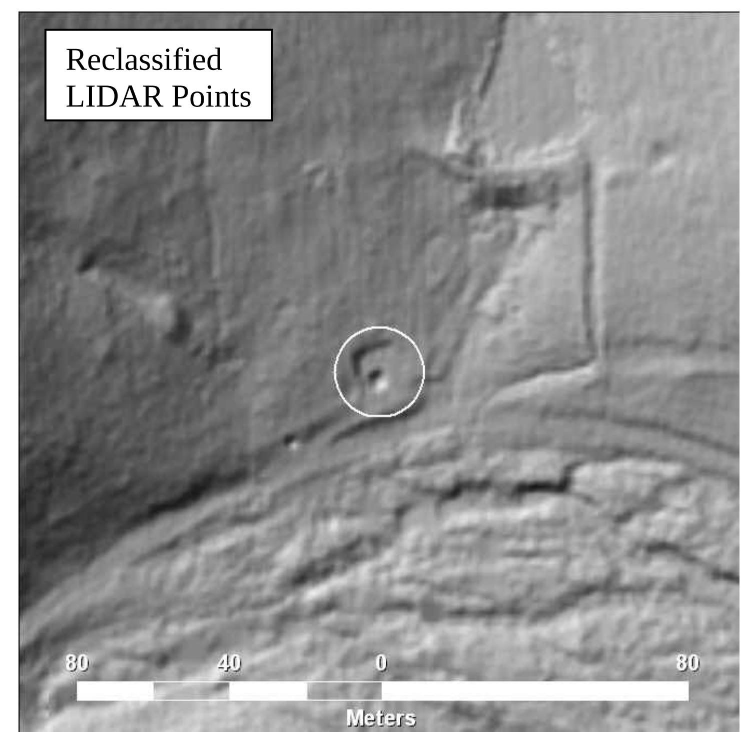

</td>
<td>
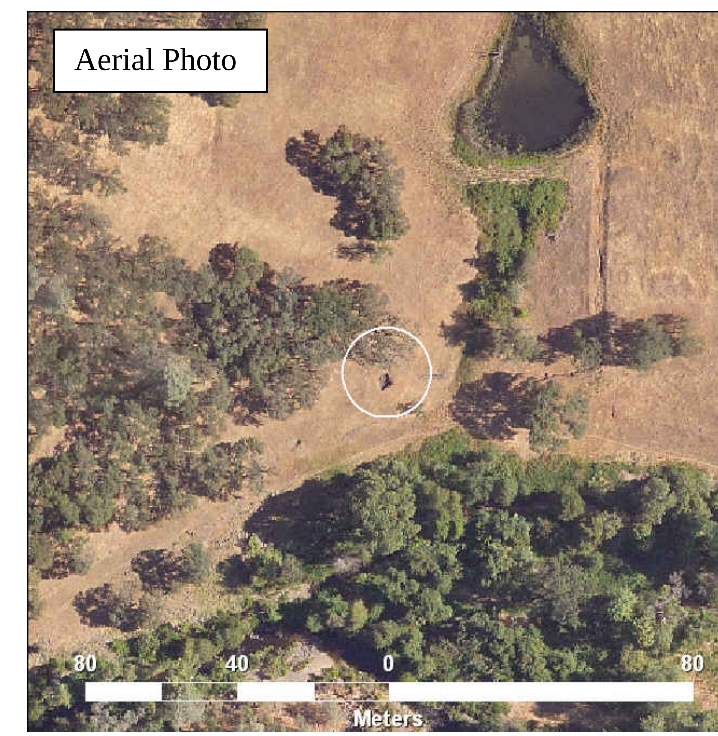

</td>
</tr>
</table>

Plot # 46 Feature size: 7.1 m Vegetation density: 44.58% Surface method: TIN DEM cell size: 1 m Lidar block reference number: 3975 Additional features visible: no Existing features more clearly visible: yes	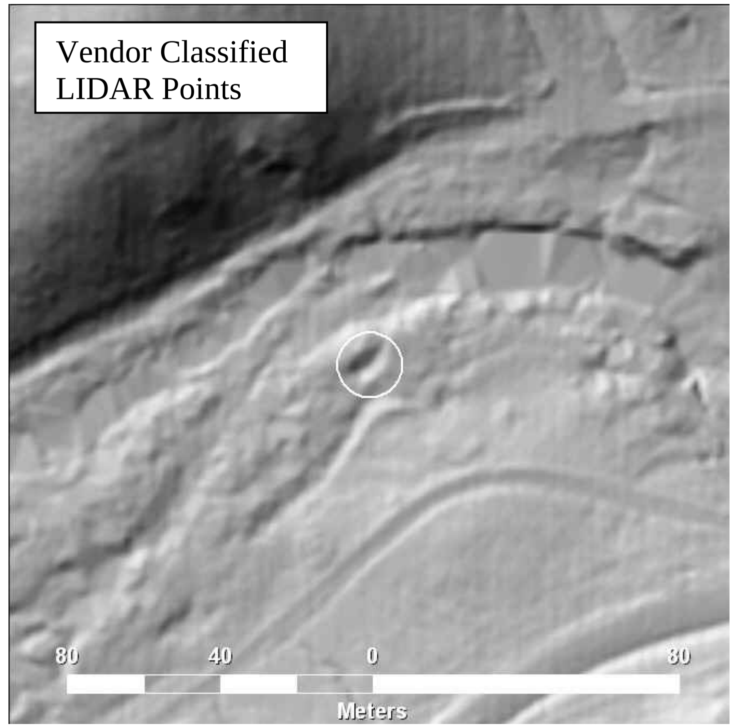	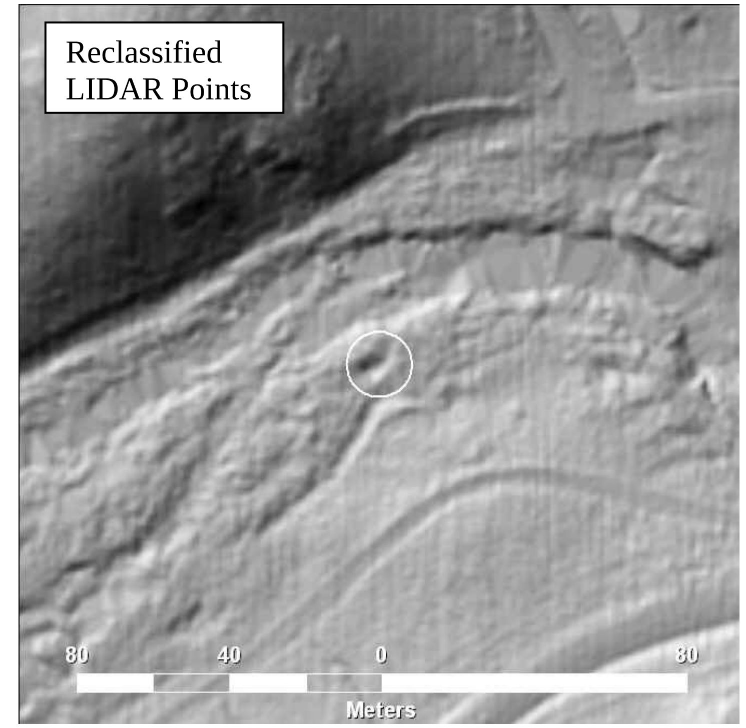	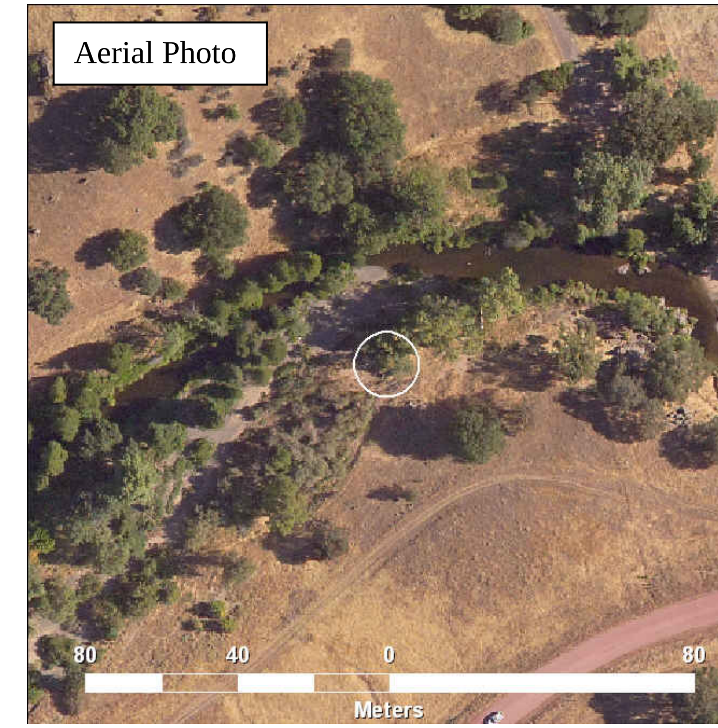
Plot # 47 Feature size: 8.0 m Vegetation density: 62.79% Surface method: TIN DEM cell size: 1 m Lidar block reference number: 5609 Additional features visible: no Existing features more clearly visible: possible	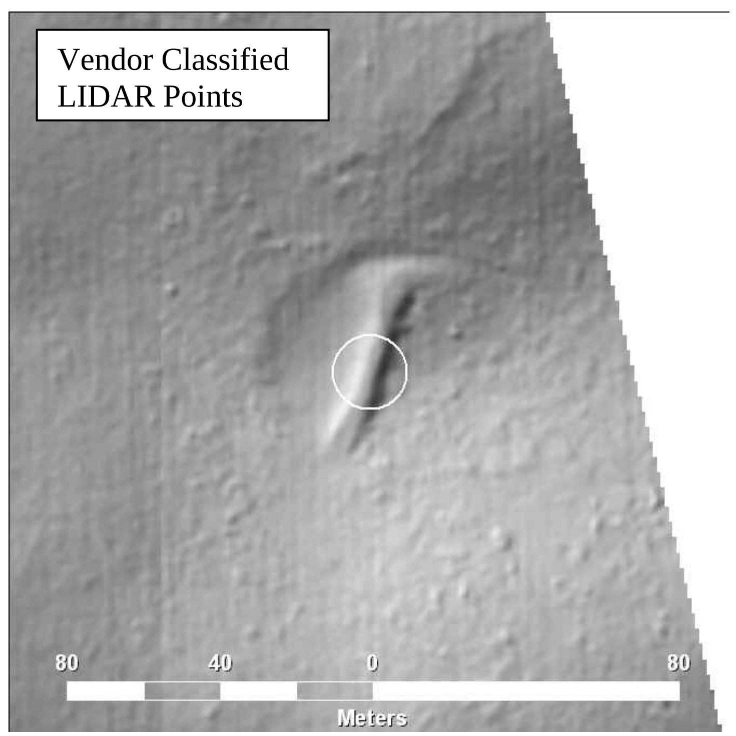	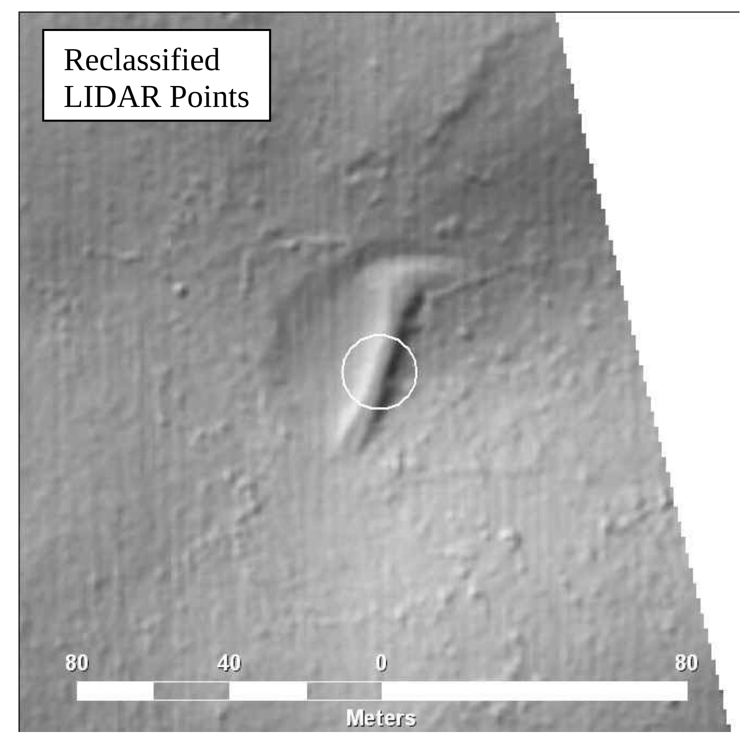	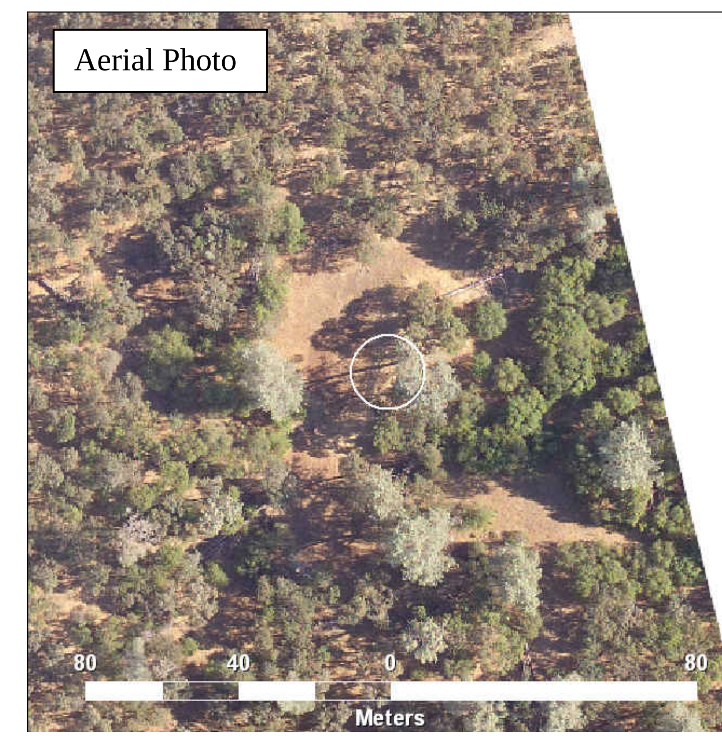

Plot # 48

Feature size: 8.2 m
Vegetation density: 46.96%
Surface method: TIN
DEM cell size: 1 m
Lidar block reference number: 5921

Additional features visible: no
Existing features more clearly visible: possible

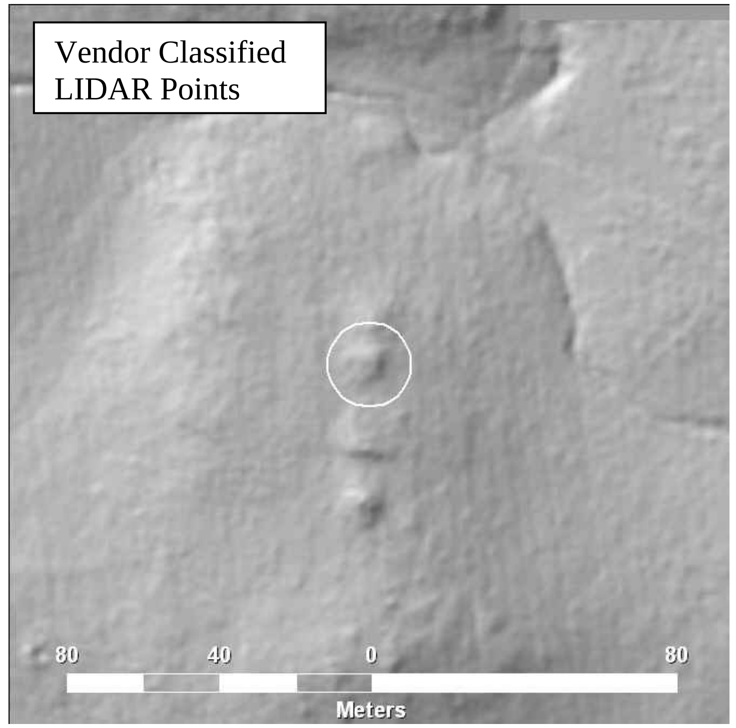

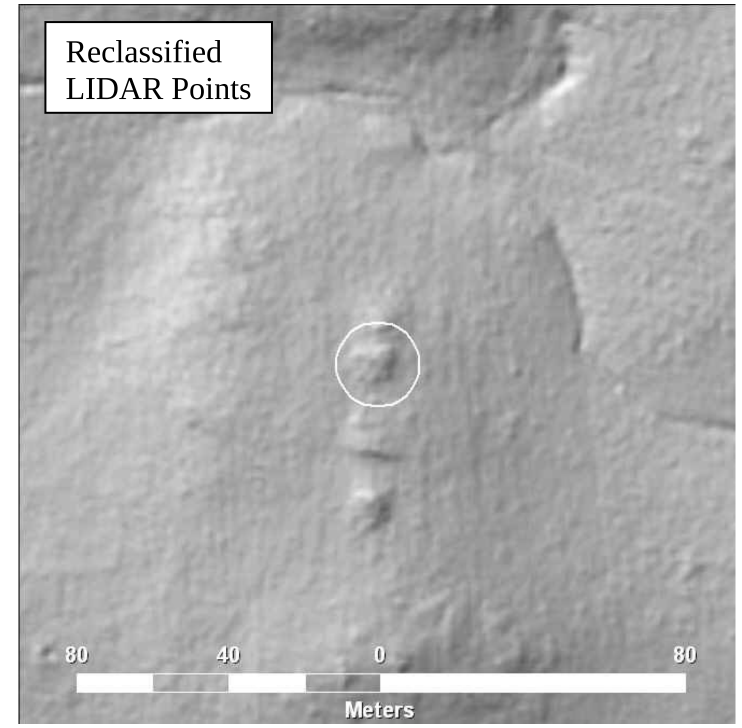

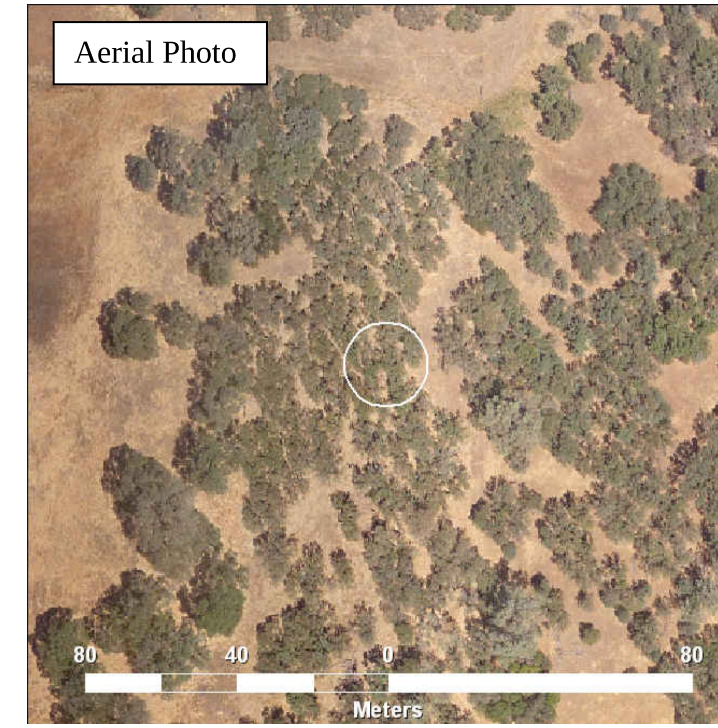

Plot # 49

Feature size: 8.2 m
Vegetation density: 51.24%
Surface method: TIN
DEM cell size: 1 m
Lidar block reference number: 4029

Additional features visible: no
Existing features more clearly visible: possible

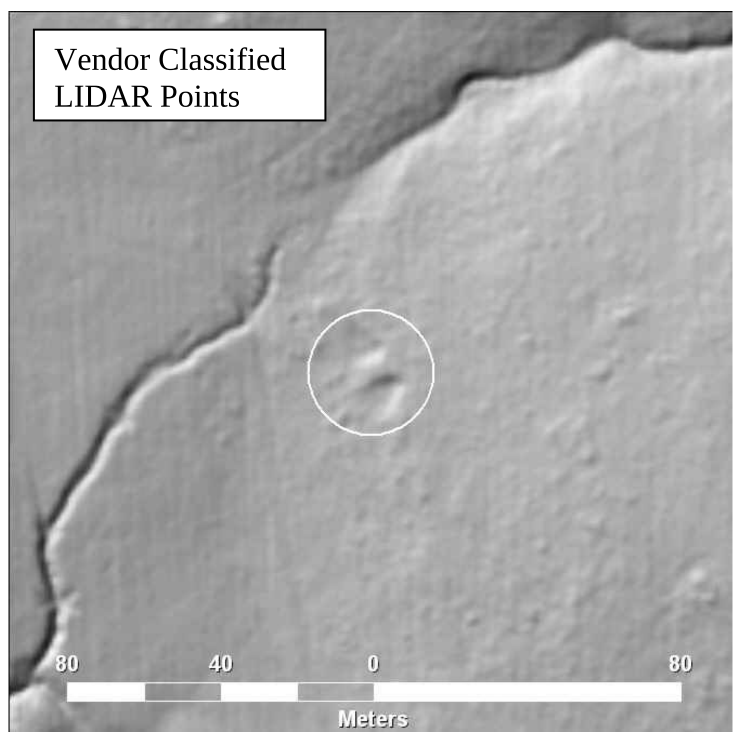

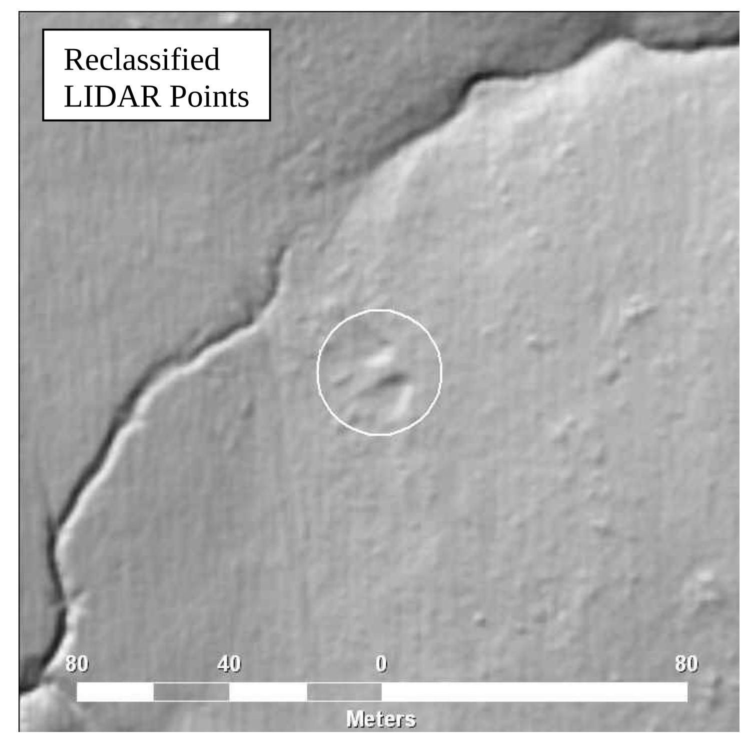

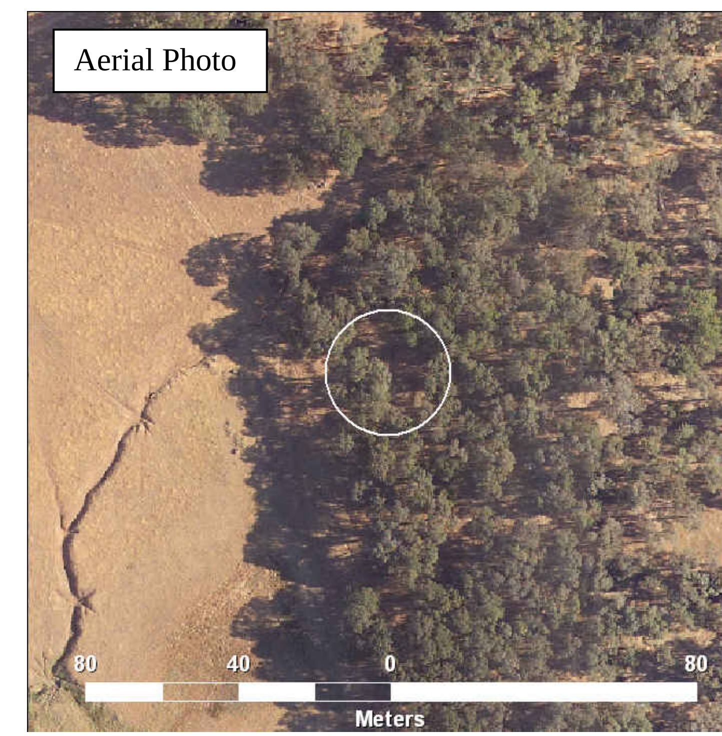

Plot # 50 Feature size: 8.6 m Vegetation density: 51.46% Surface method: TIN DEM cell size: 1 m Lidar block reference number: 5735 Additional features visible: no Existing features more clearly visible: possible	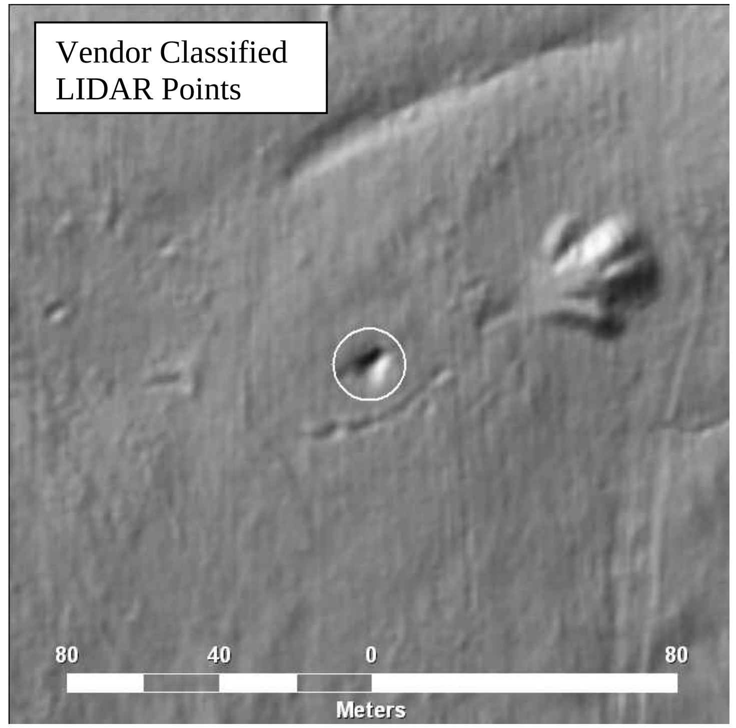	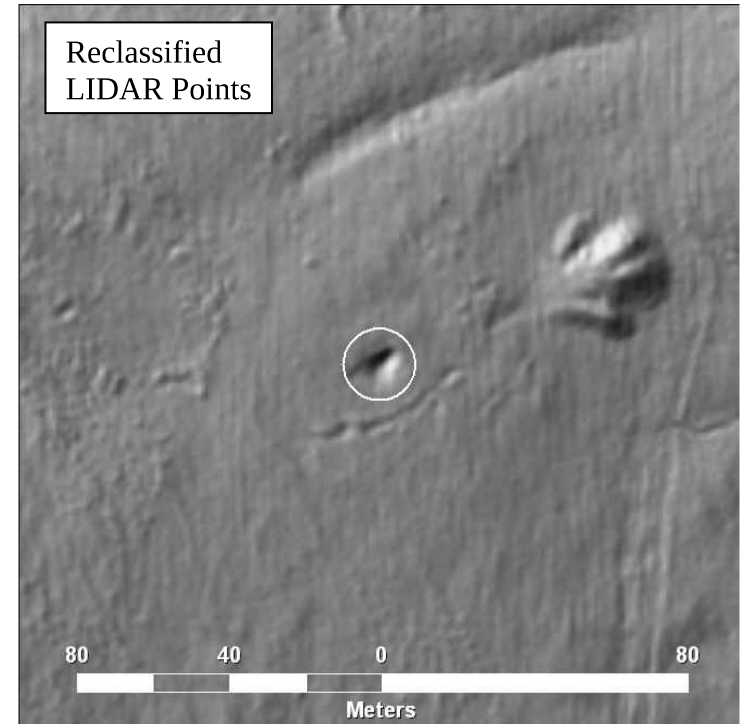	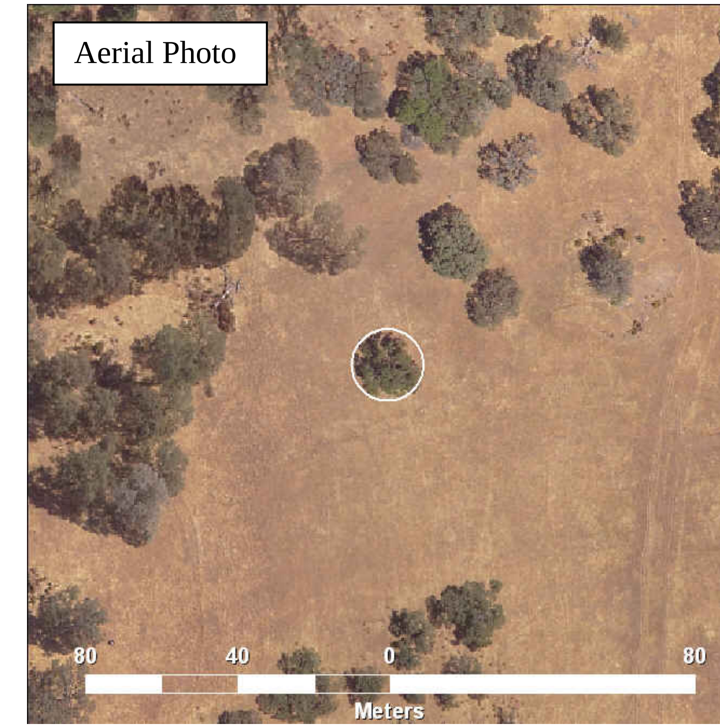
Plot # 51 Feature size: 8.7 m wide, 12.6 m long Vegetation density: 55.53% Surface method: TIN DEM cell size: 1 m Lidar block reference number: 5679 Additional features visible: no Existing features more clearly visible: possible	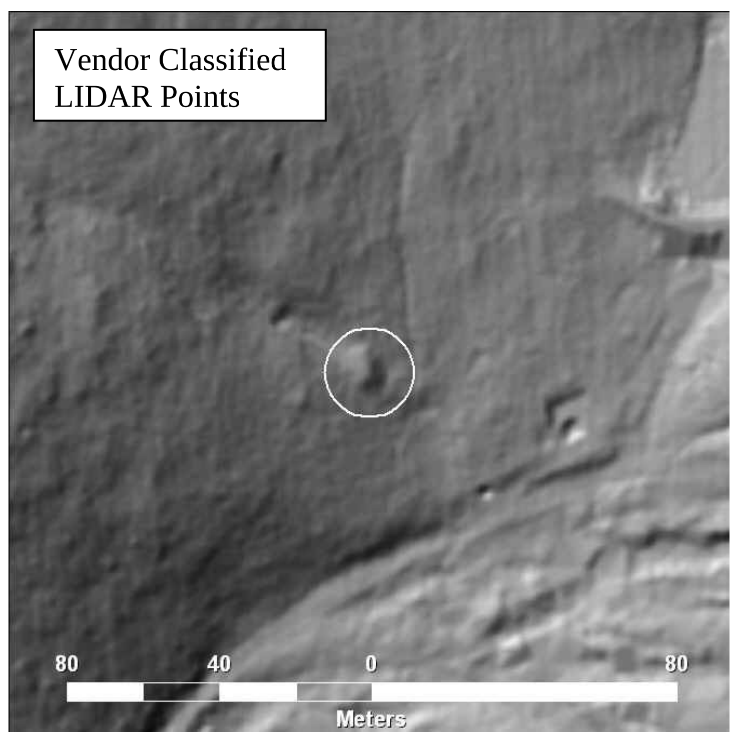	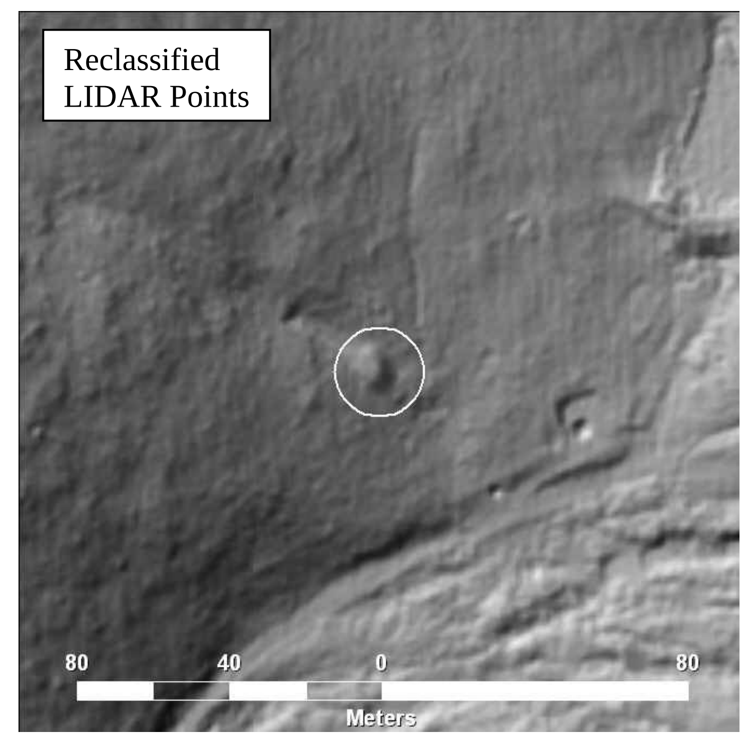	

<table>
<tr>
<td>

Plot # 52

Feature size: 8.8 m
Vegetation density: 40.96%
Surface method: TIN
DEM cell size: 1 m
Lidar block reference number: 4030

Additional features visible: no
Existing features more clearly visible: no
</td>
<td>
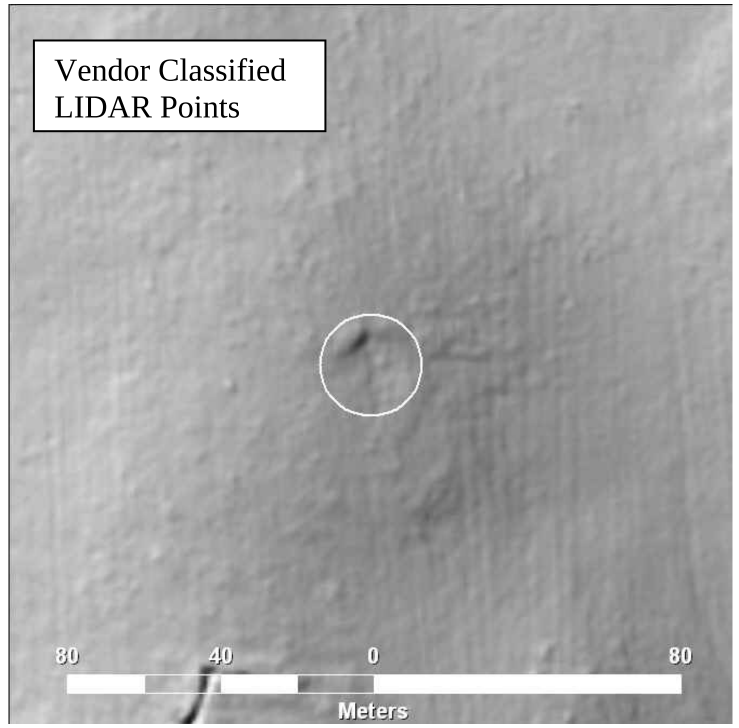

</td>
<td>
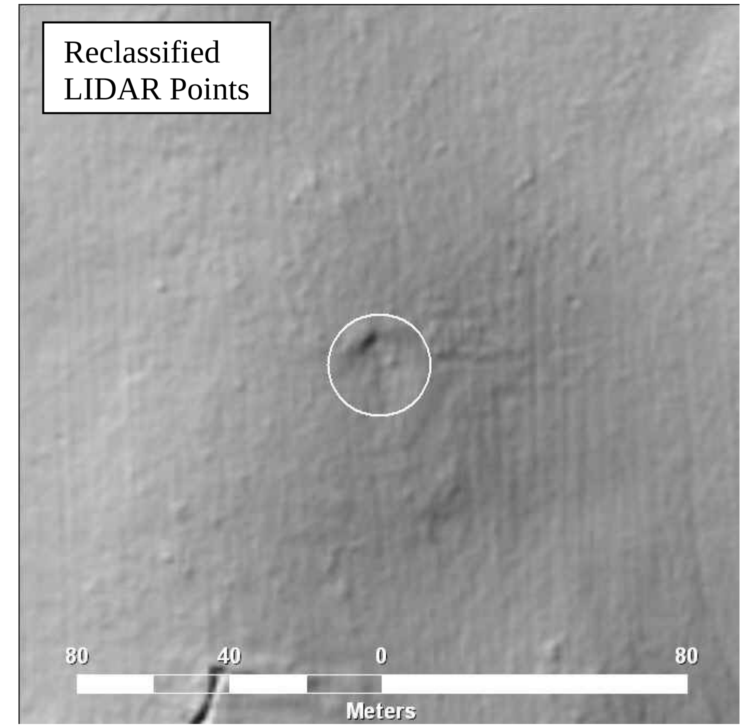

</td>
<td>
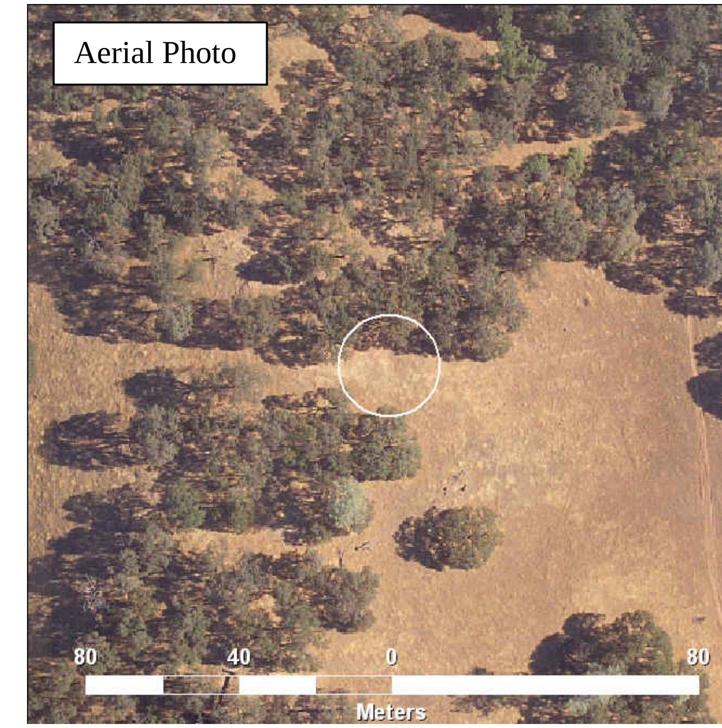

</td>
</tr>
<tr>
<td>

Plot # 53

Feature size: 10.3 m
Vegetation density: 46.88%
Surface method: TIN
DEM cell size: 1 m
Lidar block reference number: 5739

Additional features visible: possible
Existing features more clearly visible: possible
</td>
<td>
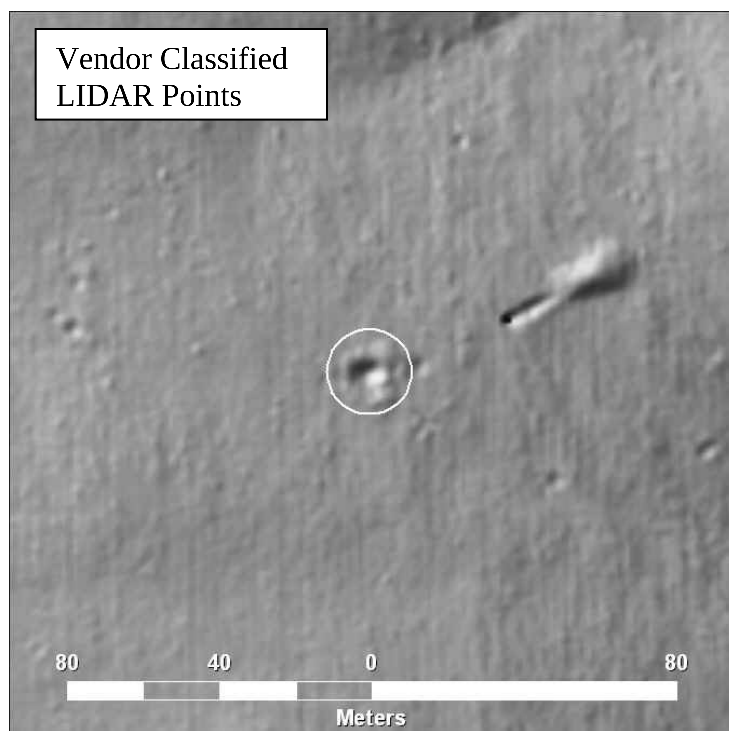

</td>
<td>
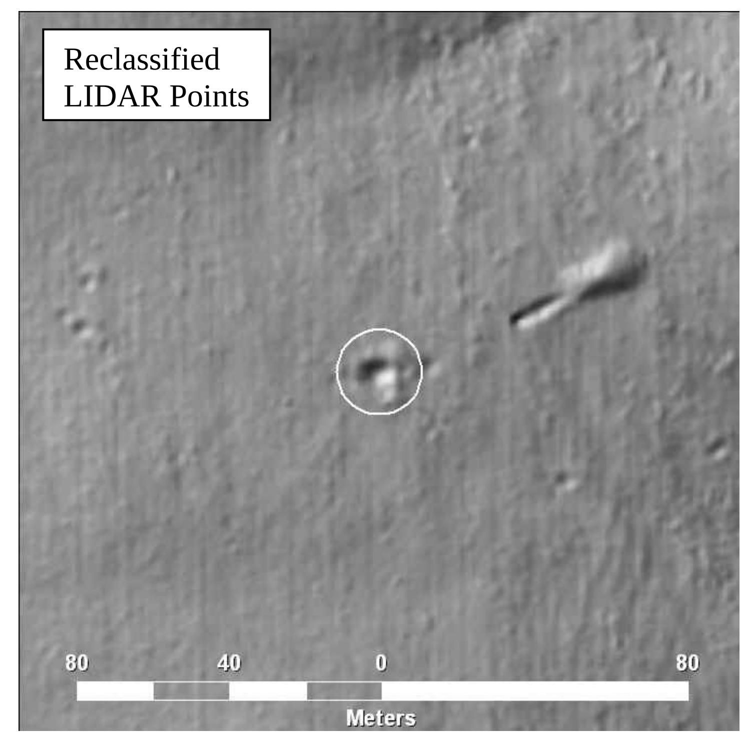

</td>
<td>
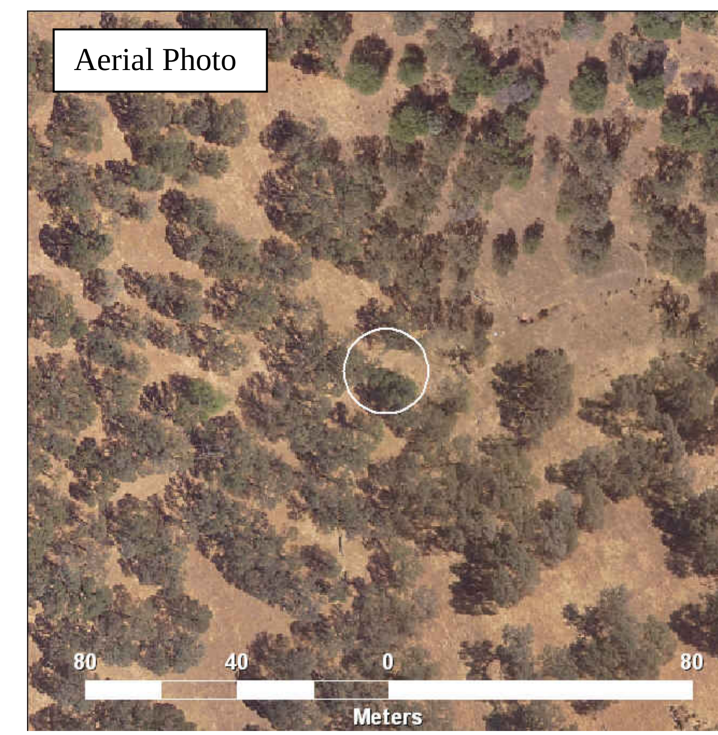

</td>
</tr>
</table>

Plot # 54

Feature size: 10.4 m
Vegetation density: 60.17%
Surface method: TIN
DEM cell size: 1 m
Lidar block reference number: 5913

Additional features visible: no
Existing features more clearly visible: possible

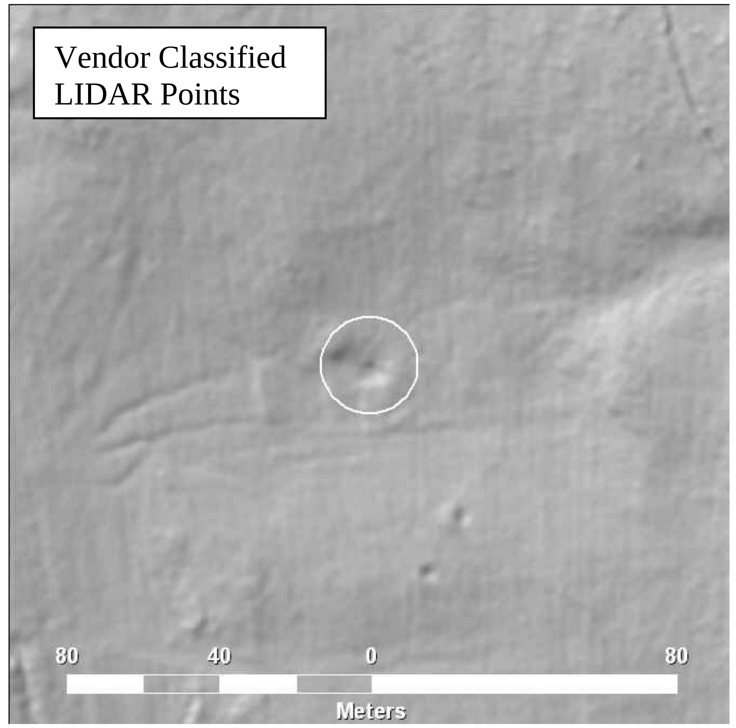

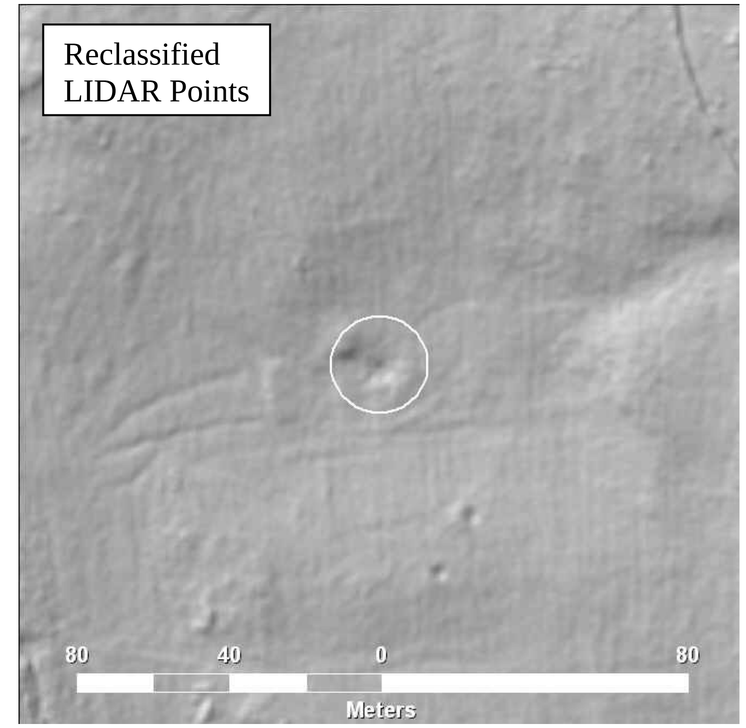

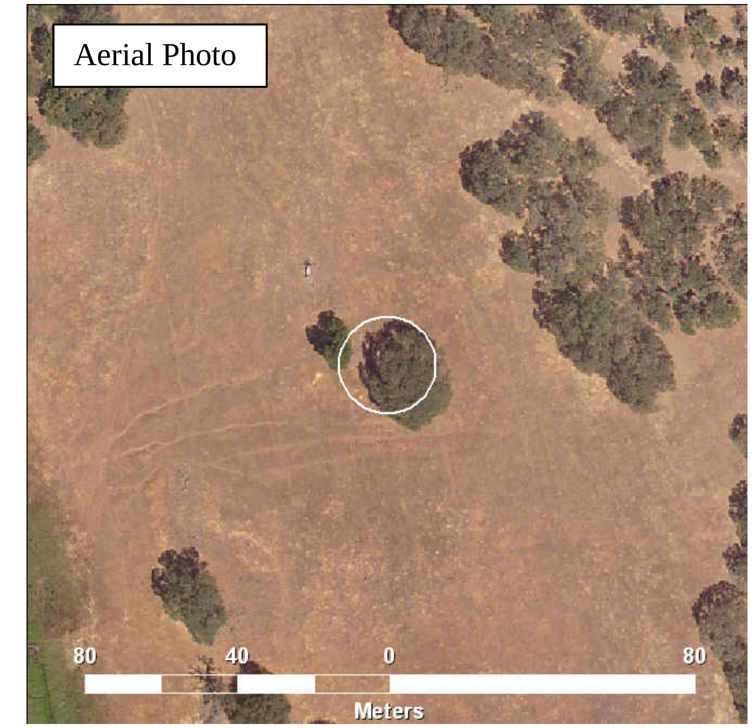

Plot # 55

Feature size: 11.3 m
Vegetation density: 36.49%
Surface method: TIN
DEM cell size: 1 m
Lidar block reference number: 5923

Additional features visible: no
Existing features more clearly visible: possible

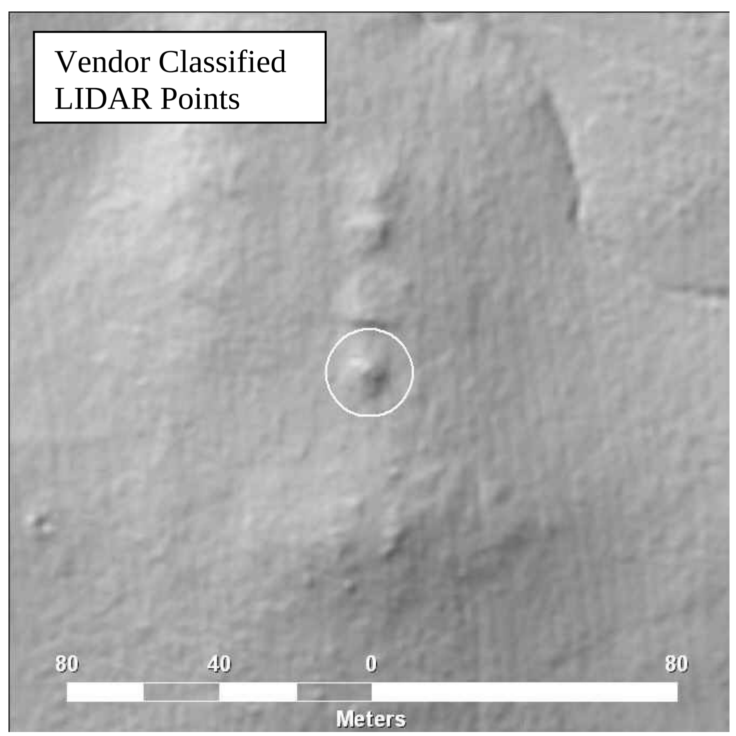

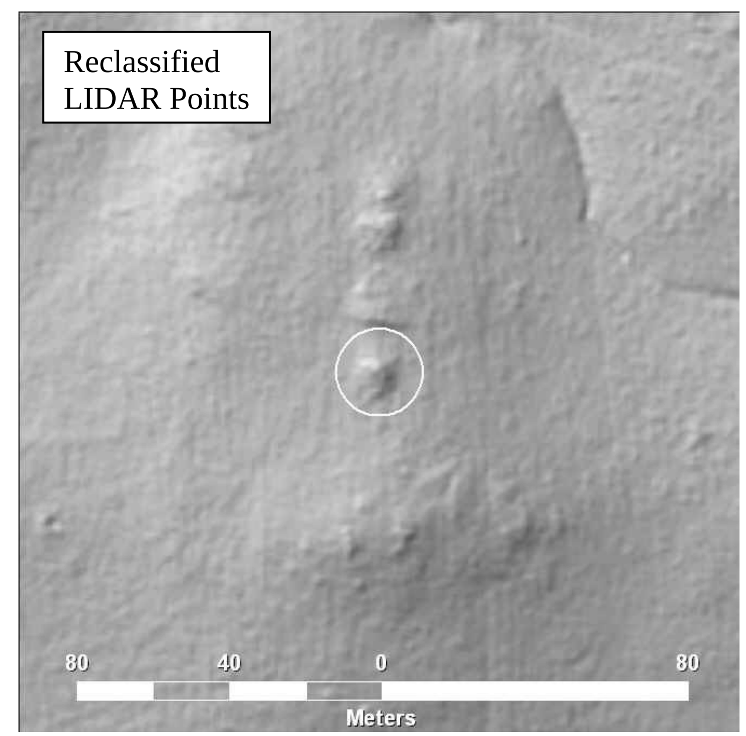

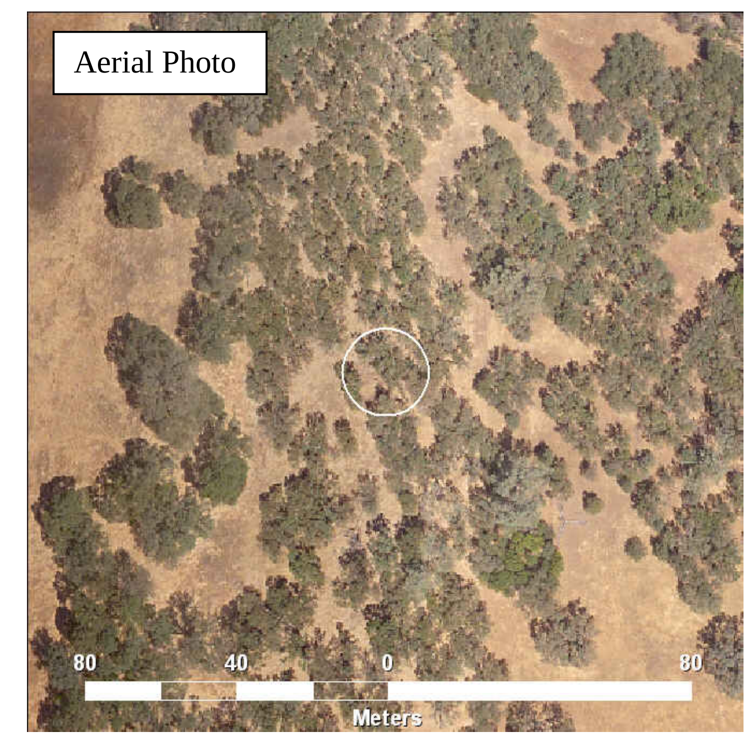

Plot # 56

Feature size: 12.20 m
Vegetation density: 43.21%
Surface method: TIN
DEM cell size: 1 m
Lidar block reference number: 5583

Additional features visible: no
Existing features more clearly visible: possible

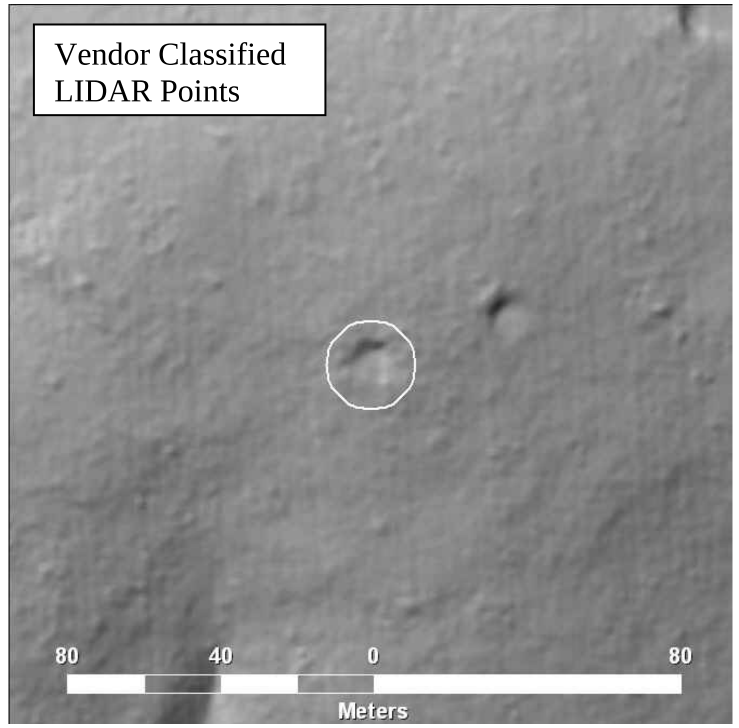

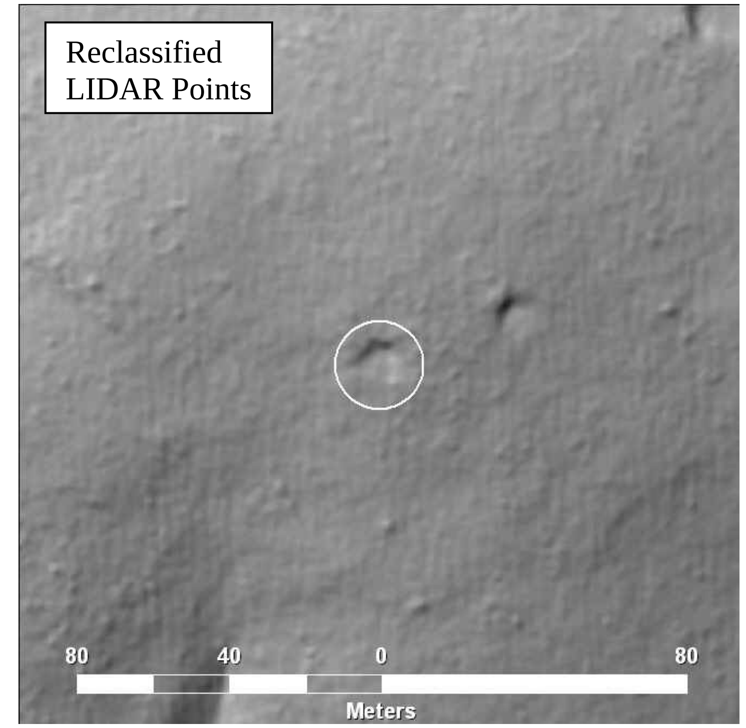

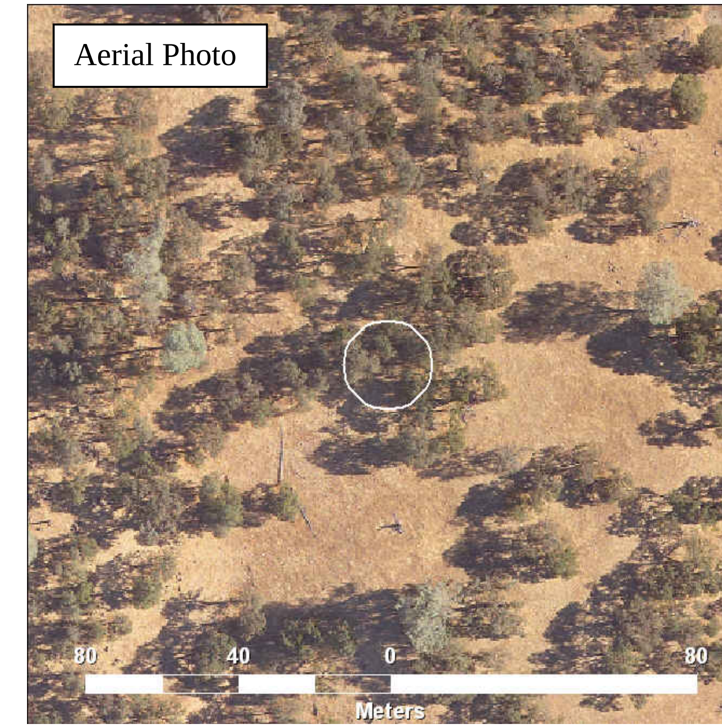

Plot # 57

Feature size: 14.3 m wide, 28.4 m long
Vegetation density: 46.03%
Surface method: TIN
DEM cell size: 1 m
Lidar block reference number: 4035

Additional features visible: no
Existing features more clearly visible: possible

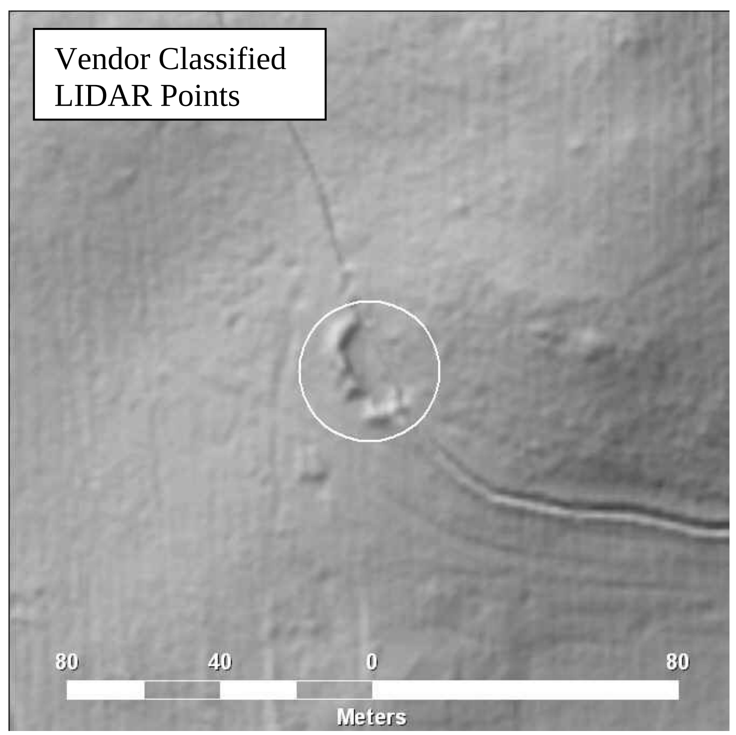

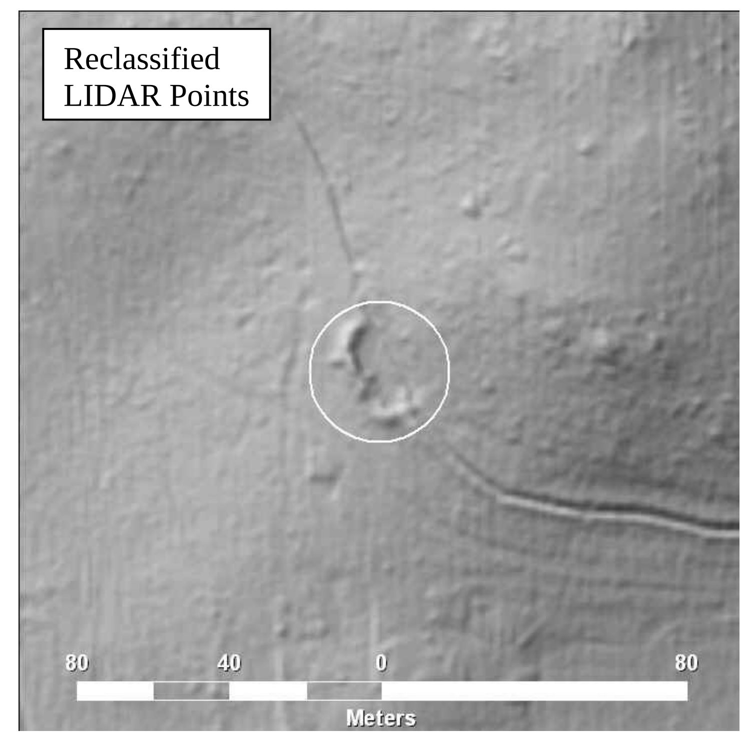

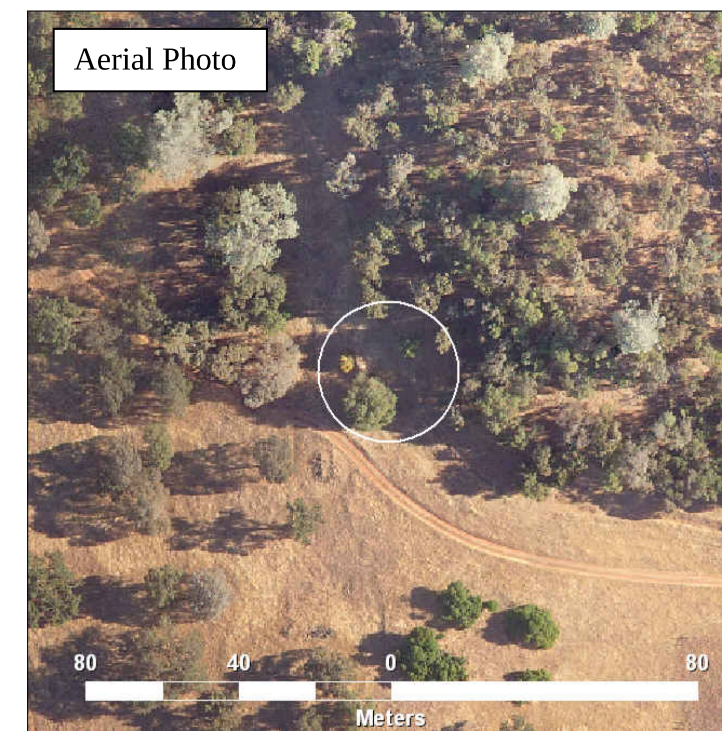

Plot # 58

Feature size: 17.4 m wide, 27.2 m long
Vegetation density: 48.85%
Surface method: TIN
DEM cell size: 1 m
Lidar block reference number: 3987

Additional features visible: possible
Existing features more clearly visible: no

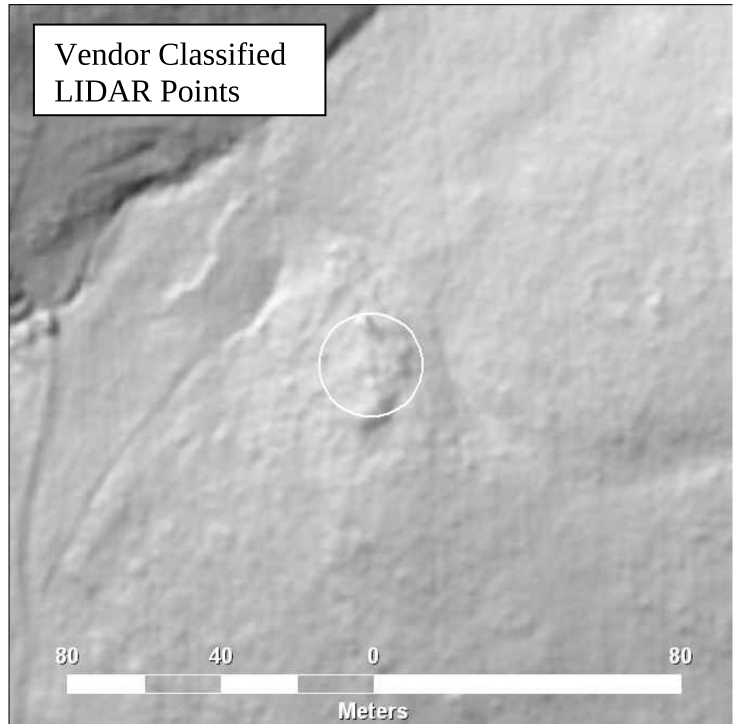

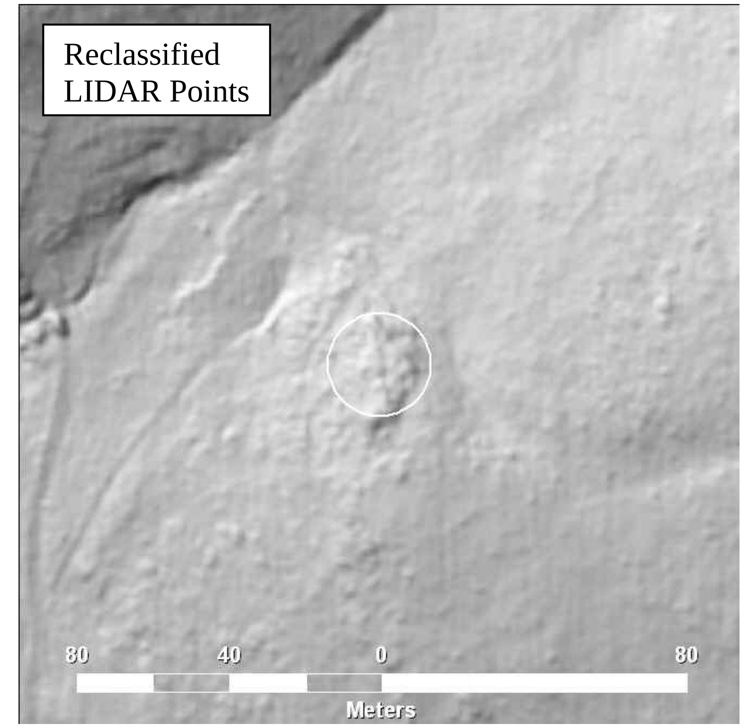

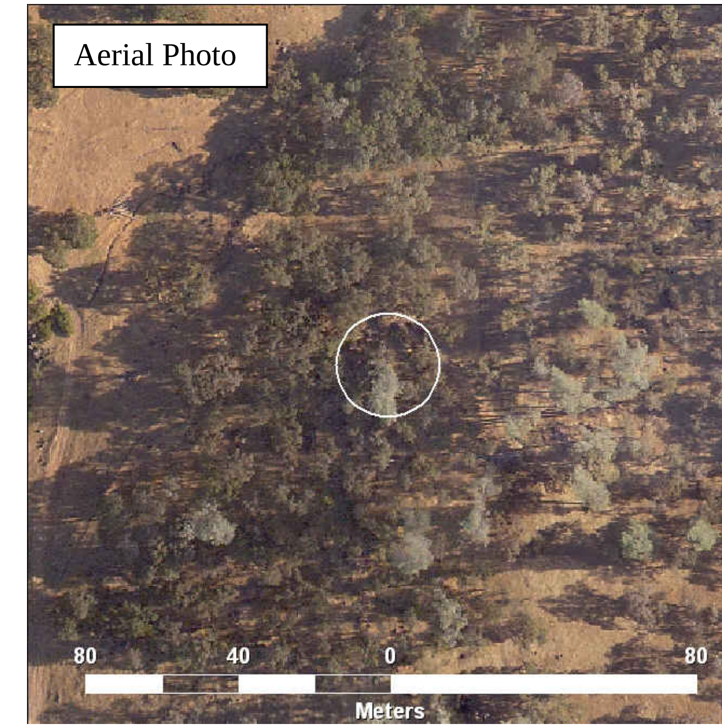

Plot # 59

Feature size: 3 m
Vegetation density: 63.28%
Surface method: TIN
DEM cell size: 1 m
Lidar block reference number: 4068

Additional features visible: no
Existing features more clearly visible: possible